School of
Civil Engineering and Geosciences

Newcastle University

Multiscale Impacts of Land Use/Management Changes on Flood Response in the River Hodder Catchment, North-West England

By

Josie Regina Martina Catharina Geris BSc MSc

School of Civil Engineering and Geosciences,
Newcastle University,
Newcastle upon Tyne,
NE1 7RU,
UK.

A thesis submitted for the degree of Doctor of Philosophy (Ph.D) at Newcastle University

April 2012

Declaration

I certify that no part of the material offered in this thesis has been previously submitted by me for a degree or other qualification in this or any other University.

Signed

Josie Regina Martina Catharina Geris

Abstract

There is substantial evidence that land use/management changes (LUMCs) can impact runoff generation at the local scale; however, it is unclear how these impacts are modified as they travel through the river channel network to affect downstream catchment flooding. There is a need for data from multiscale monitoring studies in catchments undergoing known LUMCs to assess the extent to which impacts can be detected at increasing catchment scales. This understanding is needed in developing reliable methods for assessing the potential of rural based flood prevention and mitigation measures, urgently required by catchment planners. The aim of the present study is to generate and analyse a new multiscale dataset which will serve to gain a better understanding of the effects of local LUMCs on catchment response at increasing scales.

This study investigates the impacts of recent LUMCs (drain blocking, stocking density changes, and afforestation) in the headwaters of the River Hodder (261 km^2), North-West England, UK. An unusually dense nested monitoring network (28 stream gauges) was set up at scales ranging from ~1 ha to 261 km^2. Data Based Mechanistic (DBM) modelling and a simple Storage Discharge Detection (SDD) model were used to compare pre- and post-change hydrographs at increasing scales in an effort to detect short-term change signals and their propagation to larger scales. A novel physically based Model for Upland Runoff Storage and Flow Fields (MURSAFF) was developed to further investigate the short- and long-term impacts of LUMC in complex landscapes at the micro catchment scale (~1 km^2). The results were integrated into a semi-distributed catchment impact routing model to explore the effects on the downstream catchment response.

No statistically significant evidence was found in the DBM and SDD results to suggest that any of the LUMCs had a short-term impact on catchment response at scales from 1 km^2 up to the Hodder catchment scale (261 km^2). This is attributed to the proportion of area affected by change, the timescale of impacts, and the natural variability in catchment response. Short-term small scale (< 1 km^2) field observations and MURSAFF

predictions of the impacts of drain blocking involved an increase in the local storage and change in the flow fields. However, these changes are insignificant at the micro catchment scale. The MURSAFF simulated impacts of reductions in stocking density involve attenuation of the flood hydrograph mainly. Predictions of the downstream effects suggest they will be relatively small and different for each storm, with the lack of internal synchronisation of the sub-catchment responses and the natural variability therein being dominant factors in determining the impacts on the catchment outlet response. These predictions are consistent with the failure to detect any significant impacts in the post-change records.

Acknowledgements

First and foremost I would like to thank my main supervisor Prof. Enda O'Connell for his guidance and advice, his encouragement and his immense knowledge. I would also like to sincerely thank Prof. John Ewen for his sound advice, motivation and endless inspirational ideas. It has been an enlightening experience to work with them both.

Thanks to my second supervisor Dr. James Bathurst for his guidance and for reading draft versions of this thesis and to Dr. Greg O'Donnell for his advice during numerous discussions on some of the more practical parts of this work. I would also like to thank Dr. Will Mayes for his initial advice on the field instrumentation. Thanks to Professor Andrew Metcalfe for his advice on the statistical analyses and to Dr. Lucy Manning for getting me started with the DBM work. I am grateful to Dr. Mark Wilkinson, Mr. Gareth Owen, Mr. Ian Benson and Mr. Nick Barber for their assistance during some of the field trips.

This study was funded by the UK Environment Agency under project SC060092. From the EA, I would like to acknowledge Stuart Eckersley for providing me with rainfall and discharge data. Also thanks to Adam Bayliss, Jim Walker, Wendy Brooks and Amy Shaw, who have provided me with the occasional advice during this study. Thanks to United Utilities, Natural England (Jon Hickling) and the RSPB (Pete Wilson) for field access and installation permission. From United Utilities, I would like to thank Martin McGrath, Nigel Pilling, Mike Conway, and Claire Maddison for providing information on the SCaMP project and the UU abstraction works, and making the abstraction data available. I would also like to thank all tenant farmers and other land owners in the Hodder valley for their cooperation and welcome chats during long field days.

I would like to thank my mother and father, my sister Lonney, Mark's family, my dear friend Annelien, and all the rest of my family and friends who have been there for me always. Finally, I would like to thank my future husband Mark, whom without this work might not have existed. Thank you for your love and support, for your patience and encouragement when it was most required, and for sharing the joys in life with me.

Contents

Abstract..... i

Acknowledgements..... iii

List of Figures..... ix

List of Tables..... xviii

Abbreviations..... xxi

1 Introduction 1

1.1 Land Use Management Changes and Flooding 1

1.2 Research Aims and Objectives 4

1.3 Thesis Structure 7

2 Literature Review 10

2.1 Introduction 10

2.1.1 Chapter Overview 10

2.1.2 Definition of Scale in the Context of Land Use/Management Change Impacts.. 11

2.2 Local Scale Land Use/Management Change Impacts: Plot, Hillslope and Small Catchment Experiments 13

2.2.1 Traditional Experimental Design Approaches 13

2.2.2 Typical UK Upland Rural Land Use/Management Changes and Local Impacts.. 15

2.3 Local Scale Land Use/Management Change Impacts: Peatland Management 16

2.3.1 Peatland Hydrology 16

2.3.2 Peat Drainage and Drain Blocking Effects 25

2.3.3 Stocking Density and Management Effects 29

2.3.4 Modelling Local Scale Land Use/Management Impacts in UK Uplands ... 32

2.4 Catchment Scale Land Use/Management Change Impacts: Detection and Attribution 36

2.4.1 Change Detection Approaches 37

2.4.2 Challenges in LUMC Detection 39

2.4.3 Examples of Change Detection Methods 41

2.4.4 Attribution of Catchment Scale Effects of Land Use/Management Changes. 44

2.5 Catchment Scale Land Use/Management Change Impacts: Monitoring, Modelling and Prediction 47

2.5.1 Key Issues with (Up-) Scaling Land Use/Management Change Impacts...47
2.5.2 Multiscale Nested Experimental Catchment Designs...49
2.5.3 Modelling and Predicting the Connection between LUMC effects on Hydrological Behaviour at the Small and Large Scales...51
2.6 Summary...55
3 Catchment Description and Land Use/Management Changes...57
3.1 Introduction...57
3.1.1 Chapter Overview...57
3.1.2 Catchment Selection...57
3.1.3 General Catchment Description...58
3.2 Geology and Pedology...60
3.2.1 Geology...60
3.2.2 Superficial Deposits...61
3.2.3 Soil Associations...62
3.3 Climate...63
3.3.1 Precipitation...64
3.3.2 Temperature and Evaporation...65
3.4 Land Use and Vegetation...65
3.4.1 Grassland...65
3.4.2 Moorland...65
3.4.3 Woodland...67
3.4.4 Cultivation...67
3.5 Water Supply Infrastructure...67
3.5.1 Stocks Reservoir...68
3.5.2 Bowland Abstraction System...68
3.5.3 Dunsop Abstraction System...69
3.6 Flooding...71
3.7 Land Use/Management Changes...72
3.7.1 Historical Land Use/Management Changes...73
3.7.2 Forestry Commission Felling Plan...75
3.7.3 UU SCaMP Land Use/Management Changes...77
3.8 Summary...91
4 Multiscale Experimental Monitoring Design and Data Collection...92
4.1 Introduction...92
4.1.1 Chapter Overview...92

4.1.2 Monitoring Rationale 92
4.1.3 Monitoring Design Overview 93
4.2 Existing Hydrometric Network 95
4.2.1 Rain Gauges 95
4.2.2 Flow Gauges 96
4.3 Rain Gauge Network 97
4.3.1 Network Design 97
4.3.2 Data Processing and Quality Control 98
4.3.3 Estimation of Catchment Precipitation 103
4.4 Automatic Weather Station 106
4.4.1 Location and Technical Description 106
4.4.2 Data Processing and Quality Control 107
4.4.3 Determination of Evapotranspiration 107
4.5 Stream Gauge Network 108
4.5.1 Network Design 108
4.5.2 Data Processing and Data Quality Control 112
4.5.3 Rating Curves 113
4.5.4 Discharge obtained from weirs 120
4.6 Data Collection, Data Availability and Overall Quality Control 120
4.6.1 Data Collection and Data Availability 120
4.6.2 Water Balance Checks 121
4.7 Summary 124
5 Change Detection Analysis of Land Use/Management Change Impacts at Increasing Scales 125
5.1 Introduction 125
5.2 Natural Variability in Hydrological Conditions and Catchment Response 126
5.2.1 Meteorology 126
5.2.2 Catchment response 129
5.2.3 Short term data overview 131
5.3 Evaluation of Change Detection Techniques Using Long Term Mini and Meso Scale Hodder Data 133
5.3.1 Data Based Mechanistic Modelling 134
5.3.2 Storage Discharge Detection (SDD) Model 152
5.3.3 Discussion of the use of DBM and SDD Models for Change Detection 168
5.3.4 Peak Flow Analysis 170
5.4 Multiscale Short Term Land Use Change Data Analysis 174

5.4.1 SDD Pre- and Post-Change Recession Analyses 174
5.4.2 Pre- and Post-Change SDD Model Simulations 180
5.4.3 Pre- and Post-Change Observed and SDD Simulated Peak Flows 182
5.4.4 Discussion of Short Term LUMC Impacts 183
5.4.5 Scaling of SDD parameter estimates 185
5.5 Summary 188
6 Modelling Local Scale Effects of Land Use/ Management Changes on Storage and Runoff 189
6.1 Introduction 189
6.1.1 Chapter Overview 189
6.1.2 Case Study Description 190
6.2 Observed Local Grip Blocking Effects 192
6.3 MURSAFF model 196
6.3.1 Model Requirements 196
6.3.2 Model Description 197
6.3.3 Irregular Grid Set-up 200
6.4 MURSAFF Parameterisation, Calibration and Validation 202
6.4.1 Parameterisation and Calibration for CRO_sc5 202
6.4.2 Validation for CRO_sc5 207
6.4.3 Calibration and validation for BRE_sap 211
6.5 Simulation of Pre- and Post-Grip Blocking Effects on Flood Hydrographs 212
6.5.1 Simulation Results 212
6.5.2 Discussion of Grip Blocking Simulation Results 216
6.6 Stocking Density and Management Change Effects 218
6.6.1 MURSAFF Set-Up for LOS_mid 219
6.6.2 Simulation Results 224
6.6.3 Discussion of Stocking Density Change Simulation Results 231
6.6.4 MURSAFF LOS_mid predictions and SDD 231
6.7 Summary 233
7 Up-scaling of Land Use/Management Change Impacts 234
7.1 Introduction 234
7.2 Multiscale Catchment Behaviour 235
7.2.1 Multiscale Catchment Runoff Aggregation 235
7.2.2 Multiscale Catchment Response and Precipitation Severity 239
7.2.3 Scaling Hydrograph Characteristics under Different Natural Conditions 244

7.2.4 Discussion on Up-Scaling of Potential LUMC Effects 249
7.3 Propagation of Local Scale Simulated Effects to the Catchment Outlet..... 251
7.3.1 Catchment Impact Model 251
7.3.2 Propagation of Land Use/Management Change Effects..... 254
7.3.3 Discussion..... 265
7.4 Summary..... 267
8 Conclusions and Recommendations 268
8.1 Research Summary..... 268
8.2 Conclusions..... 272
8.3 Recommendations for Future Work 279
References..... 281

Appendix 1 Newcastle University Stream Gauges..... 312

Appendix 2 Statistical Analyses related to Chapter 5..... 313

Appendix 3 Draft MURSAFF Journal Paper..... 334

Appendix 4 MURSAFF Grid Improvement Stages..... 355

Appendix 5 Additional Results of Empirical Changes at the Mini Scale on the Downstream HP Peak Flow, Related to Section 7.3.2..... 359

List of Figures

Figure 1.1 Schematic representation of the proportional level of knowledge and relative interest of catchment managers regarding LUMC effects on flooding at a range of scales 2
Figure 1.2 Schematic representation of the thesis structure and general methodology. The numbers in brackets indicate the objectives that are associated with the different chapters 8
Figure 2.1 Definition of spatial scales within the current study 12
Figure 2.2 Schematic representation of the terms used to describe different kinds of peatlands 17
Figure 2.3 Schematic representation of runoff generation at an intact peat site prior to a rainfall event (left) and during a rainfall event (right) 24
Figure 2.4 Runoff generation in drained peat prior to or early during a rainfall event (left) and during larger rainfall events (right) 27
Figure 2.5 Runoff generation in a blocked drain prior, early on in, or after a rainfall event (left) and during an event (right) 29
Figure 2.6 Schematic representation of a multiscale nested structure for instrumentation (altered from O'Connell et al. (2007b)) 50
Figure 3.1 Location of United Utilities' SCaMP areas 58
Figure 3.2 Schematic representation of the Hodder catchment 59
Figure 3.3 Geology in the Hodder catchment (source: British Geological Survey 1:50,000, through Digimap) 61
Figure 3.4 Superficial deposits in the Hodder catchment (source: BGS 1:50,000) 62
Figure 3.5 Soil Associations of the Hodder Catchment (source: Avery, 1980) 63
Figure 3.6 Average monthly precipitation (top) and days of snow lying (middle) for the uplands (black) and the lowlands (grey), and average monthly temperature (bottom) for the Hodder catchment. 64
Figure 3.7 Land Cover Map 2000 for the Hodder catchment (source: LCM 2000) 66
Figure 3.8 Schematic representation of UU Bowland Intake System, River Langden 69
Figure 3.9 Schematic representation of UU Dunsop Intake system in the River Dunsop catchment 70
Figure 3.10 EA flood inundation map showing areas prone to flooding for the 1/100 year (dark blue) and 1/1000 year flood events. Superimposed are CBHE recorded floods, colour coded according to the time of the year in which they occurred. 71
Figure 3.11 Example of typical drainage design from the upper part of the Brennand catchment 73
Figure 3.12 Stocking density rates per farm in the upper Hodder catchment over the last 40 years for sheep (left) and cattle (right). 74
Figure 3.13 Dunsop Valley Felling Plan (Forestry Commission, 2008) 76

Figure 3.14 Distributions of farms and subcatchments in the SCaMP area 78
Figure 3.15 Left: Croasdale main grip before blocking (picture taken on 13/03/2008), and right: after blocking (picture taken on 05/03/2009)..... 80
Figure 3.16 Example of a grip block and the upstream pool of water. Also indicated are the original drain direction and the direction of the redirected water flow..... 80
Figure 3.17 Tree planting on a hillslope and in the riparian zone of the upper Losterdale catchment (Sykes farm) 84
Figure 3.18 SCaMP land use/management changes for the Brennand catchment. In the upper right corner, the location of the Brennand catchment within the Hodder is shown. 85
Figure 3.19 SCaMP land use management changes for the upper Croasdale catchment. In the upper right corner, the location of the Croasdale catchment within the Hodder is shown. 86
Figure 3.20 SCaMP land use/management changes for the Hareden catchment. In the upper right corner, the location of the Hareden catchment within the Hodder is shown. 87
Figure 3.21 SCaMP land use/management changes for the Losterdale catchment. In the upper left corner, the location of the Losterdale catchment within the Hodder is shown. 88
Figure 3.22 SCaMP land use/management changes for the upper Langden catchment. In the upper left corner, the location of the upper Langden catchment within the Hodder is shown. 89
Figure 3.23 SCaMP land use/management changes for the Whitendale catchment. In the upper left corner, the location of the Whitendale catchment within the Hodder is shown. 90
Figure 4.1 Left: Hodder catchment with main subcatchments and the SCaMP area indicated by the black dashed line; Right: schematic representation of the Hodder catchment, including an overview of the hydrometric monitoring scheme 94
Figure 4.2 Existing hydrometric network in the Hodder catchment 95
Figure 4.3 Hypsometric curve of the Hodder catchment, including the elevation of the rain gauges and AWS..... 98
Figure 4.4 Rain gauge network in the Hodder catchment, including Thiessen polygons 99
Figure 4.5 Monthly snow lying days for the Hodder catchment during January 2008 – October 2010 (data source: MetOffice 5 km gridded monthly data sets) 99
Figure 4.6 Monthly precipitation totals from October 2008 – September 2009 for all tipping bucket rain gauges in the Hodder catchment 101
Figure 4.7 Average daily wind speed (left) and Maximum daily wind speed (right) against daily precipitation ratios of TBB and AWS (blue) and TBB and Footholme (red) 102

Figure 4.8 Daily prevailing wind directions against/AWS daily precipitation ratio (left) and TBB/Footholme daily precipitation ratio (right), with colour coding according to daily precipitation (P) 103
Figure 4.9 Average annual precipitation data for historical rain gauges in the Hodder catchment, plotted against the elevations at which they were measured 105
Figure 4.10 Automatic weather station at Middle Knoll 106
Figure 4.11 Schematic Hodder stream gauge monitoring network, with the stream gauges according to scale on the y axis and easting on the x-axis 109
Figure 4.12 An example of a NU stream gauge (left), with a schematic representation on the right, showing the main parts of the gauge 110
Figure 4.13 Frog and diver stage data comparison at LAN_mid 113
Figure 4.14 River cross section, stage of available discharge measurements, observed stage range, and the upper 95 and 99 percentiles of stage at CRO_out 117
Figure 4.15 Discharge and velocity for the SVA and the logarithmic stage-discharge extrapolation methods shown for the observed stage range at CRO_out 118
Figure 4.16 Daily specific discharge recorded at Croasdale weir compared to those at CRO_mid (top left) and CRO_out (top right); and at Footholme weir compared to daily discharge at WHI_mid (bottom left) , WHI_out (bottom right). The WHI_mid/Footholme comparison shows a slight, but consistent divergence from the 1:1 line. 119
Figure 4.17 Data availability for all NU gauges (AWS = green, Stream Gauge = black, TBR = blue) 121
Figure 5.1 Climatological conditions for Footholme (left) and Hodder Place (right), A: annual and average annual precipitation, B: annual and average annual snow lying days, C: annual and average annual days with ground frost, D: pre-, post- change and average monthly temperature. The annual data are presented for hydrological years. The pre-change years are shown in black, the post-change year in red. 128
Figure 5.2 Flow range and mean annual runoff rates for FH (left) and HP (right) 129
Figure 5.3 Lower part of the annual flow duration curves for FH (top) and HP (bottom) 130
Figure 5.4 Discharge, 10 * mean discharge, precipitation, and the occurrence of LUMC and show lying days for BRE_sap (top) and Hodder Place (bottom) for August 2008 – August 2010 132
Figure 5.5 Schematic representation of a parallel transfer function structure, with separation of the predicted hydrograph into a fast and a slow pathway (altered from Beven, 2001) 137
Figure 5.6 Hourly precipitation and discharge data for Hodder Place during January 1993 138
Figure 5.7 Observed and modelled discharge data for Hodder Place during January 1993 using observed precipitation data as the input of the linear DBM model 139

Figure 5.8 Top: Observed and simulated discharge data (current and Young), for Hodder Place January 1993, using effective precipitation as the input of the DBM model, bottom: the error in the simulated compared to the observed discharge 141
Figure 5.9 Left: Error in the simulated discharge (mm) plotted versus the observed discharge for the January 1993 data, Right: simulated versus observed peak flows only 141
Figure 5.10 Optimised C (left) and y (right) parameters of effective rainfall plotted against the total observed precipitation for the 6 monthly periods of hourly data at Hodder Place. 145
Figure 5.11 Relations between DBM Hodder Place model characteristics for 6 monthly periods of hourly data, Top-left: quick time constant versus delay, Top-right: contribution of quick reservoir versus delay, Bottom-left: slow time constant versus quick time constant, and Bottom-right: contribution of quick time constant versus quick time constant (all in hr) 146
Figure 5.12 DBM interpretation results (delay, quick time constant, slow time constant and percentage of flow that occurs through the slow reservoir) for yearly periods of hourly data at Footholme 147
Figure 5.13 DBM interpretation results (delay, quick time constant, slow time constant and percentage of flow that occurs through the slow reservoir) for yearly periods of hourly data at Hodder Place 148
Figure 5.14 Observed (blue) and simulated discharge at Footholme (top) and Hodder Place (bottom) for two events (one in a relatively dry year (orange, left) and one in a relatively wet year (green, right) using the DBM parameter estimates for the years in which the event occurred. The dotted black lines represent the minimum and maximum simulated discharge using the DBM parameter estimates of all other pre-change years and the red line is based on the parameter estimates of the post change year 149
Figure 5.15 Footholme frequency diagrams for the yearly DBM model characteristic results 151
Figure 5.16 Hodder Place frequency diagrams for the yearly DBM model characteristic results 151
Figure 5.17 Schematic representation of the conceptual Storage Discharge Detection model 154
Figure 5.18 Hodder Place rate of change in discharge in (mm) plotted against hourly recession discharge (mm/hr). The regression m and n parameter estimates are -0.0869 and 1.5728 respectively. 155
Figure 5.19 Top: Observed and SDD simulated discharge (both in mm/hr) for Hodder Place during January 1993, Bottom: Error of the simulated discharge 156
Figure 5.20 Top: Observed and SDD simulated discharge with a shift of 3 hrs (both in mm/hr) for Hodder Place during January 1993, Bottom: Error of the simulated discharge 157

Figure 5.21 Left: Observed discharge versus the error in the simulated discharge (mm), including the 3 hr shift, Right: Observed versus simulated peak flows only 157
Figure 5.22 SDD Footholme yearly recession data with regressions 160
Figure 5.23 SDD Hodder Place yearly recession data with regressions 160
Figure 5.24 Regressions of recession data for Footholme (left) and Hodder Place (right) for each hydrological year from October 1996 161
Figure 5.25 Footholme 1996-1997 residuals of the fitted amoeba regression, subdivided in to five classes, according to discharge. Top: discharge against residuals, Middle: frequency diagram of the residuals, Bottom: cumulative distribution of the residuals 162
Figure 5.26 Observed (blue) and simulated discharge at Footholme (top) and Hodder Place (bottom) for two events (one in a relatively dry year (orange, left) and one in a relatively wet year (green, right) using the SDD parameter estimates for the years in which the event occurred. The dotted black lines represent the minimum and maximum simulated discharge using the SDD parameter estimates of all other pre-change years and the red line is based on the parameter estimates of the post change year 164
Figure 5.27 Footholme (Top) and Hodder Place (Bottom) histograms showing the multiplier and power of the Amoeba regressions (left and right respectively). The pre-change values are in black and post-change values in red 166
Figure 5.28 Linear regressions of peak discharge on API for the 25 largest events of each hydrological year for Footholme 172
Figure 5.29 Linear regressions of peak discharge on API for the 25 largest events of each hydrological year for Hodder Place 172
Figure 5.30 Simulated versus observed peak flow for the 25 highest peak flow rates for the 2003-2003 (left) and the 2006-2007 (right) pre-change years for Footholme (top) and Hodder Place (bottom). The simulated peak flows are based on SDD model parameter estimates from all pre- and post-change years. The colour coding is consistent with all other figures (e.g. Figure 5.29 and 5.30) with the post-change year in red. 173
Figure 5.31 SDD regressions of recession data observed at nested multiscale sites (pre-change data in black and post-change data in red), undergoing grip blocking (all but CRO_mid), stocking density changes (all but CRO_mid and CRO_sc5) and tree planting (Hodder Place) 177
Figure 5.32 SDD regressions of recession data observed at nested multiscale sites (pre-change data in black and post-change data in red), undergoing grip blocking, stocking density changes (all) and tree planting (BRE_out and Footholme) 178
Figure 5.33 SDD regressions of recession data observed at nested multiscale sites (pre-change data in black and post-change data in red), undergoing grip blocking, stocking density changes (all) and tree planting (BRE_out and Footholme) 179

Figure 5.34 Pre (black) and post (red) change period NSE-morph efficiencies for the SDD model simulations using the post-change period parameter estimates plotted against those using the pre-change parameter estimates 180
Figure 5.35 Observed (blue) and simulated discharge using pre- (black) and post-change (red) SDD parameter estimates for an event during 11/11/2008 for CRO_sc5 (left) and CRO_mid (right) 181
Figure 5.36 Simulated versus observed peak flows (mm/hr) of the 25 largest peak flows during the pre-change period, using pre- (black) and post- change (red) parameter estimates. The blue line represents the 1:1 ratio. 182
Figure 5.37 SDD pre- (black) and post- change (red) m, n, b and c parameter estimates against catchment scale 186
Figure 5.38 Catchment storage and area for a range of discharge values based on the attractor curve (Equation 5.12) 187
Figure 6.1 Schematic representations of case study areas LOS_mid (top), BRE_sap (left) and CRO_sc5 (right) and their location within the Hodder catchment. The grip colours show average channel depth. 191
Figure 6.2 Examples of sheep tracks in the Hodder catchment. The tracks can be followed from gateway to gateway and crossing a stream (source: Google Earth) 192
Figure 6.3 Croasdale Swine Clough precipitation and stage data for November 2008 (pre-grip blocking, A and B) and May 2009 (post-grip blocking, C and D) 193
Figure 6.4 Left: CRO_sc3 pond drainage, and Right: CRO_sc3 stage and pond volume 194
Figure 6.5 Schematic representation of the MURSAFF model, showing an example of six interconnected rectangular grid cells, of which two are 'river' types and four are 'hill' types. 198
Figure 6.6 MURSAFF grid creation for CRO_sc5, left: stage1 representing the creation of the drainage network, right: stage 2 representing the creation of the hillslope slabs 200
Figure 6.7 Precipitation, observed and simulated discharge, and the simulated storage for CRO_sc5 (0.5 km^2) during a summer month in the calibration period (July 2009) 206
Figure 6.8 Precipitation, observed and simulated discharge, and the simulated storage for CRO_sc5 (0.5 km2) during a winter month in the calibration period (November 2009) 207
Figure 6.9 Precipitation, observed and simulated discharge, and the simulated storage for CRO_sc5 during July 2010 210
Figure 6.10 Exfiltration via a subsurface pipe, observed in the CRO_sc5 catchment, with a zoom window on the right. 210
Figure 6.11 MURSAFF grid for BRE_sap, showing the main slab types, including natural drainage network (River), the different grip types based on original grip depth, and the hillslope type. The small black squares in the zoom window show the locations of grip blocks 2111

Figure 6.12 Observed and simulated pre- and post-change discharge for CRO_sc5 (top) and Q_{post} - Q_{pre} (bottom) during November 2009 213
Figure 6.13 Observed and simulated pre- and post- change discharge for BRE_sap (top) and Q_{post} - Q_{pre} (bottom) during November 2009 213
Figure 6.14 Observed and simulated pre- and post-change discharge, Q_{post} - Q_{pre}, the average simulated pre- and post-change storage for the grip 1 m type slabs and that of the whole catchment for CRO_sc5 for a summer event (left) and a winter event (right) in 2009 214
Figure 6.15 Observed and simulated pre- and post-change discharge, Q_{post} - Q_{pre}, the average simulated pre- and post-change storage for the grip 1 m type slabs and that of the whole catchment for BRE_sap for a summer event (left) and a winter event (right) in 2009 215
Figure 6.16 Observed patterns associated with grazing in the Hodder valley *(Google Earth)* 220
Figure 6.17 MURSAFF grid for LOS_mid (zoom window on the left), showing the main slab types for the post-change simulation, including drainage network (RIVER) and hillslope slabs undergoing stock exclusion (EXCL), heft management (HEFT), inbye grazing (INBYE), restoration management (REST), and three different levels of increased soil compaction (TRACK_1 – TRACK_3). 222
Figure 6.18 Porosity (N) and optimised hydraulic conductivity (K) for the LOS_mid pre-change Winter Hill (1), Wilcocks (2), and Belmont (3) soil types 224
Figure 6.19 Observed and pre-and post-change simulated discharge for LOS_mid (top) and Q_{post} - Q_{pre} (bottom) during November 2009 225
Figure 6.20 Simulated pre- and post-change peak flows against the observed (pre-change) peak flows for the 25 largest events recorded at LOS_mid 227
Figure 6.21 Observed and pre- and post-change simulated discharge at the catchment outlet (top), Q_{post} - Q_{pre}(middle), and storage for specific slab types and the catchment average (bottom), exploring the effects of reducing stocking levels at the 'REST' (left) and the 'HEFT' slabs (right), and of stock exclusion at the 'EXCL' slabs (middle). The percentages at the top of each graph show the proportional catchment area undergoing change 228
Figure 6.22 Observed and pre- and post-change simulated discharge at the catchment outlet (top), Q_{post} - Q_{pre} (middle), and storage for specific slab types and the catchment average (bottom), exploring the effects of excluding stock at the 'INBYE' slabs (left) , the combined effect of all predicted changes (middle) and the effects of sheep tracks (right). The percentages at the top of each graph show the proportion of the total catchment area undergoing the relevant change. 229
Figure 6.23 Total slab discharge (left) and percentage of surface discharge of total slab discharge for a TRACK1 slab under high level compaction (pre-change) and as field conditions (post-change) 230

Figure 6.24 SDD observed (blue) and MURSAFF pre- (black) and post- change (red) simulated regressions of recession data (left) and simulated catchment storage against discharge (right) 232
Figure 7.1 Peak flow ranks for all subcatchments for six selected events 238
Figure 7.2 Spearman's rank correlation coefficients between the Hodder catchment outlet and the subcatchments for the peak flow ranks of 20 selected events (left) and excluding the 07/07/2009 convective event (right) 238
Figure 7.3 Precipitation (for the Hodder Place catchment) and runoff response (both in mm/hr) for seven selected events at Hodder Place 241
Figure 7.4 Total catchment event precipitations for seven selected events..... 242
Figure 7.5 Spearman's correlation coefficients between the subcatchment's peak flow ranks and precipitation ranks for 20 selected events..... 244
Figure 7.6 Peak flow against catchment area for seven events in the Hodder catchment 245
Figure 7.7 Lag time against catchment area for seven events in the Hodder catchment 246
Figure 7.8 Peak time relative to the catchment outlet at the different subcatchments within the Hodder plotted against travel distance for seven selected events, as well as the expected relative peak time based on three average travel velocities..... 247
Figure 7.9 Schematic representation of the Hodder catchment river network for the CIM model, consisting of 25 links and 16 sites. Note that the length of the network links is not according to scale..... 253
Figure 7.10 Observed (blue) and CIM pre-change simulated hydrographs black) at Hodder Place for four events. The NSE represents the Nash-Sutcliffe efficiency goodness of fit..... 254
Figure 7.11 LOS_mid (purple) and BRE_sap (blue) MURSAFF simulated pre – and post change discharge (1) and impact (2) for four different events. The impacts of change at BRE_sap are also multiplied by 5 (green) so that they can be seen more clearly..... 255
Figure 7.12 Pre- and post-change simulated peak flow (top) and the peak flow impact (middle: in m^3/s, bottom: in percentage of simulated pre-change peak flow) for LOS_mid (left) and BRE_sap (right) at different scales ranging from the micro scale to the meso scale at the catchment outlet. The impacts of change at BRE_sap are multiplied by 5. 256
Figure 7.13 The top plots show the October 2008 simulated hydrograph and the routed contribution of LOS_mid (purple, left) and BRE_sap (blue, right). The discharge and routed discharge are plotted on separate y-axes because the contribution of the routed discharge is very small. The top plots show the routed change related impact at different scales ranging from the micro scale to the meso scale at the catchment outlet. The black dotted lines connect the peak hydrograph and the associated contributing impact. The impacts at BRE_sap are exaggerated by a magnitude of five..... 257

Figure 7.14 Empirical changes (1 hr delay (cyan), 15% change (green), and both (red)) applied to the observed discharge at LAN_out during 06/07/2009 – 08/07/2009.....259
Figure 7.15 Schematic representation of the reduced Hodder catchment river network, consisting of 12 links and 7 sites for the investigation of the propagation of changes at the mini scale. Note that the length of the network links is not according to scale.....260
Figure 7.16 Pre- and post-change simulated discharge and impact of and on the Hodder Place flood hydrograph of four events, demonstrating the downstream effect of a 1 hr delay (dotted lines), a 15% change in flow (dashed lines) and a combination of both changes (full line) in the LAN_out (purple) and FH (blue) subcatchments. Note the difference in scale on the y-axis of the discharge plots.....263
Figure 7.17 Pre-change simulated Hodder Place (HP) flow and contributions of the routed flows of the different mini scale subcatchments. The figure corresponds to the potential effects of delaying the hydrograph. The dotted lines demonstrate to which part of the HP hydrograph the peak flows of the different subcatchments correspond. 264

List of Tables

Table 2.1 Examples of UK correlation (1), single (2), and paired (3) experimental catchments 14
Table 2.2 Peat hydraulic conductivity and porosity at a range of depths for a variety of worldwide study sites 21
Table 2.3 Peat effective porosity at a range of depths 22
Table 3.1 Percentages of Land Uses in the Hodder catchment, based on Figure 3.7 66
Table 3.2 Minimum compensation values for UU Bowland Intake System for the different subcatchments of the River Langden 69
Table 3.3 Estimated maximum abstractions for the different intakes within the Dunsop abstraction system 70
Table 3.4 Area of forest patches involved in Dunsop Valley Felling Plan 76
Table 3.5 SCaMP grip blocking: occurrence, timing and description 79
Table 3.6 SCaMP changes in stocking density and stocking management: occurrence, timing and description 81
Table 3.7 Recommended maximum stocking densities for different management strategies (DEFRA, 2005) 82
Table 3.8 SCaMP tree planting: occurrence, timing and description 83
Table 3.9 Occurrence of SCaMP main land use management changes per subcatchment 84
Table 3.10 Summary of the properties of Hodder headwaters and Hodder main valley and lower areas 91
Table 4.1 Environment Agency tipping bucket rain gauges 96
Table 4.2 Environment Agency stream gauges 96
Table 4.3 Newcastle University rain gauges 98
Table 4.4 Source and number of gauges for available average annual precipitation data 104
Table 4.5 Newcastle University stream gauges and weirs in the Hodder catchment 111
Table 4.6 Overall Water Balance Checks for the 2008-2009 hydrological year for all stream gauges 123
Table 5.1 Annual Precipitation (P), Discharge (Q), Potential Evapotranspiration (PET) and runoff ratios (R) for Footholme and Hodder Place from 2001-2010 131
Table 5.2 Optimisation results for the January 1993 data for a range of delays (0-6 hrs) 140
Table 5.3 DBM analysis physical interpretation results for Young (2002), Young (2003) and the current example analysis 142
Table 5.4 DBM estimated model parameters and simulation results for one year periods of hourly data for Footholme 143

Table 5.5 DBM estimated model parameters and simulation results for one year periods of hourly data at Hodder Place 144
Table 5.6 Nash Sutcliffe efficiencies for runoff predictions at Footholme and Hodder Place for a dry (2002-2003) and wet (2006-2007) pre-change year using the DBM parameter estimates of other pre-change years 150
Table 5.7 Nash Sutcliffe efficiencies for runoff predictions at Footholme and Hodder Place for the post-change year period using the DBM parameter estimates of pre-change years 152
Table 5.8 SDD analysis regression results of recession data (m and n) and the interpretation for the model (b and c) for Footholme (post-change values are presented in red) 159
Table 5.9 SDD analysis regression results of recession data (m and n) and the interpretation for the model (b and c) for Hodder Place (post-change values are presented in red) 159
Table 5.10 NSE-morph efficiencies for runoff predictions at Footholme and Hodder Place for a dry (2002-2003) and wet (2006-2007) pre-change year using the SDD parameter estimates of other pre-change years 164
Table 5.11 NSE-morph efficiencies for runoff predictions at Footholme and Hodder Place for the post-change year period using the SDD parameter estimates of pre-change years 167
Table 5.12 Pre- and post-change SDD parameter estimates for short –term data. 175
Table 6.1 Case study areas description 190
Table 6.2 Average potential storage upstream of all categories of grip and the average potential catchment storage provided by the grip blocks for CRO_sc5, BRE_sap and BRE_rhw 195
Table 6.3 CRO_sc5 MURSAFF cell types and associated parameter code for the unblocked (intact) and grip blocked cases (C = channel geometry, MC = channel Manning's n, N = porosity, K = conductivity, MS = surface Manning's n, FP = surface pooling fraction, and S = storage pond) 203
Table 6.4 Fixed MURSAFF parameters for CRO_sc5 204
Table 6.5 Optimised MURSAFF hydraulic conductivity for soil profiles at CRO_sc5 205
Table 6.6 Observed and Simulated Water Balance components (mm) and runoff ratio for CRO_sc5 during the MURSAFF post-change calibration and validation periods (observed ET is potential evapotranspiration, simulated ET is actual evapotranspiration) 208
Table 6.7 NSE-morph efficiencies for the CRO_sc5 and BRE_sap pre and post-change periods for the simulations based on the pre-change and post-change cases. 212
Table 6.8 Simulated pre- and post-change case water balance components for the CRO_sc5 and BRE_sap micro catchments during the 2008-2009 hydrological year 215
Table 6.9 Reductions in porosity and hydraulic conductivity for the different slab types based on compaction types. 223

Table 6.10 LOS_mid MURSAFF hillslope type characteristics.....224
Table 6.11 Simulated pre- and post-change scenario water balance components for the LOS_mid micro catchment during the 2008 – 2009 hydrological year 226
Table 7.1 Spearman's rank correlation coefficients of the peak flow ranks of 20 events between the different subcatchments in the Hodder catchment. The colour coding is based on level of agreement between the relative peaks observed at the two different gauges: good (dark green) = Spearman's coefficients 0.8 – 1.0, moderately good (light green) = Spearman's coefficients 0.6 – 0.8, moderately poor (light red) = Spearman's coefficients 0.4 – 0.6, and relatively poor (dark red) = Spearman's coefficients <0.4 237
Table 7.2 General information for seven selected events in the Hodder catchment ..240
Table 7.3 Spearman's rank correlation coefficients of the catchment precipitation ranks of 20 events between the different subcatchments in the Hodder catchment. The colour coding is based on level of agreement between the relative peaks observed at the two different catchments: good (dark green) = Spearman's coefficients 0.8 – 1.0, moderately good (light green) = Spearman's coefficients 0.6 – 0.8, moderately poor (light red) = Spearman's coefficients 0.4 – 0.6, and relatively poor (dark red) = Spearman's coefficients <0.4 243
Table 7.4 Impact on HP Peak flow of 1 hr delay change to the different subcatchments 261
Table 7.5 Impact on HP Peak flow of 15% change to the different subcatchments 261
Table 7.6 Impact on Hodder Place Peak flow of 1 hr delay and 15% changes to the different subcatchments.....262

Abbreviations

AONB	Area of Outstanding Natural Beauty
AWS	Automatic Weather Station
CAPTAIN	Computer- Aided Program for Time-series Analysis and Identification of Noisy systems
CBHE	Chronology of British Hydrological Events
CEH	Centre of Ecology and Hydrology
CHASM	Catchment Hydrology and Sustainable Management
CIM	Catchment Impact Model
DBM	Data Based Mechanistic
DEM	Digital Elevation Model
DF	Degrees of Freedom
DNRM	Dense channel Network Routing Model
EA	Environment Agency
FH	Footholme
FRMRC	Flood Risk Management Research Consortium
GB	Grip Blocking
HP	Hodder Place
LCM2000	Land Cover Map 2000
LUM	Land Use/Management
LUMC	Land Use/Management Change
MET Office	Meteorological Office
MLD	Mega Litres per Day
MORECS	Meteorological Office Rainfall and Evapotranspiration Calculation System
MURSAFF	Model for Upland Runoff Storage And Flow Fields
NA	Not Available
NRFA	National River Flow Archive
NSE	Nash-Sutcliffe Efficiency

NU	Newcastle University
PET	Potential Evapotranspiration
RIV	Refined Instrumental Variable
RSPB	Royal Society of the Protection for Birds
SCaMP	Sustainable Catchment Management Programme
SD(MC)	Stocking Density(/Management Changes)
SDD	Storage Discharge Detection
SSSI	Site of Special Scientific Interest
SVA	Stage-Velocity-Area
TBR	Tipping Bucket Rain gauge
TIN	Triangular Irregular Network
TP	Tree Planting
UK	United Kingdom
UU	United Utilities
YIC	Young Information Criterion

1 Introduction

1.1 Land Use Management Changes and Flooding

Recent extreme and widespread flooding incidents across Europe (notably the summer 2002 and 2010 Central European, and the autumn 2000 and summer 2007 UK floods) have raised awareness and concern about flood risk. It is suggested that episodes of severe precipitation and flooding are becoming even more frequent all over Europe (e.g. Christensen and Christensen, 2002; Ekström et al., 2005; Wilby et al., 2008) and there is growing concern that modern land use and management practices may be enhancing this trend of increased flood hazard (O'Connell et al., 2007a). Considering the economic and practical limitations for traditional structural flood defences, there is a desire to control flooding problems at the source through appropriate land use and management changes. Land Use and Management Change (LUMC) in rural areas has therefore been proposed as a mechanism that could help prevent flooding (Evrard et al., 2007; Wheater and Evans, 2009; Parrott et al., 2010).

The earliest studies concerning the hydrological effects of land use go back to the first part of the last century. They were focussed mainly on investigating the differences in overall hydrological response under forest and pasture in relatively small catchments (<10 km^2) (e.g. Bates and Henry, 1928; Law, 1957; Kirby et al., 1991). These studies have helped to gain a better understanding of the role of vegetation in controlling the evapotranspiration component of the water balance. However, in the context of flooding, it is not changes in land cover/vegetation and the water balance that are of central concern, but the way in which modern land use management practices have altered natural runoff generation processes. It has become clear that information on the changes in the timing and magnitude of storm runoff generation is needed, rather than on changes in overall volumes.

As outlined by O'Connell et al. (2004), there is considerable evidence that changes in land use and land management practices affect the local scale runoff generation characteristics. In this context, the local scale is defined as areas in the range of 1 m^2 up to a few km^2. Over the last few decades, numerous worldwide studies have linked a range of modern farming and LUM practices to changes in local runoff generation. For

example, soil compaction, resulting from farm machinery traffic (Davies et al., 1973; Young and Voorhees, 1982) and increased stocking densities (Heathwaite et al., 1989; Meyles et al., 2006), has been linked to reduced infiltration and enhanced local overland flow and runoff rates. Another example involves the local impact of drainage practices, which have been associated with both increased (e.g. Conway and Millar, 1960; Robinson, 1985) and decreased (e.g. Baden and Eggelsmann, 1968; Burke, 1975) catchment flood responses at small scales, with the effect depending on the local conditions (Holden et al., 2006).

Whereas there is clear evidence for local effects on runoff generation from hill slopes and agricultural fields, the resulting accumulated effect of distributed LUMC on flooding at larger catchment scales (>10 km^2) is not well understood (O'Connell et al., 2004; O'Connell et al., 2007a). Moreover, the impacts at larger scales, and the potential for flood mitigation through source runoff control, are of much greater interest to policy makers and catchment managers, especially because downstream flooding is more likely to result in major economic costs, loss of public and personal possessions and even loss of life (Morris and Wheater, 2007; Wheater and Evans, 2009; Parrott et al., 2010). Evidence on the downstream impacts of LUMCs is therefore urgently required by catchment managers (DEFRA, 2005b; Parrott et al., 2010). As such, there is an uneven balance between the available scientific knowledge and the policy needs and interest related to LUMC impacts when moving between spatial scales (Figure 1.1).

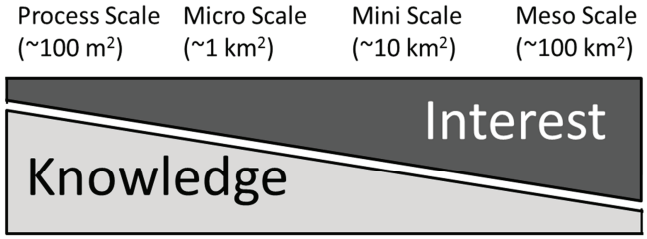

Figure 1.1 Schematic representation of the proportional level of knowledge and relative interest of catchment managers regarding LUMC effects on flooding at a range of scales

Traditionally, catchment experiments are commonly undertaken at relatively small scales (< 10 km^2) and it is difficult to transfer these results directly to larger river catchments, owing to data constraints, increasing heterogeneity, nonlinearity, and the

dominance of different processes at specific scales. As a result, the available evidence of the impacts of LUMC at larger catchment scales is anecdotal, inconsistent and has uncertain conclusions (Holden et al., 2004; O'Connell et al., 2004).

Beven et al. (2008a; 2008b) analysed historical data records of meso scale (~100 km^2) UK catchments in search of LUMC impacts. They could not detect such evidence, but this does not suggest that large scale impacts do not exist. Instead, the inability to detect LUMC impacts at larger scales may be attributed to (O'Connell et al., 2007a; Beven et al., 2008b):

1) A lack of availability of high quality data sets;
2) The effect of natural hydro-climatic variability;
3) A lack of appropriate data analysis and modelling techniques.

There has been a lack of high quality data from multiscale nested catchments that have been instrumented to investigate the effects of LUMC specifically. In addition, it is difficult to distinguish between LUMC impacts and the effect of natural climatic variability, which tends to mask any effects from LUMC. Moreover, O'Connell et al. (2007) argued that the traditional modelling and analysis methods are not adequate for predicting or estimating the impact that upstream local scale LUMCs have on larger scale downstream flooding.

Given the areas of limited knowledge as outlined above, there is an urgent need for a better understanding of the connection between local scale upstream LUMC effects and the catchment flood response at increasing downstream scales. Associated with this, three key focus areas have been identified:

1) Data are needed from a dense multiscale nested hydrological monitoring network in a catchment where land use management changes are actually taking place and can be recorded thoroughly.
2) A change detection method is required that is sensitive to changes in the systematic behaviour of runoff hydrographs, but relatively insensitive to storm-to-storm and year-to-year natural variability. Given the natural variability of rainfall and hydrological response and considering the pressing knowledge gap, the available data records from newly instrumented catchments are likely to be

relatively short. This makes working with short records an important challenge, especially as there is an almost universal lack of comprehensive, nested, long-term historical data sets worldwide that could be used to investigate the larger scale effects of LUMC on flooding.

3) There is a need for data analysis and modelling techniques that are suitable to study the detection, aggregation and propagation of LUMC (O'Connell et al., 2004), especially in complex landscapes.

Following the research recommendations of O'Connell et al. (2004), initiatives have been launched to implement multiscale nested catchment experiments in two upland areas of the UK where land use management changes are taking place. The first of these experiments has been implemented in Pontbren in upland Wales as part of the work of the Flood Risk Management Research Consortium funded by EPSRC. In this catchment, the effects of wooded buffer strips, small wetland areas and reductions in stocking densities are being studied (e.g. Carroll et al., 2004; Jackson et al., 2008; Marshall et al., 2009). However, the catchment area of this experimental site is still relatively small (12.5 km^2). The second multiscale nested catchment experiment, undertaken as part of this PhD research, and funded by the Environment Agency, has been implemented in the meso scale Hodder catchment (261 km^2), Lancashire, UK.

1.2 Research Aims and Objectives

The **main aim** of the research presented in this thesis is:

To collect and analyse a new multiscale dataset, based on a nested meso scale catchment experiment (~100 km^2), and thereby gain a better understanding of the effects of local scale LUMCs and their connection with catchment flood response at increasing scales.

The research concentrates on the impacts of LUMCs in the UK upland Hodder catchment in Lancashire, Northwest England, which has recently been undergoing several LUMCs over large areas in the upper part of the catchment (approximately 40% of the catchment). These changes have been carried out by United Utilities as part of their Sustainable Catchment Management Programme (SCaMP), and have involved restoring bogs by blocking drainage ditches (grips), reducing stocking densities and

other changes in stocking management, and afforestation. The main aim of SCaMP has been to apply and secure an integrated approach to catchment management in order to help a) deliver the government targets for Sites of Specific Scientific Interest (SSSIs), b) enhance the biodiversity, c) ensure a sustainable future for the company's agricultural tenants, and d) protect and improve the water quality (McGrath and Smith, 2006). The types of LUMCs of SCaMP are typical for UK uplands and the programme has provided an opportunity to study the effects of these on the catchment flood response at increasing scales. The Hodder catchment discharges into the River Ribble, which drains a large part of Northwest England and has high flood risk especially in the Preston area (Environment Agency, 2009), downstream of the Hodder confluence. The circumstances in the Hodder catchment were highly suitable for the purpose of the study, since historical rainfall and discharge data are available and the recent LUMC could be recorded and studied in detail, to inform the design of the multiscale catchment experiment.

The current research was carried out as part of Project SC060092 ('Multiscale Experimentation, Monitoring and Analysis of Long-term Land Use Changes and Flood Risk'), which has focussed on the effects of the SCaMP works on flood risk. Project SC060092 was funded by the Environment Agency and carried out by Newcastle University. It has provided a rare set of data that allows for the study of the relationship between upstream LUMC and downstream flood hydrograph changes. The dataset includes discharge, precipitation, and meteorological data for evapotranspiration estimates, which come from a multiscale nested monitoring network that consists of 28 stream gauges, seven tipping bucket rain gauges and an automatic weather station. The research offers a thorough evaluation of some specific change detection techniques in the context of short data records and it provides a novel physically based modelling tool that allows for the investigation of local LUMC in complex landscapes. The appropriate data analysis and modelling methods are applied to the multiscale data records in order to study impacts of the SCaMP LUMC on the catchment flood response at increasing scales. The Hodder catchment characteristics and the SCaMP changes are typical for UK uplands; hence, the study may also provide valuable information relevant to the effects of LUMC for other catchments in the UK, although it is noted that the local scale impacts may also depend on local conditions.

However, the acquired knowledge about the detection of LUMC impacts on large scale downstream flood response should prove valuable for a wide range of catchment managers and policy makers in UK upland areas.

Given the research and knowledge gaps as outlined in Section 1.1 above, the **main research question** addressed in this research work is:

What are the impacts of the upland SCaMP LUMCs on runoff generation at the local scale and can these impacts be detected at larger scales (up to ~100 km^2) through the use of multiscale nested experiments and appropriate data analyses and modelling methods?

It is **hypothesised** that knowledge of (differences in) the timing and magnitude of the pre- and post-change flood hydrographs at a range of increasing scales can lead to a better understanding of the effects of local scale LUMCs on catchment flood response at increasing scales.

The associated **objectives** of the current work are as follows:

1. Characterise the spatial physical properties of the Hodder catchment and identify the main historical and current LUMCs;
2. Design, set up and maintain a dense nested multiscale flow monitoring network that allows for the investigation of the LUMC impacts at increasing scales;
3. Investigate the functioning of the subcatchments and the Hodder catchment as a whole, especially when generating flood hydrographs;
4. Identify and apply appropriate methods, including statistical tests of significance, for LUMC change detection to the multiscale data records of the Hodder catchment;
5. Develop a new physically based modelling method that allows for the investigation of local LUMC impacts on storage, runoff and flow fields in complex landscapes;
6. Use the new physically based modelling method to explore the short and potential long term effects of LUMC in the Hodder catchment at the micro scale (~1 km^2);

7. Investigate the propagation and detectability of LUMC impacts at larger scales within the river network.

The first two objectives are concerned with data collection; the following five with data analysis and method testing and development.

1.3 Thesis Structure

A schematic representation of the thesis structure is shown in Figure 1.2. The figure also provides a brief overview of the main components of the methodological framework of the present work. Their relation to the research objectives is shown in brackets; the arrows indicate how the chapters are related to each other. An important aspect of the methodological framework is that it involves an integrated approach of field experimentation and monitoring, and several modelling and analysis methods applied at different spatial scales. Detailed descriptions of and justifications for the individual aspects of the methodology (such as specific data collection methods and analytical procedures) are discussed in the relevant chapters.

Chapter 2 provides a literature review. After a brief overview of scaling in catchment hydrology, an evaluation of local scale LUMC impacts is given. This involves a review of local scale monitoring experiments, peat hydrology and the local scale impacts of typical UK upland LUMCs, with a focus on peatland management. The subsequent sections of the literature review concentrate on the catchment scale LUMC impacts and include an overview of experimental design approaches, LUMC detection and prediction methods, and the attribution and prediction of specific catchment scale LUMC impacts relevant to the current study.

Chapter 3 gives a description of the River Hodder study catchment, which includes an overview of the main LUMCs that have taken place (Objective 1).

Chapter 4 is concerned with Objective 2. It presents the rationale for the multiscale experimental monitoring design and also deals with data collection, data processing and data quality assurance. As shown at the top of Figure 1.2, the design of the multiscale monitoring network is driven by the outcomes of Chapter 3. The data

collection also involved assembling long term hydrological records from existing monitoring stations within the Hodder catchment.

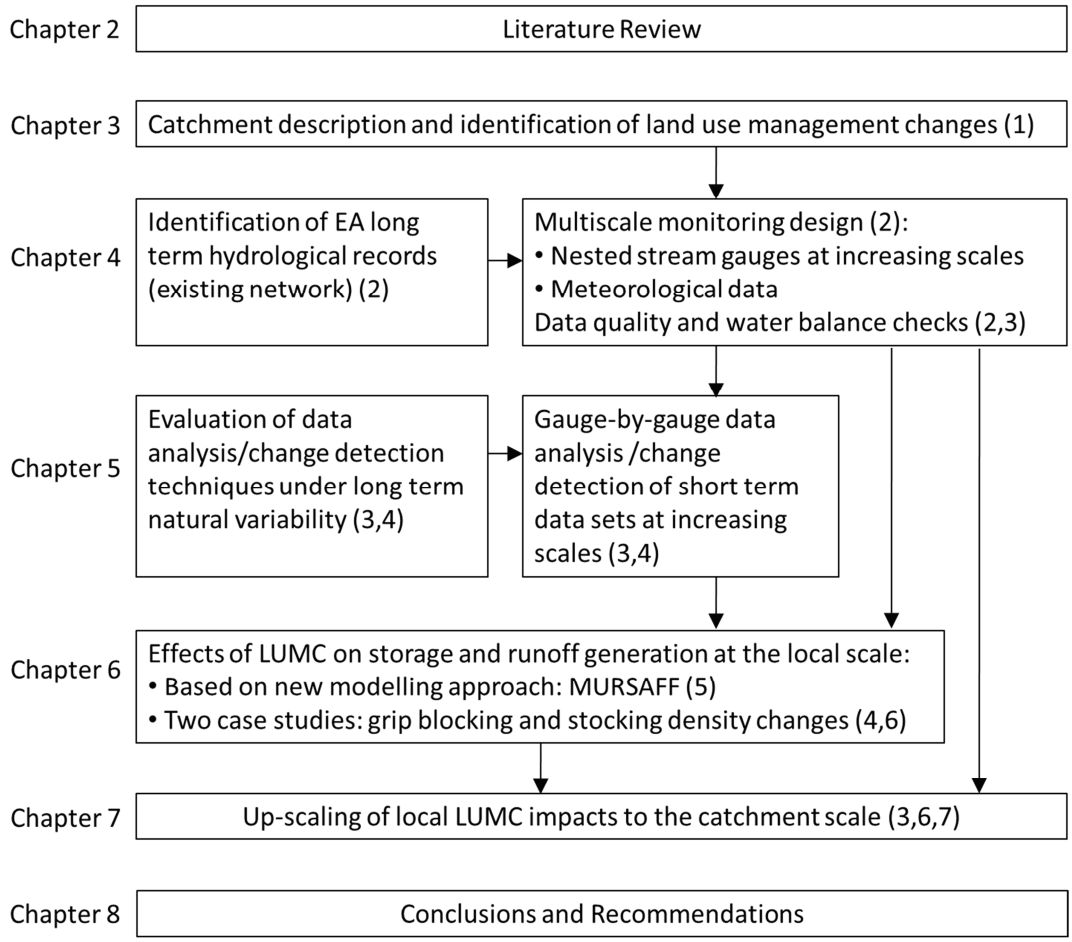

Figure 1.2 Schematic representation of the thesis structure and general methodology. The numbers in brackets indicate the objectives that are associated with the different chapters.

Chapter 5 addresses Objectives 3 and 4. It describes the analysis of the pre- and post-change hydrological behaviour at multiple scales, using the data presented in Chapter 4, and two relatively simple hydrological modelling methods (the Data Based Mechanistic (DBM) model and the Storage Discharge Detection (SDD) model). First, the sensitivity of the two models to natural climate-related hydrological variability is evaluated to assess each model's potential as a change detection method. The prime method for change detection is then used for a gauge-by-gauge analysis of the multiscale short term data set. In addition to the pre- versus post-change assessment, the results are also compared with those for gauges monitoring areas that were not

undergoing LUMC. Appropriate statistical methods are used to determine the statistical significance of differences between pre- and post-change results.

Chapter 6 is involved with the modelling of the local scale effects of LUMC on spatially distributed storage and runoff specifically. It presents a novel physically based Model for Upland Runoff Storage And Flow Fields (MURSAFF) that has been developed to allow for the investigation of within catchment impacts in a complex landscape that is represented using a flexible, irregular model grid (Objective 5). Two case studies are described. The first involves the analysis of the short-term impacts of the blocking of open drainage ditches (Objective 4). The second focuses on the potential long-term effects of stocking density and management changes (Objective 6).

In Chapter 7 the results from Chapter 6 are used to study the (potential long-term) impacts of the SCaMP LUMC at larger scales (Objective 7). First, an analysis of the multiscale Hodder catchment behaviour is presented, based on observed data and irrespective of LUMC, which also serves Objective 3. Next, the propagation of the SCaMP upland LUMC impacts are predicted through the use of a simple semi-distributed Catchment Impact Model (CIM). This involves the investigation of the downstream effects of the MURSAFF simulated impacts (as presented in Chapter 6), and the exploration of empirical changes in the mini scale catchments on the catchment response at Hodder Place.

The final Chapter, Chapter 8, presents a research summary and the main conclusions of this study. In addition, suggestions for further research are made.

2 Literature Review

2.1 Introduction

2.1.1 Chapter Overview

This chapter presents the relevant background information to the current study. In order to gain a better understanding of the impacts of local upstream land use/management change (LUMC) on downstream flooding, the study requires working at and moving between different scales. Since this is relevant to all following sections, the definition of scale in relation to LUMC impacts and the context of this study are discussed first. Next in Section 2.2 the traditional local scale experimental design approaches related to land use/management (LUM) are discussed. In addition, typical UK upland LUMCs and their local scale impacts are presented. Relevant to the LUMCs in the current study, Section 2.3 focusses on the local scale impacts of LUMCs related to upland peatland management specifically. The impacts of LUMC are strongly depending on the (dominant) runoff generation processes (i.e. the processes controlling the amount and timing of water entering the river network), flow paths and storage properties of the study catchments. It is therefore important to fully understand these in relation to the substrate before any changes in LUM are considered (Naef et al., 2002; Kirchner, 2006; Sidle, 2006; Bloschl et al., 2007). As peat is the dominant medium in the headwaters of the Hodder study catchment, a review of peatland hydrology is given prior to assessments of the impacts of peat drainage, drain blocking and stocking density and management changes. Results from grassland studies (representing the lower Hodder areas) are also given. Section 2.3 also includes a review of modelling peat hydrology and small scale LUMC impacts. While Sections 2.2 and 2.3 concentrate on local scale LUMC impacts, Sections 2.4 and 2.5 are concerned with catchment scale LUMC effects. Section 2.4 is involved with change detection and attribution. First, the available change detection techniques are discussed. The main challenges in change detection are highlighted and some examples of change detection techniques are given. Section 2.4 also includes an evaluation of the attribution of catchment scale effects of LUMCs. Section 2.5 focusses on monitoring, modelling and prediction of catchment scale LUMC impacts. This

involves a presentation of the key issues related to up-scaling local scale effects, a discussion of multiscale experimental monitoring designs and modelling studies concerned with predicting catchment scale effects. Section 2.6 provides a summary of this review, highlighting the remaining knowledge gaps regarding the present work.

2.1.2 Definition of Scale in the Context of Land Use/Management Change Impacts

The 'scale' of a phenomenon denotes the size or extent of it, especially when compared with another (Hornby, 2000). It refers to the order of magnitude (as opposed to an exact number) of an area, length, or time that defines a system, observation or a model (Bloschl and Sivapalan, 1995). Hydrological processes typically span about eight orders of magnitude in space and time (Klemes, 1983), for example the generation of infiltration excess overland flow can occur within a few minutes over an area of 1-100 m^2, while the generation or duration of floods in catchments of a million square kilometres may be days or weeks, and groundwater flow in aquifers can span over hundreds of years (Bloschl and Sivapalan, 1995).

There are a number of different ways of quantifying scale in hydrology. Bloschl and Sivapalan (1995) mention scales that are related to 'process', 'observation', and 'modelling/working'. They define the process related scale as the scale of natural phenomena beyond control (such as durations of intermittent processes (e.g. floods), or the cycle of periodic processes (e.g. related to climate). The observation scale can be defined within the constraints of measurement techniques and logistics, e.g. data resolution, distribution in space, or record length. The modelling or working scale is the most practical one, as it has defined scales that can be parameterized.

Temporally, one could work on an event based scale (e.g. a few hours or a day), seasonal scale (e.g. a hydrological year), or long-term scale (e.g. 30 years). Spatially, Dooge (1986) referred to the scales involved as the experimental plot (10 m), the basin module (100 m), the sub basin (1 km), and the basin (10-100 km) scale. Sivapalan and Bloschl (1995) defined the local (1 m), hillslope (100 m), catchment (10 km), and the regional (1000 km) scale. However, basins or catchments range from less than 1 km^2 up to 1000 km^2 and beyond, and a regional scale is not easily defined as a hydrological scale. In the context of LUMC impacts, a local scale of 10 m^2 is quite restrictive and

instead authors such as O'Connell et al. (2004) referred to the local scale for catchments up to 10 km^2. For practical reasons, the spatial scale in the current study is classified according to the schematic in Figure 2.1.

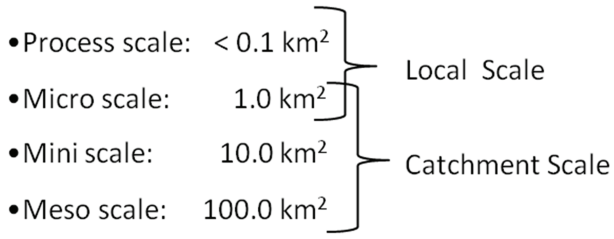

Figure 2.1 Definition of spatial scales within the current study

The catchment scale ranges from the micro scale (approximately 1 km^2) to the meso scale (in the region of 100 km^2). The term process scale here refers to the scale at which LUMC are known to impact hydrological processes directly. In the context of the present study, the local scale reflects mainly areas smaller than 0.1 km^2 (i.e. plots and hillslopes of the process scale), though in comparison with a meso scale catchment, the micro scale could also be considered local. Following the classification presented in Figure 2.1, the spatial scale of catchments in the region of 1000 km^2 and above can be referred to as the macro scale. However, the focus in the current study is primarily on the range of scales as presented in Figure 2.1, as the experimental study catchment is a meso scale catchment and LUMC impacts are hypothesised to be limited to catchments <500 km^2 (Bloschl et al., 2007).

The term 'scaling' can relate either to scale invariance or to up-scaling/down-scaling (Bloschl, 2001), though both involve a description of what happens to the characteristics of a phenomenon when its scale changes (Zhang et al., 2004; MacKinnon and Tetzlaff, 2009). The first interpretation focuses on identifying upper and lower limits for a range of scales that exhibits self-similar behaviour (Shaman et al., 2004; Church, 2008) and finding unifying relationships that underlie hydrologic processes at many scales (Bloschl, 2001). The second interpretation of 'scaling' is involved with transferring information between scales. Up-scaling involves transferring data from a small scale to a larger scale through aggregation and lumping of data, while the process of down-scaling is engaged with disaggregating and distributing data from a large scale to a smaller scale (Gupta et al., 1986; Bloschl and Sivapalan, 1995).

Scaling needs an analytical framework, though for LUMC impacts, no such framework is currently available.

Scaling is in principal different from 'rescaling', which refers to changes in the processes that are being studied (MacKinnon and Tetzlaff, 2009), and 'regionalization', which involves the transfer of information from one location to another (Kleeberg, 1992).

2.2 Local Scale Land Use/Management Change Impacts: Plot, Hillslope and Small Catchment Experiments

2.2.1 Traditional Experimental Design Approaches

The earliest studies concerning the effects of LUM were mainly focussed on forestry practices, especially in comparison with pasture. In the USA for example, Bates and Henry (1928) initiated the Wagon Wheel Gap study to measure stream flow before and after removal of trees in a search for the factors controlling erosion and floods. In the UK, Frank Law (a reservoir engineer) was concerned with the question of whether trees use more water than grass. From a small scale lysimeter study Law (1957) found that trees cause additional water losses, which he attributed to interception by the canopy and evaporation of this intercepted water. The pioneering works of Bates and Henry, Law and other researchers across the world were not always received without some controversy, and, for decades, numerous other studies have also been carried out to investigate the differences in hydrological response of forest and pasture, the reviews for which are extensive (e.g. Bosch and Hewlett, 1982; Bruijnzeel, 1990; McMulloch and Robinson, 1993; Sahin and Hall, 1996; Brown et al., 2005; Peel, 2009). Nevertheless, these early studies did provide a framework for experimental design approaches which is still used today.

The study of experimental catchments can be subdivided into three main groups: (1) correlation studies, (2) single catchment studies, and (3) paired catchment studies (Hewlett and Pienhaar, 1973; McMulloch and Robinson, 1993; Whitehead and Robinson, 1993). The first approach involves the comparison of two (or more) adjacent catchments that are subject to the same climatic inputs, are comparable in size, and have similar physical properties, and differ only in LUM. The problem is, that in

practice it is very difficult, if not impossible, to find two catchments exactly alike. Apparently small differences in catchment size, slope, or the relative distribution of north/south facing slopes could cause differences in the natural responses that could be interpreted mistakenly as a result of LUM. This problem is eliminated by the second type of catchment studies, where only one catchment is considered. The single catchment studies are generally conducted over an initial 'before' (or calibration) period, the results of which are then compared with those from an 'after' LUMC period. A disadvantage of this approach is that the climatic conditions in the 'before' period can differ from the 'after' period, especially when the records are relatively short. If time and resources permit, the third type (paired catchments), which is a combination of the former two approaches, is therefore mostly preferred (Hewlett and Pienhaar, 1973; Whitehead and Robinson, 1993). Here two (arguably) identical catchments, even in land use, are monitored so the differences between them can be properly assessed before one of the catchments undergoes a LUMC treatment. The changes in the 'treated' catchment are then compared with the observations at the 'control' or 'analogue' catchment. Examples of UK small scale experimental catchment studies whose results are significant for the present study are given in Table 2.1.

Table 2.1 Examples of UK correlation (1), single (2), and paired (3) experimental catchments in UK uplands

Catchment, location	Key references*	Study type	Area (ha)	Main study aim
Plynlimon, Wales	Kirby et al. (1991)	1	870, 1055	Comparison of hydrological behaviour of rough pasture and forestry, and effects of afforestation
Balquhidder, Scotland	Johnson and Whitehead (1993), Gusard and Wesselink (1993)	1	770, 685	Comparison of hydrological behaviour of heather moorland and forestry
Coalburn, Northumberland	Robinson et al. (1998)	2	152	Hydrological effects of drainage and afforestation
Moorhouse, Northumberland	Conway and Miller (1960), Robinson (1985), Holden et al. (2006)	1		Comparison of drained and intact peat

* These studies have led to a vast amount of publications; reviewing them all goes beyond the scope of this section. The aim is to provide examples of the key references.

The areas of these experimental catchments are conventionally small (a few ha to less than 10 km^2, see Table 2.1), and with a focus on the main components of the water balance (defined annual precipitation, evapotranspiration, any changes in storage, and runoff/water yield). In addition, point, plot and/or hillslope (process scale) experiments are carried out to better understand the internal hydrological processes within the catchments, such as interception loss, infiltration, and (preferential) flow pathways, and the effects of LUMC on these. Relevant outcomes of these studies are discussed in Section 2.3.

2.2.2 Typical UK Upland Rural Land Use/Management Changes and Local Impacts

O'Connell et al. (2004) identified key changes in UK rural LUM during the last 100 years that are related to the intensification of agricultural LUM: change from spring to autumn sown cereals, increased mechanisations, increase in grazing animals, loss of permanent pasture, more intensive use of grassland, increase in agricultural field under-drainage, afforestation, and changes in field sizes, with a disappearance of hedgerows. There is strong evidence that these changes are mainly driven by agricultural policies (O'Connell et al., 2004). Other rural LUM practices typical for the UK involve urban development, and moorland open ditch draining (Robinson et al., 2000), as well as moorland burning and, more recently, drainage ditch blocking (Holden et al., 2007).

Lane (2008) argued that within the context of flooding, and more specifically flood risk reduction, desirable effects of LUMCs include attenuation of the flood peak and increases in the time delay between precipitation inputs and the corresponding flood peak. Such measures may involve (a combination of) a change in the ratio between overland (fast) and subsurface (slow) flow, an increase in the storage potential of the catchment and a reduction in the delivery of the runoff (Lane, 2008). At larger scales however, the effects also depend on whether or not this would decrease the synchronization of tributary responses. Naef et al. (2002) demonstrated that a reduction of storm runoff through LUMC is feasible only on sites where infiltration and storage potentials can be enhanced.

At the local scale, there is substantial evidence that runoff generation is affected in such a way by LUMC. O'Connell et al. (2004) found that the intensification of agriculture as mentioned above has mainly led to decreased infiltration, increased surface runoff, and more flashy hydrological response. It is beyond the scope of this review to provide extensive information on all typical UK LUMCs and their effects on local scale runoff generation. Relevant to the present study are changes in peat drainage practices, and grazing management on peat bogs and grass. Hence, the following section describes the effects of these two LUMCs on runoff generation mainly. Specific attention is paid to changes in the annual water balance, storage and runoff generation. It is noted that change impacts in terms of percentage runoff etc. are site specific and cannot be easily extrapolated to other sites.

2.3 Local Scale Land Use/Management Change Impacts: Peatland Management

2.3.1 Peatland Hydrology

The UK has some of the world's largest peat areas (Moore and Bellamy, 1974), most of which can be found in Scotland (Robertson and Jowsey, 1968). Depending on the definition of peat, there is a range of estimations of the total peat covered area in the UK. Tibbetts (1968) and Moore and Bellamy (1974) estimated the exploitable reserves of peatland area in the UK at approximately 15,820 km^2, while Bragg (2002) provided a best estimate of 17,500 km^2 (6.5-7% of the total UK land surface area, respectively).

Peat Terminology and Physical Description

Peat consists of organic waterlogged deposits (Bragg and Tallis, 2001), accumulated in low-energy situations where organic production exceeds decomposition (Williams, 1990). Peat accumulation occurs as a result of (1) moisture availability, dependent on water replenishment from precipitation, and evaporation, (2) plant productivity and decomposition, influenced by radiation and temperature, and (3) suitable landscape characteristics (e.g. appropriate slope) (Moore and Bellamy, 1974; Price et al., 2003).

The vocabulary related to peatlands is extensive. The hierarchy of the different terms that are used in peatland terminology is shown schematically in Figure 2.2.

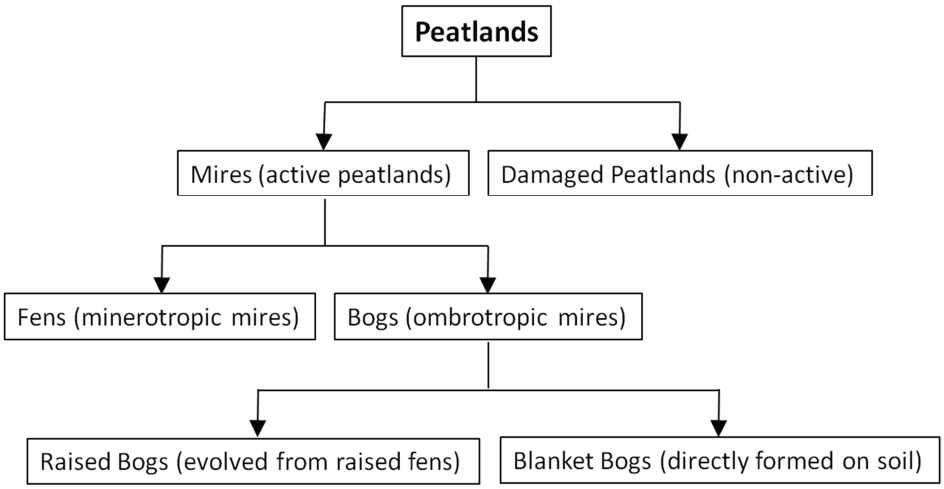

Figure 2.2 Schematic representation of the terms used to describe different kinds of peatlands

The ecosystems in which peats are actively formed are known as 'mires' (Bragg, 2002). The term 'peatlands' also includes mires which have lost their typical vegetation and are no longer peat-forming and hence non-active (Bragg, 2002). Mires can be subdivided into bogs and fens. Bogs receive water from precipitation only, and are therefore also known as ombrotropic mires. On the other hand, fens (minerotropic mires) have also access to groundwater and are therefore usually richer in their solute content. As a result of this difference in nutrient source, the ecosystems differ largely between the two types of mire and they each supply a habitat for different species. In the UK, bogs are more common (Tibbetts, 1968), and are further subdivided into 'raised bogs' and 'blanket bogs'. Raised bogs result from the upward growth of fens, when the peat becomes dependent only on rain water; blanket bogs form on mineral soils directly, on slopes that are typically less than 20° (Doyle, 1997). As the latter are present in the study catchment, this review therefore focuses mainly on the hydrology of blanket bogs.

Peatlands are often referred to as moorlands, especially in the UK. However, the term 'moorland' refers to a habitat comprising uncultivated low growing vegetation, such as heather and rough grass (Hornby, 2000), and does not have a peat soil per definition.

Peat Vegetation

Peatlands are formed in an extreme environment and the vegetation needs to cope with a number of characteristics, including: 1) limited nutrient supply, 2) an anaerobic

environment (in waterlogged sites), 3) the presence of toxic substances in the soil solution, and 4) considerable seasonal and diurnal fluctuations in temperature (Dierssen, 1992). Typical blanket bog vegetation includes *Calluna* (Heather), *Eriophorum* (Cotton grass), and *Molinia caerulea* (Purple Moor Grass). However, the prevailing species in peatlands are those of the genus *Sphagnum* (Dierssen, 1992; Clymo, 1997). *Sphagnum* species grow closely together in nearly continuous carpets, and have single cell layered leaves which form a net-like structure (Clymo, 1997). They have a large ability to retain water (up to 30-40 times their own dry weight, (Clymo, 1997) and normally grow in the top few centimetres above a water surface. *Sphagnum* is therefore very sensitive to water table changes (Bragg and Tallis, 2001). Their distinctive physical characteristics play an important role in controlling the hydrological behaviour of a peatland.

Peat Soil Profile and Soil Pipes

Usually a peat soil profile is described by the acrotelm-catotelm model (Ingram, 1978; Ingram, 1983; Bragg, 2002; Holden and Burt, 2003b), the acrotelm being the upper active, living layer and the catotelm the lower (hydrologically) inactive, dead layer. The acrotelm is affected by a fluctuating water table, while the catotelm has invariable water content with time. The lowest water table is therefore usually defined as the base of the acrotelm. Typical depths of the acrotelm are 0-0.2 m, with a maximum of 0.5 m (Price et al., 2003). Structurally, the vascular plant cover on top of the peat profile can be considered as a third layer (Ingram, 1992).

Peat soils are subject to soil piping (Gilman and Newson, 1980; Jones et al., 1997; Holden and Burt, 2003b; Holden, 2004; Holden, 2005c). This can be related to a combination of low infiltration capacity, poor internal drainage, low permeability, high shrinkage coefficients, stable roofing and an erodible subsoil (Gilman and Newson, 1980; Jones et al., 1997). Jones et al. (1997) suggested that the area which is liable to soil piping covers nearly 30% of Britain, and is concentrated in upland regions. The most common soil type associated with piping is Winter Hill (Jones et al., 1997), but in a study using ground penetrating radar, Holden (2005a) found that piping occurs in all British blanket peats.

Pipes occur on different levels within the soil profile (Holden, 2004). Most soil pipes are ephemeral and have a circular geometry, with diameters of approximately 6-8 cm (Gilman and Newson, 1980; Wilson and Smart, 1984), though this can vary rapidly over short distances (Gilman and Newson, 1980). Some pipes can evolve into perennial peat bridged streams of up to 1 m in size (Gilman and Newson, 1980; Holden, 2005c). Pipes are common in stream banks and across hillslopes. Even though thinner soils on steep slopes produce smaller, shallower pipes (Gilman and Newson, 1980), the overall slope is not a significant factor in the soil pipe frequency (Holden, 2005a).

Wilson and Smart (1984) stated that the main pipe network could remain stable for a period of five years or more, but that individual links could change, even within a rainfall event. Based on laboratory experiments, Holden and Burt (2002b) suggested that the cracking of peat during severe droughts could alter flow pathways. However, in a study testing the hypothesis that severe drying of soils can lead to cracking and thus the generation of new hydrological pathways, Worrall et al. (2007c) could find no field evidence to suggest that flow at Moor House pathways had been altered permanently after an extensive dry period in 1995. Hence, it is suggested that a pipe-network evolves slowly over time.

Physical Properties

Peat physical properties are highly variable and depend on the type of vegetation, the conditions of deposition, the growth habitat of each species, and the degree of decomposition. The key hydrological physical properties are discussed here. This review aims to include results from a variety of study sites. However, the importance of the source environment suggests that studies from one area may not be representative of the hydrological behaviour of others. In addition, some bias in the data should be taken into account, as the majority of field studies have taken place on just a few sites. This means that the range of values presented in the current section could be larger in practice. Some of the most intensely studied bogs include Moor House, North England, in the UK (e.g. Conway and Millar, 1960; Robinson, 1985; Holden and Burt, 2003c), an area in Minnesota, USA (e.g Bay, 1969; Boelter, 1972), and a site in Quebec, Canada (e.g. Schlotzhauer and Price, 1999; Kennedy and Price, 2005; Rosa and Larocque, 2008).

Hydraulic conductivity influences storage and the rate of movement of ground or soil water. Its measurement in peat has proved to be difficult (Rycroft et al., 1975) and is dependent on the composition and decomposition degree of the peat (Boelter, 1968; Boelter, 1969; Rycroft et al., 1975) and related to the local physical properties of peat, including the density (Boelter, 1968; Shibchurn et al., 2005; Surridge et al., 2005), pore size and geometry (Quinton et al., 2008), and (effective) porosity (Mulqueen et al., 1997; Deeks et al., 2004; Rizzuti et al., 2004). Table 2.2 provides observed hydraulic conductivities from a range of studies. Care should be taken with comparisons between studies, as they involve a variety of measurement techniques. Several studies have showed that the results can differ by at least one order of magnitude between techniques (Rycroft et al., 1975; Mulqueen et al., 1997; Holden and Burt, 2003a).

Table 2.2 shows that both the horizontal and vertical hydraulic conductivity exhibit great heterogeneity over short distances (Beckwith et al., 2003; Holden and Burt, 2003a; Rosa and Larocque, 2008), up to 2-3 orders of magnitude (Quinton et al., 2008), and can vary substantially between sites (Rycroft et al., 1975). Overall, the conductivity of the acrotelm is relatively high (of the order of 10^{-4} to 10^{-5} m/s), and that of the catotelm relatively low (10^{-6} – 10^{-9} m/s). At the top of the soil profile, Schlotzhauer and Price (1999) found a horizontal conductivity which was four times larger than the vertical conductivity. Some studies also show that the hydraulic conductivity of a drained peat can be lower than that of an undrained peat (Mulqueen et al., 1997; Price et al., 2003).

Holden et al. (2008) studied the relationship between overland flow velocity and vegetation cover, while also considering slope and water depth. From 256 plots (3 m^2) they observed an average velocity of 0.029 m/s (range: $1.22*10^{-4}$ - 0.191 m/s), with the highest values for bare surfaces. They also found that *Sphagnum* provided a significantly greater resistance to overland flow than peatland grasses, suggesting that *Sphagnum* is relatively better at attenuating flow velocities (Holden et al., 2008).

Table 2.2 Peat hydraulic conductivity and porosity at a range of depths for a variety of worldwide study sites

Reference	Depth profile (m) /Composition/State	Porosity	Hydraulic Conductivity (K) (m/s)	Peat Location
Boelter (1968)	Fibric Hemic Sapric	>0.9 0.85-0.9 <0.85	$1.8*10^{-5}$ $2.1\text{-}180*10^{-7}$ $<2.1*10^{-7}$	Minnesota, USA
Clymo (2004)	1 5 total 7 m peat profile	NA	$5*10^{-8}$ $0.7*10^{-8}$	Scotland, UK
Deeks et al. (2004)	0 – 0.06	0.81	3.58 m/d = $4.144*10^{-5}$	Allt Roy, Scotland, UK
Holden and Burt (2003a)	NA	NA	Approximately 3 $*10^{-8}$ (Large heterogeneity over short distances, both horizontally and vertically)	Moor House, England, UK
Holden et al. (2001) and Holden (2009)	0 0.2	NA	$0.013 – 545.6 *10^{-8}$ $4.0*10^{-6}$,$1.5*10^{-8}$	Moor House, England, UK
Ilnicki (1983)	Hemic Decomposed Peat	0.90 0.80-0.85	NA	Poland
Kennedy and Price(2005)	NA	NA	10^{-9} to 10^{-6}	Quebec, Canada
Mulqueen et al. (1997)	0 – 1.5 m	NA	$4.6*10^{-7}$ - $1.6*10^{-5}$ (K of drained peat 9-27% of undrained peat)	Barna, Galway, Ireland
Rizzuti et al. (2004)	0-0.25 0.4	High 0.31-0.68	$1.7*10^{-7} – 5.2*10^{-5}$ Practically 0	South Carolina, USA
Rosa and Larocque(2008)	See table 1 and 2 in paper	NA	Mean: Kh=$3.91*10^{-6}$, Kv=$2.75*10^{-6}$	Quebec, Canada
Rycroft et al. (1975)	Generally	NA	Range from $1*10^{-4}$ to $1*10^{-10}$	Review, mainly sites in US
Schlotzhauer and Price (1999)	0-0.05 0.3	0.9-0.95 0.9-0.95	Kh = $1.5 *10^{-6}$ Kv = $4.05*10^{-6}$ Kh= $4.05*10^{-6}$	Quebec, Canada
Quinton et al. (2008)	0 – 0.10(K)/ 0.15(n) m 0.15 (n) 0.2(K) – deeper m	0.8-0.95 0.75-0.9	$1.16– 115.7*10^{-4}$ $5.8\text{-}57.9*10^{-6}$	Yukan and NW Territories, Canada

Peat porosities and water retention capacities are relatively high (e.g. Letts et al., 2000; Schwaerzel and Bohl, 2003), which results in overall large water storage. Table 2.2 shows that porosity values for peatlands are in the range of 0.80-0.95. Compared to other substrates such as sand or clay (0.26-0.53, and 0.34-0.60 respectively (Domenico and Schwartz, 1998)) this is relatively high. However, the effective porosity, often used in modelling studies, is much lower. Example values (either calculated from field data or assumed) are given in Table 2.3. For peat bogs, most sources assume that the effective porosity is equal to the macro porosity, often defined as the percentage of pores >50µm (e.g. Deeks et al., 2004). For example, for a peat bog in Scotland, Deeks et al. (2004) concluded that these pores (>50 µm) are fundamental in determining the catchment discharge, based on a strong correlation between the soil water content and discharge, with discharge increasing rapidly when the ratio between the water filled pore volume and the pore volume in pores less than 50 µm approached unity.

Table 2.3 Peat effective porosity at a range of depths

Reference	**Depth**	**Effective Porosity**	**Observed(Calculated)/ Assumed**
Deeks et al. (2004)	0.00-0.06	0.1785	Observed
Hemond and Goldman (1985)	-	0.2	Assumed
Hoag and Price (1997)	Near surface 0.2 0.35 0.50 0.62	0.6 0.37 0.24 0.16 0.12	Observed
Ours et al. (Ours et al., 1997)	1 m soil core	0.3-0.9	Observed
Siegel and Glaser (1987)	-	0.1	Assumed
Rizzuti et al. (2004)	Acrotelm Catotelm	0.3 0.2	Observed (Average values given)
Reeve et al. (2000)	0.0-0.5 0.5-1.0 1.0-deeper	0.3 0.2 0.1	Assumed
Reeve et al. (2001)	0.0-0.5 0.5-1.0 1.0-1.5 1.5-2.5	0.6 0.4 0.3 0.2	Assumed
Ronkanen and Kløve (2008)	-	0.75-0.99	Observed

At any given potential on the soil water retention curve (van Genuchten, 1980), peaty soils have the highest moisture contents in comparison to other soil types, while *Sphagnum* peat has higher water retention and better re-wetting properties than highly decomposed peat soils (Michel, 2010).

Because of its high water content, peat is greatly compressible. Peat is known to have distinctive changes in volume, which can be attributed to 1) temporal peat expansion and compaction associated with changes in water content (Price and Schlotzhauer, 1999), 2) permanent reductions in storage capacity due to excessive drying and cracking (Holden and Burt, 2002b; Kennedy and Price, 2005), and 3) irrecoverable subsidence due to bio-oxidation of the organic material (Camporese et al., 2006). The effects depend on the composition of the peat. For example, elevation changes at the surface are relatively small (less than 0.8 cm) for consolidated or highly mineralised peat (Nuttle and Hemond, 1988). By contrast, seasonal changes of 6-12 cm (Almendinger et al., 1986; Price, 1994; Price and Schlotzhauer, 1999) have been observed in more unconsolidated peatlands. With changes in peat volume and water content, other peat characteristics such as the hydraulic conductivity are also affected (Chow et al., 1992). Where appropriate, peatland water balances should take account of peat volume changes associated storage changes (Price and Schlotzhauer, 1999).

Hydrological functioning of peat hydrology – a conceptual model

The hydrological functioning of peatlands is rather complex as the biology and hydrology are linked directly and no peatlands are alike (Boelter, 1965 ; Boelter, 1968; Bragg and Tallis, 2001). Based on literature from studies on UK peat-covered headwaters, approximately 70-80% of the annual precipitation is transformed into discharge and 20-30% is accounted for by evapotranspiration (Institute of Hydrology, 1976; Calder, 1990; Institute of Hydrology, 1991; Blackie, 1993; Holden and Burt, 2003c). Ingram (1983) highlighted that, for dry periods, stomatal control could limit transpiration, but a more recent study in the Netherlands showed that water table fluctuations had no effect on the evapotranspiration (Parmentier et al., 2009), suggesting that the actual evapotranspiration is always very close to potential evapotranspiration. There are only small changes in storage. Evans et al. (1999) showed that, for the 1994-1997 period, the water table of an upland peat was near the

surface (upper 5 cm) for 93% of the time, with a maximum depth of 40 cm during the dry summer period of 1995.

Streams draining upland peat tend to have a flashy behaviour, with minimal base flow contributions (Burt et al., 1990). This can be explained by the high water tables (restricting storage capacity) and well developed preferential flow pathways, with saturation excess overland flow and near-surface flow the dominant runoff generation mechanisms (Holden and Burt, 2002a; Holden and Burt, 2003c; Holden and Burt, 2003b). Holden et. al. (2001) suggested that saturation and percolation excess flows (in the acrotelm) over less permeable layers (the catotelm) dominate the runoff response. In addition, macropore and soil pipe flow are important pathways for runoff generation (Gilman and Newson, 1980; Holden, 2004; Holden, 2009). It has been estimated that 10-50% of flow in UK uplands occurs through soil pipes for at least some of the time (Holden, 2004). The specific role of pipe flow depends on antecedent conditions, and the storm duration and intensity (Wilson and Smart, 1984; Nieber and Sidle, 2010). The pipe discharge velocity is comparable to that of overland flow (Gilman and Newson, 1980; Smart and Wilson, 1984; Wilson and Smart, 1984).

Figure 2.3 shows a schematic interpretation of a conceptual model of runoff generation for intact peat. Figure 2.3 left represents runoff generation prior to a rainfall event. The water table (dotted white line) is high, but not at the top of the acrotelm (in grey). There are a few preferential pathways at or near the surface (dotted white arrow). Figure 2.3 right shows the runoff generation during or shortly after a rainfall event, with a high water table, much more (near) surface flow and some macropore and soil pipe flow.

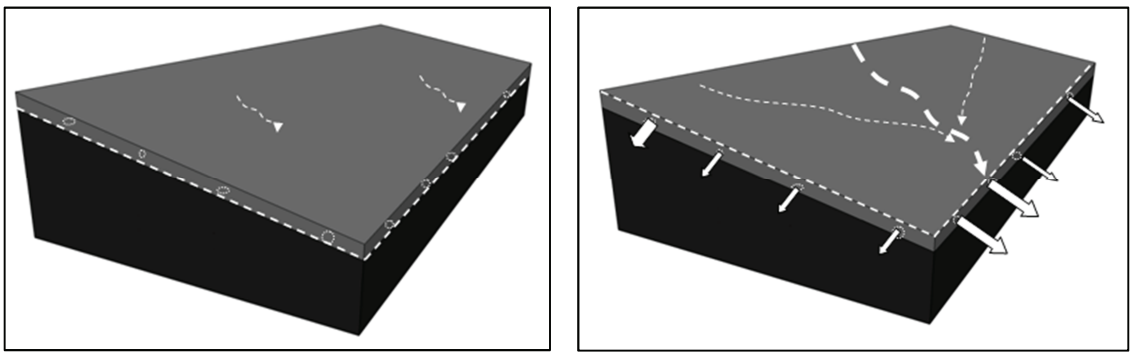

Figure 2.3 Schematic representation of runoff generation at an intact peat site prior to a rainfall event (left) and during a rainfall event (right)

2.3.2 Peat Drainage and Drain Blocking Effects

All over the world, peatlands have been drained for afforestation (Robinson et al., 1998; Beheim, 2006), peat extraction (McNally, 1997; Smout, 1997), or to improve the conditions for grazing and game (Stewart and Lance, 1983; Baldock, 1984; Rowell, 1988). It is estimated that 90% of the original peatlands in Europe have now been drained (Rochefort and Price, 2003). In the UK, peatland drainage (also known as 'gripping') goes back to Roman times (Baldock, 1984), though large scale drainage funded by agricultural schemes at the time was concentrated in the 1940s and in the 1960s-1970s (Baldock, 1984; Holden et al., 2004). Associated with peatland drainage are afforestation, grazing, cutting, and burning. The drainage ditches (or 'grips') are typically 0.4 - 1 m deep, spaced 15 - 35 m apart, and are often created at an angle to the elevation contours (Stewart and Lance, 1983; Price et al., 2003).

Hydrological Effects of Peatland Drainage

The first research on the hydrological effects of peat drainage was carried out on the Moorhouse study site by Conway and Millar (1960), who concluded that runoff production in blanket peat was more rapid where the catchments were drained, compared with catchments with untouched, natural bogs. However, contradictory results were reported from other worldwide studies. For example, Baden and Eggelsmann (1968) and Burke (1975) found a decrease in peak flow after drainage of a German and Irish bog, respectively. Numerous studies ever since have suggested that the effects of drainage depend on the local conditions, including peat type, hydraulic conductivity, vegetation, slope steepness, ditch spacing, drainage patterns and the location of the drainage within the catchment (e.g Boelter, 1972; McDonald, 1973; Ahti, 1980; Robinson, 1985; Lane et al., 2003; Holden et al., 2004; Holden et al., 2006).

In summary, peat drainage could both reduce and increase runoff generation, and, potentially, flooding. A potential flood risk reduction could be attributed to an increase in storage as a result of lower water tables. On the other hand, the artificial drainage network could also increase flooding by enhancing the runoff velocity by up to two orders of magnitude (Dunn and Mackay, 1996; Lane et al., 2003), and hence speed up the delivery of runoff to the river network.

In comparison with undrained peatlands, overland flow is significantly lower in drained peatlands, but macropore flow and pipeflow to the drains are of greater significance (Evans et al., 1999; Holden, 2006). Holden (2005a) found that moorland drainage enhances the formation of the pipe network, as a result of increased cracking induced by drying and wetting. The concentration of soil pipes has been shown to increase linearly with the age of the drainage (Holden, 2006). However, during very large storms, drained peats behave in a similar manner to intact peats, with subsurface flow through the acrotelm and, eventually, saturation excess overland flow as the main contributions to runoff (Daniels et al., 2008).

Water table fluctuations in drained peat are larger than at an intact site (Dunn and Mackay, 1996; Van Seters and Price, 2002; Daniels et al., 2008). The drawdown effects are very local near the drain edge (Jonczyk et al., 2009) as a result of the high water retention capacities of peat. These effects typically extend 0.3 - 1.0 m upslope to 1.0 - 2.0 m downslope of a grip and depend on local conditions, most noticeable slope (Stewart and Lance, 1991; Holden et al., 2006) and overall precipitation inputs (Coulson et al., 1990). In those cases where baseflow was large enough to measure, drainage resulted in an increase of baseflow (Burke, 1975; Robinson, 1986), which may be explained by a reduction in storage in the vicinity of the grip.

Peatland drainage significantly reduces the occurrence of *Sphagnum* species (Conway and Millar, 1960; Dierssen, 1992). From the findings presented in Section 2.3.1, this implies that indirectly, drainage can cause an increase in runoff velocities and a decrease in water retention and storage properties. The vegetation in the vicinity of the grips has also shown a decline in heather in favour of grasses (Coulson et al., 1990; Wilson et al., 2011), although this effect is only local. However, Wilson et al. (2011) found that, at the catchment scale, stocking densities have a much more important effect on the vegetation than drainage.

Figure 2.4 gives a schematic representation of runoff generation in the case of drained peat. The acrotelm is much larger near a drain as a result of water table drawdown. In Figure 2.4 this is represented by the light grey area at the peat surface. Some authors call this the ‘erosional acrotelm’ (Daniels et al., 2008). Prior to or early in a rainfall event, the main runoff is generated through macropores and soil pipes (Figure 2.4 left).

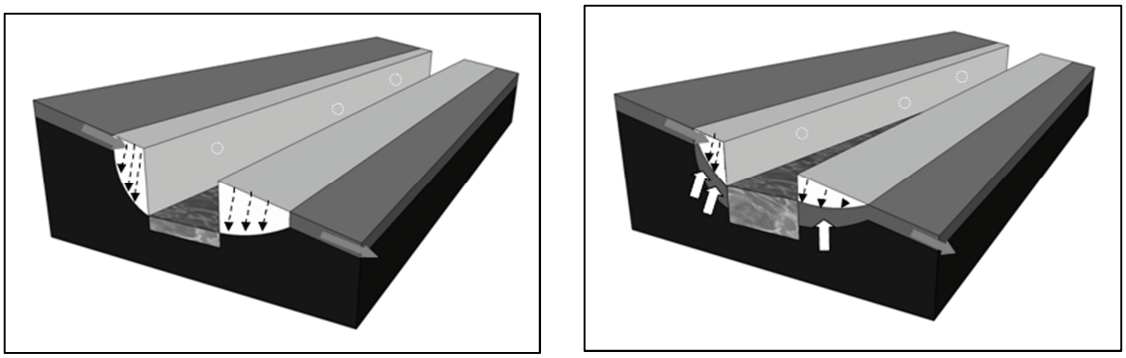

Figure 2.4 Runoff generation in drained peat prior to or early during a rainfall event (left) and during larger rainfall events (right)

Figure 2.4 right shows that the peat is rewetted later during the rainfall event and the water table rises. Macropore and soil pipe flow continues, and the peat body slowly starts to behave as intact peat with overland flow (Oberlin, 1981; Robinson, 1990).

Peatland Restoration

Since the end of the twentieth century, it has become clear that peatland drainage often doesn't have the desired water table drawdown effects to improve the conditions for grazing and game (Stewart and Lance, 1983). On the contrary, it has now been associated with increased flood risks (Lane, 2003), carbon release, water colouration (Worrall et al., 2007b), changes in aquatic communities (Ramchunder et al., 2009), sediment losses, and soil pipe development (Holden, 2006) in dried out peat. As the value of intact peatlands is increasingly recognised (Parkyn et al., 1997; Krecek and Haigh, 2006), in the UK, many peat drains are now actively being blocked in an effort to reverse this degradation. In addition, intact peatlands are large carbon stores and may act as a negative feedback as part of climate change mitigation (Milne and Brown, 1997; Worrall et al., 2003; Holden, 2005b; Yu et al., 2010; Yu et al., 2011). One of the main objectives in peatland restoration is to create suitable conditions (i.e. high water table levels) for *Sphagnum* growth and survival, as it is the key plant for peat-forming ecosystems (Eggelsmann, 1988; Joosten, 1992; LaRose et al., 1997; Money and Wheeler, 1999; Gorham and Rochefort, 2003).

Hydrological Effects of Grip Blocking

As for peat drainage, the effects of drain blocking have been shown to be site specific (Money and Wheeler, 1999; Price et al., 2003; Holden et al., 2004). It has also been

suggested by several authors that the short term effects may vary from long term effects (Spieksma, 1999; Worrall et al., 2007b). In addition, a restored peatland will not necessarily revert to intact peatland, owing to draining related irreversible changes in the physical properties (Holden, 2005b; Ramchunder et al., 2009; Holden et al., 2011).

Most studies demonstrate a reduction in total runoff after drain blocking, ranging from 25% for 8 ha of a Canadian bog (Shantz and Price, 2006), to 70-90% for a UK Pennine drain (Worrall et al., 2007b). There have been contradictory reports about changes in peak runoff flashiness post drain-blocking. Shantz and Price (2006) found an increase in peak discharge and a decrease in peak timing, attributed to relatively wetter antecedent conditions after restoration. By contrast, Jonczyk et al. (2009) and Wilson et al. (2010) described a slower and more smooth response. The difference could be related to the spatial- and temporal-scales of response. For example, Spieksma (1999) showed that, after rewetting of a German bog, the daily discharge was most flashy straight after a rise in the water table and gradually smoothed out later.

Drain blocking is generally successful in raising the water table (<0.1 m) in the vicinity of the drains (LaRose et al., 1997; Worrall et al., 2007b; Wilson et al., 2010), although it may not rise to the levels observed for intact sites (Holden et al., 2011). Wilson et al. (2010) also reported a 40% increase in the occurrence of surface water and hence overland flow. The increase in moisture content aids the recovery of vegetation such as *Sphagnum* (LaRose et al., 1997), though it lags behind the instantaneous changes in flow (Price et al., 2003; Evans et al., 2005). In turn, the occurrence of more *Sphagnum* will increase soil moisture and water retention capacities and surface roughness.

In summary, the most likely drain to hillslope scale effects of grip blocking are changes in storage and flow (direction, resistance, and to some degree type of flow and storage). It is likely that preferential flow paths (i.e. the pipe network) still remain active after drain blocking, although their role in delivering runoff post-blocking is yet unclear (Atkins, 2007). It has even been suggested that drain blocking could enhance piping (Evans et al., 2005).

Figure 2.5 shows a schematic representation of a (recently) blocked drain. Figure 2.5 left shows the runoff generation prior to or after, or early during a rainfall event when

water is stored upstream of the blocks. The water reaches the storage ponds through macropore and soil pipe flow as well as through near surface flow. The blocks are not fully impermeable. Figure 2.5 right shows the blocked drain situation when the maximum storage behind a block is reached. Water is being redirected onto the peat surface and overland flow occurs.

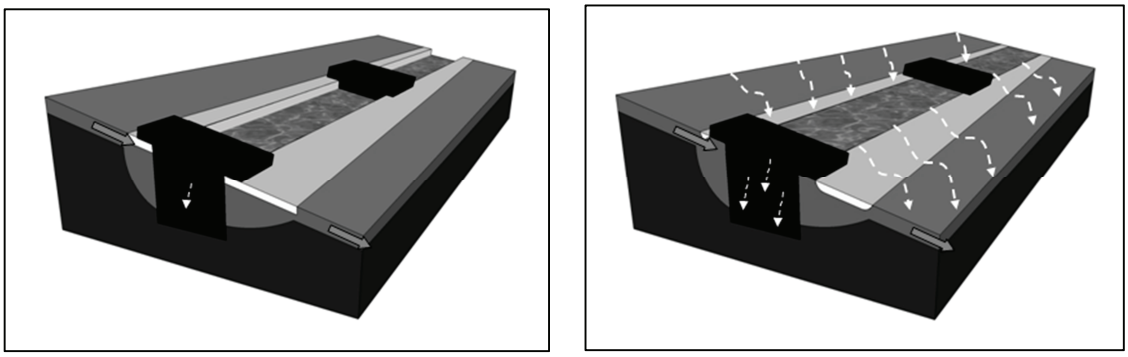

Figure 2.5 Runoff generation in a (recently) blocked drain prior, early on in, or after a rainfall event (left) and during an event (right)

2.3.3 Stocking Density and Management Effects

95% of England's blanket bog is uncultivated and used primarily for sheep grazing (Chesterton, 2009). Its management involves controlling stocking levels, which is often associated with peat drainage, heather burning and cutting of other vegetation that is unfavourable for sheep grazing. From the 1970s, stocking density numbers in the UK increased considerably owing to the introduction of headage payments (Anderson and Yalden, 1981; Fuller and Gough, 1999), which has led to overgrazing and the use of less suitable land. This has been associated with the loss of heather moorland and biodiversity (Shaw et al., 1996; Fuller and Gough, 1999), soil erosion, increased runoff, reduced aquifer recharge, and low river flows (Sansom, 1999). Birnie and Hulme (1990) also noted a change in animal type and hence weight (move from traditional to larger continental breeds), which increased the pressure on the grazing resources even more. Since the early 2000s, the national stocking levels have decreased owing to removal of these headage payments and other reforms of the EU's Common Agricultural Policy, and poor returns on livestock products (Chesterton, 2009).

As noted in the previous section, peat drainage does not have the desired effects for sheep grazing. In addition, Wilson et al. (2011) confirmed that blocking of drainage ditches does not have an effect on sheep grazing either. Heather burning is still a

common practice, as it stimulates the growth of grasses, and therefore improves the grazing conditions for sheep (Lance, 1983). In order to improve some of the current conditions of UK uplands, several authors have suggested that changing stocking levels should therefore occur in conjunction with changes to burning practices (Bragg and Tallis, 2001; Worrall et al., 2007a).

It should be noted that generalised data on overall stocking numbers hide a far more complex system. For example, there is considerable variability in how the stock is managed within a year, and also between farms. This is related to decisions governing over-wintering, lambing, and field rotation.

Vegetation

Most of the early studies on the effects of grazing focussed on the change in vegetation. Increased grazing has been associated with an overall decline in vegetation cover, a shift from *Calluna vulgaris* (heather) to more grass species (Rawes and Hobbs, 1979; Anderson and Yalden, 1981; Grant et al., 1985) and a drop in the percentage Sphagnum cover (Wilson et al., 2011). Some studies showed that these changes occurred only above a certain grazing level threshold. This depends on local conditions (e.g. 3.4 sheep/hectare at Moorhouse (Rawes and Hobbs, 1979), 2.22 sheep/hectare on a bog in southwest Scotland (Grant et al., 1985), and 1.4 sheep/hectare at a site in Northumberland (Hulme et al., 2002)). In agreement with this, decreasing stocking densities and stock exclusion have been connected with a recovery of *Calluna* species (Rawes, 1983; Hulme et al., 2002; Pakeman et al., 2003). However, Critchley et al. (2008) and Mitchell et al. (2008) argued that the restoration of vegetation by just reducing sheep numbers may be unsuccessful if competitive grasses become dominant, and a full recovery might take 5 years or longer. The vegetation type also has an influence on the soil physical characteristics of the upper part of the soil profile, the water balance, and runoff generation (see below).

Soil physical characteristics

Studies on the effects of changes in stocking density on peat bogs and grasslands have shown that, with increasing stocking levels, the following changes in soil physical characteristics generally occur:

- Soil structure degrades (Holman et al., 2003; DEFRA, 2008)
- Soil compaction increases (Langlands and Bennett, 1973; Evans, 1998; Greenwood and McKenzie, 2001; DEFRA, 2008; Houlbrooke et al., 2011)
- Bulk density increases (Langlands and Bennett, 1973; Meyles et al., 2006)
- Porosity and pore space connectivity decrease (Meyles et al., 2006; Houlbrooke et al., 2011)
- Infiltration decreases (Branson et al., 1981; Mallik et al., 1984; Heathwaite et al., 1990)

These effects are generally confined to the upper 20 cm of the soil profile, with most impacts in the upper 5 cm (Greenwood and McKenzie, 2001; Meyles et al., 2006; DEFRA, 2008; Zhao, 2008). The extent of these impacts can be vast. The reduction in infiltration capacity, for example, can be as large as 80% (Heathwaite et al., 1990). Generally, the impacts depend on local conditions such as soil type (Branson et al., 1981; Zhao, 2008), and temporal conditions, such as soil wetness (DEFRA, 2008). Compared with mineral soils, peat soils are most vulnerable (Zhao, 2008), and, when fields are wet, the effects are more extensive as wet soils lose structural stability (DEFRA, 2008). In those areas which are also burnt regularly, the decreased soil structure and infiltration are amplified (Mallik et al., 1984; Worrall and Adamson, 2008; Clay et al., 2009), while porosity is increased (Mallik and Fitzpatrick, 1996).

The recovery of these changes in soil physical characteristics generally depends on grazing management, climatic conditions and soil type (Drewry, 2006) and can range from less than a year, to about 5-10 years (Branson et al., 1981; Zhao, 2008), to more than 45 years (i.e. unrecoverable, Basher and Lynn, 1996).

Sheep behaviour causes additional variability in the grazing effects. Sheep tend to concentrate in specific local areas, such as near gateways, shelterbelts, feeders and along specific sheep tracks. The trampling and grazing effects are larger in these areas compared with the rest of the grazed fields (Heathwaite et al., 1990; Shaw et al., 1996; Pringle and Landsberg, 2004; Holden et al., 2007; Zhao, 2008; Chesterton, 2009). Pringle and Landsberg (2004) noted that, once sheep tracks are well developed, old tracks can continue to attract stock even if the factors behind their original formation have changed. It is also recognised that the changes in the physical characteristics of

the topsoil are closely related to the differences in vegetation, and are not only a direct result of the trampling of the stock (Meyles et al., 2006). However, sheep do have a vegetation preference, and gather mainly on the short grass patches.

Hydrological Effects of Changes in Stocking Density and Management

Water tables are nearer the surface (decreasing the storage potential) where both grazing and frequency of burning regimes limit the development of vegetation and hence also the evapotranspiration losses (APEM, 1998; Worrall et al., 2007a; Clay et al., 2009). Worrall et al. (2007a) estimated the average effect of grazing to be an 11% reduction in the water table depth, but make no note of grazing densities.

All of the changes in the soil physical characteristics related to increased grazing pressures are causing a reduction in hydraulic conductivity. This favours the conditions for increased (infiltration excess) overland flow and surface runoff (Heathwaite et al., 1990; Lane, 2003; O'Connell et al., 2004; Worrall et al., 2007a; DEFRA, 2008; Clay et al., 2009). Heathwaite et al. (1989) found that surface runoff from a permanently grazed pasture was 53% of the total rainfall input, compared with only 7% of the total rainfall input for ungrazed land with intact vegetation cover. Heather burning also causes faster and flashier catchment runoff, with higher peak flows (Ramchunder et al., 2009). Meyles et al. (2006) showed that intense grazing causes the right circumstances for increased delivery of runoff to quick preferential flow paths. These include sheep tracks and other rapid flow paths which, especially during large rainfall events, increase the connectivity of the hillslopes and channels. In turn, it is hypothesised that this may lead to increased flooding and decreased baseflow (Worrall et al., 2007a). Holden et al. (2008) found that the velocity of overland flow is linked to the surface roughness, which in turn is related to vegetation cover type (as discussed in Section 2.3.1), affected by stocking levels.

2.3.4 Modelling Local Scale Land Use/Management Impacts in UK Uplands

Since they allow for the investigation of various aspects of the internal behaviour, distributed physically based models are most suitable for studying the effects of small scale LUMC. Ideally, the modelling is executed in conjunction with field observations

and interpretations of hydrological processes. For the relevant two LUM changes (grip blocking and stocking density changes), these include the observation of local artificial drainage networks (grips), transient storages (ponds upstream of the grip blocks), flow fields (redirected flow), preferential surface flow pathways (sheep tracks), and other management patterns that affect vegetation and soil physical parameters.

However, a full integration of field observations in the modelling process is complicated by conflicts between the needs of catchment managers, the observations and interpretations of field scientists, and the work of catchment modellers. This is a problem that has been widely recognised (e.g. Dunne, 1983; Klemes, 1986; Beven, 1993; Seibert and McDonnell, 2002; Dunn et al., 2008). While the catchment manager needs a reliable decision support tool for practical problems such as the aggregation and propagation of LUM change impacts, the field scientist observes catchment heterogeneity and complexity, whereas the catchment modeller calls for simplification of processes. The principal components of this problem are: 1) the available models are not adequate to represent the complex dominant local runoff generation processes and flow fields as observed by field scientists (Kirchner, 2006; McDonnell et al., 2007), especially in the context of assessing the impacts of LUMCs on flooding (O'Connell et al., 2007a); 2) vegetation and soil properties have large spatial variability making it difficult to relate model parameters to local field observations (Beven, 1996; Duan et al., 2006; Sidle, 2006); 3) limitations in the applicability of model simulations, due to their 'uniqueness of place' (Beven, 2000), restrict their practical use for catchment managers.

In an attempt to tackle these issues, many authors such as Dunn et al. (2008) advocate a working framework that includes a knowledge exchange system of field-based data collection and modelling as well as the involvement of local knowledge of the end-users and/or field scientists. Nevertheless, visual field interpretations by experienced field hydrologists are often not fully accredited mainly because this information does not consist of hard data (i.e. continuous time series against which a hydrological model can be calibrated or validated). These so-called soft-data are generally catchment specific but can involve, for example, estimates of old/new water ratios (Seibert and McDonnell, 2002) and levels of snow cover or flood inundation. A dominant feature of

the two relevant LUM changes is geometrical complexity in the distribution of water flows and water storages in the channels and on and within the soil (Geris et al., 2010).

An overview of local scale modelling studies of the hydrological effects of peat drainage and blocking, as well as grazing practices, is given below. This includes an evaluation of the integration of the geometrical field complexity into the modelling.

Examples of peatland and upland land use/management change modelling

Examples of both conceptual (e.g. Guertin et al., 1987) and physically based (e.g. Ballard et al., 2011) peatland models include the three types of runoff generation in peatland: overland flow, and subsurface flow through the acrotelm and the catotelm. For physically based models, the subsurface flow to drains can be described by a variety of different methods, though most of them are based on Darcy's Law. The Hooghoudt equation (Hooghoudt, 1940) is often used for flat and gently sloping areas of less than 0.1, while the Boussinesq equation can be solved for drainage of sloping land (Schmid and Luthin, 1964). Section 2.3.1 showed that the physical properties of peatlands exhibit great heterogeneity, and that runoff generation is complex. The modelling of peat inevitably involves simplifications and reductions of this complexity. For example, the preferential flows through macropores and soil pipes are notoriously difficult to represent in models (Beven and Germann, 1982; Germann, 1990; Bonell, 1998) and including such representations results in ever more complex models, leading to over parameterization problems (Bloschl, 2001). It is therefore often assumed that they are accounted for through the hydraulic conductivity (e.g. Ballard et al., 2011).

Modelling studies concentrating on the effects of grazing have focussed mainly on the overall changes in soil physical characteristics, such as soil compaction and infiltration (e.g. Tian et al., 1998). Based on empirical relations, Pringle and Landsberg (2004) modelled the grazing pressure on sheep tracks, although this was for predicting the within-field distribution of livestock only. Even though numerous studies have modelled the effects of roads and traffic (e.g. Luce, 2002), no modelling studies have been identified that have looked at the hydrological effects of sheep tracks specifically.

Examples of hillslope modelling studies of peatland drainage for sloping land include the studies of Dunn and MacKay (1996), Lane et al. (2003; 2004), and Ballard et al.

(2011). Lane et al. (2003; 2004) developed a network-index-based modified version (SCIMAP) of the semi-distributed TOPMODEL (Beven and Kirkby, 1979), that is linked to a detailed DEM, obtained from Light Detection and Ranging (LiDAR) data. LiDAR data have proved a useful tool for identifying drains (see also Trettin et al., 2008), though the detailed (<1m resolution) LIDAR coverage for UK upland areas is sparse (Geomatics Group, 2011), which limits the application of this tool. From their study, Lane et al. (2003) concluded that a catchment scale modelling technique that represents the spatial arrangement of grips and their connectivity to the drainage network is vital to determine the catchment scale impact of gripping (or blocking) on downstream runoff. However, due to its partly conceptual nature, TOPMODEL does not allow for the direct investigation of changes in physical parameters.

Dunn and MacKay (1996) and Ballard et al. (2011) used physically based models that do allow for the investigation of (changes in) internal processes. Dunn and MacKay used SHETRAN (Ewen et al., 2000) to investigate the effects of drainage only on the hydrological behaviour of hillslopes. Ballard et al. (2011) recognized that SHETRAN does not allow for much flexibility in the representation of drain configurations and therefore developed a model that provides that flexibility so that the effects of drainage and drain blocking can be studied for a range of drainage scenarios.

The three example models (SCIMAP, SHETRAN and Ballard's physically based model) used for drainage and drain blocking use regular or finite-difference rectangular grids. Such grids are not very suitable for modelling the flow fields and storage patterns of complex landscapes with irregular drainage networks and sheep tracks, because they distort the natural geometry, and therefore degrade the detailed knowledge and information brought to the modelling by the field scientist. Other types of grids that are used for distributed modelling include restricted-geometry non-regular grids (such as GIS squares, or finite-element triangles). These types of grids allow for more flexibility in the landscape representation and would hence be more suitable. However, some degree of fixedness remains and a representation of all individual elements (such as the storage ponds in the blocked drainage network) quickly leads to high resolution grids and an increase in computational modelling time.

For a gently sloping Mediterranean catchment, Levavasseur et al. (2012) used the physically based MHYDAS model to study the impacts of artificial drainage networks. The MHYDAS model (Moussa et al, 2002) represents the catchment as a series of interconnected irregularly shaped field parts, based on man-made hydrological discontinuities that are linked to the drainage network. The irregularly shaped field parts allow for a good representation of the geometrical complexity as observed in the field. However, the model has limitations in simulating flow directions (with only one fixed downstream cell). In addition, due to the nature of the model, the same grid cannot be used for both the unblocked and grip blocked cases because the network is represented as a series of linkages so cannot easily be adapted to represent ponding behind blocks such as pictured in Figure 2.5. It is concluded that there is a need for a physically based model that can run on an irregularly-sized grid of any shape and size, which has associated with it both storage and flow properties, in order to fully represent the complex geometry of LUM practices in the landscape by features observed in the field at the local scale.

2.4 Catchment Scale Land Use/Management Change Impacts: Detection and Attribution

Sections 2.2 and 2.3 showed that the effects of rural LUMCs on the local scale hydrology are reasonably well understood. In contrast, it is unclear how these impacts aggregate downstream to affect larger scale flooding (O'Connell et al., 2007a). However, this is often of much greater interest to the catchment managers, especially when this involves infrastructure and urban areas so that flooding is more likely to result in major economic costs, loss of public and personal possessions, and even loss of life (Morris and Wheater, 2007; Wheater and Evans, 2009; Parrott et al., 2010).

Hydrological catchment change detection and prediction related to LUMC are of considerable scientific and practical importance for catchment management planning and potential flood mitigation and protection (Kundzewicz, 2004; Parrott et al., 2010; Pike et al., 2010; Ronfort et al., 2011). Hydrological change can be quantified in terms of magnitude (often relative to a baseline condition), direction (positive or negative, according to the research interest), and duration (Pike et al., 2010). Studies on the

hydrological effects of LUMCs are traditionally focussed on detecting the impacts on hydrological processes (e.g. interception, flow pathways), water quantities (e.g. annual water yield, peak flows, low flows) and the shape and timing of the flood hydrograph (e.g. lag time, recession curve). O'Connell et al. (2004) argued that, ideally, change detection should involve the full flood frequency curve, so that (change in) flood risk can be assessed across the full range of probability in a way that properly reflects the changing balance of surface and subsurface runoff conditions with changes in antecedent conditions and rainfall magnitudes.

The most obvious restriction on the ability to detect changes is the proportion of the study area subjected to LUMC. For example, in forest hydrology studies have shown that at least 20% of the area should be affected by change (in vegetation) before any hydrological change can be detected (Bosch and Hewlett, 1982; Brown et al., 2005).

2.4.1 Change Detection Approaches

There are a number of different approaches that can be used for LUMC detection. Broadly, these can be subdivided into two different groups: 1) statistical approaches, and 2) rainfall-runoff modelling approaches (O'Connell et al., 2004). Some LUMC studies use a combination of the two approaches (e.g. Zegre et al., 2010). Naturally, the method will depend on the specific area of interest and the available data.

Statistical approaches are based on the available data directly and focus on the significance of changes, between a pre- and post- change period, and/or between two different catchments over the same time period (Pike et al., 2010; Zegre et al., 2010). They involve investigating changes to a frequency distribution, e.g. of floods, derived from studying historical records of characteristics such as peak discharges (O'Connell et al., 2004). They are often focussed on trends (e.g. examining trends in peaks-over-thresholds or annual maxima (Robson et al., 1998)). Kundzewicz and Robson (2004) highlighted that every specific problem has its own appropriate statistical test and no test is perfect. The misuse of tests of statistical significance can lead to confusion in the interpretation of research data (Alila et al., 2009; Clarke, 2010). The fundamental assumption in statistical tests is that the flood generation process is stationary (i.e. the statistics are not changing with time) (Kundzewicz and Robson, 2004; O'Connell et al., 2004). However, there is large natural variability in rainfall characteristics and

antecedent conditions (Kundzewicz, 2004). It is often assumed that the records or sampling periods are long enough to capture the full range of natural variability that generally exists within hydrology (e.g. Archer and Newson, 2002), although for this assumption to be valid the records are often not long enough.

Rainfall-runoff modelling can help give insight into the hydrological functioning of the catchment landscape and the way it responds to changes in the weather, climate and LUM changes. Distributed models can provide insight into how the effects of LUM changes propagate across scales. When use in conjunction with stochastic rainfall modelling, rainfall-runoff modelling can be used to obtain the frequency distribution of peak discharges etc. (O'Connell et al., 2004). Rainfall-runoff modelling is therefore a potentially useful tool for the assessment and prediction of (future) LUMC impacts on hydrologic behaviour. The rainfall-runoff modelling approach can either be event based or involve continuous rainfall-runoff simulations. There are two extremes in the hydrological modelling approach. The method can be: 1) top-down, which generally involves lumped conceptual models or 2) bottom-up, through distributed physically based models (Beven, 2001b). A lumped model typically uses parameters for lumped representations of catchment functioning. These parameters are derived through calibration and influenced by several features of the catchment behaviour. They often have no physical meaning. In contrast, distributed physically based models account for the spatial variation of hydrological processes and model parameters, though they require more information and contain more parameters than lumped models.

It is accepted that the current monitoring and modelling techniques used to detect catchment scale changes may be too crude for detecting changes in hydrological functioning (O'Connell et al., 2004; Atkins, 2007; Halcrow, 2008). An advantage of statistical and lumped modelling detection methods is that they are relatively easy to transfer to other catchments and larger scales (e.g. Uhlenbrook et al., 1998; Archer, 2003). However, they do not allow for within catchment complexities, such as runoff generation and land cover heterogeneity (Beven, 2001b), which can lead to an underestimation of the impacts of LUMC (O'Connell et al., 2004; van Dijk et al., 2011). In addition, if change is detected, it is difficult to determine the exact cause of the change as cumulative effects cannot be disentangled. It has been argued that, for

lumped models, the main uncertainty source is the simple model concept itself and the missing consideration of spatial structures (Bormann et al., 2009). Especially for change prediction, distributed physically based models are therefore preferred (Beven and Binley, 1992; O'Connell et al., 2004; Bormann et al., 2009).

However, the complexity in the representation of physical processes and the number of parameters that have to be evaluated in distributed physically based modelling are both the method's strength and weakness (Ewen and Parkin, 1996; Beven, 2001b). The use of physically based models in general (Grayson et al., 1992; Beven, 1993; Beven, 2001a), and in particular for change detection and prediction (Ewen et al., 2006b; O'Connell et al., 2007a) has received much critique. It is almost impossible to obtain enough data (especially relating to subsurface processes) to accurately inform process based models, and there are knowledge gaps in the understanding of which processes are relevant to flooding, and in the conceptual understanding of the physical processes and parameters (Lane, 2008). Good results (high Nash-Sutcliffe values, good fits) are quite easily obtained when a large number of parameters are involved, though they may not produce an adequate model representation of the internal processes (Klemes, 1983; Beven, 1989; Parkin et al., 1996). Over-parameterisation, parameter uncertainty and hence model output uncertainty are all associated (Beven, 1993).

2.4.2 Challenges in LUMC Detection

In addition to the general shortcomings of the currently available change detection methods as described above, the ability to detect changes is a function of other interrelated factors. The main challenges lie in: 1) data uncertainty, 2) de-coupling change impacts from natural variability, 3) working with short records, as well as 4) differentiating between different change effects, and 5) the transferability and scaling of impacts. Details are given below.

There are always uncertainties in the estimates of the catchment inputs and observations of discharge outputs (Robson et al., 1998; Kundzewicz and Robson, 2004; O'Connell et al., 2007a), for example, as a result of limited spatial sampling and altered measurement techniques. In addition, at larger scales, there are also uncertainties in the characterisation of LUMC patterns in space and time (van Dijk et al., 2011). Both

data related uncertainties generally increase with the age and length of the records. However, from a sampling point of view, longer records are required.

The main challenge is to make a distinction between natural variability and effects of LUMC, as climate is a dominant factor in determining the temporal variability in runoff response, and the frequency and magnitude of flood events within any given catchment (Robson et al., 1998; Gilman, 2002; Kundzewicz and Robson, 2004; Woods, 2004; Atkins, 2007; O'Connell et al., 2007a; Beven et al., 2008b; Lane, 2008; van Dijk et al., 2011). However, at the plot or hillslope scale, LUMCs can be significant (Peel, 2009). Peak flows may be seriously affected by the spatial and temporal variability in rainfall and antecedent conditions (e.g. soil moisture). A study of effects of LUMCs should consider the effects of natural climatic variability. In addition, LUMC impacts are likely to be more obvious under some natural hydrological conditions than others (Gilman, 2002; O'Connell et al., 2007a). Several studies have shown significantly different effects of LUMC between seasons (Bronstert et al., 2002; Pfister et al., 2004; Evrard et al., 2007) and types of storms (Beven et al., 2008a; Bathurst et al., 2010). Data records that only cover one season or specific types of storms that do not reflect the full range of variability might over- or under- estimate the LUMC impacts.

In relation to the above, long enough data records are an important condition for change detection. For both detection approaches, it is important that the full range of natural hydrological conditions is covered in the data record. Several authors have argued that timescales required for LUMC change detection in hydrological records, as for climate (Robson, 2002; Pfister et al., 2004; Wilby, 2006), should be significantly longer than the timescales over which responses to the drivers of those changes occur. It is not uncommon to have a long time lag (>5 years) between the implementation and the effects of LUMCs (Bloschl et al., 2007). Radziejewski and Kundzewicz (2004) noted that some (statistical) tests are not able to detect weak or short lived trends, although it should not be interpreted as proof of change absence. Based on a statistical methodology, in a study looking for (long term) trends in UK flooding, Robson (2002) showed that trends (and change detection) depend on the duration over which the evaluation is made. For example, no trends could be detected in flow series longer than 50 years, but there is clear evidence of recent trends for 30-40 year periods.

Another challenge is to differentiate between the effects of different LUMCs (Sullivan et al., 2004). Quite often, several LUMCs occur in conjunction with each other (e.g. field drainage and afforestation), and their impacts may buffer each other out (Fohrer et al., 2001; Pfister et al., 2004; Atkins, 2007). For larger catchments, this is complicated by a patchwork of different types of LUM (and LUMCs) (e.g. Pfister et al., 2004), in addition to the natural heterogeneity in the physical characteristics and the tributary response phasing. Here, up-scaling and extrapolation is difficult as a result of the non-linearity and complexity of the processes involved (Schulze, 2000; O'Connell et al., 2007a; Halcrow, 2008).

As a result of these challenges, a distinct gap often exists between the level of certainty of information that hydrologists can provide and the certainty of detection and predictions that managers seek. Archer and Newson (2002) listed a number of properties or conditions for effective LUMC detection, including: 1) focus on attributes of flow considered to have been influenced by LUMC, 2) use of an appropriately short measurement interval, 3) decoupling of the effect of climate and weather (natural variability), 4) allowance for detection of step changes and trends, 5) allowance for comparison between sites (in space and scale), and 6) allowance for statistical validation. Based on the discussion above, the need for long enough records is added to this list.

2.4.3 Examples of Change Detection Methods

Statistical approaches

The most commonly used traditional statistical change detection method is closely related to the data from the traditional paired catchment approach. The method involves (Zegre et al., 2010): 1) fit a regression model through pre-change data (e.g. a linear regression through monthly precipitation versus monthly discharge) from each catchment, 2) use the regression model to compute prediction intervals and predict the catchment behaviour of the changed catchment based on observations from the control catchment during the post-change period, 3) calculate the model residuals, and 4) evaluate the proportion of post-change residuals that exceed the prediction limits. For example, using 95% prediction intervals, change is predicted when more than 5% of the post-change residuals exceed the prediction limits (Zegre et al., 2010). However,

chronological pairing of events is difficult as a result of variability in storm timing, duration, intensity or spatial distribution (Thomas and Megahan, 1998; Alila et al., 2009), which is why this method is generally applied to monthly or annual data sets (e.g. Kirby et al., 1991; Hubbart et al., 2007; Zegre, 2009). Where records are long enough for single catchment studies to capture the full natural variability, the pre-change record can be used to predict the post-change record for a comparison with the observed post-change data. Examples include the work of Sullivan et al. (2004) who analysed annual maxima in the discharge record, and Howorth and Manning (2005) and Lane et al. (2005) who studied flow duration curves to allow for the detection of changes in low and high flows. More examples of common statistical tests applied to change detection in hydrological records are given by Kundzewicz and Robson (2004).

Archer and co-authors (e.g. Archer and Newson, 2002; Archer, 2003; Archer, 2007; Archer et al., 2010) described a novel statistical method for detecting LUMC effects in different aspects of the hydrograph, through the use of indices of flow variability. The method involves a comparison of the annual number, and average and total duration of pulses above selected threshold flows between pre- and post- LUMC years. With some adjustments to the main method, it can also be used to detect changes in rates of short-term rise and fall in the flow hydrograph (Climent-Soler et al., 2009; Archer et al., 2010). Advantages of this 'indices of flow variability' method are 1) it allows for the full time series of hydrograph variability to be examined and the application to different aspects of the flow regime including magnitude, frequency and duration of flow pulses, 2) the decoupling of natural variability in precipitation (based on a regression between annual precipitation and annual pulse numbers above each threshold) 3) its application to and comparisons of catchments at different spatial scales (as it relates to median flow) and 4) its ability to work with small (sub-daily) data intervals (Archer, 2004). However, this method, as with all statistical methods, still requires a significantly long enough record (30+ years) to establish the relationship between annual precipitation and the pulses over threshold relation and hence account for natural variability. Using this method, change in the flow characteristics has only been clearly attributed to LUMC in small research catchments (e.g. Coalburn, 1.5 km^2 (Archer and Newson, 2002), and the Severn at Plynlimon, 8.7 km^2 (Archer,

2007)), where the proportions of area impacted by LUMC are large and changes to pulses can be clearly identified on very short time intervals. However, it is more challenging for the method to evidently detect changes in meso scale catchments (e.g. the Irthing, 333.8 km^2 (Archer, 2003) and the Axe, 288.5 km^2 (Archer et al., 2010)), because the effects of LUMC become more diffused when the catchment scale increases and the proportional area affected becomes smaller.

Rainfall-Runoff models

There are two ways of using hydrological models for change detection (Zegre et al., 2010): 1) calibrate and validate a hydrological model for the pre-change period and compare the simulated and observed post-change data without changing any of the model parameters (e.g. Siriwardena et al., 2006), or 2) calibrate and validate the model separately for the pre- and the post-change periods (Post et al., 1996).

Examples of (semi) lumped models used in change detection include the unit hydrograph (e.g. Robinson, 1990) and its extension method, the Identification of unit Hydrographs And Component flows from Rainfall, Evaporation and Streamflow data (IHACRES, Jakeman et al., 1990) (e.g. Post et al., 1996). The Data Based Mechanistic modelling framework (DBM, e.g. Young, 1992; Young and Beven, 1994; Young, 2003; Ratto et al., 2007) has also been used recurrently for change detection (Beven et al., 2008b; McIntyre and Marshall, 2010). Ewen et al. (2010) used a lumped Storage Discharge Detection (SDD) model for change detection. A detailed description of the DBM and SDD methods is provided in Chapter 6. For large catchment scales, most modelling studies of LUMCs are semi-distributed conceptual, though there are some examples of studies were fully distributed physically based models are used (O'Connell et al., 2004; O'Connell et al., 2007a; Halcrow, 2008; Breuer et al., 2009).

Zegre et al. (2010) combined semi-distributed conceptual daily rainfall-runoff modelling (HBV-EC, Hamilton et al., 2000), uncertainty analysis and time series regression to distinguish between the effects of forest clearing, data errors and natural variability of daily discharge from a small subcatchment (0.23 km^2) of the Hinkle Creek catchment in Oregon, USA. They could not detect changes in a neighbouring control catchment (1.56 km^2), arguably strengthening their approach. However, owing to the

nature of the rainfall-runoff model, it is not possible to detect changes in flashy catchments for responses at the sub-daily level. In addition, it is impossible to unravel the exact cause of the change by using semi-distributed conceptual models.

2.4.4 Attribution of Catchment Scale Effects of Land Use/Management Changes

From their review on the effects of rural LUM practices, O'Connell et al. (2007a) concluded that there is an almost complete lack of evidence that local scale effects aggregate to cause impacts at larger scales downstream, though they did not suggest that they therefore do not exist. Instead, they attributed the lack of evidence to a limitation in the number of studies, and those studies that did focus on larger scales have inconsistent or uncertain conclusions (O'Connell et al., 2007a). Commonly, catchment scale studies are limited to areas <10 km^2 (O'Connell et al., 2004), although occasionally they extend to a maximum of approximately 100 km^2 (Kiersch, 2001).

In a response to the review study by O'Connell et al., Beven et al. (2008b) analysed historical UK data sets to look for impacts of LUMC on flood generation. They used the DBM method for change identification for data with relatively short time intervals (hourly). From the 9 catchments (75 - 1134 km^2) in the UK that they selected for their analysis, most catchments showed no clear change in the hydrograph characteristics that could be attributed to changes in LUMCs. In addition, the results for those few catchments that did show some tendency for change in the hydrograph characteristics were masked by year to year variability. Beven et al. (2008b) also attributed the failure to detect impacts to the poor quality of the available data and noted that some of the statistical assumptions made within the analysis may not have been met.

Worldwide, most large scale catchment studies on the effects of LUMCs involve modelling and are predictive only. There are a few cases of studies that investigate a direct link between large scale hydrological change and LUMC effects. For example, using a statistical change detection method, Tu et al. (2005) analysed whether recent changes in the frequency and magnitude of floods in the Meuse River (33,000 km^2) were aggravated by LUMC. They found that these different hydrological responses could be ascribed to climate variability. Costa et al. (2003) found a 24% increase in annual mean discharge and a 28% increase in the high-flow season discharge between

two consecutive 20 year periods of the Tocantins River (175360 km^2) in Brazil. Because they found that the mean daily precipitation between the two periods was not statistically different, they attributed these changes to an increase in agricultural practices. However, the study did not consider changes in spatial and temporal rainfall patterns and the respective percentages of land used for agricultural purposes were based on rough estimations, so the evidence for LUMC attribution is not strong.

O'Connell et al. (2004) highlighted that most UK catchment scale monitoring and modelling studies had so far focussed mainly on the effects of changes in vegetation and on soil degradation related to different crop types and regimes. Autumn-sown and late harvested crops are typically identified as runoff enhancers. Archer et al. (2010) studied the effect of these on the flood response of the river Axe (288.5 km^2), using the 'pulse over threshold' method and found higher rates of discharge rises, coinciding with an increase of these crops. However, a comparison with potential differences in rainfall intensities between the pre-and post-change periods was not made.

An overview of catchment scale studies of the LUMC relevant to the current study is given below.

Effects of moorland drainage on catchment scale response

Despite considerable increases in land drainage and arable farming, Hiscock et al. (2001) found no change in the long-term hydrological behaviour of three meso scale lowland rivers in eastern England. Lane (2003) suggested that the increase in the frequency and magnitude of flood events in the River Ouse catchment could have been caused by catchment drainage or increases in stocking levels, though no clear conclusions could be made, as a result of difficulties in disentangling the LUMC signal from the record. Archer (2003) studied the effects of moorland drainage and afforestation in the River Irthing (335 km^2) catchment (19% of catchment area subjected to change) and the nested Coalburn catchment 1.5 km^2. He observed long term changes due to afforestation (a less flashy response) at both scales, though the proportional change was much smaller for the Irthing. Conversely, the short term increased flashy response observed at Coalburn just after drainage could not be detected at the catchment scale. Archer (2003) speculated that the small or no

response at the catchment scale could be attributed to the respective percentage area undergoing change, the patchwork of forest development and the spread in time and the change in balance of hydrological processes.

In summary, there are no studies that have observed effects of drainage and/or drain blocking specifically at the larger catchment scale.

Effects of stocking density changes on catchment scale response

There has been anecdotal speculation that grazing practices might be related to some changes that have been observed at larger scales. For example, Samson (1996) remarked that an increase in the magnitude and occurrence of floods in the river Ure (915 km^2) could have been caused by increased runoff rates as a result of overgrazing. Sansom (1999) related a 25% increase in annual water yields of a catchment in North Yorkshire with doubled stocking levels over the same period. However, these studies of Samson did not involve an evaluation of rainfall variability, making these suggestions highly questionable. Climatic variability leads to natural hydrological variability. If not accessed properly, this can be easily confused with the impacts of LUMC. Sullivan et al. (2004) found an 8.7% increase in the median mean daily flow of the De Lank River (22 km^2) that coincided with a 43% rise in the intensity of maximum upland grazing levels. It is noted that no equivalent rise in the maximum daily flow could be observed. The effects of temporal changes in daily rainfall totals were ruled out as no corresponding rise in the maximum daily flow was detected. For the downstream Camel catchment (210 km^2), Sullivan et al. (2004) could not distinguish between the impacts of subtle changes in climate, increased farming activity and urban expansions, to explain the long-term changes in flood frequency and magnitude. In addition, Holman et al. (2003) linked the autumn 2000 floods in several parts of the UK to structural degradation of the soils, partly caused by sheep and livestock rearing. They argued that the soil degradation occurred over large areas of the catchments of the River Severn (11420 km^2), Yorkshire Ouse (3400 km^2), Uck (88 km^2), and Bourne (50 km^2), and contributed to enhanced runoff in each of these catchments. Because the study of Holman et al. (2003) lacked a qualitative link between the soil degradation and flood response, their reports do not provide solid evidence of the large scale effects of LUMC impacts.

At a much smaller catchment scale, McIntyre and Marshall (2010) investigated differences in catchment responses related to land management through a paired catchment approach, using the DBM method for change detection. Based on the average DBM parameters for 17 short periods for nine different gauges (0.04 - 5.77 km^2) in the Pontbren study, they found a more flashy response for improved grasslands compared with that for more natural conditions. These outcomes agree with the other small scale studies on the effects of grazing (see Section 2.3.3), though the catchments are too small for these results to contribute to the knowledge on large scale impacts of LUMCs. In addition, Grayson et al. (2010) argued they found evidence that overstocking and increased erosion of peatland at Moorhouse coincided with a flashier response (higher discharge peaks and shorter lag times) at the catchment scale (11 km^2). It is noted that there is some bias in their data, leading to the inability of assessing whether this effect is evident over the full range of hydrological conditions. In their analysis, Grayson et al. (2010) only included singled peaks, while the majority of events in UK upland catchments typically have multiple peaks. In addition, even though they state that as many single peaked storm hydrographs covering as many months as possible were selected, on average only 16 storms per year were included in the analysis and it is unclear during which seasons these events occurred, and whether the relative distribution is similar for the different time periods that were analysed.

Overall, there seems to be vague evidence of flashier catchment responses associated with increasing stocking density changes. These impacts were found on mini catchment scales at most. The potential effects at the meso scale are unproven.

2.5 Catchment Scale Land Use/Management Change Impacts: Monitoring, Modelling and Prediction

2.5.1 Key Issues with (Up-) Scaling Land Use/Management Change Impacts

Owing to the lack of data from large scale catchments undergoing known LUMC, and of evidence of large scale LUMC impacts, there is an inevitable desire for a way of up-scaling the effects observed at the local scale. It is often assumed that the results of plot and hillslope scale studies can be scaled to the catchment level. However, even

when it is assumed that catchments are not undergoing change, scaling in catchment hydrology has been a major challenge for a long time and continues to be so (Klemes, 1983; Dooge, 1986; Bloschl and Sivapalan, 1995; Bloschl, 2001; Bloschl et al., 2007). The key problems associated with the scaling complexity are data constraints, heterogeneity, nonlinearity and the dominance of different processes at specific scales.

The data constraints pose limitations on the conceptualisation of processes mainly, especially at larger scales where management decisions are needed but the level of detailed information is much smaller than for small scales (Bloschl, 2001; Sidle, 2006). Because of heterogeneity, nonlinearity and differences in dominant processes, a large catchment cannot be considered simply as the sum of many individual fields (Cerdan et al., 2004; Shaman et al., 2004; Soulsby et al., 2006). Details on these two issues are given below.

There is heterogeneity at all scales, owing to variability in climate (precipitation), geology, topography, soil, vegetation, and land-use (Beven et al., 1988; Sivapalan, 2003; McDonnell et al., 2007; Pike et al., 2010). This landscape heterogeneity results in spatio-temporal variability of hydrological states and fluxes, scale-dependent flow and incomplete process understanding (Bloschl and Sivapalan, 1995; Troch et al., 2009). To adequately capture this variability, Dooge (1986) stated that there is a need to either solve extremely complex physically based models which take full account of the spatial variability of various parameters, or else derive realistic models at the catchment scale in which the global effect of these spatially variable properties is parameterized in some way. Correspondingly, upscaling often involves identifying dominant processes that are evident at the catchment scale, rather than attempting to capture all small-scale variability and complexity (Bloschl, 2001; Sivapalan, 2003; Tetzlaff et al., 2010). However, the heterogeneity and unique characteristics of a catchment or a particular scale should be considered in order to understand LUMC impacts, because it is the internal behaviour of catchments at local scales (flow paths etc.) that are directly affected by LUMC (Bloschl, 2001; Buttle, 2006; Sidle, 2006). It is generally accepted that both up-scaling and down-scaling are needed in order to reach a good understanding of scaling (Klemes, 1983; Dooge, 1986; Sivapalan, 2003).

If a system was entirely linear, it would be simple to integrate small scale equations for conditions over larger areas and the large scale parameters would be the spatial averages of the corresponding parameters at the small scale (Dooge, 1986). However, most processes in hydrologic systems are nonlinear and the properties of proportionality and superposition do not hold (Dooge, 1967). The hydrologic response at the catchment scale is dominated by different processes (e.g. channel processes) than those observed at the small scale (e.g. infiltration)(Klemes, 1983; Sidle, 2006). There are numerous cases where using data collected at the small scale to describe processes at the large scale is misleading or incorrect. For example, a plot scale study may show that a large proportion of the runoff generation is overland flow, up to a few orders of magnitude higher than those appropriate for hillslopes or catchments (Sidle, 2006). In addition, there are indications that hydraulic conductivities obtained from point scale field tests are up to two orders of magnitude different from those derived from larger scale field investigations (Bonell, 1998; Nilsson et al., 2001).

2.5.2 Multiscale Nested Experimental Catchment Designs

When the scale of a study catchment increases, it becomes more challenging to isolate effects and find catchments for paired experiments (Schindler, 1998; Pike et al., 2010). Sidle (2006) promoted the idea of implementing field measurements at the scales appropriate to the interest of the study. However, this can raise some level of conflict. Unless plot and hillslope scale studies are included, the catchment scale behaviour can be a black box. A lack of understanding of the within catchment processes could potentially lead to a false sense of confidence that models or analyses are giving the 'right answers', though 'for the wrong reasons' (Kirchner, 2006; Sidle, 2006).

A number of studies have focussed on the way hydrological processes at different scales are linked and integrated. To elucidate the spatial distribution and the inter-linkages of processes, these studies implemented multiscale nested experimental catchment monitoring designs (Soulsby et al., 2006; Bloschl et al., 2007; O'Connell et al., 2007b). A schematic representation of a monitoring structure that involves nested groups of catchments at multiple scales is shown in Figure 2.6. Compared with the traditional small scale approaches (Section 2.2.1), the multiscale nested monitoring systems are relatively uncommon, owing to high costs and maintenance demands.

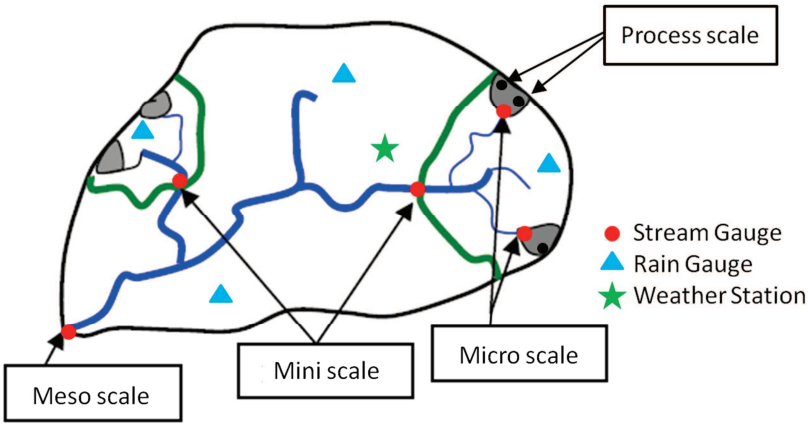

Figure 2.6 Schematic representation of a multiscale nested structure for instrumentation (altered from O'Connell et al. (2007b))

A few examples of multiscale nested monitoring systems include the MARVEX project in the Mahurangi catchment (50 km^2) in New Zealand (Woods et al., 2001) and the Reynolds Creek catchment (239 km^2) experiment in Idaho, USA (Slaughter et al., 2001). Several projects in the UK have instrumented meso scale catchments following the same generic design as presented in Figure 2.6. For example, from 2003-2004, the CHASM programme started monitoring the Oona Water (92 km^2), Upper Severn (187 km^2), Feshie (200 km^2), and the upper Eden (322 km^2) catchments (O'Connell et al., 2003; O'Connell et al., 2007b). These were selected based on the existence of previous micro scale monitored catchments (such as those presented in Table 2.1), among others. The main aims of CHASM were to gain new understandings of the hydrological and ecological functioning of meso scale catchments and how catchment response changes with scale (Mayes et al., 2006; O'Connell et al., 2007b).

There is a shortage of data from multiscale nested catchments that have been instrumented to investigate the effects of LUMC specifically (Gilman, 2002; O'Connell et al., 2004; Atkins, 2007; O'Connell et al., 2007a). Although the catchment area is still relatively small (12.5 km^2), the Pontbren study site in Wales, where the effects of wooded buffer strips, small wetland areas and reductions in stocking densities are being studied (e.g. Carroll et al., 2004; Jackson et al., 2008; Marshall et al., 2009), is one of a few examples. The historical records of the actual LUMCs are generally poor for other catchments with existing monitoring networks, and the timing and distribution of LUMC rarely occur in an ordered fashion (Archer, 2003).

2.5.3 Modelling and Predicting the Connection between LUMC effects on Hydrological Behaviour at the Small and Large Scales

Change Prediction Modelling Methods

Hydrological modelling is mainly used for LUMC change prediction, sometimes in combination with statistical methods. O'Connell et al. (2004) recommended that modelling for predicting impacts should be distributed, (partly) physically based and include detailed modelling of surface water flow so that the effects can be tracked downstream. This should also be supported by a considerable amount of high-quality field data on local scale impacts. However, Croke et al. (2004) suggested that, where data limitations limit the application of distributed and physically based models, lumped or semi-distributed models may be a more appropriate method.

For change prediction, the pre-change model's parameters are often calibrated after which they are altered to their post-change values without calibration (Ewen et al., 2006b; O'Connell et al., 2007a). In addition to validation, adequate testing and estimation of uncertainty in predictions should be included, although these are typically not executed rigorously (O'Connell et al., 2004). In addition, some modelling and prediction studies are solely based on theory, as they do not even include a validation of the model on pre-change data, but are instead based on empirical relationships related to catchment features (e.g. Hess et al., 2010; Ronfort et al., 2011).

Bormann et al. (2009) demonstrated that the uncertainties in predictions can be reduced by bringing together the results of physically based models and lumped models, and they therefore advocated a multi-model ensemble. In agreement, Huisman et al. (2009) applied an ensemble of 10 hydrological models (including lumped, semi-distributed and fully distributed models) to the same set of LUMC scenarios for the Dill catchment (693 km^2) in Germany. They found that the models generally agreed about the direction of changes in the mean annual discharge and 90% discharge percentile predicted by the ensemble members. However, the range in the magnitude of predictions for the scenarios and catchments under consideration was considerable. Nonetheless, they concluded that the use of a model ensemble increases confidence in the reliability of the model predictions regarding LUMC.

Linking small and large catchment scale models for LUMC prediction

From numerous small scale plot- and hillslope scale studies, it has become clear that the responses at these scales are characterized by complexity and heterogeneity (Sections 2.3.4 and 2.5.1), and so are the physically based models designed to aid in the understanding of these (Sivapalan, 2003). On the other hand, large catchment scale models are much simpler (Bloschl et al., 2007) and focus on different hydrological aspects (e.g. routing and interactions between streams and aquifers) rather than small scale processes (such as macropore and soil pipe flow). According to Beven and Kirkby (1979) the effect of the river network becomes important from the mini scale (10 km^2).

In the modelling context, there are two main approaches to establishing the connection between the small and large scale hydrological behaviour: the upward and the downward approach (see Section 2.1.2). Up-scaling the small scale complexity (and the relatively complex physically based models) is challenging for a number of reasons (Grayson et al., 1992; Clark et al., 2009). Firstly, with increased complexity there is a need for more parameters. Estimating the parameter values in complex models is quite challenging, and this problem increases with larger spatial scales. The non-linear nature of a small scale, highly parameterised physically based model, leads to more uncertainties and a potential inability to upscale any of this information (e.g. Jackson et al., 2008). Secondly, physically based models have large data and computational requirements. On the other hand, the downward approach does not facilitate a proper investigation of the changes in the internal processes.

Modelling studies aiming to gain a better understanding of the connection between local hillslope LUMC and the impacts on downstream catchment response have recurrently installed an intermediate step in the modelling procedure to link small and large scale processes efficiently and systematically. For example, Dunn and Mackay (1996) established pseudo or effective parameters in their SHETRAN model to transfer hillslope scale peatland drain information to meso scale catchment (114 km^2) response.

A variety of UK studies has recently been carried out within the UK EPSRC Flood Risk Management Research Consortium (FRMRC, 2008). One of the objectives of FRMRC was to gain a better understanding of the link between LUMCs and flooding at the

catchment scale. A collaborative project between Imperial College London and Newcastle University in the second phase of FRMRC (FRMRC2) focussed specifically on LUMC issues in the Pontbren catchment in Wales and in the Rivers Hodder and Eden in Northwest England (FRMRC2, 2011). Within the project, a new multiscale modelling methodology was developed, which involves linking small scale physically based runoff generation models with dense channel network routing models to study the propagation of impacts to the catchment scale. First, physics based hillslope models are parameterised and calibrated against observations. The outputs of these small scale models are then used to train conceptual models to replicate the response from the physically based models. The parameters of these 'metamodels' are then regionalized (Bulygina et al., 2011) and used to represent hydrological runoff elements that are linked to a dense channel network routing model (DNRM)(FRMRC2, 2011).

The DNRM model (O'Donnell et al., 2011; Ewen et al., 2012) was developed to study in detail how a flood develops and how local (LUMC induced) changes in runoff generation propagate through the river channel network to affect flooding downstream. It focusses on the physically-based modelling of the open-channel flow network. The spatial patterns of rainfall, soil types, land use and land conditions are represented by grid squares (typically 500 m or less), and the impact of LUMC can be applied to the grid cells through the metamodels as described above, resulting in a conceptual runoff generation at the grid cell scale. The drainage network is represented in fine detail and the hydraulic routing is represented by the St. Venant Equations (O'Donnell et al., 2011). In an adjoint (backwards integration) version of DNRM, the sensitivity of the catchment model output to changes in the model input and parameters can be calculated through backwards information tracking, and mapped onto the catchment landscape (O'Donnell et al., 2011). This new tool is useful in two ways: it determines where the flood water arriving at a downstream location comes from and it can help in estimating which areas in the catchment are most sensitive to LUMC and hence for which areas within the catchment land management interventions might be most effective (O'Donnell et al., 2011).

Predicted Large Catchment Scale LUMC Impacts

As LUMCs are generally local phenomena, the impact of any LUMC is likely to decrease with catchment size (Archer, 2003; Bloschl et al., 2007). The LUMC impacts at larger scales will also depend on the percentage area undergoing change, the spatial distribution and temporal variation in individual physical catchment characteristics, LUM activities and their effects on runoff generation (magnitude and timing), the connectivity of local scale flow paths with the stream network, and the routing of runoff through the channel network (Gilman, 2002; O'Connell et al., 2004; Bloschl et al., 2007; Halcrow, 2008). Significant impacts at the small (hillslope or plot) scale may not therefore have a significant impact at the catchment scale. Even if the flood hydrograph of a small subcatchment can be altered as a result of LUMCs, it is possible that the effect is filtered out by the cumulative effect of the different (de-synchronised) flood hydrographs from the other subcatchments at the main catchment outlet (Fohrer et al., 2001; Halcrow, 2008). For that reason, the large scale effects will depend on the exact location within the catchment (Gilman, 2002; Lane, 2003; FRMRC2, 2011)

Several modelling studies have suggested that extensive upland LUMCs are required to produce an only modest but significant impact at the downstream catchment scale (Gilman, 2002; JBA Consulting, 2007; O'Donnell et al., 2011). In a study where they tested the sensitivity of the downstream hydrograph to upstream changes in runoff generation, O'Donnell et al. (2011) showed that this is due to considerable attenuation of small scale runoff changes during the propagation, attributed to hydrodynamic (the effect of channel friction) and geomorphologic (the geometry of the channel network which affects the timing of downstream runoff delivery) dispersion. It is also suggested that the impacts of LUMC (as for the local scale) are greatest for the more intermediate and frequent flood events than for more extreme events (Archer and Newson, 2002; JBA Consulting, 2007; Hess et al., 2010; Bathurst et al., 2011a; Bathurst et al., 2011b), and depend on seasonal/antecedent conditions (Climent-Soler et al., 2009).

In a modelling study on the effects of grip blocking in the upper part (40%) of the Ripon catchment (120 km^2), JBA Consulting (2007) predicted that the effects at the catchment scale could be a 1-8% reduction of the peak flow magnitudes. They based

these predictions on the assumption that grip blocking would potentially improve the structural properties of peaty soils, although there is no scientific evidence to suggest that this will actually happen (see Section 2.3.2).

Recent modelling studies have suggested potential flood mitigation effects of changing the soil conditions (i.e. reverse soil degradation), (e.g. Gilman, 2002; Hess et al., 2010; Holman et al., 2011) which can be achieved partly by reduced stocking levels. Gilman (2002) simulated the effects of a 10% increase in infiltration rates over headwater catchment areas of over 200 km^2, which led to a 2-4% decrease in modelled peak flows downstream. Hess et al. (2010) predicted that improvements to the soil conditions would have the greatest relative impact in low rainfall areas and on more permeable grassland soils, though the peak flow reduction would be no greater than 5%. Holman et al. (2011) predicted that improved soil conditions could increase the baseflow index from less than 5% up to 10%, depending on soil and climatic conditions. It is noted that these studies use (largely conceptual) models, none of which are calibrated against real data of change, and the predicted changes in parameters are based on large assumptions. These predictions are therefore only able to indicate the potential direction of change; the percentage change is subject to large uncertainty.

2.6 Summary

Traditionally, the experimental design of LUMC studies can be subdivided into three main groups: correlation studies, single catchment studies, and paired catchment studies. However, the areas of these experimental catchments are conventionally small and there is a lack of data from multiscale nested catchments that have been instrumented to investigate the effects of LUMC specifically at larger catchment scales. Change detection and prediction methods are subdivided into two different groups: statistical approaches, and rainfall-runoff modelling approaches. Both methods have their advantages and limitations and the change detection method will depend on the specific area of interest and the available data. The main challenges in change detection and prediction are related to data uncertainty, de-coupling change impacts from natural variability, working with short records, differentiating between different change effects, and the transferability and scaling of impacts.

The hydrological functioning of peatlands is rather complex and no peatlands are alike owing to a strong link between the biology and hydrology, mediated by climate. In general, streams draining upland peat tend to have a flashy behaviour, with minimal contributions of base flow. A vast amount of research has led to the establishment of convincing links between LUMC and changes to the runoff regime at the plot and hillslope scale, and in some cases even at small catchment scales (<10km^2), depending on the spatial extent of the changes. Increases in grazing pressures are typically associated with faster and flashier catchment runoff and increased delivery of runoff to quick preferential flow paths (sheep tracks). Peat drainage (and potentially drain blocking) can both reduce and increase runoff, depending on local conditions, such as peat type and the location of the drainage within the catchment. In order to fully represent the complex geometry of LUM practices in the landscape by features as observed in the field (sheep tracks and (blocked) drainage systems), a physically based model that can run on an irregularly-sized grid of any shape and size is needed.

There is an almost complete lack of evidence that local scale effects aggregate to cause impacts at larger scales downstream. The available evidence is anecdotal, inconsistent and has led to uncertain conclusions. In addition to the overall complexity with up-scaling (resulting from data constraints, heterogeneity, nonlinearity and the dominance of different processes at specific scales), the local scale LUMC impacts at downstream larger scales are a function of the percentage area undergoing change, the spatial distribution and temporal variation in individual physical subcatchment characteristics, LUM activities and their effects on runoff generation (magnitude and timing), the connectivity of local scale flow paths with the stream network, and the routing of runoff through the channel network. It is suggested that a large extent of upland LUMC is required to produce an only modest but significant impact at the downstream catchment scale, and that the effects vary between storms and antecedent conditions.

3 Catchment Description and Land Use/Management Changes

3.1 Introduction

3.1.1 Chapter Overview

After a note on the catchment selection and a general catchment overview as part of this introduction, Chapter 3 gives a detailed description of the experimental study catchment of the River Hodder. This includes its geology and pedology, climate, main land uses and vegetation. The water supply infrastructure that is operated by United Utilities and the flooding issues in the Hodder are also described. Finally, the land use/management changes that the catchment has been subjected to, both historically and under the SCaMP programme, are reported. A summary is given at the end of the chapter.

3.1.2 Catchment Selection

Chapter 2 stressed the need for hydrometric data from catchments that are undergoing known rural Land Use/Management Changes (LUMC), for the investigation of the impacts of these changes on downstream flooding. The identification of catchments for the collection of those data at relatively large catchment scales is a major challenge, as there is often no record or clear structure in the timing and distribution of the implementation of LUMC.

A rare opportunity to study the impacts of LUMCs in a meso scale catchment arose when United Utilities (the main water supplier in northwest England), in collaboration with the Royal Society for the Protection of Birds (RSPB), announced substantial land use/management changes in four of their key rural areas, the Bowland, Longdendale, Goyt and a few small Peak District Estates (Figure 3.1), as part of their Sustainable Catchment Management Programme (SCaMP). The main aim of SCaMP was to apply and secure an integrated approach to catchment management in order to help a) deliver the government targets for Sites of Specific Scientific Interest (SSSIs), b) enhance the biodiversity, c) ensure a sustainable future for the company's agricultural tenants, and d) protect and improve the water quality (McGrath and Smith, 2006).

Figure 3.1 Location of United Utilities' SCaMP areas

The SCaMP changes are typical for UK uplands and included the blocking of open moorland drainage ditches (grips), tree planting and changes in stocking density and management.

Prior to the start of the present study, Ewen et al. (2006a) evaluated the potential of the four SCaMP management areas for monitoring the effects of the land/use management changes on flooding at a range of scales. The Bowland Estate, situated in the upper part of the Hodder catchment in the Forest of Bowland, Lancashire, NW England, was concluded to have the most potential. The catchments in which the other possible areas are situated, all contain considerably more reservoirs, which would greatly affect the downstream signal from the effect of the land use management changes (Ewen et al., 2006a).

The Hodder catchment in the Forest of Bowland, Lancashire, NW England, UK (Figure 3.2) was therefore designated as the field experimental site for the current study.

3.1.3 General Catchment Description

The River Hodder is a major tributary of the River Ribble that drains into the Irish Sea near Lytham, Lancashire, NW England. Just upstream of the confluence with the River Ribble, approximately 4 km southwest of the town of Clitheroe, the River Hodder drains an area of 261 km^2 at the Environment Agency flow gauge at Hodder Place (Figure 3.2). The elevations in the Hodder catchment range from 37 m at the catchment outlet in the south, to 541 m in the north of the catchment. The area is largely rural with only a few small hamlets and villages, including Chipping, Whitewell,

Dunsop Bridge, Newton in Bowland, and Slaidburn (Figure 3.2). One of the main characteristics of the area is Stocks Reservoir, which is part of the abstraction works of United Utilities, who own a large part of the uplands (SCaMP area in Figure 3.2), and abstract water for supply to parts of Lancashire and Greater Manchester.

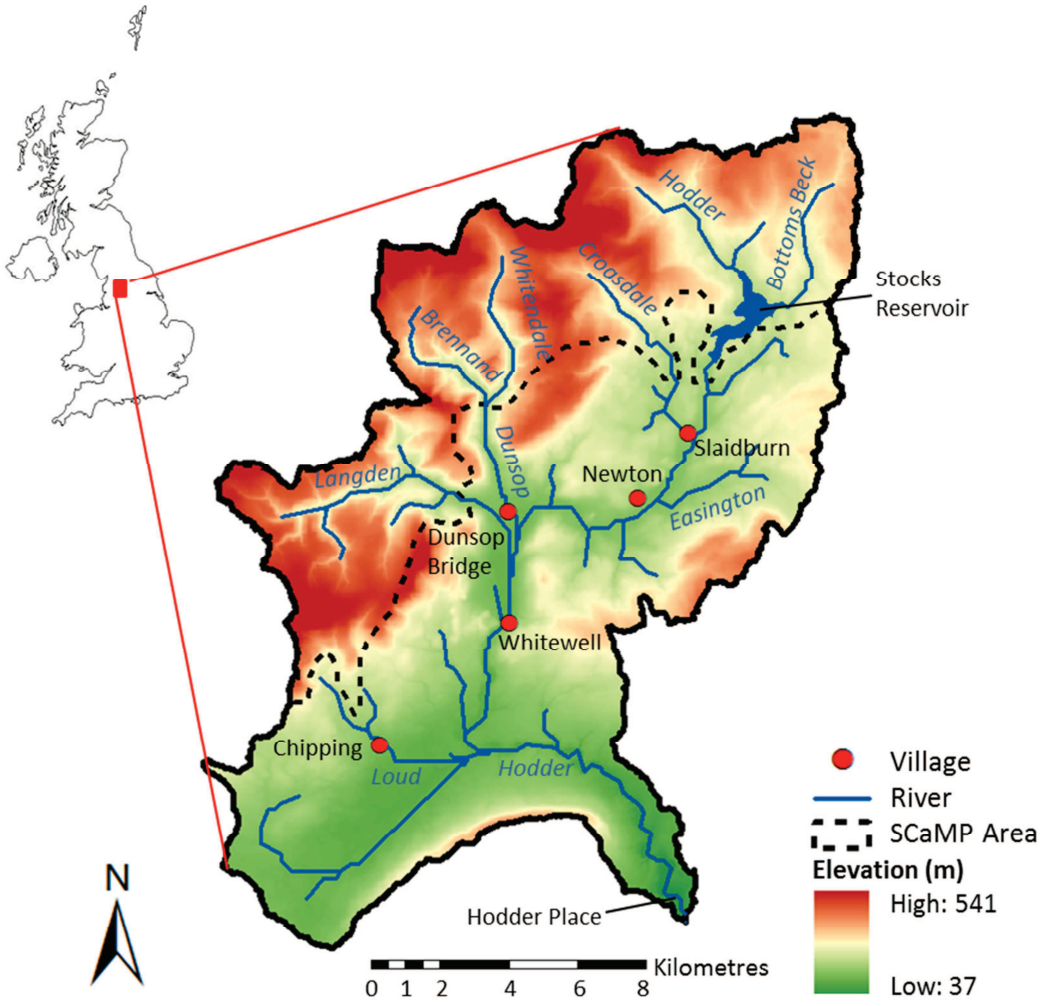

Figure 3.2 Schematic representation of the Hodder catchment

The headwaters are characterized by steeply incised valleys that cut through rough moorland and blanket bog-covered plateaus and flanking slopes. For a large extent, the uplands also lie in the Forest of Bowland, which is recognized as an Area of Outstanding Natural Beauty (AONB) and as an SSSI. Land uses are sheep and cattle livestock farming, game rearing and tourism. The fells of the Forest of Bowland are also internationally important habitats for many bird species, including Red Grouse (*Lagopus logupus scoticus)*, Golden Plover (*Pluvialis apricaria)*, Merlin (*Falco columbarius)*, Ring Ouzel (*Turdus torquatus)*, Whinchat (*Saxicola rubetra)* and Hen Harrier (*Circus cyaneus)* (RSPB, 2011a).

The main subcatchments that drain the upper part of the catchment and that were also subjected to the UU's SCaMP works are the River Hodder upstream of Stocks Reservoir (37.5 km^2), Croasdale Brook (21.1 km^2), Langden Brook (27.7 km^2), and the River Dunsop (25 km^2) (Figure 3.2). The latter consists of the River Brennand (11 km^2) and the River Whitendale (13.6 km^2). With the exception of Croasdale Brook all of these subcatchments have been used for surface water abstraction since the 1870s (Conway, 2008). The main Hodder valley, Easington Brook (13.3km^2), and the River Loud (47.3 km^2) are situated in the lower part of the catchment (Figure 3.2). The lowlands are characterized by mineral soils covered with improved grasslands. The land uses are sheep and cattle livestock farming and minor arable farming (winter sown cereals, maize and horticulture).

3.2 Geology and Pedology

3.2.1 Geology

The Hodder catchment is situated in the central Pennines, which form a north-south orientated anticline across England, broadly consisting of Carboniferous Millstone Grit underlain by Limestone (Johnson, 1987; Aitkenhead and Wray, 2002).

Figure 3.3 shows that the main geological strata in the upper part of the Hodder catchment are those of the Carboniferous Pendle and Brennand Grit formations of the Millstone Grit Group, consisting of interbedded sequences of sandstones, silty mudstones and siltstone (brown, orange and light green in Figure 3.3).

The limestones of the Chatburn Limestone Group outcrop in the central areas of the catchment (dark blue in Figure 3-3). The villages Slaidburn and Newton in Bowland extract water from these formations for domestic use.

The lower part of the catchment consists of mudstones and siltstones mainly (dark green and orange in Figure 3-2). A large area is covered by the Bowland Shale, which consists of mudstone with sandstone, limestone and limestone debris beds, and feeds some springs in the Loud catchment.

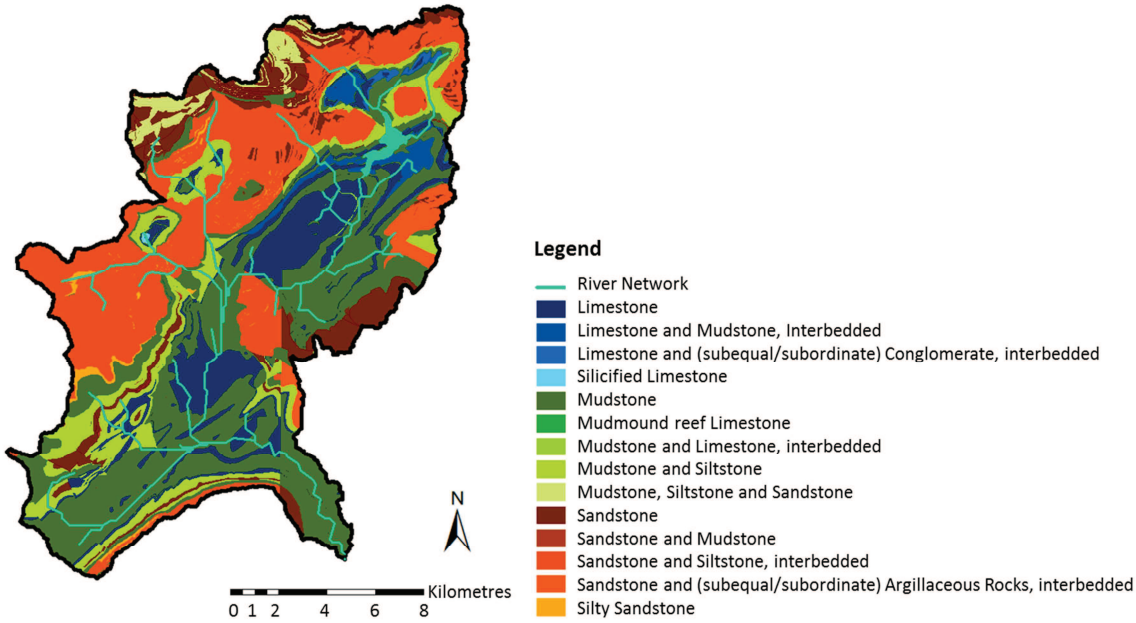

Figure 3.3 Geology in the Hodder catchment (source: British Geological Survey 1:50,000, through Digimap)

3.2.2 Superficial Deposits

The geology in the Hodder catchment is largely overlain by superficial deposits. From Figure 3.4 it is clear that there are three main superficial deposits, including peat (dark green), head (purple) and glacial till (orange).

In the upper part of the catchment peat rests on the fells, with a thickness ranging from approximately 1 – 3 m on slopes, although in those places where it fills holes it can be as thick as 8 m (Aitkenhead et al., 1992). The bog formation started from the period just after the retreat of the glaciers approximately 9000 years ago. The peat prevails largely on top of the Millstone Grit sandstones. There are head deposits in the valleys of the River Dunsop and the River Langden.

The most widespread superficial deposit is glacial till (4-14 m thick) in the eastern and southern parts of the catchment, deposited in the latest Ice Age. The head deposits, consisting of weathered near-surface bedrock and/or drift material (Aitkenhead et al., 1992), overlap the glacial till in the lower valleys of the River Dunsop and Langden Brook mainly. The thickness of these deposits ranges from 4-12 m (Aitkenhead et al., 1992). In the main river valleys there are some river terrace and alluvium deposits, which give an indication of (recent) river activity.

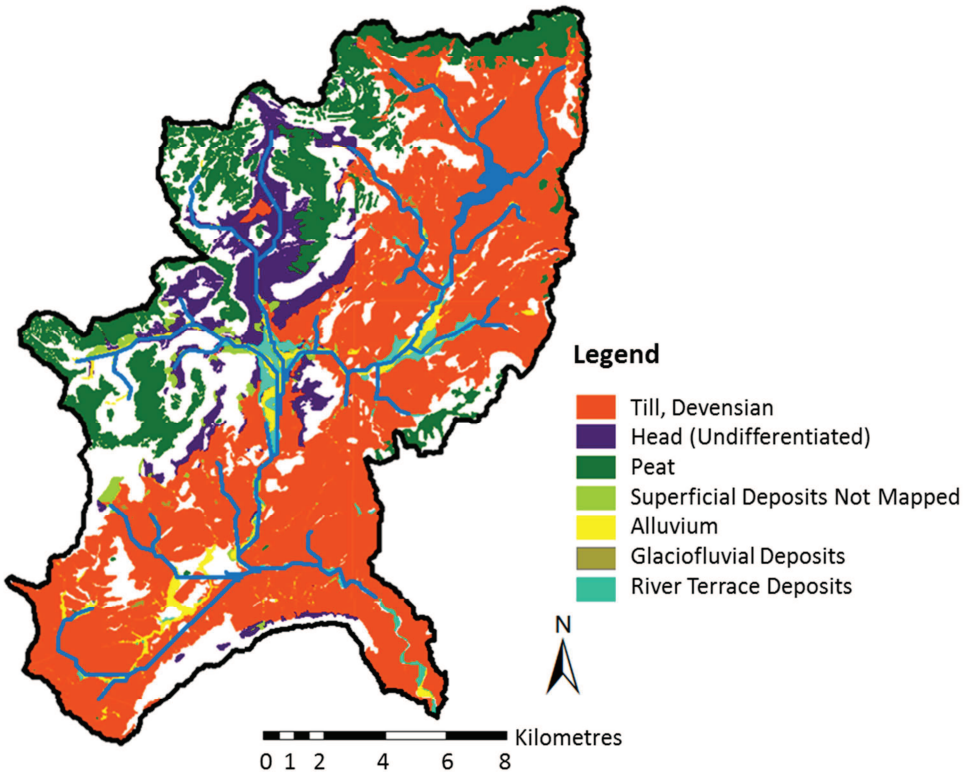

Figure 3.4 Superficial deposits in the Hodder catchment (source: BGS 1:50,000)

3.2.3 Soil Associations

Figure 3.5 shows the soil associations of the Hodder catchment. There are four main soil associations that prevail in the area, including the Winter Hill, Belmont, Wilcocks 1, and Brickfield 2 and 3 associations.

The Winter Hill association has formed as part of the peat deposits in the upper part of the catchment mainly, primarily as a result of high rainfall combined with low (summer) temperatures and poor drainage. Erosion of the peat is taking place especially in the top headwaters and on slopes.

The Belmont association is primarily present in the valleys of the headwaters. It comprises peaty gleyed podzols, with a characteristic thin iron-pan at approximately 0.2 m below the surface of the mineral soil (Crompton, 1966). The soils develop there where the subjacent material is reasonably well drained and the surface is covered with thin, acid hill peat (Crompton, 1966). Compared with the Winter Hill association, these soils are situated on relatively well drained sites with moderate slopes.

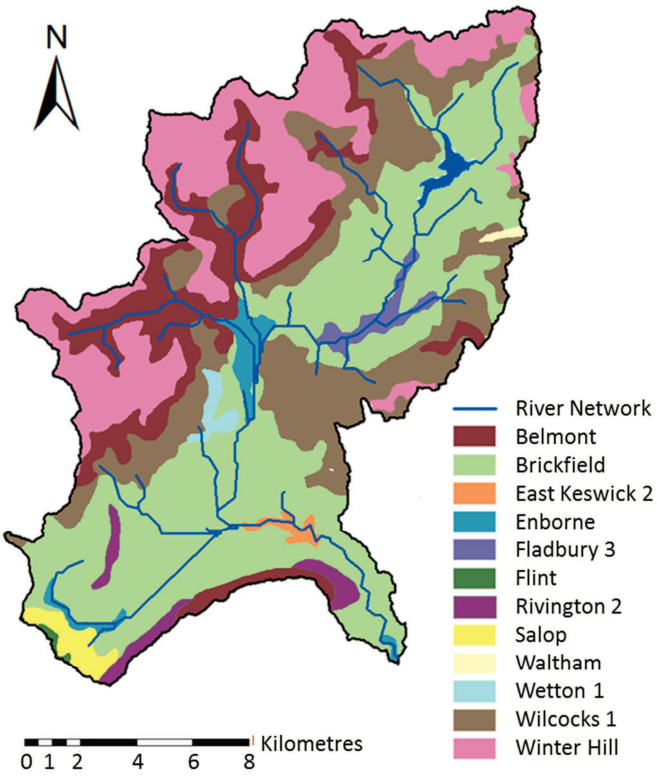

Figure 3.5 Soil Associations of the Hodder Catchment (source: Avery, 1980)

The Wilcocks association (a peaty/very humose loam underlain by a sandy humose loam) occurs in the lower parts of the headwater valleys. The soils are formed in the till and are poorly drained and remain wet for most of the year (Crompton, 1966). As a result, these soils are mainly suitable for rough grazing.

The Brickfield 2 and 3 associations are generally poorly drained soils developed on the glacial till (Crompton, 1966), and are present on the gentle and moderate slopes of the main Hodder valley. Of the four soils described here, Brickfield can produce the best crops (mainly grass), but only when the soils are improved by tile drainage and frequent applications of lime and fertilizers (Crompton, 1966). Both of these management techniques are practised throughout the Hodder valley.

3.3 Climate

The climate of the UK is classified as a mid-latitude oceanic climate (*Cfb* in the Koppen-Geiger climate classification (Peel et al., 2007)). The higher elevation regions of Northwest England, including the upper part of the Hodder catchment, are known as some of the wettest and windiest areas in England (Tufnell, 1997). Figure 3.6 shows the average monthly precipitation for an upland and a lowland gauge (top), the

average snow lying days in the uplands and lowlands (middle), and the average monthly temperature for the Hodder catchment (bottom).

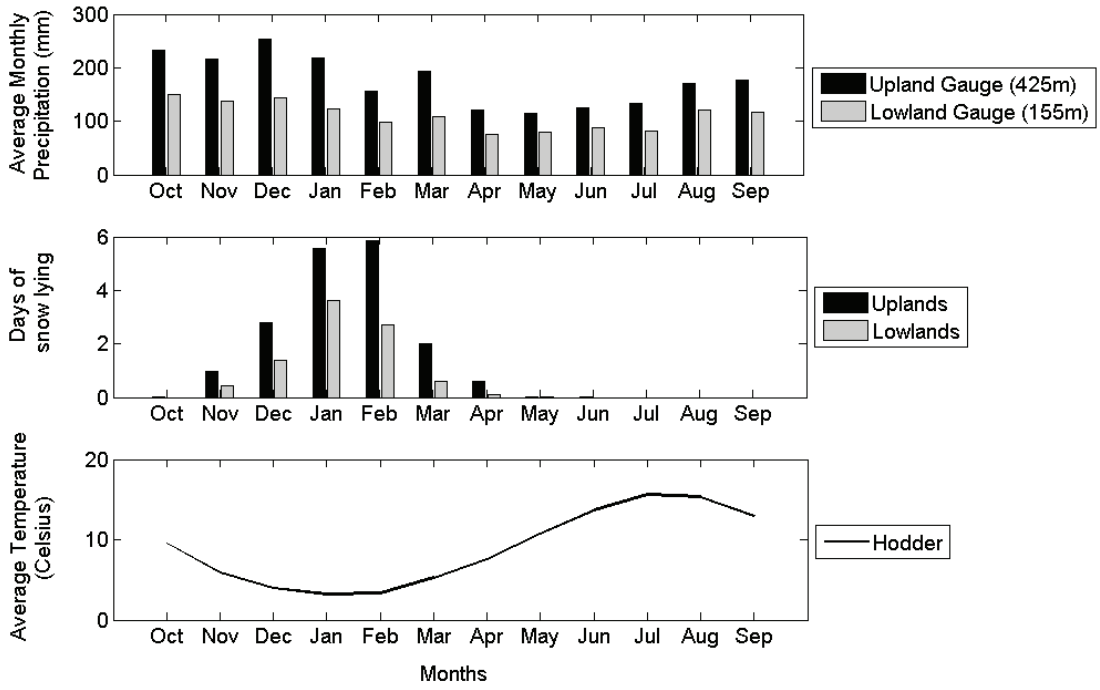

Figure 3.6 Average monthly precipitation (top) and days of snow lying (middle) for the uplands (black) and the lowlands (grey), and average monthly temperature (bottom) for the Hodder catchment.

3.3.1 Precipitation

Overall, the Hodder catchment receives an average annual rainfall of 1675 mm (UKCIP dataset 1961-1990). Large variations in average annual rainfall exist across the catchment, ranging from 1150 mm per year in the lowlands to 2090 mm in the uplands. An example of this variability is shown in Figure 3.6 - top, where average monthly precipitation totals are plotted for a typical gauge in the uplands (425 m) in black; and for a typical gauge in the lowlands (155 m) in grey. The data averages are based on monthly data for 1960-2006. Throughout the catchment, the period from August to January is generally the wettest (Figure 3.6 - top).

Some snowfall is common from November to April (Figure 3.6 - middle). A snow lying day is defined as snow cover of greater than 50% of the ground surface per day (Tufnell, 1997). On average, there are about 13.2 snow lying days per year for the Hodder catchment (UKCP09 dataset 1971-2006). The upper part has generally more snow than the lower part of the catchment (17.8 and 8.9 snow lying days per year respectively) (UKCP09 dataset 1971-2006).

3.3.2 Temperature and Evaporation

The average mean monthly temperature ranges from 3.2 degrees Celsius in January to 15.6 degrees Celsius in July (UKCP09 dataset 1914-2006) (Figure 3.6-bottom). In winter temperatures can drop as low as -15 °C, while in summer they can reach a maximum of about 30°C. It was at Stocks Reservoir in the Hodder catchment where some of the initial studies of evaporation in the UK started (Calder, 1990). Early experiments on rainfall, interception and evaporation losses at the plantation of *Sitka Spruce* trees at Stocks Reservoir estimated 430 mm of potential evaporation for the calendar year 1956 (Law, 1957). The average yearly potential evaporation for the Hodder is about 400 mm.

3.4 Land Use and Vegetation

Figure 3.7 shows the Centre of Ecology and Hydrology (CEH) Land Cover Map 2000 (LCM2000), based on satellite images, for the Hodder catchment. The main land uses have been classified into grassland (65.7 %), moorland (other than grassland) (19.5 %), woodland (10.1%) and cultivation (2.5%) (Table 3.1).

3.4.1 Grassland

With a coverage of nearly two thirds of the Hodder catchment, grassland is the main land use. At lower elevations and in the main Hodder valley, the grasslands have been improved with drainage and fertilizer to become permanent grasslands (or pasture) (dark green in Figure 3.7). They are used mainly for cattle and sheep farming. At higher elevations, the combination of poor drainage and steeper slopes has resulted in rough grasslands which are suitable only for sheep grazing (light green in Figure 3.7).

3.4.2 Moorland

Bog (red in Figure 3.7) and dwarf shrub (purple in Figure 3.7) are the main land uses classified as moorland. Depending on the definition, about 20 % (excluding grasslands) – 35% (including acid and calcareous grasslands) of the catchment may be classified as moorlands. These are part of a larger peatland (ca 15,000 ha), which is the largest expanse of heather moorland in Lancashire, and one of the largest in England (Mackay and Tallis, 1994). According to Mackay and Tallis (1994; 1996), it is one of the few areas in England where dwarf-shrub heath and blanket peat are extensive together.

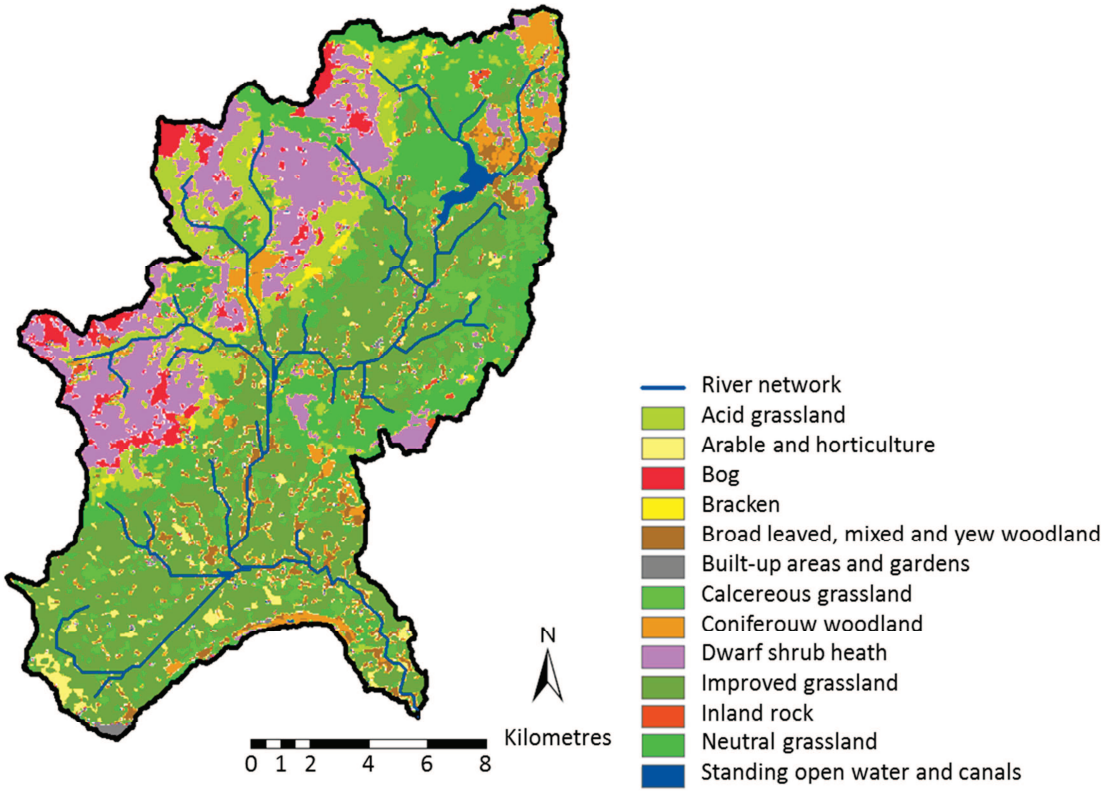

Figure 3.7 Land Cover Map 2000 for the Hodder catchment (source: LCM 2000)

Table 3.1 Percentages of Land Uses in the Hodder catchment, based on Figure 3.7

Land Use		Percentage Area Hodder Catchment
Grassland	Improved grassland	33.3
	Neutral grassland	15.6
	Acid grassland	10.1
	Calcareous grassland	6.7
	Total grassland	**65.7**
Moorland (other than grassland)	Dwarf shrub heath	15.2
	Bog	3.3
	Bracken	0.9
	Total moorland (other than grassland)	**19.5**
Woodland	Broad leaved, mixed and yew woodland	6.3
	Coniferous woodland	3.9
	Total woodland	**10.1**
Other	Arable and horticulture	2.4
	Built-up areas and gardens	1.2
	Inland rock	0.8
	Standing open water and canals	0.3

Over the last two millennia, Sphagnum was a widespread component of the vegetation, but, since the beginning of the 20th century, species have declined from many areas owing to a relatively dry period in the early 1900s and a change in management standards, including peatland drainage, burning practices and stocking densities (Mackay and Tallis, 1996). Also, the growth of bracken, which occurs on the relatively drier parts of the moorlands, has been associated with these land management practices.

3.4.3 Woodland

Approximately 10 % of the Hodder catchment area is forested. There are numerous small patches of broad leaved, mixed and yew woodland (dark brown in Figure 3.7). The Forestry Commission manages three main coniferous forested areas (light brown in Figure 3.7) including Gisburn Forest (upstream of Stocks Reservoir), Dunsop Valley Forest (in the Dunsop valley), and Longridge Fell Forest (in the south of the catchment). These are all commercial coniferous forests, which were planted in about 1950. They are now slowly being converted into woodlands with more native species (see Section 3.7) and are used for recreational purposes mainly.

3.4.4 Cultivation

Only a relatively small area of the total surface area (about 2.5%) is cultivated (light yellow in Figure 3.7). Agricultural production consists of wheat, maize and horticulture and is concentrated in the Loud catchment and the main Hodder valley.

3.5 Water Supply Infrastructure

United Utilities abstracts water from the Hodder headwaters. The abstraction works could potentially influence the hydrological behaviour of the Hodder catchment by removing water from the system. In addition, it is likely that Stocks Reservoir buffers the (changing) signal in the hydrograph. A good understanding of the abstraction works is therefore needed. In the headwaters of the River Hodder, there are three major abstraction systems: 1) Stocks Reservoir (Section 3.5.1), 2) the Bowland system in the catchment of the River Langden (Section 3.5.2) and 3) the Dunsop system in the River Dunsop catchment (Section 3.5.3). The information on the latter two abstraction

systems is based on personal communication with Mr. Mike Conway, the operational controller of United Utilities abstraction works, on the 1st July 2008.

3.5.1 Stocks Reservoir

Stocks Reservoir is situated in the North Eastern part of the Hodder catchment. It is fed by the upper River Hodder and Bottoms Beck, from the north and west of the reservoir respectively (Figure 3.2). Construction of the reservoir commenced in 1922 and it was officially opened in July 1932 (United Utilities, 2008). It is the only reservoir in the Hodder catchment and is United Utilities' main water supply feature in the Bowland Estate. It controls about 15 % of the entire Hodder catchment. It has a surface area of 1.4 km^2 and a catchment area of 37.5 km^2. When full, the reservoir holds up to 12,000,000 m^3 of water (United Utilities, 2008). The reservoir outlet is manually controlled and discharge release data are available at a 15 minute interval.

3.5.2 Bowland Abstraction System

The original Bowland abstraction system dates from the 1870s and was upgraded to its current form in 1920. It can take a maximum of 109.1 MLD (Mega Liters per Day). However, this rarely occurs since the system is often closed down in high flow as a result of bad water quality in those conditions. A schematic representation of the Bowland Intake system is given in Figure 3.8. The structure takes water from several streams within the River Langden catchment, including the upper Langden, Losterdale, Hareden and Penny Brook. In total, the intake system consists of seven surface water intakes and two minor ground water intakes (Figure 3.8). The system feeds Longridge reservoir, 11 miles away from its source.

The abstraction license legislates the compensation water needed at the three main surface water intakes of the Bowland System. The minimum compensation values at these locations are given in Table 3.2.

Figure 3.8 also shows the presence of a fish farm. This dates from approximately 1930 and is situated just upstream of the Langden outlet. It abstracts roughly 2.3 MLD from the culvert pipe and releases it back into the river. The daily operation of the system depends on local conditions including water quality, water demand and the prevailing weather conditions. Daily abstraction data are available from United Utilities.

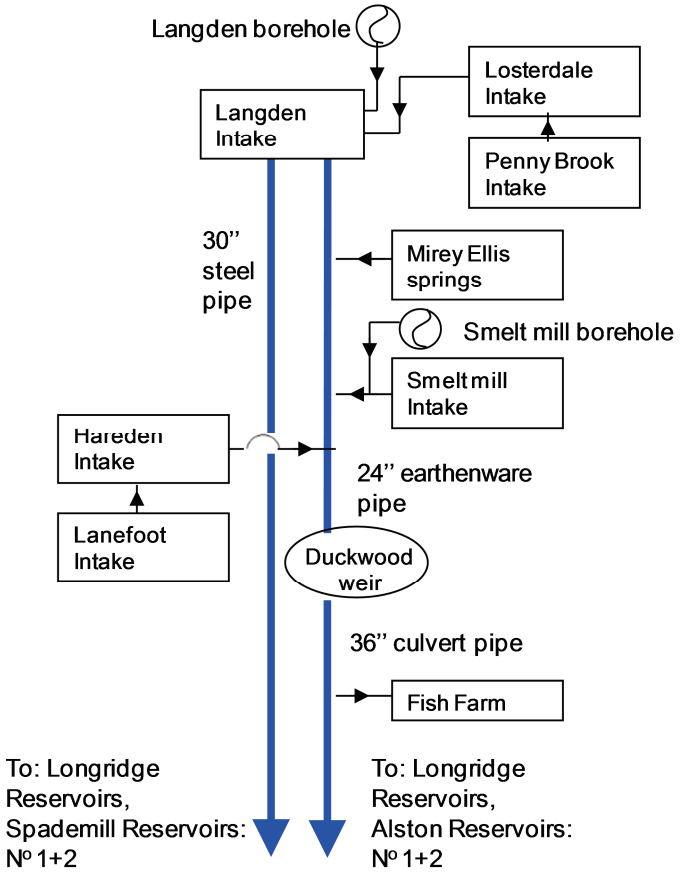

Figure 3.8 Schematic representation of UU Bowland Intake System, River Langden

Table 3.2 Minimum compensation values for UU Bowland Intake System for the different subcatchments of the River Langden

Intake	Minimum Compensation (MLD)
Langden	8.60
Losterdale	0.91
Hareden	2.70

3.5.3 Dunsop Abstraction System

The Dunsop system dates from 1880 and, up until approximately 2000, 22 intakes, spread over the Whitendale and Brennand catchments, were active. Since the year 2000 the Dunsop intake system is reduced to its current structure (Figure 3.9), reducing its ability to approximately 92 % of its original capacity. The structure takes water from River Brennand and the River Whitendale. Figure 3.9 shows the present Dunsop intake system, which contains two surface water intake points in the Brennand catchment and three in the Whitendale. Near Footholme, there is a borehole taking additional ground water. The intakes in the Dunsop system are gravity based and there is no control of how much water is taken. Only the maximum intake is controlled by

the size of the pipelines and is approximately 35 MLD. Based on the catchment areas, this could be a maximum intake of 11.8 MLD for the Brennand intake system and 23.2 MLD for the Whitendale system (Table 3.3).

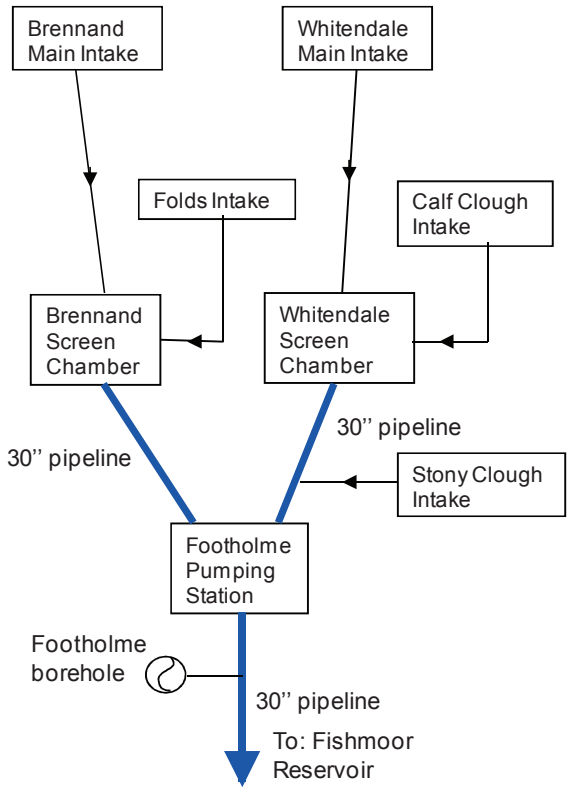

Figure 3.9 Schematic representation of UU Dunsop Intake system in the River Dunsop catchment

Table 3.3 Estimated maximum abstractions for the different intakes within the Dunsop abstraction system

Intake	Catchment area (ha)	Maximum estimated intake (MLD)
Brennand system	1073	11.8
Whitendale main system	1748	19.3
Whitendale Calf Clough	197	2.2
Whitendale Costy Clough	148	1.7
Total	3166	35

Within the intake structure, there is only one compensation point, which is located at Footholme. There, the discharge is not allowed to drop below 6.1 MLD. To meet these compensation requirements, in low flow water from the Brennand intakes is led back into the outlet of Whitendale River, just upstream of the Brennand and Whitendale confluence. The intake systems are operative throughout the year and shut approximately twice a year. Daily abstraction data are available from United Utilities.

3.6 Flooding

Figure 3.10 shows the Environment Agency flood map (2009) for the Hodder catchment. The dark blue areas indicate regions likely to be affected by the 1/100 year flood; the light blue areas show regions that are likely to be flooded by the 1/1000 year flood. Along the main stem of the Hodder, there are two areas liable to flooding, which include the areas just downstream of Slaidburn village (Whiteholme) and Dunsop Bridge village (Figure 3.10). In addition, there is an area in the River Loud catchment, just downstream of the village of Chipping that is prone to flooding. Since the catchment is mainly rural, there are not many properties at risk. However, high flow inputs from the Hodder may contribute to flooding further downstream along the River Ribble (Figure 3.10). In addition to a range of infrastructure, there are numerous properties at risk in Lytham St. Annes and Preston (>1000 properties for both), and Blackpool (500-1000 properties) (Environment Agency, 2009).

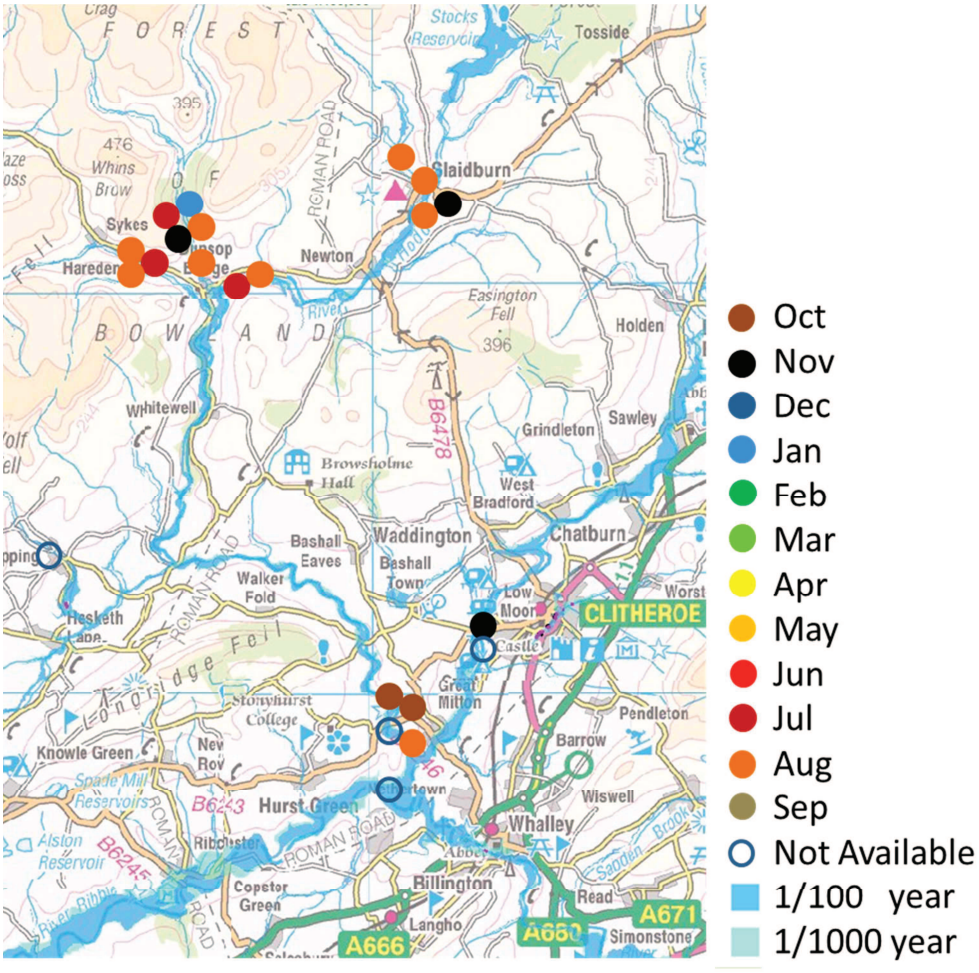

Figure 3.10 EA flood inundation map showing areas prone to flooding for the 1/100 year (dark blue) and 1/1000 year flood events. Superimposed are CBHE recorded floods, colour coded according to the time of the year in which they occurred.

The Chronology of British Hydrological Events (CBHE) holds several historical flood records within the Hodder catchment, with recorded floods from 1851 to 2004 (Black and Law, 2004). Although the CBHE records do not include all events, it gives an idea of the distribution of major floods. The events are plotted in Figure 3.10, where they are colour coded according to the month in which they occurred. The main recorded historical floods took place in the upper part of the catchment, at the confluences of the River Dunsop, Langden Brook and Croasdale Brook with the main Hodder, with most of them occurring in the winter period Oct-Jan and in Jul-Aug.

3.7 Land Use/Management Changes

The Hodder catchment has long been subject to LUMCs. For example, woodland clearance and increased grazing pressure have been assigned to the Iron Age and Romano-British period (400 B.C to A.D. 400), but mainly to the Medieval Period (A.D. 800-1300 and 1500 onwards) (Mackay and Tallis, 1994; Chiverrell et al., 2009). The few small patches of woodland in the area of the Hodder catchment do not justify the name, 'Forest of Bowland', by which it is known. Prior to United Utilities' SCaMP project, alterations over the last 50-100 years have been associated with enhancing farming, game, and woodland reserves. The associated LUMCs mainly include moorland gripping, changes in stocking density and afforestation (Section 3.7.1). The most recent changes include a Forestry Commission felling plan (Section 3.7.2) and, far more extensively, the United Utilities' SCaMP programme (Section 3.7.3).

This section focuses only on changes that have occurred and are occurring in the Hodder headwaters (i.e. the SCaMP area as indicated in Figure 3.2), including the Langden Brook, River Dunsop, and Croasdale Brook subcatchments. The part of SCaMP upstream of Stocks Reservoir is not considered in much detail, as any changes to the hydrological behaviour of the reservoir headwaters will be buffered by the regulating effect of the reservoir. A review of the LUMCs in the non-SCaMP subcatchments (Easington Brook and River Loud) is beyond the scope of the current study. However, potential changes in the hydrological behaviour of those catchments are examined later (Chapter 5).

3.7.1 Historical Land Use/Management Changes

Gripping

As part of government schemes that encouraged UK upland drainage, large areas of the upper part of the Hodder catchment have been converted by open moorland drainage ditches (grips). For the main part of the 20th century, this has been a common practice in many parts of the UK for the improvement of upland conditions for game rearing (see Chapter 2).

In a study based on historical maps, aerial photographs and some ground truth exercises, Ewen et al. (2010) found that gripping in the upper Hodder occurred in the period 1956-1969. These activities were mainly concentrated in the Dunsop catchment (Brennand 28.3 km of grips, Whitendale 10 km of grips), the Croasdale catchment (0.5 km of grips) and upstream of Stocks Reservoir (approximately 10 km of grips).

The moorland open drainage ditches are typically 1 m deep and spaced roughly 20 m apart. The orientation of the drains is irregular. An example of a common drainage design from the upper part of the Brennand catchment is shown in Figure 3.11. The grips run parallel to each other and drain into a larger carrier grip which runs at an angle to the smaller grips. The main grips, often canalised natural streams themselves, eventually drain into the natural streams. This drainage design is known as a herringbone drainage structure (Castle et al., 1984).

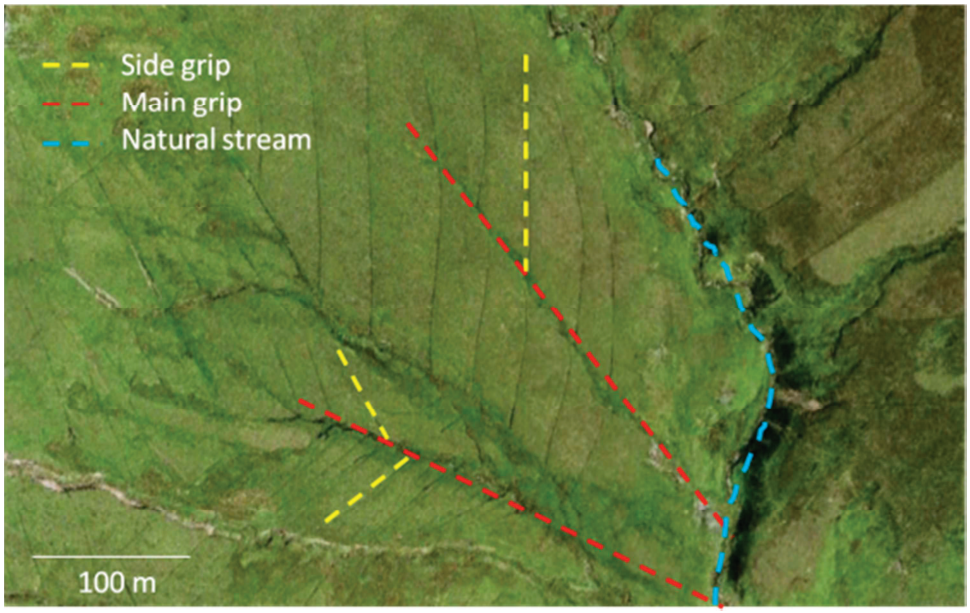

Figure 3.11 Example of typical drainage design from the upper part of the Brennand catchment

Stocking Density Changes

Mackay and Tallis (1996) studied the stocking density changes from 1890 to 1990 in the Bleasdale Parish, situated in the Wyre catchment, adjacent to the River Hodder catchment in the West. They found that total sheep numbers rose from approximately 5000 in 1880, to 8000 in 1960. From 1960 to 1990, the total stock numbers nearly doubled to a maximum of 15,000 sheep, which is equivalent to a stocking density of 5 sheep/ha for the total area or, 15 sheep/ha in areas set aside for rough grazing (Mackay and Tallis, 1996).

Figure 3.12 shows the available stocking density rates for sheep and cattle on farms in the upper Hodder catchment over the last 40 years. These numbers are based on personal communication with tenant farmers. For privacy reasons, total stock numbers and farm sizes are deliberately not mentioned. Brennand, Whitendale and Croasdale farms are situated in the eponymous catchments. Hareden and Sykes farm are both situated in the Langden Brook catchment (see also section 3.7.3 below). A slight decrease in stocking levels has occurred for most farms from the 1970s to the 2000s. The stocking density rates of 2010 are determined by the SCaMP programme and are discussed in Section 3.7.3.2.

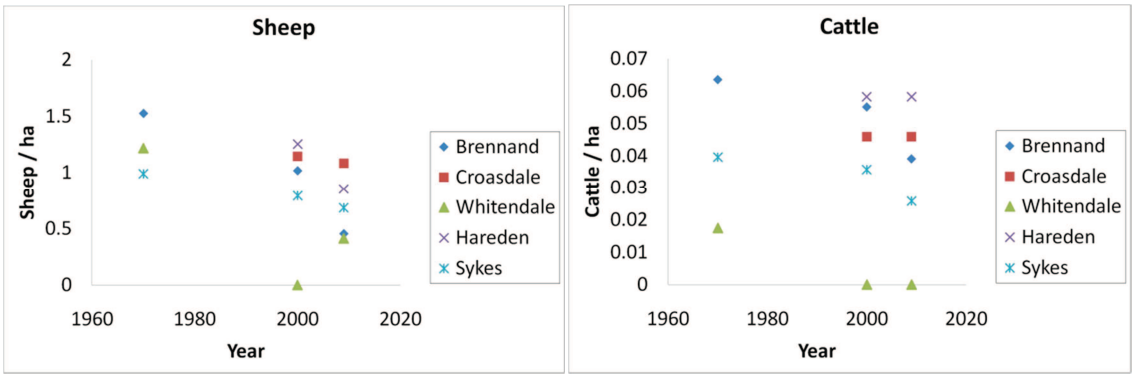

Figure 3.12 Stocking density rates per farm in the upper Hodder catchment over the last 40 years for sheep (left) and cattle (right).

The stocking densities in Figure 3.12 are considerably lower than those reported by Mackay and Tallis (1996). This may be attributed to a combination of two reasons. Firstly, the soils in the Bleasdale Parish can generally support more sheep than those in the Hodder headwaters. The main Hodder valley has similar soils to the majority of the

Bleasdale Parish, and it is therefore likely that the stocking density values reported by Mackay and Tallis (1996) are more representative for the main Hodder valley than the Hodder headwaters. Secondly, the numbers available for the upper Hodder catchment are farm related and not total area related as for Bleasdale Parish. However, it is assumed that the overall trend in stocking densities is similar for all areas: a steady increase in stocking densities from the late 1800s to the late 1900s. Only from the early 2000s, the numbers have started to decrease slightly. This can be attributed to the government stewardship scheme's aim to keep stock low and the occurrence of foot and mouth disease in 2001 (personal communication with tenant farmers).

Afforestation

In the upper part of the Hodder catchment, the UK Forestry Commission manages two large patches of land: 1) a strip of forest alongside the river Dunsop, known as the Dunsop Valley Forest (1.7 km^2), and 2) Gisburn Forest, upstream of Stocks Reservoir, in the area of Bottoms Beck (12.5 km^2). The former has been owned by the Forestry Commission since 1952; the latter area has been leased from UU since 1949. Both forests were planted in the late 1950s in order to increase the timber resources. Ever since then, the trees have never been cut collectively (Colledge, 2008). The forest in both of these areas is currently dominated by Sitka Spruce, Norwegian Spruce and Larch species.

3.7.2 Forestry Commission Felling Plan

The following information on the Forestry Commission practices in the upper Hodder catchment is based on a personal conversation with M. Colledge, the Forestry Commission Area Forester for Bowland and Dalton, North West England, on October 23rd 2008.

As part of their 'Forest Design Plan', the Forestry Commission is currently gradually replacing the conifers of Dunsop Valley Forest and Gisburn Forest by more native species, including birch, oak, ash, alder, and hazel.

Figure 3.13 shows a map of Dunsop Valley Forest and the current felling plan of the Forestry Commission. The area is divided into six patches and every five years the trees of one of those areas will be felled, after which they will be replaced by native species.

According to management guidelines, during forest clearance remnant branches are placed on the extraction routes to minimise erosion and soil compaction (Forestry Commission, 1991).

The first two patches of the Forest Design Plan were felled in 2001 and 2007-2008 respectively. These two have an area of 39 ha in total. Table 3.4 shows the areas affected and the proposed timing of felling.

Table 3.4 Area of forest patches involved in Dunsop Valley Felling Plan

Timing of felling	2001	2007-08	2008-11	2012-16	2017-21	2022-26
Patch Area (ha)	5.9	32.9	45.5	42.2	9.0	35.6

The River Dunsop has a total catchment area of 25 km^2. The forested area in the lower Dunsop valley subject to change comprises only 7% of the total catchment area. The area that has already been felled is 1.5 % of the Dunsop catchment area.

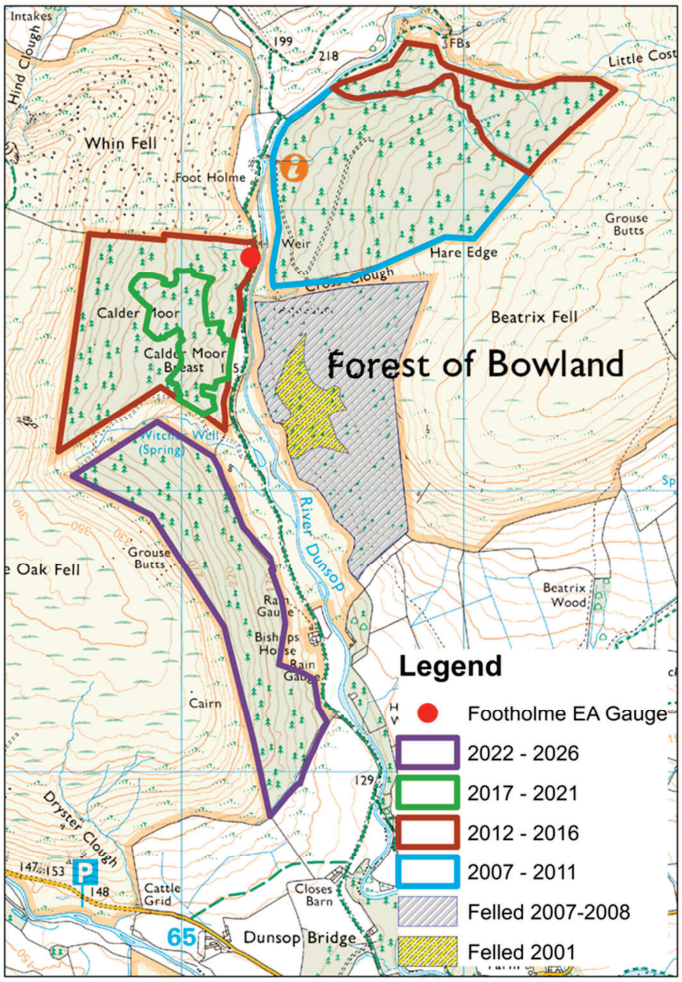

Figure 3.13 Dunsop Valley Felling Plan (Forestry Commission, 2008)

The felling of Gisburn Forest is also subject to a five year period felling programme similar to the Dunsop Felling Plan. Compared to the Dunsop Felling Plan, the Gisburn Felling Plan is more gradual and subtle (i.e. there will be no large neighbouring areas felled). Gisburn Forest is situated upstream of Stocks Reservoir, which makes the area of less interest for the current research, since any hydrological effects of the changes upstream of Stocks reservoir would be buffered by the reservoir.

3.7.3 UU SCaMP Land Use/Management Changes

From 2005-2010, several land use management changes have been implemented in the headwaters of the Hodder, as part of the Sustainable Catchment Management Programme (SCaMP) of United Utilities in collaboration with the RSPB. The types, locations and timing of the SCaMP LUMCs were beyond the control of the present study. The majority of the work was carried out from spring 2008 to spring 2009.

The Bowland SCaMP area is situated in the headwaters of the River Hodder (Figure 3.2). The area undergoing changes (i.e. the SCaMP area) covers 101.26 km^2, approximately 40% of the total catchment area of the River Hodder.

The main restoration work of SCaMP involved (McGrath and Smith, 2006; United Utilities, 2011):

1. Blocking gullies and grips to increase the water levels on the moorlands, in order to restore the blanket bogs
2. Fencing to reduce or relocate livestock to keep them away from special habitats, rivers and streams
3. Establishing woodlands on hillslopes and in riparian zones
4. Creating scrapes (shallow depressions with gently sloping edges (RSPB, 2011b)) with the intention of providing habitat for wading birds
5. Restoring vegetation (e.g. through re-seeding) on eroded and exposed peat, hay meadows and heather moorlands
6. Controlling the extent and frequency of heather burning
7. Controlled bracken spraying

Since the first three SCaMP works have been implemented over relatively large areas, the focus of the current study is on grip blocking, changes in stocking density and

management, and tree planting. At the end of this section an overview of these main interventions per subcatchment is also given.

The data on the SCaMP land use/management changes are based on a number of different sources:

1. United Utilities' farm plans for the works
2. The Higher Level Scheme (HLS) agreements of the farms with Natural England
3. Discussions with UU's SCaMP site manager, Mr. N Pilling on several occasions (13th March 2008, 17th April 2008, 11th May 2009)
4. Discussions with tenant farmers on several occasions
5. A number of field walk-over surveys (for detailed information and verification)

As the SCaMP plans were originally drawn up for individual farms (and hence not necessarily for catchments), some information on the SCaMP works is farm-based. The schematic in Figure 3.14 shows the distribution of farms and subcatchments in the upper Hodder. It is noted that Brennand and Whitendale farms coincide well with the River Brennand and the River Whitendale subcatchments respectively. Croasdale farm is situated in the upper part of the Croasdale Brook catchment only. The Langden Brook catchment has two main farms: Sykes farm, which corresponds with the Losterdale Brook and part of the upper Langden Brook catchments, and Hareden farm, which corresponds with the Hareden Brook and part of the Langden Brook catchments.

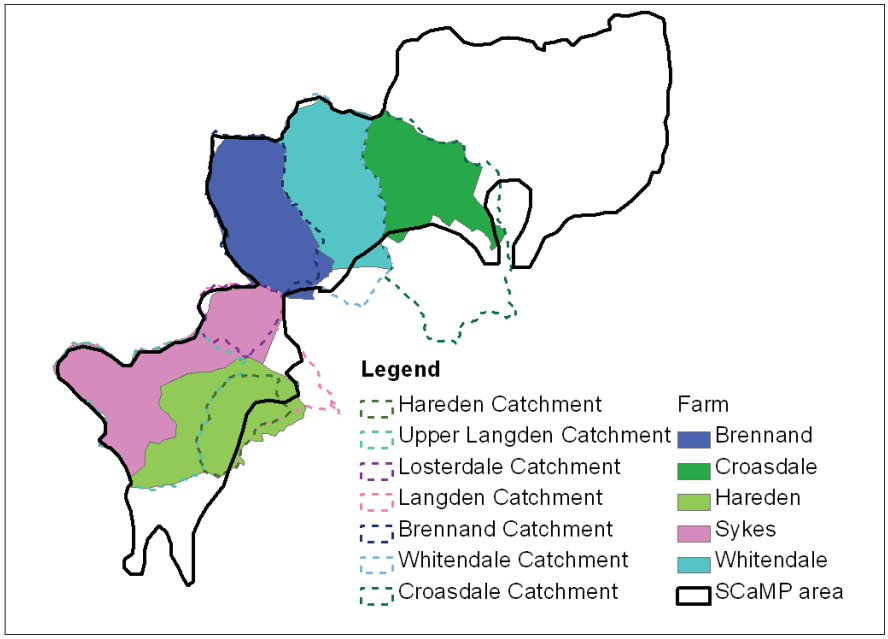

Figure 3.14 Distributions of farms and subcatchments in the SCaMP area

Grip Blocking

Table 3.5 shows the extent and timing of the grip blocking in the SCaMP area in detail. All grips in the upper Hodder with an original depth less than 3 m were blocked. As indicated in Section 3.7.1, the main areas that were originally gripped are located in the Brennand, Whitendale and Croasdale catchments. The area upstream of Stocks Reservoir was excluded from grip blocking. The blocking of the Whitendale grips occurred prior to this study as part of a grip blocking techniques trial exercise. More information on this study can be found in Armstrong et al. (2006), Worrall et al. (2007b) and Worrall et al. (2007d). In the Brennand catchment, the grips were blocked in November 2008 and in the Croasdale catchment in February 2009.

Table 3.5 SCaMP grip blocking: occurrence, timing and description

Catchment	Timing	Description
Brennand	November 2008	A total length of 28.3 km of grips was blocked in the Sapling Clough (13.9 km), Round Hill Water (11.5 km), and Lee End (2.9 km) subcatchments.
Croasdale	February 2009	Approximately 0.5 km of grips were blocked in the Swine Clough subcatchment
Whitendale	2005	Approximately 10 km of grips were blocked in the upper part of the Whitendale catchment. A more detailed description of this work (a trial study) is provided by Armstrong et al. (2006) and Worrall et al. (2007b; Worrall et al., 2007d).

The grip blocks all consist of locally obtained peat and heather bales. Based on field observations, three main grip blocking techniques were used (Ewen et al., 2010):

1. A dam is built from peat bales that are dug from intact bog nearby
2. A dam is built from material scraped from the area surrounding the original channel
3. The channel banks are made to collapse inward

The resulting crescent-shaped dams (or blocks) are spaced approximately 10 m apart, regardless of the size of the grip. Figure 3.15 shows an example of a grip before and after blocking (left and right, respectively). The proportions of a block depend on the size of the original grip. Depending on water availability, a pool of water is generated

upstream of each block. When a pool has reached its capacity, the excess water is redirected by the block onto the peat, away from the grip in the downslope direction (Figure 3.16).

Figure 3.15 Left: Croasdale main grip before blocking (picture taken on 13/03/2008), and right: after blocking (picture taken on 05/03/2009)

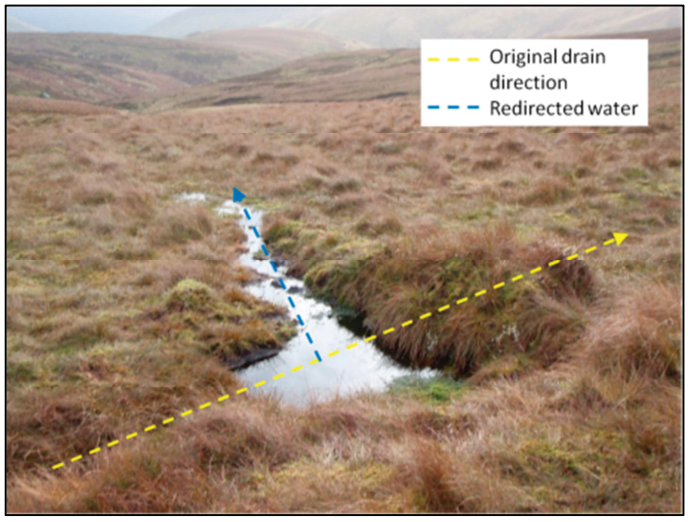

Figure 3.16 Example of a grip block and the upstream pool of water. Also indicated are the original drain direction and the direction of the redirected water flow

At the end of this section (Figure 3.18 and 3.19) the location of the blocked grips is shown for each subcatchment. More detailed information on blocked grips at specific sites in the Brennand and Croasdale subcatchments is given in Chapters 5 and 6. In Chapter 5 this concerns monitoring of hydrogical response; in Chapter 6, local scale effects of grip blocking.

Stocking Density and Stocking Management Changes

Table 3.6 shows the occurrence, timing and description of the SCaMP changes in stocking density and stocking management for each farm in the upper Hodder. The fells are the unimproved higher grounds of the farms. In the case where the stock management involves sheep and cattle, density numbers in Table 3.6 are given in Livestock Units per hectare (LU/ha). A sheep livestock unit is approximately 0.1; a cattle livestock unit is approximately 0.7-0.8.

Table 3.6 SCaMP changes in stocking density and stocking management: occurrence, timing and description

Farm (Catchment)	Timing	Change in overall number of stock	Management on Fell	
			Summer	Winter
Croasdale	Spring 09	6% reduction in sheep, no change in cattle	Maximum of 0.15LU/ha (1st April – 31st October), includes sheep and cattle	Maximum of 0.075LU/ha = 0.75 ewes/ha (1st November – 31st March), cattle exclusion
Whitendale	Spring 08	100% introduction of sheep, no cattle	Maximum of 0.480 ewes/ha (1st of May – 30th September)	Total stock exclusion (31st October – 1st May)
Brennand	Spring 08	55% reduction in sheep, 30% reduction in cattle	Maximum of 0.564 ewes/ha	0.564 ewes/ha
Sykes (Losterdale)	Spring 09	Overall: 20% reduction in sheep, no change in cattle	Maximum of 0.564 ewes/ha	Total Stock exclusion
Sykes (Upper Langden)	Spring 09		Maximum of 1.128 ewes/ha	1st Oct – 28th Feb removal of 25% of total sheep
Hareden (Upper Langden)	Spring 09	32% reduction in sheep, no change in cattle	Maximum of 0.15LU/ha = 1.5 ewes/ha (1st March – 30th Sept), no cattle	Maximum of 0.075LU/ha = 0.75 ewes/ha (1st Oct – 28th Feb), no cattle

For most farms, changes in stocking density involve reductions in actual stocking levels. In Table 3.6 these are given as percentages of total stock before the SCaMP LUMC were introduced (see also Figure 3.12). Brennand farm has the greatest reduction in

stocking levels. However, these sheep have been relocated to Whitendale farm, where sheep were reintroduced at low levels after a period of stock exclusion (see Figure 3.12).

Changes to stocking management involve relocation of stock and changes to the stocking calendar. In Table 3.6 the SCaMP fell management is given as an example, as the exact stocking densities are different for each field. The maximum stocking levels for an area or a field are determined by management strategies, which depend on the Higher Level Stewardship (HLS) guidelines (DEFRA, 2005a) for the local conditions of the land such as soil type, vegetation and erosion. Table 3.7 shows these management strategies, with the recommended maximum sheep stocking levels.

Table 3.7 Recommended maximum stocking densities for different management strategies (DEFRA, 2005)

Management Strategy	Recommended stocking density (ewes/ha)
Restoration of blanket bog	0.134
Maintenance of blanket bog	0.267
Restoration of dry heath	0.564
Maintenance of dry heath	1.128

The main management strategy for Brennand, Whitendale, Croasdale and the Losterdale side of Sykes farm is habitat restoration. For Hareden farm and the upper Langden side of Sykes farm, it is maintenance of the uplands. On all farms, the main riparian zones and/or some hillslopes have been excluded from stock. These areas generally coincide with tree planting activities. Each farm has designated inbye areas, which are improved land slabs that provide more food and shelter for sheep than moorland, and have more flexible stocking levels. The sheep flocks are sometimes hefted around the edges of the inbye land, which enables livestock to be kept in unfenced areas without constant shepherding.

At the end of this section the stocking management strategies are shown for each subcatchment. More detailed information on changes in stocking density is given in Chapter 6, where the effects of the SCaMP stocking density and management changes on local scale runoff generation, specifically for the Losterdale subcatchment on Sykes farm, are discussed.

Tree Planting

The tree planting within the SCaMP programme was confined in part to some hillslopes, but mainly to the riparian zones in the River Brennand, Whitendale, and Langden catchments (Table 3.8). For the first two catchments, fences were put up in the spring of 2008, after which planting commenced. This occurred in the winter/spring of 2009 for the Langden Brook catchment. The trees planted in all areas include a variety of native species such as oak, birch, pine and hazel. Some ash, alder, rowan, wild cherry, and hawthorn trees were also planted. Within the fenced off areas for tree planting, there is also stock exclusion.

Table 3.8 SCaMP tree planting: occurrence, timing and description

Catchment	When	Description
Brennand	Spring 2008	Along the main stem of the River Brennand and along some tributaries in the north-western side of the catchment (50 ha in total)
Whitendale	Spring 2008	Along the main stem of the River Whitendale and on the south-eastern hill slopes (30 ha in total)
Losterdale	March 2009	The main planting is located in the Swine Clough subcatchment (ha). Some minor (patchy) planting has occurred in the eastern part of the catchment
Upper Langden	Spring 2009	Some minor tree planting has occurred in the riparian zones along the main stem of Langden Brook.

Figure 3.17 shows some of the tree planting in Losterdale. It also gives an indication about the density of the planting.

In addition to the tree planting activities, there has been minor logging of some isolated patches of deciduous trees in the Croasdale and Hareden catchments (approximately 1-2 ha each). This took place in November 2008 and December 2009, respectively. The patches will be replanted with either deciduous or coniferous species.

Figures 3.18 – 3.23 show the exact locations of tree planting activities for each subcatchment.

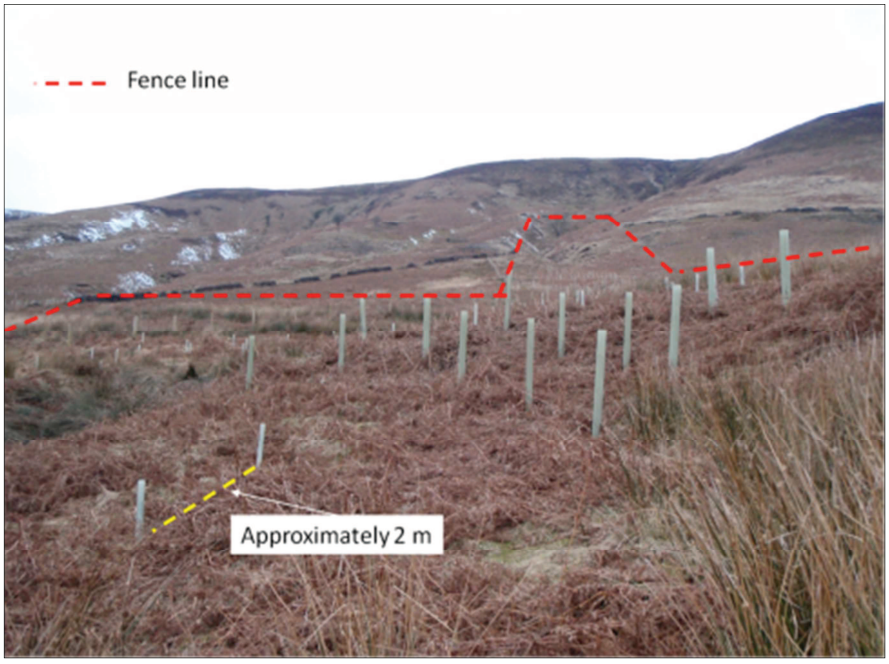

Figure 3.17 Tree planting on a hillslope and in the riparian zone of the upper Losterdale catchment (Sykes farm)

Main SCaMP Interventions per subcatchment

Table 3.9 gives a brief summary overview of the occurrence and timing of the main SCaMP works per subcatchment. The distribution of the changes is shown in Figures 3.18 – 3.23, where the main changes are shown schematically for each subcatchment.

Table 3.9 Occurrence of SCaMP main land use management changes per subcatchment

Subcatchment	Grip blocking	Stocking density / Stocking management	Tree planting
Brennand	November 2008	Spring 2008	Spring 2008
Croasdale	February 2009	Spring 2008	-
Hareden	-	Spring 2009	-
Losterdale	-	February 2009	March 2009
Upper Langden	-	Spring 2009	Spring 2009
Whitendale	(2005)	Spring 2008	Spring 2008

The stocking densities shown on the land use management maps in Figure 3.18-3.23 represent only management strategies, such as low stocking levels for uplands maintenance or for habitat restoration. As described in Section 3.7.3.2, no exact stocking density numbers are given, since these numbers are generally different for each farm/field.

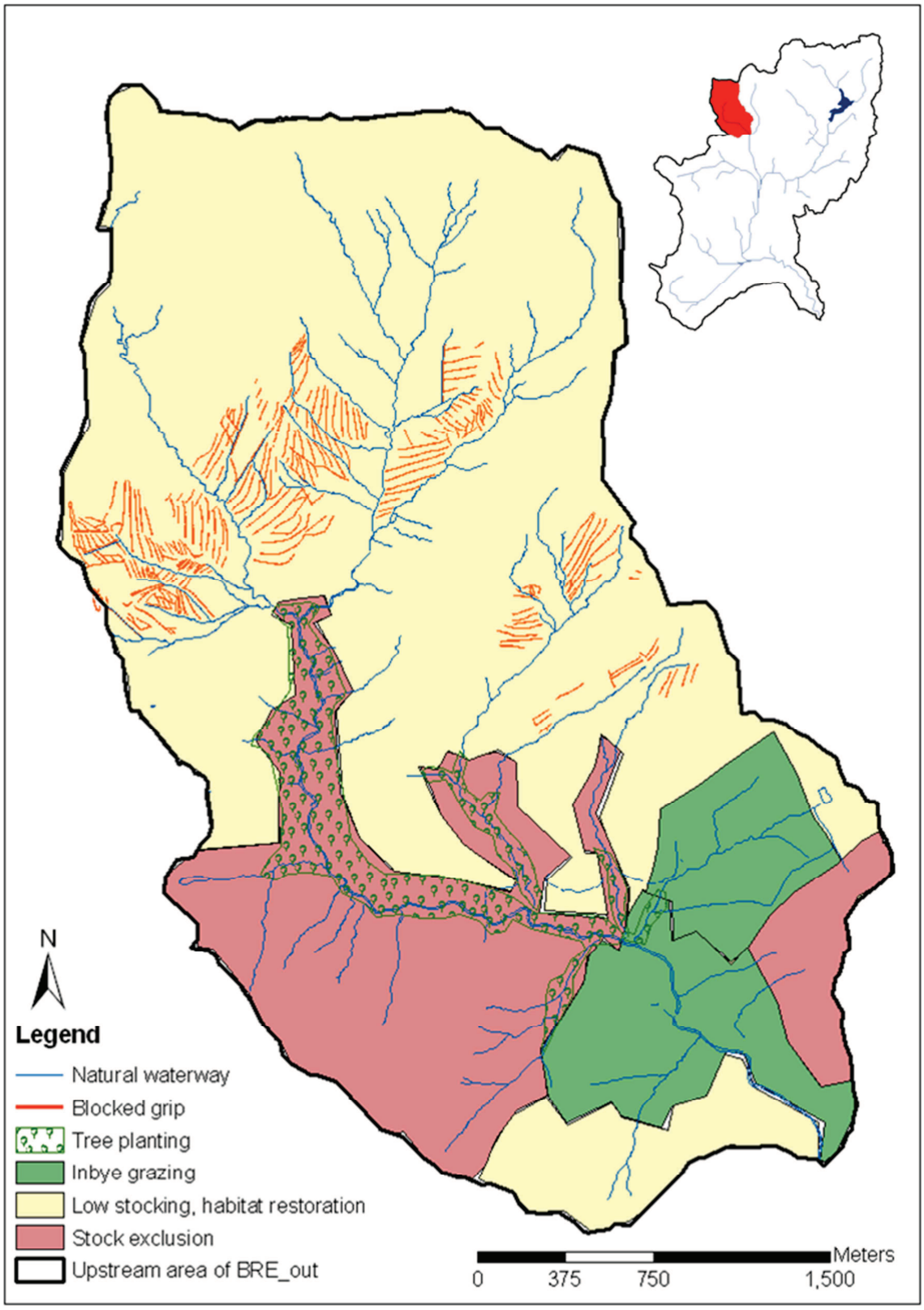

Figure 3.18 SCaMP land use/management changes for the Brennand catchment. In the upper right corner, the location of the Brennand catchment within the Hodder is shown.

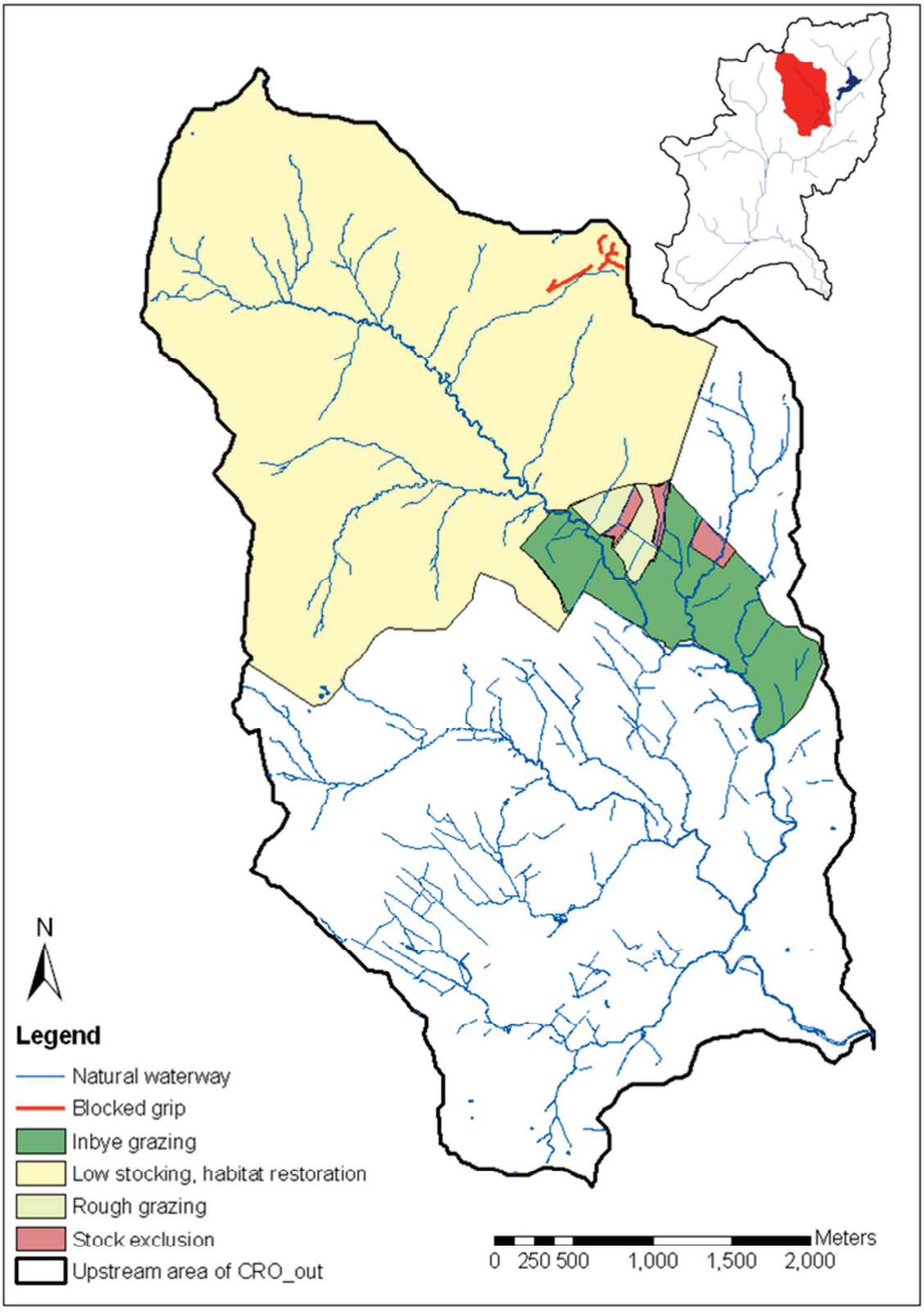

Figure 3.19 SCaMP land use management changes for the upper Croasdale catchment. In the upper right corner, the location of the Croasdale catchment within the Hodder is shown.

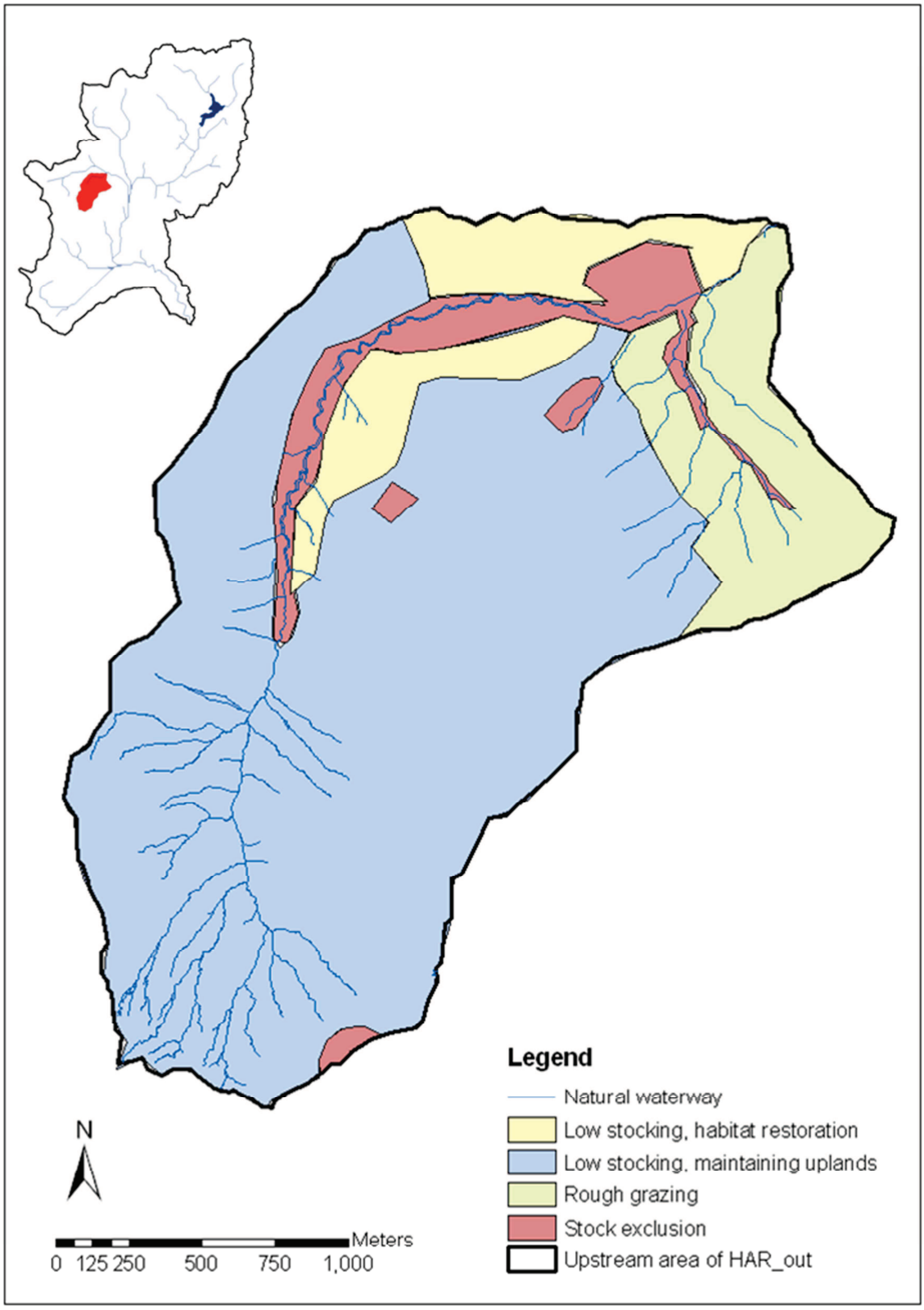

Figure 3.20 SCaMP land use/management changes for the Hareden catchment. In the upper right corner, the location of the Hareden catchment within the Hodder is shown.

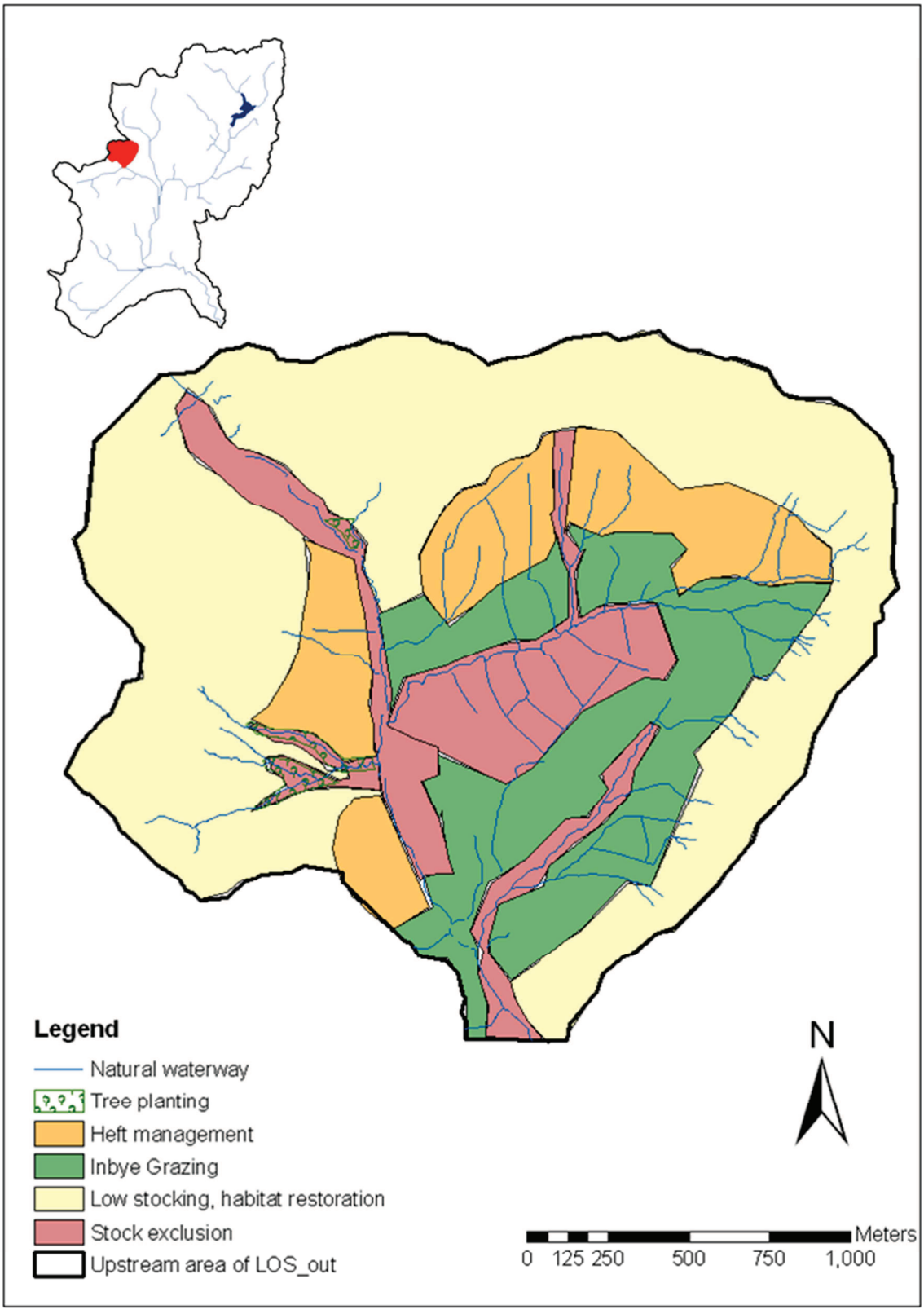

Figure 3.21 SCaMP land use/management changes for the Losterdale catchment. In the upper left corner, the location of the Losterdale catchment within the Hodder is shown.

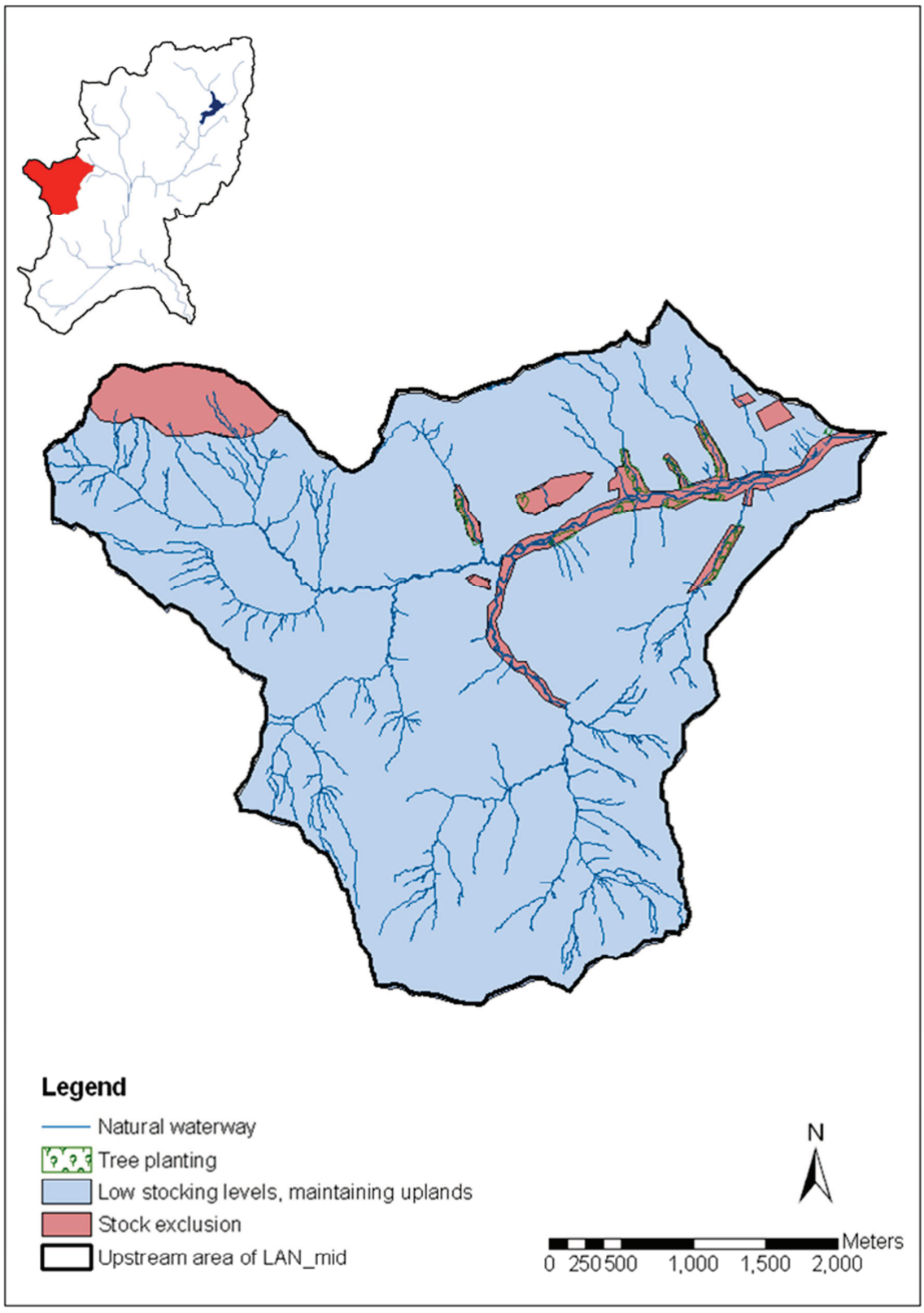

Figure 3.22 SCaMP land use/management changes for the upper Langden catchment. In the upper left corner, the location of the upper Langden catchment within the Hodder is shown.

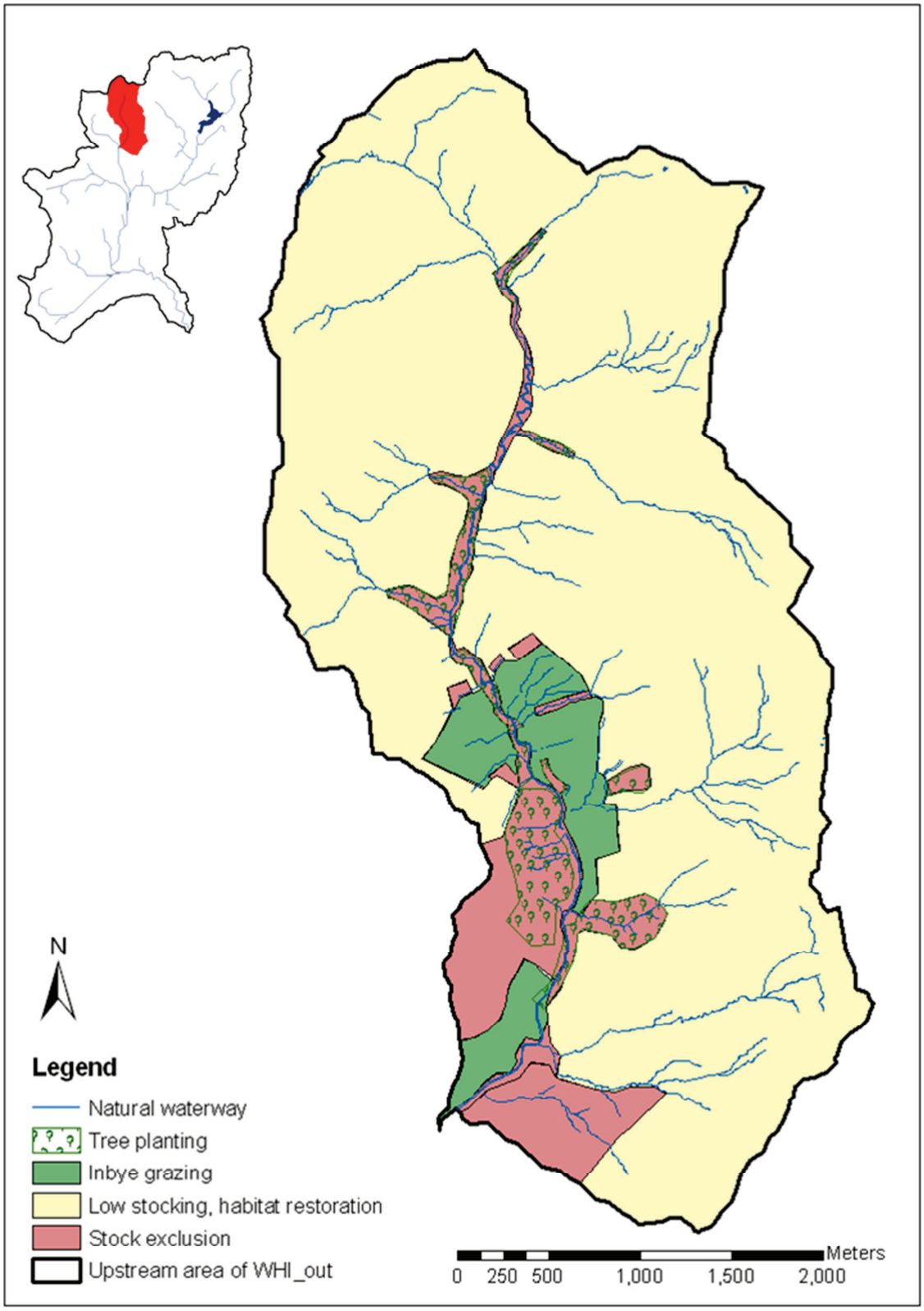

Figure 3.23 SCaMP land use/management changes for the Whitendale catchment. In the upper left corner, the location of the Whitendale catchment within the Hodder is shown.

3.8 Summary

The River Hodder catchment (261 km^2) in Northwest England was designated as the study catchment. A clear distinction can be made between the catchment properties of the headwaters, and those of the lower areas and main Hodder valley. The geology and pedology, climate, land use and vegetation, water supply infrastructure and flooding issues for these two main areas are summarised in Table 3.10. In the headwaters of the Hodder catchment, several land use/management changes have taken place under UU's SCaMP programme, over an area that covers approximately 40% of the total catchment area. The main land use/management changes included grip blocking, reductions in stocking density, and tree planting (Table 3.10).

Table 3.10 Summary of the properties of Hodder headwaters and Hodder main valley and lower areas

Properties		Hodder headwaters	Hodder main valley and lower areas
Geology and pedology	**Geology**	Sandstone	Limestone, Mudstone
	Superficial deposits	Peat, Head	Till, River terrace and Alluvium deposits
	Soils	Winter Hill, Belmont	Wilcocks, Brickfield
Climate	**Annual precipitation**	2090 mm	1150 mm
	Annual snow lying days	17.8 days	8.9 days
Land Use and vegetation		Bog, Dwarf shrub heath, Acid grasslands, Woodland	Improved grasslands, Neutral grasslands, Woodland
Water abstractions		United Utilities: Stocks Reservoir, and Dunsop and Bowland abstractions, some local springs	Some local springs
Flooding		At subcatchments outlet	Near confluences with headwaters, at catchment outlet
Land Use/ Management changes		UU's SCaMP programme: grip blocking, tree planting and stocking density and management changes	Some local, patchy tree planting

4 Multiscale Experimental Monitoring Design and Data Collection

4.1 Introduction

4.1.1 Chapter Overview

The aim of this chapter is to describe the multiscale nested monitoring network that has been implemented in the Hodder catchment and give an overview of the data, which includes data availability, processing, quality assurance and quality control. Section 2 presents the existing EA hydrometric network. Sections 3, 4, and 5 describe the extended rain gauge network, the automatic weather station, and the extended stream gauge network, respectively. These sections include the site selection procedure and a technical description of the gauges, the data processing, and a discussion of the data quality assurance and control. Section 6 discusses the data collection, availability and overall quality control of the fully processed data. A summary is given in Section 7.

4.1.2 Monitoring Rationale

The main purpose of the monitoring network is to provide the appropriate data that can be used to (1) study how the subcatchments and the catchment as a whole function, especially when generating flood hydrographs, (2) study the effects of land use/management changes (LUMC) on runoff generation at the small (i.e. micro) scale, and (3) investigate how these changes propagate through the river network and affect the catchment behaviour at larger scales. Eventually this can lead to a better understanding of how the factors controlling the catchment behaviour are affected by land use/management changes at increasing scales.

To meet the data requirements for 1 and 3, a multiscale nested monitoring design is needed. Chapter 2 discussed a range of experimental monitoring strategies for the effects of LUMCs on runoff generation. The traditional approach would be to densely instrument a (few) hillslope(s) or plot(s) and monitor the effects of the different land use/management changes on local variables such as groundwater level, infiltration, subsurface and overland flow, etc. In addition, these results could be compared with a

'control' site not undergoing any change. Although labour-intensive and expensive, this type of work would be acceptable for the second requirement of the monitoring network, as there are numerous examples of these kinds of studies which have provided valuable insights (Chapter 2). However, there are problems with distinguishing between differences caused by land use/management change and by heterogeneities in the physical properties within and between plots, hillslopes and catchments, and how this information can be scaled. It would be impossible financially and practically, to apply this method over the entire area undergoing change and include detailed monitoring of local variables for all different types of land use/management changes, while also incorporating multiscale nested monitoring farther down the river network.

The approach in the current study is quite unusual in the way it focuses on dense multiscale monitoring of flow and does not include any monitoring of local variables. In this way, the changes induced by LUMC can be detected at larger and increasing scales, while the causes at small (plot and hillslope) scales can be inferred through modelling and knowledge based on field walkovers and the rich literature available for small scale studies. Also, in case changes in flow are detected at larger scales (i.e. micro, mini and meso scale), the monitoring rationale still allows for expansion to more detailed and targeted monitoring of local variables.

In addition to the stream gauges, an Automatic Weather Station (AWS) and several Tipping Bucket Rain (TBR) gauges have been installed to obtain potential evaporation estimates and precipitation records, respectively. The main products of the monitoring network are continuous measurements of discharge, rainfall and evapotranspiration.

4.1.3 Monitoring Design Overview

The design and implementation of the monitoring network started in January 2008 and occurred in five stages (following Shaw et al., 2011):

1. Initial background research on the location and characteristics of the study area
2. Identification of existing measuring stations
3. Identification of new sites: first based on maps, and then adjusted to ground conditions during field visits

4. Planning and design of installations, including acquiring installation permissions
5. Implementation of the equipment

The first stage has been described in Chapter 3. The present chapter describes the results of stage 2-5.

A number of constraints on the network had to be considered. Firstly, there were limitations in the available equipment and staff time to install and maintain the network. Secondly, it was not possible to install any monitoring equipment that was detrimental to the land, especially for areas designated both as a SSSI and an AONB. Any installations and subsequent work had to be in agreement with UU, tenant farmers, game keepers, Natural England and the RSPB. Thirdly, the monitoring depended on the delivery of UU's SCaMP. Finally, the design had to make full use of the existing monitoring network by incorporating it within the experimental design.

The total full monitoring network consisted of seven tipping bucket rain gauges, an AWS, and 28 stream gauges. A schematic representation of the River Hodder catchment showing the locations of these gauges is given in Figure 4.1 (right). The details of these gauges are discussed in Sections 2-6 below.

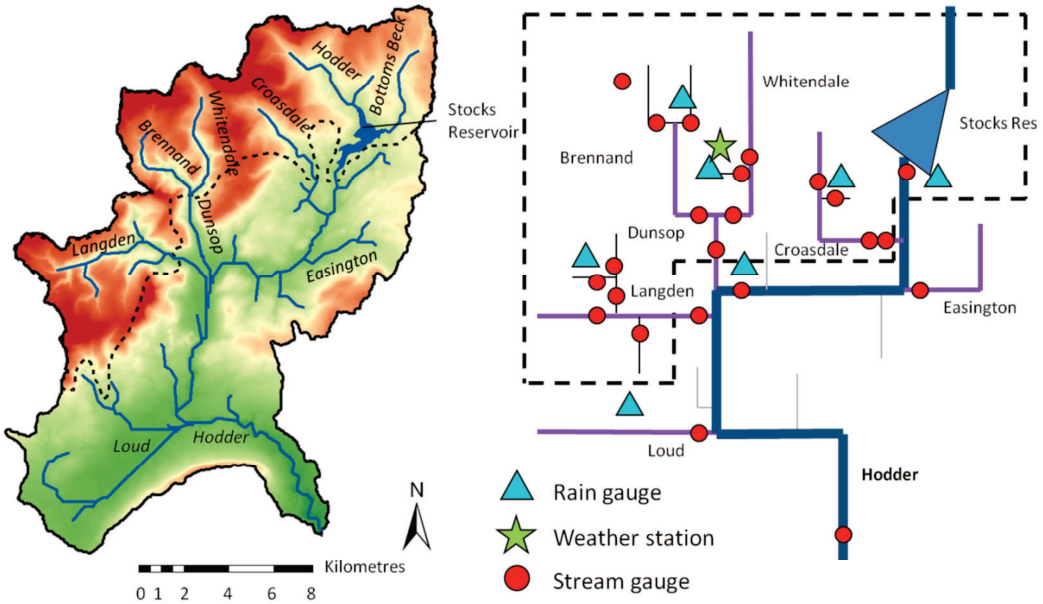

Figure 4.1 Left: Hodder catchment with main subcatchments and the SCaMP area indicated by the black dashed line; Right: schematic representation of the Hodder catchment, including an overview of the hydrometric monitoring scheme

4.2 Existing Hydrometric Network

Several stream and rain gauges have been monitoring the Hodder catchment for a number of years (Tables 4.1 and 4.2). Figure 4.2 shows the locations of 4 EA tipping bucket rain gauges (Section 4.2.1) and 5 EA stream gauges (weirs) (Section 4.2.2). Their data sets are of great value, especially because the present project started monitoring only 6-12 months prior to the implementation of the land use/management changes. Long term data records are important for the current study as these provide a good background (pre- change) data set in order to study the natural variability in the catchment behaviour prior to the implementation of the changes (Chapter 5).

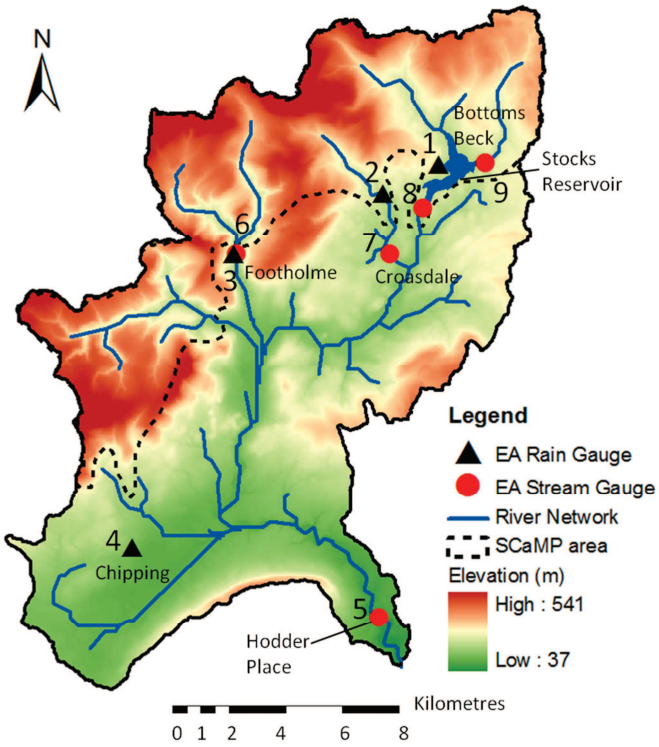

Figure 4.2 Existing hydrometric network in the Hodder catchment

4.2.1 Rain Gauges

Table 4.1 presents information on the EA tipping bucket rain gauges, all operational since the early 1990s. The rain gauge at Footholme has had some problems and has considerable data gaps in the record up to February 1997, after which it was replaced by a more reliable gauge. The rain gauge at Croasdale House has been inactive since 2000 and has therefore not been included in the current monitoring network. However, the historical data are still important for the study of natural rainfall variability in the Hodder catchment.

Table 4.1 Environment Agency tipping bucket rain gauges

Location	EA reference number	Reference in Figure 4.2	Grid reference	Elev. (m)	Catch-ment	Data record
Stocks Reservoir	573342	1	SD 716 547	192	Hodder	1991 – present
Croasdale House	573426	2	SD 704 550	183	Croasdale	1990 - 2000
Footholme	573719	3	SD 652 528	167	Dunsop	1990 - present
Chipping	574006	4	SD 704 550	166	Loud	1990 - present

4.2.2 Flow Gauges

Table 4.2 provides information on the EA flow gauges. The longest available flow records go back to 1976 for the catchment outlet (Hodder Place). For each gauge, Table 4.2 gives the National River Flow Archive (NRFA) number in addition to the gauge information.

Table 4.2 Environment Agency stream gauges

Location	NRFA Num-ber	Reference in Figure 4.2	Grid reference	Area (km^2)	River	Data record
Hodder Place	71008	5	SD 710 382	261	Hodder	1976 – present
Footholme	71015	6	SD 653 529	25.3	Dunsop	1995 – present
Croasdale*	71003	7	SD 704 549	10.4	Croasdale Brook	1982 -1989; 2003 – present
Stocks Reservoir	71002	8	SD 719 544	37.5	Hodder	1977 – present
Bottoms Beck*	71005	9	SD 745 565	10.6	Bottoms Beck	1982 – present

* Stage only

The records for Stocks Reservoir, Footholme and Hodder Place are all for discharge; the Bottoms Beck and Croasdale datasets are stage only. Bottoms Beck is situated upstream of Stocks Reservoir and the data are therefore not used in the current study. Discharge measurements at a range of stages for the Croasdale weir have been made available by the EA. In the current study, these were used to obtain a rating curve. The discharge for Croasdale weir is calculated according to Equations 4.1.1 and 4.1.2:

$Q = 1.3853h^{2.2221}$ (h ≤ 0.9) (Equation 4.1.1)

$Q = 1.8914h^{5.0737}$ (h > 0.9) (Equation 4.1.2)

For Equation 4.1.1 and 4.1.2 Q is the discharge in $m^3 s^{-1}$ and h is the stage in m. The break in the rating curve is caused by the weir design (a trapezoidal flume with a low flow throat), which has a distinctive change in profile at a height of 0.9 m.

4.3 Rain Gauge Network

4.3.1 Network Design

Several authors have highlighted the need for rain gauge coverage of the full range of elevation in order to get a good representation of the catchment rainfall (e.g. Mayes et al., 2006; Wilkinson, 2009). The existing EA rain gauge network (Section 4.2.1) is especially sparse in the upper part of the catchment, as it covers only the bottom 40% of the elevation range (Figure 4.3). The main requirement for the complementary rain gauge network was therefore to extend it to higher elevations. Secondly, it was desirable to have a good spatial rain gauge coverage over the entire area of the Hodder catchment, as rainfall is also irregularly distributed in space (Shaw et al., 2011) and time (Wilkinson, 2009). Finally, there was a need for representative rain data records at specific small scale monitoring sites. Owing to management and budgetary reasons, the number of additional gauges was restricted to four (including the rain gauge as part of the AWS, Section 4.4).

For spatial distribution and the occurrence of LUMCs, the Langden, Brennand and Croasdale subcatchments were initially selected as the three main areas for these gauges. After field inspections and discussions with land owners, managers and elevation consideration, the specific sites in these three catchments were identified.

Tipping bucket rain gauges of *IH (CEH)* aerodynamic design (as shown on Figure 4.10 as part of the AWS), fitted with an *Environmental Measurements Ltd.* (EML) DT2 type loggers, were installed at locations TBB (Tipping Bucket Brennand), TBC (Croasdale), and TBL (Langden) (Table 4.3 and Figure 4.4). The gauges were programmed to record 0.2 mm 'event based' tips, to allow for aggregation at any required time interval.

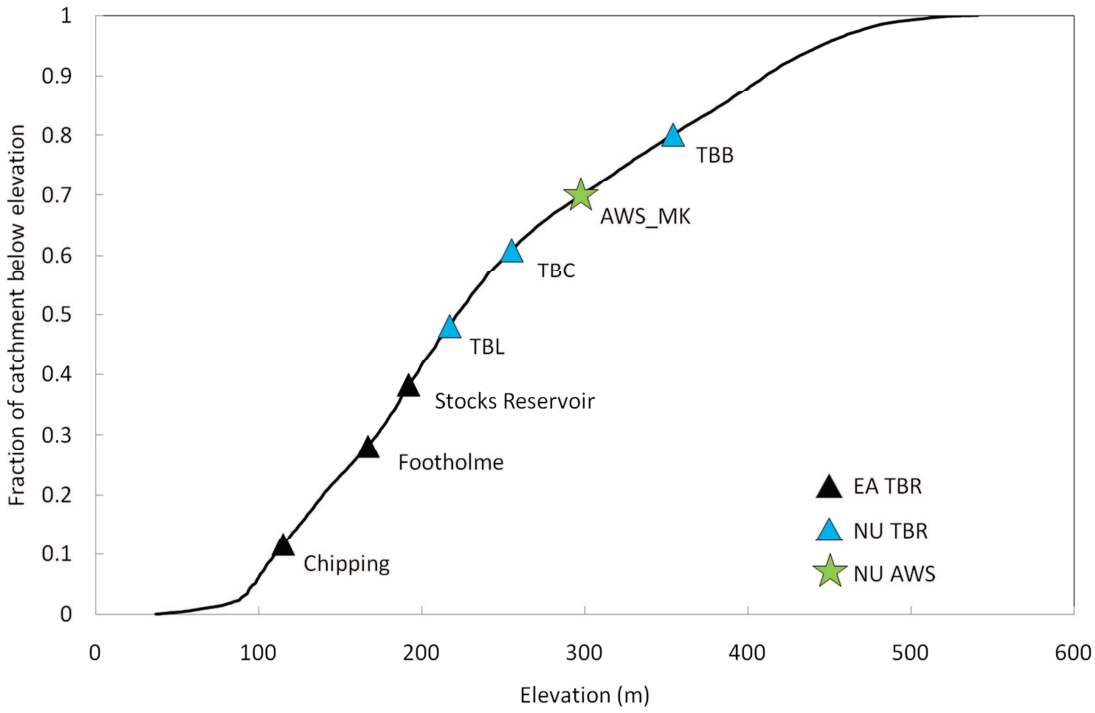

Figure 4.3 Hypsometric curve of the Hodder catchment, including the elevation of the rain gauges and AWS

Table 4.3 Newcastle University rain gauges

Catchment	Location Code	Grid reference	Elevation (m)
Brennand	TBB	SD 634 558	354
Croasdale	TBC	SD 687 565	255
Langden	TBL	SD 627 522	217

Figure 4.4 shows the spatial distribution of the full rain gauge network, including the rain gauge as part of the AWS (Section 4.4) and the active EA TBR gauges. From Figure 4.3 it is clear how the extended rain gauge network now provides a good coverage with regard to elevation.

4.3.2 Data Processing and Quality Control

Processing of Raw Data

The event-based precipitation data were aggregated to 5 min, 15 min, hourly, daily and monthly time series. Upon data downloads, the raw data were checked for unphysical values that could be associated with data logger failures first. If there were any errors, those data were disregarded.

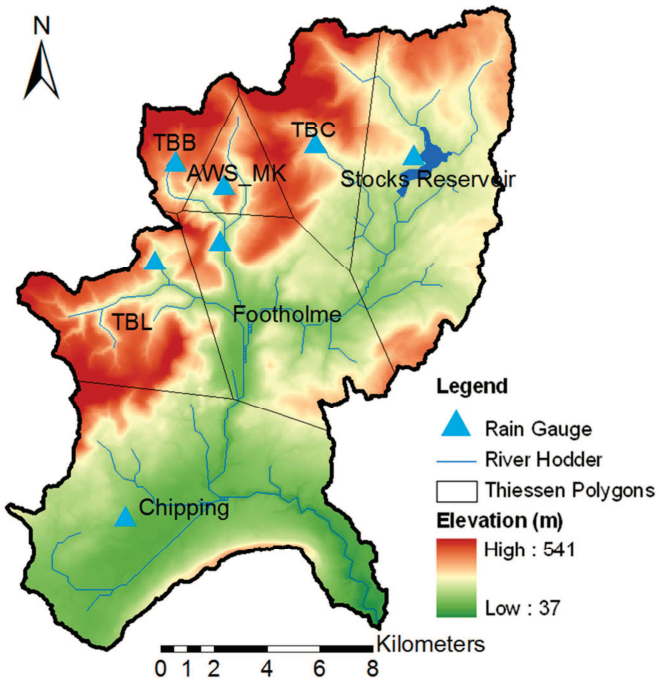

Figure 4.4 Rain gauge network in the Hodder catchment, including Thiessen polygons

Snow cover and snow melt

Snow cover within the experimental period was recorded during January - April 2008, October 2008 - March 2009 and November 2009 - April 2010, with significant snow cover of more than five snow lying days per month during December 2008 – February 2009 and December 2009 – February 2010 (Metoffice 5 km gridded monthly data sets, (Perry and Hollis, 2005))(Figure 4.5). Especially during these latter two periods, the recorded data at the rain gauges may represent rainfall and/or snow melt. The latter could involve significant error in the water input as a result of snow drift. The gauges are not heated, which causes a delay in the measurements depending on snow melt.

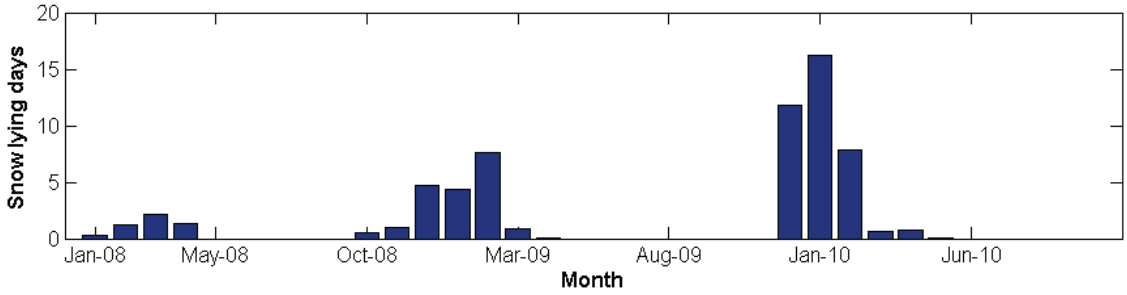

Figure 4.5 Monthly snow lying days for the Hodder catchment during January 2008 – October 2010 (data source: MetOffice 5 km gridded monthly data sets)

Data Uncertainty and Quality Control Checks

Data uncertainty in the TBR gauge data could be caused by wind effects and/or (to a lesser extent) calibration errors. It is generally known that wind effects (turbulence and rainfall direction) can cause a significant underestimation of rainfall depths (e.g. Larson and Peck, 1974; Nespor and Sevruk, 1999; Chang and Flannery, 2001; Guo et al., 2001; Wilkinson, 2009). The average wind induced rainfall undercatch ranges from approximately 2 to 15% for wind speeds up to 7 m/s (Nespor and Sevruk, 1999; Guo et al., 2001) and increases about 2.2% with every m/s of wind speed (Larson and Peck, 1974). However, this also depends on other conditions, such as rain gauge height and exposure, raindrop size and velocity, vegetation cover (Guo et al., 2001), and type of rain gauge (Chang and Flannery, 2001). It is beyond the scope of the current research to quantify the exact undercatch of the rain gauges. However, some underestimation of the actual precipitation should be taken into account in the data analyses of all rain gauges.

For an overall quality control check, a comparison is made between all tipping bucket rain gauges in the Hodder catchment. The monthly totals for each gauge are plotted in Figure 4.6 for the 2008-2009 hydrological year. Apart from some snow lying days during December 2008 – February 2009, there are no particular peculiarities during this period. For TBC, there are missing data for December 2008 and January, March, and April 2009; for TBL for February and March 2009 (see Section 4.6 below).

From Figure 3.6 in Chapter 3, it is expected to find considerably more precipitation in the upper part of the catchment (e.g. TBB and AWS_MK) compared with that observed in the lower part (e.g. Chipping). However, there is also some variation in precipitation totals spatially. It is noted, though, that the TBB gauge (at an elevation of 353 m) recorded only about 80% of the precipitation observed at AWS_MK (297 m) and about 95% of that observed at Footholme (167 m). These three gauges are all located in the Brennand subcatchment (11 km^2) and as precipitation is expected to increase with elevation, these observations may appear slightly unusual. If they can be related to any equipment failure or additional wind induced errors at TBB, a correction for one or some of the gauges may be needed. Alternatively, the differences might be explained by differences in the local topography (e.g. aspect).

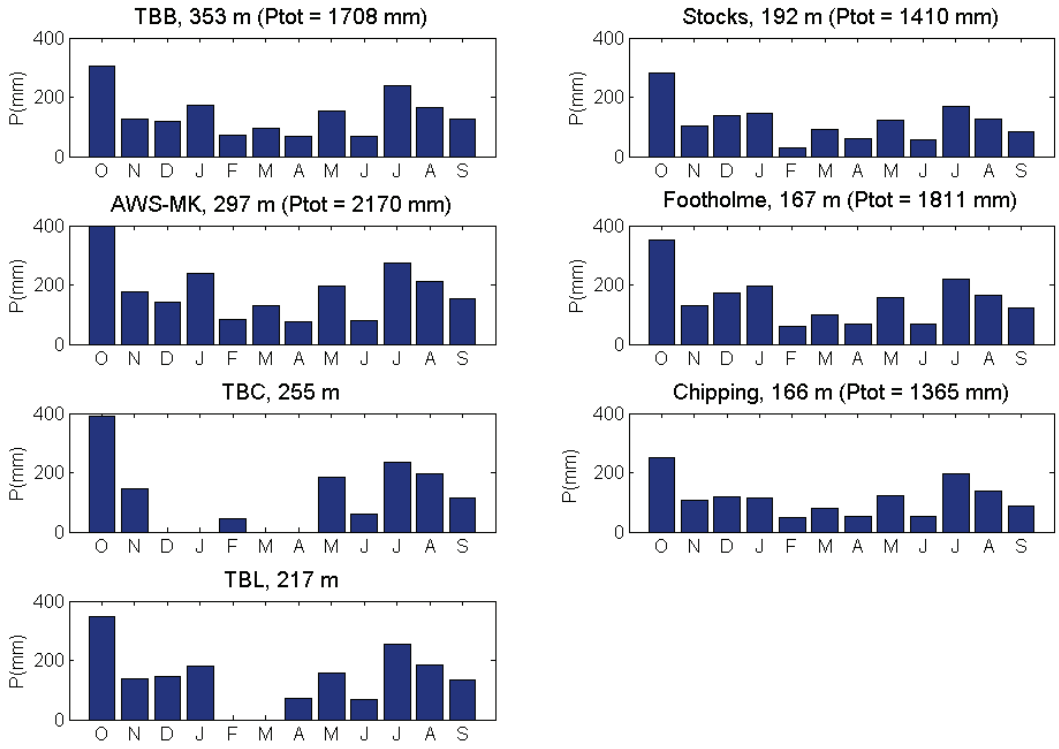

Figure 4.6 Monthly precipitation totals from October 2008 – September 2009 for all tipping bucket rain gauges in the Hodder catchment

For the TBB, AWS_MK and Footholme gauges, three tests were done to check for 1) equipment failures, 2) additional wind induced errors at TBB, and 3) influences of aspect.

Additional tipping bucket rain gauges were installed at TBB (TBB_2, during 17/06/2010 – 02/10/2010) and AWS_MK (AWS_MK_2, during 06/02/2011 – 28/04/2011). During their test periods, TBB_2 recorded 95.2% of the precipitation record at TBB and AWS_2 recorded 89.9% of that of AWS. The latter appears a little low, but the differences are within the error range associated with wind undercatch. In addition, tipping bucket rain gauges are known to suffer from mechanical errors (up to 10-15%) especially during high rainfall intensities (Molini et al., 2001; La Barbera et al., 2002). The daily precipitation data at TBB and TBB_2 are very similar, which suggests that the precipitation measured by the TBB rain gauge is consistent. The tipping bucket rain gauge at Footholme is quality assured by the EA, which compares the data with a daily storage rain gauge.

If TBB is more affected by wind speed than the other gauges, it may be expected that the ratio between the daily precipitation of TBB with AWS and/or Footholme would change with increasing wind speed. However, as can be seen from Figure 4.7, there is no relation between average daily wind speed or maximum daily wind speed and the daily precipitation ratios during the 2008-2009 hydrological year, for days at which the observed precipitation at TBB > 1mm. However, there are four outliers. For the TBB/Footholme ratios these can be attributed to localised convective storms during the summer months at the top of the catchment (TBB) only. For the TBB/AWS ratio, the recorded data are from a snow lying day and may be related to snow melt differences.

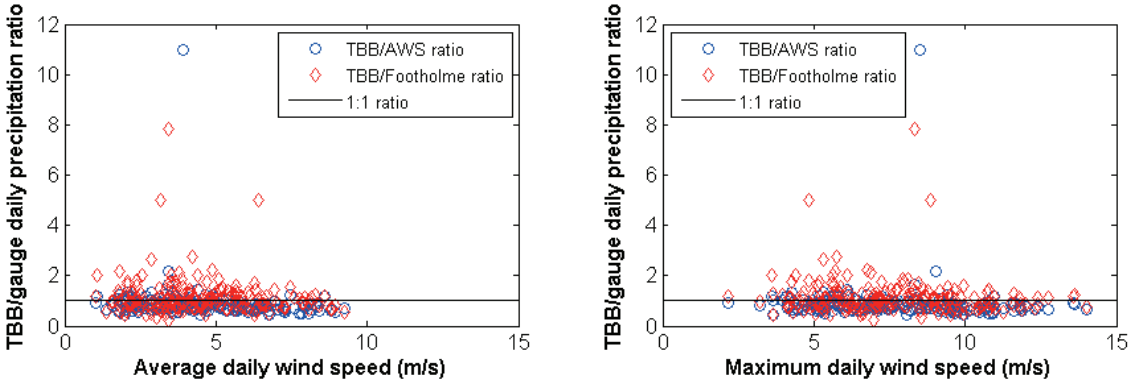

Figure 4.7 Average daily wind speed (left) and Maximum daily wind speed (right) against daily precipitation ratios of TBB and AWS (blue) and TBB and Footholme (red)

An uncomplicated way of checking any influences of aspect of the rain gauge location is by comparing the daily precipitation ratios (as shown in Figure 4.7) with their main wind directions. Excluding the days with extreme ratios, the daily precipitation ratios for TBB/AWS (left) and TBB/Footholme (right) are plotted against the daily prevailing wind direction in Figure 4.8. It is clear that the most common wind direction is either SW or W. It is noted that the overall variability in the ratios is much higher for TBB/Footholme than for TBB/AWS, which may be attributed to much higher differences in location and elevation between the prior two stations. If aspect would be responsible for the ratios between the daily precipitations of the different gauges, there might be higher or lower ratios respectively with alternating wind directions. However, based on this one year of data, there is no clear indication of this kind of aspect effects in Figure 4.8.

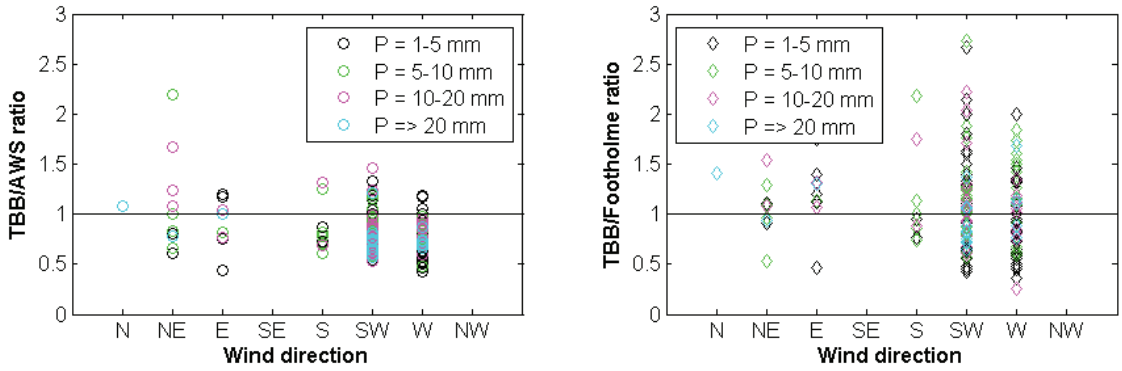

Figure 4.8 Daily prevailing wind directions against/AWS daily precipitation ratio (left) and TBB/Footholme daily precipitation ratio (right), with colour coding according to daily precipitation (P)

In summary, from the comparison of daily precipitation at TBB with AWS_MK and Footholme, there are no solid grounds for any corrections to the precipitation data of any of the gauges. The errors of the rain gauges (such as those potentially caused by wind undercatch) are assumed the same for each site. No clear signal of aspect arose from the simple analysis. However, as the topography of upland areas is rather complex other features such as slope could interact with aspect (Buytaert et al., 2006). Overall, the maximum uncertainty in the precipitation data is in the order of 10%.

4.3.3 Estimation of Catchment Precipitation

For analysis and modelling purposes, it is necessary to obtain an estimate of catchment precipitation from the point measurements of the TBR gauge network. A straightforward and common way of interpolating point rainfall observations is through the Thiessen polygon method (Thiessen, 1911), which assigns weights to the rainfall measured at each gauge according to the proportion of the catchment area that is nearest to that gauge. Figure 4.4 shows the Thiessen polygons based on the rain gauge network in the Hodder catchment. However, the Thiessen polygon method does not account for physical factors that are known to influence the rainfall, such as topography. More advanced methods of rainfall interpolation include Kriging, which is a geostatistical linear weighting method based on the correlation between of the catches of individual rain gauges that generally decreases with distance between pairs of gauges (Shaw et al., 2011). Through a multivariate extension process called Co-Kriging, other variables such as topography can be taken into account (e.g. Goovaerts, 2000). This method is computationally more intensive and requires relatively more

gauges than the simple Thiessen method. However, there is no clear conclusion about which method might be best (Shaw et al., 2011).

Here, an extended version of the Thiessen polygon method is used, that does account for elevation. A rainfall correction factor (r) is applied to the Thiessen polygon precipitation estimate, that accounts for the difference between average catchment elevation (E_c in m) and the rain gauge elevation (E_g in m). r Is then applied to the rainfall measured at the gauge (P_g in mm) to obtain the corrected contribution to the catchment average rainfall (P_c in mm), according to:

$$P_c = r\, P_g \qquad \text{(Equation 4.2)}$$

where r is determined as:

$$r = \frac{aE_c+b}{aE_g+b} \qquad \text{(Equation 4.3)}$$

where a and b are two coefficients obtained from the relation between the mean annual precipitation ($\overline{P_{ann}}$ in mm) and the elevation of gauges in the Hodder catchment, which is described as the linear regression of these data, according to:

$$\overline{P_{ann}} = aE + b \qquad \text{(Equation 4.4)}$$

Note that, in the application of r, it is assumed that the elevation is the main predictor of the mean annual rainfall. It is recognized that there are a number of other factors such as slope and aspect which give rise to differences in rainfall in an area with complex terrain, though it is beyond the scope of the present study to include the more complex analysis of their effects.

Table 4.4 Source and number of gauges for available average annual precipitation data

Time Period	Source/Reference	Number of gauges
1916 - 1950	Hydrological year book 1969	43
1941 - 1970	Hydrological year book 1990	10
1989 - 2009	BADC	7

For the determination of the relation between E and $\overline{P_{ann}}$ historical data sets for the Hodder were used that were available for three different time periods, including 1916-1950, 1941-1970, and 1989-2009 (Table 4.4 and Figure 4.9).

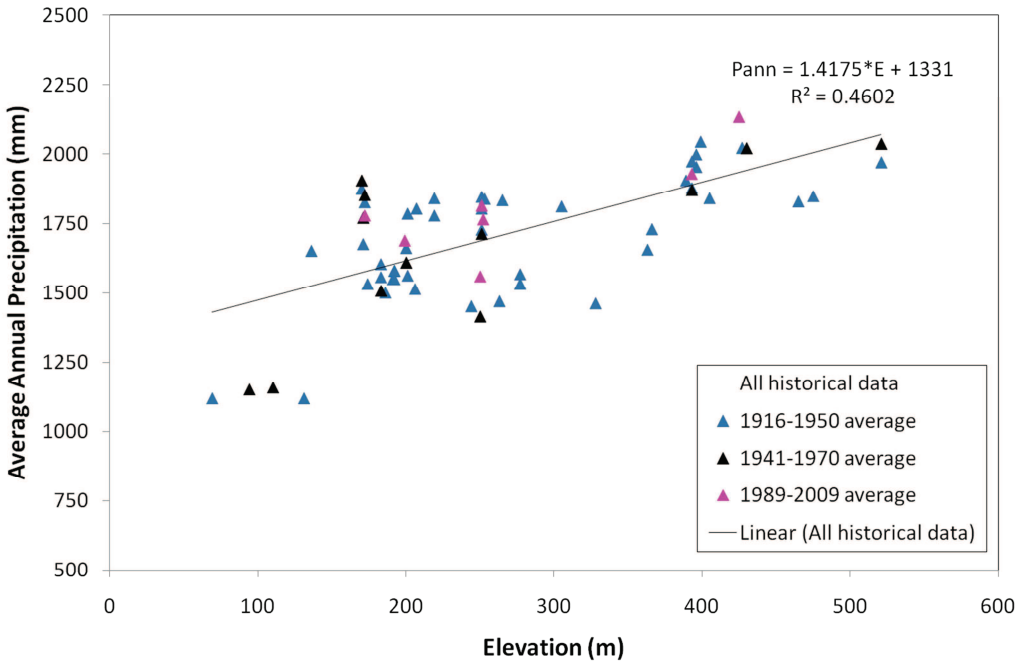

Figure 4.9 Average annual precipitation data for historical rain gauges in the Hodder catchment, plotted against the elevations at which they were measured

Table 4.4 and Figure 4.9 show that the dataset for the earliest period is most extensive. This is related to the creation of Stocks reservoir in the 1920-1930s. However, the regression is to be used for the more recent data of 2008-2010. It was therefore tested if it may be assumed that the areal average rainfall of 1916-1950 is the same of that of 1941 – 1970 and that of 1989 – 2009 by comparing $\overline{P_{ann}}$ for three gauges that were operational during all time periods and 1 which was operational during the first and last period only. It was found that the average annual rainfall totals at these gauges were within 5% of each other for all three time periods, from which it was concluded that the above assumption is realistic. In addition, this also indicates that all historical data sets can be used to obtain the current relationship between $\overline{P_{ann}}$ and E.

The time periods for which the $\overline{P_{ann}}$ data were obtained are not the same in length. In the determination of the regression line this was accounted for by assigning a weight to the three different data sets, proportional to the length of the period for which the $\overline{P_{ann}}$ data were calculated.

As shown in Figure 4.9, for the Hodder catchment, the regression equation for the relation between the elevation and the mean annual rainfall becomes:

$$\overline{P_{ann}} = 1.4175E + 1331 \qquad \text{(Equation 4.5)}$$

The R^2 value for the regression (0.46) is rather low, probably owing to the influence of aspect, slope, and other unknown factors. Applying Equations 4.2-4.5 to an example where E_g= 350 m and E_c = 450 m, the rainfall correction would be 1.08. For those catchment areas covered by two or more Thiessen polygons, the appropriate rainfall correction numbers were based on the average catchment elevation within each polygon.

4.4 Automatic Weather Station

4.4.1 Location and Technical Description

An AWS was installed on Middle Knoll (AWS_MK in Figure 4.4) at an elevation of 297 m (grid reference SD 631 550) (Figure 4.10). At this location the AWS could be located within an existing enclosure, out of reach of sheep, and also out of public sight.

The *EML* automatic weather station, fitted with a *Campbell* CR10X logger, measures maximum, minimum and average wind speed (m s^{-1}), wind direction (degrees), relative humidity (%), air temperature (degrees Celsius), net radiation (W m^{-2}), and precipitation (mm) at a 15 min interval.

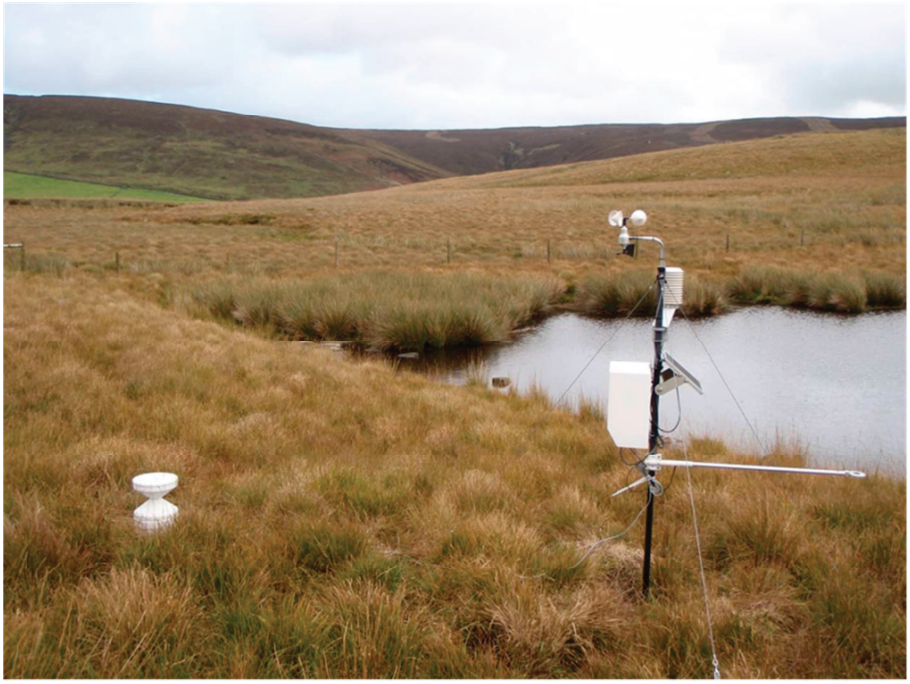

Figure 4.10 Automatic weather station at Middle Knoll

4.4.2 Data Processing and Quality Control

The raw meteorological data did not need any data processing. However, they were checked for irregularities. The anemometer has a minimum start-up wind speed of 0.5 m/s. For periods where the maximum wind speed was less than that, the minimum, maximum and average wind speed is 0. Unrealistically high wind speed data were recorded in July 2009. These data were disregarded.

4.4.3 Determination of Evapotranspiration

The potential evapotranspiration (PE_0, W m^{-2}) was obtained through the Penman-Monteith equation (Calder, 1990):

$$\lambda E = \frac{\Delta R_n + \rho C_p VPD / r_a}{(\Delta + \gamma)(1 + \frac{r_s}{r_a})} \qquad \text{(Equation 4.6)}$$

in which R_n is the mean net radiation (W m^{-2}), Δ the slope of the saturated vapour pressure curve (kPa K^{-1}), ρ the density of air (kg m^{-3}), C_p the specific heat of air at constant pressure (J kg^{-1} K^{-1}), *VPD* the mean vapour pressure deficit (kPa), λ the latent heat of vaporization of water (J kg^{-1}), γ the psychrometric constant (kPa K^{-1}), r_a the aerodynamic resistance (s m^{-1}), and r_s the (bulk) surface resistance (s m^{-1}).

The vapour pressure deficit is defined by Equation 4.7:

$$VPD = e_s - e_a \qquad \text{(Equation 4.7)}$$

where e_s is the saturation vapour pressure (Pa) and e_a is the actual vapour pressure (Pa).

The reference evapotranspiration was calculated for a reference vegetation height (h) of 0.12 m, a fixed bulk surface resistance of 70 s m^{-1}, and an albedo (α) of 0.23 (Allen et al., 1998). For this reference crop, the aerodynamic resistance was calculated according to Equation 4.8 (Allen et al., 1998):

$$r_a = \frac{208}{u_2} \qquad \text{(Equation 4.8)}$$

where u_2 is the wind speed (m s^{-1}) at a height of 2 m, measured by the AWS.

It was assumed that the potential evapotranspiration calculated from the AWS data at Middle Knoll could be applied to the entire Hodder catchment.

4.5 Stream Gauge Network

4.5.1 Network Design

The locations of the stream gauges were dependent on a number of factors, including:

- The location, types and timing of the SCaMP interventions
- A full coverage of scale (from approximately 100 m^2 to 100 km^2) was needed
- The monitoring had to cover the main subcatchments of the Hodder
- The monitoring had to complement the existing monitoring network of the EA
- Logistics, access, and safety
- Limitations on the amount of gauges (management and budget)

After numerous field walkovers and a discussion with the Bowland Estate SCaMP coordinator (Chapter 3), 21 stream gauges and an additional three weirs were installed throughout the Hodder catchment, which greatly enhance the EA flow gauge network.

The location of each gauge is schematically represented in Figure 4.1. In Figure 4.11, this stream gauge network is redrawn in such a way that it demonstrates the scale at which each gauge is monitoring. For the gauges (circles), the y-axis shows scale (catchment area) and, on the x-axis, the easting gives an idea of the gauge location in space. In total, the full network consists of 7 process scale, 8 micro scale, 11 mini scale, and 2 meso scale nested sites. The links between the gauges (and scales) are also shown, with the streams of each of the major subcatchments colour coded. In addition, the gauges themselves have been colour coded to show the type of land use management changes that occurred upstream of each gauge.

All gauges have been given a location name and code (Figure 4.11). The code holds information on the gauge location: the first three letters are of the stream in the subcatchment of which the gauge is located, and the last three letters give information on the location within that subcatchment. For the process scale monitoring, the last three letters refer to the specific type of LUMC monitoring. For example, BRE_sap is the code for the outlet of Sapling Clough in the River Brennand catchment, and WHI_tree is the monitoring site in the River Whitendale catchment where the effects of tree planting are being monitored. In the three cases where a weir has replaced or superseded a gauge, the code has that information added (e.g. WHI_tree_weir).

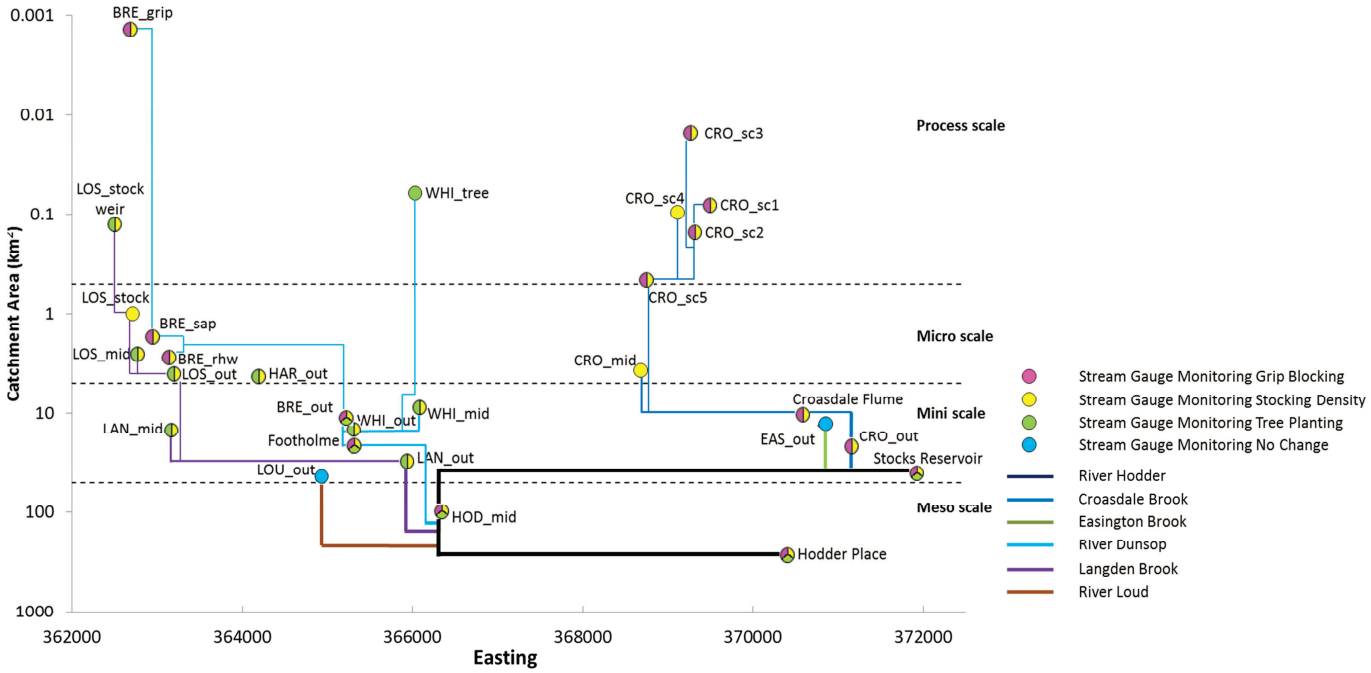

Figure 4.11 Schematic Hodder stream gauge monitoring network, with the stream gauges according to scale on the y axis and easting on the x-axis

The main land use management changes have been implemented in the Langden Brook, Brennand River, Whitendale River, and Croasdale Brook catchments (Chapter 3). Hence these catchments were instrumented most densely. It was impossible to gauge all inflows to the Hodder, but the main contributions, including Easington Brook and the River Loud, have been instrumented. No efforts were made to monitor any water courses upstream of Stocks Reservoir because of the regulating effect of the reservoir. Figure 4.11 shows that nesting of up to seven gauges deep (CRO_sc1 – CRO_sc2, CRO_sc5, Croasdale_Weir, CRO_out, HOD_mid and Hodder Place) results from the network design.

Table 4.5 provides general information about the stream gauges, including grid reference, elevation, catchment area, monitoring interval and the effects of which type of land use management changes it is monitoring (GB = Grip Blocking, SDMC = Stocking Density/Management Changes, and TP = Tree Planting). More detailed information on each individual gauge is given in Appendix 1.

The stream gauges consist of pressure transducers which are housed in protective tubes. Figure 4.12 shows a photograph of a stream gauge in the field (left) and a schematic representation of a stream gauge (right). The gauge consists of a black plastic tube with a series of holes that allow water to enter and exit with rising or falling stage. The tube has a lid with a detachable top that allows easy access. Drilled through the tube and lid is a bolt from which a string with a pressure transducer (diver) is hung. The entire gauge is attached in a fixed position to a steel post which is hammered into both the river bank and bed.

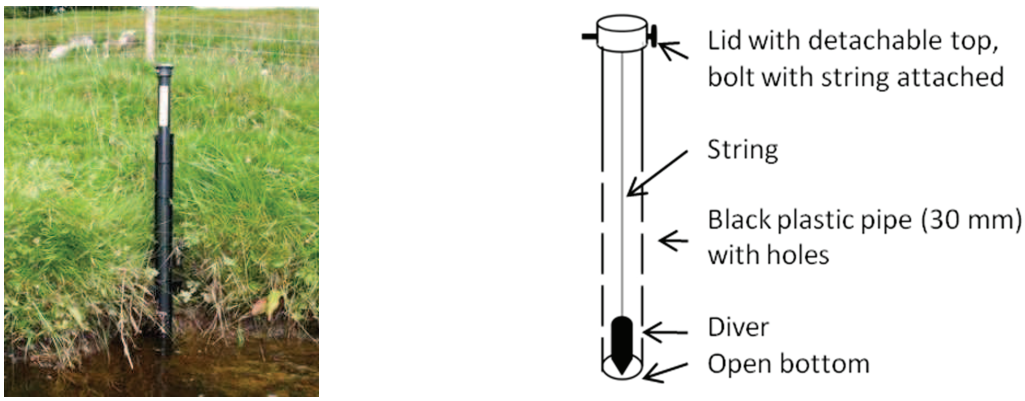

Figure 4.12 An example of a NU stream gauge (left), with a schematic representation on the right, showing the main parts of the gauge

Table 4.5 Newcastle University stream gauges and weirs in the Hodder catchment

Location Code	Grid reference	Elevation (m)	Catchment Area (km^2) (scale)	Interval (min)	LUMC
BRE_grip	SD 627 559	384	0.0014 (process)	5 min	GB, SDMC
BRE_grip_weir	SD 627 559	381	0.0014 (process)	5 min	GB, SDMC
CRO_sc1	SD 695 573	411	0.08 (process)	5 min	GB, SDMC
CRO_sc2	SD 693 572	395	0.15 (process)	5 min	GB, SDMC
CRO_sc3	SD 693 572	396	0.015 (process)	5 min	GB, SDMC
CRO_sc4	SD 691 571	370	0.10 (process)	5 min	GB, SDMC
LOS_stock_weir	SD		0.012 (process)	5 min	SDMC
WHI_tree	SD 660 547	208	0.06 (process)	5 min	TP
WHI_tree_weir	SD 660 546	205	0.06 (process)	5 min	TP
BRE_rhw	SD 631 558	333	2.8 (micro)	5 min	GB, SDMC
BRE_sap	SD 630 557	340	1.7 (micro)	5 min	GB, SDMC
CRO_mid	SD 687 566	248	3.6 (micro)	5 min	SDMC
CRO_sc5	SD 687 567	256	0.5 (micro)	5 min	GB, SDMC
HAR_out	SD 642 566	147	4.9 (micro)	5 min	SDMC
LOS_mid	SD 627 520	188	2.5 (micro)	5 min	SDMC, TP
LOS_out	SD 632 512	165	4.0 (micro)	5 min	SDMC, TP
LOS_stock	SD 627 520	198	1.0 (micro)	5 min	SDMC, TP
BRE_out	SD 653 532	173	11.0 (mini)	15 min	GB, SDMC, TP
CRO_out	SD 712 525	137	21.1 (mini)	5 min	GB, SDMC
EAS_out	SD 708 503	134	13.3 (mini)	5 min	None
LAN_mid	SD 631 511	166	15.0 (mini)	15 min	SDMC, TP
LAN_out	SD 659 493	117	27.7 (mini)	15 min	SDMC, TP
LOU_out	SD 649 431	87	47.3 (mini)	15 min	None
WHI_mid	SD 661 546	205	10.0 (mini)	5 min	SDMC, TP
WHI_out	SD 653 532	178	13.6 (mini)	15 min	SDMC, TP
HOD_mid	SD 663 500	116	110.3 (meso)	5 min	GB, SDMC, TP
Baro Footholme	SD 653 532	176	-	5 min	-
Baro Croasdale	SD 687 566	249	-	5 min	-
Baro Losterdale	SD 627 522	217	-	5 min	-
Baro Loud	SD 649 431	90	-	15 min	-

The *Eijkelkamp Agrisearch* (*Slumberger)* pressure transducers (DIVERS) have an integral battery & logger. The benefits of these DIVERS are their robustness, inexpensiveness, ease of use, and unobtrusiveness. The main disadvantage is that their data need to be corrected for barometric pressure (see below), using barometric pressure transducers that are housed in dry air wells (Table 4.5). Other small disadvantages are that divers need to be taken out of their position to download the data and have minor temperature dependence.

4.5.2 Data Processing and Data Quality Control

The raw diver data comprise water temperature (T) and pressure (P_d). P_d Is the sum of the pressure exerted by the water column and atmospheric pressure (P_b). To obtain stage data, P_d needs to be corrected for P_b, which is measured by the barometer. A second issue with the divers is that they are slightly sensitive to temperature and are calibrated only between 15 and 35°C (Slumberger Water Services, 2010). As T is generally <15°C for most of the year, the conversion of raw diver data to stage should take this into account.

Every time the site of a stream gauge was visited, a manual measurement of stage, relative to a fixed local datum (the top of the tube of the gauge), was taken. These manual measurements were done over a range of stage and temperature values and further used to calibrate the raw diver data correction procedure. To reduce effort and errors, the raw data compensation process was automated and software developed within project SC060092 for the Environment Agency (Ewen et al., 2010) was used. Equation 4.9 gives the compensation equation for obtaining stage (h) in m, where parameters a and b are calibrated based on the manual measurements.

$$h = a + 0.01(P_d - P_b) + bT \qquad \text{(Equation 4.9)}$$

In Equation 4.9 P_d and P_b are in cm, which explains the 0.01 multiplier. a Adjusts the data relative to the datum and bT compensates for temperature.

Ewen et al. (2010) found that the maximum errors after compensation occurred during summer low flows (Appendix D, Ewen et al., 2010). Overall, the errors generally decrease for sites with larger catchment areas. They also recognized that the errors decrease with the number of manual measurements made.

To evaluate the overall quality assurance of the diver data and their raw data correction procedure (Equation 4.9), a comparison was made with independent stage data. Alongside the diver stream gauge at LAN_mid an *ISODAQ* FROG RX GSM/GPRS telemetry logger with an *Impress* depth level pressure sensor was installed on 24th April 2010. Unlike the diver pressure sensor, the FROG logger cable has an integrated air tube for atmospheric pressure reference, which avoids the need for a separate

barometer gauge and the associated data corrections. However, a disadvantage of the frog loggers is that the vent must not be submerged.

In Figure 4.13, over 2000 corrected diver stage data are plotted against frog stage data (>0.1 m) at LAN_mid. With a slope of 1, the regression (R^2 = 0.993; standard error = 0.0078) shows a good relation between the two equipment types for measuring stage. The offset is caused by the difference in datum for each of the gauges. For a given stage the error is < 0.04 m and there is no bias with stage. From the plot in Figure 4.13, it may be concluded that the data obtained from the divers and the associated data correction procedure are in good agreement with the frog logger data.

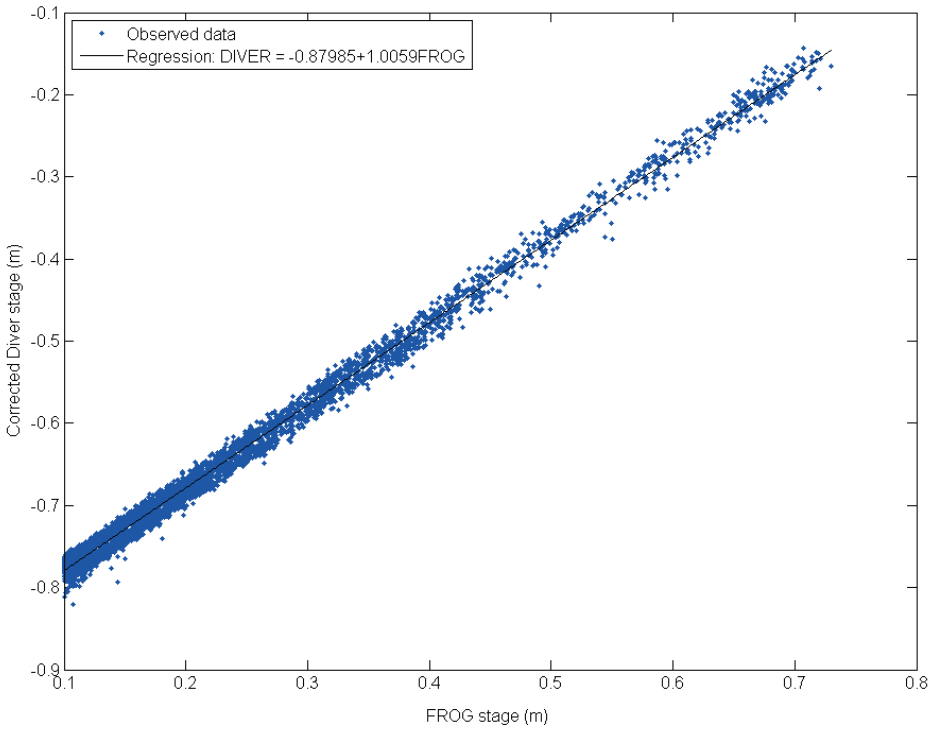

Figure 4.13 Frog and diver stage data comparison at LAN_mid

4.5.3 Rating Curves

The NU gauges produce stage data only. However, discharge data are required for data analysis and modelling purposes. The establishment of a reliable relationship between stage and discharge is difficult and takes time, especially for flashy streams where the highest flows are of short duration and predictable with only short notice. Considerable work was done to obtain stage-discharge relationships (or rating curves) for each individual gauge.

Discharge Gauging for Calibration

Rating data were obtained through the velocity-area method of streamflow measurement using current meter gauging. In the UK, this is one of the most widely used techniques for the establishment of stage discharge relationships (Whalley et al., 2001) and around 90% of the gauged rivers in the world depend on this method (Shaw et al., 2011).

For process and micro scale sites, a *Valeport* electromagnetic current meter (model 801) was used at approximately ten selected verticals (depending on the stream width and the time available) to measure the average velocity ($\bar{v}$ in m/s). Measurements were taken over at least 30 s, at 0.6 of depth from the surface (d in m) across the cross section of the stream. It is sometimes suggested that more than one measurement should be made in the vertical (e.g. at 0.2 and 0.8 of the depth). However, Whalley et al. (2001) found that the error introduced by a reduction in the number of points in the vertical is within the error to be expected from a current meter gauging, so in order to save time, this was not done. The error of the gauging does increase exponentially with a reduction in the number of verticals across the cross section (Whalley et al., 2001), hence this was never compromised. The discharge was then calculated through the 'mean section' method (Shaw et al., 2011) using Equation 4.10:

$$Q = \sum q_i = \sum \bar{v}a = \sum_{i=1}^{n} \frac{(\bar{v}_{i-1} - \bar{v}_i)}{2} \frac{(d_{i-1} - d_i)}{2} (b_i - b_{i-1}) \quad \text{(Equation 4.10)}$$

where b_i is the distance (m) of the measuring point (i) from the bank, and there are n subareas.

For the mini and meso scale sites, in addition to the method described above, a mobile *Teledyne* RD Stream Pro ADCP (Acoustic Doppler Current Profiler) was used that, when pulled across the stream surface, automatically produces numerous velocity profile verticals along the river width. As it also detects the proportions of the river bed, it automatically generates a discharge value for the time of gauging. At least 3 cross-sections were done for every gauging and an average value was used for the rating curve calibration.

For every discharge gauging, a manual measurement of stage was made in order to obtain stage discharge sets that could be used in the calibration of the rating curve. In excess of 170 discharge measurements were performed at different stages for 21 stream gauges (excluding the two sites at which a weir superseded the original gauge), which gives on average approximately eight calibration stage-discharge data sets for each rating curve.

Establishment and Extrapolation of Rating Curves

The most common technique used to obtain a stage discharge relationship from the calibration measurements is the logarithmic method, where a linear regression is fitted through the stage and discharge data in log space (Herschy, 1995). Accordingly, the rating curve is often represented by some form of the following equation:

$$Q = a(c + h)^b \qquad \text{(Equation 4.11)}$$

where Q is the discharge in m^3/s, h the stage of the water in the river in m, c is a datum correction, and a and b are constants, which are characteristic for the specific site (Herschy, 1995; Shaw et al., 2011). Typical values for b range from 1.5-2.5 (Herschy, 1995).

This logarithmic method is suitable for the part of the stage range for which calibration data are available. However, it is suggested that it may be less appropriate for extrapolation purposes. Especially near the extreme lower and upper ends of the stage range, the logarithmic fits often provide discharge values that are unrepresentative of the actual hydraulic conditions at the site (Herschy, 1995; Whalley et al., 2001).

Several alternative methods have been developed to improve the extrapolation of the rating curves. According to Herschy (1995), the best method for extending rating curves is the Stage-Velocity-Area (SVA) method. In the SVA method, the discharge is calculated according to:

$$Q = v * A \qquad \text{(Equation 4.12)}$$

where v is the mean velocity of the entire cross section in m/s and A is the wetted area of the cross section in m^2. Both the wetted area and the velocity increase with stage. However, at higher stages the rate of velocity increase quickly diminishes and a

maximum velocity is reached. Depending on the channel properties, for UK upland channel networks, the maximum velocity is about 1.5 – 2 m/s (Beven, 1979; Beven et al., 1979; Herschy, 1995).

For the SVA method, the wetted area for each stage can be obtained from a field survey study. There are two main options to establish the mean velocity for each level of stage. Firstly, for a given stage, the mean velocity can be approximated as a function of the channel roughness and the slope of the water surface, e.g. according to the Manning equation method, using Manning's n for roughness (Leonard et al., 2000) or the Stevens method, using Chezy's C for roughness. As the roughness changes with stage, these roughness parameters need to be determined for the full range of stage, to obtain a full velocity profile. Although labour intensive, this method can be useful in the absence of observed stage/mean velocity data. However, the establishment of appropriate values of n and C requires skill and experience and is subject to uncertainties (Herschy, 1995; Fisher and Dawson, 2003; Owen, 2008). Alternatively, the relation between stage and mean velocity can be calibrated, using calculated velocities of the observed stage/area - discharge data pairs (Herschy, 1995), based on Equation 4.12. This method fully utilises the available data and avoids the need for estimations of roughness parameters. However, it does not provide the data for the stage range of interest for high flows. Ewen et al. (2010) developed software that can be used to obtain extended rating curves through the SVA method, that makes use of a calibrated velocity equation, with a sigmoid function that varies smoothly between the minimum and maximum set velocities (e.g. 1.5 m/s). A sigmoid velocity profile is normal for relatively shallow, steep, cobble and boulder bed streams in mountainous areas (e.g. Marchand et al., 1984; Bathurst, 1988), such as in the Hodder catchment. Simultaneously, the optimisation of the rating curve also aims to preserve mass balance using abstraction, evaporation and precipitation data from the nearest gauge. This is done by checking the water mass balance for a specific period (e.g. a hydrological year) for which zero changes in storage are assumed.

The two main different rating curve extrapolation techniques (the Logarithmic rating curve method, and the SVA method implemented through the Ewen et al. (2010) software as described above) have been applied to the CRO_out stage-discharge data

pairs set as an example. Figure 4.14 shows the cross section for CRO_out (21.1 km^2), with the observed stage range, the available discharge gauging data, and the upper 95 and 99 percentiles of the observed stage data over the full data availability period. These percentiles give an indication of the range of the highest flows. The cross-section is fairly regular, apart from two minor breaks in the profile, one at a height of approximately -0.5 m and the other at approximately -0.1 m.

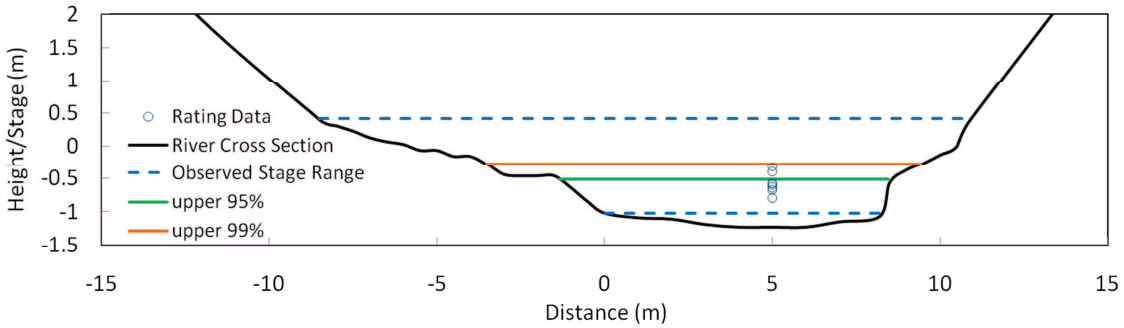

Figure 4.14 River cross section, stage of available discharge measurements, observed stage range, and the upper 95 and 99 percentiles of stage at CRO_out

Figure 4.15 shows the rating data and the extrapolated discharge values against stage for the SVA (solid black line) and the logarithmic (solid red) methods. For the relatively low stage range (-1.2 to -0.4 m) both methods give similar discharge predictions. However, for the stage range > -0.4 m, the logarithmic method predicts much higher values of discharge than the SVA method and these differences increase with stage. When the stage-velocity relationships (dashed lines in Figure 4.15) are plotted for these two methods, it becomes clear that the SVA method provides far more realistic values of velocity (and hence discharge) than the logarithmic method. For the highest observed stages, the logarithmic method predicts cross sectional average velocities of 2-7 m/s, which is highly unphysical as maximum average flow velocities in UK upland channel networks are in the region of 1.5 m/s (Beven, 1979; Beven et al., 1979).

For all stream gauges, rating curves have been extrapolated using the SVA method, implemented through the software described by Ewen et al. (2010), as it predicts realistic discharge values representing the hydraulic conditions while preserving mass balance. The cross sections, discharge gauging data and the extrapolated rating curves for each stream gauge are given in Appendix 1. Some information on the rating data and their relation to the observed stage range is also given.

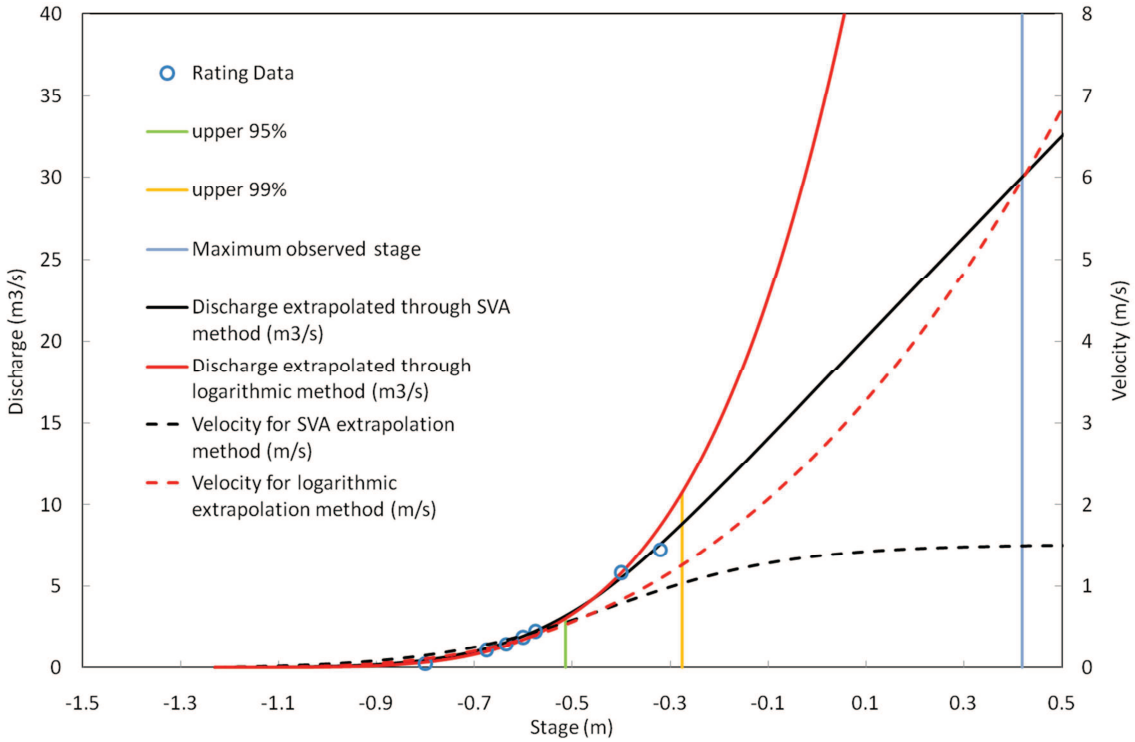

Figure 4.15 Discharge and velocity for the SVA and the logarithmic stage-discharge extrapolation methods shown for the observed stage range at CRO_out

Uncertainties and Quality Control

Uncertainty in the rating curves is composed of the following:

1. Data uncertainty
2. Uncertainty in the inter- and extra-polation of the rating curves
3. Temporal uncertainty

The data uncertainty is caused by errors in the stage observations and calibration measurements. The uncertainty in the extrapolation of the rating curves is, undoubtedly, the largest of the three kinds of uncertainty. However, as described in the previous section, attempts are made to reduce this error. The temporal uncertainty in the rating curves is caused by erosion and deposition and the modifications they make to the geometry of the river bed and cross section (e.g.Jalbert et al., 2011; Westerberg et al., 2011). However, the movement of sediment along the river bed has relatively more effect on the lower end of the rating curve. Considering the scope of the study, this is less of a concern.

Given the relatively small number of calibration points, it is inappropriate to attempt a full statistical uncertainty analysis for the rating curves of each gauge, for example

such as suggested by Di Baldassarre and Montanari (2009) and Herschy (1995). For a statistically acceptable uncertainty analysis, at least 20 current meter observations or more should have been available in each range (Herschy, 1995). However, it is possible to check the consistency between flows in nested subcatchments of the NU gauges and those of EA gauges (Figure 4.16), which have well established and calibrated rating curves with less potential errors as they involve concrete structures. Assuming uniform precipitation and catchment behaviour over the nested catchments, the observed daily specific discharge (mm) of nested gauges in Figure 4.16 are expected to fall on the 1:1 line in the case that all rating curves of the gauges are correct. The daily data in Figure 4.16 are for the period 04/10/2008 – 12/08/2010 (678 data points). Although a high level of consistency is indicated by Figure 4.16, some divergence from the 1:1 line is observed for the WHI_mid/Footholme comparison (Figure 4.16, bottom left). This can be explained by the fact that the gauges monitor at different scales and have varying rainfall inputs. Taking that into account, the daily specific discharge data of the NU gauges are in good agreement with those recorded at the EA gauges.

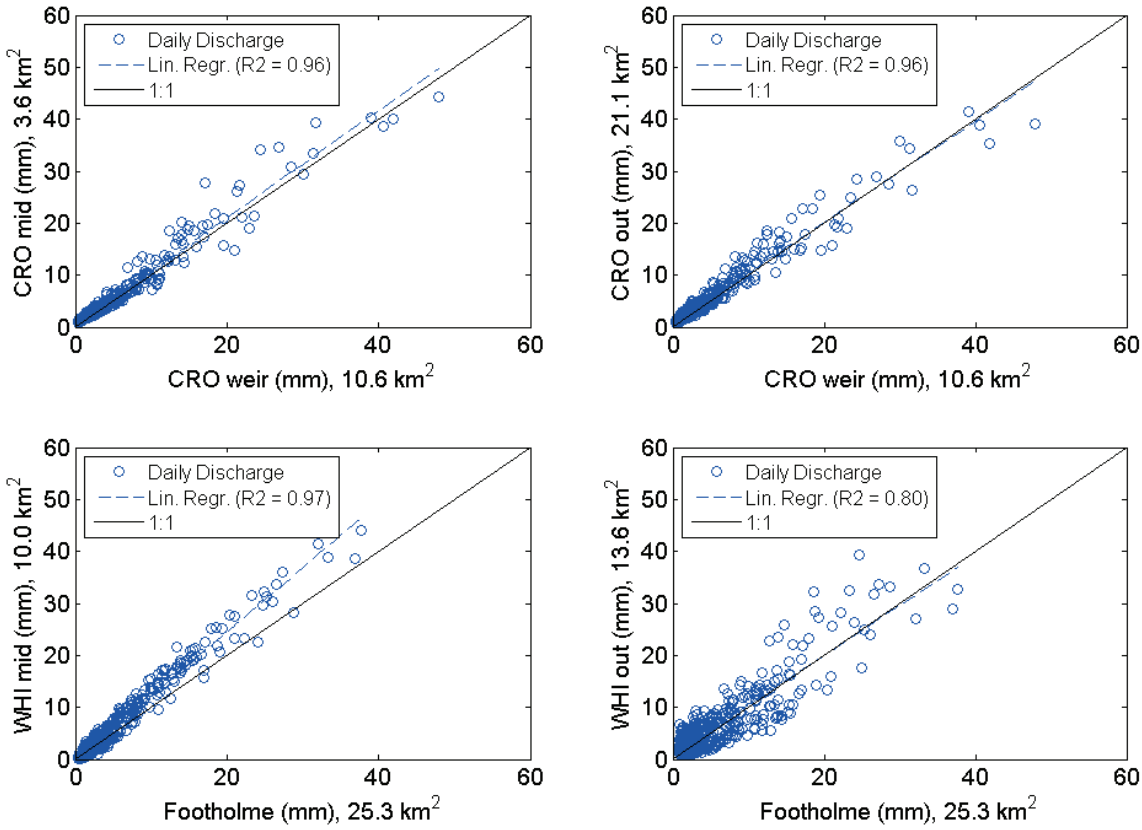

Figure 4.16 Daily specific discharge recorded at Croasdale weir compared to those at CRO_mid (top left) and CRO_out (top right); and at Footholme weir compared to daily discharge at WHI_mid (bottom left) , WHI_out (bottom right). The WHI_mid/Footholme comparison shows a slight, but consistent divergence from the 1:1 line.

4.5.4 Discharge obtained from weirs

As an alternative to creating rating curves for each gauge, thin plate weirs were installed at three small scale sites within the network, according to British Standard 3680. These involve one rectangular weir (LOS_stock_weir) and two v-notch weirs (BRE_grip_weir and WHI_tree_weir). The characteristic shapes of these weirs have a theoretical stage discharge relationship that can be used after some calibration. For the relevant gauges, Appendix 1 provides information on the dimensions of the weirs and the associated equations for the conversion of stage to discharge.

4.6 Data Collection, Data Availability and Overall Quality Control

4.6.1 Data Collection and Data Availability

Data collection took place over the course of more than 2.5 years, from January 2008 to August 2010. The planning and design of the monitoring network was completed during the first few months of the study. However, the full installation was completed only at the end of July 2008 as it took considerable time and effort to obtain installation permission from all parties involved in the area. As described in Chapter 3, the LUMCs in the study catchment were implemented near the end of 2008 and early 2009. Within the present research, it has therefore still been possible to obtain data prior to, during and after the implementation of SCaMP. The maximum pre-change record is 14.5 months.

After the initial field surveys and instrumentation period, the catchment was visited at regular intervals to maintain and download the monitoring network, and obtain discharge gauging data for the rating curves. On average, this involved a 2-3 day trip every 2 weeks over the entire monitoring period (55+ trips).

Figure 4.17 shows the data availability of all the Newcastle University gauges, with the stream gauges in black, the TBR gauges in blue and the AWS in green. As the gauges were not installed simultaneously, the records have different starting points. Data gaps are the result of equipment failures, which occurred especially during the cold winter periods.

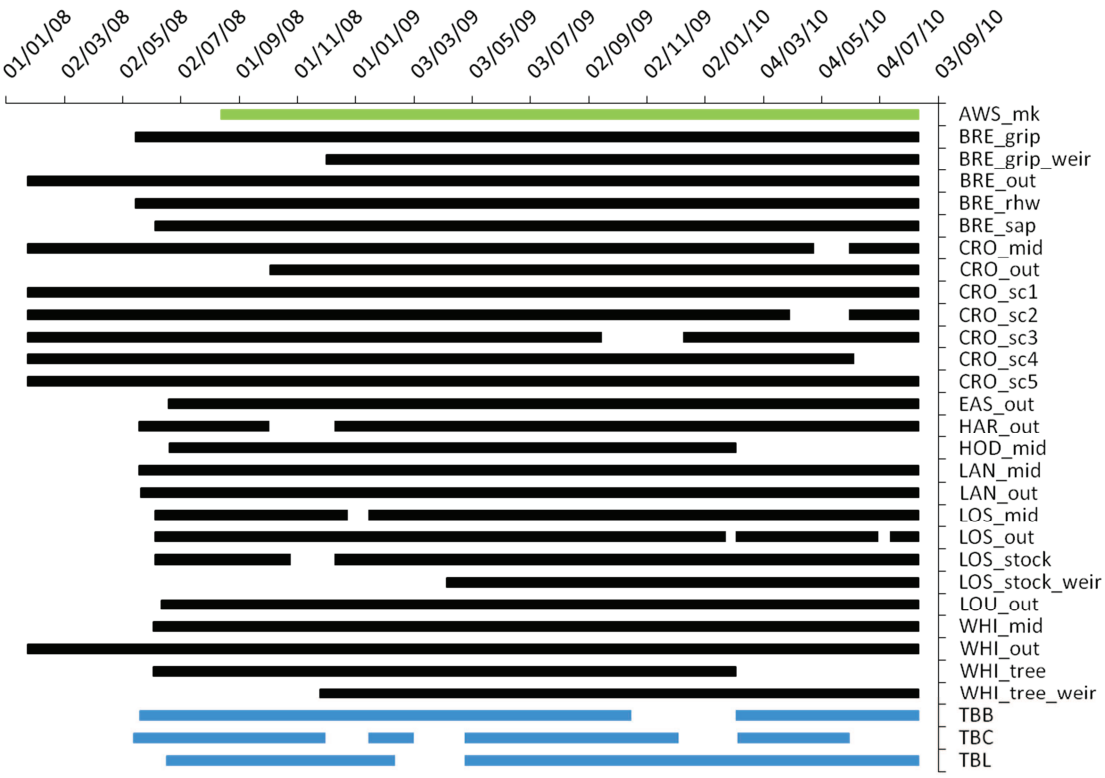

Figure 4.17 Data availability for all NU gauges (AWS = green, Stream Gauge = black, TBR = blue)

Apart from national data sets, hydrological data are usually project specific and unavailable for other researchers. One of the main aims of EA project SC060092 was to share the data collected with other users. All data have been made available through an Electronic Project Record as described by Ewen et al. (2010).

Currently, a skimmed-down version of the monitoring network is in place, which includes stream gauges at the main Hodder subcatchments and at specific sites that monitor the effects of the different land use management changes, all (event based) rain gauges (except TBC), and the weather station.

4.6.2 Water Balance Checks

As described in the previous sections, all gauges were quality assured individually. Insight into the overall quality of the data can be gained through a rough annual water balance check (assuming no leakages or groundwater contributions) of the fully processed data according to Equation 4.13:

$$Q = P - E - A \qquad \text{(Equation 4.13)}$$

where Q is the discharge, P is the catchment precipitation (as described in Section 4.5.3 and Section 4.3.3, respectively), E is the actual evapotranspiration, and A represents the abstractions for water supply (all in mm).

The actual evapotranspiration is here assumed to be equal to the potential evapotranspiration. For the headwaters this may be more acceptable than for the lower lying subcatchments, as the water table of upland peat is near the surface for most of the year (Evans et al., 1999).

Table 4.6 gives an overview of these water balance checks for all gauges for the 2008-2009 hydrological year. The abstraction data are not available for all subcatchments and for BRE_out and WHI_out there are no discharge data available for relatively dry days. It is therefore not possible to obtain full water balances for every site. For those sites where all data are available, considering the assumptions and data uncertainties mentioned in previous sections, the water balance is generally acceptable as Q is plus or minus 10% of $P - E - A$ for all subcatchments (column 8 in Table 4.6). However, it has to be noted that this is not a fully independent test, as preserving mass balance is part of the rating curve calibration procedure. However, the data in Table 4.6 do allow for an overall evaluation of the data values in relation to each other.

It is expected to find annual runoff ratios (Q/P or $(Q + A)/P$) between 0.7 and 0.8 for upland peatland process-mini scale catchments in the UK (Holden and Burt, 2003c). However, some UK upland catchments can reach runoff ratios in excess of 0.9 (Newson, 1981). In general, for catchments in Northwest England, the runoff ratios are between 0.5 and 0.75 (Ward, 1981). The runoff ratios in column 10 of Table 4.6 agree well with these figures, with generally higher values for the process and micro scale upland catchments (0.78-0.86) than the for the mini scale catchments (0.69-0.76).

From these final water balance checks, it is concluded that the error in the hydrometric data is relatively small, considering the simplifying assumptions made for the water balance, the time available for the discharge gauging and the common errors associated with a hydrometric network such as the one described here.

Table 4.6 Overall Water Balance Checks for the 2008-2009 hydrological year for all stream gauges

Location Code	Scale	Catchment Elev (m)	Q (mm)	P (mm)	E (mm)	A (mm)	Q/(P-E-A)	E/P	(Q+A)/P	Notes
BRE_grip	Process	385.0		1745.0	413.0	-		0.24		-
CRO_sc4	Process	450.0	1845.4	2208.8	413.0	-	1.03	0.19	0.84	-
WHI_tree	Process	297.0		2165.4	413.0	-		0.19		-
BRE_rhw	Micro	430.6	1415.0	1805.1	413.0	-	1.02	0.23	0.78	-
BRE_sap	Micro	444.0	1488.1	1822.8	413.0	-	1.06	0.23	0.82	-
CRO_mid	Micro	408.5		2171.1	413.0	-		0.19		-
CRO_sc5	Micro	401.6	1751.7	2138.6	413.0	-	1.02	0.19	0.82	-
HAR_out	Micro	342.1	921.4	1385.0	379.4	YES/NA	NA	0.27	NA	Data from 17/12/2008 00:00
LOS_mid	Micro	334.3	1711.9	1997.7	413.0	-	1.08	0.21	0.86	-
LOS_out	Micro	315.3	998.2	1988.6	413.0	YES/NA	NA	0.21	NA	-
LOS_stock	Micro	325.0		2001.5	413.0	-		0.21		-
BRE_out	Mini	365.5	NA	1861.7	413.0	192.6	NA	0.22	NA	-
Croasdale weir	Mini	350.9	1553.1	1640.4	413.0	-	0.95	0.20	0.76	-
CRO_out	Mini	291.6	1426.6	1867.9	411.4	-	0.98	0.22	0.76	Data from 03/10/2008 09:05
EAS_out	Mini	227.9	1085.2	1505.5	413.0	-	0.99	0.27	0.72	-
Footholme	Mini	367.6	1169.0	2010.2	413.0	248.4	0.87	0.21	0.71	-
LAN_mid	Mini	377.9	1447.3	2085.2	413.0	81.0	0.91	0.20	0.69	-
LAN_out	Mini	342.3	1480.3	2027.7	413.0	YES/NA	NA	0.20	NA	-
LOU_out	Mini	167.4	1026.9	1364.3	413.0	-	1.08	0.30	0.75	-
WHI_mid	Mini	382.4	1241.9	2122.0	413.0	386.0	0.94	0.19	0.77	-
WHI_out	Mini	369.4	NA	2126.3	413.0	306.3	NA	0.19	NA	-
HOD_mid	Meso	261.1	1062.2	1712.0	413.0	YES/NA	NA	0.24	NA	-
Hodder Place	Meso	244.1	1037.9	1636.9	413.0	YES/NA	NA	0.25	NA	-

4.7 Summary

A multiscale nested monitoring design was set up in the Hodder catchment to monitor the effects of UU's SCaMP land use/management changes on the hydrological behaviour of the Hodder catchment at a range of scale. For this, the experimental design focussed on dense monitoring of flow, precipitation and evapotranspiration. It did not include the monitoring of local internal catchment variables, which are typically associated with large heterogeneities, making it difficult to scale such local information. The full monitoring network comprised 28 stream gauges, seven tipping bucket rain gauges, and a weather station. The rain gauges were spatially distributed throughout the catchment while providing a good spread over the elevation range. An automatic weather station was placed in the upper part of the catchment to provide data for calculation of potential evapotranspiration. The nested stream gauges were placed in such a way that it was possible to monitor the flood hydrograph from the process scale to the meso scale. The project involved an extensive field campaign. The data are available for approximately 0.5-1 year before and 1-1.5 year after the implementation of the land use/management changes. Quality control checks of all types of gauges individually and one of the overall data showed acceptable data results within the range of error that is expected.

5 Change Detection Analysis of Land Use/Management Change Impacts at Increasing Scales

5.1 Introduction

This chapter describes the data analysis of land use/management change (LUMC) effects at increasing scales. For this, a large amount of high quality data has been collected, as described in the previous chapter. Nevertheless, these data cover only a relatively short period of time. There is approximately 6-12 months of data prior to and about 20 months of data post the implementation of the LUMCs available from the full monitoring network. However, Chapter 4 showed that a few EA stream and precipitation gauges have been monitoring the hydrological conditions of the Hodder catchment at several sites for a much longer period of time. The Footholme (25 km^2) (FH) and Hodder Place (261 km^2) (HP) have the most complete long term data records and are therefore of specific interest. The FH and HP data are used here to investigate the longer term natural variability in meteorological and hydrological conditions, in which the detection of changes, potentially related to land use/management changes, should be considered (Section 2). Section 2 also briefly discusses the post-change hydrological conditions and puts them into context of the variability between pre-change hydrological years. The challenge is to detect potential effects of land use management changes within the context of natural variability. In Section 3, tests are performed on the longer term FH and HP data sets in order to examine the prospects of applying different change detection techniques to the short term datasets. The 'best' of the evaluated change detection techniques is then applied to the short term data records at a range of scales, to determine whether any changes to the hydrological regime can be detected as a result of the SCaMP LUMCs (Section 4). Finally, a summary is given at the end of the chapter in Section 5.

5.2 Natural Variability in Hydrological Conditions and Catchment Response

Before the potential effects of LUMC on the hydrological behaviour of any catchment can be considered, especially when only relatively short term data records are available, an analysis of the natural variability of the hydrological conditions and catchment behaviour is needed.

This section has two main aims. The first is to show the year to year natural variability in meteorological conditions and hydrological response for a mini scale subcatchment (FH) and the meso scale Hodder catchment (HP). This information can then be used in Section 3 in order to evaluate to what extent the different change detection techniques are sensitive to the natural variability. The second aim is to put the post-change hydrological year (2009-2010) into the context of the natural variability of the available data of the pre-change hydrological years. It is essential to consider this in relation to the short term land use/management change analysis in Section 4.

As the pre- and post-change data records are approximately 1 year in length, it is appropriate to review the variability in catchment response between years in relation to the general meteorological conditions. The full precipitation and discharge records for FH and HP are available only from 2001 (Chapter 4). A complete analysis can therefore include only the data from then onwards. Longer meteorological data records are available, which are presented to put the more recent climatic conditions into a longer term context.

5.2.1 Meteorology

Figure 5.1 gives an overview of the annual precipitation, annual snow lying days, annual days with ground frost, and the monthly average temperature for the average of the 5 km^2 grid cells covering Footholme (left) and Hodder Place (right). Average values for the 1981 to 2009 period are also given. These data are mainly obtained from the Met Office 5 km^2 gridded data sets (UKCP09 dataset 1981-2006 (Perry and Hollis, 2005)). The Metoffice data post 2006 include only the monthly temperature, snow lying days and days of ground frost. The annual precipitation record post 2006 was unavailable and is therefore complemented with data from EA gauges situated in the Hodder catchment (see Chapter 4). The EA data source is available only from 2001, but

is considered to be more accurate (the Met office uses regression and interpolation of selected gauges, also situated outside the catchment (Perry and Hollis, 2005)). A comparison of annual precipitation obtained through the Met Office and the EA was made for the 2001-2002 to 2005-2006 years to check if they give comparable records. For Hodder Place, the data from these sources was comparable, as the average precipitation of the Met office gridded data was within 3% of the precipitation calculated with the data from the EA rain gauges. For Footholme, the Met office data showed an average (consistent) underestimation of 18% compared with the EA gauges. This shows that it is unacceptable to assume that the data from the two different sources are equivalent. The Met office data record is much longer and hence should be used. The Footholme precipitation data in Figure 5.1 prior to 2001 therefore consist of Met Office data, corrected for the 18% difference with the EA data, in order to compare the precipitation between years.

The annual precipitation at Footholme (for 1981-2009) ranges from 1299 to 2645 mm and has an average value of 2076 mm. For Hodder Place, the figures are 1032-2129 and 1643 mm, respectively. Figure 5.1 (A) shows that the pre-change precipitation data from 2001 to 2008 for these two catchments include both dry (e.g. 2002-2003) and wet (e.g.2006-2007) years, relative to the average. The post-change hydrological year (2009-2010) is relatively dry, though not as extreme as 2002-2003.

The bottom three data sets (B-D) in Figure 5.1 together give an idea about the winter conditions of each hydrological year. Cold years that endure many snow lying days and days with ground frost tend to have more and prolonged storage capacities in the form of snow and/or ice. The hydrological responses are therefore likely to be different during times when part of the catchment storage is solid and unable to move freely. Also, snow melt water, especially in combination with rain on melting snow, can result in rapid discharge increases, different from catchment responses under normal conditions. From Figure 5.1 it can be seen that there is large variability between years in the annual snow lying days, ranging from 1 to 45 for FH and from 1 to 37 for HP. All 2001-2008 pre-change years are below average (approximately 12 days for both catchments). However, the post-change hydrological year has the most snow lying days on record for both FH and HP.

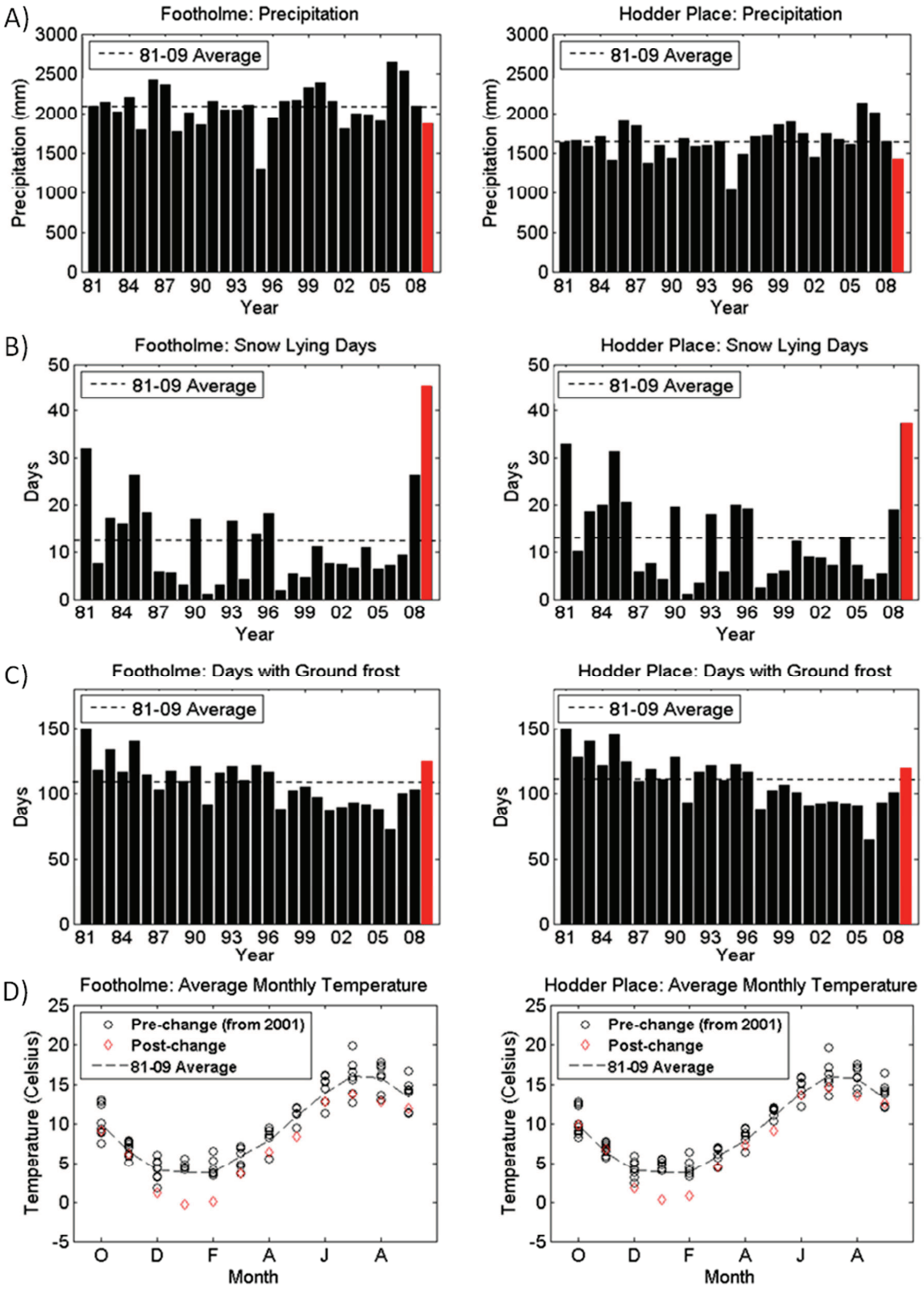

Figure 5.1 Climatological conditions for Footholme (left) and Hodder Place (right), A: annual and average annual precipitation, B: annual and average annual snow lying days, C: annual and average annual days with ground frost, D: pre-, post- change and average monthly temperature. The annual data are presented for hydrological years. The pre-change years are shown in black, the post-change year in red.

The days with ground frost for 2009-2010 are also above average (approximately 110 days for both catchments). The temperatures, especially during January and February 2010, are below average. In contrast, the 2001-2008 records show relatively little snow lying days and generally above average winter temperatures. Overall, the post-change hydrological year experienced more harsh winter conditions compared with the 2001-2008 pre-change years. It was also relatively dry, but the total precipitation lies within the range of annual precipitation natural variability. It should be noted, though, that there is the possibility of an underestimation of the precipitation during the post-change year, considering the potential errors in precipitation records associated with snow (as discussed in Chapter 4).

5.2.2 Catchment response

Figures 5.2 and 5.3 demonstrate some of the natural variability in flow. For each hydrological year post 2001, Figure 5.2 shows the observed runoff range on the x-axis and the mean annual runoff rates on the y-axis. In addition, these data are plotted in black for the total observed flow record (from 1995 and 1990 for FH and HP respectively). Compared with Hodder Place, Footholme has higher annual mean runoff rates (in mm/hr) and a larger range in the observed flows. The differences in annual mean runoff rates between years are similar for each gauge. For HP, the largest observed runoff ranges generally coincide with higher annual mean runoff rates (Figure 5.2, right). This is different for the FH record. For example 2004-2005 (pink) and 2005-2006 (light blue) show below average (black) annual mean runoff rates, but the maximum observed flows are much higher than for 2006-2007 (green) or 2007-2008 (yellow), where maximum annual mean runoff rates are observed (Figure 5.2, left).

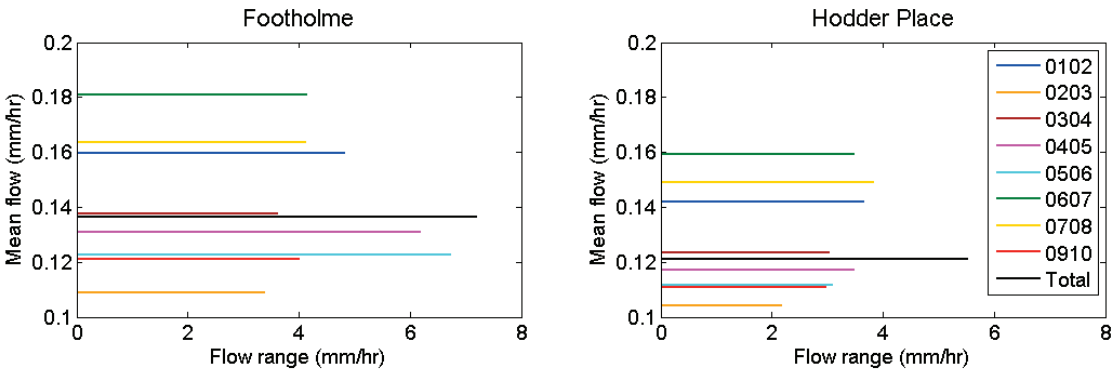

Figure 5.2 Flow range and mean annual runoff rates for FH (left) and HP (right)

Figure 5.3 shows the bottom part of the flow duration curve (flow < 1 mm/hr) for each year. Flows above 1 mm/hr occur for approximately 2% of the Footholme flow record, and 1.5% of that of Hodder Place. Again, the variability in the annual flow duration curves is larger for Footholme than for Hodder Place (Figure 5.3). In addition, the shape of the flow duration curve has differences between years at FH, while the shape at HP is similar for each year. Overall, Figure 5.2 and Figure 5.3 show that compared with Hodder Place, Footholme is more responsive or 'active' and has a larger natural variability in flow, which is most likely related to the differences in precipitation inputs and catchment area.

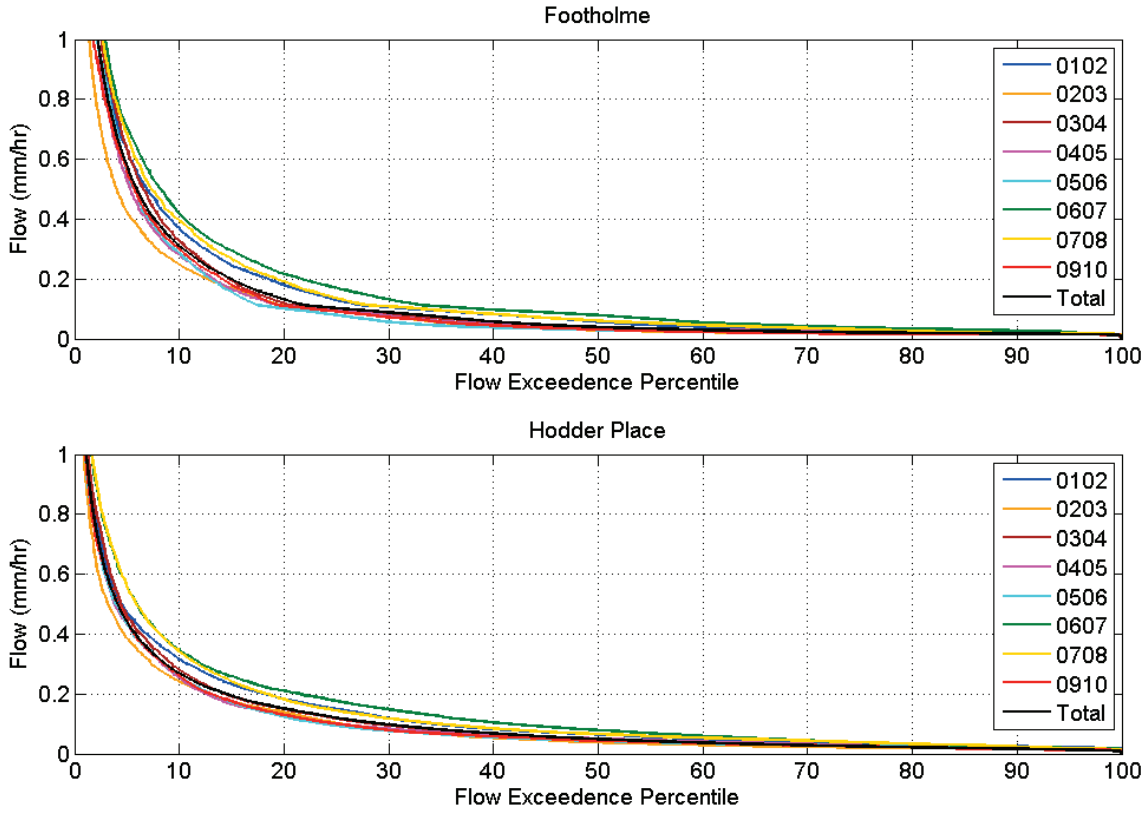

Figure 5.3 Lower part of the annual flow duration curves for FH (top) and HP (bottom)

In theory, if a catchment is not undergoing any major changes that can affect the catchment runoff generation or storage potential, the overall catchment response to precipitation inputs should be similar for each year. Table 5.1 shows the annual precipitation, discharge, evaporation and runoff ratios for FH and HP for 2001-2002 to 2009-2010. The evaporation data are obtained from daily MORECS estimates, proportional to the land use covers (Chapter 3) of the different catchments. The runoff

ratios for FH vary between 0.53 and 0.65 and for HP between 0.61 and 0.72. The lower runoff ratios for FH can be related to considerably higher abstractions in relation to catchment size. For a particular catchment, low runoff ratios coincide with relatively dry years and relatively high evapotranspiration losses. Other variations could be related to differences in the total abstractions upstream.

Table 5.1 Annual Precipitation (P), Discharge (Q), Potential Evapotranspiration (PET) and runoff ratios (R) for Footholme and Hodder Place from 2001-2010

Hydrological Year	Footholme				Hodder Place			
	P (mm)	Q (mm)	PET (mm)	R (-)	P (mm)	Q (mm)	PET (mm)	R (-)
2001-2002	2157	1398	409	0.65	1736	1242	421	0.72
2002-2003	1794	955	445	0.53	1443	912	458	0.63
2003-2004	1989	1210	427	0.61	1732	1085	441	0.63
2004-2005	1984	1148	465	0.58	1659	1025	479	0.62
2005-2006	1898	1074	466	0.57	1600	976	480	0.61
2006-2007	2646	1584	412	0.60	2130	1394	424	0.65
2007-2008	2537	1438	359	0.57	2005	1310	370	0.65
2008-2009	2095	1169	377	0.56	1643	1038	389	0.63
2009-2010	1865	1069	348	0.57	1420	949	363	0.67

In summary, the following years (post 2001) have specific characteristics to be considered in the evaluation of change detection techniques and the LUMC effects data analysis:

- 2002-2003 (orange in Figures 5.2 and 5.3) is the driest year, with relatively low total precipitation, total discharge and mean annual flow (FH, HP)
- 2005-2006 (cyan) has similar total precipitation and catchment response observations as the 2009-2010 post change year (FH)
- 2006-2007 (green) and 2007-2008 (yellow) are the wettest years, with relatively high total precipitation, total discharge, mean annual flow (FH, HP) and a large range in the observed flow (HP)
- 2009-2010 (red) is the post change year and has experienced the most harsh winter on record (FH, HP)

5.2.3 Short term data overview

An overview of the short-term data availability of the full monitoring network is given in Chapter 4. Here, some of those data are presented in order to show the pre- and

post- change records along with the occurrences of the different LUMCs and any other peculiarities during the monitoring period for which the network was fully operational (August 2008 – August 2010). Note that the definition of the pre-change and post-change periods is variable for different subcatchments, as the LUMCs have not occurred simultaneously throughout the catchment (see Chapter 3 and Appendix 1).

As an example, Figure 5.4 shows the hourly catchment precipitation (blue) and discharge (black) for two nested sites at the micro and meso scale for the duration of the monitoring period. The threshold of ten times the mean discharge recorded at the gauge during the full monitoring period (indicated by the dashed black line) is shown to highlight the largest events for each catchment. The figure also shows the incidents of LUMCs (dark grey) and snow lying days (light grey) during the monitoring period.

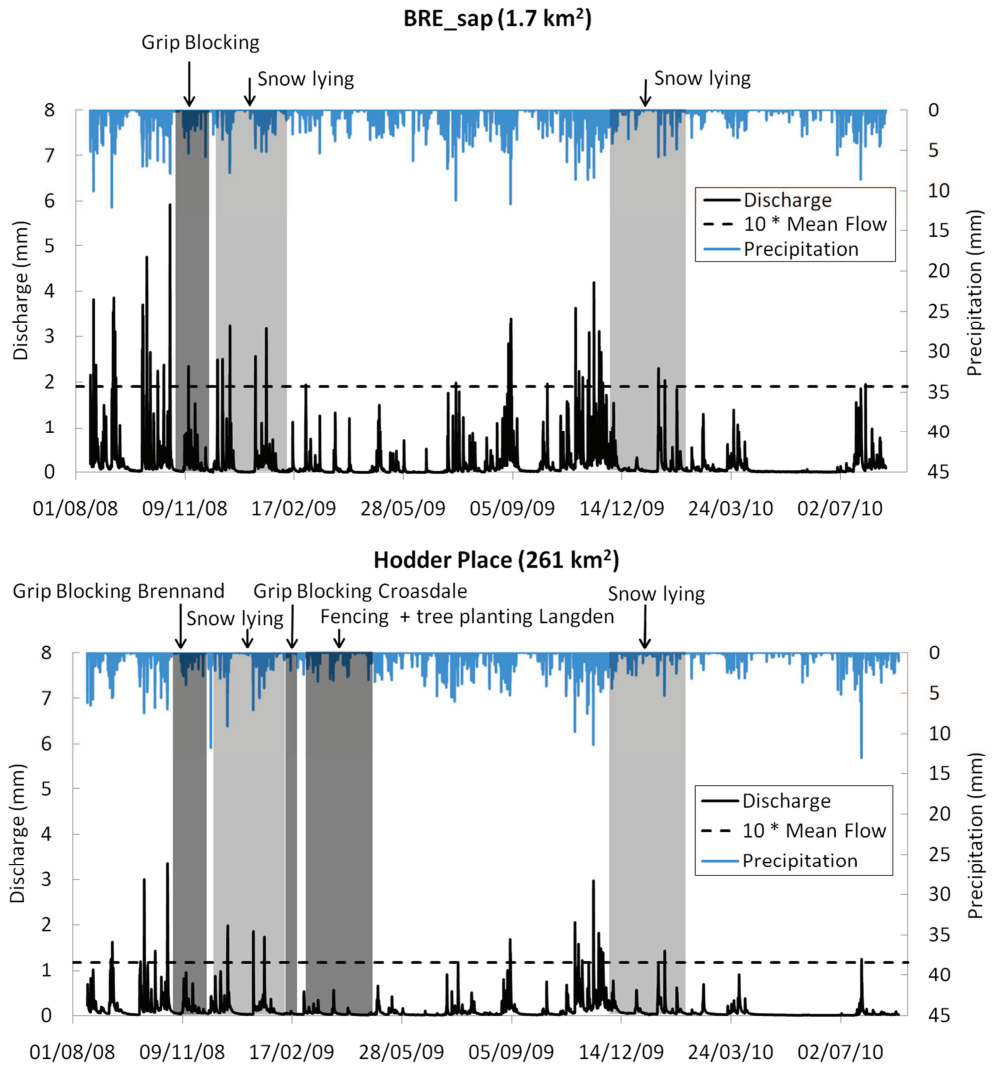

Figure 5.4 Discharge, 10 * mean discharge, precipitation, and the occurrence of LUMC and show lying days for BRE_sap (top) and Hodder Place (bottom) for August 2008 – August 2010

From Figure 5.4 it is clear that, even though the pre-change monitoring period may be relatively short, for both catchment scales, there are at least four events with peak flows higher than 10 times the mean flow. In fact, the largest event during the period August 2008- August 2010, was recorded during the pre-change period (at 26/10/2008). For all gauges, care must be taken when peak flows are studied during periods with snow lying days (see Chapter 4). In addition, the period from April to June 2010 was relatively dry (Figure 5.4). Figure 5.4 also shows higher specific discharges and flashier catchment behaviour at the micro scale than at the meso scale. The catchment precipitation between scales is also different with generally more precipitation which is also more intense, at the micro scale in the upper part of the catchment.

5.3 Evaluation of Change Detection Techniques Using Long Term Mini and Meso Scale Hodder Data

Section 5.2 showed that there is considerable variability in the natural meteorological conditions and catchment response between hydrological years. As the lengths of the short term pre- and post-change records are of the same time scale (i.e. approximately 1 year), it is important to evaluate potential change detection techniques for their sensitivity to this natural variability. Note that from here on, the 2001-2008 dataset is defined as the long term pre-change record. To test the capabilities of different data analysis methods, first, the Footholme and Hodder Place post 2001 historical records are divided into yearly (Oct – Sep) periods. Subsequently, two different data driven models are applied to these individual periods. The underlying assumption is that if a model is relatively insensitive to natural variability, the estimated model parameters describing the catchment response will be the same (or very similar) for all yearly periods for which the catchment has been in the same 'state' (i.e. no catchment changes occurred between or during any of these periods). Correspondingly, if LUMCs significantly affect the catchment response, this will be reflected in the parameter estimates of the post-change period of these models. In addition, if a model is relatively insensitive to natural variability, no LUMC impacts will have been detected if the post-change period can be accurately predicted with the pre-change model parameter estimates.

The two top-down methods that are evaluated are the Data Based Mechanistic (DBM) and the Storage Discharge Detection (SDD) models. From the range of change detection techniques discussed in Chapter 2, these two methods were selected as they 1) are data driven, 2) avoid examining individual hydrographs and allow for the study of systematic catchment behaviour, 3) do not necessarily need long term data records, and 4) have been applied in other studies related to the effects of LUMC on catchment response (e.g. DBM in Beven et al. (2008b), and SDD in Ewen et al. (2010)).

The main aim of this section is to investigate the possibility of using the DBM and/or SDD modelling approaches for the detection of potential changes in the hydrograph characteristics as a result of LUMC on the short term data sets. Additionally, the DBM and SDD models are applied to the post-change hydrological year to explore potential impacts as a result of the SCaMP changes. First, the DBM and SDD models are reviewed separately (Section 5.3.1 and Section 5.3.2 respectively), after which they are compared directly in Section 5.3.3.

5.3.1 Data Based Mechanistic Modelling

DBM Method

The Data Based Mechanistic (DBM) modelling framework is a set of statistical methods that identify linear transfer functions, whose individual components may be interpreted in a conceptual way (e.g. Young, 1992; Young and Beven, 1994; Young et al., 1997; Young and Garnier, 2006). The method involves the use of available data to relate input with output data without the need for prior physical arguments or theories about the processes involved (Beven, 2001b). Part of the process is identifying an appropriate transfer function model order and structure. Here, a summary of the DBM approach, specifically for its use in a rainfall – runoff context, is given. This section also provides a demonstration of how the DBM modelling works in practice, based on an example using data from the catchment outlet at Hodder Place. The DBM analyses are carried out using various estimation algorithms, provided by the Computer-Aided Program for Time-series Analysis and Identification of Noisy systems (CAPTAIN) toolbox, a set of MATLAB functions for non-stationary time series analysis and forecasting (Taylor et al., 2007).

The DBM method is based on a general linear transfer function given by Equation 5.1:

$$y_t = \frac{b_0+b_1z^{-1}+b_2z^{-2}\ldots+b_mz^{-m}}{1+a_1z^{-1}+a_2z^{-2}+\cdots+a_nz^{-n}}x_{t-\delta} + \xi_t \qquad \text{(Equation 5.1)}$$

where x is the model input (in the rainfall – runoff context usually the rainfall (P_t)), y is the model output (commonly the estimated discharge (Q_t)), a and b are model parameters, t is the time-step value, δ is the time lag value (or the delay), z is the backward shift operator, and ξ is the error. The a and b parameters of Equation 5.1 can be estimated based on the refined instrumental variable (RIV) methods as described by Young (1984), provided by the RIV subroutine as part of the CAPTAIN package (Taylor et al., 2007).

The transfer function of Equation 5.1 assumes that the input and output are linearly related. However, it has been argued by others (e.g. Young and Beven, 1994; Young and Tomlin, 2000; Young, 2002; Young, 2003; Romanowicz et al., 2006) that the relationship between rainfall and discharge is actually non-linear. In a natural system other processes, such as evaporation and the antecedent soil moisture (storage) of the catchment, affect the discharge in a non-linear manner. In order to overcome this problem, the authors as above assume that the nonlinearities characterizing the relationship between effective and observed rainfall can be approximated by using discharge (or stage) as a surrogate measure of the antecedent wetness or soil water storage in the catchment. In this way, the effective rainfall (P^*) can be described by:

$$P^* = P_{obs}(cQ_{obs}{}^{\gamma}) \qquad \text{(Equation 5.2)}$$

where P_{obs} and Q_{obs} are the observed rainfall and discharge respectively, and c and γ are coefficients which are unique for each individual P_{obs} and Q_{obs} data set. From Equation 5.2 it is noted that when $\gamma > 0$, a relatively higher proportions of P_{obs} will result as P^* when the catchment is wet. Secondly, a high value of γ will result in large differences in effective rainfall between relatively wet and dry periods.

As noted before, the DBM modelling approach allows for various orders of Equation 5.1, where the final form is driven by the data. The optimal model structure and order (i.e. the values of m and n in Equation 5.1) can be identified by the Young Information Criterion (YIC) and the coefficient of determination (RT2). The YIC is based on how well

the parameter estimates are defined statistically by combining elements of goodness of fit and standard errors on the coefficients, and should be as negative as possible (Beven, 2001b; Young, 2001; Young, 2004). The RT2 value is a statistical measure of how well the model explains the data (Young and Beven, 1994, Appendix 1) and is comparable with the more commonly used Nash-Sutcliffe efficiency in hydrology (following Nash and Sutcliffe, 1970). The RT2 value ranges between 0 and 1. Values that tend towards 1 represent a good fit (i.e. a low variance of model residuals compared with the variance of the data).

In the rainfall – runoff case, the optimal model is commonly a second order model with two parallel linear stores, representing one fast flow pathway and one slow flow pathway (Young, 1992; Young and Beven, 1994; Young, 2002; Young, 2003; McIntyre and Marshall, 2010). For this case, combining Equation 5.1 and 5.2 results in the following model structure:

$$Q_t = \frac{b_0 + b_1 z^{-1}}{1 + a_1 z^{-1} + a_2 z^{-2}} P^*_{t-\delta} + \xi_t \qquad \text{(Equation 5.3)}$$

In order to obtain the description of the two different pathways, the first part of the right hand side of Equation 5.3 can be rewritten as the sum of a quick flow path ($Q_{q,t}$) and a slow flow path ($Q_{s,t}$):

$$Q_{q,t} = \frac{\beta_1}{1 + \alpha_1 z^{-1}} P^*_{t-\delta} \qquad \text{(Equation 5.4.1)}$$

$$Q_{s,t} = \frac{\beta_2}{1 + \alpha_2 z^{-1}} P^*_{t-\delta} \qquad \text{(Equation 5.4.2)}$$

where α_1, α_2, β_1, and β_2 are parameters derived from Equation 5.3.

Some physical meaning may be obtained from the identified transfer function and its parameters; however this should be interpreted with care (Young, 1992; Beven, 2001b). For example, Young (1992) showed that the proportion of effective rainfall going through the slow and quick flow pathways is subject to considerable uncertainty. For the rainfall – runoff application, catchment response characteristics that can be deduced include the lag time (δ), reservoir residence time constants (TC) and the relative contribution of flow of each reservoir (PCT). A schematic illustration of a DBM model with a parallel transfer function structure of two pathways is given in Figure 5.5.

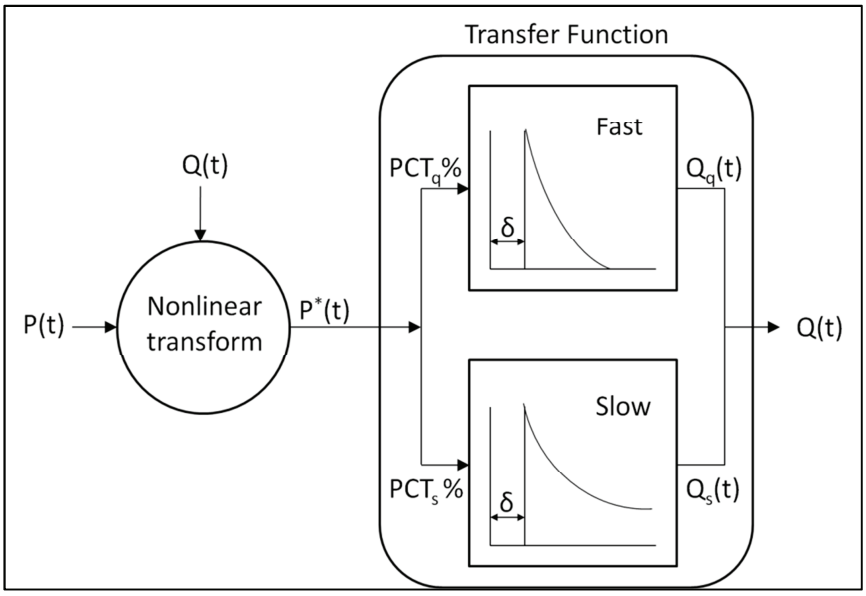

Figure 5.5 Schematic representation of a parallel transfer function structure, with separation of the predicted hydrograph into a fast and a slow pathway (altered from Beven, 2001)

The time constant represents the average residence time and is given by Equation 5.5.1 for the quick reservoir (TC_q) and by Equation 5.5.2 for the slow reservoir (TC_s):

$$TC_q = -\frac{1}{\ln(\alpha_1)} \quad \text{(Equation 5.5.1)}$$

$$TC_s = -\frac{1}{\ln(\alpha_2)} \quad \text{(Equation 5.5.2)}$$

The percentage of effective rainfall that leaves the catchment through the quick reservoir (PCT_q) and the slow reservoir (PCT_s) can be obtained through:

$$PCT_q = \frac{SSG_q}{SSG_s + SSG_q} \quad \text{(Equation 5.6.1)}$$

$$PCT_s = \frac{SSG_s}{SSG_s + SSG_q} \quad \text{(Equation 5.6.2)}$$

where the steady state gain (SSG) is a ratio between the output sum and the input sum of the model and is given by:

$$SSG_q = \frac{\beta_1}{1 - a_1} \quad \text{(Equation 5.7.1)}$$

$$SSG_s = \frac{\beta_2}{1 - a_2} \quad \text{(Equation 5.7.2)}$$

Practical Example

To demonstrate the DBM modelling as used in the current study, an example is given for the catchment outlet at Hodder Place (261 km^2). For this site, some work involving DBM analysis has been done previously (including Young and Tomlin, 2000; Young, 2002; Young, 2003). The data sets used in those studies are hourly rainfall and discharge data for January 1993 (Figure 5.6).

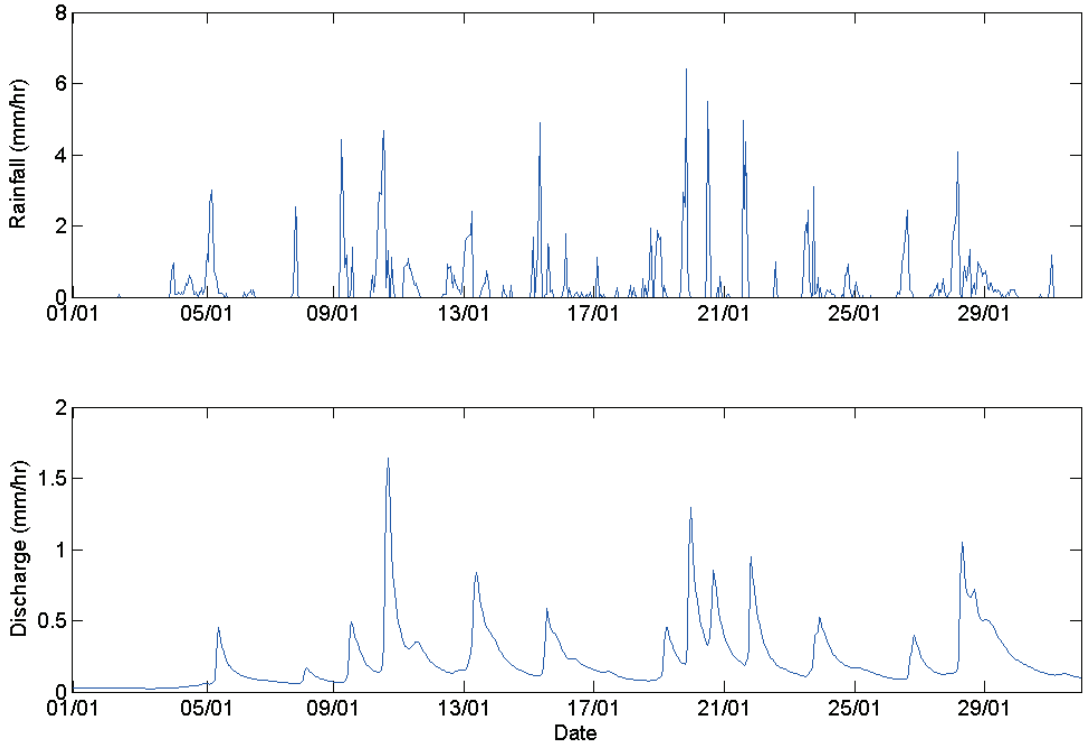

Figure 5.6 Hourly precipitation and discharge data for Hodder Place during January 1993

The rainfall data were based on a Thiessen polygon average of the Croasdale House (0.36), Footholme (0.31) and Chipping (0.33) rain gauges. In order to compare the results of the present study with those of Young and his colleagues in previous studies, the EA data for the same period are used in the current example. This also involves using the standard Thiessen polygon method (excluding the elevation correction, as described in Chapter 4) for the precipitation. The total observed discharge during January 1993 is 164 mm; the total observed precipitation is 230 mm.

First, the relationship between the Hodder Place precipitation and discharge was tested for linearity, and therefore, whether there is a need for using effective rainfall. Assuming in the first instance that rainfall is linearly related to flow, the data were fed

directly through the transfer function model, with use of the refined instrumental variable (RIV) tool of the CAPTAIN package. The best fitted model structure has a YIC value of -8.92 and a RT2 value of 0.80. The optimal model is first order and with a delay of 3 hours for the January 1993 data. Figure 5.7-top shows the observed and simulated discharge (Q_{obs} and Q_{sim} respectively). Figure 5.7-bottom shows the model output compared with the observed data, calculated according to Equation 5.8:

$$Error = Q_{sim} - Q_{obs} \qquad \text{(Equation 5.8)}$$

From Equation 5.8 it is noted that if the model underestimates the observed discharge, the error is negative, and when the model is overestimating, the error is positive.

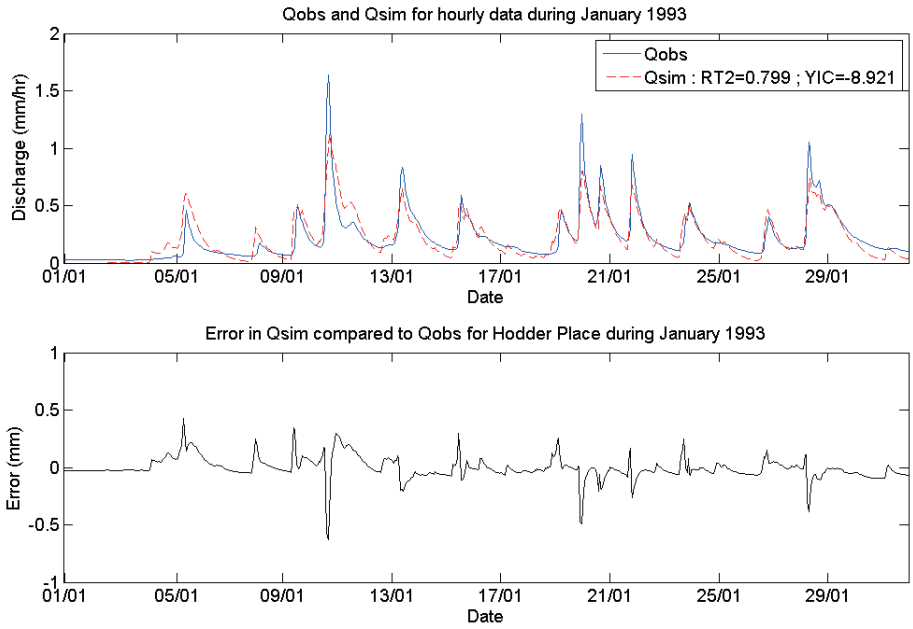

Figure 5.7 Observed and modelled discharge data for Hodder Place during January 1993 using observed precipitation data as the input of the linear DBM model

Figure 5.7 shows that the model fits the data reasonably well, though the majority of the peak flows are underestimated and the recession is too quick. Indeed, it could be concluded that the rainfall might not be linearly related to the discharge, and the model could be improved by using effective rainfall.

The effective rainfall was determined by parameterising the *C* and *γ* coefficients of the effective precipitation within the model structure identification and the optimisation of the parameters of the transfer function. In this way, *C* and *γ* were parameterised

simultaneously with the RIV parameterisation. During this stage, b_0 was always set to 1, so Equation 5.3 can be rewritten as:

$$Q_t = \frac{1+B_1 z^{-1}}{1+a_1 z^{-1}+a_2 z^{-2}} P^*_{t-\delta} + \xi_t \qquad \text{(Equation 5.9)}$$

For a range of delays (0-6), Table 5.2 shows the optimisation results of the other parameters of Equation 5.9 (*C, y, a1, a2,* and *B1).* The best YIC and RT2 values are observed for the parameter estimates with a delay of 3 hrs. The optimisation of with a 3 hr delay also has the smallest mean squared normalised residual (MSNR). The 3hr delay results in parameter estimates $\propto_1$= 0.8612 and β_1=0.9714 for the quick reservoir in Equation 5.4.1, and $\propto_2$= 0.9939 and β_2=0.9714 for the slow reservoir in Equation 5.4.2.

Table 5.2 Optimisation results for the January 1993 data for a range of delays (0-6 hrs)

Delay	C	γ	a1	a2	B1	YIC	RT2	MSNR
0	-0.0386	0.1845	-1.4105	0.4539	-2.0415	-4.6116	0.8116	0.0087
1	0.0065	0.2053	-1.3755	0.4232	6.0135	-3.6924	0.8146	0.0085
2	-0.0780	0.5868	-0.6487	-0.2209	-3.4629	-3.6306	0.7200	0.0144
3	0.1108	0.3095	-1.8551	0.856	-0.9901	-6.6962	0.8550	0.0065
4	0.2661	0.2205	-0.8081	-0.1101	-0.6924	-2.8064	0.7331	0.0121
5	0.1344	-0.5200	0.3549	-1.255	-0.7913	-3.5323	-0.2478	0.0631
6	0.1186	0.0933	-1.4589	0.4762	-0.8785	-4.5312	0.6634	0.0152

The simulated discharge data (using the parameter estimates set with a delay of 3) are plotted in Figure 5.8. Compared with the data in Figure 5.7, where observed, instead of effective precipitation was used, the top plot in Figure 5.8 has significantly improved (RT2 increase from 0.80 to 0.86). In addition, the overall error has also decreased. The simulated data of Young (2002) (RT2: 0.84) are comparable (Figure 5.8-top).

To check if there are any systematic errors in the models that could be improved, Figure 5.9-left shows the error of the simulated discharge against the observed discharge. The right plot in Figure 5.9 shows the observed and simulated discharge for the peak flows only. From the left plot it may be concluded that the model is not systematically under- or over-estimating the observed discharge, as there is no obvious bias. However, Figure 5.9-right shows that the simulated peak flows, especially for the largest events, are generally underestimated by the DBM model.

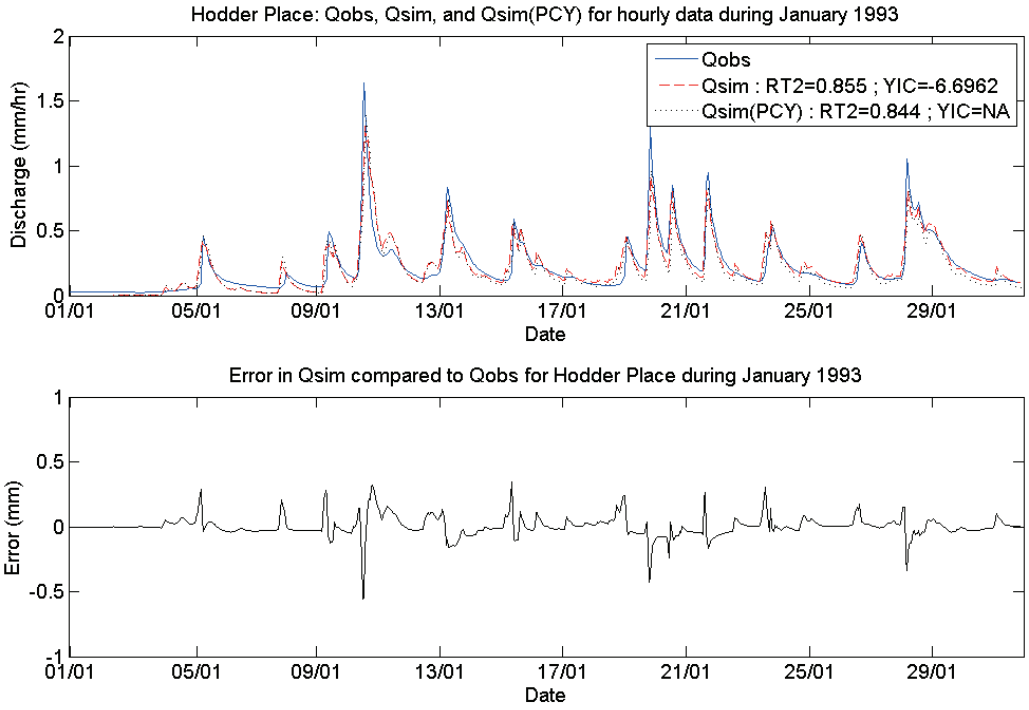

Figure 5.8 Top: Observed and simulated discharge data (current and Young), for Hodder Place January 1993, using effective precipitation as the input of the DBM model, bottom: the error in the simulated compared to the observed discharge

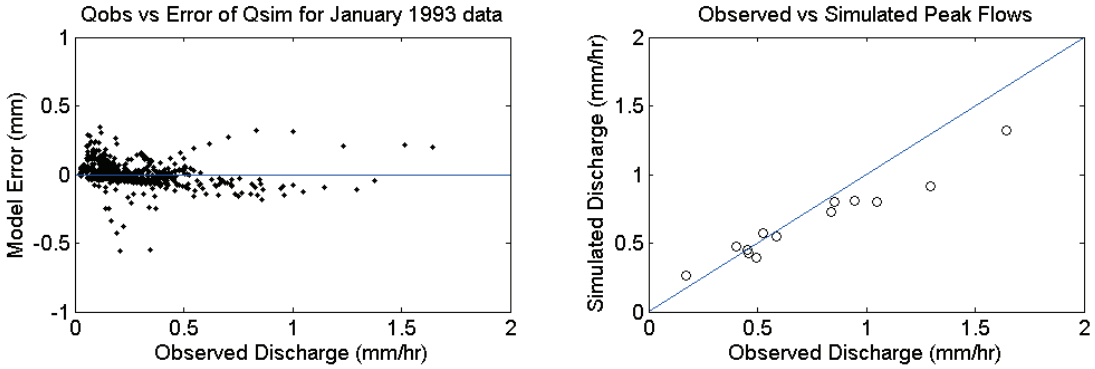

Figure 5.9 Left: Error in the simulated discharge (mm) plotted versus the observed discharge for the January 1993 data, Right: simulated versus observed peak flows only

Table 5.3 shows the physical interpretation of the analyses on the Hodder Place January 1993 data, which were used for the current analysis, those of Young (2002), and Young (2003). The DBM analysis shows that the quick time constant is approximately 5-7 hrs, while the slow time constant is more variable (84-230 hrs). Approximately 56-60% of the discharge originates from the quick reservoir. The same data set is used for the three different analyses and the results are very similar, but not exactly the same, not even by the same author on two different occasions. This may be a result of differences in the parameterisation processes, especially while obtaining the

effective rainfall. The delay (or lag time) of the current analysis is one hour less than the delay predicted by Young (2002). This can be explained by the actual lag time being somewhere in between 3 and 4 hours.

Table 5.3 DBM analysis physical interpretation results for Young (2002), Young (2003) and the current example analysis

Analysis	Data set	Delay (hr)	RT2	TCs (hr)	TCq (hr)	Ps	Pq
Young (2002)	January 1993	4	0.844	84	5.5	0.44	0.56
Young (2003)	January 1993	4	NA	230	5.2	0.41	0.59
Current example	January 1993	3	0.855	164	6.7	0.40	0.60

DBM Analysis of Long Term Hodder Data

According to the manner described in the previous section, the DBM method was applied to the yearly post 2001 hourly data sets for Footholme and Hodder Place. In addition, it was also applied to the full pre- and post-change hourly data sets. The analyses exclude the year in which the changes took place (2008-2009).

The simulation results are presented in Tables 5.4 and 5.5 for Footholme and Hodder Place respectively. These tables show the parameter estimates of Equation 5.9, the YIC and RT2 values, and the average error, as well as the physical interpretation of these parameter estimates (reservoir time constants and percentage of flow through each reservoir).

From the overall simulation results in Table 5.4, it is noted that the Footholme catchment behaviour generally has a lag time of about 1 hr. Approximately 60% of the runoff is generated from a quick reservoir with a time constant of 2-4 hrs. The remaining 40% of the runoff generated from a slow reservoir has a time constant of roughly 80-90 hrs. For Hodder Place (Table 5.5) the delay is about 3 hrs, and approximately 55% of runoff is generated through the quick reservoir (time constant 4-6 hrs) and 45% through the slow reservoir (time constant of 100-150 hrs). A much slower response is expected from the larger Hodder Place catchment, with longer travel distances and travel times. The enlarged contribution of the slow reservoir could be explained by a relatively larger input of groundwater at the larger scale.

Table 5.4 DBM estimated model parameters and simulation results for one year periods of hourly data for Footholme

Parameter	pre-all (2001-2008)	post-all (2009-2010)	2001-2002	2002-2003	2003-2004	2004-2005	2005-2006	2006-2007	2007-2008	2009-2010
Delay	1	1	1	1	2	1	3	1	1	2
a1	-1.7203	-1.737	-1.6778	-1.7262	-1.5964	-1.6520	-1.2496	-1.7293	-1.7419	-1.6082
a2	0.7232	0.7401	0.6816	0.7290	0.6096	0.6643	0.2872	0.7338	0.7445	0.6187
B1	-0.9829	-0.9786	-0.9805	-0.9824	-0.9408	-0.9361	-0.871	-0.9721	-0.9834	-0.9434
C	0.1312	0.1176	0.1579	0.1278	0.1572	0.1387	0.1749	0.1174	0.1128	0.1347
y	0.2933	0.3725	0.2814	0.3968	0.2423	0.3092	0.1349	0.2683	0.2937	0.3010
YIC	-11.4201	-9.5920	-9.6676	-9.4928	-8.5455	-8.6893	-6.1819	-9.8243	-9.8389	-8.5007
RT2	0.8616	0.8457	0.8697	0.8800	0.8089	0.8460	0.6660	0.8864	0.8792	0.8219
MSNR	0.0134	0.0092	0.0140	0.0069	0.0174	0.0167	0.0303	0.0118	0.0114	0.0124
TC_q	3.2	3.5	2.7	3.3	2.2	2.7	0.8	3.4	3.5	2.2
TC_s	92.4	80.0	81.2	91.9	27.4	24.5	18.0	55.5	95.5	33.9
PCT_q	0.62	0.56	0.61	0.60	0.56	0.57	0.37	0.61	0.61	0.47
PCT_s	0.38	0.44	0.39	0.40	0.44	0.43	0.63	0.39	0.39	0.53

Table 5.5 DBM estimated model parameters and simulation results for one year periods of hourly data at Hodder Place

Parameter	pre-all (2001-2008)	post-all (2009-2010)	2001-2002	2002-2003	2003-2004	2004-2005	2005-2006	2006-2007	2007-2008	2009-2010
Delay	3	3	3	3	7	3	3	2	3	3
a1	-1.7945	-1.8234	-1.7790	-1.8485	-1.9007	-1.7860	-1.7918	-1.8380	-1.7883	-1.7414
a2	0.7963	0.8246	0.7812	0.8489	0.9012	0.7878	0.7935	0.8394	0.7905	0.7443
B1	-0.9839	-0.9880	-0.9825	-0.9953	-0.9865	-0.9849	-0.9849	-0.9852	-0.9809	-0.9782
C	0.1117	0.1053	0.1260	0.1059	0.0359	0.1122	0.1109	0.0956	0.1139	0.1381
y	0.3061	0.3793	0.2761	0.3895	0.2005	0.2895	0.3258	0.3301	0.3224	0.3627
YIC	-11.2545	-9.3125	-9.2815	-9.0236	-4.9414	-9.2273	-9.4621	-9.5000	-9.5622	-9.1160
RT2	0.8828	0.8562	0.8768	0.8823	0.5516	0.8824	0.8839	0.8986	0.8892	0.8675
MSNR	0.0064	0.0043	0.0073	0.0039	0.0227	0.0062	0.0050	0.0061	0.0067	0.0051
TC_q	4.6	5.4	4.2	6.2	10.2	4.4	4.5	6	4.5	3.5
TC_s	107.7	148.4	96.3	385.8	180.4	114.3	118.1	108.2	93.3	84.6
PCT_q	0.55	0.54	0.57	0.54	0.37	0.56	0.53	0.60	0.53	0.52
PCT_s	0.45	0.46	0.43	0.46	0.63	0.44	0.47	0.40	0.47	0.48

Next, the DBM analysis results of the different periods are evaluated within the natural variability first. Second, it is investigated if the parameter estimates of one pre-change period are able to accurately predict the catchment response of the other pre-change periods. Finally, post-change year DBM analysis results are evaluated within the pre-change variability across years to potentially detect changes as a result of LUMCs.

DBM analysis results in the context of natural variability

Both Table 5.4 and Table 5.5 show that, for a specific catchment, there is quite some variability in the DBM parameter estimates and catchment characteristics between years. For example, for pre-change years, the delay ranges from 1 to 3 hrs for Footholme and from 2 to 7 hrs for Hodder Place, and the slow reservoir time constant varies between 18 and 96 hrs and between 93 and 386 hrs, respectively.

To explore if some of these differences may be explained in terms of natural variability, the *y* and *C* parameter estimates of the effective precipitation are first plotted against the total precipitation in Figure 5.10. The data are for 6 monthly periods of Hodder Place. The figure shows that periods with relatively large precipitation totals, result in higher *C* and lower γ values for the effective precipitation, though the trend in the former is not strong. This means that, for generally wet 6 monthly periods, a relatively larger proportion of the observed precipitation results in effective precipitation, but the differences in the ratio of the effective and observed precipitation between wet and dry periods within a specific period are smaller.

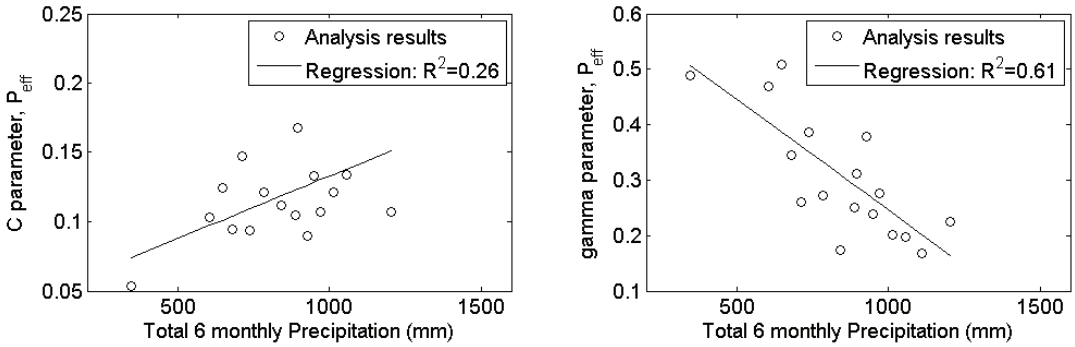

Figure 5.10 Optimised C (left) and y (right) parameters of effective rainfall plotted against the total observed precipitation for the 6 monthly periods of hourly data at Hodder Place.

In addition, it should be noted that the delay and other parameters of Equation 5.9, and hence the DBM model catchment characteristics, are all related to each other.

Some examples of these relations are given in Figure 5.11 for 6 monthly periods of hourly data at Hodder Place. The four plots of Figure 5.11 combined show that when the delay is relatively low, TC_q and TC_s are relatively high, and PCT_q is also relatively high. It is noted that the relation between the TC_q and PCT_q (Figure 5.11, right bottom) is obvious, as they are both derived from the same parameter.

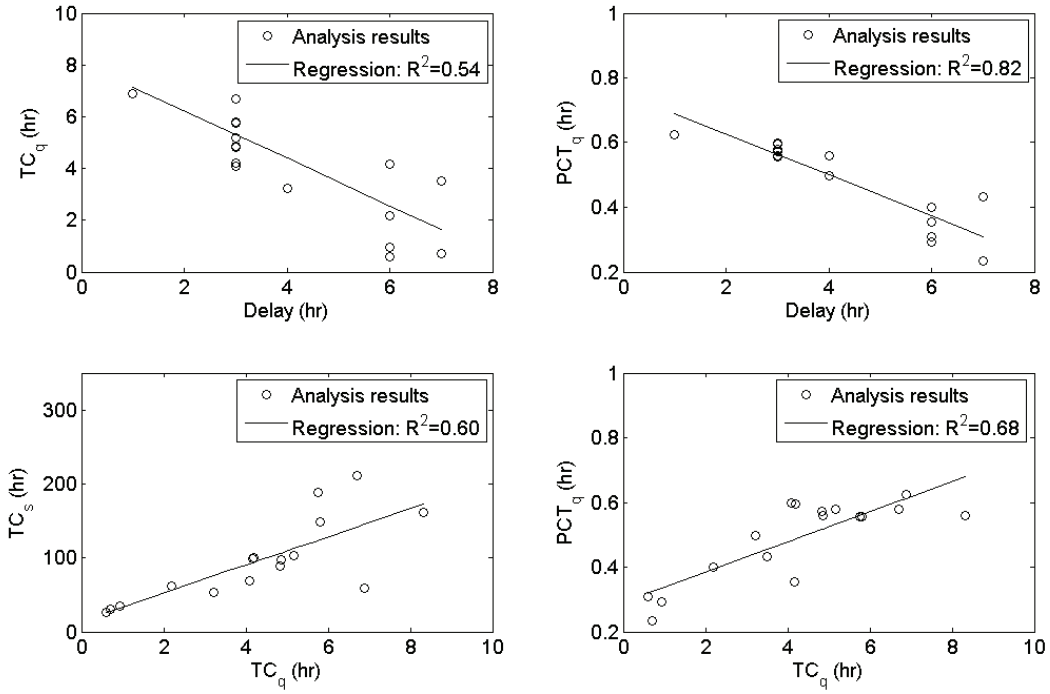

Figure 5.11 Relations between DBM Hodder Place model characteristics for 6 monthly periods of hourly data, Top-left: quick time constant versus delay, Top-right: contribution of quick reservoir versus delay, Bottom-left: slow time constant versus quick time constant, and Bottom-right: contribution of quick time constant versus quick time constant (all in hr)

Assuming that no actual change in catchment behaviour has occurred between periods, the plots also demonstrate that the overall catchment response can be represented in different ways (e.g. a short delay with a high percentage of the runoff generated through the quick reservoir and overall relatively high time constants; or a long delay with a relatively small proportion of the runoff generated through the quick reservoir, but with low time constants).

As the parameters and DBM model characteristics are all interrelated, the natural variability in catchment behaviour (Section 5.2.2) should be compared with all DBM model catchment characteristics of a particular period simultaneously. In the previous studies concerning hydrological change in relation to LUMC where the DBM method was applied, the interrelation between DBM parameters such as the delay and time

constants was not considered, and only differences in the estimates of one parameter at a time were evaluated (e.g. Beven et al, 2008).

The yearly DBM physical interpretations are shown in Figure 5.12 (FH) and Figure 5.13 (HP). Some specific years are highlighted, including the dry year of 02-03 (orange), the wet years of 06-07 (green) and 07-08 (yellow), and the post change year of 09-10 (red). By comparing Figures 5.12 and 5.13 with the differences in meteorology and catchment response between years (Section 5.2), it appears that the DBM parameter estimates are sensitive to natural variability. For example, while the delay for Hodder Place is average (3 hrs), the reservoir time constant is relatively high for the dry year of 2002-2003 (Figure 5.13), representing a slow response, with high catchment storage potential. In addition, the reservoir time constants and contributions of the slow reservoir are relatively low for the wet years (2006-2008), signifying a much quicker response. These observations are less apparent for the Footholme data. It is also noted that the 2005-2006 delay and quick time constant for FH and those of 2003-2004 for HP are distinctly different from the other years for the two sites. It is suggested that this could be a reflection of the type of events occurring within these two years at the respective catchments. Alternatively, this might be a reflection of a change in the overall hydrological functioning compared to previous years.

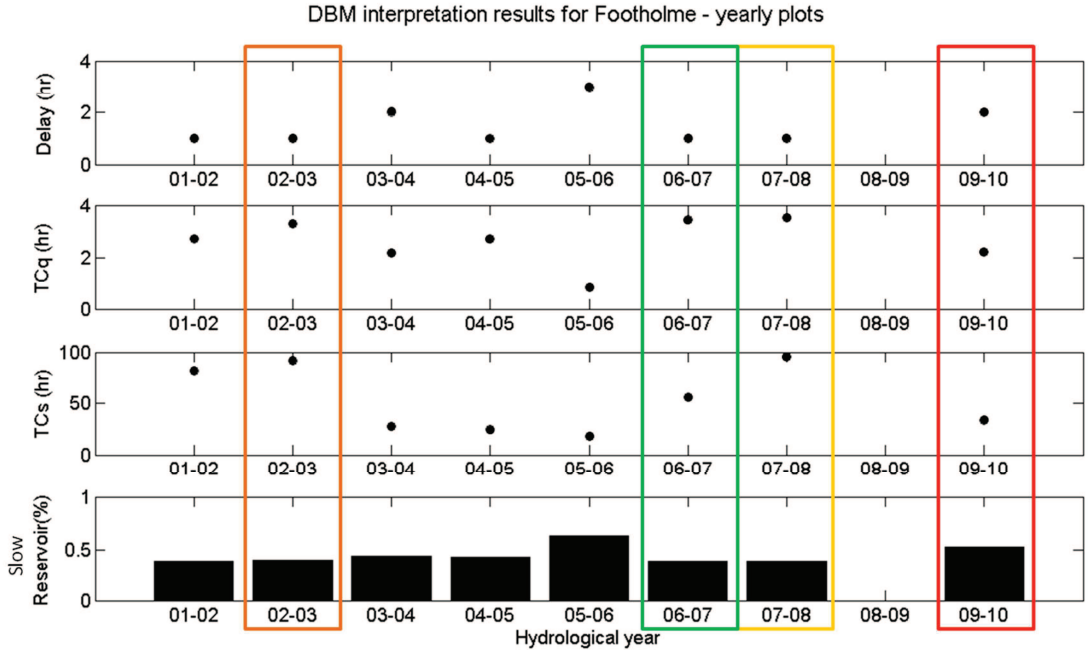

Figure 5.12 DBM interpretation results (delay, quick time constant, slow time constant and percentage of flow that occurs through the slow reservoir) for yearly periods of hourly data at Footholme

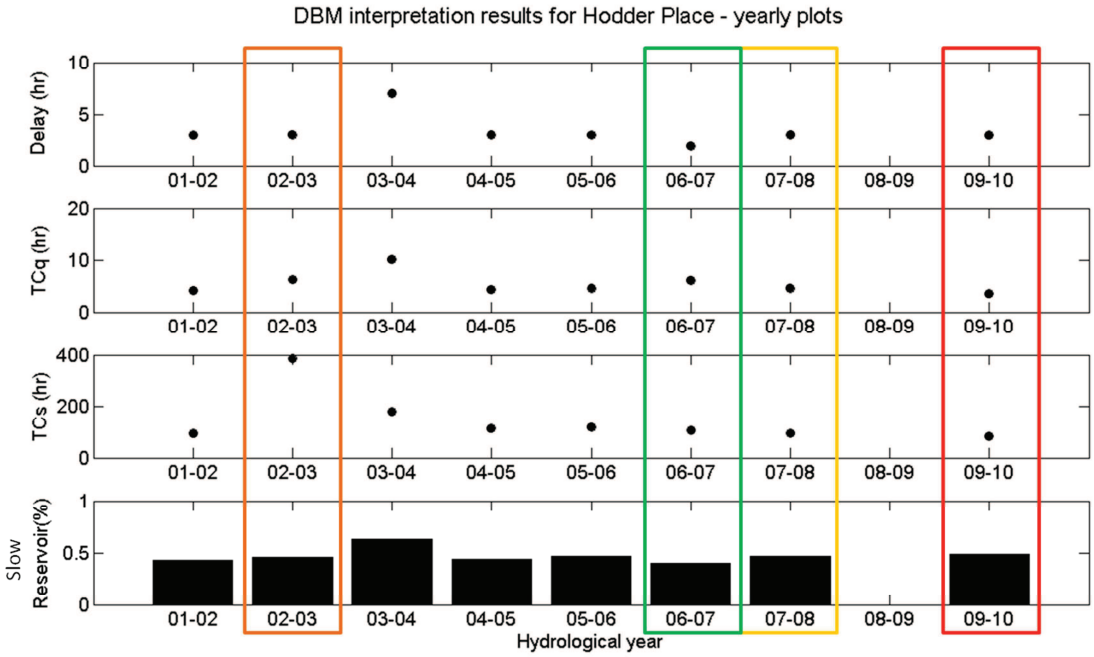

Figure 5.13 DBM interpretation results (delay, quick time constant, slow time constant and percentage of flow that occurs through the slow reservoir) for yearly periods of hourly data at Hodder Place

Hydrograph predictions using DBM parameter estimates of all pre-change years

In addition to the evaluation of the parameter estimates themselves, the question is also investigated as to whether the model parameter estimates for one pre-change period are able to accurately predict the catchment response of the other pre-change periods. As an example, the two most extreme years (the 2002-2003 dry year and the 2006-2007 wet year) are studied here. Figure 5.14 shows the largest FH and HP observed hydrographs for these years in blue. The simulated hydrographs that were based on the parameter estimates of the year in which the event occurred are indicated in orange (02-03) and green (06-07). They show a reasonably good fit. However, the range of simulations for which all parameter estimates of all other pre-change years were used (dotted black lines) is quite large, especially for the simulations for HP, where the minimum simulated peak hydrograph is more than twice as low as the maximum simulated peak hydrograph. The simulations based on the post-change parameter estimates (red) fall within the range of the simulations based on all pre-change years.

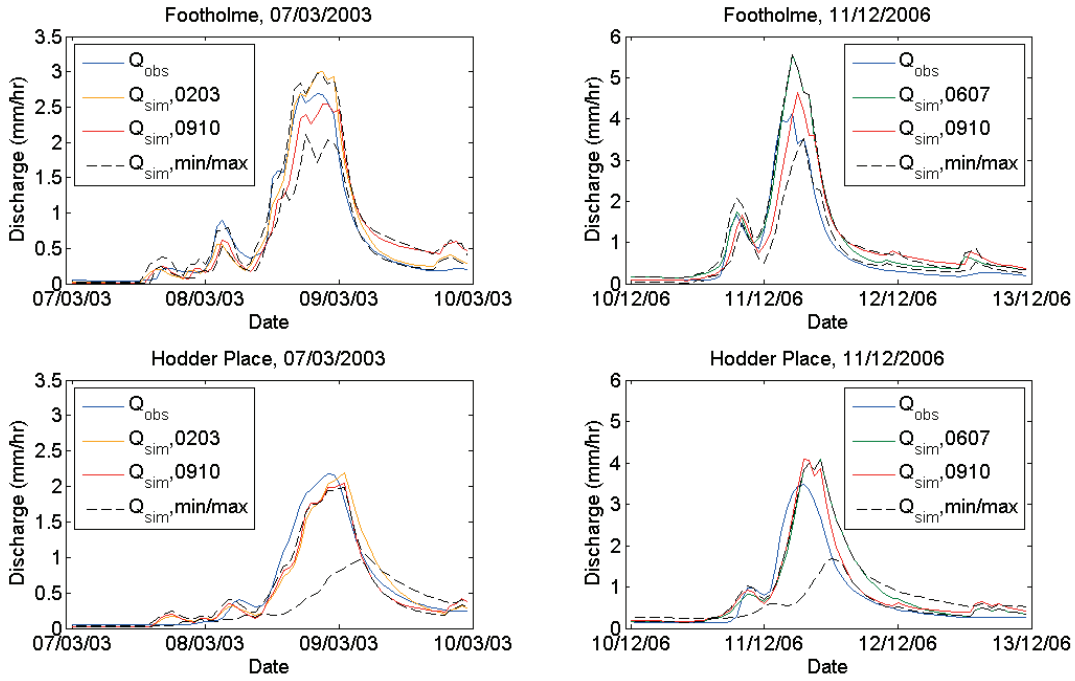

Figure 5.14 Observed (blue) and simulated discharge at Footholme (top) and Hodder Place (bottom) for two events (one in a relatively dry year (orange, left) and one in a relatively wet year (green, right) using the DBM parameter estimates for the years in which the event occurred. The dotted black lines represent the minimum and maximum simulated discharge using the DBM parameter estimates of all other pre-change years and the red line is based on the parameter estimates of the post change year.

The Nash-Sutcliffe efficiency (NSE) for the simulated discharges of the two full hydrological years, using the parameter estimates of all other pre-change years, are presented in Table 5.6. In general, the NSEs are good (close to one), in particular when the parameter estimates of the year to be predicted are used (highlighted in green). However, the parameter estimates of 2005-2006 for FH, and those of 2003-2004 for HP are less able (or unable) to predict the runoff for these two years (in red).

Figure 5.14 and Table 5.6 show that the model parameter estimates of one pre-change period are not always able to accurately predict the catchment response of the other pre-change periods. This can be related to the model parameter estimates being sensitive to the natural variability. These observations indicate that the DBM model is not suitable as a LUMC change detection method for short term records. For example, if the 2002-2003 year had been a pre-change year and 2003-2004 a post-change year, the HP DBM pre- and post-change results could have been falsely interpreted as an occurrence of 'change' related to LUMC. However, in reality, the DBM results would only represent differences as the product of natural variability.

Table 5.6 Nash Sutcliffe efficiencies for runoff predictions at Footholme and Hodder Place for a dry (2002-2003) and wet (2006-2007) pre-change year using the DBM parameter estimates of other pre-change years

Parameter estimates used in simulation (period)	Nash-Sutcliffe Efficiencies			
	Footholme		Hodder Place	
	2002-2003	2006-2007	2002-2003	2006-2007
2001-2002	0.858	0.880	0.844	0.888
2002-2003	0.860	0.872	0.856	0.875
2003-2004	0.797	0.830	-0.046	0.009
2004-2005	0.857	0.884	0.805	0.874
2005-2006	0.589	0.633	0.810	0.876
2006-2007	0.833	0.875	0.838	0.894
2007-2008	0.815	0.857	0.829	0.886
2009-2010	0.759	0.794	0.837	0.885

Post-change DBM results within pre-change variability

It was shown that the effect of natural variability is large for short term DBM analyses. However, in theory, if the LUMC would have induced a significant change in the catchment behaviour beyond the range of natural variability effects, this could still be picked up from the pre- versus post-change DBM analyses. Figure 5.15 (FH) and Figure 5.16 (HP) show the post change DBM model characteristics plotted together with the same pre-change yearly results, represented as frequency diagrams.

For Footholme (Figure 5.15), all post-change DBM model catchment characteristics fall within the pre-change range. This means that no change has been detected, either because no change occurred, or because the LUMC effects are masked by natural variability. The Hodder Place (Figure 5.16) post-change reservoir time constants are slightly quicker than the pre-change ones, but the other catchment characteristics fall within the pre-change range. As they are all related, it is difficult to determine whether this represents a real change.

Table 5.7 shows that there is no systematic change to be detected in the post-change catchment behaviour, as the parameters for some pre-change years are able to accurately predict the post-change behaviour. In addition, there is no considerable difference between the results for the full pre-change and the full post-change periods (Table 5.4 and Table 5.5). Figure 5.14 also shows that the simulations of the two events

at Footholme and Hodder Place based on the post-change parameters fall within the range of pre-change parameter simulations.

In conclusion, the DBM model has not been able to pick up any short term systematic changes in the catchment behaviour due to changes in land use/management, for Footholme as well as Hodder Place. However, this does not mean that changes have not occurred, as the DBM simulations are highly sensitive to natural variability.

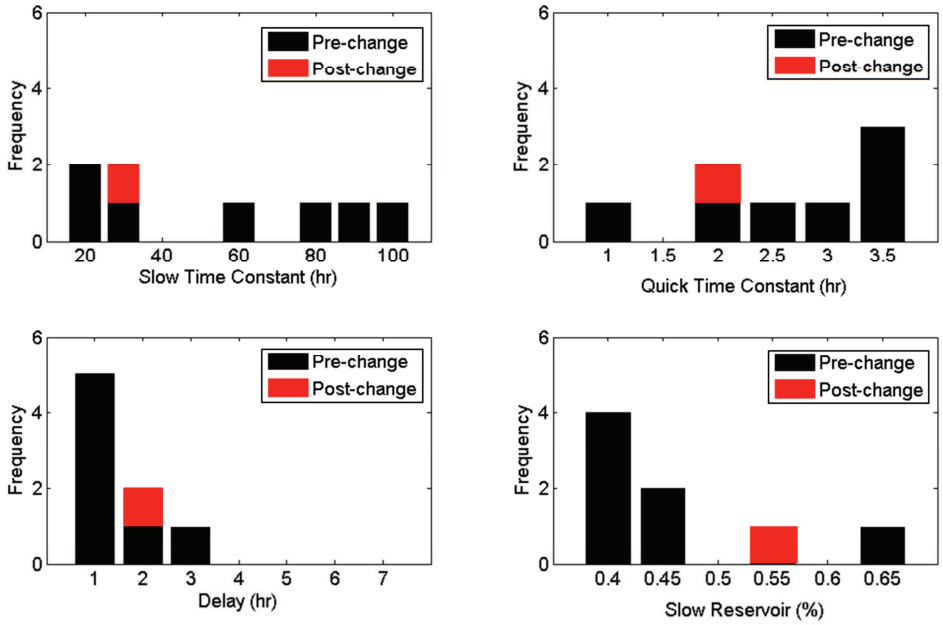

Figure 5.15 Footholme frequency diagrams for the yearly DBM model characteristic results

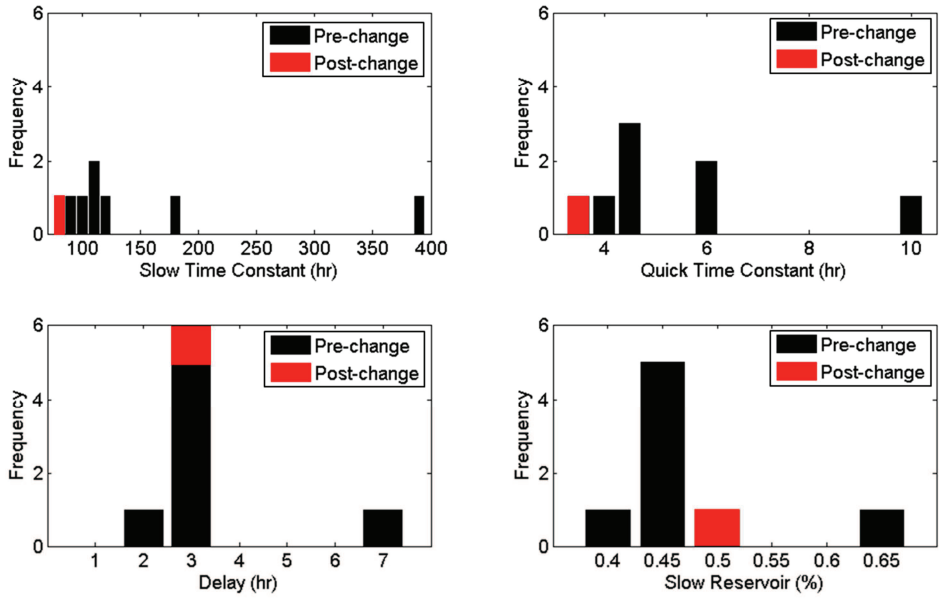

Figure 5.16 Hodder Place frequency diagrams for the yearly DBM model characteristic results

Table 5.7 Nash Sutcliffe efficiencies for runoff predictions at Footholme and Hodder Place for the post-change year period using the DBM parameter estimates of pre-change years

Parameter estimates used in simulation (period)	Nash-Sutcliffe Efficiencies	
	Footholme	Hodder Place
	2009-2010 period	2009-2010 period
2001-2002	0.851	0.871
2002-2003	0.859	0.872
2003-2004	0.796	0.274
2004-2005	0.853	0.854
2005-2006	0.583	0.858
2006-2007	0.834	0.873
2007-2008	0.816	0.867
2009-2010	0.876	0.871

5.3.2 Storage Discharge Detection (SDD) Model

SDD Model Structure

The DBM model showed sensitivity to natural variability, as its structure and model parameter estimates are based on the full effective precipitation and discharge datasets in the simulation period, which are all subjected to natural variability (Section 5.3.1). It is hypothesised here that the part of the hydrograph least sensitive to natural variability is the falling limb (i.e. the recession), on the basis that it is not affected by precipitation variability. A conceptual catchment model that is based on recession analysis should therefore be less sensitive to natural variability.

One way of expressing the recession curve is by the rate of change in discharge for a specific discharge, according to Equation 5.10:

$$\frac{dQ}{dt} = mQ^n \qquad \text{(Equation 5.10)}$$

where Q is discharge, t time and m and n are parameters.

A variety of studies use recession analysis to inform the structure of conceptual models (e.g. Lamb and Beven, 1997; Wittenberg, 1999; Ewen and Birkinshaw, 2007; Clark et al., 2009). Ewen et al. (2010) describe a simple Storage Discharge Detection (SDD) model, that involves the use of the m and n parameters of Equation 5.10 to build a simple conceptual catchment storage discharge model. The SDD model is based

on a nonlinear storage discharge relationship, governed by the assumption that the behaviour of peak discharges depends on that of the recessions. A version of this model is used in the present section.

The SDD model relies on a water mass balance equation, which in its simplest form can be described by Equation 5.11.

$$\frac{dS}{dt} = -Q \qquad \text{(Equation 5.11)}$$

The equation describes the rate of change in catchment storage (S) when the stream discharge is the only output from the catchment (i.e. assuming no precipitation, evapotranspiration, or other catchment losses such as abstractions).

Ewen and Birkinshaw (2007) and Ewen et al. (2010) showed that the discharge itself can be represented as the following function of the storage:

$$Q = (S/b)^c \qquad \text{(Equation 5.12)}$$

Equation 5.12 is referred to as the 'attractor curve' by Ewen and Birkinshaw (2007), since they found that the dynamic storage-discharge relationship (plotted on a graph) is always 'attracted' to the curve plotted for Equation 5.12. They showed that the storage-discharge relationship is hysteretic for their test catchment (Slapton Wood catchment, Devon UK), as it deviates away from the attractor curve during periods with precipitation. For subcatchments in the Hodder catchment, however, Ewen et al. (2010) found that the hysteresis is not strong, as the observed storage-discharge relationships show only narrow loops.

Inserting Equation 5.11 into Equation 5.12 gives:

$$\frac{dS}{dt} = -(S/b)^c \qquad \text{(Equation 5.13)}$$

In effect, Equation 5.13 characterizes the catchment behaviour during the recession. The parameters b and c are directly related to the m and n parameters of Equation 5.10, according to:

$$c = 1/(2-n) \qquad \text{(Equation 5.14)}$$

$$b = -c/m \qquad \text{(Equation 5.15)}$$

The c parameter indicates the degree of non-linearity, and takes the value 1 for a linear system. The b parameter reflects the flashiness (or responsiveness) of the system, with low values indicating flashy behaviour.

The full water mass balance equation for a Hodder subcatchment must allow for precipitation input (P), and evapotranspiration (ET) and water abstraction (A) outputs, resulting in the principal equation for the SDD model as presented in Equation 5.16:

$$\frac{dS}{dt} = P - ET(PET, Q) - A - Q(S) \qquad \text{(Equation 5.16)}$$

where $Q(S)$ is the attractor equation (Equation 5.12) and ET is a function of the potential evaporation (PET) and discharge (discharge used here as a surrogate for the catchment wetness), according to:

$$ET = aPET \qquad \text{(Equation 5.17)}$$

for which a is assumed to rise linearly from 0 at Q = 0 to 1 at Q = Q_{Th}, where Q_{Th} is a specified threshold discharge. For Q>Q_{Th}, the value of a is fixed at 1 because the catchment is assumed saturated and the actual evapotranspiration equals the potential evaporation. Finally, Equation 5.16 requires an initial condition, for which it is assumed that the attractor equation can be used.

A schematic representation of the SDD model is given in Figure 5.17.

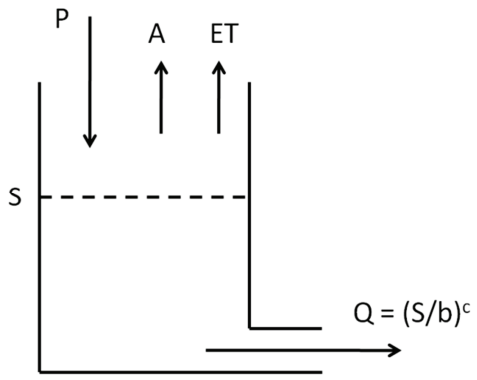

Figure 5.17 Schematic representation of the conceptual Storage Discharge Detection model

Practical Example

In order to explain the SDD modelling in more detail and to compare the model simulations directly with those of the DBM model, a practical example is given here for the same hourly data as presented in Figure 5.6 (January 1993) for the DBM example. In addition to precipitation and discharge, the SDD model also requires evaporation and abstraction data. The evaporation data are based on MORECS estimations for the Hodder catchment. The abstractions are estimated based on daily abstraction data from UU, which were evenly spread over the hourly intervals.

Figure 5.18 shows the HP January 1993 recession data that were extracted from the observed discharge record for periods with decreasing flow. The regression line through these data points was obtained using a multidimensional downhill simplex optimisation method, based on Nelder and Mead (1965), as programmed for FORTRAN in the subroutine 'amoeba' (Press et al., 1992). This non-linear regression method assumes that the noise standard deviation is constant and avoids giving biased regression results. From the amoeba regression, the m and n parameters of Equation 5.10 can be derived (-0.0869 and 1.5728 respectively), resulting in b = 26.94 and c = 2.34 for the parameters of the attractor equation.

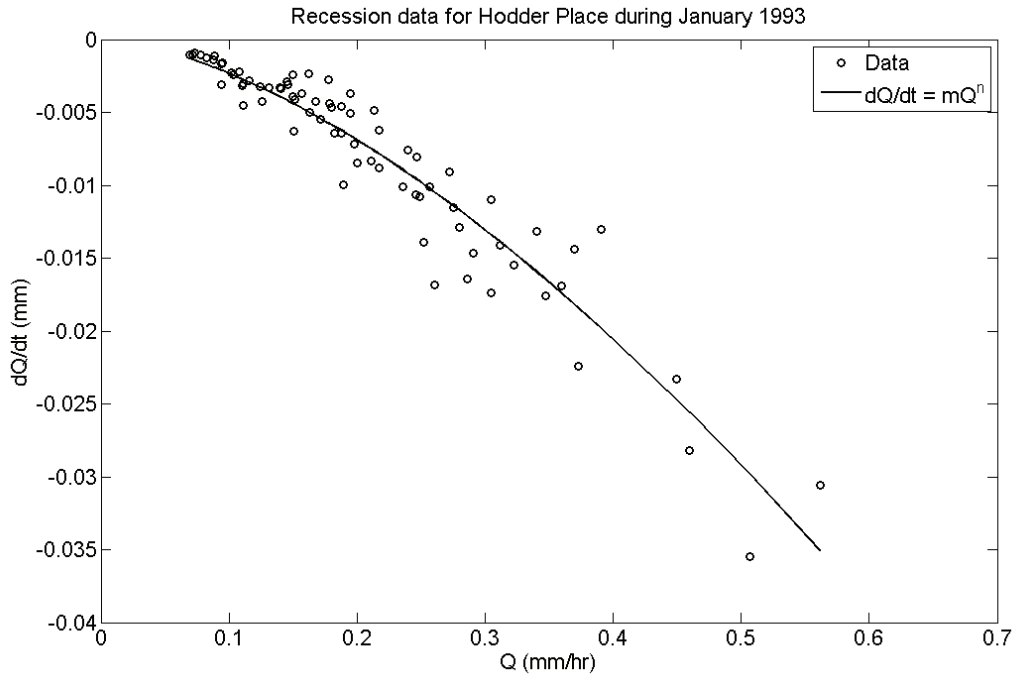

Figure 5.18 Hodder Place rate of change in discharge in (mm) plotted against hourly recession discharge (mm/hr). The regression m and n parameter estimates are -0.0869 and 1.5728 respectively.

The recession data extraction method does not discard any specific recession data, as long as there is decreasing flow for a number of time steps. For high resolution data sets (e.g. 15 min) in relatively small catchments, this becomes a problem for those sections of the recession that experienced periods with continuous rainfall. For the hourly data of Hodder Place (and Footholme), however, an adjusted recession data selection procedure was unnecessary as these data are relatively smooth (i.e. compared to 15 min records). It could be argued that other periods of recession data, such as those experiencing extreme evapotranspiration rates, should be excluded from the analysis. However, for the present study this is a trivial concern.

Figure 5.19-top shows the observed discharge as well as the SDD simulated discharge, using the above mentioned optimised *b* and *c* parameter estimates of the attractor equation (and for Q_{Th} = 0.05 mm/hr, which is about 0.5 times the mean annual flow rate). The overall NSE is 0.685. The bottom plot shows the error of the simulated discharge (according to Equation 5.8).

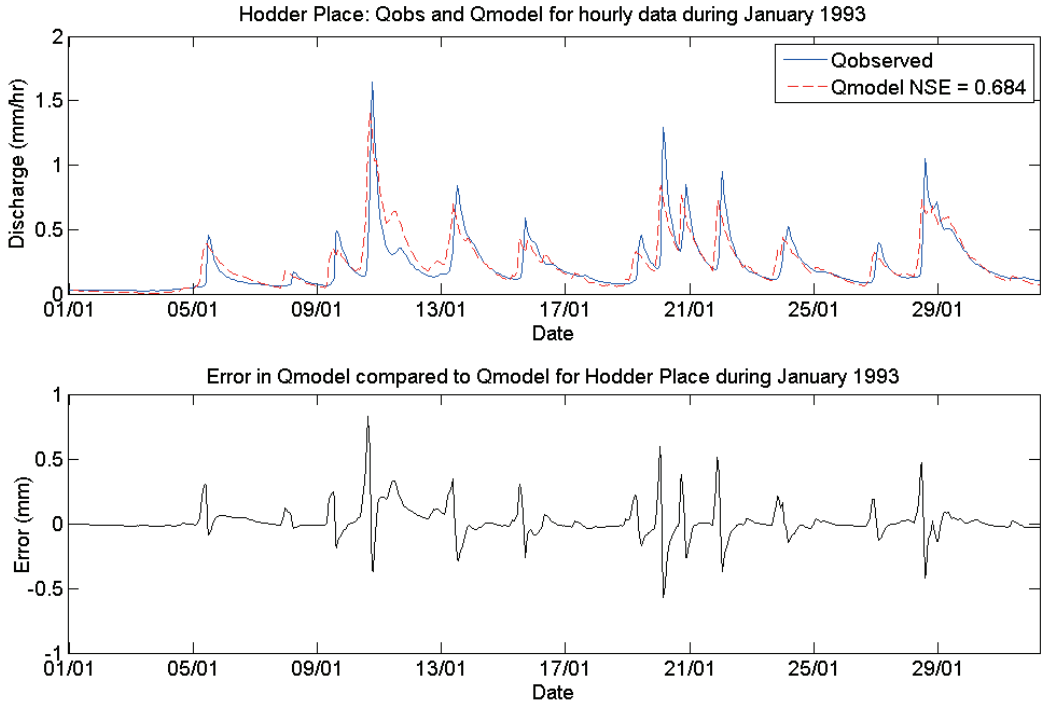

Figure 5.19 Top: Observed and SDD simulated discharge (both in mm/hr) for Hodder Place during January 1993, Bottom: Error of the simulated discharge

From Figure 5.19, it is noted that there appears to be a systematic error in the simulations of the hydrographs, related to a timing difference. The average difference between the observed and simulated peak timings is 3 hours, which corresponds with

the ‘delay’ value of the DBM simulation. The SDD simulation can be improved significantly by introducing a 3 hour shift (Figure 5.20), which increases the NSE from 0.684 to 0.826. In addition, the overall error decreases and the systematic errors are absent.

The plots in Figure 5.21 show that the SDD model (including the 3-hr shift) tends to underestimate relatively higher discharges, including all peak flows, and slightly overestimate the relatively lower discharges. Although overall smaller, similar errors were observed for the DBM analysis. As the DBM model involves considerably more parameters than the SDD model, the better fit is in line with what is expected.

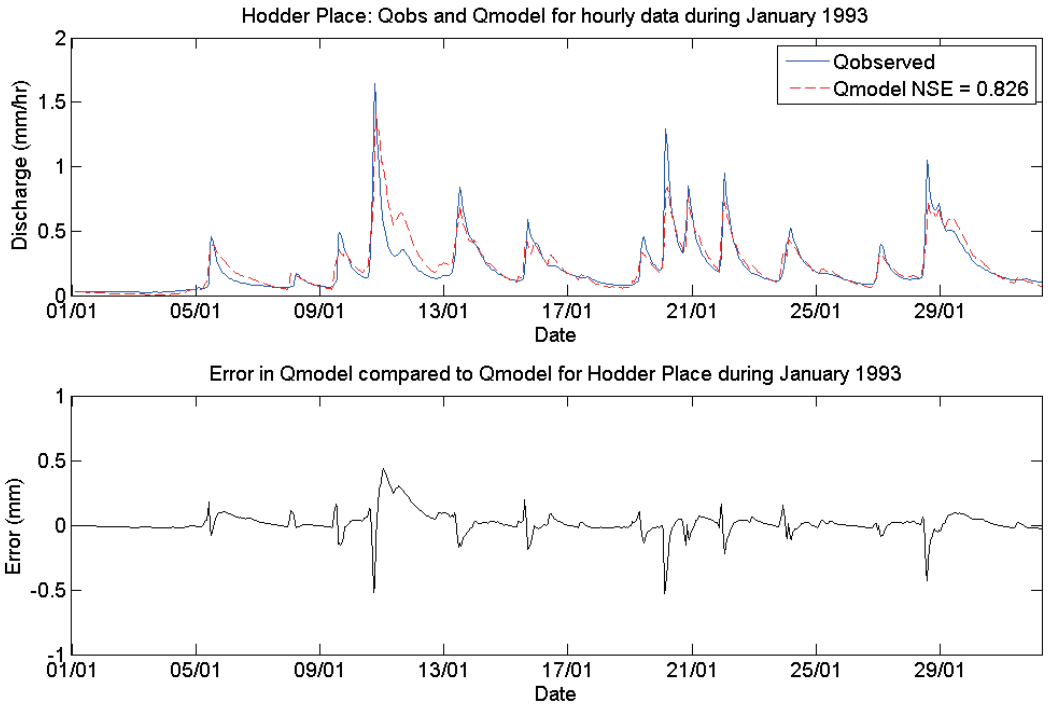

Figure 5.20 Top: Observed and SDD simulated discharge with a shift of 3 hrs (both in mm/hr) for Hodder Place during January 1993, Bottom: Error of the simulated discharge

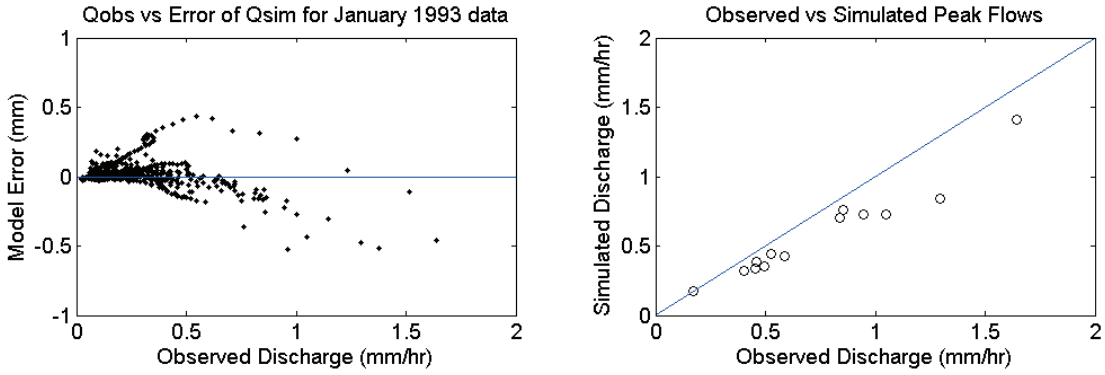

Figure 5.21 Left: Observed discharge versus the error in the simulated discharge (mm), including the 3 hr shift, Right: Observed versus simulated peak flows only

The SDD model is able to predict the overall catchment behaviour well, taking into account that it is based on only the two parameters derived from the recession analysis. As shown in Figure 5.20, a third parameter (a time shift) could be introduced to improve the model fit. However, the estimate of this third parameter is likely to be sensitive to natural variability, in a similar way as the DBM 'delay' parameter estimate. For this reason, the time shift was not applied to the further SDD analysis in this chapter.

For flashy catchments, timing errors are common in model simulations, and they tend to be penalised too harshly by the NSE: the realistic aim in modelling (as it is in this study) is often simply to reproduce the general features, and flashiness, of the hydrograph rather than to reproduce the hydrograph exactly. Ewen (2011) developed a method that calculates an efficiency which is based directly on the NSE, the NSE-morph, but which does not penalise small differences in the timing. If up to 3 time steps of timing difference are allowed, the NSE-morph for the above example is 0.863. As a measure of the goodness of fit, the analyses results in the following sections are therefore presented as NSE-morph efficiencies.

SDD Analysis of Long Term Hodder Data

The SDD analysis was applied to the hourly Footholme and Hodder Place pre- and post-2001 data sets. The precipitation and discharge datasets (also used for the DBM analysis) were supplemented with potential evaporation data, based on MORECS estimates, and abstraction estimates derived from the UU abstraction data.

Tables 5.8 and 5.9 show the optimised regression parameter estimates m and n, and the b and c parameter estimates of the attractor curve to which they are converted, for all the pre-change and post-change years. From the overall pre-change simulation results in the tables, it is noted that the Footholme recession has a more flashy response (smaller b values) than Hodder Place. This is in line with the results of the overall DBM analyses of FH and HP. The overall catchment behaviour at Hodder Place is more nonlinear than at Footholme, indicated by the larger c values for HP.

Table 5.8 SDD analysis regression results of recession data (m and n) and the interpretation for the model (b and c) for Footholme (post-change values are presented in red)

period	m	n	b	c	RMSE
full pre	-0.0849	1.2117	14.9412	1.2686	0.0030
full post	-0.0805	1.2458	16.4807	1.3260	0.0030
2001-2002	-0.0829	1.2125	15.3143	1.2698	0.0033
2002-2003	-0.0926	1.3079	15.6108	1.4449	0.0022
2003-2004	-0.0891	1.2120	14.2365	1.2691	0.0030
2004-2005	-0.0841	1.2278	15.4010	1.2951	0.0029
2005-2006	-0.0926	1.2620	14.6373	1.3549	0.0023
2006-2007	-0.0836	1.2857	16.7485	1.4000	0.0029
2007-2008	-0.0814	1.2342	16.0342	1.3059	0.0032
2009-2010	-0.0768	1.2558	17.5003	1.3438	0.0031

Table 5.9 SDD analysis regression results of recession data (m and n) and the interpretation for the model (b and c) for Hodder Place (post-change values are presented in red)

period	m	n	b	c	RMSE
full pre	-0.0707	1.3479	21.6804	1.5335	0.0023
full post	-0.0751	1.4233	23.0780	1.7341	0.0017
2001-2002	-0.0709	1.3183	20.6856	1.4668	0.0021
2002-2003	-0.0772	1.4355	22.9489	1.7716	0.0015
2003-2004	-0.0691	1.3066	20.8590	1.4422	0.0028
2004-2005	-0.0707	1.4174	24.2884	1.7163	0.0019
2005-2006	-0.0778	1.3858	20.9274	1.6283	0.0016
2006-2007	-0.0655	1.3275	22.7019	1.4871	0.0030
2007-2008	-0.0688	1.3486	22.3026	1.5351	0.0021
2009-2010	-0.0724	1.4270	24.1154	1.7453	0.0017

As for the DBM analysis section, the SDD results for the different periods are evaluated in the context of natural variability, to see whether the parameter estimates of one pre-change period are able to accurately predict the catchment response of the other pre-change periods. In addition, the pre- and post-change SDD analysis results are compared to potentially detect changes as a result of LUMCs.

SDD analysis results in the context of natural variability

Figures 5.22 and 5.23 show the amoeba regressions through the post 2001 yearly recession data for Footholme and Hodder Place respectively. For each of these plots, it is clear that there appears to be little variation between the data from year to year. There is little scatter and all regression lines are very similar. It is noted though, that

for Footholme, the post-change year (red) shows a generally slower response than the pre-change years.

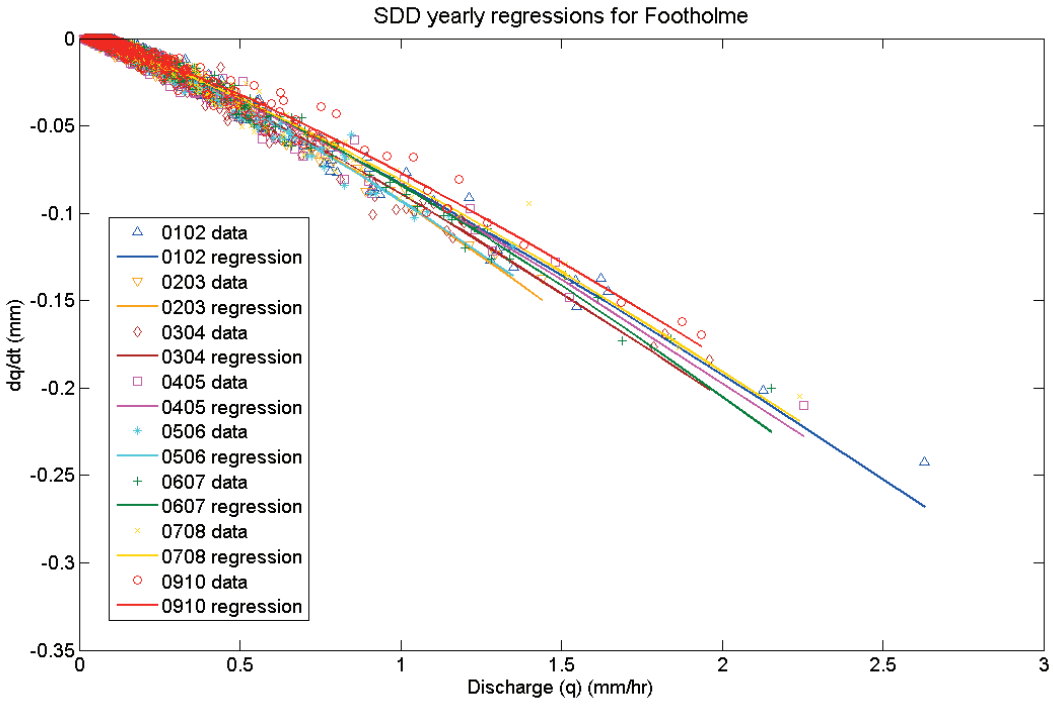

Figure 5.22 SDD Footholme yearly recession data with regressions

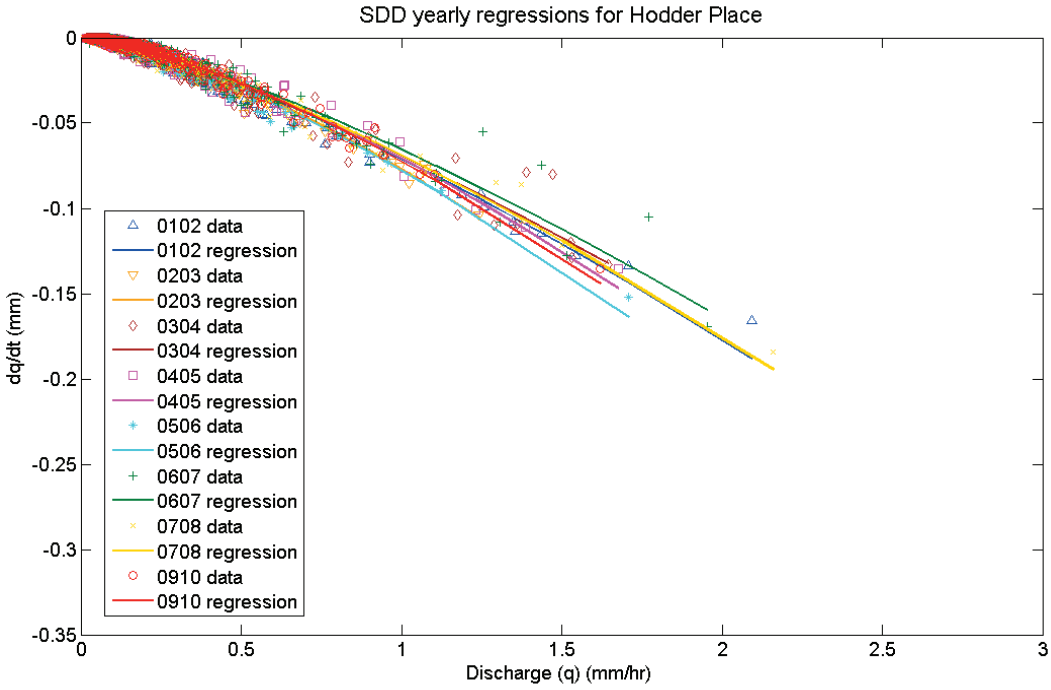

Figure 5.23 SDD Hodder Place yearly recession data with regressions

First, statistical analyses of significance are needed to determine whether all pre-change yearly data sets are from the same population and hence if the SDD parameter estimates are sensitive to natural variability. For such statistical analyses, it would be beneficial to have data available for a longer period than the 7 pre-change years from 2001. As the SDD model parameter estimates rely only on recession discharge data (and not on precipitation data which is incomplete pre 2001), the recession analysis can be extended to the full period for which discharge data are available. The earliest hydrological year for which a full discharge record is available starts in October 1996 (Chapter 4). Figure 5.24 shows the regressions of FH (left) and HP (right) for all 12 pre-change hydrological years and the 1 post-change hydrological year.

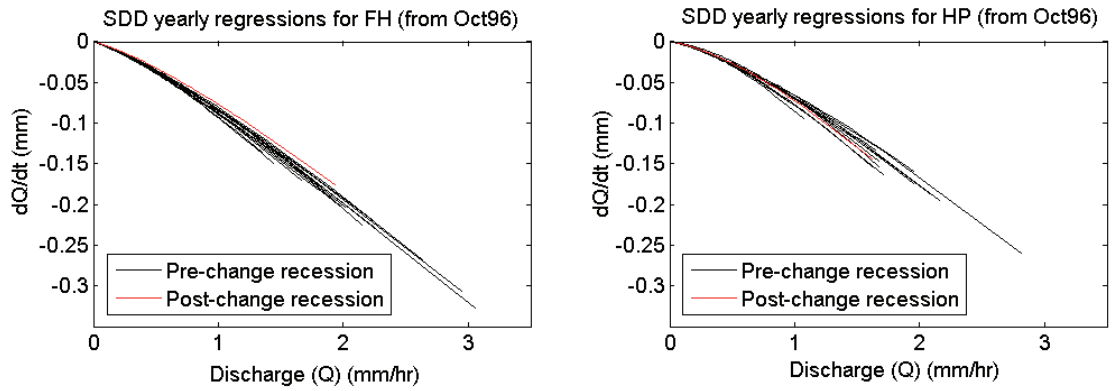

Figure 5.24 Regressions of recession data for Footholme (left) and Hodder Place (right) for each hydrological year from October 1996

Figure 5.24 shows that the yearly regressions for Footholme as well as Hodder Place are still very similar, though the Footholme post-change regression still shows the slowest response. For the statistical test regarding equality of all pre-change regressions, the null hypothesis is that all the pre-change samples are from the same population (i.e. there is no significant difference between the parameter estimates of the regression lines). The statistical analysis is somewhat complicated by the fact that the regressions are non-linear while the available standard procedures for regression lines are based on linear regression theory. The analysis is therefore done on the *m* and *n* regression parameter estimates rather than the regression as a whole. Appendix 2 describes the full statistical methodology. A brief overview of the statistical methodology is given here.

In summary, a test was carried out to establish whether the sample variance of the *m* and *n* parameter estimates of all pre change years was the same as the average variance of the *m* and *n* parameter estimates of each individual year. The latter were obtained through bootstrap estimation (e.g. Efron and Tibshirani, 1993) and provide an estimate of the estimated *m* and *n* parameter population variance.

For the data of each hydrological year, the bootstrap procedure involved resampling the observed residuals to generate 1000 random data samples, for which *m* and *n* parameter estimates were obtained. As a result of the non-linear character of the regressions, the residuals are, however, not independently distributed, their variance is not constant across the range of the discharge, and they cannot be fitted satisfactorily with a normal (or any other) distribution. To represent the dependency of the variance of the residuals on the discharge, the observed residuals were subdivided into five classes, based on the discharge, in such a way that the variance is approximately constant in each class (see example in Figure 5.25). The corresponding cumulative distribution of the residuals within each class was then used to resample the residuals, so that the bias and distribution of the residuals is well represented in the bootstrap samples.

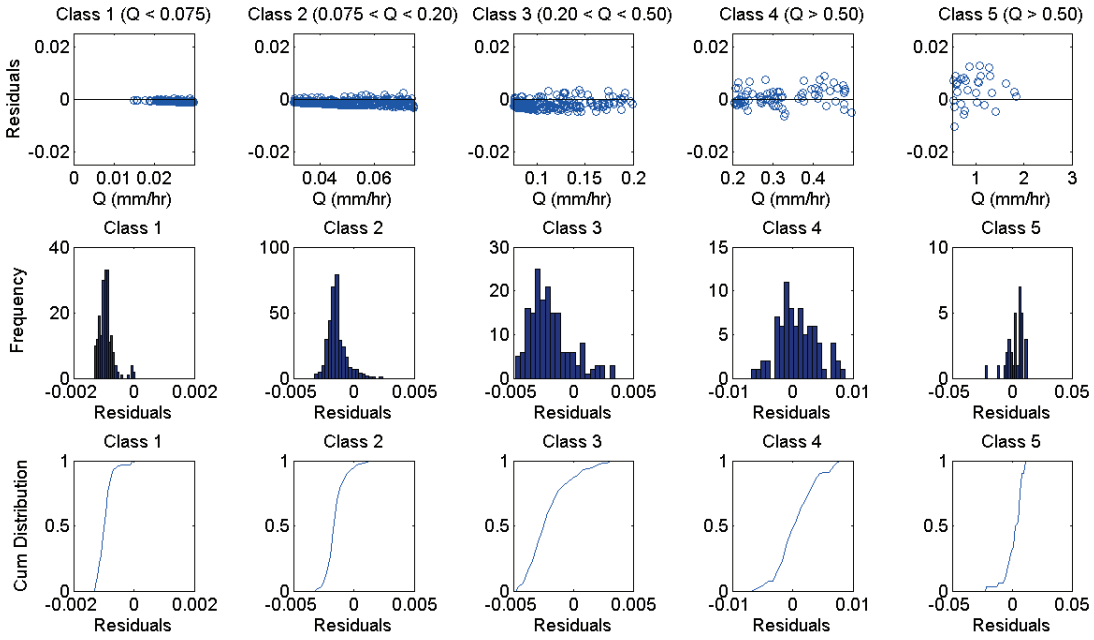

Figure 5.25 Footholme 1996-1997 residuals of the fitted amoeba regression, subdivided in to five classes, according to discharge. Top: discharge against residuals, Middle: frequency diagram of the residuals, Bottom: cumulative distribution of the residuals

From the 1000 bootstrap estimates of each year, the variance of *m* and *n* could be determined. If all pre-change years are statistically the same, the ratio between the sample variance of the *m* and *n* parameter estimates of all pre change years and the average variance of the *m* and *n* parameter estimates of each individual year should be (close to) 1. The significance of the ratio can be tested using an F-test. The test results showed that the sample variance of the m and n parameter estimates of all pre change years is much higher than the average variance of the m and n parameter estimates of each individual year (Appendix 2). This means that not all pre-change years are statistically the same, indicating sensitivity to natural variability.

Catchment hydrograph predictions using SDD parameter estimates of all pre-change periods

Even though the analysis showed that not all pre-change year parameter estimates are statistically the same, the pre-change parameter estimates are still very similar, especially when compared with the large differences between the DBM parameter estimates of pre-change years. Corresponding to the plots in Figure 5.14, Figure 5.26 presents the FH (top) and HP (bottom) observed (blue) and SDD simulated hydrographs of the 2002-2003 (wet) and 2006-2007 (dry) years.

Again, the SDD simulated hydrographs using parameter estimates of the year in which the event occurred are shown in orange and green for the 2002-2003 and 2006-2007 events, respectively. The dotted black lines represent the minimum and maximum simulations using the parameter estimates of all other pre-change years and the red lines are based on the parameters of the post-change year.

In comparison with the DBM simulations of Figure 5.14, Figure 5.26 shows that, although the SDD simulations based on the parameter estimates of the year in which the events occurred are not as accurate as the DBM simulations, there is far less variability between the simulations based on parameter estimates from other pre-change years. This is also reflected in the comparison between the DBM NSE (Table 5.6) and SDD NSE-morph (Table 5.10) goodness of fit efficiencies for the two hydrological years, using the parameter estimates of all other pre-change years. Overall, the

efficiencies are lower for the SDD simulations, but there is far less variability between the efficiencies when parameter estimates of other years are used.

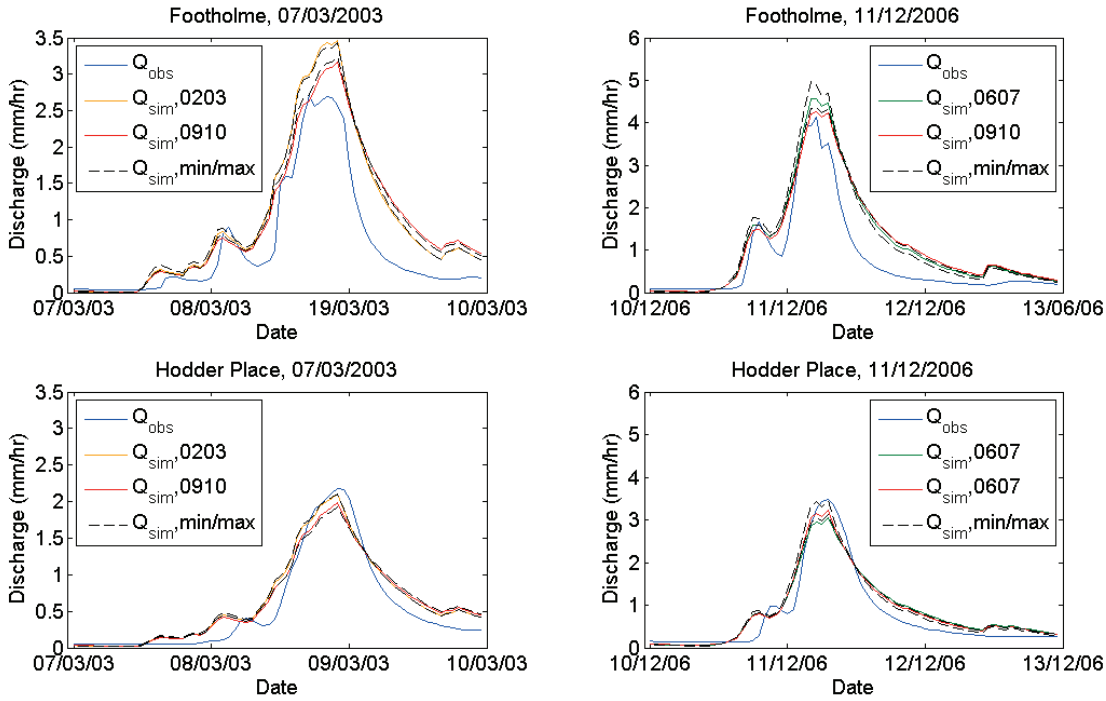

Figure 5.26 Observed (blue) and simulated discharge at Footholme (top) and Hodder Place (bottom) for two events (one in a relatively dry year (orange, left) and one in a relatively wet year (green, right) using the SDD parameter estimates for the years in which the event occurred. The dotted black lines represent the minimum and maximum simulated discharge using the SDD parameter estimates of all other pre-change years and the red line is based on the parameter estimates of the post change year

Table 5.10 NSE-morph efficiencies for runoff predictions at Footholme and Hodder Place for a dry (2002-2003) and wet (2006-2007) pre-change year using the SDD parameter estimates of other pre-change years

Parameter estimates used in simulation (period)	**NSE-morph**			
	Footholme		Hodder Place	
	2002-2003 period	2006-2007 period	2002-2003 period	2006-2007 period
2001-2002	0.714	0.815	0.805	0.853
2002-2003	0.739	0.827	0.824	0.863
2003-2004	0.711	0.818	0.799	0.849
2004-2005	0.717	0.818	0.815	0.860
2005-2006	0.726	0.818	0.815	0.856
2006-2007	0.733	0.835	0.802	0.866
2007-2008	0.718	0.817	0.805	0.854
2009-2010	0.723	0.815	0.821	0.851

Post-change SDD results compared with pre-change variability

The Hodder Place post-change SDD model parameter estimates lie within the pre-change range (Table 5.9 and Figures 5.23 and 5.24(right)). On the other hand, from Table 5.8, and Figures 5.22 and 5.24-left, it appears that the regression through the Footholme post change recession data may be different from those through the pre-change hydrological years. The results for Footholme could designate relatively slower recession behaviour than that observed for the pre-change hydrological years. This indicates that the rate at which the water is released from storage is slower. In theory, when the stored water is unable to contribute fully to the discharge, it is likely to be bound up somewhere, but gradually released later during the recession, which could potentially be attributed to LUMC (e.g. grip blocking). Alternatively, the water could also be stored in snow, or a frozen layer, as a result of the strong winter in the post-change period (Section 5.2).

Figure 5.27 shows the histograms of the *m* and *n* parameter estimates of the amoeba regressions through the recession Footholme (top) and Hodder Place (bottom) data. It is noted that the pre-change spread of parameter estimates is smaller for Footholme than for Hodder Place. For Hodder Place, all post-change parameter estimates lie within the range of pre-change parameter estimates (consistent with Figures 5.22 and 5.23). However, for Footholme, the post-change estimate of the multiplier (m parameter) of the regression lies outside the range of the pre-change estimated parameters.

Another statistical analysis of significance is needed to determine whether the post-change Footholme yearly parameter estimates are from the same population as the Footholme yearly pre-change parameter estimates.

For both the FH and HP data sets, three statistical tests were used for the pre- versus post- change parameter estimate means, all according to Chatfield and Collins (2000). The null hypothesis is that all the samples are from the same population (i.e. there is no significant difference between the pre- and post-change regression lines). A full description of the statistical analysis is given in Appendix 2.

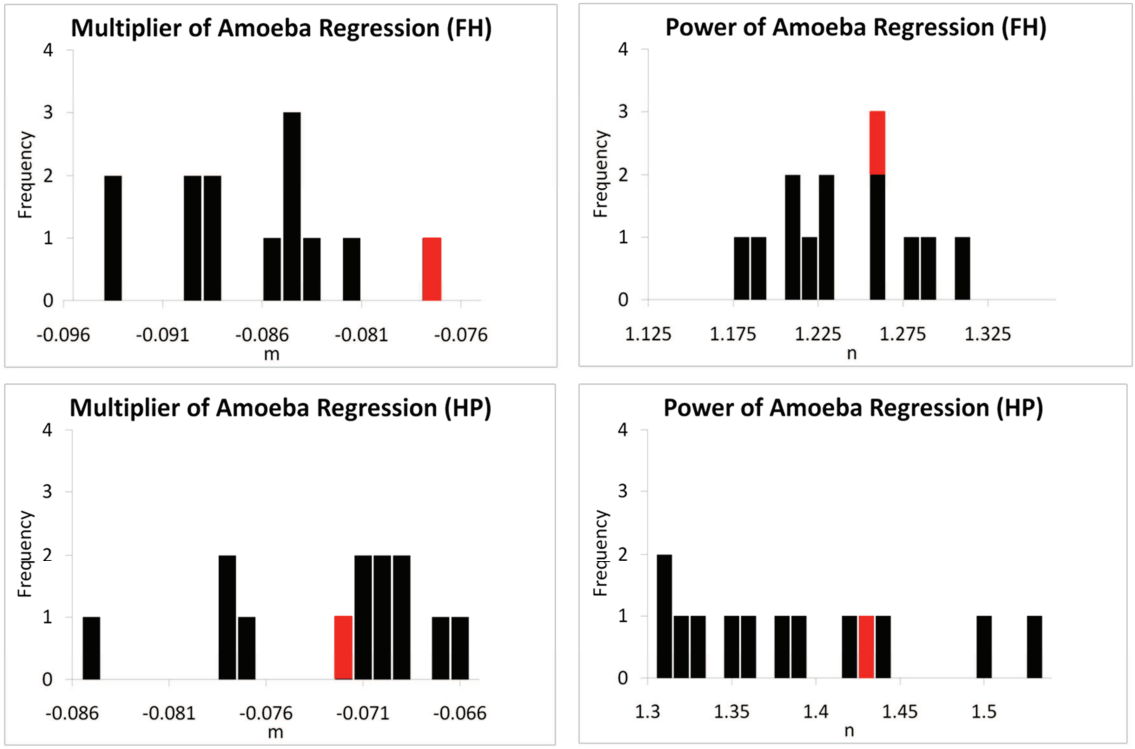

Figure 5.27 Footholme (Top) and Hodder Place (Bottom) histograms showing the multiplier and power of the Amoeba regressions (left and right respectively). The pre-change values are in black and post-change values in red

The first statistical test involved a t-test of the difference in the means of two independent samples, with the means based on sample sizes of 12 and 1 (for the pre- and post- change number of years, respectively), to test the hypothesis of no difference between the mean m parameter estimates. The second test was carried out as the first, to test the hypothesis of no difference between the mean n parameter estimates. Finally, a multivariate Hotelling T^2-test was done to determine whether the two parameter estimates taken together have no significant difference between the pre- and post- change periods.

The first two tests showed that, for Footholme, the post-change mean m parameter estimate is significantly different at the 5% significance level from the pre-change mean m parameter estimate (p = 0.036), while the mean n parameter estimate is the same for both periods (p = 0.692). For Hodder Place, both the pre- and post-change mean m and n parameter estimates are statistically the same (p=0.985 and p=0.619 respectively). These results are in line with the frequency diagrams in Figure 5.27. However, the Hotelling T^2-test showed that, for both Footholme and Hodder Place, the

post-change combination of m and n parameter estimates is not significantly different (5% level) from the pre-change parameter estimates (p=0.060 (FH) and p=0.827 (HP)).

In addition to the statistical tests on the means, a pair-wise comparison of the bootstrap estimated parameter variance ratios of individual years was made, which included the ratios between pre-change years as well as the ratios between pre- and post-change years (see Appendix 2). As the post-change ratios fell within the range of the pre-change ratios, it may be concluded that no change has been detected.

Finally, Table 5.11 also shows that no systematic change can be detected in the post-change catchment behaviour, as the parameter estimates of some pre-years are able to predict the post-change behaviour as accurately as the parameter estimates of the post-change year.

Table 5.11 NSE-morph efficiencies for runoff predictions at Footholme and Hodder Place for the post-change year period using the SDD parameter estimates of pre-change years

Parameter estimates used in simulation (period)	NSE-morph	
	Footholme	Hodder Place
	2009-2010 period	2009-2010 period
2001-2002	0.763	0.841
2002-2003	0.769	0.849
2003-2004	0.761	0.837
2004-2005	0.766	0.846
2005-2006	0.771	0.844
2006-2007	0.778	0.837
2007-2008	0.766	0.839
2009-2010	0.781	0.849

Overall, it may be concluded that the statistical tests have not provided the evidence against the null hypotheses of no difference between the pre- and post- change SDD parameter estimates. It is therefore assumed that there are no significant changes observed between the pre- and post- change catchment behaviour as described by the SDD parameter estimates derived from the recession data, either at FH or at HP.

5.3.3 Discussion of the use of DBM and SDD Models for Change Detection

The focal point of the evaluation of the DBM and SDD models as change detection techniques should be their applicability to short term records such as those collected for the current study. For the purpose of change detection, the overall goodness of fit is of minor concern. The results presented in the two sections above show that overall, for a specific short period in time the DBM model can provide slightly better fits than the SDD model. This is probably a function of the number of parameters involved in the two models respectively. For example, when 10 random x and y data pairs are considered, given enough parameters, it is not difficult to obtain a much better relation between x and y with a high-degree polynomial relation than a simple linear relation (Klemes, 1983). However, the DBM analysis has shown large variability in the parameter estimates between the pre-change years and the catchment behaviour of one year cannot consistently be predicted with parameter estimates of other pre-change years. On the other hand, the parameter estimates of the SDD model showed much more consistency between periods, because the focus has been on getting good fits to the recessions, which tend to be stable and less sensitive to year to year variability.

Detecting the effects of LUMCs requires detecting systematic changes in the presence of natural variability. A model that is sensitive to systematic change effects, but insensitive to natural variability is therefore needed. The DBM method makes use of the effective precipitation and the discharge data, which include the full spectrum of the hydrograph. These are known to be sensitive to natural variability (e.g. due to variability in antecedent conditions and precipitation). If the pre and post-change records are long enough so that the full natural variability is properly sampled for both periods, the DBM model, as any other statistical model, could rely on being insensitive to natural variability. The problem with short records, though, is that they are not long enough to sample the full range of natural variability (i.e. by analogy with the example of curve fitting, they sample only a segment of the full curve). Consequently, the DBM parameter estimates obtained for a certain (short) time period reflect the average conditions only within the sampled period, masking any sensitivity to LUMC effects between periods.

In agreement with the findings here, McIntyre and Marshall (2010) and McIntyre et al. (2011) also found differences in DBM parameter estimates and performances between short data periods for specific sites in the Pontbren study. The most pronounced differences were observed between winter and summer periods and when a prolonged dry spell was included in one of the periods. McIntyre et al. (2011) attributed this to the complexity of wetting and drying dynamics as well as potential changes to physical soil properties, between wet and dry periods. Beven et al. (2008a; 2008b) made a first step in illuminating some of the dependency of DBM parameter estimates on natural variability by event classification, based on antecedent conditions and the maximum peak discharge. However, they still found considerable scatter between periods for one event class, resulting in a continued inability to differentiate clearly between effects of LUMC and natural variability.

Against the background of year to year and season to season variability, it is not recommended to use the DBM method (or any other statistical method that relies on a full sampling of the natural variability) for change detection on the relatively short dataset from the multiscale nested monitoring design. Any changes that could be detected between the 6-12 month period prior to and approximately 18 months post the implementation of the LUMCs could be reflecting only natural (climatic) variability.

In contrast, the SDD model relies only on data from recession curves, which are less likely to be insensitive to natural variability. Even though the analysis showed that not all pre-change year SDD parameter estimates are statistically the same, this does not instantly make the SDD model unsuitable as a change detection technique. Compared with the DBM variability in pre-change parameter estimates, the SDD variability is much smaller and the catchment behaviour of one pre-change year can be predicted more consistently using the parameter estimates of other pre-change years. The analysis has shown though, that the SDD model would not be able to pick up very subtle changes in catchment behaviour as a result of LUMC, owing to some dependency on natural variability.

For short records (and arguably also for longer term records), it remains unfeasible to fully eliminate the effect of natural variability. In addition, as highlighted in Chapter 2, it should be noted that data records that cover only one season or specific types of

storms that do not reflect the full range of variability might over- or under-estimate the overall effects of LUMC, or not detect them at all.

However, compared with many (statistical) methods including the DBM method, the SDD method (based on data from the recession only and involving few parameters) offers a better alternative for LUMC detection. Even though statistically the SDD method cannot avoid some dependency on natural variability, the differences in the parameter estimates as a result of natural variability are relatively small. For this reason the SDD model was selected as the change detection method for the short term records in the current study, with the assumption that potential effects of LUMC would be picked up more quickly through the SDD method than the DBM method.

5.3.4 Peak Flow Analysis

In the evaluation of the two change detection methods the main focus has so far been on the general catchment response and the shape of the hydrograph. However, as discussed in Chapter 2, LUMC are prone to affect not only the shape of the hydrograph, but also the timing and magnitude of the peak flow. Therefore, an analysis of effects on the peak flows should also be included as part of the LUMC change detection.

It was shown in Section 5.3.1 that the lag time of the peak flow is quite sensitive to natural variability. It can be approximated by the 'delay' DBM parameter estimate. Based on the results of the DBM analysis, the FH peak flow lag time ranged between 1 and 3 hrs for the different years, while that of HP ranged between 3 and 7 hrs. The post-change DBM 'delay' parameter estimate fell within the pre-change range for both sites. This might be interpreted as no change detected, but as discussed above, it is difficult to draw solid conclusions because of the natural variability.

The following focusses on change detection on the magnitude of the peak flow. Simple methods that allow for comparisons between relative peak flow rate responses include evaluations of the relationships between peak flows and the total rainfall in a certain time window preceding the peak flow and/or the maximum rainfall intensity (during that time window) prior to the occurrence of the peak flow. For Footholme and Hodder Place, the flow rates of the 25 largest peaks of each year were taken from the records. To exclude multiple peaks within a single event, only the highest peak within a

window of 16 hr for FH and a window of 24hr for HP was considered. Linear regressions through the FH data show a reasonable relation between the peak flow rate and the total rainfall in a window (optimum 8hr) prior to the peak (average R^2 for the annual regressions = 0.60). The relation with the maximum rainfall intensity is poor (average R^2 = 0.28). For Hodder Place the R^2 values were 0.76 and 0.32 respectively, for a 12 hr window prior to the occurrence of the peak.

However, a better relationship could be obtained between the peak flow rate and the Antecedent Precipitation Index (API), for which the regressions showed average R^2 values of 0.65 for Footholme and 0.83 for Hodder Place. The API can be used as a measure of the soil wetness prior to a rainfall event and is described by Equation 5.18 (Linsley et al., 1949; Shaw, 1988):

$$API_t = k * API_{t-1} + P_{t-1} \qquad \text{(Equation 5.18)}$$

where API_t and API_{t-1} are the antecedent precipitation index values in (*mm)* at time *t* and *t-1* respectively, P_{t-1} is the precipitation in (*mm)* at *t-1, and k* (-) is a time decay factor, inversely representing the rate at which the catchment wetness declines in the absence of precipitation. The value of *k* depends on catchment characteristics such as soil type (Shaw, 1988). Relatively flashy catchments have low values for k resulting in less importance of precipitation during previous time intervals in comparison with the catchment wetness.

Beschta (1990) demonstrated that one possible way to obtain the value of k is from the slope of the relation between the discharge at Q_{t-1} and Q_t. Using this technique the values of k for *hourly* Footholme and Hodder Place data are 0.92 and 0.93, respectively. Though very similar, the relative dependence on antecedent precipitation is smaller for Footholme.

In this section, the peak flows are compared with the API at the peak time (and hence not at a time prior to a precipitation event). In this way, the precipitations during the event, as well as the relative catchment wetness, are taken into account. $API_{t,0}$ was set to 10 mm for both catchments. Figure 5.28 and 5.29 show the peak discharge versus the API at the peak time for the 25 largest events for each hydrological year since 2001. The data have the same colour coding as used in Section 5.2.

A 95% confidence ANOVA test of the linear regression lines through the data in Figures 5.28 and 5.29 showed that there is no statistical similarity between the regressions of all pre-change years ($p < 0.05$, see Appendix 2). This can be attributed to the natural year to year variability. For example, 2002-2003 has been recorded as a relatively dry year with overall low runoff ratios (see Section 5.2). Accordingly, in Figures 5.28 and 5.29 the regressions through the data of this hydrological year (dark blue line) show a relatively low intercept and a less steep slope, for FH as well as HP.

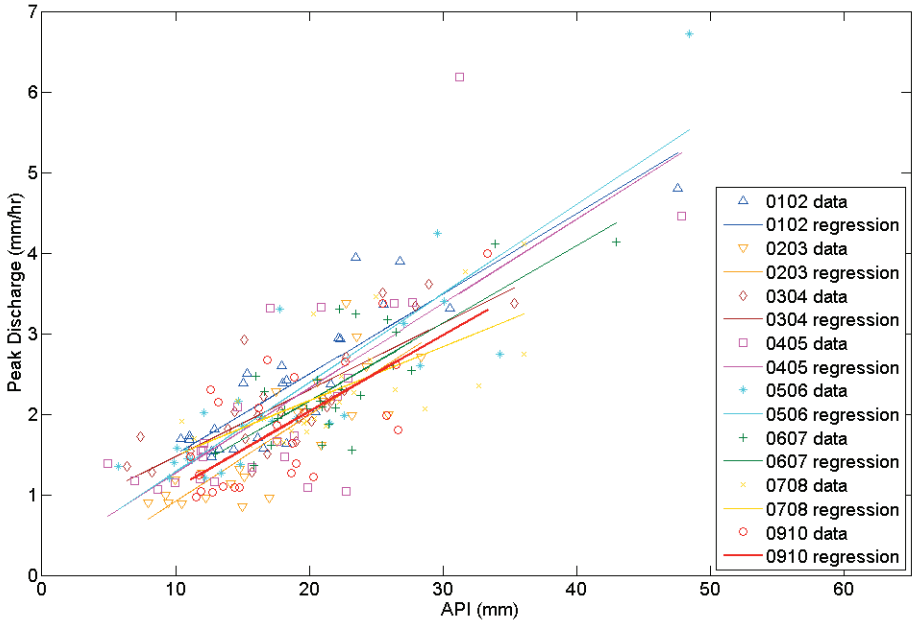

Figure 5.28 Linear regressions of peak discharge on API for the 25 largest events of each hydrological year for Footholme

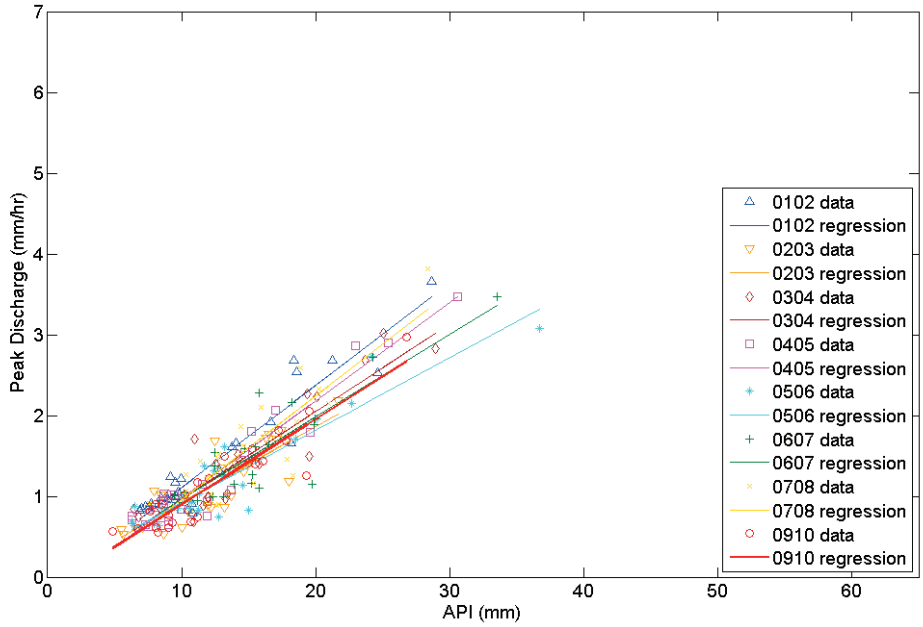

Figure 5.29 Linear regressions of peak discharge on API for the 25 largest events of each hydrological year for Hodder Place

As shown in Figure 5.21 the SDD model is also able to predict the peak flows well, although some scatter may be observed. Figure 5.30 shows the 25 highest observed peaks for the 2002-2003 (relatively dry) year (left) and the 2006-2007 (relatively wet) year (right), for Footholme (top) and Hodder Place (bottom). The SDD simulated data, for which the model parameter estimates of all other pre-change as well as the post-change year were used, are plotted against the observed data. To allow for timing differences between the observed and simulated peak flows (see Section 5.3.2), the simulated peaks flows were matched manually with the observed peaks flows.

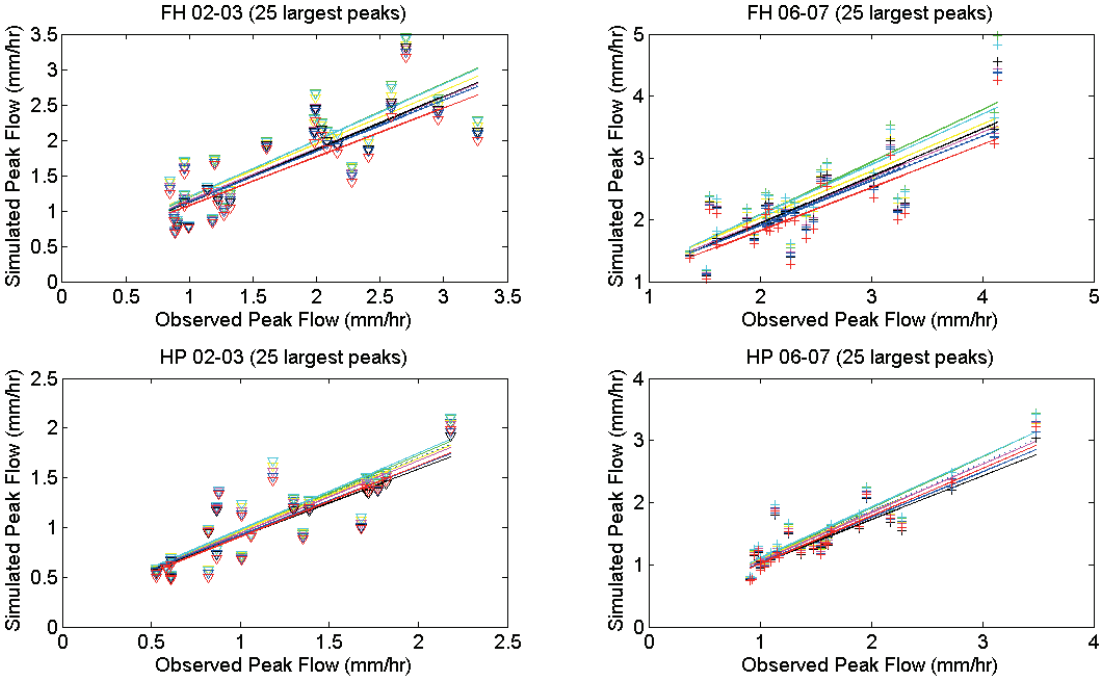

Figure 5.30 Simulated versus observed peak flow for the 25 highest peak flow rates for the 2003-2003 (left) and the 2006-2007 (right) pre-change years for Footholme (top) and Hodder Place (bottom). The simulated peak flows are based on SDD model parameter estimates from all pre- and post-change years. The colour coding is consistent with all other figures (e.g. Figure 5.29 and 5.30) with the post-change year in red.

From Figure 5.30 there is no clear difference between the relation of the observed and simulated peak flows, using the parameter estimates of any pre- or post-change year. ANOVA tests showed that the intercept and slope of all regressions for one subplot in Figure 5.31 are statistically the same ($p > 0.05$). The full ANOVA test results are shown in Appendix 2. As the post-change parameter estimates are just as able to adequately predict the peak flow response as the pre-change parameter estimates, the analysis also shows that there is no reason to suggest that the changes in LUM have had an effect on the peak flow response.

5.4 Multiscale Short Term Land Use Change Data Analysis

The SDD method has been applied to all pre- and post-change short term data of the full monitoring network (excluding the gauge at LOS_out, see Appendix 1). Section 5.4.1 describes the recession analyses for change detection. Section 5.4.2 evaluates the overall pre- and post-change simulations, and Section 5.4.3 focuses on potential impacts on the peak flows. To allow for between-site comparison, the time interval for all sites is 15 min. Unless otherwise stated, the SDD model has been applied according to the procedures described in Section 5.3.2. The selection of recession data from flow data has been slightly adjusted for the 15 min records. At this time interval, prolonged recession periods with continued rainfall occurred, which significantly affects the shape of the recession curve. For that reason, these data were discarded during the optimisation of the SDD parameters.

5.4.1 SDD Pre- and Post-Change Recession Analyses

Table 5.12 shows the *m* and *n* parameter estimates (Equation 5.10), and the *b* and *c* parameters of the attractor equation (Equation 5.12) for the pre- and post- change periods of all gauges. The length of each of these periods is also given, as well as the upstream area and the type of LUMC (grip blocking (GB), tree planting (TP) and changes in stocking density/management (SD)) that occurred upstream of each of the gauges (also see Chapters 2 and 4 and Appendix 1). The gauges of CRO_mid, EAS_out and LOU_out have not undergone any land use/management change, but the data record has been subdivided into a 'pre-change' and a 'post-change' period, defined by the pre- and post-change periods of the nearest gauge that has undergone change. For CRO_mid this is CRO_sc5, for EAS_out this is CRO_out and for LOU_out this is LAN_out.

On initial inspection, the pre- and post-change individual parameter estimates for most gauges are quite similar. A few larger differences may be observed for sites with a relatively short pre- or post- change period, such as CRO_out, HAR_out and HOD_mid. The largest difference in the parameter estimates is observed for CRO_sc5, a gauge downstream of a grip blocking site.

Table 5.12 Pre- and post-change SDD parameter estimates for short –term data.

Gauge	Area (km^2)	LUMC	Pre- and post- change periods, dates		m	n	b	c
CRO_sc5	0.5	GB, (SD)	pre	15/08/08 -31/01/09	-0.155	1.451	11.79	1.82
			post	01/03/09 -11/08/10	-0.119	1.301	12.04	1.43
BRE_sap	1.7	GB, (SD)	pre	15/08/08 -31/10/08	-0.164	1.101	6.78	1.11
			post	01/12/08 -11/08/10	-0.156	1.211	8.12	1.27
LOS_mid	2.5	SD	pre	14/01/09 -31/03/09	-0.117	1.723	30.91	3.61
			post	01/06/09 -02/03/10	-0.120	1.675	25.70	3.08
BRE_rhw	2.8	GB, (SD)	pre	15/08/08 -31/10/08	-0.201	1.226	6.42	1.29
			post	01/12/08 -11/08/10	-0.188	1.324	7.85	1.48
CRO_mid	3.6	(SD)/(-)	pre	15/08/08 -31/01/09	-0.139	1.406	12.11	1.68
			post	01/03/09 - 26/04/10	-0.129	1.507	15.72	2.03
HAR_out	4.9	SD	pre	16/12/08 - 01/02/09	-0.149	1.442	11.99	1.79
			post	01/04/09 - 11/08/10	-0.135	1.351	11.40	1.54
WHI_mid	10.0	SD, TP	pre	15/08/08 -31/10/08	-0.132	1.306	10.90	1.44
			post	01/12/08 -11/08/10	-0.137	1.208	9.24	1.26
CRO_weir	10.4	GB, SD	pre	15/08/08 -31/01/09	-0.146	1.530	14.59	2.13
			post	01/03/09 -11/08/10	-0.139	1.558	16.30	2.26
BRE_out	11.0	GB, TP, SD	pre	15/08/08 -31/10/08	-0.155	1.691	20.88	3.24
			post	01/12/08 - 06/06/09	-0.165	1.743	23.58	3.89
EAS_out	13.3	-	pre	15/08/08 -31/01/09	-0.182	1.330	8.21	1.49
			post	01/03/09 -11/08/10	-0.161	1.449	11.30	1.82
WHI_out	13.6	SD, TP	pre	15/08/08 -31/10/08	-0.173	1.231	7.52	1.30
			post	01/12/08 -11/08/10	-0.127	1.344	12.01	1.53
LAN_mid	15.0	SD, (TP)	pre	15/08/08 -31/01/09	-0.158	1.547	14.00	2.21
			post	01/04/09 - 11/08/10	-0.154	1.499	12.96	1.20
CRO_out	21.1	GB, SD	pre	04/10/08 - 31/01/09	-0.142	1.394	11.62	1.65
			post	01/03/09 -11/08/10	-0.124	1.417	13.87	1.71
FH	25.3	GB, TP, SD	pre	15/08/08 -31/10/08	-0.150	1.401	11.14	1.67
			post	01/12/08 -11/08/10	-0.148	1.381	10.91	1.62
LAN_out	27.7	SD, (TP)	pre	15/08/08 -31/01/09	-0.140	1.542	15.59	2.18
			post	01/04/09 - 11/08/10	-0.147	1.629	18.38	2.70
LOU_out	47.0	-	pre	15/08/08 -31/01/09	-0.133	1.224	9.71	1.29
			post	01/04/09 - 11/08/10	-0.131	1.309	11.08	1.45
HOD_mid	110.3	(GB), (SD)	pre	15/08/08 -31/01/09	-0.114	1.355	13.56	1.55
			post	01/03/09 -11/08/10	-0.124	1.368	12.77	1.58
HP	261.0	GB, TP, SD	pre	15/08/08 -31/10/08	-0.105	1.434	16.86	1.77
			post	01/04/09 - 12/08/10	-0.105	1.445	17.17	1.80

More information can be obtained from the regression lines of the recession data as a whole. Figures 5.31, 5.32 and 5.33 show the pre- and post-change recession plots, using the *m* and *n* parameter estimates as presented in Table 5.12 for the nested sites

of the Croasdale, Dunsop (Brennand and Whitendale), and Langden subcatchments respectively. For each of these subcatchments, the downstream and associated gauges are also shown in such a way that all micro, mini, and meso scale gauges are shown. For each figure, the plots have been schematically presented in the way they are nested. The main LUMCs for the Dunsop subcatchment are grip blocking, tree planting and stocking density/management changes (see Figure 4.11). For the Langden subcatchment these are stocking density/management changes and some minor tree planting, and for the Croasdale subcatchment, grip blocking and slight changes in stocking density and management (Figure 4.11). Figures 5.31, 5.32, and 5.33 show that, visually, the regression lines through the pre and post change recessions appear very similar (if not the same) for most gauges. The main exception is CRO_sc5. Small differences between the pre- and post-change regression lines of HAR_out, CRO_out, and HOD_mid are also observed. As noted before, though, these sites have relatively short data records. Care should also be taken with any physical interpretation of the SDD parameter estimates and/or model simulations of BRE_out, WHI_out, LAN_mid, and LAN_out. The first two gauges record only relatively high flows (see Appendix 1) and the latter two are downstream of major abstraction works, for which only unreliable abstraction data are available.

In spite of any LUMC effects, the analysis of different pre-change periods in Section 5.3.2 showed that significant differences are likely to be observed in the regressions of short term recession data, as a result of natural variability. However, it is possible to look at a particular gauge and compare the results of the statistical tests with the results of the other gauges. T and Hotelling T^2 tests were performed on the bootstrap estimated properties of the SDD parameters (Appendix 2). In agreement with the results above, the statistical tests showed that the difference in the mean bootstrap estimated pre- and post- change parameters seems to be particularly large for CRO_sc5 (e.g. Hotelling's T^2 F statistic = 304485), especially when the test results are compared with those of the neighbouring catchment CRO_mid (F statistic = 80865), which has not undergone any changes, and with the downstream site of CRO_weir (F statistic = 11436). On the other hand, the test statistics of all other gauges for which land use/management change did occur are of the same order of those of the three gauges for which no changes occurred (see Appendix 2).

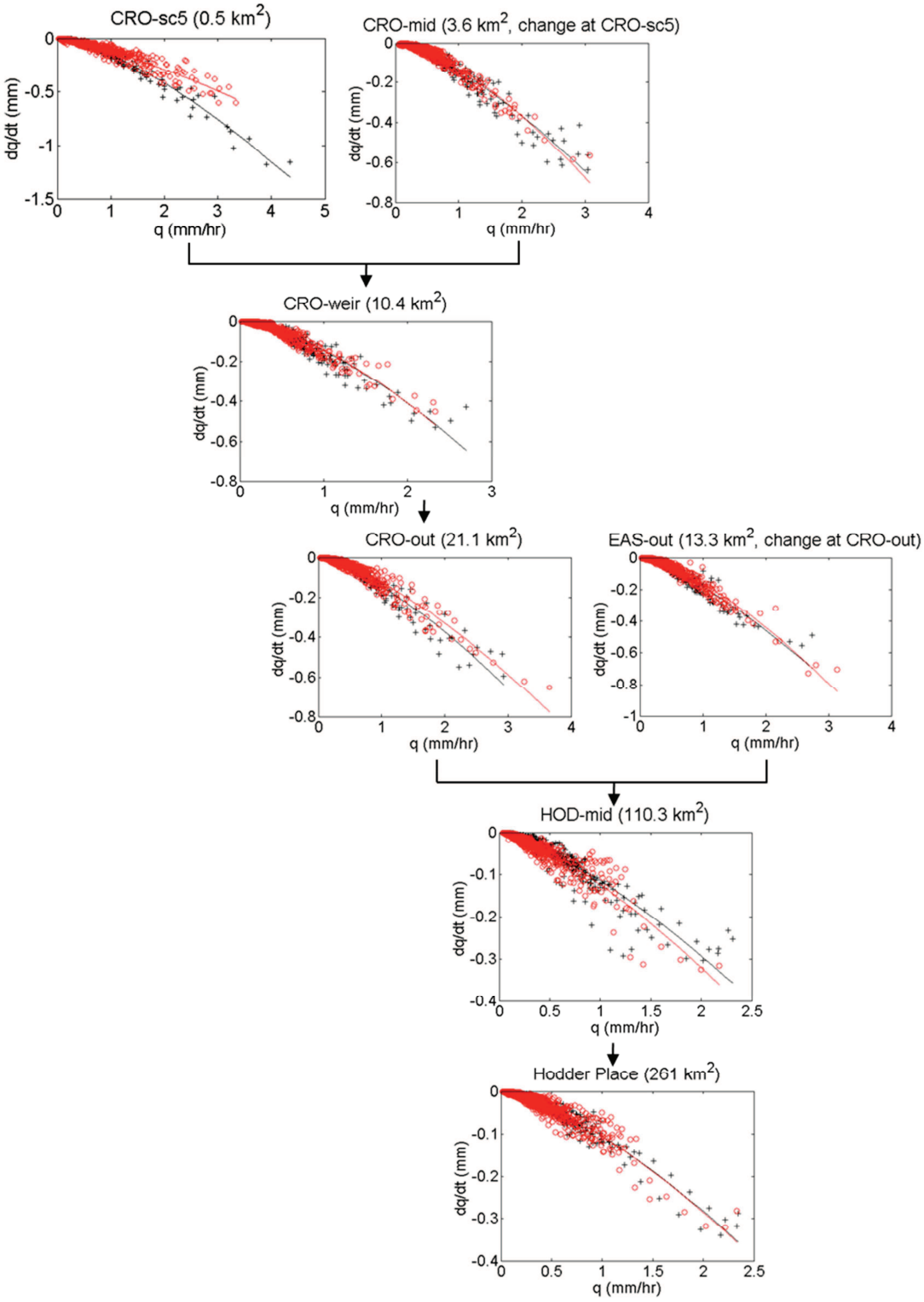

Figure 5.31 SDD regressions of recession data observed at nested multiscale sites (pre-change data in black and post-change data in red), undergoing grip blocking (all but CRO_mid), stocking density changes (all but CRO_mid and CRO_sc5) and tree planting (Hodder Place)

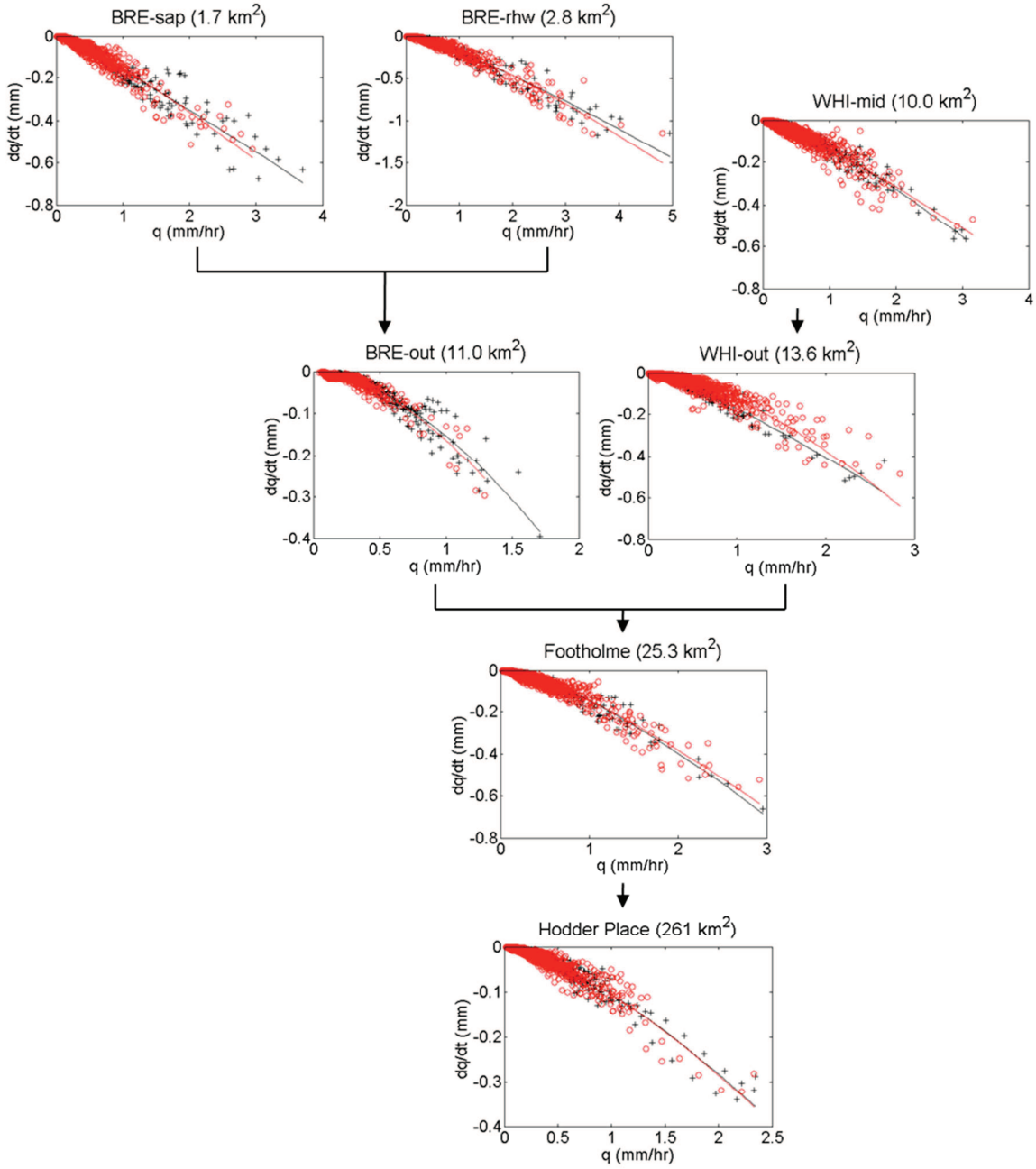

Figure 5.32 SDD regressions of recession data observed at nested multiscale sites (pre-change data in black and post-change data in red), undergoing grip blocking, stocking density changes (all) and tree planting (BRE_out and Footholme)

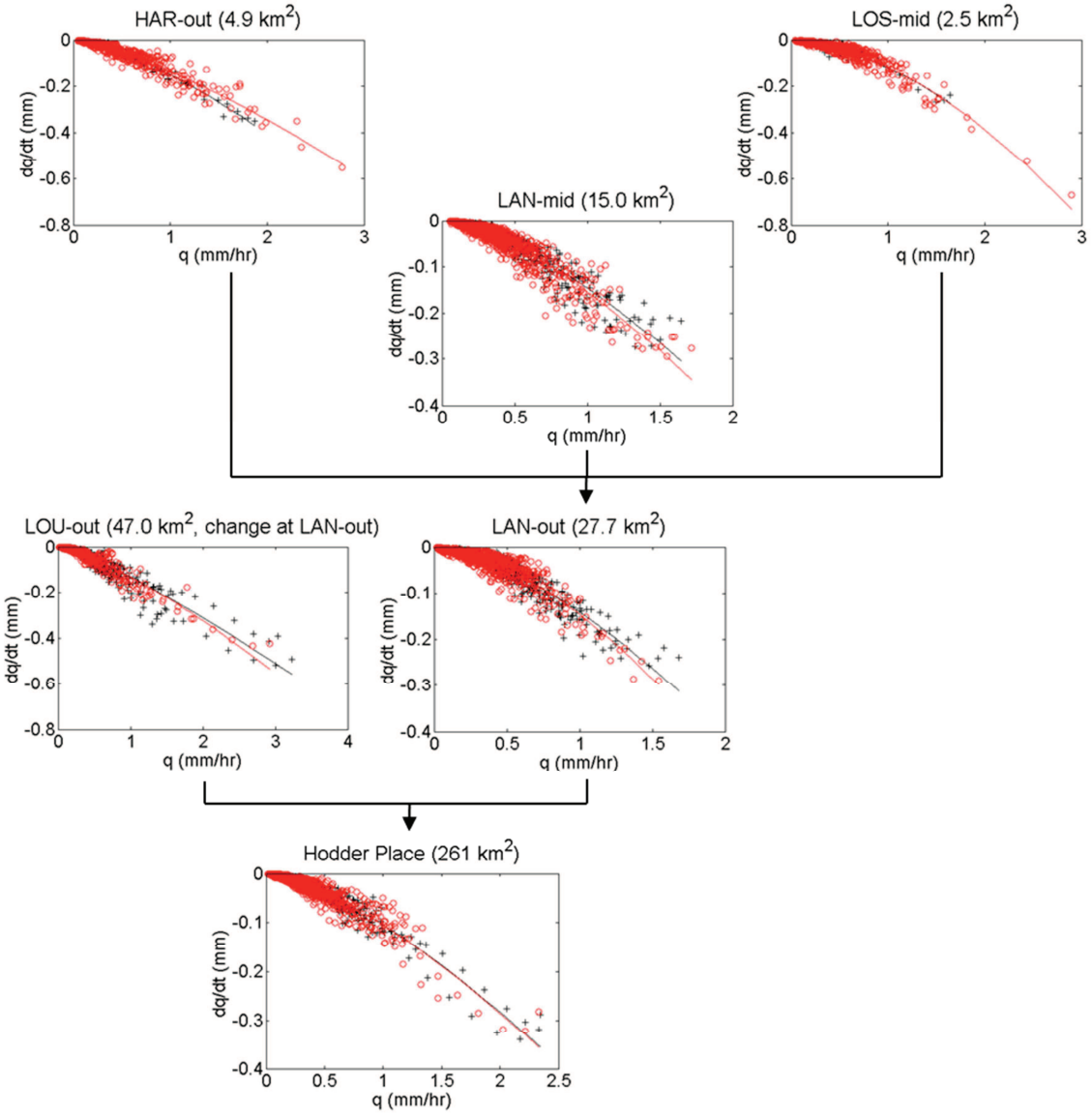

Figure 5.33 SDD regressions of recession data observed at nested multiscale sites (pre-change data in black and post-change data in red), undergoing grip blocking, stocking density changes (all) and tree planting (BRE_out and Footholme)

5.4.2 Pre- and Post-Change SDD Model Simulations

Figure 5.34 shows the NSE-morph efficiencies for the pre- (black) and post- change periods based on the pre-change SDD parameter estimates versus those based on the post-change parameter estimates. These data exclude the sites of BRE_out, WHI_out, LAN_mid and LAN_out (see above). Overall, the pre-change periods have higher NSE-morph efficiencies than the post-change periods (Figure 5.34). This could be related to the prolonged winter period with extensive snow lying (and hence snow melt) during the post-change period. The SDD does not allow for any snow related effects. The potential of LUMC effects is ruled out, as the pre- and post-change parameter estimates fit the post-change period similarly well, demonstrated by the fact that the NSE-morph efficiencies in Figure 5.34 largely fall around the blue 1:1 line. However, it is difficult to draw firm conclusions about the pre- versus post- change simulations from just the NSE-morph efficiencies. This is because the NSE-morph, as the NSE, is just a single-valued goodness-of-fit measure index that can be sensitive to a number of factors, including sample size, outliers, magnitude bias, and time-offset bias (McCuen et al., 2006).

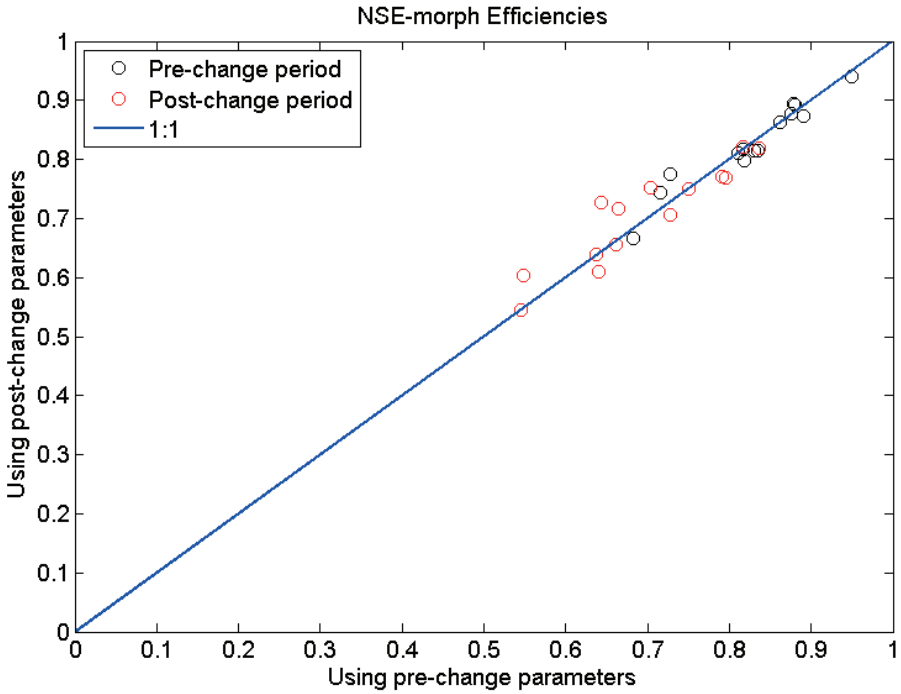

Figure 5.34 Pre (black) and post (red) change period NSE-morph efficiencies for the SDD model simulations using the post-change period parameter estimates plotted against those using the pre-change parameter estimates

For example, for the CRO_sc5 pre-change period, the NSE-morph ratio is close to 1, which could be interpreted as no change detected between the pre-and post-change period. However, the previous section showed that the pre- and post- change recessions and SDD parameter estimates of the CRO_sc5 grip blocking site were quite different. More valuable information on the relative fits of the pre- and post-change simulations can be gained from Figure 5.35 which shows the observed and simulated discharge using pre and post change SDD parameter estimates for a pre-change event for CRO_sc5 (left) and CRO_mid (right).

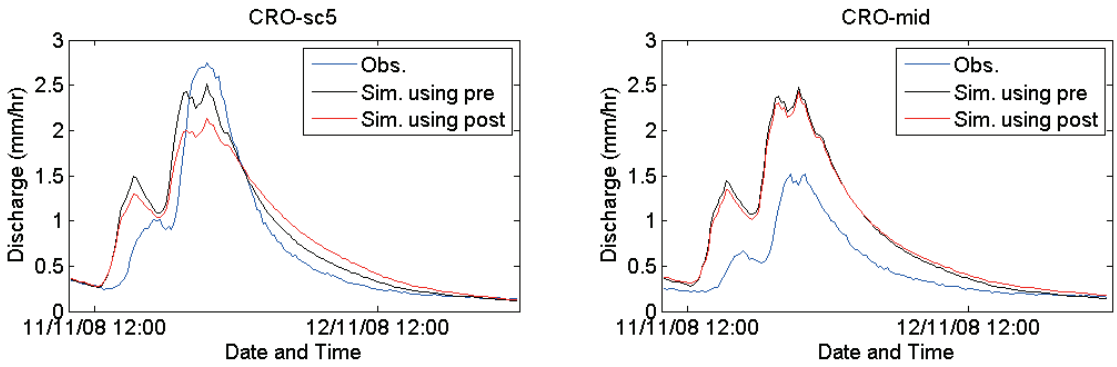

Figure 5.35 Observed (blue) and simulated discharge using pre- (black) and post-change (red) SDD parameter estimates for an event during 11/11/2008 for CRO_sc5 (left) and CRO_mid (right)

The overall fits are better for CRO_sc5 than for CRO_mid. However, there is a significant difference in the CRO_sc5 hydrograph simulations of those based on the pre- and post- change parameter estimates respectively. In contrast, the simulations at CRO_mid are the same for the two parameter estimate sets, although both show a relatively poor fit. The plots in Figure 5.35 suggest that no change is detected at CRO_mid, although potentially there has been at CRO_sc5. It is noted though, that the difference between the CRO_sc5 pre and post change parameter estimates model simulations is of the same order as the difference between the observed and simulated hydrographs.

5.4.3 Pre- and Post-Change Observed and SDD Simulated Peak Flows

In Figure 5.36 the 25 largest pre-change simulated peaks are plotted against the observed peaks, with the simulated peaks based on the parameter estimates of the pre- and post-change periods separately. Overall, considering the limitations of the SDD model (Section 5.3.2 and 5.3.3), the observed and simulated peak flows correspond reasonably well as they are close to the 1:1 line.

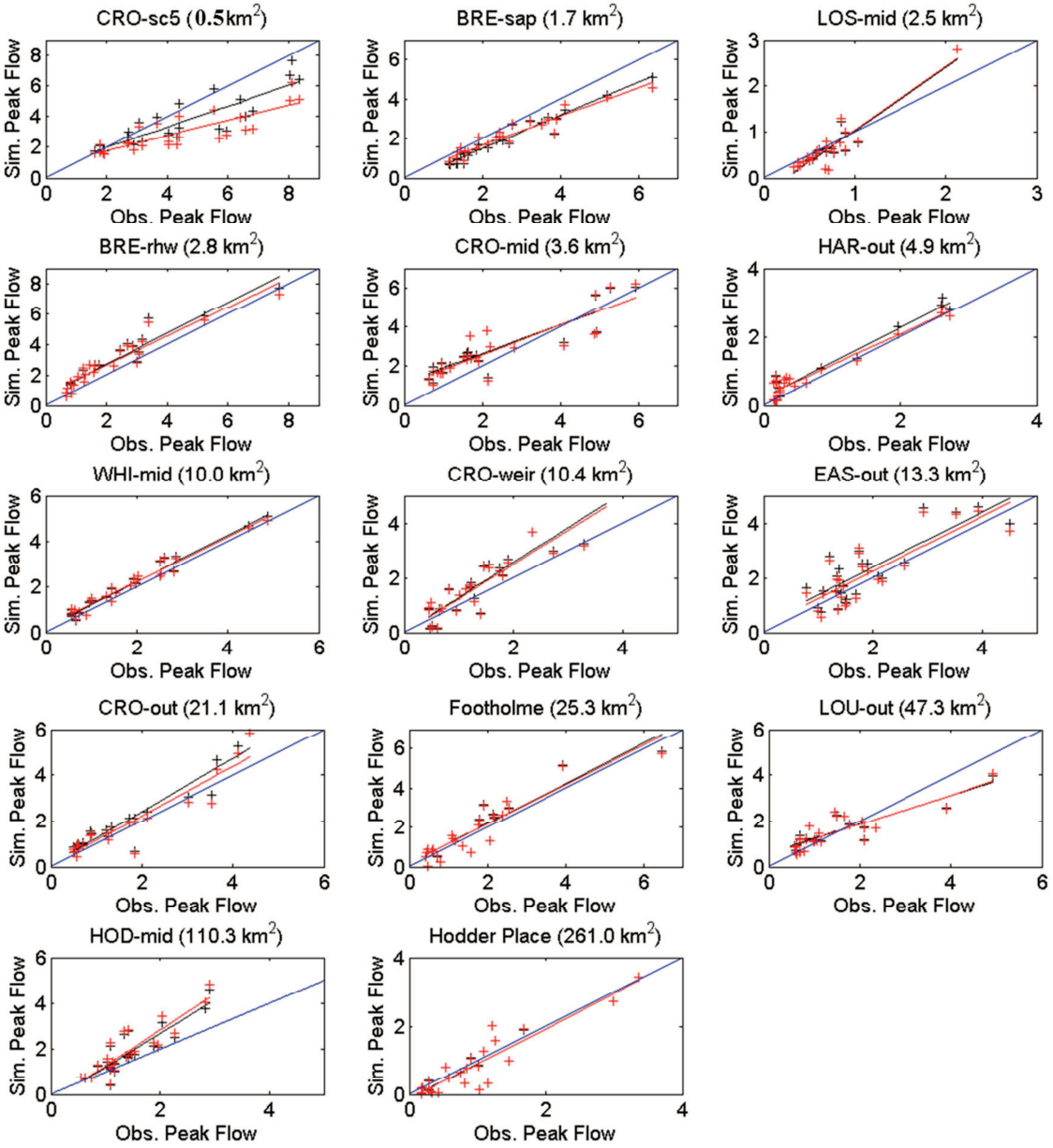

Figure 5.36 Simulated versus observed peak flows (mm/hr) of the 25 largest peak flows during the pre-change period, using pre- (black) and post- change (red) parameter estimates. The blue line represents the 1:1 ratio.

The plots in Figure 5.36 show that for most gauges the simulated peaks slightly overestimate the observed peaks, but there are no large differences between the simulated peaks using the pre-and post-change parameter estimates respectively. The results of statistical t-tests (according to Kleinbaum et al., 1988 p. 266-269) on the intercept and slope of the pre- versus post- change regression lines in Figure 5.36 confirm these visual observations for most gauges ($p>0.05$, H_0 = equality of slope and intercepts). For three gauges (HAR_out, HOD_mid, and CRO_out) the slopes of the regressions are significantly different, although the intercepts are the same. As noted above, for these three gauges, either the pre- or post- change period is relatively short (see Table 5.12), which may have resulted in insufficient recession data for the reliable optimisation of the SDD parameters.

Figure 5.36 shows that the regressions based on pre- and post-change parameter estimates simulations for CRO_sc5 are visually different, suggesting that the peak flows of the post-change period at CRO_sc5 have reduced in comparison with the peak flows of the pre-change period. However, statistical analyses showed that both the slope ($p=0.387$) and the intercept ($p=0.505$) of the peak flow regressions are not significantly different (Appendix 2).

5.4.4 Discussion of Short Term LUMC Impacts

The results of the previous three sections showed that there is not enough evidence to suggest that the SCaMP LUMC in the Hodder catchment have had a statistically significant short-term impact on the overall catchment response of any of the subcatchments other than potentially at CRO_sc5.

The suggestion that no change has been detected could be the interpreted in a number of ways, including 1) there are no LUMC effects on the overall catchment behaviour, 2) it takes a long time before the full impacts of LUMC are established and can hence be detected, and/or 3) owing to the sensitivity of the SDD method to natural variability, the method is unable to detect the LUMC impacts. It is clear that longer records are needed to make a solid case for any (combination) of these interpretations. Here, arguments are raised for and against that may lead to some preliminary

conclusions about the SCaMP LUMC impacts in the Hodder catchment at increasing scales.

Based on the findings in Chapter 2, it is expected that those catchments that have undergone changes in tree planting and/or stocking density/management will not experience immediate short-term impacts as the time for the transfer from the pre-change situation to the fully established post-change situation is likely to exceed the short term monitoring period. In contrast, from observations in the field, some effects of grip blocking are quite immediate as the quick displacement of water through the drains is halted and the water is redirected onto the adjacent peat. In addition, small storage ponds are created upstream of the drain blocks (Figures 3.15 and 3.16).

The three micro scale catchments in which grip blocking took place are CRO_sc5 in the Croasdale subcatchment, and BRE_sap and BRE_rhw in the Brennand subcatchment. Approximately 38, 35 and 20% of these catchments was gripped and hence subject to change (Chapter 3 and Appendix 1). Although this could not be confirmed with statistical tests, visually, the analyses may suggest that the CRO_sc5 catchment behaviour post grip blocking is less flashy than that in the pre-change period. Possibly, a reduction in the peak flows has also occurred. This has not been observed in the BRE_sap and BRE_rhw catchments. These differences could be a function of the percentage area that has been subjected to change. Alternatively, the difference in impacts could also be attributed to differences in the drain network, original drain orientation or the location of the drainage network within the catchment (Chapter 2). Furthermore, it is possible that there might be some degree of resilience in the hydraulic catchment characteristics in responding to grip blocking. For example, peat drainage has been associated with increased macropore and soil piping (Holden, 2005a) and it is unclear if and for how long the pipe network will remain active. The pipe network accommodates quick preferential flow pathways (Chapter 2). It could therefore be suggested that a reduction in the pipe network would lead to a less flashy response, although this could be counteracted by increased overland flow.

A better understanding of the within-catchment processes (such as runoff generation and storage) and the effects on these of the grip blocking practices is needed that leads to an improved interpretation of the SDD pre- and post- change modelling results of the different catchments. Chapter 6 investigates these processes using a new physically based model that is developed specifically to study the effects of LUMC on runoff generation, storage and flow fields in upland areas. The modelling exercise also allows for the study of potential long-term effects of LUMC (Chapter 6).

Finally, there is the suggestion that the SDD method might not be capable of detecting land use management changes within the context of natural variability. This is supported by the results of the statistical analyses of the regression lines through the recession data in Section 5.3.2. The DBM and SDD methods were initially selected from a range of available methods as the two most suitable for the current analysis of the short data sets. Section 5.3 showed that of the two, the SDD method was the most robust one, with a minimum dependency on natural variability. Even though statistically the pre- and post- change SDD parameter estimates might not be the same, it has been demonstrated that the pre- and post-change responses of most gauges are very similar, despite natural variability (and potential LUM effects). The fact that the catchments not undergoing change showed similar statistical differences to catchments that did undergo LUMC supports the indication that no change has been detected at any of the sites.

5.4.5 Scaling of SDD parameter estimates

From Table 5.12 it is observed that the SDD parameter estimates of the gauges in the Hodder catchment appear scale dependent. Figure 5.37 shows all pre- (black) and post-change (red) SDD parameter estimates, with the *m* and *n* parameter estimates of Equation 5.10 in the top plots and their derived *b* and *c* parameter estimates of Equation 5.12 in the bottom plots. The graphs show that there is quite some scatter, though in general both *m* and *n* (and hence *b* and *c* as well) increase with scale. Note that the parameter estimate relationships with scale for the post-change period do not differ much from the post- change period, apart from the *m* parameter estimate, which is dominated by the difference observed at CRO_sc5.

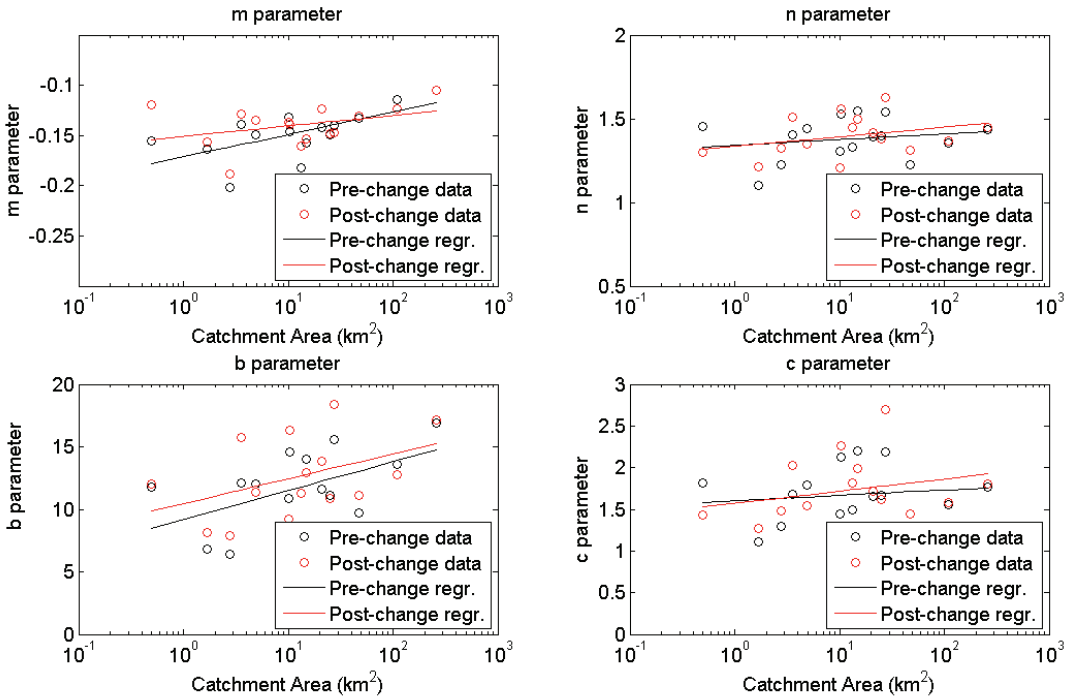

Figure 5.37 SDD pre- (black) and post- change (red) m, n, b and c parameter estimates against catchment scale

An increase of *c* with scale can be interpreted as an increase in the degree of non-linearity; an increase in *b* with scale as a decrease in the flashiness of the catchment behaviour (see also Section 5.3.2). These scale related observations are in agreement with other studies for different catchments that are based on recession analysis (Wittenberg, 1999; Clark et al., 2009).

Figure 5.38 presents an example of how this information can be interpreted in physical terms. The plot shows the relationship between area and catchment storage for five different discharge rates (1, 2, 4, 6, and 8 mm/hr). The catchment storage is calculated according to the attractor equation (5.12), using the pre-change *b* and *c* parameter estimates of the appropriate gauges for each scale in Table 5.12. The figure shows that for a specific discharge, relatively more catchment storage is needed for larger catchments. The slope of the relations becomes steeper for higher specific discharges.

The plots of Figures 5.37 and 5.38 indicate that there is some systematic variation in the hydrological behaviour with catchment size. These relatively simple relationships can potentially support the analysis of the downstream propagation of potential LUMC impacts. This is further investigated in Chapter 7.

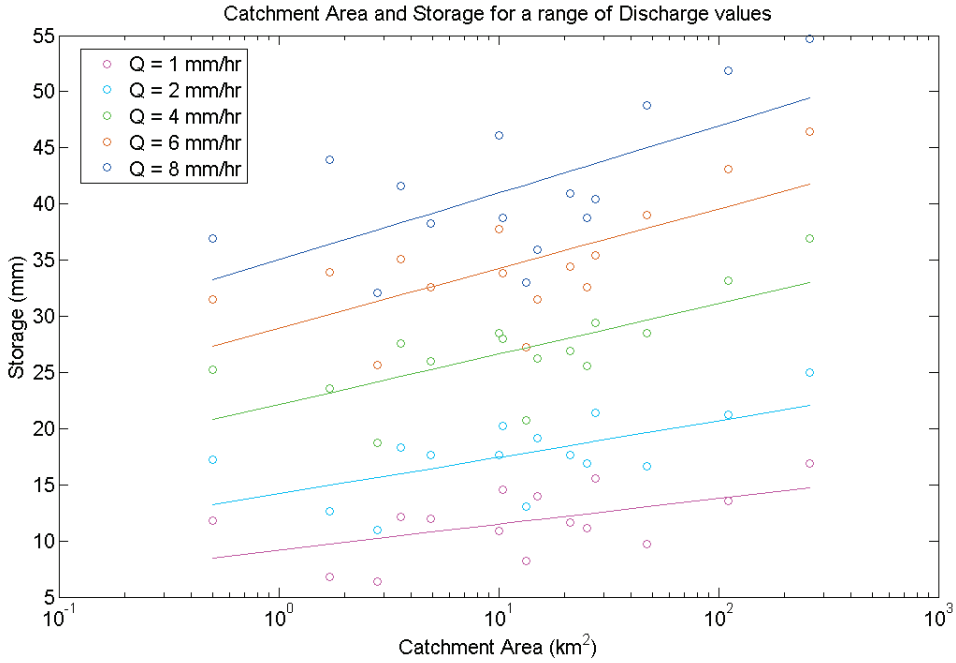

Figure 5.38 Catchment storage and area for a range of discharge values based on the attractor curve (Equation 5.12)

In the plots of Figure 5.37 and 5.38, the parameter estimates of LOS_mid are not included. This is because the values of the LOS_mid SDD parameter estimates lie beyond the patterns and range of parameter estimates of the other gauges (see Table 5.12). It might be suggested that the catchment behaviour at LOS_mid is inconsistent with those at other sites and scales within the Hodder catchment, potentially related to differences in catchment physical characteristics. On the other hand, it is quite likely that the SDD model is not able to describe the full complexity of the catchment behaviour. In essence, the SDD model is just a simple, one store, lumped model (Section 5.3.2). The exceptionally high n and c parameter estimates of LOS_mid indicate a high degree of non-linearity, which suggests that the catchment behaviour might be better described by a multiple store/reservoir system. The catchment behaviour of LOS_mid is studied in more detail in Chapter 6.

5.5 Summary

This chapter has reported on the results of change detection analysis of LUMC impacts at a range of scales within the Hodder catchment. The pre- and post- change records are relatively short (6-12 months pre- and about 20 months post-change). Long term data for Footholme (25 km^2) and Hodder Place (261 km^2) revealed that there is considerable variation in the natural hydrological conditions and the catchment response at these short term time scales. This highlighted the need for a change detection technique that is sensitive to systematic changes in catchment response, but insensitive to natural variability. An evaluation of two preselected potential change detection techniques (DBM and SDD models) showed that it remains unfeasible to fully eliminate the effects of natural variability. However, even though statistically, the SDD method cannot avoid some dependency on natural variability, the differences in the parameter estimates as a result of natural variability are relatively small, especially when compared with the DBM model. The SDD model was therefore considered as the most suitable method for change detection and hence it was applied to the analysis of the multiscale short term pre- and post-data. The analysis showed that there is no evidence to suggest that any short-term changes with respect to the SCaMP LUMCs have been detected at any of the gauges other than potentially at a small scale grip blocking site (CRO_sc5, 0.5 km^2). More information is needed on the within catchment processes and the potential effects on these for a better understanding of the short term grip blocking and long term LUMC effects.

6 Modelling Local Scale Effects of Land Use/ Management Changes on Storage and Runoff

6.1 Introduction

6.1.1 Chapter Overview

This chapter studies how the effects of LUMC on storage and runoff generation at the process scale (up to ~0.1 km^2), where the impacts of LUM practices are relatively well understood, aggregate and propagate downstream to have an impact on flood peak flows and volumes at the micro scale (~ 1 km^2). For two case studies (CRO_sc5 and BRE_sap), the effects of grip blocking are investigated; another case study (LOS_mid) investigates the impacts of stocking density and stocking management changes.

The main aims of this chapter are to 1) present a new modelling tool that allows for the investigation of the effects of LUMC on storage and runoff generation at the process and micro catchment scale in complex landscapes, 2) study the short-term effects of grip blocking at two micro scale catchments and 3) study the potential micro scale long-term effects of changes in stocking density and management.

After a brief overview of the case study catchments, Section 6.2 first describes the observed local effects of grip blocking. In Section 6.3 the modelling tool requirements are highlighted, after which a new Model for Upland Runoff Storage And Flow Fields (MURSAFF) is presented. The section also involves a description of the creation of the grid which is used by MURSAFF. The MURSAFF parameterisation, calibration and validation for the grip blocking case studies are presented in Section 6.4. MURSAFF is then used to investigate the short- term effects of grip blocking in Section 6.5. Here, the simulated short effects are compared also with the local field observations as presented in Section 6.2. The potential long-term effects of changes in stocking density and stocking management based on MURSAFF simulations are explored in Section 6.6. A summary is given at the end of the chapter, in Section 6.7.

6.1.2 Case Study Description

Chapters 2 and 5 highlighted the need for a better understanding of the changes in storage and runoff generation resulting from grip blocking at the local (micro) catchment scale. Field observations suggest that the post-blocking behaviour could potentially be less flashy than in the pre-change period, owing to the creation of storage ponds and the redirection of the water flow away from the drainage network (Figures 3.15 and 3.16). Although the significance of these observations was obscured by natural variability, Chapter 5 suggested that this was potentially also observed at the CRO_sc5 catchment outlet (0.5 km^2), but not at BRE_sap (1.7 km^2). The pre- and post- grip blocking catchment behaviour at CRO_sc5 and BRE_sap is therefore studied in more detail here. The two other main types of SCaMP LUMC involved tree planting and changes in stocking density and management (Chapter 3). Chapter 2 indicated that the overall impacts of the former are relatively well understood. Previous studies related to grazing were carried out mainly at the plot scale and ignored specific grazing patterns (such as sheep tracks). For that reason, the third case study site is that of LOS_mid, which is undergoing changes in stocking density and management.

Table 6.1 and Figure 6.1 give a brief catchment overview for the three case study areas (see also Chapter 3). Dominant features related to the case studies are highlighted in Figure 6.1. For CRO_sc5 and BRE_sap these are the grips, classified by the mean depth (map provided by *Dinsdale Moorland Services Ltd*.); for LOS_mid the field boundaries.

Table 6.1 Case study areas description

	CRO_sc5	**BRE_sap**	**LOS_mid**
Catchment area (km^2)	0.5	1.7	2.5
Elevation range (m)	263-451	329-524	191-474
Stream gauges	CRO_sc1 – CRO_sc5	BRE_grip, BRE_sap	LOS_mid
Subcatchment	Croasdale Brook	River Brennand	Langden Brook
Main land use(s)	Bog, grasslands	Bog	Grasslands
Main soil type(s)	Wilcocks, Winter Hill	Winter Hill	Belmont, Wilcocks, Winter Hill
LUMC (proportion of catchment area subject to change)	GB (0.4), SDMC (1)*	GB(0.35), SDMC (1) *	SDMC (1) *
Change period	February 2009	November 2008	Spring 2009
Total grip length (km)	1.3	13.9	-

* GB = grip blocking, SDMC = stocking density/management changes

CRO_sc5 drains the area of Swine Clough in the upper Croasdale catchment (Figure 6.1). The grip system consists mainly of a relatively large grip that joins the natural channel of Swine Clough. A few smaller side grips feed into the main grip.

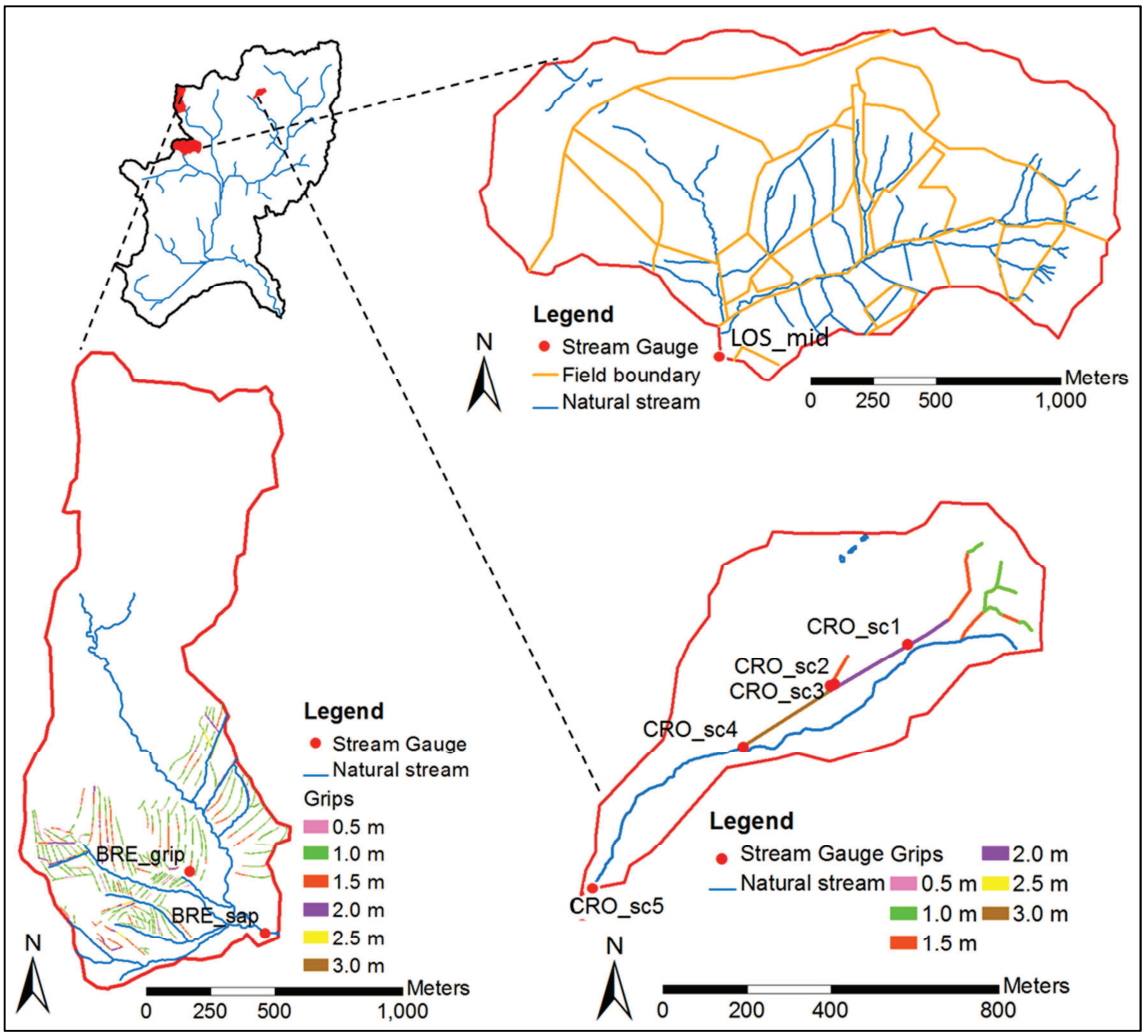

Figure 6.1 Schematic representations of case study areas LOS_mid (top), BRE_sap (left) and CRO_sc5 (right) and their location within the Hodder catchment. The grip colours show average channel depth.

BRE_sap drains the area of Sapling Clough in the upper Brennand catchment (Figure 6.1). There are many individual grips with a total length of 13.9 km.

LOS_mid drains the upper part of Losterdale Brook subcatchment of the Langden Brook (Figure 6.1). The catchment has been subjected to changes in stocking density and management, with overall reductions in stocking density and changes in spatial patterns (Chapter 3). In addition, there are sheep tracks (see example in Figure 6.2).

Figure 6.2 Examples of sheep tracks in the Hodder catchment. The tracks can be followed from gateway to gateway and crossing a stream (source: Google Earth)

6.2 Observed Local Grip Blocking Effects

There are four stream gauges upstream of CRO_sc5 (Figure 6.1): 1) CRO_sc1 at the top of the main grip, downstream of the site of a block, 2) CRO_sc2, halfway down the main grip, downstream of the site of a block, 3) CRO_sc3, at the outlet of a side grip to the main grip, just downstream of CRO_sc2 and upstream of the site of a block, and 4) CRO_sc4 in the natural stream, upstream of the confluence with the main grip (see also Appendix 1). Figure 6.3 shows the Croasdale catchment precipitation (for CRO_sc5) and the channel water level stage at the five stream gauges during November 2008 (prior to blocking) and May 2009 (post blocking). Note the difference in scale of the y axes of Figure 6.3 B and D.

Figure 6.3 demonstrates that when the drains are still intact and part of the drainage network, all gauges respond to the precipitation in a similar fashion. However, after the grips are blocked, the levels at CRO_sc1 (blue) and CRO_sc2 (green) remain low (dry), while at CRO_sc3 (red) the filling and drainage of the pond upstream of a block can be observed. Visually, no obvious differences can be observed between the pre- and post- blocking responses at CRO_sc4 and CRO_sc5 from the plots in Figure 6.3 (cyan and pink respectively).

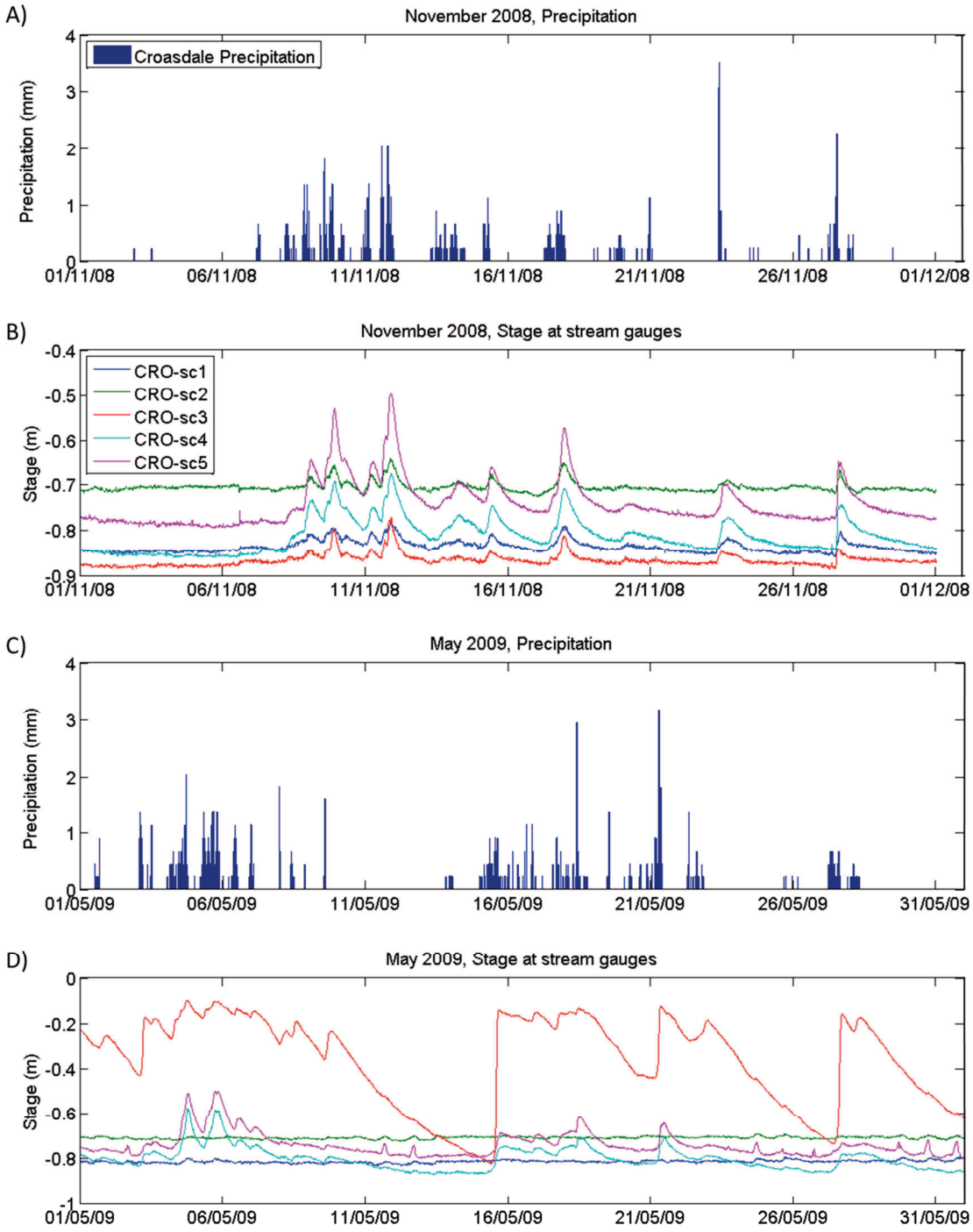

Figure 6.3 Croasdale Swine Clough precipitation and stage data for November 2008 (pre-grip blocking, A and B) and May 2009 (post-grip blocking, C and D)

Figure 6.3 shows that the grips in the upper part of Swine Clough have been successfully cut off from the drainage network and the blocks appear to provide additional available catchment storage. More information on the additional storage

facilitated by the grip blocks can be obtained from the stage data at CRO_sc3 and field surveys on the geometry of the ponds upstream of the blocks. Figure 6.3 shows that the CRO_sc3 pond fills almost instantaneously following rainfall, although it drains at a much slower rate. To analyse the drainage behaviour of the CRO_sc3 pond, a single segment of the falling stage time series is not representative of the general pond drainage. To overcome this problem, a master drainage curve was constructed in a similar fashion as a master recession curve, which embodies the falling stage data (during periods with no rainfall) from several individual recessions (Figure 6.4 left). From full, it takes approximately 15 days without rainfall for the CRO_sc3 pond to drain.

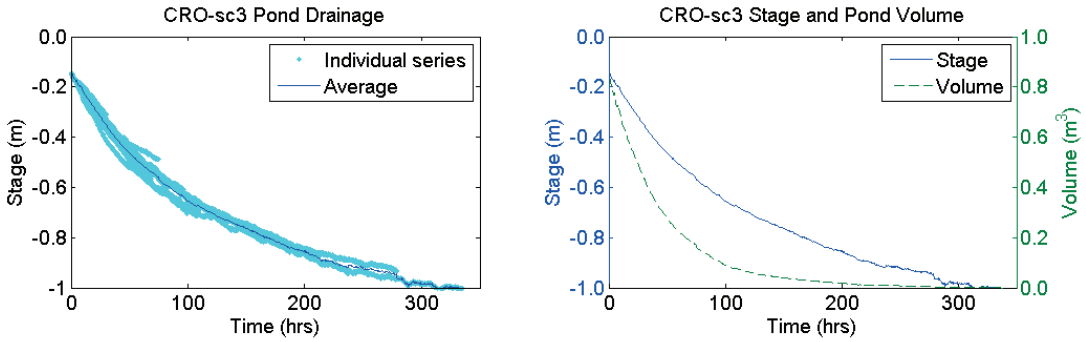

Figure 6.4 Left: CRO_sc3 pond drainage, and Right: CRO_sc3 stage and pond volume

Based on field measurements, the pond at CRO_sc3 starts spilling at -0.145 m. The potential storage upstream of the pond was determined by averaging the wet cross sections of the upstream and downstream sides, and multiplying it with the length of the storage pond. The field survey showed that the pond volume at -0.145 m is 0.85 m^3. Although it takes 15 days to fully drain the CRO_sc3 pond, in terms of volume, 50% drains within the first 31 hrs and 90% within the first 4 days (Figure 6.4 right) after rainfall cessation.

Assuming no pond leakages and negligible evaporation, the pond drainage depends mainly on the hydraulic conductivity of the soil. From visual observations in the field, it is noted that not all ponds upstream of a grip block drain at the same rate. Some blocks might be leaky or the ponds may be connected to a soil pipe, and others could be surrounded by peat with varying hydraulic conductivities.

To translate this process scale potential storage information to the (micro) catchment scale, a field survey was done in order to calculate the maximum potential storage upstream of all grip blocks in the CRO_sc5 and BRE_sap (and BRE_rhw) catchments. The storage upstream of a grip block depends on the original physical characteristics of the grip. *Dinsdale Moorland Services Ltd.* (2006) divided the grips into 6 different categories, based on grip depths of 0.5, 1.0, 1.5, 2.0, 2.5, and 3.0 m, respectively (Figure 6.1). A field survey was done to measure the potential maximum storage upstream of a grip block for 3-6 randomly selected ponds of each of the grip categories (Table 6.2). Table 6.2 shows the resulting average volumes of these ponds.

Table 6.2 Average potential storage upstream of all categories of grip and the average potential catchment storage provided by the grip blocks for CRO_sc5, BRE_sap and BRE_rhw

		Grip (block) category						Catch-ment totals
		0.5m	1.0 m	1.5 m	2.0 m	2.5 m	3m	
Average potential storage upstream of a block (m^3), (standard deviation)		0.05	0.23 (0.08)	0.81 (0.08)	6.79 (2.46)	-	-	
CRO_sc5	Total length (m)	-	306	421	334	-	259	1321
	Number of blocks	-	30	42	33	-	-	
	Total storage (m^3)	-	6.9	34.0	224.1	-	-	**265**
BRE_sap	Total length (m)	584	9109	2691	1058	358	58	13858
	Number of blocks	58	910	269	106	35	-	
	Total storage (m^3)	2.9	209.3	217.9	719.7	755.0	-	**1905**
BRE_rhw	Total length (m)	137	7543	2680	977	175	-	11511
	Number of blocks	13	754	267	97	17	-	
	Total storage (m^3)	0.7	173.4	216.3	658.6	366.7	-	**1416**

The (relatively small) variability is most likely related to discrepancies in the slope or geometry of the original grip. During the field survey, it became clear that the grips of a depth of 3 m were not blocked. It was not possible to measure the storage potentials for the smallest category (0.5 m depth), but it was possible to make a reasonable estimation. Based on the occurrence of the specific grip categories in the catchments (Figure 6.1), and assuming that the spacing of grip blocks is 10 m, the total potential storage for the CRO_sc5, BRE_sap and BRE_rhw catchments was calculated (Table 6.2).

The total potential catchment storage created by the grip blocking, calculated as a depth over the entire catchment, is 0.53 mm for CRO_sc5 (0.5 km^2), 1.12 mm for BRE_sap (1.7 km^2), and 0.51 mm for BRE_rhw (2.8 km^2). For the downstream CRO_weir (for CRO_sc5) and BRE_out (for BRE_sap and BRE_rhw) mini scale catchments this is only 0.03 mm and 0.34 mm respectively. In comparison to the maximum peak flows observed in these catchments (in the range of 4-8 mm/hr), this is relatively small. In addition, a dry period for over two weeks is rare in this area, which means that the ponds are nearly always filled with water to some degree (see Figure 6.3). Hence, at the start of a rainfall event, the additional storage created by the grip blocks is generally even smaller.

The above analysis focuses on the available catchment storage that grip blocking can provide through the ponds upstream of the grip blocks. However, some additional storage will also be available in the peat body. When grips are installed, the peat in the vicinity of the grip dries out (see Figure 2.5). Data from other studies have shown that grip blocking causes an almost immediate rise in the water table within the vicinity of the grips (Worrall et al., 2007b; Jonczyk et al., 2009). During a storm, therefore, when the ponds behind blocks fill up, there will be some additional increase in storage associated with the rise in the phreatic surface in the peat body adjacent to the pond.

6.3 MURSAFF model

Driven by the model requirements as discussed in Section 6.1.3 above, the MURSAFF model (Geris and Ewen, Appendix 3) was developed as a physically based distributed model that allows specifically for investigating (changes in) runoff, storage and flow fields for upland regions. Developing, testing and improving on the various stages of the model and grid development formed a substantial part of the present work.

6.3.1 Model Requirements

The main aim in the modeling is to represent the flow fields, storage and flow response in as realistic a fashion as possible, based on local knowledge and field information (such as those presented in Figure 6.1 and Table 6.1). From Figure 6.1 it is clear that the most notable feature of the case study areas is the complex geometry of the

patterns related to land use and changes in land uses. For CRO_sc5 and BRE_sap, this includes the geometry of grip networks and the temporary surface water volumes that are distributed across the landscape during storms, such as the ponds upstream of the grip blocks (Figures 3.15 and 3.16). For LOS_mid, the geometrical complexity arises from the field boundaries, the flexible stocking (density) management, sheep tracks, and the associated differences in vegetation and soil properties. It is hypothesised that these complexities play an important role in the storage patterns and flow fields within the catchment, as they could potentially affect the distribution of water flows and water storage in the channels on and within the soil.

It is difficult to include such complexity in a simple lumped model (as discussed in Chapters 2 and 5) and, instead, physically distributed modelling is required. However, it is impossible to model the geometric complexity adequately using traditional distributed models that require the landscape to be represented using regular grids, or geometry-restricted non-regular grids, such as GIS squares, finite-difference rectangles or finite-element triangles. These grids tend to distort the natural geometry of complex landscapes, and thus degrade the detailed knowledge and field information. To allow for a good representation of these fine details, the model should be able to use a flexible irregular polygon-celled grid that can be adapted to match the various different areas of the landscape such as hillslopes and fields and the linear features such as grips and sheep tracks. The appropriate storage and flow properties can then be associated with these individual irregular features to simulate the subsurface flow and the temporary surface storage on and flow over the complex rough surfaces.

6.3.2 Model Description

MURSAFF uses an irregular grid with polygon cells (or slabs) of different shapes and sizes, all interconnected to allow flow to run down slope from one cell into the next. MURSAFF uses Darcy's law for flow through porous media and Manning's equation for overland flow and flow in open channels. The cells can take any freeform regular or irregular polygon shape, so this includes simple shapes such as triangles, squares, rectangles and hexagons.

A basic representation of the MURSAFF model is given in Figure 6.5, for six interconnected rectangular grid cells. The two middle cells (in red) represent a river and the other four (in blue) make up the hillslopes. All potential water in- and out-flow pathways for each cell are signified schematically by the colour coded arrows.

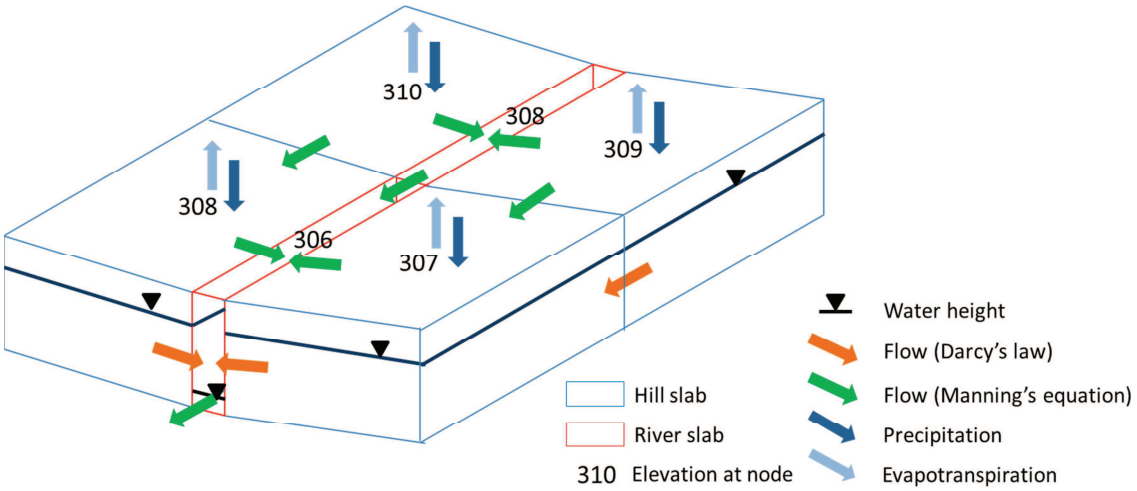

Figure 6.5 Schematic representation of the MURSAFF model, showing an example of six interconnected rectangular grid cells, of which two are 'river' types and four are 'hill' types.

The water height shown in Figure 6.5 is for the phreatic surface. There is also surface water. Depending on the coarse roughness specified for the cell, which accounts for the effects of rills, depressions, vegetation clumps, etc., the surface area and volume of surface storage increases with the water surface elevation. Each slab carries relevant information for the catchment at its location, such as the surface elevation at its node, the coordinates of each vertex, and the slab type (any number of types can be specified). One of the limitations of the current version of MURSAFF is that flow is represented as a cascade from slab to slab, with flow directions that are fixed depending on the ground surface (or channel bed) elevations of the slabs. The differences in the fixed surface elevation at the adjacent node therefore determine the flow directions at slab interfaces (see Figure 6.5). A slab face is defined as the side of a slab that is common to an adjacent slab. The rates of flow are determined by the water elevations in the neighbouring grid cells. Each slab type (e.g. 'river' or 'hill') can have its own set of physical properties, defined over a depth profile to allow for variations in the layering of porous media, and the geometry of the various water stores such as

surface water (i.e. the coarse roughness effect), channel water and ponds. Seven MURSAFF properties can be parameterised. The main properties (see Appendix 3) are the effective porosity and hydraulic conductivity of the porous media, Manning's n for surface and channel flow, and a surface ponding proportion to allow for the coarse roughness. Other properties, where applicable, include the river channel geometry and the volume of a surface storage pond.

The surface water store allows for ponding water, for example associated with saturation and infiltration excess runoff (e.g. related to low hydraulic conductivities at the top of the soil profile resulting from soil compaction), as well as the effect of coarse roughness as noted above. For each cell, the MURSAFF relationship between storage and flow is tabulated, to give tables with a resolution of 1 millimetre depth that specify the flow directions and flow rates for the surface and subsurface waters. When MURSAFF is running, these tables are used to calculate the flow fields and storage distributions, time step by time step.

Evaporation is taken from the surface store, but, when this is dry, it is taken from the subsurface store. To allow for differences related to vegetation types, the potential evapotranspiration rate can be assigned slab by slab. A simple approach is used to calculate the actual evaporation rate from the potential rate, assuming linear proportionality to the ratio of water storage to the maximum storage. MURSAFF is designed for application to small areas, so assumes that precipitation is distributed evenly over the catchment. This limits the application to areas of less than about 10 km^2, especially in UK upland areas where the spatial rainfall variability can be high. The MURSAFF output data include phreatic surface, storage and runoff time series for all individual slabs.

A technical description of the MURSAFF model is given by Geris and Ewen (Appendix 3). The effect of LUMC is represented by changing the properties of the slabs. The following sections describe the set-up of the irregular grid, the model parameterisation, calibration and validation as well as the model assumptions and limitations based on the CRO_sc5 case study as an example.

6.3.3 Irregular Grid Set-up

Grid Creation

Creating and classifying the grid slabs are quite major undertakings that need detailed local knowledge. The process used is as follows. Initially, using *ESRI* ARCGIS software, the grid is drawn in 2-D, based on local field and map information. The shape and size of the grid cells, as well as the way in which the grid is created, thus depend heavily on the local conditions and allow for flexibility related to the specific case to be studied.

The creation of the irregular grid for CRO_sc5 is shown schematically in Figure 6.6, as an example. This occurred in two main steps. First, the cells or slabs that comprise the river network (including the drains) were drawn (Figure 6.6 left). The location of these slabs is based on maps of the river network and locations of the grips. The width of these slabs is determined by local cross sections (e.g. Appendix 1) and field walkovers. The length of the grip slabs is determined by the location of the grip blocks, so that the same slabs can be used for pre-blocking and post-blocking modelling. The slab type will be different; for pre-blocking, the slab represents a section of channel (the grip) and post-blocking it represents the pool caused by the block.

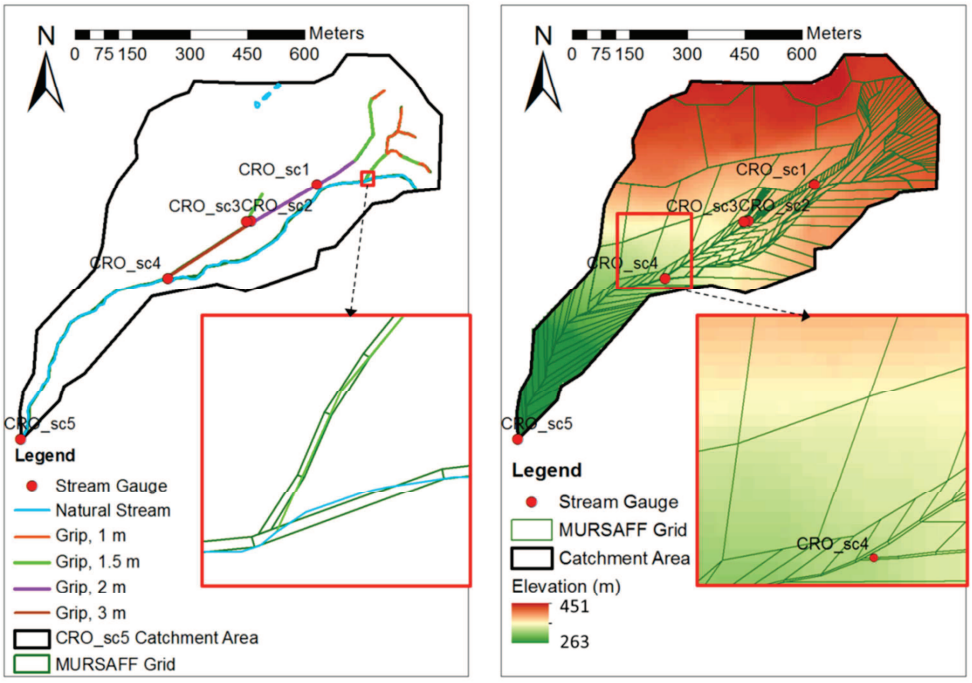

Figure 6.6 MURSAFF grid creation for CRO_sc5, left: stage1 representing the creation of the drainage network, right: stage 2 representing the creation of the hillslope slabs

Second, the hillslope slabs were drawn (Figure 6.6 right). A hybrid approach is needed in this key stage in the creation of the mesh of slabs. The resulting grid must depend in the main part on information extracted automatically from a DEM, but also in part on information handled manually that takes into account the problem being studied and information from the field. For example, the orientations of the hillslope slabs depend mainly on the topography so they were based on a 10 m DEM and derived elevation contour lines and flow directions. The hillslope slabs were drawn so that they eventually drain to the river network (see Figure 6.6 right). When studying the effects of stocking density, for example, the other types of information relevant are soil types and land use, field boundaries, sheep tracks and LUMC maps (Figures 6.1 and 6.2). These are checked against the outcome from the automatic generation (based on the DEM) and adjusted manually (or inserted manually, as in the case of sheep tracks).

The final CRO_sc5 grid (Figure 6.6 right) comprises 372 slabs, with a total of eight different types, comprising: (1) four grip types; (2) two river types; and (3) two hillslope types. The grip slabs are classified according to their original depth (Figure 6.6 left). The river slabs have been subdivided into different channel geometries; and the two hillslope types are differentiated by soil type and land use.

Grid Improvements

Once the polygons are drawn, a MURSAFF input file is created that contains relevant information about each individual cell. The data it contains for each cell include its slab number, slab type, elevation at the gravitational centroid, x and y coordinates at the gravitational centroid, number of polygon vertices, and the x and y coordinates for all vertices. Apart from the slab type, most of this information is extracted from the DEM, using *ESRI ARCGIS* software.

No MURSAFF tools are available for grid creation, although the input file (as above) of a (manually drawn) grid can be tested and improved. There are six stages that involve testing and improving the set-up file of a grid. These are: 1) identification of isolated vertices, 2) check for mismatched faces and add extra vertices if necessary, 3) find neighbouring slabs and match faces, 4) digitally walk over and depit the main drainage

network (e.g. slabs with type “river”), 5) apply general pit filling, and 6) digitally walk over and depit the entire grid. For every stage, all improvements to the grid are checked for agreements with field observations.

During MURSAFF stage 7, the flow directions for each cell are set up. The areas for each cell are calculated during stage 8. MURSAFF also tests the viability of the channel network capacity for a predefined maximum discharge, which coincides with the maximum observed flow during the simulation period.

Appendix 4 gives more information on the individual stages of the grid improvement.

The overall purpose in grid improvement is to ensure the grid is as it is meant to be, that slabs that are meant to exchange flow will exchange flow, and that networks that are intended to drain the catchment will drain the catchment. The need for this testing is, if anything, higher in MURSAFF than in models that have an arbitrary mesh, because the aim is to represent reality over a wide range of spatial scales. In the current version of MURSAFF, there is also the difficulty that the directions of lateral flow (on a compass) are defined by the ground surface elevations, so care has to be taken that the node elevations for the slabs give a coherent draining pavement, in much the same way as DEMs are sometimes tested and depitted to ensure that a channel drainage network can be generated.

6.4 MURSAFF Parameterisation, Calibration and Validation

6.4.1 Parameterisation and Calibration for CRO_sc5

The MURSAFF slab type physical property tables are initially set up based on field observations and values from the literature (such as described in Chapter 2). For the CRO_sc5 example, Table 6.3 shows the eight different slab types and the associated seven properties for the grip blocked and unblocked cases. The model parameters are indicated by codes of the form Ab where A is a character (see title for Table 6.3) and b a number. If the number b is 0 it means that the item does not exist. For example, S0 means that the slab type does not contain a pond, and S3 means it contains a pond with the third set of property values. It is assumed that the only difference between

the two cases is the physical change for grip blocking: that is a change from the grip channels being represented as drains connected to the river network to being represented as disconnected transient storage ponds.

Table 6.3 CRO_sc5 MURSAFF cell types and associated parameter code for the unblocked (intact) and grip blocked cases (C = channel geometry, MC = channel Manning's n, N = porosity, K = conductivity, MS = surface Manning's n, FP = surface pooling fraction, and S = storage pond)

Slab type	Unblocked (Intact) Grips	Grip Blocked
River_small	C1, MC1, N1, K1, MS1, FP1, S0	C1, MC1, N1, K1, MS1, FP1, S0
River_medium	C2, MC2, N2, K2, MS2, FP1, S0	C2, MC2, N2, K2, MS2, FP1, S0
Grip_1_0	C3, MC3, N1, K1, MS1, FP1, S0	C0, MC0, N1, K1, MS1, FP1, S1
Grip_1_5	C4, MC4, N1, K1, MS1, FP1, S0	C0, MC0, N1, K1, MS1, FP1, S2
Grip_2_0	C5, MC5, N1, K1, MS1, FP1, S0	C0, MC0, N1, K1, MS1, FP1, S3
Grip_3_0	C6, MC6, N1, K1, MS1, FP1, S0	C6, MC6, N1, K1, MS1, FP1, S0
Grass_hill	C0, MC0, N2, K2, MS2, FP1, S0	C0, MC0, N2, K2, MS2, FP1, S0
Bog_hill	C0, MC0, N1, K1, MS1, FP1, S0	C0, MC0, N1, K1, MS1, FP1, S0

The majority of the CRO_sc5 parameters were fixed as shown in Table 6.4. The channel geometries and (drain blocked) pond volumes were based on average observations from intensive field campaigns (Appendix 1 and Section 6.2 respectively), as were the channel and surface Manning's roughness coefficients (based on tabulations according to Chow, 1988). Note that grips with a depth of 3 m were not blocked. The peat Winter Hill soil thickness is 2 m (Chapter 3) and the Wilcocks soil 1 m, with the latter situated on much steeper slopes. It was assumed that the soils are underlain by a relatively impermeable base. The effective porosity of the soil was based on literature values (see Table 2.3). The proportion of surface ponding was assumed, based on observations of actual surface coarse roughness, to increase linearly from 0 to 1 between 0 and 0.15 m relative to the ground surface.

Table 6.4 Fixed MURSAFF parameters for CRO_sc5

Channel geometry (C)	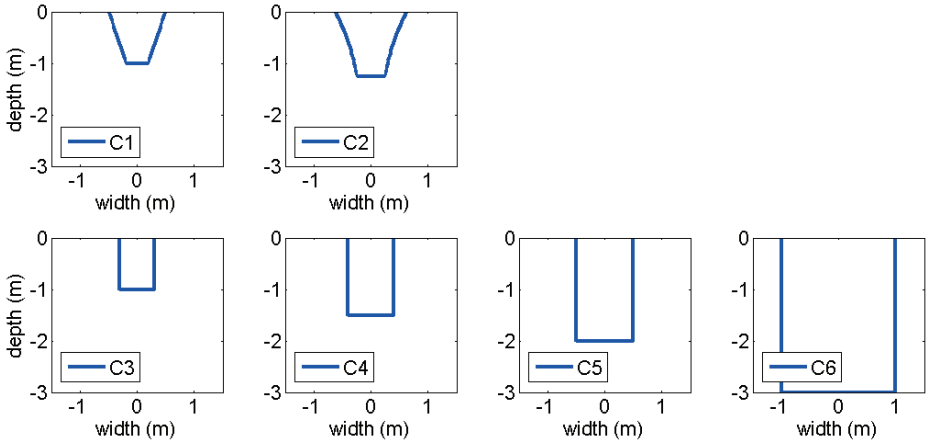		
Channel manning's n (MC)	MC1	River small	0.035
	MC2	River medium	0.040
	MC3	Grip, 1 m depth	0.035
	MC4	Grip, 1.5 m depth	0.035
	MC5	Grip, 2.0 m depth	0.035
	MC6	Grip, 3.0 m depth	0.040
Surface manning's n (MS)	MS1	Bog	0.04
	MS2	Grass	0.035
Ponding Proportion (FP)	FP1	Depth 0.15 to 0: Decrease linearly from 1 to 0	
Soil porosity (N)	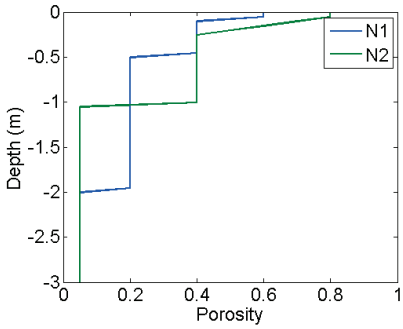 N1 = Winter Hill, N2 = Wilcocks		
Storage ponds (S)	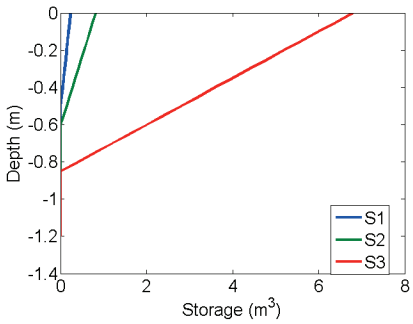 S1 = blocked grip 1 m depth, S2 = blocked grip 1.5 m, S3 = blocked grip 2 m		

There are two parameters that were automatically optimised through shuffled complex optimisation (Nelder and Mead, 1965; Press et al., 1992). The calibrated parameters are the hydraulic conductivities of the two soil types. These were calibrated for two reasons. Firstly, an initial sensitivity analysis showed that the MURSAFF simulations are sensitive to hydraulic conductivity. Secondly, although there have been extensive studies of the conductivity of the soil profile, reported values vary widely (by several orders of magnitude) both laterally and vertically (Chapter 2).

Chapter 2 showed that a peat soil profile and its properties are layered in two main zones: the acrotelm and the catotelm. Within the acrotelm, substantial changes in the hydraulic conductivity have also been observed within the upper 5-10 cm. The hydraulic conductivity of the Winter Hill peat profile was therefore optimised with the lower acrotelm and the catotelm values as fixed fractions of that of the upper acrotelm layer (Table 6.5). The Wilcocks soil profile has only one layer. The calibration of the two parameters involved working towards a best-fit (NSE-morph, see Ewen 2011 and Chapter 5) set of parameter values within a priori set bounds (Table 6.5) representing a physically realistic range as obtained from the literature. The automatic calibration of the hydraulic conductivity was carried out for the case with the longest data record, which is the blocked case. This involved a period of a full year of 15 min data (01/03/2009 – 28/02/2010). Table 6.5 shows the a priori bounds and optimised hydraulic conductivities (with associated profiles).

Table 6.5 Optimised MURSAFF hydraulic conductivity for soil profiles at CRO_sc5

Parameter		A priori range/ fraction	Optimised	Depth profile with optimised parameters
K1	Bog $K_{(0.005 - 0.150)}$ Winter Hill	0.1000E-05 – 0.1000E-02	0.969E-04	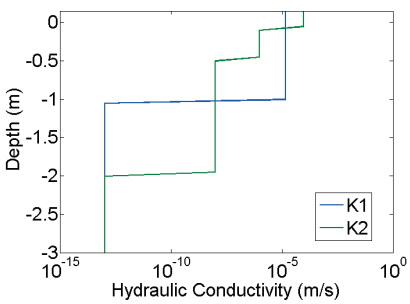
	Bog $K_{(-0.30 – (-0.10))}$ Winter Hill	K1*0.01	0.969E-06	
	Bog $K_{(-1.95 – (-0.35))}$ Winter Hill	K1*0.0001	0.969E-08	
K2	Grass Wilcocks	0.1000E-05 – 0.1000E-02	0.147E-04	

K1 = Winter Hill, K2 = Wilcocks

As shown in Table 6.5, the a priori ranges for K1 and K2 is the same. In the top 10 cm of the soil profile, the Winter Hill (peat) soil has a higher optimised conductivity than the Wilcocks soil. Overall, the Wilcocks soil drains better than the Winter Hill soil, which agrees with the relative properties of the different soil types (Chapter 3).

The NSE-morph for the full calibration period is 0.851 (allowing up to 3 time steps (i.e. 45 minutes) of timing difference); the NSE is 0.738. It can be seen that the simulated discharge fits the observed discharge well during both of the selected months, although the largest peak flows are overestimated.

Figures 6.7 and 6.8 show the observed and simulated discharge for a summer (July 2009) and a winter (November 2009) month, respectively for the unblocked case. The figures also show the observed precipitation and the simulated catchment storage.

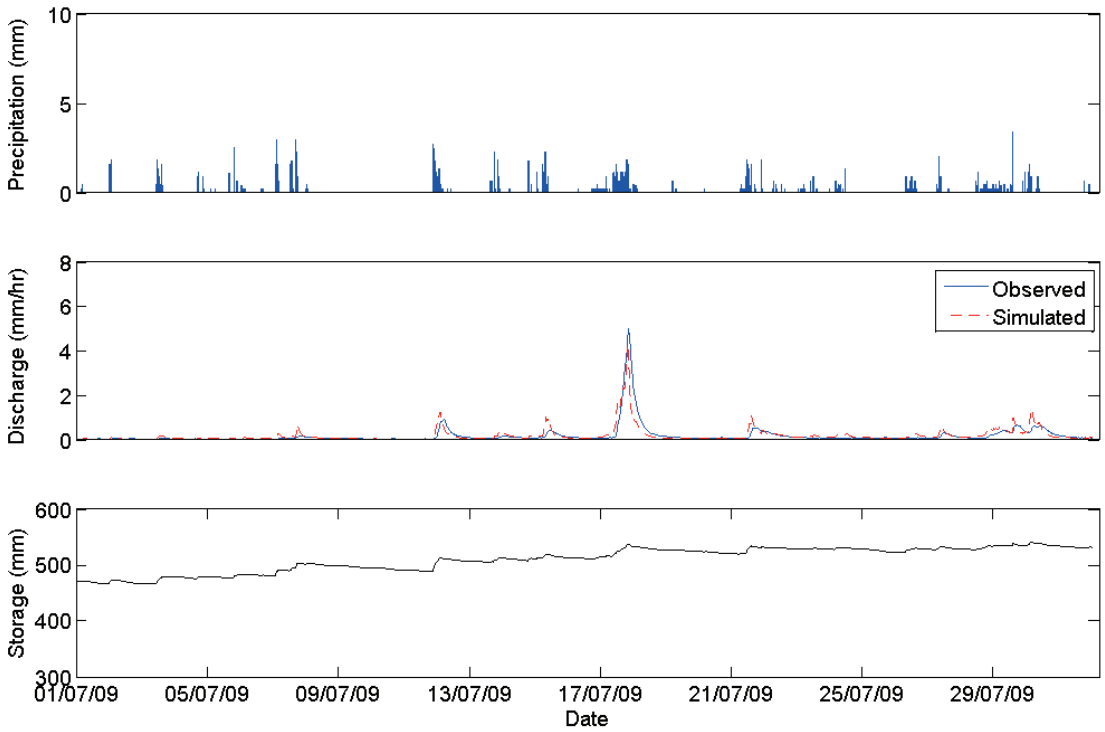

Figure 6.7 Precipitation, observed and simulated discharge, and the simulated storage for CRO_sc5 (0.5 km^2) during a summer month in the calibration period (July 2009)

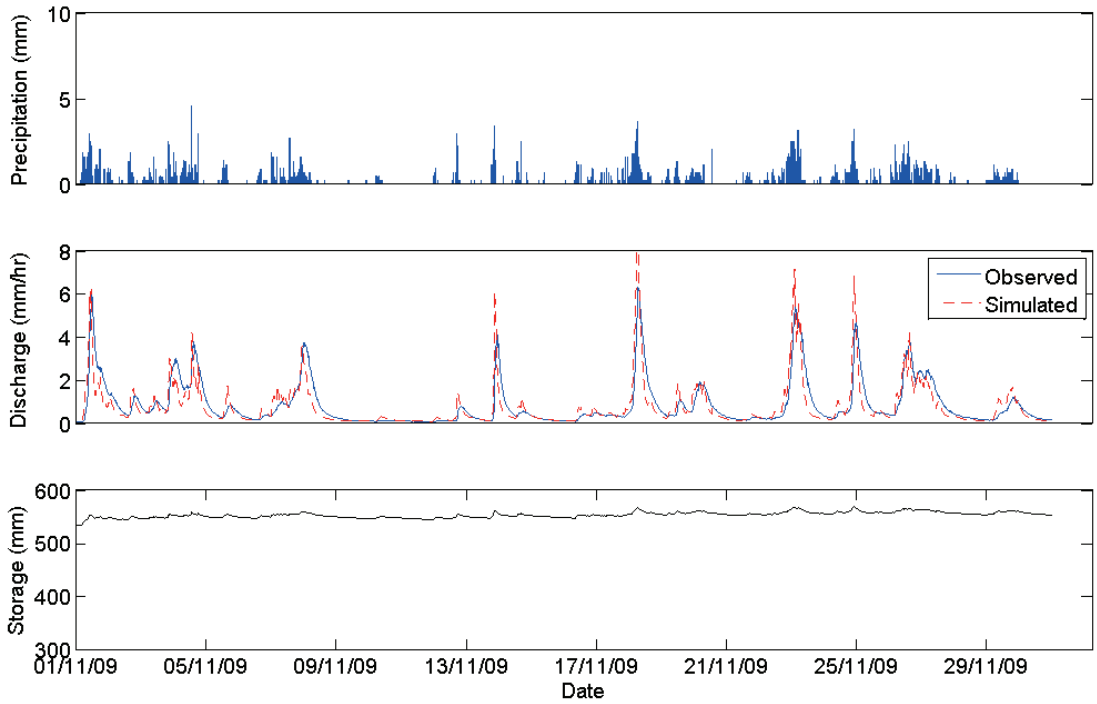

Figure 6.8 Precipitation, observed and simulated discharge, and the simulated storage for CRO_sc5 (0.5 km^2) during a winter month in the calibration period (November 2009)

6.4.2 Validation for CRO_sc5

To test the parameterised and calibrated MURSAFF model outside the calibration period, validation should be carried out for a period during which the catchment was in the same physical state as during the calibration period (Klemes, 1986) (i.e. blocked drains). The period directly following the calibration period (01/03/2010 to 31/07/2010) is relatively dry (453 mm of precipitation in 6 months, compared to 2281 mm in 12 months during the calibration period, see Table 6.5). The water balance losses from evapotranspiration during this period are larger than those from discharge and in excess of 60% of the precipitation, which is unusual for a generally wet upland catchment such as CRO_sc5. In comparison, approximately 18% of the precipitation during the calibration period was lost through evapotranspiration, which agrees more with observations of annual precipitation losses through evapotranspiration at other UK upland moorlands (e.g. 18% (Institute of Hydrology, 1976), 22% (Institute of Hydrology, 1991), 29 ± 7% (Heal et al., 2004)).

The main purpose of the validation testing is to test the calibrated model under similar climatic conditions. After that, further validation involves testing whether the calibrated model can be applied under different climatic conditions.

Additional data were collected during the period 01/08/2010 – 28/04/2011. During this period, the conditions were more similar to the calibration period (see Table 6.5). The NSE-morph for this validation period is 0.808, which is only slightly less than the NSE-morph for the calibration period. Table 6.6 shows the main observed and simulated water balance components during the calibration and validation periods. The observed and simulated components agree well for the calibration and validation periods. The table shows that, in agreement with the observations from Figure 6.8, MURSAFF overestimates the discharge. It is noted that the observed difference in storage in Table 6.6 is based on the assumption that evapotranspiration takes place at the potential rate all through the year. As the model simulates the actual evapotranspiration, the storage values in the table are not fully comparable.

Table 6.6 Observed and Simulated Water Balance components (mm) and runoff ratio for CRO_sc5 during the MURSAFF post-change calibration and validation periods (observed ET is potential evapotranspiration, simulated ET is actual evapotranspiration)

Water balance components (mm)	**Calibration period** (01/03/2009 – 28/02/2010)		**Dry period** (01/03/2010 – 31/07/2010)		**Validation period** (01/08/2010 – 28/04/2011)	
	Observed	**Simulated* (0.851)**	**Observed**	**Simulated* (0.461)**	**Observed**	**Simulated* (0.808)**
P	2281.0	-	451.6	-	1335.6	-
ET	411.5	380.6	280.9	225.5	219.9	201.6
Q	1843.0	1891.3	251.7	274.9	1067.9	1149.1
dS	26.5	9.0	-79.6	-48.8	47.8	-15.8
Runoff Ratio (Q/P)	0.81	0.83	0.56	0.61	0.80	0.86

* Number in brackets is the NSE-morph efficiency

As with any hydrological model with multiple parameters, it is recognised that different realistic combinations of parameter estimates can give similar outcomes in calibration/validation testing (Beven, 1993; Beven, 2006). However, confidence that the calibrated parameter values are appropriate stems from (1) calibrating only two

parameters and (2) using field data and widely-reported literature values for fixing parameters and to provide bounds for these when they were optimized. In addition, the NSE/NSE-morph efficiencies are comparable for the simulation and validation periods. The aim was to limit the automatic calibration to as few parameters as possible. The parameter values obtained will also, in part, depend on the nature of the modelling; for example, they will depend on the time step, the model structure, and the grid itself (Geris and Ewen (Appendix 3)).

Another valuable validation test is to check whether the calibration model is valid for conditions other than those during the calibration period. For this test, the simulations during the above mentioned dry period are studied. The NSE-morph for the simulation during the period 01/03/2010 to 31/07/2010 is low: 0.461. As noted above, there are large differences in climatic circumstances between the calibration/validation and this dry period (Table 6.5). The observed precipitation during April – June 2010 was only 100 mm. Figure 6.9 shows the model performance during July 2010 to focus on the transition period from relatively dry to wetter conditions. The simulated catchment storage at the start of July 2010 is low, especially in comparison with that during the same time in the previous year (Figure 6.7) and November 2009 (Figure 6.8).

Figure 6.9 shows that the rainfall in mid July 2010 results in only a small response in the discharge. The precipitation from 14-21 July 2010 leads to much higher observed runoff response than simulated. It would be simple to fix this in the tabulations within MURSAFF so that the simulated summer hydrograph and the calibration/validation metrics would be better. However, this could easily lead to unrealistic physical representations. One possible explanation for the observed July 2009 response in Figure 6.9 is macropore and pipe flow, which are known to take place prior to fully saturated conditions (Beven and Germann, 1982). Exfiltration via pipe flow has been observed in the CRO_sc5 catchment (see Figure 6.10). This will be considered alongside other improvements associated with representing the dynamics of flow, especially allowing the flow direction to vary over time in response to the state of wetness. However, since the main focus here is on representing conditions associated

with high flows, the parameterization for the more normal, year round wet conditions found in this upland catchment is retained.

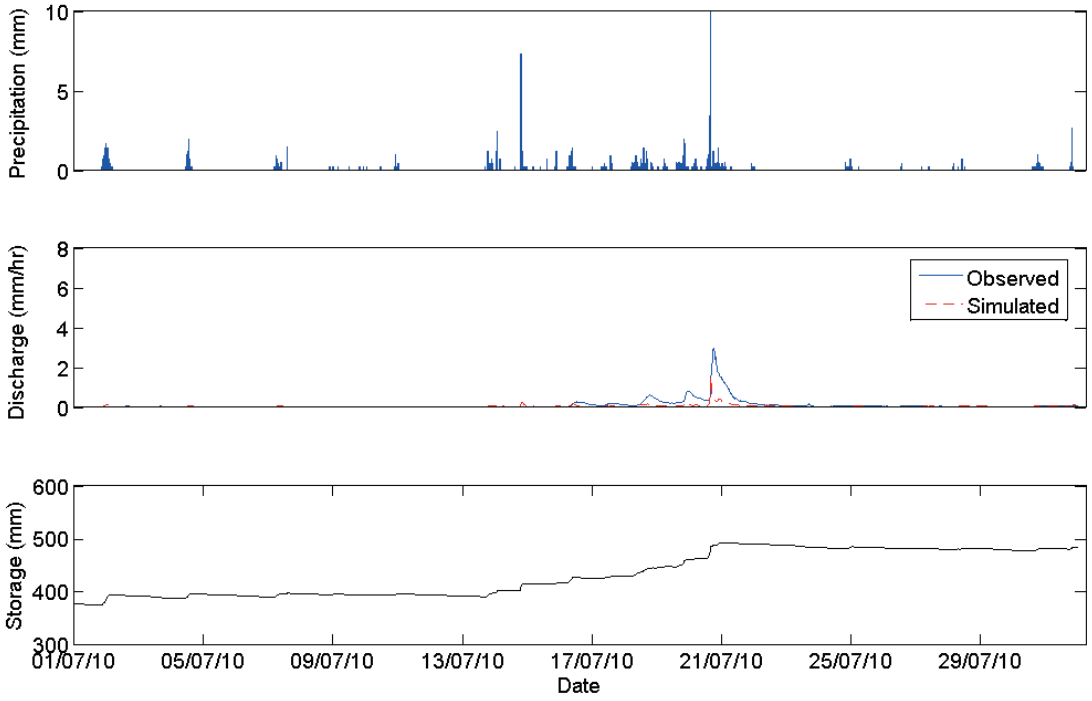

Figure 6.9 Precipitation, observed and simulated discharge, and the simulated storage for CRO_sc5 during July 2010

Figure 6.10 Exfiltration via a subsurface pipe, observed in the CRO_sc5 catchment, with a zoom window on the right.

6.4.3 Calibration and validation for BRE_sap

The grid of BRE_sap was created in a similar fashion to that of CRO_sc5. Here, digital information on the exact locations of the grip blocks (see Figure 6.11) was taken into account. The BRE_sap grid as shown in Figure 6.11 comprises 3877 slabs, with a total of 8 different types: (1) five grip types; (2) two river types; and (4) one hillslope type.

The parameterisation, calibration and validation for the BRE_sap grid were carried out according to the method described in Section 6.2.3, although for BRE_sap the automatic optimisation of the soil hydraulic conductivity involved a single parameter (K1). The BRE_sap optimised hydraulic conductivity of the peat soil profile (K1 = 0.568E-04 m/s) is of the same order as that optimised for CRO_sc5. The NSE/NSE-morph for the calibration period (01/12/2008 – 30/11/2009) and the validation period (01/08/2010 – 28/04/2011) is 0.853/0.916.

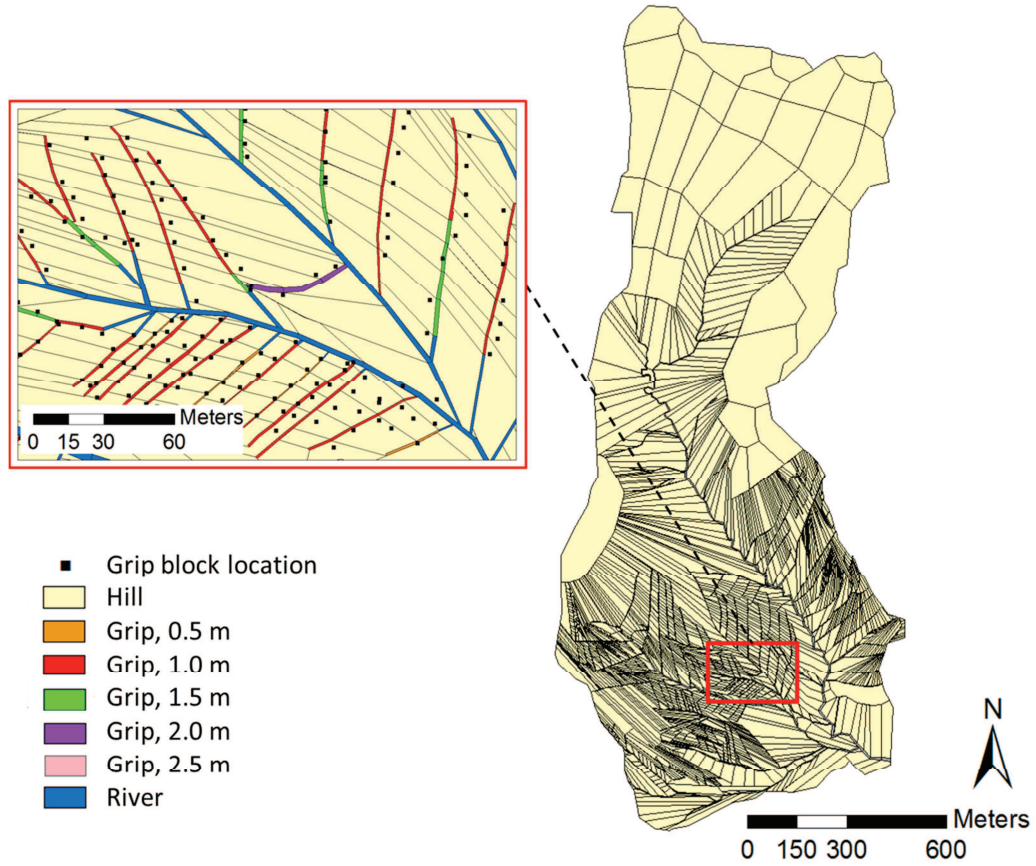

Figure 6.11 MURSAFF grid for BRE_sap, showing the main slab types, including natural drainage network (River), the different grip types based on original grip depth, and the hillslope type. The small black squares in the zoom window show the locations of grip blocks.

6.5 Simulation of Pre- and Post-Grip Blocking Effects on Flood Hydrographs

6.5.1 Simulation Results

For the full simulation period (August 2008 – August 2010) the CRO_sc5 and BRE_sap discharge was simulated for both the blocked and unblocked case. The only difference between the two cases is the physical change for grip blocking: that is a change from the grip channels being represented as drains connected to the river network to being represented as disconnected transient storage ponds. Figures 6.12 and 6.13 show the CRO_sc5 and BRE_sap observed and simulated pre- and post-grip blocking case discharge as well as the difference (Q_{post} - Q_{pre}) in pre- and post- change simulated discharge during November 2009. Within the simulation period, November 2009 was the wettest month on record with some of the highest recorded peak flows. During this period, the grips of both catchments were blocked. The two figures show that the reduction in simulated discharge during November 2009 associated with grip blocking reduction is very small. In fact, for both CRO_sc5 and BRE_sap, the pre- and post-change simulated discharges fit the observed discharge similarly well. This is also reflected by the NSE-morph efficiencies for the two simulation cases for the two scenarios (Table 6.7).

Table 6.7 NSE-morph efficiencies for the CRO_sc5 and BRE_sap pre and post-change periods for the simulations based on the pre-change and post-change cases.

		Full Pre-change period	Full Post-change period
CRO_sc5	Pre-change case simulation	0.831	0.841
	Post-change case simulation	0.831	0.842
BRE_sap	Pre-change case simulation	0.961	0.960
	Post-change case simulation	0.960	0.960

Overall, the impacts of grip blocking at CRO_sc5 are negligible (Figure 6.12). Figure 6.13 shows that BRE_sap grip blocking results in a slight reduction in peak flow. The maximum reduction is 5% for a relatively small peak flow (during 12/11/2009). For the recessions, the post-blocking simulated discharge is somewhat higher than the pre-blocking discharge (maximum 2% of the simulated pre-change peak flow).

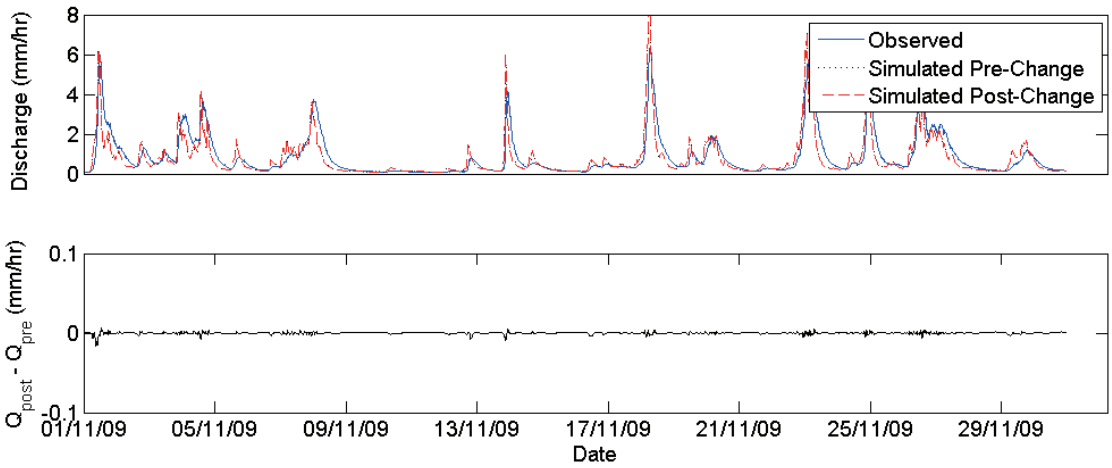

Figure 6.12 Observed and simulated pre- and post-change discharge for CRO_sc5 (top) and Q_{post} - Q_{pre} (bottom) during November 2009

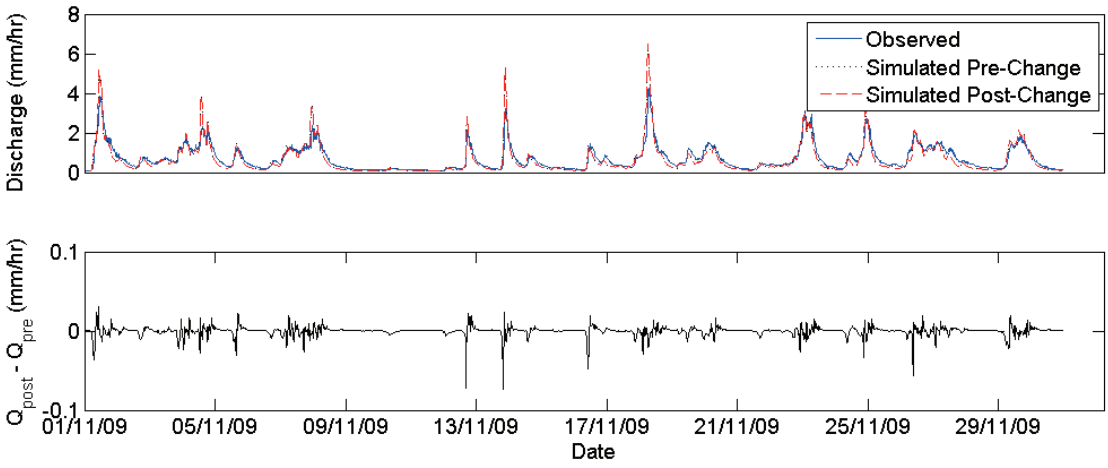

Figure 6.13 Observed and simulated pre- and post- change discharge for BRE_sap (top) and Q_{post} - Q_{pre} (bottom) during November 2009

For the full simulation period, the max reduction in flow for CRO_sc5 is 0.046 mm/hr (1% of the pre-change peak flow during 17/07/2009) and for BRE_sap 0.082 mm/hr (5% of the pre-change peak flow during 14/07/2009). For both catchments, the largest reductions have been observed during July 2009, which suggests that the effects are more pronounced during summer conditions, although still relatively small. To further investigate the differences between summer and winter conditions at CRO_sc5 and BRE_sap, the responses of the individual summer events, for which the largest reductions were observed, are compared with a winter event of comparable size.

Figure 6.14 (top) shows the CRO_sc5 pre- and post-change simulated discharge for the 17/07/2009 (left) and 01/11/2009 (right) events. The 1m grip type average storage as well as the catchment average storage are also shown, to demonstrate differences between the process and the micro catchment scale responses. It is shown that, even for the summer event, the reduction in simulated discharge is trivial (maximum of 1% of the simulated pre-change discharge). However, in agreement with field observations, there are significant increases in storage at the process scale for both events. The extra local average storage associated with the blocking of the 1m grips is 332 mm. For the other grip types, these effects are proportional. However, at the catchment scale the average post-change increase in storage is only 1.15 mm, which is small, especially in comparison with the gross variations in storage between storms. The relatively larger pre- and post-change reduction in discharge between the summer and winter event may also be explained by the overall catchment storage, which is much lower during the summer event than the winter event (bottom plots Figure 6.14).

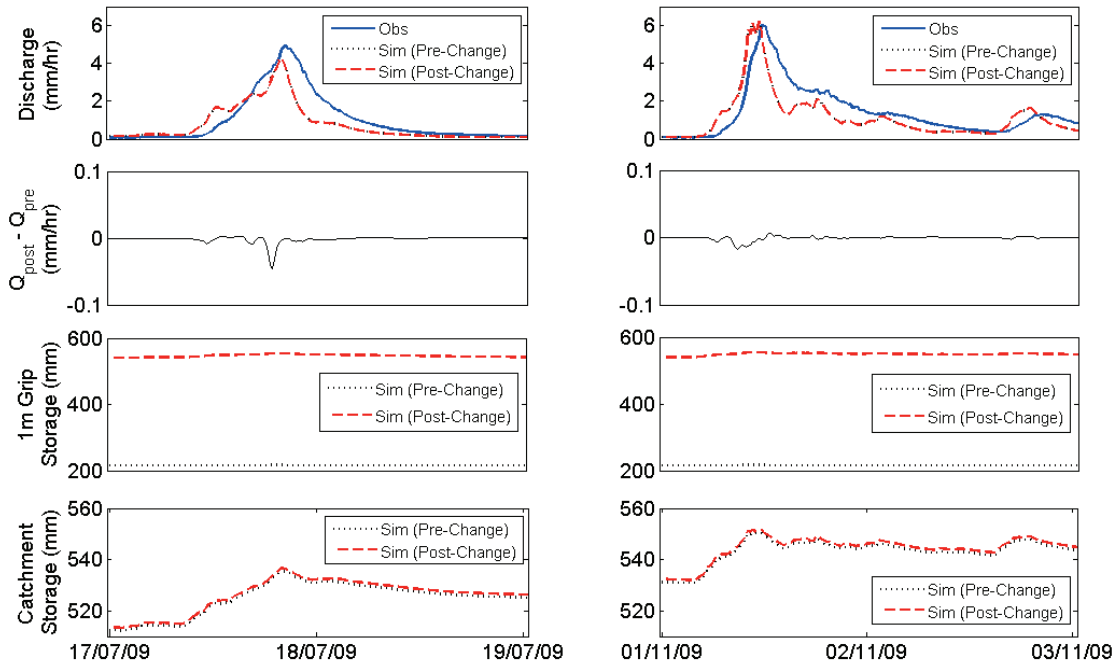

Figure 6.14 Observed and simulated pre- and post-change discharge, Q_{post} - Q_{pre}, the average simulated pre- and post-change storage for the grip 1 m type slabs and that of the whole catchment for CRO_sc5 for a summer event (left) and a winter event (right) in 2009

For BRE_sap (Figure 6.15), the largest impact of grip blocking (a reduction of 4.7% in the peak flow) is simulated during a relatively small event on 14/07/2009. The average extra storage associated with the blocking of the 1m type grip locally is 335 mm, an effect that is reduced by a factor 70 to 4.9 mm at the catchment scale.

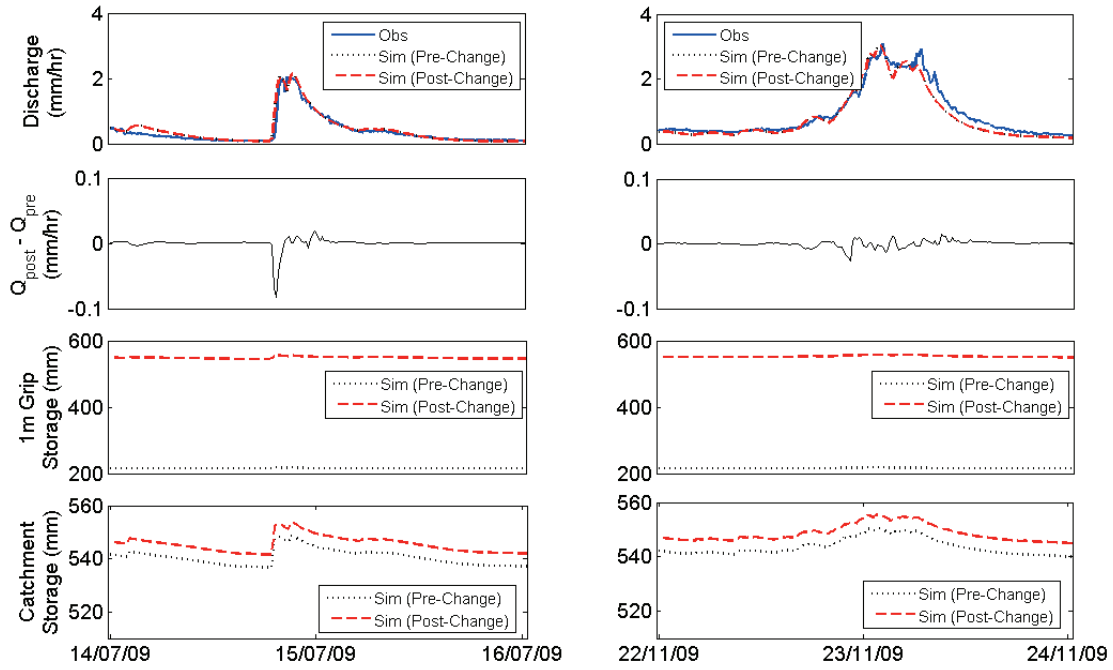

Figure 6.15 Observed and simulated pre- and post-change discharge, Q_{post} - Q_{pre}, the average simulated pre- and post-change storage for the grip 1 m type slabs and that of the whole catchment for BRE_sap for a summer event (left) and a winter event (right) in 2009

Table 6.8 shows the simulated pre- and post-change case water balances for CRO_sc5 and BRE_sap at the micro catchment scale during the 2008-2009 hydrological year. The table shows that there are no large overall impacts of grip blocking on any of the components of the water balance. As a result of grip blocking, there is a negligible increase in evapotranspiration and a reduction in the discharge for both catchments, which can be associated with the higher water tables at the process scale post blocking.

Table 6.8 Simulated pre- and post-change case water balance components for the CRO_sc5 and BRE_sap micro catchments during the 2008-2009 hydrological year

Water balance components (mm)	CRO_sc5		BRE_sap	
	Simulated (blocked)	**Simulated (unblocked)**	**Simulated (blocked)**	**Simulated (unblocked)**
P	2133.4	2133.4	1827.3	1827.3
ET (actual)	382.9	382.0	404.0	400.4
Q	1810.1	1811.0	1445.7	1449.2
dS	-59.7	-59.6	-22.3	-22.3
Runoff Ratio	0.85	0.85	0.79	0.79

6.5.2 Discussion of Grip Blocking Simulation Results

Overall, this simulation work with the MURSAFF model has demonstrated some clear impacts of grip blocking at the process scale (in the local grips). However, there are no significant short-term impacts of grip blocking at the BRE_sap and CRO_sc5 micro scale catchments.

Figures 6.14 and 6.15 show that there are substantial increases in storage at the process scale, within and in the vicinity of the grips. This is in agreement with the field observations as presented in Section 6.2. However, Figures 6.12-6.15 and Table 6.8 show that the impacts of grip blocking at the micro catchment scale of CRO_sc5 and BRE_sap are small and almost undetectable, especially for large winter events. For example, Figure 6.13 shows that for the largest event during the post-blocking period (18/11/2009), the simulated impact of grip blocking in the BRE_sap catchment involves a reduction in the peak flow of less than 0.02 mm/hr. The observed peak flow during that event is 4.3 mm/hr, so the impact involves a peak flow reduction of less than 0.5%. Those events that show higher (though still small) percentages of impact (e.g. 5%) are relatively small (approximately 2mm/hr). The results show that during the larger events, where the flood reduction effects of LUMC are more desirable, the impacts are almost negligible. Overall, the simulation results suggest that the grip blocking impacts are relatively larger during drier antecedent conditions in summer, where more catchment storage is available.

These results suggest that the overall catchment behaviour is more important in controlling the flood response, compared to the (blocked) additional drainage network created by the grips and the local arrangement of flow direction. For most of the year, there is little available catchment storage, as the catchment is almost permanently saturated. Variations in natural catchment conditions (such as in rainfall characteristics and antecedent catchment wetness) are likely to lead to larger differences in catchment response than those potentially caused by grip blocking (see Figure 6.14).

The grip blocking covers only a small part of the catchments, so the percentage area affected by change is small. As discussed in Chapter 2, the effects of installing ditches are limited to the near vicinity of the drains and do not affect the water tables of entire hillslopes. It appears that the same applies to the impacts of grip blocking. Even though approximately 38 and 35% of the catchments were covered by grips, the actual grips themselves cover less than 1% at the CRO_sc5 and only 2% over the BRE_sap catchments respectively. The field observations of Section 6.3.1 also predicted that the catchment scale impacts of grip blocking on the overall storage in relation to large peak flows is small.

Even though the physically based model analyses in this section are data driven, the modelling exercise does not involve an assessment of the model simulation uncertainties. However, as argued by authors such as Bormann et al. (2009) and Huisman et al. (2009), the uncertainties in LUMC impact predictions can be reduced by bringing together the results of physically based models and lumped models. The MURSAFF simulation results agree well with the findings in Chapter 5, where no evidence was found to suggest that the pre- and post-change SDD conceptual model simulations at BRE_sap were significantly different. However, the SDD analysis results for the CRO_sc5 subcatchment were inconclusive, highlighting the need for a further investigation of the grip blocking effects. The analyses in this section indicate that it is unlikely that the grip blocking in the upper part of CRO_sc5 has had a significant impact on the runoff generation at the micro catchment scale. This also suggests that the SDD differences between the pre- and post-change periods can be attributed to natural variability. The model analyses using MURSAFF also agree well with the

predictions of the relative catchment scale effects of grip blocking, which were based directly on field observations (Section 6.3.1). In addition, other studies that have simulated the effects of grip blocking, using different techniques to those used in the present study, also concluded that the impacts of grip blocking at the micro catchment scale are likely to be very small (e.g. Ballard et al., 2010).

It is noted though, as discussed in Chapter 2, that the long term impacts of grip blocking may be different from the short term impacts as studied here (Spieksma, 1999; Worrall et al., 2007). The generally wetter antecedent conditions induced by drain blocking might, in time, give rise to more vigorous vegetation cover, and this will change the flow hydraulics, so vegetation changes may need to be incorporated in the analysis. There might also be some degree of resilience in the hydraulic catchment characteristics in responding to drain blocking, so feedback effects may need to be considered. Peat drainage has been associated with an increase in macropores and soil piping (Holden, 2005b), but it is unclear if and for how long this will remain active, so preferential flow may need to be modelled. And it is also noted that a restored peatland will not necessarily revert to an intact peatland, owing to irreversible changes in the physical properties as a result of draining (Holden, 2005a; Holden et al., 2011; Ramchunder et al., 2009), so, again, subtle variations in properties may need to be included in the modelling.

6.6 Stocking Density and Management Change Effects

As discussed in Chapter 2, through grazing and trampling, sheep are likely to influence the (local) storage and runoff. The patterns of these impacts from sheep are influenced by the following dominant features in the LOS_mid catchment: the field boundaries (Figure 6.1), the stocking management plans (Figure 3.21), and sheep tracks (Section 6.1.2). The prior two will mainly influence the overall runoff generation pattern, while the sheep tracks will act as preferential flow pathways (Chapter 2).

The purpose of this section is to explore the potential fully established long-term impacts of the stocking density and management change plans for LOS_mid and to investigate the effect of sheep tracks. No short-term change in the hydrological

response of LOS_mid has been detected and, because the transition from pre-change to fully-established post-change conditions is expected to take several years, no such post-change data are available. In the modelling that follows, the representations for the pre- and post-change conditions are based on a range of assumptions. Consequently, the results in this section cannot be interpreted as exact or accurate predictions. Instead, the aim is to aid a better understanding of relative impacts.

6.6.1 MURSAFF Set-Up for LOS_mid

Grid Creation

The LOS_mid grid creation process took into account the field boundaries, the SCaMP stocking density management plans, the soil associations, the land use distribution, the topography and the sheep tracks. Apart from for the sheep tracks, all the necessary information was available digitally (see also Chapter 3). Brief field inspections showed that sheep tracks were abundant in the LOS_mid catchment. However, for grid creation, a full field survey would have been time consuming, so satellite imagery (G*oogle Earth, version 2010*) was used. As a result of the relatively tall vegetation in the Losterdale catchment, and image quality limitations, it is difficult to identify sheep tracks and other grazing patterns from satellite imagery. Assuming that sheep tend to behave similarly from one field to another, examples of fields with shorter vegetation were used to identify the main sheep grazing patterns that could be applied to the LOS_mid MURSAFF grid.

Figure 6.16 shows the common patterns associated with grazing, that were identified during a survey using G*oogle Earth* in the main Hodder valley where the vegetation consists of shorter grasses. The most obvious effects of trampling and poaching are near gateways. Tile A in Figure 6.16 shows that there are clear trampling and erosion effects near each gateway from one field to another. The effects occur in star shape patterns, fanning out away from the gateway (Figure 6.16 B).

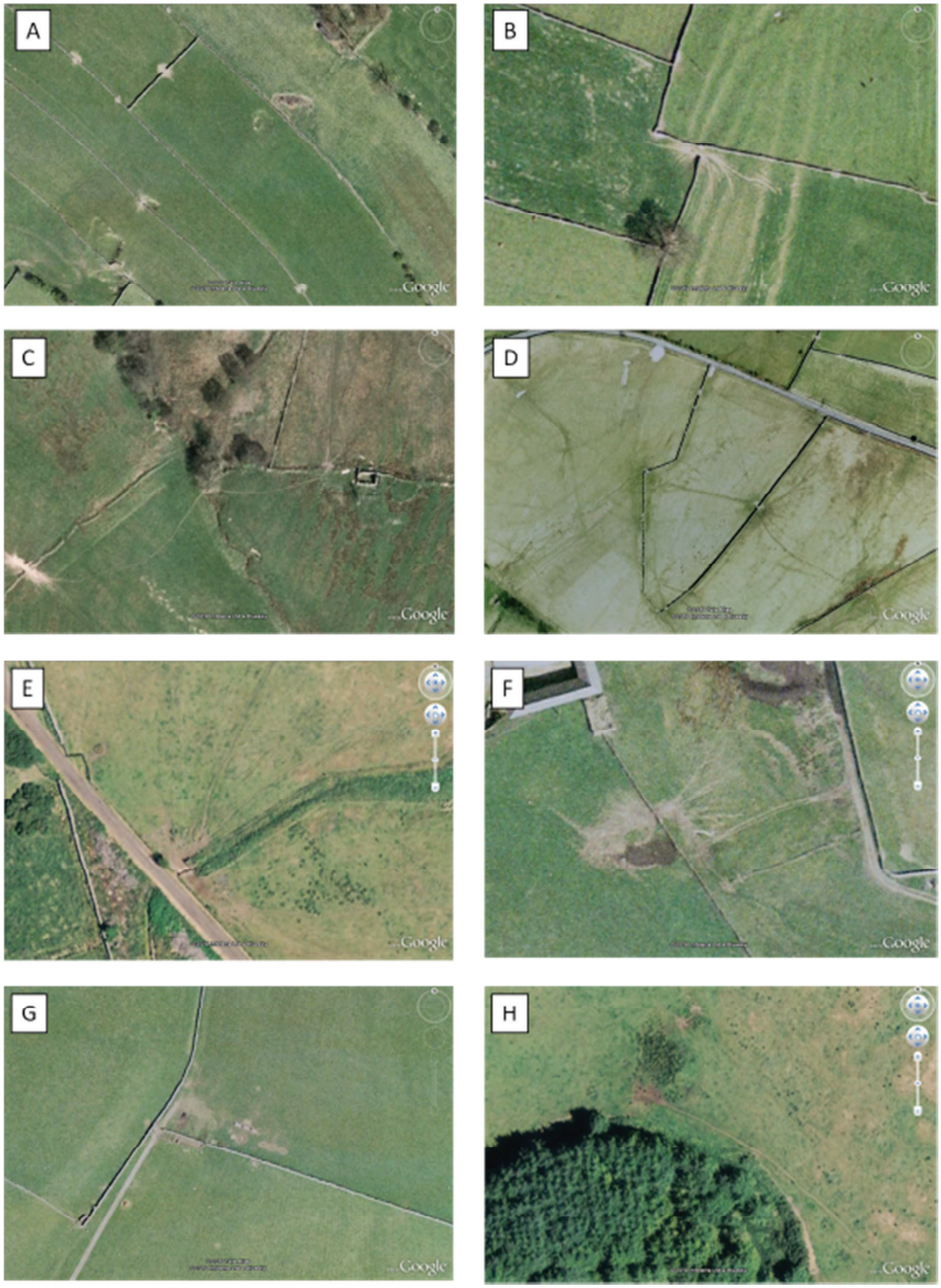

Figure 6.16 Observed patterns associated with grazing in the Hodder valley *(Google Earth)*

The tracks either fade within a few meters from the gateway, or, as can be seen from Figure 6.16 C and D, they can continue all the way to the next gateway. Similar star

shape patterns appear in corners of fields where sheep gather (Figure 6.16 E), and at locations where sheep can cross a waterway (Figure 6.16 C and F). It should be noted that the patterns observed as sheep tracks, and the effects on soil compaction and erosion, are likely enhanced by small farm vehicles such as quad bikes. Figure 6.16 F, G and H show that the patterns around feeding and watering troughs may also appear as a concentrated trampling area, with star shape patterns and long tracks towards the feeding and/or watering places. Finally, from Figure H it can be seen how the sheep tend to walk close to trees that provide shelter.

These findings have been used in creating the LOS_mid MURSAFF grid, in the following way:

- Identify gateways, crossing, feeding and gathering places and possible shelter areas
- Apply an area of extremely high soil compaction at and in the near vicinity of these areas
- Add longer tracks with high soil compaction towards the feeders, gateways, and crossing places, which fan out and fade away from the concentration area
- Apply sheep tracks running from gateway to gateway and along potential shelterbelts

On steep hillslopes, some sheep tracks with an orientation parallel to the contour lines have also been observed. These have been ignored here, and the impacts of only those sheep tracks that are connected directly to the river network are investigated.

Figure 6.17 shows the resulting LOS_mid MURSAFF grid that is based on the drainage network, the DEM, the field boundaries, the SCaMP stocking density management plans, the sheep tracks, the soil associations, and the land use distribution. The grid in Figure 6.17 comprises 891 slabs, with 6 different main slab types, comprising: (1) two river types; and (2) four hillslope types. The four hillslope types have been classified according to their (post-change) type of stocking density management. The coding corresponds with the SCaMP stocking density land management types (EXCL = stock

exclusion, HEFT = heft management, INBYE = inbye grazing, and REST = restoration management). Overall, these four types coincide with the different soil types and land uses (see Figures 3.5 and 3.7 respectively), although some generalisations were made to keep the number of hillslope types low. The colour coding in Figure 6.17 conforms to that of Figure 3.21 and represents the post-change stocking density management. To accommodate the sheep tracks, all hillslope types have associated with them 3 extra levels of compaction. In Figure 6.17, these three levels are represented by the bow tie-shaped areas near gateways and watering or river crossing places as well as by the sheep tracks that connect these areas. They involve the following levels of compaction:

1) Extra High (at the feeders and gateways)
2) High (in the near vicinity of feeders and gateways, and for the tracks)
3) Medium (farther away from the feeders and gateways)

Including these sublevels, there are 18 slab types in total for the LOS_mid grid.

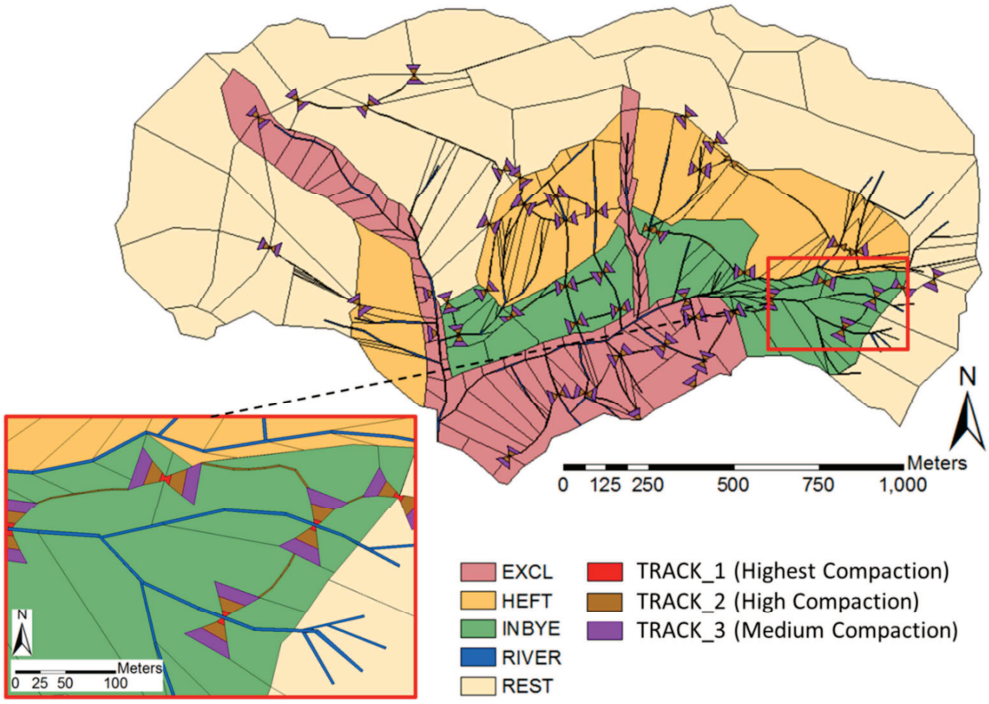

Figure 6.17 MURSAFF grid for LOS_mid (zoom window on the left), showing the main slab types for the post-change simulation, including drainage network (RIVER) and hillslope slabs undergoing stock exclusion (EXCL), heft management (HEFT), inbye grazing (INBYE), restoration management (REST), and three different levels of increased soil compaction (TRACK_1 – TRACK_3).

Parameterisation, Calibration and Validation

The parameterisation of the LOS_mid grid largely follows the procedure as described in Section 6.4. The main differences are that 1) the LOS_mid grid involves 3 soil types, and hence the need for 3 parameters to be automatically optimised, and 2) it is assumed that the upper 20 cm of the soil profiles are affected by soil compaction, with the strongest impact on the upper 5 cm. The hydraulic conductivity of the upper layer of the soil profile was therefore set as a fraction of the lower soil profile that is assumed to be unaffected by compaction effects. These assumed fixed reductions in porosity and optimised reduced hydraulic conductivity of the 3 soil profiles are given in Table 6.9. These numbers are based on local scale field observations from the literature (see Chapter 2). The largest reduction is applied to the sheep tracks with the highest level of soil compaction.

Table 6.9 Reductions in porosity and hydraulic conductivity for the different slab types based on compaction types.

Slab type	Upper 0.05 m	0.10-0.20 m depth
Field	40%	20%
Track_1	80%	60%
Track_2	70%	50%
Track_3	60%	40%

Table 6.10 summarises the main characteristics of the hillslope types and the estimated average annual pre- and post-change stocking density levels (see also Chapter 3). Although the pre-change stocking levels for the REST hillslope types are lower, poorly drained peat soils are more vulnerable to trampling effects (Chapter 2) and it is therefore assumed that initially the proportional effects on the compaction levels for the different soil types are the same (i.e. the assumed fixed reductions in porosity and hydraulic conductivity of the soil profiles as presented in Table 6.9).

Table 6.10 LOS_mid MURSAFF hillslope type characteristics

Hillslope type	Soil type	Land Use	Pre-change stocking density (sheep/ha)	Post-change stocking density (sheep/ha)	Percentage of reduction in stocking density
EXCL	Wilcocks	Grass	5.8	0.0	100
HEFT	Belmont	Grass	4.5	3.5	33
INBYE	Wilcocks	Grass	5.8	4.5	22
REST	Winter Hill	Bog	1.7	0.2	88

As an example, Figure 6.18 shows the fixed porosity and optimised hydraulic conductivity profiles of the Winter Hill (1), Belmont (2) and Wilcocks (3) soils for the slabs representing fields (FIELD) and the highest level of compaction (TRACK1).

The NSE/NSE-morph values for the calibration (01/03/2009 – 28/02/2010) and validation periods (01/09/2008 – 28/02/2009, excluding a period with heavy snowfall: 25/12/2008 – 13/01/2009) are 0.878/0.920 and 0.834/0.886 respectively. A plot of observed and simulated discharges at LOS_mid during November 2009 is shown in Figure 6.19 below.

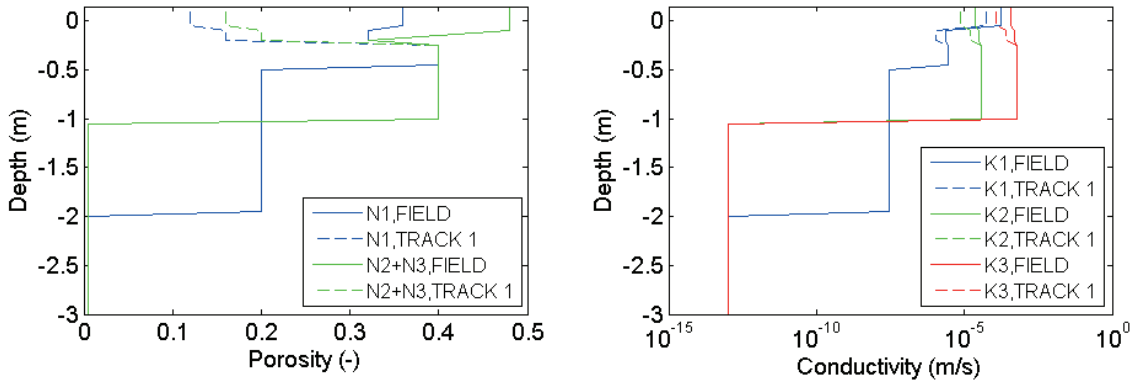

Figure 6.18 Porosity (N) and optimised hydraulic conductivity (K) for the LOS_mid pre-change Winter Hill (1), Wilcocks (2), and Belmont (3) soil types

6.6.2 Simulation Results

From the discussion in Chapter 2, it is proposed that the reductions in stocking density are likely to have the following long-term effects at the process scale:

1) Reduction in soil compaction and hence increase in porosity and infiltration in the top 0.2 m
2) Change in vegetation (from grass to heather) for the HEFT areas
3) Even when overall levels of stock are reduced, the sheep tracks remain active

Changes in vegetation are likely to have an impact on the hydraulic roughness and potential evapotranspiration, while the soil compaction level affects the hydraulic conductivity and the porosity of the top 0.2 m of the soil profile. The post-change scenario was simulated by implementing the following changes to the LOS-mid pre-change MURSAFF set-up:

1) Increase the hydraulic conductivity and porosity of the upper 20 cm of all hillslope and sheep track slabs in proportion to the decrease in stocking density changes (Table 6.10). For example, if the pre-change field conditions involved a 40% reduction of porosity in the upper 5 cm of the soil profile, a 22% reduction in stocking density decreases this reduction of porosity associated with compaction for the post-change conditions to 31%.
2) Change the land use of the HEFT hillslope slabs (from grass to bog) resulting in an increase in the roughness (from 0.035 to 0.040) and an increase in the PET

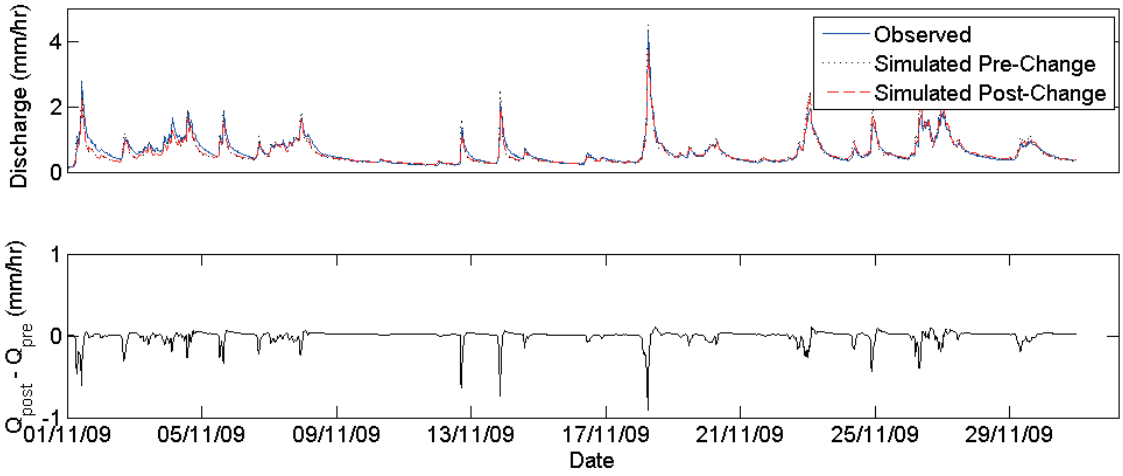

Figure 6.19 Observed and pre-and post-change simulated discharge for LOS_mid (top) and Q_{post} - Q_{pre} (bottom) during November 2009

Figure 6.19 shows the LOS_mid observed and pre- and post-change simulated discharge, as well as Q_{post} - Q_{pre} for November 2009. Note that the scale of the y-axis in the bottom plot of Figure 6.19 is an order of magnitude larger than for those in Figures 6.12-6.15. The simulated stocking density changes result in a clear reduction of the peak flows. Although relatively small compared to the decreases in peak flow, there are increases in the hydrograph recession and base flow (Figure 6.19).

Overall, Table 6.11 shows that none of the water balance components are substantially different between the pre- and post- change simulations. There is a small increase in the total runoff, associated with a reduction in the actual evapotranspiration. Even though the post-change potential evapotranspiration is increased for the HEFT slabs (16% of the catchment), there is slightly less actual evapotranspiration for the post-change scenario. This can be attributed to the increases in infiltration as a result of reduced compaction levels, so that there is less standing water which is available directly for evapotranspiration.

Table 6.11 Simulated pre- and post-change scenario water balance components for the LOS_mid micro catchment during the 2008 – 2009 hydrological year

Water balance components (mm)	Simulated Pre-change	Simulated Post-change
P	2002.6	2002.6
ET (actual)	246.1	239.6
Q	1805.6	1815.1
dS	-49.1	-52.2
Runoff Ratio	0.90	0.91

Figure 6.20 shows the pre- and post-change simulated peak flows against their corresponding 25 largest peak flows during the calibration period. The pre-change peak flows slightly overestimate the observed peak flows, while the post-change peak flows are clearly reduced.

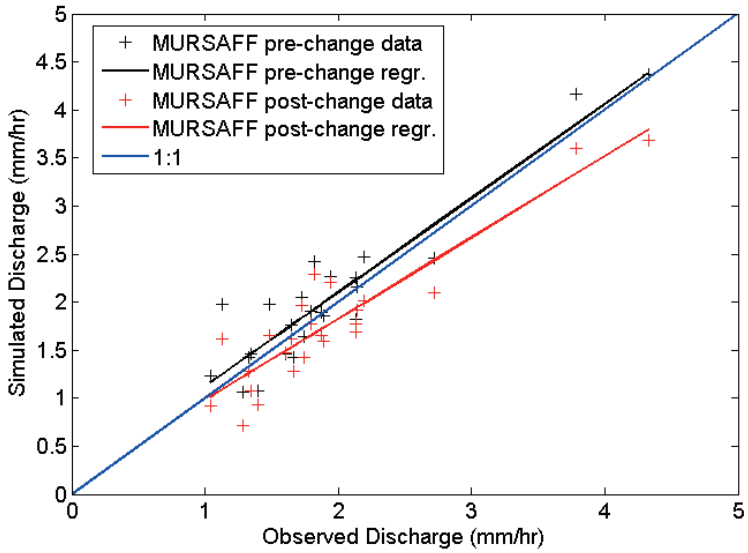

Figure 6.20 Simulated pre- and post-change peak flows against the observed (pre-change) peak flows for the 25 largest events recorded at LOS_mid

To gain a better understanding of the relative impacts of the specific stocking density changes of the different hillslope types, Figure 6.21 shows the impact of the compaction changes in the REST (left), the EXCL (middle) and the different changes in the HEFT slabs (right) for two days during September 2009. For the same events, Figure 6.22 shows the impact of compaction changes in the INBYE slabs (left), all changes combined (as for Figure 6.19) (middle) and for the removal of the higher level compaction (compared to the field compaction) of sheep tracks specifically (right).

The plots in Figures 6.21 and 6.22 show that the impacts at the catchment outlet arise mainly from the changes in the REST hillslope slabs. This can be explained as follows. Firstly, the REST slabs cover more than half of the catchment. Secondly, the proportional change in the soil parameters of the top 20 cm is relatively large (88% increase, see Table 6.10). Thirdly, in comparison with the other hillslope slabs, the storage changes for the individual REST slabs are the highest (bottom left panel of Figure 6.21). This might be attributed to differences in the overall hydraulic conductivity of the respective soil profiles, indicating that the Winter Hill peat soils are more sensitive to changes than the other soil profiles.

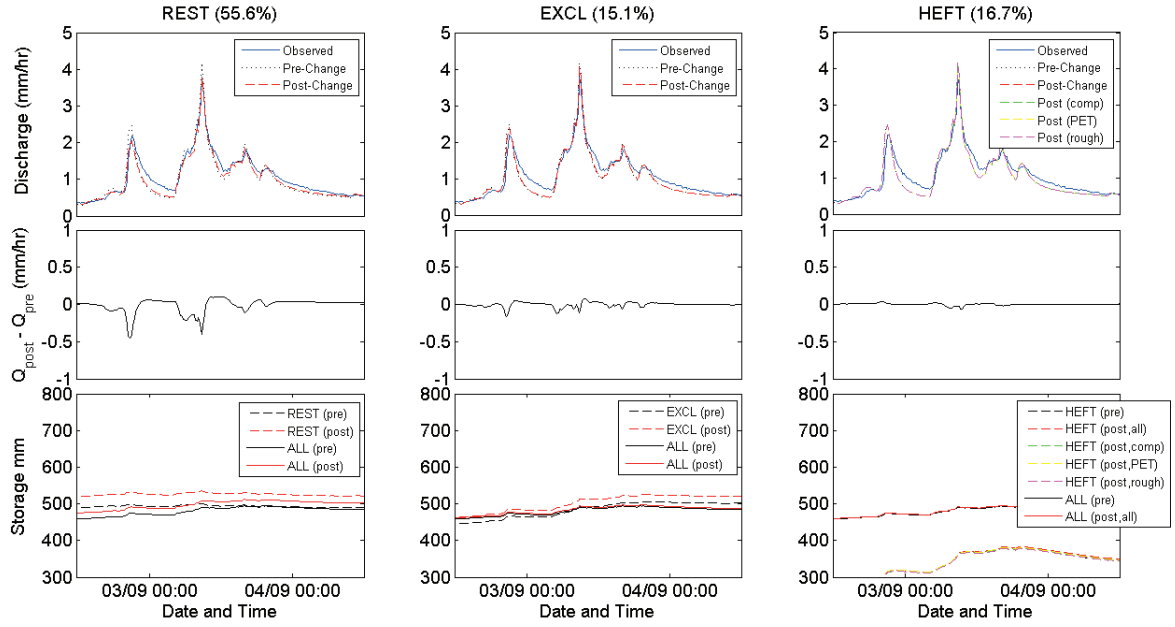

Figure 6.21 Observed and pre- and post-change simulated discharge at the catchment outlet (top), Q_{post} - Q_{pre}(middle), and storage for specific slab types and the catchment average (bottom), exploring the effects of reducing stocking levels at the 'REST' (left) and the 'HEFT' slabs (right), and of stock exclusion at the 'EXCL' slabs (middle). The percentages at the top of each graph show the proportional catchment area undergoing change.

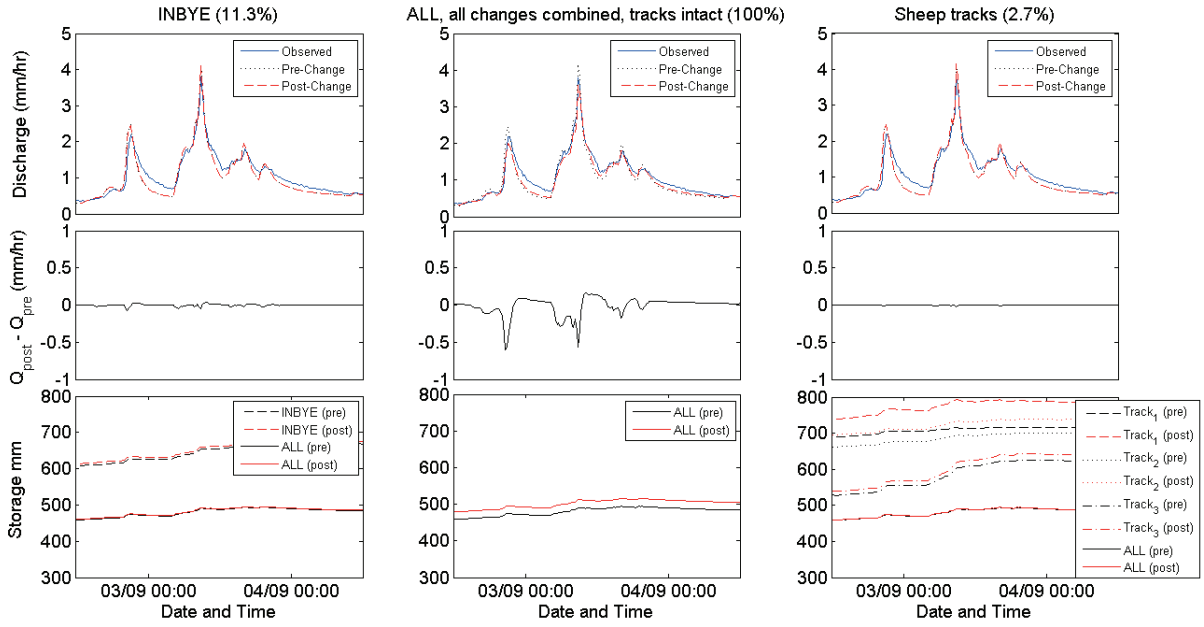

Figure 6.22 Observed and pre- and post-change simulated discharge at the catchment outlet (top), Q_{post} - Q_{pre} (middle), and storage for specific slab types and the catchment average (bottom), exploring the effects of excluding stock at the 'INBYE' slabs (left) , the combined effect of all predicted changes (middle) and the effects of sheep tracks (right). The percentages at the top of each graph show the proportion of the total catchment area undergoing the relevant change.

Figure 6.21 shows that the effects of the changes on the storage of the HEFT hillslope slabs are relatively small. This may be related to the relatively high conductivity of the Belmont soil (see Figure 6.18), which might also explain the overall lower storages in the HEFT slabs as well (Figure 6.21). Overall, the changes in roughness and evapotranspiration had little effect, especially in comparison with changes in the compaction levels (i.e. in the effective porosity and hydraulic conductivity).

Figure 6.22 (right) shows that the higher level soil compaction for the different sheep tracks clearly increases the slab storages, while there are little impacts of the sheep tracks at the catchment scale. As the sheep tracks cover only 2.7% of the LOS_mid catchment, large effects are not expected. At the process scale of individual slabs, the impact of the extra high compaction levels on runoff generation is substantial. For example, for an INBYE TRACK1 slab, Figure 6.23 shows the difference in total slab discharge (left) as well as the percentage of total discharge generated in the surface store (right) under highly compacted conditions (pre) and under normal field conditions (post). The figure shows that reductions in soil compaction not only reduce the total slab discharge, but it also decreases the percentage of discharge that is generated in the surface store (i.e. as overland flow) even during periods where the total discharge is similar. No changes in the timing of the runoff generation have been observed at 15 min time intervals.

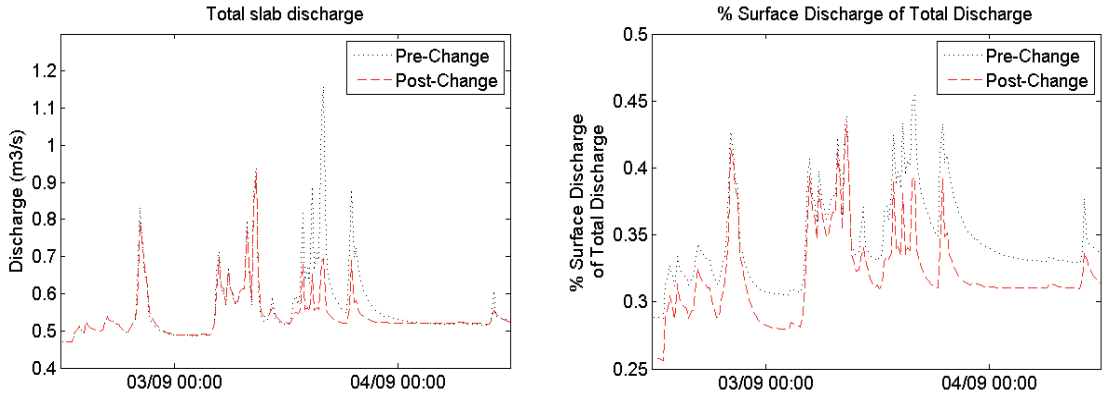

Figure 6.23 Total slab discharge (left) and percentage of surface discharge of total slab discharge for a TRACK1 slab under high level compaction (pre-change) and as field conditions (post-change)

6.6.3 Discussion of Stocking Density Change Simulation Results

According to the simulated post-change predictions, the potential micro catchment scale impacts of changes in stocking density involve a reduction in the peak flows and a corresponding overall increase in the recession flows, so that the main water balance components remain similar. The direction of change agrees with local scale field observations reported in the literature (e.g. Heathwaite et al., 1989; Clay et al., 2009). The reduced soil compaction levels allow for relatively more infiltration and higher soil water storages, so that the water is released more steadily. The simulations suggest that the effects of soil compaction are relatively larger than those of changes in vegetation (i.e. changes in potential evapotranspiration and roughness), although the relative effects also depend on soil type.

In agreement with local scale observations (e.g. Meyles et al., 2006; Zhao, 2008), the simulated process scale effects of sheep tracks demonstrate increased discharges with high percentages of overland flow runoff generation (Figure 6.23). As they are all connected, the tracks create preferential flow paths. However, at the micro catchment, these effects appear insignificant, as the tracks represent only a small proportion of the total catchment area.

As the stocking density change impact prediction at LOS_mid and the effects of sheep tracks are subjected to many assumptions, information on percentages of change could be misleading. Nevertheless, the results suggest that the impacts of reductions in stocking levels on runoff generation can be substantial, especially compared with those of grip blocking.

The LOS_mid simulation results have demonstrated that MURSAFF is a useful tool for exploring the relative impacts of the different stocking density changes such as those in the LOS_mid catchment. However, for these results to inform or be used as more accurate predictions, future work should focus on improved model reconciliations with field observations and a study of uncertainty.

6.6.4 MURSAFF LOS_mid predictions and SDD

The MURSAFF LOS_mid long-term predictions of stocking density impacts provide an opportunity to test the sensitivity of the pre- and post- change SDD simulations, ruling

out the effects of natural variability as there are no differences between the climatic conditions between the two simulations. The observed and MURSAFF simulated pre- and post-change LOS_mid recession data were extracted for the period January 2009 - August 2010. The left plot in Figure 6.24 shows the recession data and their regression lines fitted according to the method described in Section 6.3.2 and as shown in Section 6.5.1. The recession line of the MURSAFF simulated pre-change or current situation is very similar to the recession through the observed data. Visually, the post-change recession deviates from the pre-change data, showing a less flashy response, in agreement with the observations in Section 6.4.2. From this it may be concluded that if short term changes (such as those simulated for LOS_mid) had occurred in the Hodder catchment, the SDD model analyses would have been able to detect them. To fully rule out the effects of natural variability, this could be supported by a comparison against data for neighbouring sites that are not undergoing change.

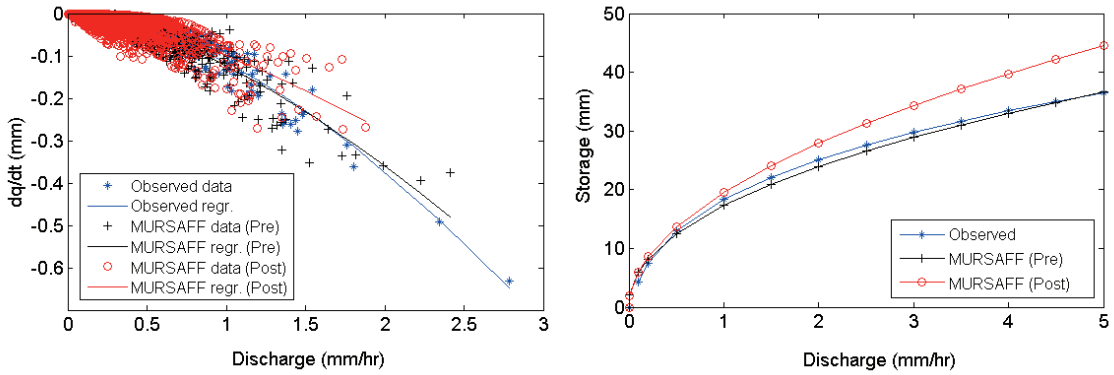

Figure 6.24 SDD observed (blue) and MURSAFF pre- (black) and post- change (red) simulated regressions of recession data (left) and simulated catchment storage against discharge (right)

Unlike the pre- versus post-change recession results presented in Chapter 5, the difference between the pre- and post-change MURSAFF-simulated SDD recessions can be attributed directly to the potential impacts of LUMC, as there are no differences between the climatic conditions. Based on Equation 5.12, the right plot in Figure 6.24 can provide an estimate for the relative difference in storage needed to generate a specific discharge. Note that the storage in the right hand tile in Figure 6.24 does not represent the actual catchment storage (such as those presented by MURSAFF in the previous sections), but rather an arbitrary storage. The plot shows that the post-change simulated catchment response is slightly more buffered. For example, to

generate a discharge of 3.0 mm/hr, the plot shows that the catchment requires approximately 5 mm more storage post-change than it does pre-change. The magnitude of this difference changes with discharge. One explanation is that the soil water storage is increased when stocking density is reduced, as also shown in Figures 6.21 and 6.22.

6.7 Summary

This chapter has presented a novel modelling tool (Model for Upland Runoff Storage And Flow Fields (MURSAFF)) that can be used to investigate the (potential) effects of LUMC on storage and runoff generation for process scale and micro scale catchments. It is unique in the way it uses a grid with irregular grid cells which can represent the complex spatial patterns observable in the field, such as irregular drainage networks, field boundaries and sheep tracks. The creation of the irregular MURSAFF grids depended strongly on field observations, interpretations and digital field maps. The grid parameterisation was also based on field observations, in addition to literature values. Both of these phases of the MURSAFF set-up involved testing with the aim to represent reality over a wide range of spatial scales. Pre- and post-change MURSAFF simulations for the CRO_sc5 and BRE_sap subcatchment case studies showed that while the impacts of grip blocking are instant and significant at the process scale, they are small and almost undetectable at the micro catchment scale. It was concluded that this is partly because the proportion of area directly affected by LUMC is small. The simulation results obtained agree with direct field observations in the two study catchments, and with the SDD pre- versus post-change data analyses in Chapter 5. The long-term effects of changes in stocking density in the LOS_mid subcatchment are predicted to involve attenuation of the flood hydrograph. The effects of sheep tracks are significant locally while the micro catchment scale impacts will depend on the proportional area affected.

7 Up-scaling of Land Use/Management Change Impacts

7.1 Introduction

From the analyses and modelling work reported in Chapters 5 and 6, it became clear that no statistically significant short-term change could be detected as a result of LUMC at any of the scales investigated. However, the potential long-term effects of changes in stocking density at the micro scale were explored in Chapter 6. This chapter is concerned with the propagation of those potential local scale changes downstream to the catchment outlet. Even though the record length is short, the unique data set collected in the present study provides an opportunity to investigate some fundamental issues (highlighted in Chapter 2) concerning the aggregation and scaling of flood hydrographs that affect how impacts of LUMC propagate downstream.

In Section 7.2 the multiscale catchment behaviour is considered based on observed data and irrespective of LUMC impacts. Firstly, this involves an investigation of within-catchment runoff aggregation by comparing relative peak flow ranks at multiple scales and spatial locations. Secondly, simple scaling relationships of peak flows, lag times and peak timings relative to the peak time at the catchment outlet are considered under a range of natural conditions. This work expands on the findings in Chapter 5, suggesting a systematic variation in the hydrological behaviour with catchment size, as derived from the multiscale SDD model parameters. Thirdly, Section 7.2 also includes an evaluation of these simple scaling relationships for their support in the analysis of the downstream propagation of potential LUMC impacts.

In Section 7.3 a simple semi-distributed Catchment Impact Model (CIM) for routing flood waves from multiple subcatchments is used to (1) investigate the downstream effects of the MURSAFF simulated impacts for LOS_mid, and BRE_sap (as presented in Chapter 6), and (2) explore the impacts of empirical changes to the different mini catchment responses on the HP catchment output. Section 7.3 ends with a discussion on the potential detection of impacts at HP of the long term upstream SCaMP LUMCs.

Finally, Section 7.4 provides a summary of the main findings presented in this chapter.

7.2 Multiscale Catchment Behaviour

7.2.1 Multiscale Catchment Runoff Aggregation

Chapter 5 showed that the SDD model parameters varied systematically with catchment size. If the hydrological response of the catchment behaviour changes systematically with scale, simple scaling relationships can be derived that can potentially aid in the analysis of the downstream propagation of LUMC impacts. However, the relative contribution proportions from the various subcatchments within the Hodder catchment most likely depend on the space-time pattern of precipitation and the spatial pattern of antecedent wetness. A better understanding of the relative hydrological state and response severity at different scales (irrespective of LUMC) during flood generation is therefore needed.

An important question related to the relative response severities at different spatial scales is whether the T-year flood on the micro scale catchments can be scaled to give the T-year flood on the meso scale catchment, and thereby provide a basis for scaling of T-year floods. In order to be able to answer this question correctly, long term records are needed so that the T-year floods at different scales can be determined. The multiscale data set of the present study is too short to perform such an analysis, though a first indication can be obtained by analysing the correlation of peak flow ranks for the different subcatchments.

During the post-change time period 14/01/2009 – 03/02/2010 multiscale data are available for a maximum number of stream gauges in the monitoring network (all excluding BRE_out, which has a data gap in June 2009, see Appendix 1). For this period, the 20 highest peak flows at the catchment outlet (Hodder Place) were identified. To avoid including multiple high peaks in single events, the peak flows were extracted as described in Chapter 5, with the highest peak flows identified in a time window of 16 hrs. For the 20 events, the peak flows for all subcatchments were extracted and ranked from high to low (i.e. highest recorded peak flow = rank 1).

The correspondence between the hydrological response severities at different scales is simple when the ranking of peak flows is similar for each subcatchment. A measure of

the statistical dependence between ranks of two variables can be given by the Spearman's rank correlation coefficient (R_s), according to Equation 7.1:

$$R_S = \frac{6 \sum d_i^2}{n(n^2-1)} \qquad \text{(Equation 7.1)}$$

where for sample size n, d_i is the difference in ranks given to the two variable values for each item of the data. R_s can range between -1 and 1, with positive values showing positive relationships and a value of 1 representing a perfect match.

Table 7.1 shows the Spearman's rank correlation coefficients between the 20 ranked events of all subcatchments within the Hodder catchment. There is a positive correlation between the ranks of all subcatchments, though there is quite some variability in the degree of correlation. The Spearman's coefficients in Table 7.1 are colour coded according to good (dark green, R_s = 0.8 - 1.0), moderately good (light green, R_s = 0.6 - 0.8), moderately poor (light red, R_s = 0.4 – 0.6) and poor (dark red, R_s < 0.4) positive correlations between sites. The table shows that there is generally good agreement in the peak flow ranks between nested sites within mini scale subcatchments (e.g. CRO_sc5, CRO_mid, CRO_weir, and CRO_out), and to some degree also between neighbouring mini scale catchments at the same scale (e.g. CRO_out and EAS_out). For the EAS_out, LOS_mid, HAR_out, LAN_mid and LAN_out subcatchments specifically, there is an overall disagreement in the ranks of the 20 peak flows with most other catchments. EAS_out is situated in the most Eastern part of the catchment and could therefore have been subjected to different relative rainfall patterns than the rest of the catchment. The poor agreement in ranks for the LOS_mid, HAR_out, LAN_mid and LAN_out can be attributed to a local convective summer event (07/07/2009) in the Langden catchment.

For six of the 20 different events, Figure 7.1 shows the spatial patterns of the peak flow ranks to demonstrate the spatial variability of the subcatchment's response severity during a range of natural conditions. The peak flow ranks in Figure 7.1 are colour coded with a high rank in brown and a low rank in blue. Apart from the largest event during 18/11/2009, there are clear differences in the spatial patterns of the peak flow ranks between events, which demonstrates the variability between the hydrological response spatially and at different scales.

Table 7.1 Spearman's rank correlation coefficients of the peak flow ranks of 20 events between the different subcatchments in the Hodder catchment. The colour coding is based on level of agreement between the relative peaks observed at the two different gauges: good (dark green) = Spearman's coefficients 0.8 – 1.0, moderately good (light green) = Spearman's coefficients 0.6 – 0.8, moderately poor (light red) = Spearman's coefficients 0.4 – 0.6, and relatively poor (dark red) = Spearman's coefficients <0.4

	CRO_sc5	BRE_sap	LOS_mid	BRE_rhw	CRO_mid	HAR_out	WHI_mid	CRO_weir	EAS_out	WHI_out	LAN_mid	CRO_out	FH	LAN_out	LOU_out	HOD_mid	HP
CRO_sc5	x	0.79	0.54	0.81	0.96	0.29	0.9	0.93	0.8	0.74	0.61	0.93	0.86	0.45	0.84	0.91	0.85
BRE_sap	0.79	x	0.78	0.96	0.86	0.34	0.94	0.75	0.58	0.82	0.71	0.81	0.97	0.64	0.71	0.72	0.74
LOS_mid	0.54	0.78	x	0.78	0.61	0.23	0.71	0.5	0.43	0.68	0.75	0.6	0.79	0.57	0.58	0.53	0.59
BRE_rhw	0.81	0.96	0.78	x	0.88	0.2	0.92	0.77	0.59	0.78	0.71	0.82	0.95	0.52	0.74	0.74	0.74
CRO_mid	0.96	0.86	0.61	0.88	x	0.24	0.95	0.91	0.77	0.83	0.61	0.95	0.92	0.46	0.84	0.9	0.85
HAR_out	0.29	0.34	0.23	0.2	0.24	x	0.26	0.34	0.36	0.24	0.59	0.29	0.31	0.84	0.51	0.37	0.54
WHI_mid	0.9	0.94	0.71	0.92	0.95	0.26	x	0.86	0.73	0.89	0.59	0.92	0.98	0.52	0.82	0.85	0.84
CRO_weir	0.93	0.75	0.5	0.77	0.91	0.34	0.86	x	0.86	0.77	0.62	0.93	0.82	0.52	0.89	0.93	0.89
EAS_out	0.8	0.58	0.43	0.59	0.77	0.36	0.73	0.86	x	0.68	0.49	0.89	0.67	0.43	0.86	0.92	0.86
WHI_out	0.74	0.82	0.68	0.78	0.83	0.24	0.89	0.77	0.68	x	0.55	0.84	0.89	0.5	0.79	0.8	0.83
LAN_mid	0.61	0.71	0.75	0.71	0.61	0.59	0.59	0.62	0.49	0.55	x	0.59	0.69	0.84	0.68	0.59	0.68
CRO_out	0.93	0.81	0.6	0.82	0.95	0.29	0.92	0.93	0.89	0.84	0.59	x	0.89	0.48	0.9	0.95	0.91
FH	0.86	0.97	0.79	0.95	0.92	0.31	0.98	0.82	0.67	0.89	0.69	0.89	x	0.59	0.8	0.8	0.82
LAN_out	0.45	0.64	0.57	0.52	0.46	0.84	0.52	0.52	0.43	0.5	0.84	0.48	0.59	x	0.59	0.49	0.64
LOU_out	0.84	0.71	0.58	0.74	0.84	0.51	0.82	0.89	0.86	0.79	0.68	0.9	0.8	0.59	x	0.93	0.99
HOD_mid	0.91	0.72	0.53	0.74	0.9	0.37	0.85	0.93	0.92	0.8	0.59	0.95	0.8	0.49	0.93	x	0.95
HP	0.85	0.74	0.59	0.74	0.85	0.54	0.84	0.89	0.86	0.83	0.68	0.91	0.82	0.64	0.99	0.95	x

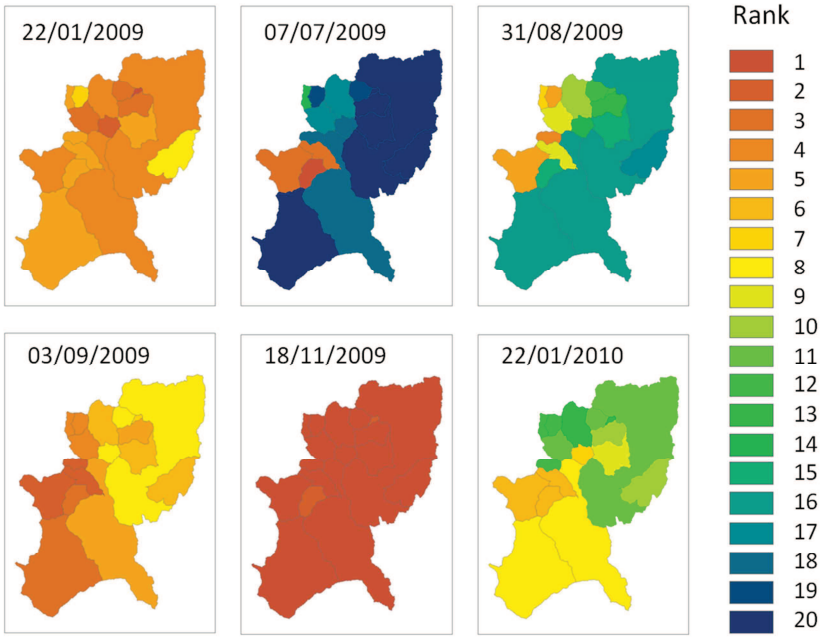

Figure 7.1 Peak flow ranks for all subcatchments for six selected events

Figure 7.2 (left) shows the Spearman's coefficients between the 20 ranked events of all subcatchments within the Hodder catchment and those at the catchment outlet (bottom row in Table 7.1). Overall, there is a tendency for better correlation coefficients with increasing catchment scale, although the coefficients in the Langden subcatchments in the western part of the catchment are relatively low. From the plot on the right of Figure 7.2, it is evident that the convective event during 07/07/2009 distorts the overall picture, because when the event is excluded from the determination of the correlation coefficients, the overall pattern becomes clearer.

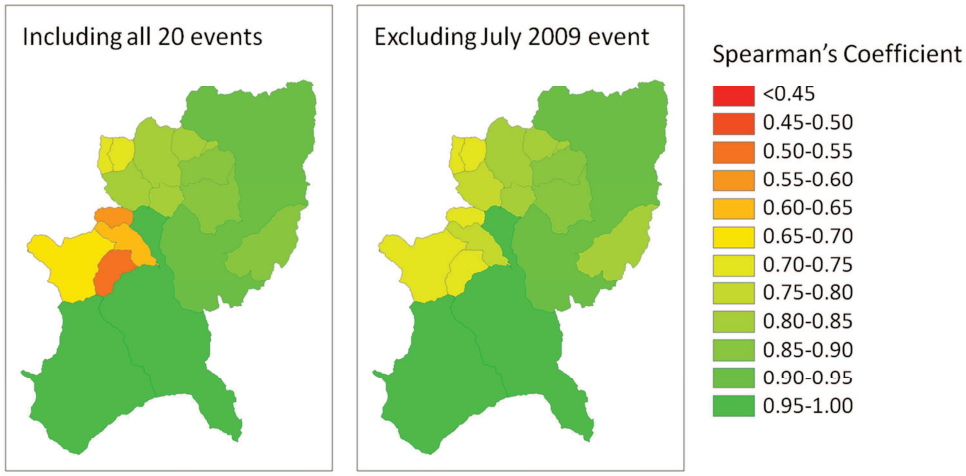

Figure 7.2 Spearman's rank correlation coefficients between the Hodder catchment outlet and the subcatchments for the peak flow ranks of 20 selected events (left) and excluding the 07/07/2009 convective event (right)

Figure 7.2 right shows that the correlation coefficients between the subcatchments and the catchment outlet increase with catchment scale. However, for a specific event in time, Figure 7.1 shows that the response severity of the Hodder catchment can be very different at different spatial scales. On a storm to storm basis, the response severity at the large scale (HP) appears not to have a straightforward time correlation to the response severity at the small scale. In addition, the relative contributions of the various subcatchments to the Hodder catchment outflow is therefore variable. From these results it may also be suggested that it is unlikely that the T-year flood on the micro scale catchments can be scaled to give the T-year flood on meso scale catchment, although analyses on longer records are needed to derive a more definite conclusion on this.

7.2.2 Multiscale Catchment Response and Precipitation Severity

In order to determine how dominant the precipitation is in determining the catchment response at the different catchment scales, the correlation between the peak flow ranks and the corresponding catchment precipitation is investigated.

Table 7.2 gives an overview with general information about seven selected events in the Hodder catchment. These include the six events for which the peak flow ranks were presented in Figure 7.1, as well as the largest pre-change event (recorded on 26/10/2008). This also allows for an additional evaluation of pre- versus post-change catchment response. Another reason for including this event in the analysis is that it is the largest event recorded during the entire data collection period. Overall, the seven events were selected so that they represent a range of natural conditions. They therefore include summer and winter events, convective local events and large scale synoptic events, single- as well as multi-peak events, a snowmelt event, and a range of different peak flows, including the highest recorded flows.

Table 7.2 General information for seven selected events in the Hodder catchment

Date	Catchment Precipitation (mm)	Peak discharge at HP (mm/hr)/(m^3/s) (rank, Section 7.2.1)*	Note
26/10/2008	61.4	3.36/244 (-)	The largest event on record, Pre-change event
22/01/2009	24.6	1.77/128 (4)	A winter event with a relatively 'even' distribution of rainfall over the catchment
07/07/2009	11.1	0.89/64.4 (18)	A convective summer event
31/08/2009	17.6	1.03/74.6 (16)	A summer event with a relatively 'even' distribution of rainfall
03/09/2009	39.5	1.68/122 (5)	A large event with double peak response
18/11/2009	44.3	2.99/217 (1)	A large event with a single peak response
22/01/2010	28.1	1.45/105 (8)	A large event that includes snow melt

Figure 7.3 shows the precipitation and discharge response for Hodder Place in time. From the plots in Figure 7.3 it is clear that there is considerable variability in the rainfall intensity and timing. Overall, the precipitation for the summer events is of much shorter duration and more intense than the winter events. Some events consist of multiple waves of intense precipitation, notably those recorded for 26/10/2008, 31/08/2009 and 03/09/2009. It is noted that the 22/01/2010 precipitation in Figures 7.3 and 7.5 is subjected to large uncertainties related to snowmelt (see also Chapter 4).

Figure 7.4 shows the total event precipitation as determined for each subcatchment, according to the procedure described in Section 4.3.3. The catchment precipitation is generally higher in the uplands compared to the lowlands, though some events show more within catchment variability than others. The largest relative difference in catchment precipitation is for the event at 07/07/2009, where the precipitation in the Langden catchment in the West is 5.5 times of that in the Easington catchment in the East. This is reflected in the respective peak flow ranks for the July event in Figure 7.1, with much higher ranks in western Langden subcatchment. The 18/11/2009 event has a relatively high and more evenly distributed precipitation event, also reflected by the relative peak flow ranks of Figure 7.1.

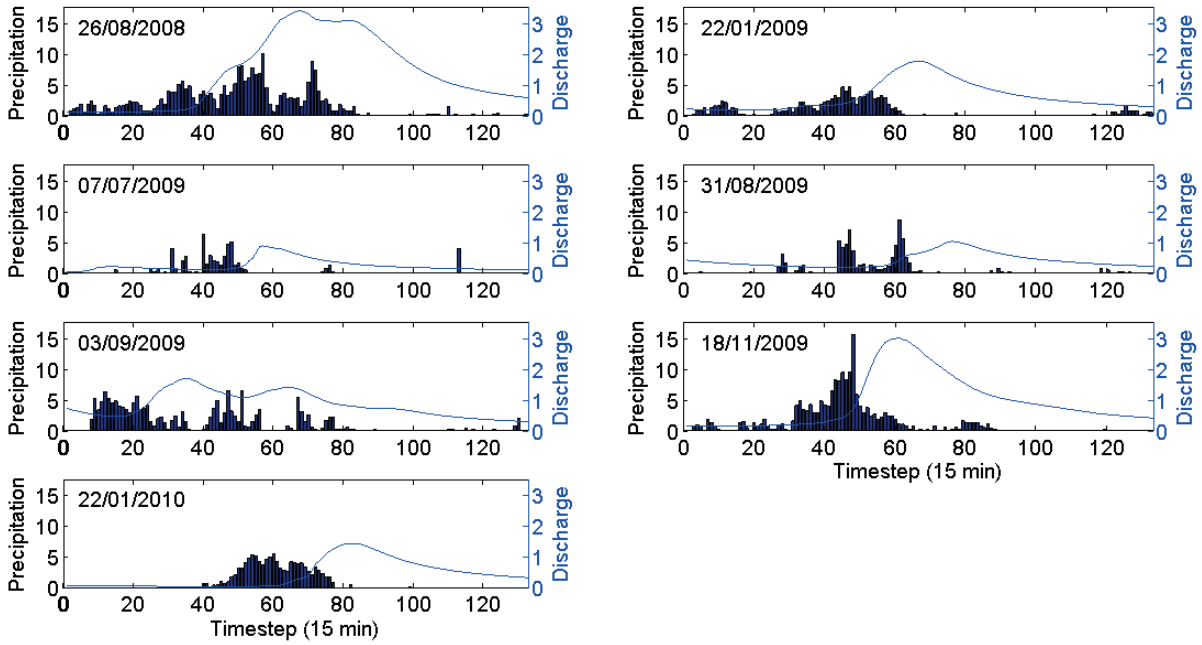

Figure 7.3 Precipitation (for the Hodder Place catchment) and runoff response (both in mm/hr) for seven selected events at Hodder Place

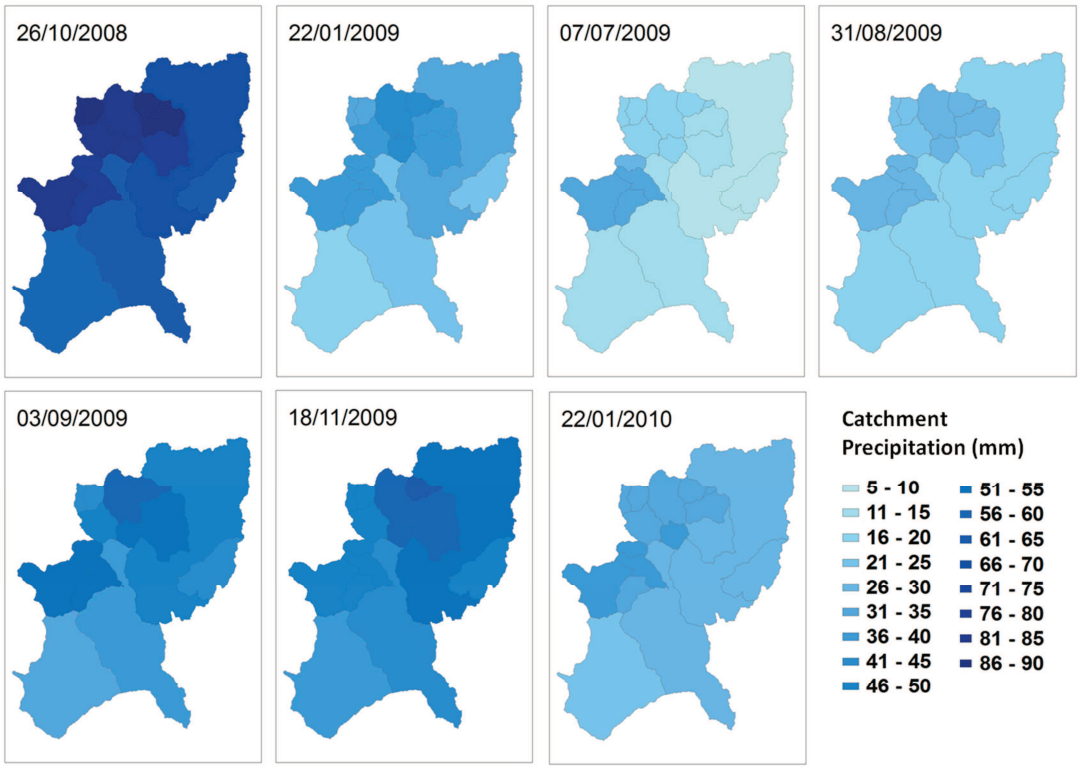

Figure 7.4 Total catchment event precipitations for seven selected events

To be able to make an informed judgement on the correlation between the spatial patterns of the event rainfall distribution and the catchment response severities, the catchment precipitation of the 20 events used to construct the peak flow ranks for the subcatchments were also ranked. Table 7.3 shows that the catchment precipitation ranks show much higher positive Spearman's rank correlation coefficients (Equation 7.1) between the subcatchments than the peak flow ranks in Table 7.1. Part of this high correlation is induced by the averaging of the point rainfall measurement values for individual subcatchments. The largest differences are between the Loud catchment, which is situated in the southern, lower lying part of the Hodder catchment, and the other subcatchments.

In Figure 7.5 the spatial pattern of the correlation between the 20 ranked peak flow events and the corresponding ranked catchment precipitation for the events is shown for the different subcatchments. The figure shows a rather complex pattern, with a relatively better correlation between total precipitation and catchment response severity in the eastern part than in the western part of the catchment. To some degree there is also a better correlation in the upper part than in the lower part.

Table 7.3 Spearman's rank correlation coefficients of the catchment precipitation ranks of 20 events between the different subcatchments in the Hodder catchment. The colour coding is based on level of agreement between the relative peaks observed at the two different catchments: good (dark green) = Spearman's coefficients 0.8 – 1.0, moderately good (light green) = Spearman's coefficients 0.6 – 0.8, moderately poor (light red) = Spearman's coefficients 0.4 – 0.6, and relatively poor (dark red) = Spearman's coefficients <0.4

	CRO_sc5	BRE_sap	LOS_mid	BRE_rhw	CRO_mid	HAR_out	WHI_mid	CRO_weir	EAS_out	WHI_out	LAN_mid	CRO_out	FH	LAN_out	LOU_out	HOD_mid	HP
CRO_sc5	x	0.83	0.81	0.83	1	0.78	0.96	0.99	0.91	0.97	0.78	0.99	0.95	0.82	0.61	0.96	0.92
BRE_sap	0.83	x	0.85	1	0.83	0.81	0.93	0.85	0.83	0.91	0.81	0.86	0.95	0.84	0.69	0.85	0.87
LOS_mid	0.81	0.85	x	0.85	0.81	0.98	0.88	0.8	0.79	0.9	0.98	0.83	0.9	1	0.68	0.83	0.89
BRE_rhw	0.83	1	0.85	x	0.83	0.81	0.83	0.85	0.83	0.91	0.81	0.86	0.95	0.84	0.69	0.85	0.87
CRO_mid	1	0.83	0.81	0.83	x	0.78	0.96	0.99	0.91	0.97	0.78	0.99	0.95	0.82	0.61	0.96	0.92
HAR_out	0.78	0.81	0.98	0.81	0.78	x	0.85	0.77	0.76	0.86	1	0.79	0.86	0.99	0.7	0.8	0.88
WHI_mid	0.96	0.93	0.88	0.83	0.96	0.85	x	0.97	0.91	0.99	0.85	0.97	0.99	0.88	0.68	0.95	0.94
CRO_weir	0.99	0.85	0.8	0.85	0.99	0.77	0.97	x	0.91	0.97	0.77	1	0.95	0.81	0.63	0.96	0.92
EAS_out	0.91	0.83	0.79	0.83	0.91	0.76	0.91	0.91	x	0.9	0.76	0.93	0.9	0.8	0.65	0.98	0.95
WHI_out	0.97	0.91	0.9	0.91	0.97	0.86	0.99	0.97	0.9	x	0.86	0.97	0.99	0.89	0.65	0.95	0.94
LAN_mid	0.78	0.81	0.98	0.81	0.78	1	0.85	0.77	0.76	0.86	x	0.79	0.86	0.99	0.7	0.8	0.88
CRO_out	0.99	0.86	0.83	0.86	0.99	0.79	0.97	1	0.93	0.97	0.79	x	0.96	0.83	0.66	0.97	0.94
FH	0.95	0.95	0.9	0.95	0.95	0.86	0.99	0.95	0.9	0.99	0.86	0.96	x	0.9	0.67	0.94	0.93
LAN_out	0.82	0.84	1	0.84	0.82	0.99	0.88	0.81	0.8	0.89	0.99	0.83	0.9	x	0.67	0.83	0.89
LOU_out	0.61	0.69	0.68	0.69	0.61	0.7	0.68	0.63	0.65	0.65	0.7	0.66	0.67	0.67	x	0.68	0.78
HOD_mid	0.96	0.85	0.83	0.85	0.96	0.8	0.95	0.96	0.98	0.95	0.8	0.97	0.94	0.83	0.68	x	0.96
HP	0.92	0.87	0.89	0.87	0.92	0.88	0.94	0.92	0.95	0.94	0.88	0.94	0.93	0.89	0.78	0.96	x

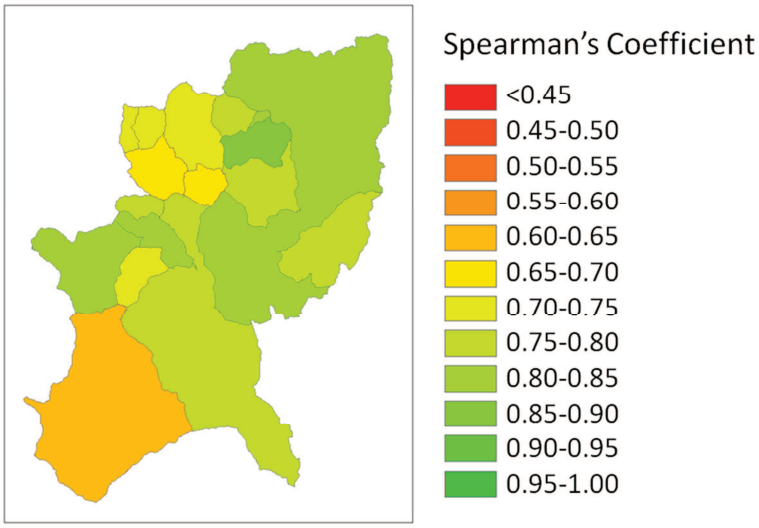

Figure 7.5 Spearman's correlation coefficients between the subcatchment's peak flow ranks and precipitation ranks for 20 selected events

Overall, the correlations between peak flow ranks and catchment precipitation ranks in Figure 7.5 are good, with Spearman's rank correlation coefficients in the region of 0.62 to 0.89. From this it may be concluded that the catchment precipitation is the dominant factor in determining the response severity. However, the complexity in the map of Figure 7.4 suggests that other factors, such as the rainfall intensity (Figure 7.3), the antecedent conditions of the subcatchments, or differences in the geology or soils may also determine the catchment response severity.

7.2.3 Scaling Hydrograph Characteristics under Different Natural Conditions

As highlighted in Chapter 2, desirable LUMC effects in the context of flooding involve an attenuation of the flood peak and increases in the time delay between precipitation inputs and the corresponding flood peak. However, this also depends on whether or not this would decrease the synchronization of tributary responses. This section therefore explores simple scaling relationships of the flood peak and lag time with area, and of the peak timing relative to the peak occurrence at the catchment outlet with travel distance. The seven different events as presented in the previous sections were further used for this investigation of scaling response patterns within the Hodder catchment.

It has been shown that, during single events, peak discharge (Q in m^3/s) and catchment area (A in km^2) are correlated according to Equation 7.2:

$$Q(A) = aA^{\theta} \qquad \text{(Equation 7.2)}$$

where parameters a and θ change between events (Furey and Gupta, 2005; Gupta et al., 2010). As shown in Figure 7.6, the peak flow data for the seven events in the Hodder catchment comply rather well with this relationship, though there is considerable scatter for the event on 07/07/09, resulting from the highly uneven rainfall distribution in space. The relationship and scatter is similar for all other events, while the vertical shifts between the events are related to overall differences in event size (e.g. the lower regression lines are for the relatively smaller summer events, while the lines with the highest intercept are for the large (winter) events).

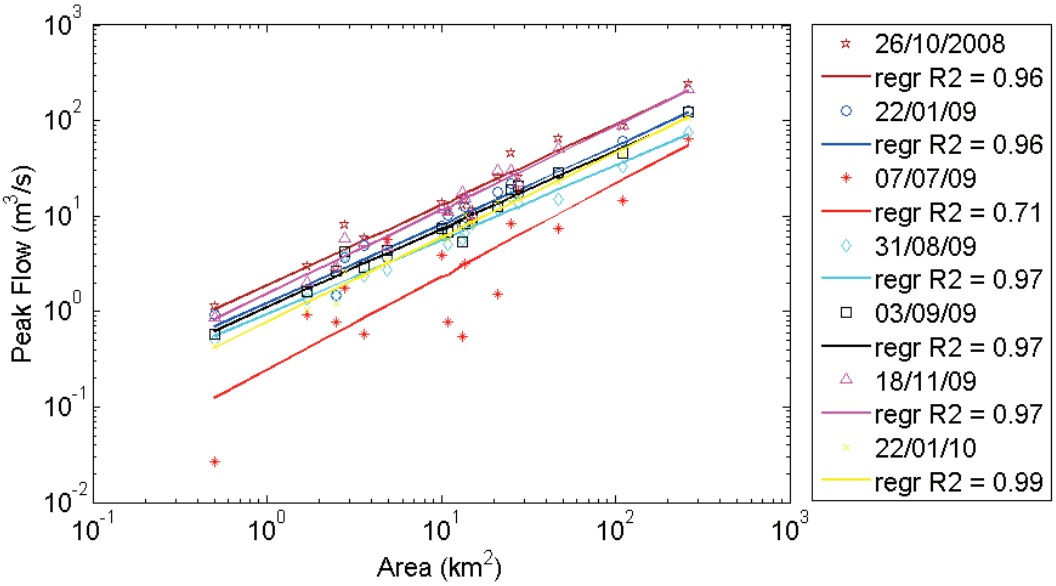

Figure 7.6 Peak flow against catchment area for seven events in the Hodder catchment

Figure 7.7 shows the peak lag time against catchment area for the seven selected events. The lag time is defined as the time difference between the mass centroid of the rainfall event and the peak flow occurrence of the resulting hydrograph. There is a reasonable correlation for the majority of the individual events, based on the expected increase in lag time with area. This corresponds with the findings in Chapter 5, which showed a more flashy response at smaller scales. However, there is considerable

scatter around the regression as well as large variability between events. It is suggested that the difference in the regression intercept may be a function of the antecedent catchment wetness, with shorter lag times when the catchment is already wet. There is also a correspondence with the peak flow size. For example, the relatively large 26/10/2008 and 18/11/2009 events have the highest peak flows (Figure 7.6) and the shortest lag times (Figure 7.7), while the largest lag times were observed for the relatively small 31/08/2009 event. The main outliers are the convective and the snowmelt events, which show less steep regression lines and generally poor relationships. This indicates less variation in lag time with catchment scale and suggests that there might be other factors, such as snow melt rainfall patterns, rainfall intensity, and antecedent conditions, which can dominate the lag time.

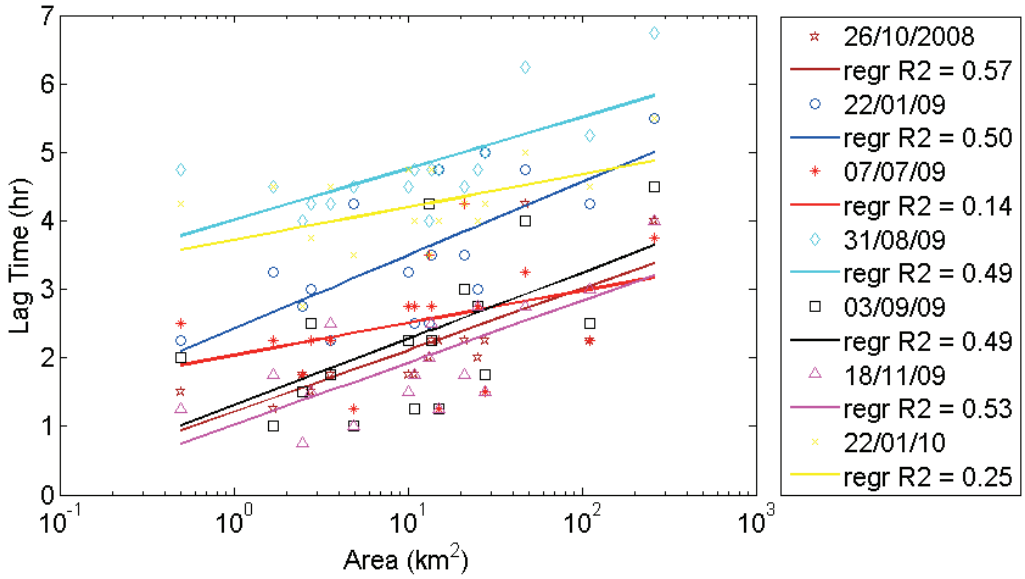

Figure 7.7 Lag time against catchment area for seven events in the Hodder catchment

For the seven events, Figure 7.8 shows the peak time of the multiscale Hodder subcatchments (colour coded) against the travel distance. The peak time is presented relative to the peak time at the catchment outlet. For example, during the event on 22/01/2009, the Croasdale catchment, 33.5 km upstream of the catchment outlet, peaks 3 hours and 15 mins earlier (at CRO_mid) than the peak at the catchment outlet.

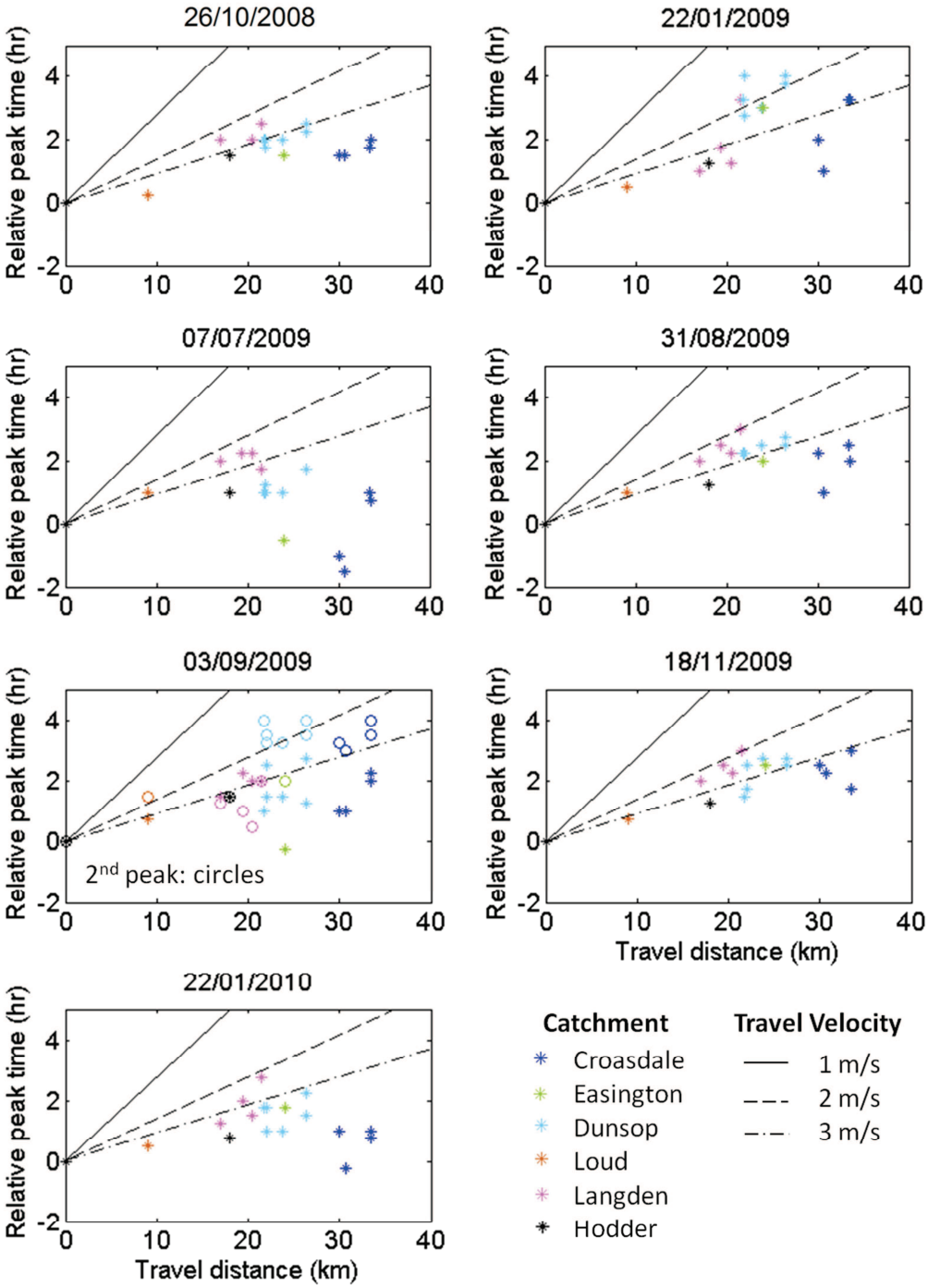

Figure 7.8 Peak time relative to the catchment outlet at the different subcatchments within the Hodder plotted against travel distance for seven selected events, as well as the expected relative peak time based on three average travel velocities

Figure 7.8 also shows the expected relative peak time against the travel distance for three average travel velocities: 1, 2 and 3 m/s. Typical velocities for streams draining UK uplands (<10 km^2) are 1-1.5 m/s (Beven et al., 1979), while average velocities of up

to 3 m/s have been measured for meso scale catchments (Richards, 1982; Kirkby, 1993). It is widely recognised that the propagation of a flood hydrograph is a complex and dynamic process with the velocity of the flood wave continuously changing with time and distance (Beven and Wood, 1993). However, assuming that typical average travel velocities for the Hodder catchment are between 1 and 3 m/s, the average travel velocities as shown in Figure 7.8 can aid towards a better understanding of the (lack of) synchronisation of the different subcatchments. Where the relative peak flow timings all lie around an average travel velocity line, this indicates that the peak flows are all more or less synchronized, so that the timing of the peak flow of a particular upstream site corresponds directly with that of the peak flow downstream. Some scatter is expected around the average velocities, arising from uneven distributions of the space-time pattern of rainfall, differences in rainfall intensity, and antecedent wetness as discussed above.

Figure 7.8 shows that during none of the events are the timings of all the subcatchment peaks synchronized, and there is quite some variability in the relative peak timing pattern between storms. For some events (26/10/2008, 31/08/2009 and 18/11/2009) the relationship between relative peak time and travel distance is relatively flat. For example, on 28/10/2008 the Croasdale catchment (dark blue) and the Easington catchment (green) peak at the same time as the Hodder catchment downstream (black). Considering the difference in travel distance (10-15 km) the upstream and downstream peak flows cannot be directly linked. However, the peak flow timings during these three events, (especially during the event on 18/11/2009) lie more or less within the expected range based on average travel velocities, and are closer to synchronisation than those during the other events (with more a more complex space-time rainfall pattern). During the events on 07/07/2009, 03/09/2009 and 22/01/2010, the peak flow at the gauges of some of the subcatchments occurs even later than that at the catchment outlet (i.e. they have a negative relative peak time). This means that these peak flows upstream contribute only to somewhere in the tail end of the catchment outlet hydrograph recession.

Although the analysis only involves one pre-change event, it is noted that the pre-change multiscale catchment behaviour (26/10/2008) is not particularly different from

the post-change behaviour, as shown in Figures 7.6, 7.7 and 7.8. In fact, the pre-change response is very similar to those of the largest recorded post-change event (18/11/2010). This supports the earlier findings that there is no evidence to suggest that the SCaMP LUMC have had a short-term impact on the magnitudes and timings of peak discharges.

7.2.4 Discussion on Up-Scaling of Potential LUMC Effects

Although some are more apparent than others, scaling relationships have been established for peak flow, lag time (Section 7.2.2) and overall catchment behaviour (Chapter 5). The correlations of peak flow and lag time with catchment area differ between events, while the relationship of the overall catchment behaviour with area has been established in more general terms, by using the SDD model parameters (Chapter 5). Here, the potential of using these relatively simple scaling relationships to up-scale potential LUMC effects is discussed.

Gupta et al. (2007) hypothesised that the physical basis of power laws in flood peaks (Equation 7.2) has its origin in the self-similarity (self-affinity) of channel networks. The good relationships between peak discharge and catchment area in Figure 7.6 therefore reflect the strong footprint of the channel network geometry in determining the way peak flows can be scaled. If, for a particular event, the associated peak flow scaling relationship could be used to predict the downstream impacts of upstream LUMC effects, the relative impact downstream is expected to change between events, as the relationships are different between events. However, it is suggested that these relationships are likely to be relatively insensitive to the small scale perturbations as predicted in the current study, owing to the nature of the power-law relationship on the log-log plot, which tends to disguise small changes. The lag time scaling relationship is not particularly strong and also differs between events. As with the peak flow scaling relationship, the use of these scaling relationships will also result in a relative impact downstream that is different for each event.

Overall, there is some scope for the use of scaling relationships in peak flow and lag time if events are considered individually. However, both scaling relationships ignore the fact that during a particular event, some subcatchments may have more severe

responses than others (Section 7.2.1) and there is also considerable variability in the (lack of) synchronisation of the different subcatchments (Section 7.2.3).

The relative timings and response severities are important when assessing what happens to the contributions of the different subcatchments. In general, the channel network geometry is understood to be fundamentally related to the travel times of the subcatchment contributions and whether or not they arrive before, at, or after the downstream peak of the flood hydrograph. If precipitation was uniform, and the responses per unit area were all the same, then the travel times would dominate the overall catchment response. However, the above analysis has shown that spatial variability in precipitation and the heterogeneity in the hydrological response disturbs this expected behaviour.

This variability in precipitation and heterogeneity in the hydrological response has important consequences for the downstream propagation of LUMC impacts. For example, consider the situation where upstream LUMCs increase the lag time of an upland subcatchment. If the relative peak flow timing of that particular subcatchment would then be desynchronized with the peak timing at the catchment outlet, this effect could contribute to an attenuation of the catchment outlet flood hydrograph downstream. However, if the subcatchment's pre-change peak flow would have contributed to the rising limb of the catchment outlet hydrograph, a delay in the lag time could result in a larger peak flow response downstream. Clearly, the latter effect is less desirable in terms of flood management as it would increase the downstream peak flow.

In addition, if for a particular event, a subcatchment is relatively more or less responsive, the downstream impacts will also vary. For example, during the event on 07/07/2009, the flow from the Langden catchment made the largest contribution to the flood hydrograph response at the catchment outlet. Meanwhile, the Croasdale catchment was relatively inactive (low rank peak flow) and peaked much later than the peak flow at the catchment outlet. Therefore, potential effects of LUMCs in the Croasdale catchment would have made no impact on the catchment outlet peak flow

response, while LUMC impacts downstream of the Langden catchment could have been significant.

Because of a strong dependence on differences in rainfall distribution (in space and time) and the antecedent wetness conditions, the multiscale peak flow, lag time and timing of peak flow responses show some degree of uniqueness for each event. It is therefore argued that it is not possible to simply use these scaling relationships to assess downstream LUMC impacts, as a result of a complex interaction of the differences in the relative subcatchment activity (or response severity) and a lack of synchronisation of relative peak timings. The same will account for the scaling relationship based on the SDD parameters. Instead, the prediction of the propagation of upland LUMC impacts (as predicted through the MURSAFF simulations in Chapter 6), will draw on a Catchment Impact Model (CIM) that can deal with the complex distribution of rainfall inputs and responses and the interaction of subcatchments.

7.3 Propagation of Local Scale Simulated Effects to the Catchment Outlet

7.3.1 Catchment Impact Model

The Catchment Impact Model (CIM) is a simple semi-distributed model for routing flood hydrographs from multiple subcatchments. It was developed recently by John Ewen (Personal Communication December 2011) to meet the need to track small impacts propagating through river networks where there are large space-time variations in flow. The CIM treats subcatchments independently and calculates the total flow at a network outlet as the sum of the routed flows from each subcatchment. The CIM model can be used to estimate the downstream impact of LUMC in a subcatchment by routing its pre- and post-change runoff hydrographs. In this context, impact, whether measured at a subcatchment or downstream, is defined as the difference between the post- and pre-change discharge.

For each subcatchment, the CIM model tracks kinematic waves to a downstream measuring point by using an analytic solution to the non-linear advection-dispersion equation:

$$\frac{\partial q}{\partial t} = D(x,t)\frac{\partial^2 q}{\partial x^2} - u(x,t)\frac{\partial q}{\partial x} \qquad \text{(Equation 7.3)}$$

for which q (m^3/s) is the estimated contribution runoff, t (s) is time, D (m^2/s) is the hydrodynamic dispersion coefficient, x (m) is the distance along the path from the subcatchment to the measurement point and u (m/s) is the kinematic wave velocity. This general approach to routing has a long history stretching back to the early work of Hayami (see Chow, 1959 p. 601). The second term on the right-hand side of Equation 7.3 describes the downstream movement of the wave (advection); and the first term the spread of the wave and hence the decay of its amplitude (dispersion). In the CIM model, the hydrodynamic dispersion is determined as the sum of a storage hydrodynamic dispersion coefficient (D_0) and the friction hydrodynamic dispersion coefficient ($\overline{D}$):

$$D = (D_0 + \overline{D}) \qquad \text{(Equation 7.4)}$$

D_0 accounts for dead spaces in the channel (pools) and complex geometries (such as rough bends). It is a fixed value (50 m^2/s for the work reported here) and independent of flow. During high flows its effect is relatively small compared to the friction hydrodynamic dispersion coefficient, defined as:

$$D = Q/(2ws_0) \qquad \text{(Equation 7.5)}$$

where w (m) is the channel water surface width and s_0 is the bed slope (Henderson, 1966 p. 384). The CIM model assumes the following relationship between the kinematic wave velocity u and the bulk flow velocity v (m/s):

$$u = \frac{3}{2}v \qquad \text{(Equation 7.6)}$$

This relationship is used widely in routing models and methods, and can be derived for rectangular channels undergoing uniform flow. In routing the effects of change in runoff, the flow velocities and hence kinematic wave velocities will rise and fall with the flow rate. This has several effects, captured within CIM, such as tending to cause the steepening of rising limbs in the flood hydrograph as faster kinematic waves to gradually catch up with slower kinematic waves (i.e. the mechanism that causes kinematic shock).

The CIM river network for the Hodder catchment that is used here is schematically presented in Figure 7.9. The network consists of 16 sites (which have associated with them pre- and post- change runoff) and 25 links (which have a discharge rate). The CIM model is unusual for a routing model in that it is driven directly by observed field data. All links have associated with them channel properties (length (m), s_0, w, Manning's n) which are based on field observations (see for example Appendix 1 and Owen (2008)). These properties are used to calculate the bulk flow velocities from the observed discharge rates for the individual links. The discharges for the links are set using observed data. For example, the discharge for link 16 is that observed at CRO_out, while that at link 17 is the observed release from Stocks Reservoir. For those links where no observed discharge data are directly available (e.g. link 18), the discharge is approximated as the sum of the discharges for two upstream links (e.g. for link 18 this is the sum for links 16 and 17). The discharge for link 25 is the observed discharge at the catchment outlet (Hodder Place).

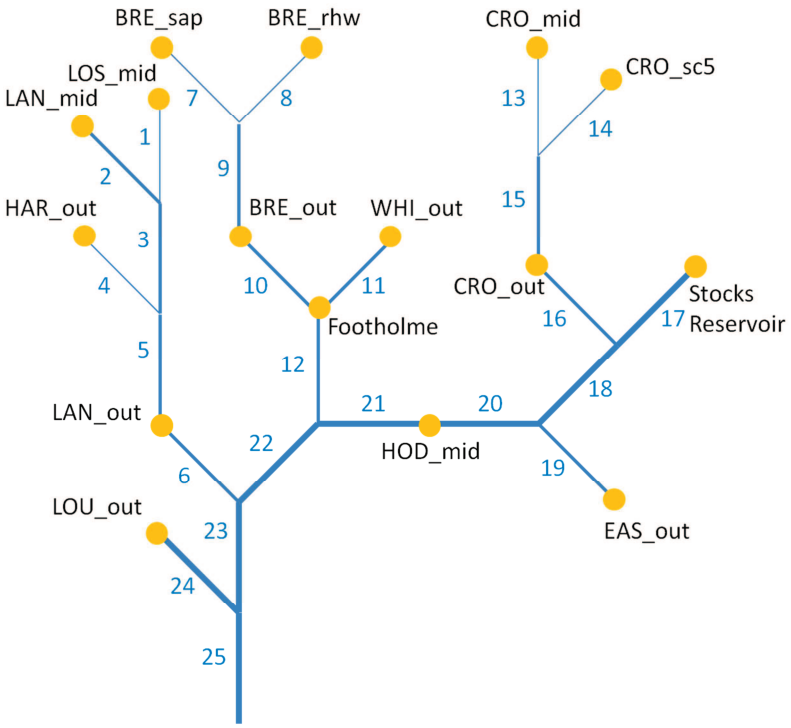

Figure 7.9 Schematic representation of the Hodder catchment river network for the CIM model, consisting of 25 links and 16 sites. Note that the length of the network links is not according to scale.

7.3.2 Propagation of Land Use/Management Change Effects

The CIM model was used for two different types of impact propagation analyses. First, it was used to investigate the downstream impacts of the MURSAFF simulated changes at LOS_mid, and BRE_sap as presented in Chapter 6. The MURSAFF analyses in Chapter 6 showed that the effects of grip blocking in CRO_sc5 and BRE_sap were negligible at the micro scale; hence the downstream effects of CRO_sc5 are here not further explored and the BRE_sap impacts of grip blocking are multiplied by five, so that the relatively small impacts at that site are more visible graphically. Second, the CIM was used to explore the propagation of empirical impacts at the mini scale to the catchment outlet. Both analyses were performed for four selected storms out of the seven presented in Section 7.2. These are the 26/10/2008, 22/01/2009, 07/07/2009 and 18/11/2009 events, so that a range of conditions, including those during the highest recorded events at the catchment outlet (Hodder Place), can be explored. For these four storms, Figure 7.10 shows the observed and CIM simulated hydrographs, as well as the Nash-Sutcliffe Efficiencies (NSE). Considering the relatively simple nature of the CIM model, it is shown that it can reproduce the downstream hydrograph relatively well for the observed conditions. Generally, the CIM overestimates the observed response for the large winter events, while the response for the smaller summer event is underestimated.

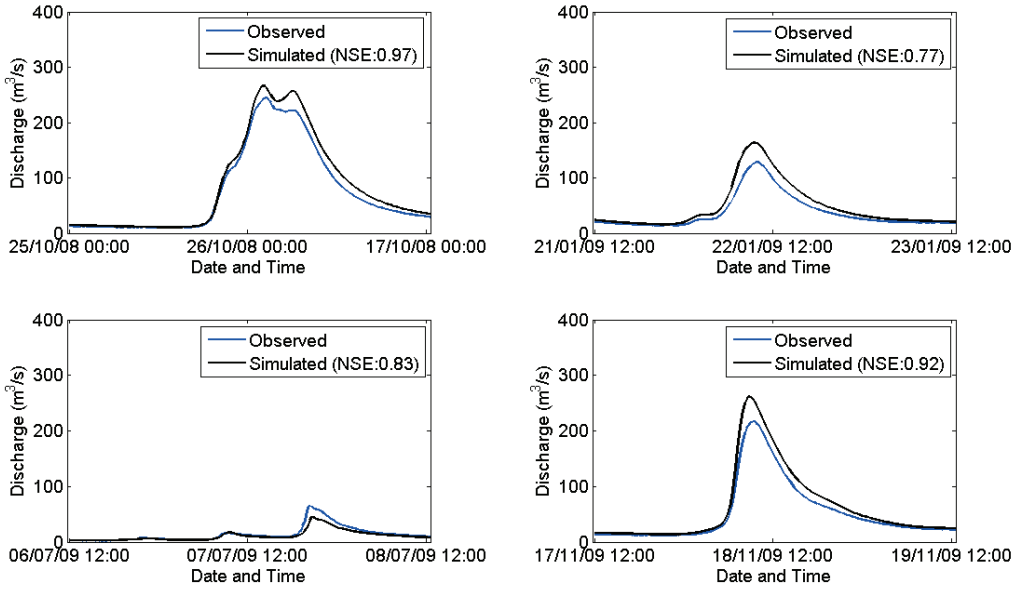

Figure 7.10 Observed (blue) and CIM pre-change simulated hydrographs black) at Hodder Place for four events. The NSE represents the Nash-Sutcliffe efficiency goodness of fit.

Propagation of MURSAFF simulated micro scale change effects

Figure 7.11 shows the MURSAFF simulated pre- and post-change stocking density changes and grip blocking effects for the four events for LOS_mid (purple) and BRE_sap (blue) respectively. As the simulated impacts at BRE_sap are small and trivial (Chapter 6), the fivefold impacts at BRE_sap are shown in green. The figure shows that the simulated impacts at LOS_mid and BRE_sap are different for each storm (see also Chapter 6) and, during an event, these can be either negative or positive. For LOS_mid, decreases in flow are generally associated with the rising limb and the peak of the hydrographs, while increases in flow occur during the falling limb.

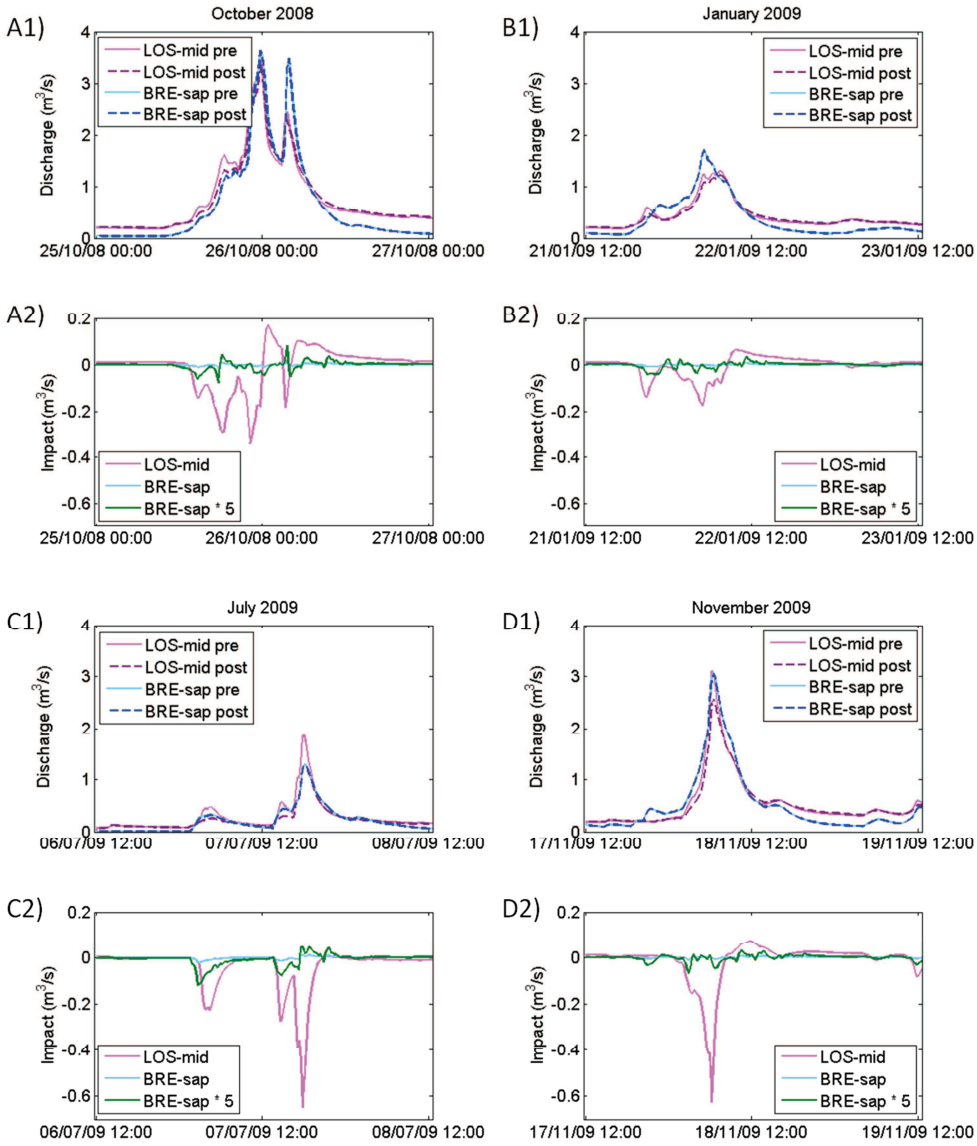

Figure 7.11 LOS_mid (purple) and BRE_sap (blue) MURSAFF simulated pre – and post change discharge (1) and impact (2) for four different events. The impacts of change at BRE_sap are also multiplied by 5 (green) so that they can be seen more clearly.

The pre- and post-change MURSAFF simulated discharges of LOS_mid and BRE_sap were routed through the river network for the four events. Figure 7.12-top shows the pre- and post-change peak flows within the river network ranging from the micro scale at LOS_mid (left) and BRE_sap (right) to the meso scale at the catchment outlet. The peak flow impacts are very small, in the order of 0.05 - 0.5 m3/s (Figure 7.12-middle), as expected from the plots in Figure 7.11. The impact percentage of pre-change peak flow for BRE_sap is insignificant at all scales, even when the impact is multiplied by five (Figure 7.12 bottom right). At LOS_mid the impacts become trivial at the mini scale (approximately 10 km^2). This can be related to the percentage area undergoing change, which is decreasing with increasing scale.

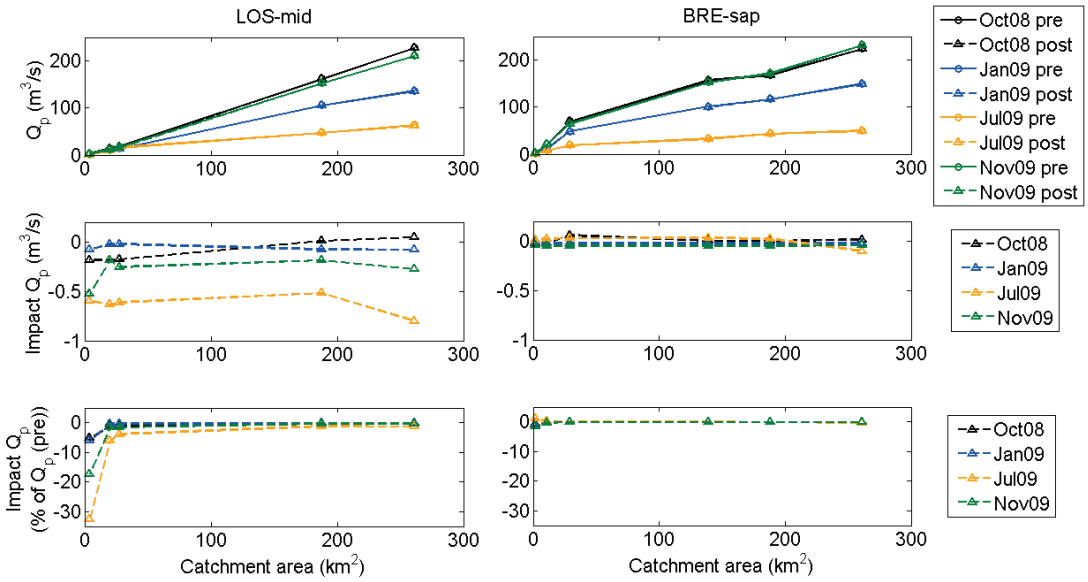

Figure 7.12 Pre- and post-change simulated peak flow (top) and the peak flow impact (middle: in m^3/s, bottom: in percentage of simulated pre-change peak flow) for LOS_mid (left) and BRE_sap (right) at different scales ranging from the micro scale to the meso scale at the catchment outlet. The impacts of change at BRE_sap are multiplied by 5.

Another observation from Figure 7.12 is that, while the upstream impacts all involve a decrease in peak flow, the associated downstream impact is different for each storm, and can result in a decrease or increase. An example is the peak flow impact at LOS_mid and the downstream sites for the October 2008 event (Figure 7.12 middle left in black). Figure 7.13 shows that this depends on where the contribution of the routed upstream hydrograph sits in the downstream hydrograph. The latter is plotted on the primary y-axis; while the former is plotted on the secondary y-axis. Compared to the peak discharge, the impacts are very small.

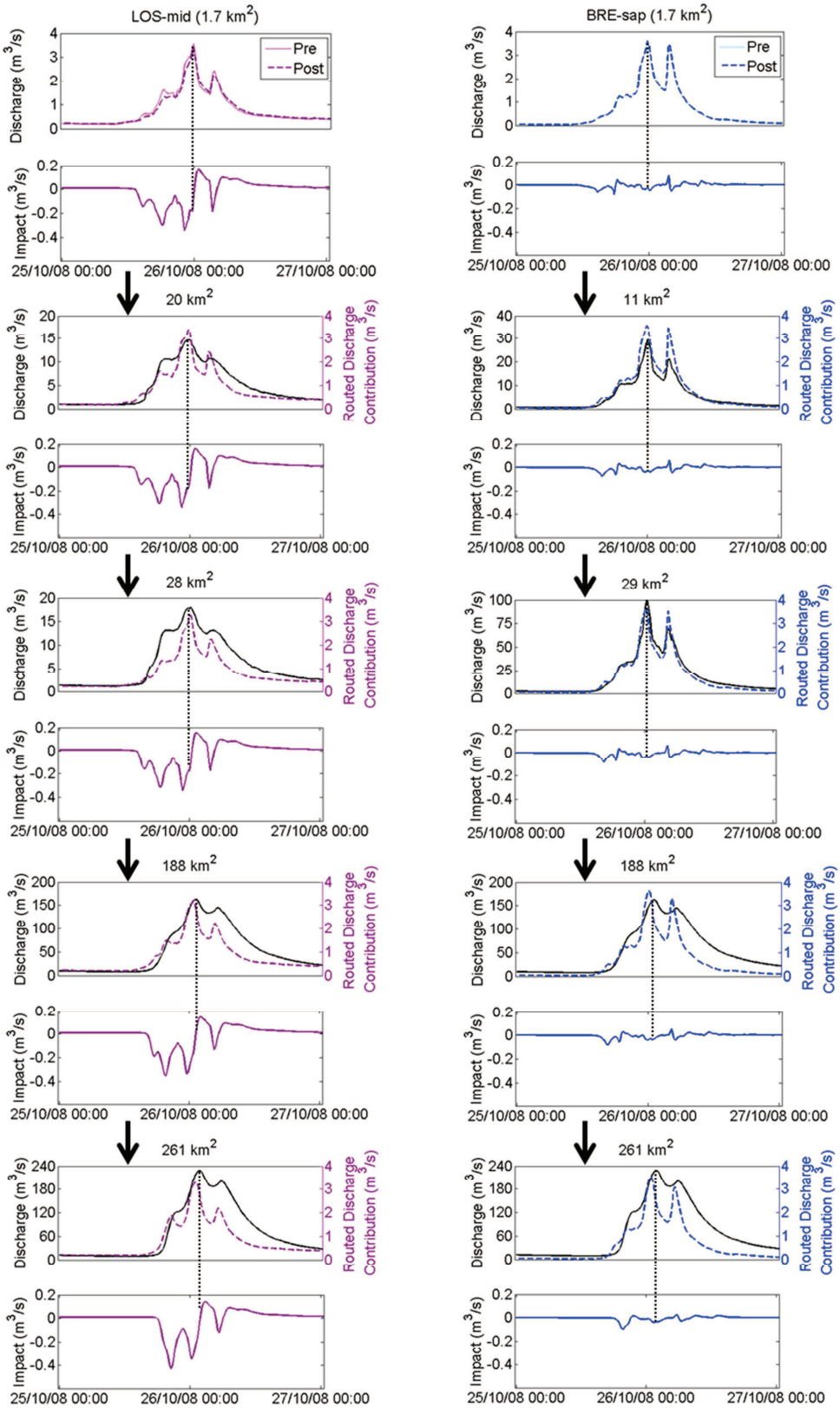

Figure 7.13 The top plots show the October 2008 simulated hydrograph and the routed contribution of LOS_mid (purple, left) and BRE_sap (blue, right). The discharge and routed discharge are plotted on separate y-axes because the contribution of the routed discharge is very small. The top plots show the routed change related impact at different scales ranging from the micro scale to the meso scale at the catchment outlet. The black dotted lines connect the peak hydrograph and the associated contributing impact. The impacts at BRE_sap are exaggerated by a magnitude of five.

For the October event in 2008, Figure 7.13 illustrates the simulated hydrograph and the routed contribution of LOS_mid (left) and BRE_sap (right) as well as the routed change related impact at different scales, ranging from the micro scale to the meso scale at the catchment outlet. The hydrograph and impact are both smoothed as they move down the system. This is the result of hydrodynamic dispersion and the effect of nonlinear kinematic dispersion related to variations in the kinematic wave velocity.

For LOS_mid on the left, Figure 7.13 shows that, at the micro and mini scale (1.7, 20 and 28 km^2), the part of the routed impact that involves a decrease in flow (i.e. negative routed impact) contributes to the peak of the hydrograph (i.e. the peak flow is reduced). In Figure 7.13 this is indicated by the black dotted lines, which connect the peak hydrograph and the associated contributing impact. At the meso scale sites (188 and 261 km^2) however, the peak of the hydrograph corresponds with a positive routed impact. This is in agreement with the location of the contribution of the routed upstream hydrograph peak in the downstream hydrograph (i.e. the falling limb of LOS_mid contributes to the peak discharge at HP). At scales larger than the mini scale, the hydrograph is not synchronized with the routed contribution of LOS_mid, as it consists of contributions of subcatchments from all over the Hodder catchment. This shows that the downstream impact for each subcatchment will depend on the timings of the runoff from all the contributing subcatchments.

Propagation of empirical mini scale impacts

The analyses above showed that the downstream micro scale changes of LOS_mid and BRE_sap depend on the timing of the other contributing subcatchments but are insignificant at the catchment outlet scale. However, the impacts at these two catchments alone do not represent the full extent of the SCaMP changes in the entire catchment (40% of the total catchment area), which have taken place over large areas of the upper part of the catchment (e.g. entire area upstream of LAN_out (11% of total catchment area), Footholme (10%), and CRO_out (8%)).

The current research has provided no evidence for changes at the mini scale, though the timescale of impacts are expected to be longer than the present data record. To explore the potential downstream impacts of changes in the different subcatchments

and for different storms, empirical changes were applied to the runoff of the mini scale subcatchments (LOU_out, LAN_out, FH, CRO_out and EAS_out). These involved (a) a delay (or time shift) of 1 hour, (b) a 15% change in flow and (c) a and b combined (see example in Figure 7.14 for the 7th July 2009 event in the LAN_out catchment). The alteration of 15 % was applied to the full data time series record and involved a 15% reduction in the flows above the mean and a 15% increase of flow below the mean flow during the full data record period.

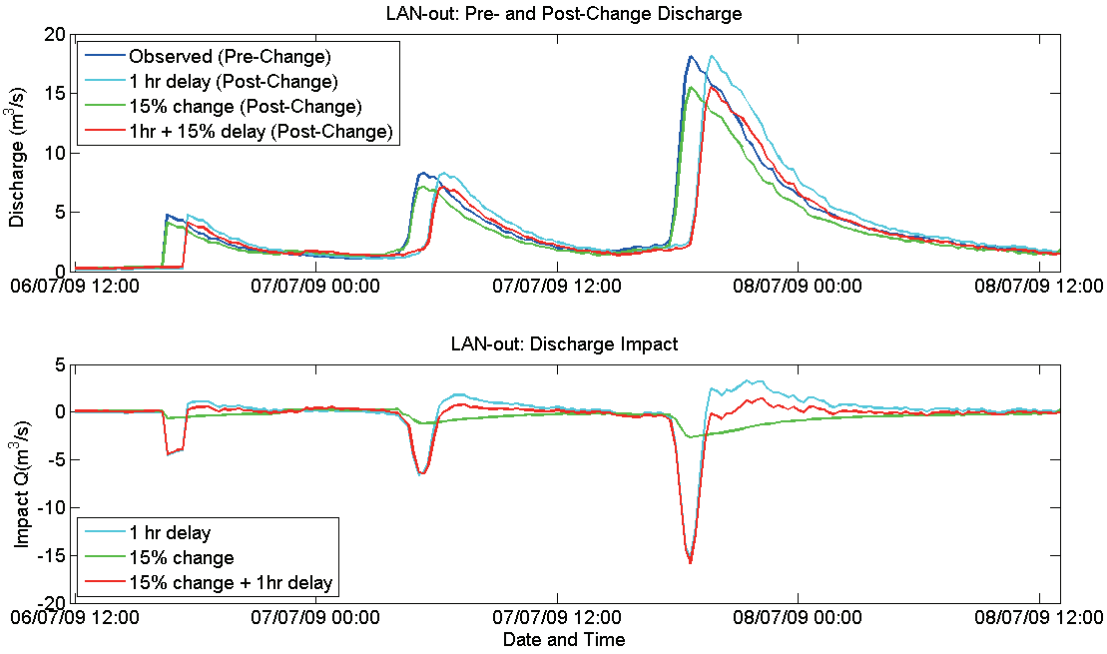

Figure 7.14 Empirical changes (1 hr delay (cyan), 15% change (green), and both (red)) applied to the observed discharge at LAN_out during 06/07/2009 – 08/07/2009.

The 1 hr delay and 15% change are expected to represent some of the most extreme LUMC induced impacts possible at the mini scale and they are likely to substantially overestimate the SCaMP LUMC impacts. The 15% change is based on the average decrease in peak flow simulated for stocking density changes at the LOS_mid micro scale catchment. As the impacts of LUMC generally decrease with scale, at the mini scale, this is likely to be less than 15%, so that the empirical simulations at this scale are thought to represent the upper limit of impacts. The aim is to explore the relative downstream impacts between storms and catchments. As there is no supporting evidence for these changes, the further analysis does not aid in providing accurate predictions of downstream impacts in terms of volumes or percentage impacts. The

three empirical changes focus mainly on decreasing the peak flow and delaying the response time, two of the generally assumed most desirable effects of LUMC at the local scale in the context of flooding (e.g. Lane 2008) (Lane, 2008).

The three types of changes were applied to all main subcatchments in the Hodder catchment separately and simultaneously for the four events (26/20/2008, 22/01/2009, 07/07/2009, and 18/11/2009). The pre- and post-change runoff from the subcatchments were routed through a reduced river network (Figure 7.15) compared to that of Figure 7.9. The network in Figure 7.15 excludes the micro scale sites, as the effect of LUMCs at the micro scale sites are assumed to be accounted for by the changes to the mini scale sites.

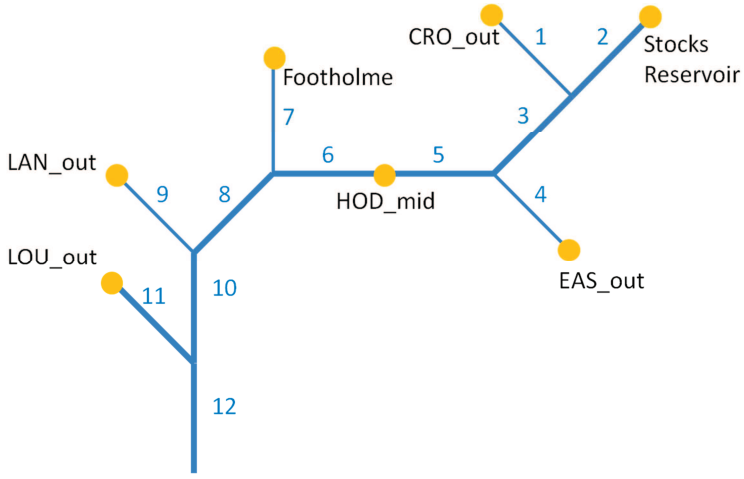

Figure 7.15 Schematic representation of the reduced Hodder catchment river network, consisting of 12 links and 7 sites for the investigation of the propagation of changes at the mini scale. Note that the length of the network links is not according to scale.

The impact results of the three types of changes to all the subcatchment hydrographs individually and simultaneously are presented in Appendix 5. In the current section, the impacts of the changes at LAN_out, FH, and CRO_out separately and the combined impact of changes at LAN_out, FH and CRO_out, are discussed. LAN_out is downstream of LOS_mid and Footholme of BRE_sap (see Figure 7.9). The combined effects of changes at LAN_out, FH and CRO_out are thought to represent the upper limit of impacts of the SCaMP LUMCs in the entire Hodder catchment.

For the four storms, Tables 7.4, 7.5 and 7.6 show the downstream impacts on the peak flow of HP of the 1 hr delay, 15% change and a combination of the two, respectively. Figure 7.16 shows the simulated downstream impacts on the full hydrograph at Hodder Place for changes at LAN_out and Footholme.

Table 7.4 Impact on HP Peak flow of 1 hr delay change to the different subcatchments

IMPACT at HP, from 1 hr delay at subcatchment	**October 2008**		**January 2009**		**July 2009**		**November 2009**	
	Delay Q_p (hr)	ΔQ_p (m^3/s)*	Delay Q_p (hr)	ΔQ_p (m^3/s)*	Delay Q_p (hr)	ΔQ_p (m^3/s)*	Delay Q_p (hr)	ΔQ_p (m^3/s)*
LAN_out	0.25	+1.02 (+0.4%)	0.00	-1.23 (-0.8%)	1.25	-3.93 (-8.9%)	0.25	-7.19 (-2.7%)
FH	0.75	-1.18 (-0.4%)	0.00	+1.95 (+1.2%)	0.00	-1.62 (-3.7%)	0.25	-4.67 (-1.8%)
CRO_out	0.00	-5.52 (-2.0%)	0.25	-4.04 (-2.5%)	0.00	+0.04 (+0.1%)	0.25	-9.20 (-3.5%)
LAN_out + FH + CRO_out	1.00	-1.45 (-0.6%)	0.25	-3.29 (-2.0%)	1.25	-7.37 (-16.6%	0.75	-14.83 (-5.7%)

* Percentage change of pre-change peak flow in brackets

Table 7.5 Impact on HP Peak flow of 15% change to the different subcatchments

IMPACT at HP, from 15% change at subcatchment	**October 2008**		**January 2009**		**July 2009**		**November 2009**	
	Delay Q_p (hr)	ΔQ_p (m^3/s)*	Delay Q_p (hr)	ΔQ_p (m^3/s)*	Delay Q_p (hr)	ΔQ_p (m^3/s)*	Delay Q_p (hr)	ΔQ_p (m^3/s)*
LAN_out	0.00	-3.46 (-1.4%)	0.00	-2.28 (-1.4%)	0.00	-2.83 (-6.4%)	0.00	-3.24 (-1.2%)
Footholme	0.00	-6.01 (-2.3%)	0.00	-2.95 (-1.8%)	0.00	-0.47 (-1.1%)	0.00	-4.32 (-1.7%)
CRO_out	0.00	-3.11 (-1.2%)	0.00	-2.50 (-1.5%)	0.00	+0.22 (+0.5%)	0.00	-4.43 (-1.7%)
LAN_out + FH + CRO_out	0.00	-12.36 (-4.6%)	0.00	-7.73 (-4.7%)	0.00	-3.09 (-7.0%)	0.00	-12.00 (-4.6%)

* Percentage change of pre-change peak flow in brackets

Table 7.6 Impact on Hodder Place Peak flow of 1 hr delay and 15% changes to the different subcatchments

IMPACT at HP, from 15% change +1hr delay at subcatchment	**October 2008**		**January 2009**		**July 2009**		**November 2009**	
	Delay Q_p (hr)	ΔQ_p (m^3/s)*	Delay Q_p (hr)	ΔQ_p (m^3/s)*	Delay Q_p (hr)	ΔQ_p (m^3/s)*	Delay Q_p (hr)	ΔQ_p (m^3/s)*
LAN_out	0.25	-2.48 (-0.9%)	0.00	-3.34 (-2.0%)	1.25	-6.11 (-13.8%)	0.25	-9.48 (-3.6%)
Footholme	0.75	-6.64 (-2.5%)	0.25	-1.25 (-0.8%)	0.00	-1.72 (-3.9%)	0.25	-8.27 (-3.2%)
CRO_out	0.00	-7.80 (-2.9%)	0.25	-6.01 (-3.7%)	0.00	+0.26 (+0.6%)	0.00	-12.36 (-4.7%)
LAN_out + FH + CRO_out	1.00	-13.62 (-5.1%)	0.25	-10.49 (-6.4%)	1.25	-9.80 (-22.1%)	0.75	-25.08 (-9.6%)

* Percentage change of pre-change peak flow in brackets

Tables 7.4-6 and Figure 7.16 show that there is variability in the downstream response between subcatchments and between storms. To further demonstrate and investigate this variability the key outcomes are highlighted below:

- The largest downstream effect of mini scale changes can be achieved during relatively small (and convective) events such as the July 2009 event (~10-20% change in peak discharge) with LUMC in the upstream subcatchment receiving most rainfall (LAN_out). Overall, however, the downstream impacts of the empirical changes at the mini scale are likely to be small (~5% or less).
- The impact of changes in all three subcatchments is generally larger than for changes in individual subcatchments. Overall, this can be attributed to a larger percentage area undergoing change. However, there are cases where the changes in multiple subcatchments can balance each other out. For example, for the October 2008 event, a 1 hr delay for CRO_out alone has a larger impact on the peak flow downstream (-2.0%) than a delay for all subcatchments (-0.6%) (Table 7.4).

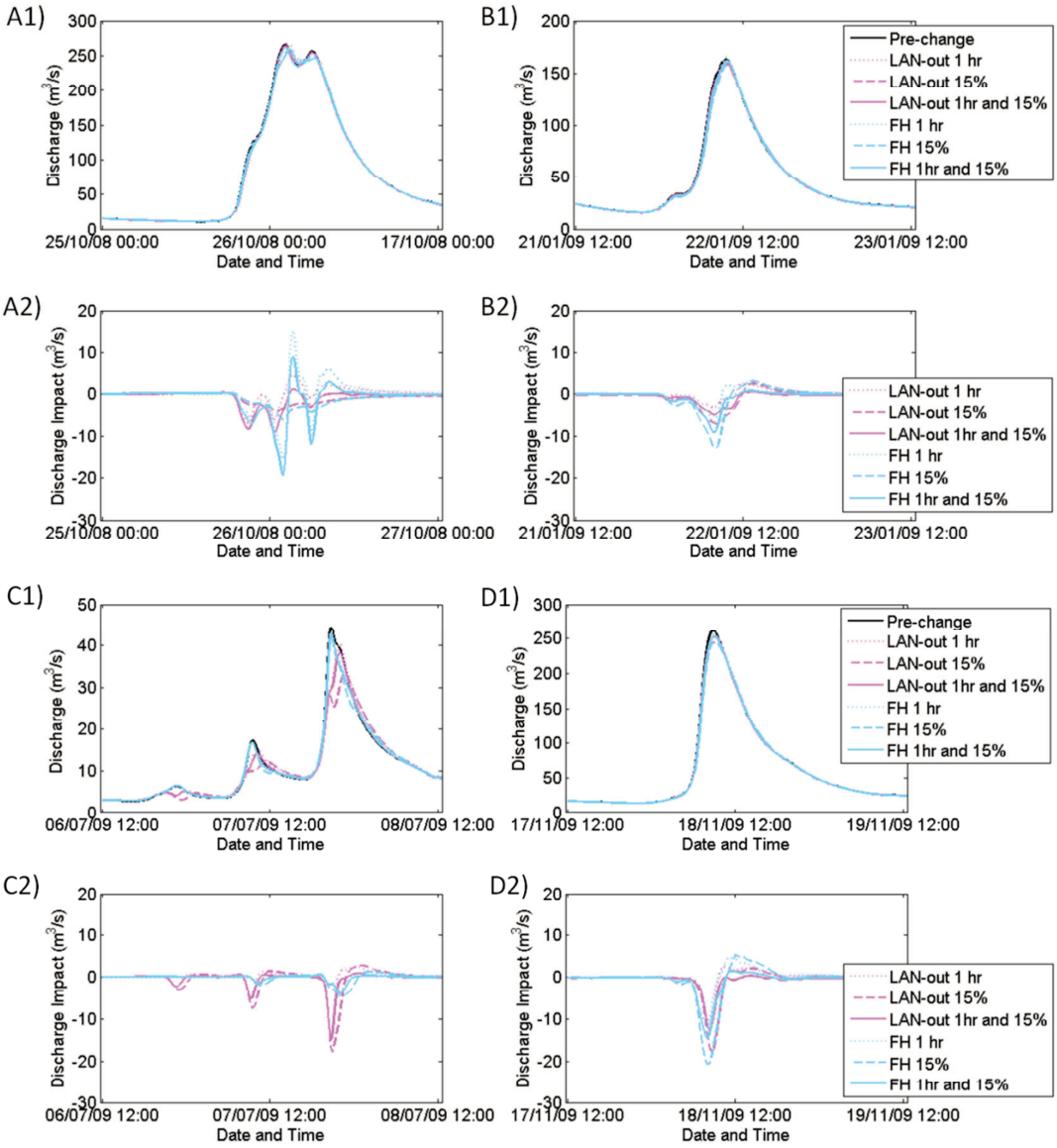

Figure 7.16 Pre- and post-change simulated discharge and impact of and on the Hodder Place flood hydrograph of four events, demonstrating the downstream effect of a 1 hr delay (dotted lines), a 15% change in flow (dashed lines) and a combination of both changes (full line) in the LAN_out (purple) and FH (blue) subcatchments. Note the difference in scale on the y-axis of the discharge plots.

- A 1 hr upstream shift (delay) can result in an increase or decrease of peak flow downstream. In agreement with the downstream impacts of LOS_mid, a one hour shift at LAN_out can result in a downstream increase in peak flow during the October 2008 event and a decrease in peak flow during the January 2009 event (Table 7.4). For a 1 hr shift at Footholme, the downstream impacts for the two events are the reverse (Table 7.3). Again, this can be attributed to the

relative locations of the contributions of the two subcatchments to the catchment outlet hydrograph. Figure 7.17 shows the contribution of the routed hydrographs of all mini scale subcatchments for the four events. For the October 2008 event, the figure demonstrates that the LAN_out peak flow contributes to the rising limb of the HP hydrograph, while the contributing FH peak flow corresponds with the exact peak flow at HP. For the January 2009 event, this is the reverse (Figure 7.17). For the October 2008 event, a one hour delay at LAN_out will therefore result in a synchronisation of the peak flows (and hence an increase in peak flow), while a one hour delay at FH will result in a decrease in peak flow (see also Figure 7.16).

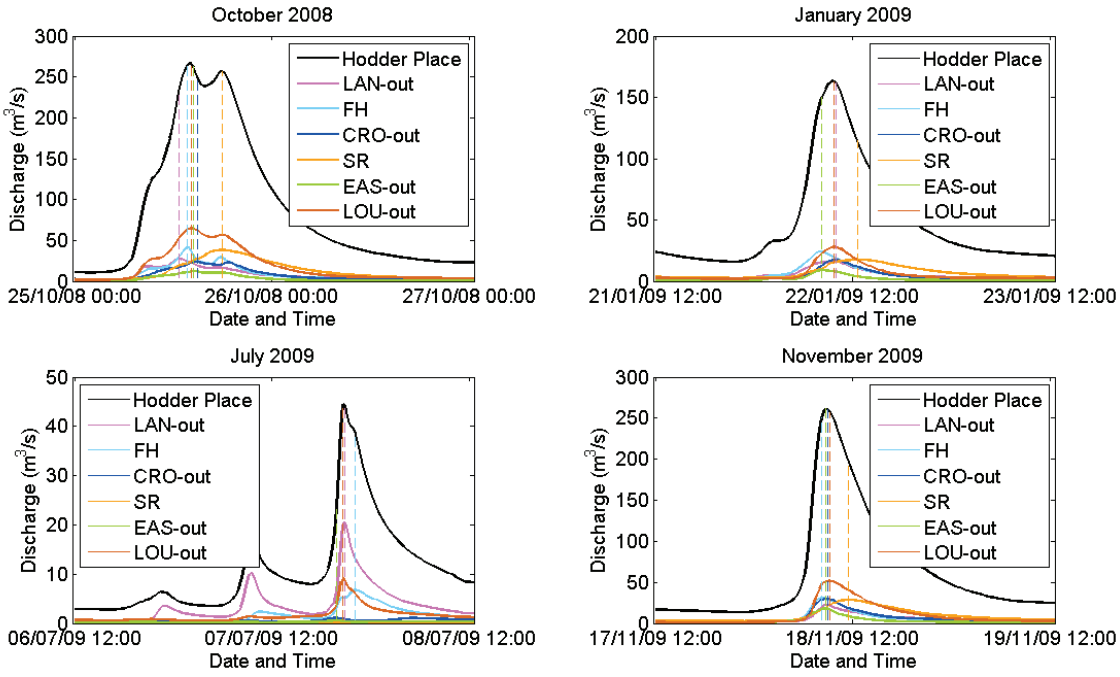

Figure 7.17 Pre-change simulated Hodder Place (HP) flow and contributions of the routed flows of the different mini scale subcatchments. The figure corresponds to the potential effects of delaying the hydrograph. The dotted lines demonstrate to which part of the HP hydrograph the peak flows of the different subcatchments correspond.

- Table 7.5 shows that, for a specific subcatchment, even though the percentage change of the upstream mini scale subcatchments is stable at 15% for all events, the associated downstream relative impacts on the peak flows are variable across the events. This can be attributed to differences in the relative

contributions of each subcatchment to the Hodder Place hydrograph. For example, for the October 2008 event, a 15% decrease in peak flow at LAN_out results in a 1.4% decrease in peak flow downstream, while this is a 6.4% decrease for the July 2009 event (Table 7.5). From Figures 7.16 and 7.17 it becomes clear that this is because the relative contribution of the discharge at LAN_out is much higher for the July 2009 event than for the October 2008 event.

- Tables 7.4 and 7.6 show that a 1 hr delay of a subcatchment also has a variable effect of a delay in peak flow downstream. For example, for the 1 hr delay at LAN_out, this results in a 15 min delay at HP during the October 2008 event, and a 1 hr and 15 min delay at HP during the July 2009 event. This may also be related to the timing and the relative contributions of the subcatchments, and the effects of nonlinear kinematic dispersion.

7.3.3 Discussion

The analyses in this section have shown that the downstream impact of an upstream change in LUMC is rather complex and a function of the percentage area undergoing change as well as the timing and relative magnitudes of the contributions from the upstream subcatchments to the downstream hydrograph (and hence their location within the catchment). As discussed in Section 7.2.4, the average travel time is controlled by the network geometry, which determines the average arrival time of the subcatchment's hydrograph contribution to the downstream flood response. However, on a storm to storm basis, the subcatchment hydrographs and contributions are a function of natural variability in precipitation and heterogeneity in the catchment response patterns. The downstream impacts of LUMCs are therefore different for each storm.

Overall, it is suggested that the downstream impacts of LUMCs such as those of the SCaMP project in the Hodder catchment are small (< 5%), with the largest downstream impacts occurring during relatively small summer events. The MURSAFF simulated changes are insignificant at the catchment outlet, mainly related to the percentage

area subjected to change (~1% of the catchment area). The empirical changes at the mini scale are meant to reflect changes over much larger areas and their effects are therefore more pronounced at the catchment outlet. However, overall, the downstream impacts of these empirical changes on large events are still small (in the order of 5%). There is large uncertainty regarding these empirical changes as there is no direct evidence to support these changes. However, it is suggested that the empirical changes are likely to overestimate the actual future (fully established) changes as a result of the SCaMP LUMCs, since a delay of 1 hr as well as a consistent decrease of peak flow of approximately 15% are thought to represent the upper limits of impacts at the mini scale. This implies that it is unlikely that significant (future, fully established) impacts of the upstream SCaMP changes (specifically in stocking density) will be detected at the catchment outlet, given the difficulty of identifying changes in the presence of natural hydro-climatic variability (Chapter 5).

From this discussion, it may be concluded that a specific upland LUMC may have impacts downstream that, in terms of flood management, can be slightly beneficial for one storm and the reverse for another, although overall, extensive upstream changes can be expected to achieve only relatively small impacts downstream.

The above analyses results, which are based on the unique data set collected as part of this study, have provided an important part of the missing evidence in that they justify the speculations and predictions of other modelling studies such as those discussed in Chapter 2. For example, several authors (Gilman, 2002; O'Connell et al., 2004; Bloschl et al., 2007; Halcrow, 2008) have suggested that the downstream LUMC impacts depend on the percentage area undergoing change, the spatial distribution and temporal variation in individual physical catchment characteristics, LUM activities and their effects on runoff generation (magnitude and timing), the connectivity of local scale flow paths with the stream network, and the routing of runoff through the channel network. It has also been suggested that extensive upland LUMCs are required to produce small impact at the downstream catchment scale (Gilman, 2002; JBA Consulting, 2007; O'Donnell et al., 2011).

7.4 Summary

This chapter has investigated the propagation of local micro-catchment LUMC impacts to larger catchment scales. An analysis of the multiscale Hodder catchment behaviour, based on observed data and irrespective of LUMC, revealed that scaling relationships for peak flows and lag times could be established, although they are different for each storm. It was argued, however, that these simple scaling relationships cannot be used to inform the propagation of downstream LUMC effects, because they ignore the demonstrated within catchment variability in catchment response severity and the variability in the peak timings of the different subcatchments. These are both a function of natural variability in precipitation patterns, (antecedent) catchment conditions and hydrological functioning. To predict the propagation of the SCaMP upland LUMC impacts, a simple semi-distributed Catchment Impact Model (CIM) was therefore used, for its ability to capture the complex distribution of responses and the interaction of subcatchments. The CIM model routes flood hydrographs from multiple catchments to determine the catchment outlet hydrograph. It was used to investigate the downstream effects of the MURSAFF simulated impacts of LOS_mid and BRE_sap (as presented in Chapter 6), and to explore the impacts of empirical changes in the mini scale catchments on the catchment response at Hodder Place, which are assumed to represent the upper limits of the full scale SCaMP LUMC effects. The results suggest that the downstream effects of the Hodder SCAMP LUMCs will be relatively small and different for each storm. An upstream change in peak flow can result in a downstream decrease or increase in peak flow, depending on the location of the contribution of the routed upstream hydrograph within the downstream hydrograph. The largest downstream effects can be achieved during relatively small and convective summer events with LUMCs in the subcatchment that receives most rainfall. It was concluded that the internal synchronisation of the subcatchment responses and the natural variability therein are dominant factors in determining the catchment outlet response and hence also the downstream impacts of upstream LUMCs.

8 Conclusions and Recommendations

8.1 Research Summary

This study has focussed on the multiscale impacts of Land Use/Management Changes (LUMCs) on the flood response in the River Hodder catchment, North-West England.

The literature review described the current state of knowledge regarding local scale LUMC impacts and their connection with downstream catchment response. It also provided an overview of the associated monitoring and analyses techniques. The key remaining challenges and areas of limited knowledge were identified as:

1. Although a vast amount of research has led to the establishment of convincing links between LUMCs and changes to runoff regimes at the local scale, there is an almost complete lack of evidence that local scale effects aggregate to cause impacts at larger scales downstream;
2. There is a lack of data from multiscale nested meso scale catchments that have been instrumented to investigate the effects of LUMC specifically;
3. LUMC detection and prediction are complicated by data uncertainty, de-coupling change impacts from natural variability, working with short records, differentiating between different change effects, and the transferability and scaling of impacts;
4. In order to fully understand and represent the complex geometry of LUM practices in the landscape as defined by features observed in the field (such as sheep tracks and (blocked) drainage systems), a physically based model that can run on an irregularly-sized grid of any shape and size is needed;
5. Up-scaling local scale LUMC impacts is a complex process as a result of data constraints, heterogeneity, nonlinearity and the dominance of different processes at specific scales.

Given these key challenges and areas of limited knowledge, this study aimed to gain a better understanding of the effects of local scale LUMCs and their connection with catchment flood response at increasing scales through the collection and analysis of a

new multiscale dataset, based on a nested meso scale (~100 km^2) catchment experiment and appropriate data analyses and modelling methods.

The River Hodder catchment (261 km^2) in North-West England was designated as the study catchment, because of the unique opportunity to monitor and study the multiscale impacts of known LUMCs, and the availability of long term historical rainfall and discharge data. A clear distinction can be made between the catchment properties of the headwaters and those of the lower areas and main Hodder valley. Historical changes in the catchment involved the instalment of grips, increases in stocking density and afforestation. The more recent changes in the headwaters of the Hodder catchment have included grip blocking, reductions in stocking density, and tree planting as part of United Utilities' SCaMP programme. The SCaMP changes were implemented over an area that covers approximately 40% of the total catchment area, which includes the area upstream of Stocks Reservoir (15% of the catchment area).

To be able to study the impact of the SCaMP LUMCs on the catchment flood response at increasing scales, a multiscale nested monitoring design (including the existing monitoring network: 28 stream gauges, seven tipping bucket rain gauges, and a weather station for evapotranspiration estimates) was set up in the Hodder catchment. The experimental design is unusual in the way it has focussed mainly on dense and continuous monitoring of flow and did not include the monitoring of local internal catchment variables (e.g. hydraulic conductivity, phreatic levels), which are typically associated with large heterogeneities, making it difficult to scale such local information. The study involved an extensive field campaign. The data from the multiscale network are available for approximately 0.5-1 year before and 1-1.5 year after the implementation of the LUMC. In the context of long term historical conditions, the monitoring period endured relatively cold winters with an above average number of snow lying days and snow depths (especially during the post-change period). Quality control checks of all data from different types of gauges showed acceptable data results within the range of error that is expected.

In the context of detecting LUMC impacts in hydrological records, the pre- and post-change timeseries from the multiscale experiment are relatively short. The analysis of

historical long term data for two sites in the Hodder catchment (Footholme (25 km^2) and Hodder Place (261 km^2)) revealed that there is considerable variation in the natural hydrological conditions and the catchment response at the short-term time scales for which the data from the multiscale network are available. This highlighted the need for a change detection technique that is sensitive to systematic changes in catchment response, but relatively insensitive to natural variability. An evaluation of two preselected potential change detection techniques (DBM and SDD models) showed that it remains infeasible to fully eliminate the effects of natural variability from such short records. However, the SDD model, the parameters of which are derived from recession data (which are generally least sensitive to natural variability) was considered as the most suitable method for change detection. This is based on the assumption that, for a specific change detection method, it is important to have consistency in the description of catchment behaviour between two short term periods during which no change has occurred. As such, the differences in parameter estimates as a result of natural variability are relatively small for the SDD model, especially compared with those of the DBM model. The SDD model was therefore selected for the analysis of the multiscale short term pre- and post-change data.

The pre- versus post-change catchment flood response multiscale analysis showed that, based on statistical tests of significance, there is no evidence to suggest that any short-term changes associated with the SCaMP LUM changes have been detected at any of the gauges. This was attributed to the small proportion of area affected by change, the timescale of impacts, and the natural variability in catchment response. The SDD analysis results suggested that some changes could have been detected at a small scale grip blocking site (CRO_sc5, 0.5 km^2). However, further analysis of detailed field data regarding the changes in storage, as well as the simulation results of an extensive physically based modelling exercise, revealed that no such changes had occurred. As such, the differences in the pre- and post-change catchment behaviour as described by the SDD model at CRO_sc5 were attributed to natural variability.

In order to be able to better understand the short term grip blocking and other potential long term LUMC effects on the within catchment storage and runoff generation processes, a novel modelling tool (Model for Upland Runoff Storage And

Flow Fields (MURSAFF)) was co-developed. The main aim of the MURSAFF model was to be able to capture the complex spatial patterns observable in the field (such as irregular drainage networks, field boundaries and sheep tracks) and represent reality as much as possible. The MURSAFF model is unique in the way it uses a grid with irregularly sized polygon grid cells, the creation of which depends strongly on field observations and interpretations.

Pre- and post-change MURSAFF simulations were performed to further investigate the short term effects of grip blocking and the potential long term effects of stocking density changes at the micro scale (~1 km^2). The effects of tree planting were not further investigated as these are relatively well understood at the micro scale. For two case studies (including CRO_sc5), MURSAFF simulations showed that, while the impacts of grip blocking are quickly realised and significant at the process scale, they are small and almost undetectable at the micro catchment scale. It was concluded that this is partly because the proportion of area directly affected by LUMC is small, which agrees with direct field observations in the two study catchments. The potential long-term effects of changes in stocking density are predicted to involve attenuation of the local scale flood hydrograph. The effects of sheep tracks as preferential flow paths are significant locally while the micro catchment scale impacts will depend on the proportional area affected.

Irrespective of LUMCs, the study revealed that there are some systematic catchment responses that change with scale. For example, the runoff ratios and the flashiness of the catchment response both decrease with scale. Simple scaling relationships for peak flow and lag times have also been established, although they are different for each storm. The multiscale data also revealed considerable variability in catchment response severity and in the peak timings of the different subcatchments, which can be attributed to natural variability in precipitation patterns and antecedent catchment conditions. This complicates the use of simple scaling relationships to explore the propagation of LUMC effects downstream.

A simple semi-distributed Catchment Impact Model (CIM), which is able to capture the complex distribution of responses and the interaction of subcatchments, was therefore

used to predict the propagation of the SCaMP upland LUMC impacts. It was used to investigate the downstream effects of the MURSAFF simulated impacts of the micro scale case studies, and to explore the impacts of empirical changes (a delay and decrease in peak flow) in the mini scale catchments on the catchment response at Hodder Place. The results suggest that the downstream effects of the Hodder SCAMP LUMCs will be relatively small and different for each storm. An upstream change in peak flow can result in a downstream decrease or increase in peak flow, depending on the location of the contribution of the routed upstream hydrograph within the downstream hydrograph. The largest downstream effects were achieved during relatively small summer events. Although the geometry of the river channel network fundamentally controls the catchment response, variations in travel times and runoff contributions from the subcatchments occur due to the spatial variability in rainfall, antecedent conditions and hydrological functioning. On a storm to storm basis, it was concluded that the internal synchronisation of the subcatchment responses and the natural variability therein are dominant factors in determining the catchment outlet response and hence also in determining the downstream LUMC impacts.

8.2 Conclusions

The conclusions related to the research objectives presented in Chapter 1 are stated below.

Objective 1: Characterise the spatial physical properties of the Hodder catchment and identify the main historical and current LUMCs

- Overall, the physical properties are relatively homogeneous throughout the catchment, though there are some clear differences between the properties of the uplands and those of the lower parts of the catchment (e.g. geology: sandstone versus limestone and mudstone, superficial deposits: peat versus till, soils: Winter Hill and Belmont versus Wilcocks and Brickfield, land use and vegetation: bog and dwarf shrubs versus grasslands, respectively)
- The historical changes in the catchment involved the installation of grips, increases in stocking density and afforestation, while the more recent changes

in the headwaters (approximately 40%) of the Hodder catchment included grip blocking, reductions in stocking density, and further tree planting as part of United Utilities' SCaMP programme.

- The properties as well as the historical and current LUMCs in the Hodder catchment are typical for UK uplands.

Objective 2: Design, set up and maintain a dense nested multiscale flow monitoring network that allows for the investigation of the LUMC impacts at increasing scales

- An extensive field campaign that concentrated on the design, set-up and maintenance of a dense multiscale nested monitoring network has been successfully executed. This has provided a unique data set that can be used to study the impacts of LUMCs at increasing scales. The data are available for approximately 0.5-1 year before and 1-1.5 year after the implementation of the SCaMP LUMCs.
- Quality control checks of the multiscale data set showed acceptable data results within the range of error that is expected for the different types of gauges.

Objective 3: Investigate the functioning of the subcatchments and the Hodder catchment as a whole, especially when generating flood hydrographs

- The Hodder catchment has a flashy runoff response with relatively high runoff ratios, typical for upland catchments in North-West England.
- For long term data sites, there is considerable variation in the natural hydrological conditions and the overall catchment response between hydrological years.
- The catchment response of the Hodder subcatchments changes systematically with scale. The runoff ratios and the flashiness of the catchment response both decrease with increasing scale. For a specific storm, the peak flow and lag time both increase with scale. The latter scaling relationships are subjected to natural variability and therefore different for each storm.

- For a specific storm, there is considerable variability in the catchment response severity and the in the peak timings of the different subcatchments. This can be attributed to natural variability in precipitation patterns mainly. However, there is also some dependence on other factors such as precipitation intensity, antecedent conditions, and other variations in catchment characteristics (e.g. soil or geology). The catchment response severity and peak timings are therefore not just a function of catchment scale.

Objective 4: Identify and apply appropriate methods, including statistical tests of significance, for LUMC change detection to the multiscale data records of the Hodder catchment

- When working with short records, there is a need for a change detection method that is sensitive to systematic changes in catchment response, but relatively insensitive to natural variability.
- Based on the results obtained from the application of the DBM and SDD modelling methods to both the longer term EA flow records, and the shorter term data collected during this study, the use of the SDD model is preferred over the DBM model when used as change detection technique on short records. The SDD model requires the estimation of fewer parameters which are derived from properties least sensitive to natural variability (such as the hydrograph recession).
- It remains difficult to fully eliminate the effects of natural variability in change detection on short records.
- The results of pre- and post-change statistical analyses of SDD model results have not provided any statistically significant evidence to suggest that any of the LUMCs had a short-term impact on the catchment flood response (full hydrograph, including peak flows) at scales from 1 km^2 up to the Hodder catchment scale (261 km^2). This is attributed to the proportion of area affected by change, the timescale of impacts, the natural variability in catchment response, and the dispersion in the arrival times for impacts from the various

subcatchments which depend on the travel distances between the subcatchments and the downstream sites.

Objective 5: Develop a new physically based modelling method that allows for the investigation of local LUMC impacts on storage, runoff and flow fields in complex landscapes

- A new physically-based model (Model for Upland Runoff Storage And Flow Fields, MURSAFF) was developed (jointly with Prof. J. Ewen) that allows the geometric complexity of the landscape (various different areas of the landscape such as hillslopes, fields, irregular drainage networks, and sheep tracks) to be represented more accurately than is possible using standard computation grids such as squares, rectangles or triangles.
- The MURSAFF modelling represents the flow fields, storage and flow response in as realistic a fashion as possible, based on local knowledge and field information. This is also reflected in the grid creation, dominant process representation and the model parameterisation.
- The observed and MURSAFF simulated outputs (storage and runoff) agree well for calibration and validation periods during normal, year round wet conditions, although improvements in the dynamics for flow are needed for low flow conditions.
- The MURSAFF model can reproduce credible simulations of change for storage and runoff. For example, the changes in within channel storage from intact to blocked grips agree with local measurements of such storage capacities.

Objective 6: Use the new physically based modelling method to explore the short and potential long term effects of LUMC in the Hodder catchment at the micro scale (~1 km^2)

- Short-term small scale (<1 km^2) field observations and MURSAFF predictions of the impacts of grip blocking involved an increase in the local storage and change in the flow fields. The impact on local storage depends on the depth of the original grip. As the channel is disconnected from the network, the post

blocking runoff is only generated as subsurface and overland flow. However, at two case studies at the micro catchment scale (BRE_sap, 1.7 km^2 and CRO_sc5, 0.45 km^2) the effects are insignificant as the proportion of area directly affected by LUMC is small. These results are in agreement with those of the SDD analysis, where no statistically significant change between the pre- versus post-change catchment response could be detected, as well as with a field data analysis of the potential differences in catchment storage, in that they predict that grip blocking has little effect on the discharge at the micro catchment scale.

- Potential long term (fully established) impacts of reductions in stocking density at a micro scale case study site (LOS_mid, 2.5 km^2), with 100% of the area affected, involve an attenuation of the flood hydrograph (e.g. an average 15% decrease in the flood peaks). This can be attributed mainly to reduced levels of soil compaction, which leads to an increase in infiltration capacities and hence storage.
- The effects of sheep tracks involve local increases in overland flow and total discharges. At the micro catchment scale however, the impacts of sheep tracks on the overall catchment response will depend on the proportional area affected, which is likely to be small.

Objective 7: Investigate the propagation and detectability of LUMC impacts at larger scales within the river network

- For the assessment of downstream LUMC impacts, it is not possible to use simple scaling relationships of peak flow, lag time and catchment response, as a result of a complex interaction of the differences in the relative subcatchments response severities and a lack of synchronisation of relative peak timings. These are different for each storm, because of a strong dependency on rainfall distribution (in space and time) and to a lesser degree also on other factors such as the antecedent wetness conditions.
- The downstream impacts of LUMC depend on the nature of the change and the location within the catchment, which effects are different for each storm. Consistent with the failure to detect any significant impacts in the post-change

records, it appears that the future downstream SCaMP LUMC effects at the catchment outlet (Hodder Place, 261 km^2) will be relatively small and different for each storm. An upstream change in peak flow can result in a downstream decrease or increase in peak flow, depending on the locations and magnitudes of the contributions of the routed upstream hydrographs within the downstream hydrograph. This is fundamentally controlled by the geometry of the river channel network, but variations in travel times and runoff contributions occur due to the spatial variability in rainfall, antecedent conditions and hydrological functioning.

- On a storm to storm basis, the lack of internal synchronisation of the subcatchment's responses and the natural variability therein are dominant factors in determining the Hodder catchment outlet response and hence also in determining the relative downstream impacts of LUMC.

The main research question of this study was:

What are the impacts of the upland SCaMP LUMCs on runoff generation at the local scale and can these impacts be detected at larger scales (up to ~100 km^2) through the use of multiscale nested experiments and appropriate data analyses and modelling methods?

In summary, no statistically significant impacts of the SCaMP LUMCs have been detected on the runoff generation at scales from 1 km^2 up to the Hodder catchment scale (261 km^2), although longer records are needed to investigate the impacts of fully established LUMCs. Overall, the multiscale nested data analyses and modelling exercises have shown that the knowledge of (differences in) the timing and magnitude of the pre- and post-change flood hydrographs at a range of increasing scales has led to a better understanding of the effects of local scale LUMCs on catchment flood response at increasing scales. It is expected that the future downstream SCaMP LUMC effects at the catchment outlet will be relatively small and different for each storm.

In the wider context of the existing knowledge on the effects of local scale land use and management changes and their connection with downstream catchment flood responses, the study has provided the following advances:

- The study has provided a unique high quality data set from a multiscale monitoring experiment designed especially to investigate the impacts of LUMC in a meso scale catchment. In addition, a detailed record of the nature of the LUMCs has been obtained. These data can be a valuable source for further research regarding the impacts of LUMCs and for other studies requiring a dense multiscale nested hydrological data set.
- It was demonstrated that detecting statistically significant LUMC changes on short records remains difficult, because the effects of natural variability cannot be fully eliminated. However, there is most scope in change detection methods (e.g. the SDD model) that are based on characteristics that are least sensitive to natural variability (such as the hydrograph recession).
- The study has provided a new modelling tool (MURSAFF) that can be used to study the effects of distributed LUMC in complex landscapes, and to investigate impacts such as localised soil compaction that heretofore have been difficult to represent in existing distributed models. The model can be used for applications other than those presented in the current study (e.g. the distributed impacts of tree planting or other land use practices such as ploughing and farm machinery trafficking).
- It has been shown that upscaling the impacts of LUMCs in mesoscale catchments such as the Hodder catchment is the product of a complex process, with the impacts depending on the nature of the LUMCs, the affected areas and their locations within the catchment, and the natural variability in the contributions of other subcatchments. Although the downstream impacts are expected to be relatively small, in terms of catchment flood response they can result in a small increase for one storm, but a small decrease for another. As such, multiple distributed LUMCs could also balance each other out, but, in the long-term, the average impact taken across many storms at larger catchment scales would be expected to reflect the geometry of the river channel network, and the dispersion processes taking place within it.

The findings in this study have several broader implications for catchment managers and planners, relating to the effectiveness and reliability of LUMC as a method for flood management in upland UK catchments. Over the short term of the monitoring

period, no impacts of the SCaMP LUMCs were detected at scales between 1 km^2 and 261 km^2. A second important finding, based on multiscale data analysis and model simulations, is that the impacts of the SCaMP LUMCs will likely remain small in the longer term, once their effects on vegetation, soils and hydrology become fully established. Together, these findings suggest that LUMC might generally be an inefficient method for flood management for large scale flooding caused by runoff from upland rural catchments. There is also doubt about whether LUMC is a reliable method for flood management at smaller scales. For example, even if there are significant impacts when LUMCs are made over a large percentage area of a mini-scale catchment (~10 km^2), the magnitude of these impacts might vary significantly from storm to storm because of natural variability in the hydrological response of the catchment. Another reason why LUMC can be inefficient for flood management is that there can be a lack of synchronisation in the timing of the impacts for sub-catchments. This means that when several sub-catchments undergo major change the resulting impact at larger scales downstream will be different between storms and does not necessarily increase efficiently with scale. Of course, there are other benefits from LUMCs which must be considered alongside any potential benefits for flood management. For example, grip blocking can have beneficial impacts in terms of carbon storage, sediment control, water quality and habitat creation.

8.3 Recommendations for Future Work

There are several ways in which the work presented in this study can be taken forward:

- Continued long-term monitoring of LUMC impacts at the various spatial scales would be recommended for several reasons. Firstly, this would allow for further investigation into the long term (fully established) impacts of the SCaMP LUMCs in the Hodder catchment. Secondly, the effects of natural variability become smaller with increasing record lengths. The effects could be more easily reduced in future work, for example by averaging responses across a larger number of storms.
- Associated with continued monitoring, further work could focus on the level of data detail that is needed to study future (fully established) downstream impacts of LUMCs in meso scale catchments. Owing to budgetary, management and

practical reasons, there are often limitations in the number of monitoring sites that can be maintained. Of particular interest therefore, is the worth of the different components in the multiscale monitoring network. A study into the minimum level of monitoring should aim to provide guidelines for the identification of key monitoring locations in the Hodder catchment network. In addition, this could lead to setting up guidelines for experimental design structures concerned with LUMC impacts in other meso scale catchments.

- Regarding the MURSAFF modelling, one area for further development would be to explore the possibilities for automation of the irregular MURSAFF grid creation process. During the initial phase as presented in this study, it was required to manually draw the grid cells to investigate ways in which field observations can be represented. The steps for automation of the grid creation process could be informed by those taken here.
- Work should also focus on reconciling the MURSAFF simulations with local field measurements. For example, in the study of stocking density changes and sheep tracks, local field measurements of soil compaction levels would better inform the MURSAFF parameterisation.
- The results of the MURSAFF and CIM modelling work would be more useful if a full uncertainty analysis could be done, which would demonstrate the levels of uncertainty in the simulations and hence in the predictions of change.
- One type of SCaMP LUMCs that has not been explicitly investigated in this study is tree planting. It has been suggested that the relative impacts of tree planting vary with time (e.g. Robinson et al., 1998) and hence it would be interesting to explore the development of the downstream impacts on flood response over time.
- Although the opportunities for monitoring controlled LUMCs over large areas in meso scale catchments are rare, the testing of current findings in other catchments would be highly recommended. This would provide more information on the transferability of the conclusions drawn here. Of particular interest would be to study the impacts of LUMCs in lowland meso scale catchments. Modelling studies have been done for the lowland Parrott and Tone catchments (e.g. Park et al., 2009; Park et al., 2010), though other multiscale data studies are needed.

References

Ahti, E. (1980) 'Ditch spacing experiments in estimating the effects of peatland drainage on summer runoff', *International Association of Hydrological Sciences Publication,* 130, pp. 49-53.

Aitkenhead, N., McBridge, D., J., R. N. and Kimbell, S. F. (1992) *Geology of the country around Garstang - memoir for 1:50 000 geological sheet 67 (England and Wales)*, London: HMSO. (British Geological Survey).

Aitkenhead, N. and Wray, D. A. (2002) *The Pennines and adjacent areas.*4th Edition ed: British Geological Survey, Natural Environment Research Council.

Alila, Y., Kuras, P. K., Schnorbus, M. and Hudson, R. (2009) 'Forests and floods: A new paradigm sheds light on age-old controversies', *Water Resources Research,* 45, pp. W08416.

Allen, R. G., Pereira, L. S., Raes, D. and Smith, M. (1998) 'FAO Penman-Monteith equation ', in FAO(ed), *Crop evapotranspiration - Guidelines for computing crop water requirements - FAO Irrigation and drainage paper 56.* Rome: FAO.

Almendinger, J. C., Almendinger, J. E. and Glaser, P. H. (1986) 'Topographic fluctuations across a spring fen and a raised bog in the Lost River Peatland, Northern Minnesota', *Journal of Ecology,* 74, pp. 393-401.

Anderson, P. and Yalden, D. W. (1981) 'Increased sheep numbers and the loss of heather moorland in the Peak District, England', *Biological Conservation,* 20, pp. 195-213.

APEM. (1998) *The impact of grazing and upland management on erosion and runoff, Environment Agency research and development technical report 123.* Bristol: Environment Agency

Archer, D. (2003) 'Scale effects on the hydrological impact of upland afforestation and drainage using indices of flow variability: the River Irthing, England', *Hydrology and Earth System Sciences,* 7, (3), pp. 325-338.

Archer, D. R. (2004) 'New hydrological insights from the analysis of flow variability on the impact of land use change and river regulation', *British Hydrological Society Conference on Hydrology: Science and Practice for the 21st century.*

Archer, D. R. (2007) 'The use of flow variability analysis to assess the impact of land use change on the paired Plynlimon catchments, mid-Wales', *Journal of Hydrology,* 347, pp. 487-496.

Archer, D. R., Climent-Soler, D. and Holman, I. P. (2010) 'Changes in discharge rise and fall rates applied to impact the assessment of catchment land use', *Hydrology Research,* 41, pp. 13-26.

Archer, D. R. and Newson, M. D. (2002) 'The use of indices of flow variability in assessing the hydrological and instream habitat impacts of upland afforestation and drainage', *Journal of Hydrology,* 268, pp. 244-258.

Armstrong, A., Worrall, F. and Holden, J. (2006) 'The effectiveness of grip blocking in the Whitendale catchment, Forest of Bowland, UK', *Geophysical Research Abstracts,* 8, pp. 06336.

Atkins. (2007) *R&D Update review of the impact of land use and management on flooding.* Bristol: Environment Agency

Avery, B. W. (1980) *Soil Classification for England and Wales (Higher Categories).* Harpenden: Soil Survey Technical Monograph

Baden, W. and Eggelsmann, R. (1968) *Proceedings of the 3rd international peat congress.* Quebec, Canada:International Peat Society.

Baldock, D. (1984) *Wetland drainage in Europe.* Notthingham: International Institute for Environment Development.

Ballard, C. E., McIntyre, N. and Wheater, H. (2010) 'Peatland drain blocking: Can it reduce peak flood flows?*', BHS Third International Symposium, Managing Consequences of a Changing Global Environment.* Newcastle University, Newcastle upon Tyne, pp. 6.

Ballard, C. E., McIntyre, N., Wheater, H. S., Holden, J. and Wallage, Z. E. (2011) 'Hydrological modelling of drained blanket peatland', *Journal of Hydrology,* In Press.

Basher, L. R. and Lynn, I. H. (1996) 'Soil changes associated with cessation of sheep grazing in the Canterbury high country, New Zealand', *New Zealand Journal of Ecology,* 20, pp. 179-189.

Bates, C. G. and Henry, A. J. (1928) 'Forest and streamflow experiment at Wagon Wheel Gap, Colorado', *Monthly Weather Review Supplement,* 30, pp. 1-79.

Bathurst, J. C. (1988) *Hydrology of mountainous areas.* Strbske Pleso, Czechoslovakia:IAHS.

Bathurst, J. C., Amezaga, J., Cisneros, F., Gavino Novillo, M., Iroume, A., Lenzi, M. A., Mintegui Aguirre, J., Miranda, M. and Urciuolo, A. (2010) 'Forests and floods in Latin America: science, management policty and the EPIC FORCE project', *Water International,* 35, pp. 114-131.

Bathurst, J. C., Birkinshaw, S. J., Cisneros, F., Fallas, J., Iroumé, A., Iturraspe, R., Novillo, M. G., Urciuolo, A., Alvarado, A., Coello, C., Huber, A., Miranda, M., Ramirez, M. and Sarandón, R. (2011a) 'Forest impact on floods due to extreme rainfall and snowmelt in four Latin American environments 2: Model analysis ', *Journal of Hydrology,* 400, pp. 292-304.

Bathurst, J. C., Iroumé, A., Cisneros, F., Fallas, J., Iturraspe, R., Novillo, M. G., Urciuolo, A., de Bièvre, B., Borges, V. G., Coello, C., Cisneros, P., Gayoso, J., Miranda, M. and Ramírez, M. (2011b) 'Forest impact on floods due to extreme rainfall and snowmelt in four Latin American environments 1: Field data analysis', *Journal of Hydrology,* 400, pp. 281-291.

Bay, R. R. (1969) 'Runoff from small peatland watersheds', *Journal of Hydrology,* 9, pp. 90-102.

Beckwith, C. W., Baird, A. J. and Heathwaite, A. L. (2003) 'Anisotropy and depth-related heterogeneity of hydraulic conductivity in a bog peat. I: laboratory measurements', *Hydrological Processes,* 17, pp. 89-101.

Beheim, E. (2006) 'The effects of peat land drainage and afforestation on runoff dynamics: consequences on floods in the Glomma river', in Krecek, J. and Haigh, M.(eds) *Environmental role of wetlands in headwaters.* Dordrecht: Springer, pp. 59-75.

Beschta, R. L. (1990) 'Peakflow estimation using an antecedent precipitation index (API) model in tropical environments', *Research needs and applications to reduce erosion and sedimentation in tropical steeplands.* Suva, Fiji:IAHS Publication

Beven, K. (1979) 'On the generalized kinematic routing method', *Water Resources Research,* 15, pp. 1238-1242.

Beven, K. (1989) 'Changing ideas in hydrology - The case of physically based models', *Journal of Hydrology,* 105, pp. 157-172.

Beven, K. (1993) 'Prophecy, reality and uncertainty in distributed hydrological modelling', *Advances in Water Resources,* 16, pp. 41-51.

Beven, K. (2001a) 'How far can we go in distributed hydrological modelling', *Hydrology and Earth System Sciences,* 5, pp. 1-12.

Beven, K. and Binley, A. (1992) 'The future of distributed models: Model calibration and uncertainty prediction', *Hydrological Processes,* 6, pp. 279-298.

Beven, K. and Germann, P. F. (1982) 'Macropores and water flow in soils', *Water Resources Research,* 18, pp. 1311-1325.

Beven, K., Gilman, K. and Newson, M. D. (1979) 'Flow and flow routing in upland channel networks', *Hydrological Sciences - Journal - des Sciences Hydrologiques,* 24 pp. 303-325.

Beven, K., Romanowicz, R., Young, P., Holman, I., Posthumus, H., Morris, J., Rose, S., O'Connell, E. and Ewen, J. (2008a) 'An event classification approach to the identification of hydrological change*', EGU General Assembly.* Vienna

Beven, K. and Wood, E. F. (1993) 'Flow routing and the hydrological response of channel networks', in Beven, K. and Kirkby, M. J.(eds) *Channel network hydrology* Chichester, UK: Wiley & Sons Ltd., pp. 99-128.

Beven, K., Young, P., Romanowicz, R., O'Connell, P. E., Ewen, J., O'Donnell, G. M., Holman, I., Posthumus, H., Morris, J., Hollis, J., Rose, S., Lamb, R. and Archer, D. (2008b) *Analysis of historical data sets to look for impacts of land use and management change on flood generation - Final Report.* Department for Environment, Food and Rural Affairs

Beven, K. J. (1996) 'A discussion of distributed modelling', in Refsgaard, J. C. and Abbot, M. B.(eds) *Distributed hydrological modelling.* Dordrecth: Kluwer, pp. 255-279.

Beven, K. J. (2000) 'Uniqueness of place and process representations in hydrological modelling', *Hydrology and Earth System Sciences,* 4, pp. 203-213.

Beven, K. J. (2001b) *Rainfall - runoff modelling.* Chichester, West Sussex, UK: John Wiley & Sons.

Beven, K. J. (2006) 'A manifesto for the equifinality thesis', *Journal of Hydrology,* 320, pp. 18-36.

Beven, K. J. and Kirkby, M. J. (1979) 'A physically-based, variable contributing area model of basin hydrology', *Hydrological Sciences Bulletin,* 24, pp. 43-69.

Beven, K. J., Wood, E. F. and Sivapalan, M. (1988) 'On hydrological heterogeneity - catchment morphology and catchment response', *Journal of Hydrology,* 100, pp. 353-375.

Birnie, R. V. and Hulme, P. D. (1990) 'Overgrazing of peatland vegetation in Shetland', *Scottish Geographical Magazine,* 106, pp. 28-36.

Black, A. R. and Law, F. M. (2004) 'Development and utilization of a national web-based chronology of hydrological events', *Hydrological Sciences - Journal - des Sciences Hydrologiques,* 49, pp. 237-246.

Blackie, J. R. (1993) 'The water balance of the Balquhidder catchments ', *Journal of Hydrology,* 145, pp. 238-257.

Bloschl, G. (2001) 'Scaling in hydrology', *Hydrological Processes,* 15, pp. 709-711.

Bloschl, G., Ardoin-Bardin, S., Bonell, M., Dorninger, M., Goodrich, D., Gutknecht, D., Matamoros, D., Merz, B., Shand, P. and Szolgay, J. (2007) 'At what scales do climate variability and land cover change impact on flooding and low flows?', *Hydrological Processes,* 21, pp. 1241-1247.

Bloschl, G. and Sivapalan, M. (1995) 'Scale issues in hydrological modelling: a review', *Hydrological Processes,* 9, pp. 251-290.

Boelter, D. H. (1965) 'Hydraulic conductivity of peats', *Journal of Soil Science,* 100, pp. 227-231.

Boelter, D. H. (1968) *Third International Peat Congress.* Quebec, Canada:Department of Engery, Minds and Resources and National Research Council of Canada.

Boelter, D. H. (1969) 'Physical properties of peats as related to degree of decomposition', *Soil Science Society of America Proceedings,* 33, pp. 606-609.

Boelter, D. H. (1972) 'Water table drawdown around an open ditch in organic soils', *Journal of Hydrology,* 15, pp. 329-340.

Bonell, M. (1998) 'Selected challenges in runoff generation research in forests from the hillslope to headwater drainage basin scale', *Journal of the American water resources association,* 34, pp. 765-785.

Bormann, H., Breuer, L., Giertz, S., Huisman, J. A. and Viney, N. R. (2009) *Uncertainties in evironmental modelling and consequences for policy making.* Dordrecht:Springer.

Bosch, J. M. and Hewlett, J. D. (1982) 'A review of catchment experiments to determine the effect of vegetation changes on water yield and evapotranspiration', *Journal of Hydrology,* 55, pp. 3-23.

Bragg, O. M. (2002) 'Hydrology of peat-forming wetlands in Scotland', *The Science of the Total Environment,* 294, pp. 111-129.

Bragg, O. M. and Tallis, J. H. (2001) 'The sensitivity of peat-covered upland landscapes', *Catena,* 42, pp. 345-360.

Branson, F. A., Gifford, G. F., Renard, K. G. and Hadley, R. F. (1981) *Rangeland Hydrology.* Dubuque: Kendal Hunt.

Breuer, L., Huisman, J. A., Willems, P., Bormann, H., Bronstert, A., Croke, B. F. W., Frede, H.-G., Graff, T., Hubrechts, L., Jakeman, A. J., Kite, G., Lanini, J., Leavesley, G., Lettenmaier, D. P., Lindstrom, G., Seibert, J., Sivapalan, M. and Viney, N. R. (2009) 'Assessing the impact of land use change on hydrology by ensemble modeling (LUCHEM). I: Model intercomparison with current land use', *Advances in Water Resources,* 32, pp. 129-146.

Bronstert, A., Niehoff, D. and Burger, G. (2002) 'Effects of climate and land-use change on storm runoff generation: present knowledge and modelling capabilities', *Hydrological Processes,* 16, pp. 509-529.

Brown, A. E., Zhang, L., McMahon, T. A., Western, A. W. and Vertessy, R. A. (2005) 'A review of paired catchment studies for determining changes in water yield resulting from alterations in vegetation', *Journal of Hydrology,* 310, pp. 28-61.

Bruijnzeel, L. A. (1990) *Hydrology of moist tropical forests and effects of conversion: a state of knowledge review.* Amsterdam: Vrije Universiteit Amsterdam.

Bulygina, N., McIntyre, N. and Wheater, H. (2011) 'Bayesian conditioning of a rainfall-runoff model for predicting flows in ungauged catchments and under land use changes', *Water Resources Research,* 47, pp. W02503.

Burke, W. (1975) 'Effect of drainage on the hydrology of blanket-bog', *Irish Journal of Agricultural Research,* 14, pp. 145-162.

Burt, T. P., Heathwaite, A. L. and Labadz, J. G. (1990) 'Runoff production in peat covered catchments', in Anderson, M. G. and Burt, T. P.(eds) *Process studies in hillslope hydrology.* Chichester: Wiley, pp. 463-500.

Buttle, J. (2006) 'Mapping first-order controls on streamflow from drainage basins: the T3 template.', *Hydrological Processes,* 20, (3415-3422).

Buytaert, W., Celleri, R., Willems, P., De Bievre, B. and Wyseure, G. (2006) 'Spatial and temporal rainfall variability in mountainous areas: a case study from the south Ecuadorian Andes', *Journal of Hydrology,* 329, pp. 413-421.

Calder, I. R. (1990) *Evaporation in the Uplands.* Chichester, UK: John Wiley & Sons Ltd.

Camporese, M., Ferraris, S., Putti, M., Salandin, P. and Teatini, P. (2006) 'Hydrological modeling in swelling/shrinking peat soils', *Water Resources Research,* 42, pp. W06420.

Carroll, Z. L., Bird, S. B., Emmett, B. A., Reynolds, B. and Sinclair, F. L. (2004) 'Can tree shelterbelts on agricultural land reduce flood risk?', *Soil Use and Management,* 20, pp. 357–359.

Castle, D. A., McCunnall, J. and Tring, I. M. (1984) *Field drainage: principles and practices.* London: Batsford Academic and Educational.

Cerdan, O., Le Bissonnais, Y., Govers, G., Lecomte, V., van Oost, K., Couturier, A., King, C. and Dubreuil, N. (2004) 'Scale effect on runoff from experimental plots to catchments in agricultural areas in Normandy', *Journal of Hydrology,* 299, pp. 4-14.

Chang, M. and Flannery, L. A. (2001) 'Spherical gauges for improving the accuracy of rainfall measurements', *Hydrological Processes,* 15, pp. 643-654.

Chatfield, C. and Collins, A. J. (2000) *Introduction to multivariate analysis.* Boca Raton, Florida: Chapman and Hall/CRC Press.

Chesterton, C. (2009) *Environmental impacts of land management.* Sheffield: Natural England

Chiverrell, R. C., Foster, G. C., Marshall, P., Harvey, A. M. and Thomas, G. S. P. (2009) 'Coupling relationships: Hillslope-fluvial linkages in the Hodder catchment, NW England', *Geomorphology,* 109, pp. 222-235.

Chow, T. L., Rees, H. W., Ghanem, I. and Cormier, R. (1992) 'Compactibility of cultivated Sphagnum peat material and its influence on hydrologic characteristics', *Soil Science Society of America Proceedings,* 153, pp. 300-306.

Chow, V. T. (1959) *Open-Channel Hydraulics.* New York: McGraw-Hill.

Chow, V. T. (1988) *Open-channel hydraulics.* McGraw-Hill

Christensen, J. H. and Christensen, O. B. (2002) 'Severe summertime flooding in Europe', *Nature,* 421, pp. 805–806.

Church, M. (2008) 'Multiple scales in rivers', in Habersack, H., Piegay, H. and Rinaldi, M.(eds) *Gravel-Bed Rivers VI: From Process Understanding to River Restoration.* Amsterdam: Elsevier.

Clark, M. P., Rupp, D. E., Woods, R. A., Tromp - van Meerveld, H. J., Peters, N. E. and Freer, J. E. (2009) 'Consistency between hydrological models and field observations: linking processes at the hillslope scale to hydrological responses at the watershed scale', *Hydrological Processes,* 23, pp. 311-319.

Clarke, R. T. (2010) 'On the (mis)use of statistical methods in hydro-climatological research', *Hydrological Sciences - Journal - des Sciences Hydrologiques,* 55, pp. 139-144.

Clay, G. D., Worrall, F., Clark, E. and Fraser, E. D. G. (2009) 'Hydrological responses to managed burning and grazing in an upland blanket bog', *Journal of Hydrology,* 376, pp. 486-495.

Climent-Soler, D., Holman, I. and Archer, D. R. (2009) 'Application of flow variability analysis to identify impacts of agricultural land use change on the River Axe, southwest England', *Hydrology Research,* 40, pp. 380-393.

Clymo, R. S. (1997) 'The roles of *Sphagnums* in peatlands', in Parkyn, L., Stoneman, R. E. and Ingram, H. A. P.(eds) *Conserving Peatlands.* Oxon CAB International, pp. 95-102.

Clymo, R. S. (2004) 'Hydraulic conductivity of peat at Ellergower Moss, Scotland', *Hydrological Processes,* 18, pp. 261-274.

Colledge, M. (2008) Forestry commission activities in the upper Hodder catchment, 23/10/2008.

Conway, M. (2008) UU's Bowland and Dunsop Intake systems, 01/07/2008.

Conway, V. M. and Millar, A. (1960) 'The hydrology of some small peat-covered catchments in the northern Pennines', *Journal of the Institute of Water Engineers,* 14, pp. 415-424.

Costa, M. H., Botta, A. and Cardille, J. A. (2003) 'Effects of large-scale changes in land cover on the discharge of the Tocantins River, Southeastern Amazonia', *Journal of Hydrology,* 283, pp. 206-217.

Coulson, J. C., Butterfield, J. E. L. and Henderson, E. (1990) 'The effect of open drainage ditches on the plant and invertebrate communities of moorland and on the decomposition of peat', *Journal of Applied Ecology,* 27, pp. 549-561.

Critchley, C. N. R., Adamson, H. F., McLean, B. M. L. and Davies, O. D. (2008) 'Vegetation dynamics and livestock performance in system-scale studies of sheep and cattle grazing on degraded upland wet heath', *Agriculture, Ecosystems and Environment,* 128, pp. 59-67.

Croke, B. F. W., Merritt, W. S. and Jakeman, A. J. (2004) 'A dynamic model for predicting hydrologic response to land cover changes in gauged and ungauged catchments', *Journal of hydrology,* 291, pp. 115-131.

Crompton, E. (1966) *The soils of the Preston district of Lancashire (sheet 75).* Harpenden: Soil survey of England and Wales.

Daniels, S. M., Agnew, C. T., Allott, T. E. H. and Evans, M. G. (2008) 'Water table variability and runoff generation in an eroded peatland, South Pennines, UK', *Journal of Hydrology,* 361, pp. 214-226.

Davies, D. B., Finney, J. B. and Richardson, S. J. (1973) 'Relative effects of weight and wheel slip in causing soil compaction', *Journal of Soil Science,* 24, pp. 339-409.

Deeks, L. K., Bengough, A. G., Low, D., Billett, M. F., Zhang, X., Crawford, J. W., Chessell, J. M. and Young, I. M. (2004) 'Spatial variation of effective porosity and its implications for discharge in an upland headwater catchment in Scotland', *Journal of Hydrology,* 290, pp. 217-228.

DEFRA. (2005a) *Higher Level Stewardship Handbook.* Department for Environment Food and Rural Affairs

DEFRA. (2005b) *Making space for water, taking forward a new government strategy for flood and coastal erosion risk management in England.* London: DEFRA

DEFRA. (2008) *BD2304, Appendix to SID5: Scoping study to assess soil compaction affecting upland and lowland grassland in England and Wales.*

Di Baldassarre, G. and Montanari, A. (2009) 'Uncertainty in river discharge observations: a quantitative analysis', *Hydrology and Earth System Sciences,* 13, pp. 913-921.

Dierssen, K. (1992) 'Peatland vegetation and the impact of man', in Bragg, O. M., Hulme, P.D., Ingram, H.A.P. and Robertson, R.A(ed), *Peatland Ecosystems and Man: An Impact Assessment. Proceedings of the BES/IPS symposium held in Dundee, September 1989.* Department of Biological Sciences, University of Dundee, pp. 213-225.

Domenico, P. A. and Schwartz, F. (1998) *Physical and chemical hydrogeology.*Second ed New York: John Wiley and Sons, Inc.

Dooge, J. C. I. (1967) 'A new approach to nonlinear problems in surface water hydrology: hydrologic systems with uniform nonlinearity', *International Association of Scientific Hydrology Publication,* 76, pp. 409–413.

Dooge, J. C. I. (1986) 'Looking for hydrologic laws', *Water Resources Research,* 22, pp. 46S-58S.

Doyle, G. (1997) 'Blanket bogs: an interpretation based on Irish blanket bogs', in Parkyn, L., Stoneman, R. E. and Ingram, H. A. P.(eds) *Conserving Peatlands.* Oxon: CAB International pp. 25-34.

Drewry, J. J. (2006) 'Natural recovery of soil physical properties from treading damage of pastoral soils in New Zealand and Australia: A review', *Agriculture, Ecosystems and Environment,* 114, pp. 159-169.

Duan, Q., Schaake, J., Andreassian, V., Franks, S., Goteti, G., Gupta, H. V., Gusev, Y. M., Habets, F., Hall, A., Hay, L., Hogue, T., Huang, M., Leavesley, G., Liang, X., Nasonova, O. N., Noilhan, J., Oudin, L., Sorooshian, S., Wagener, T. and Wood, E. F. (2006) 'Model parameter estimation experiment (MOPEX): an overview of science strategy and major results from the second and third workshops', *Journal of Hydrology,* 320, pp. 3-17.

Dunn, S. M., Freer, J., Weiler, M., Kirkby, M. J., Seibert, J., Quinn, P., Lischeid, G., Tetzlaff, D. and Soulsby, C. (2008) 'Conceptualization in catchment modelling: simply learning?', *Hydrological Processes,* 22, pp. 2389-2393.

Dunn, S. M. and Mackay, R. (1996) 'Modelling the hydrological impacts of open ditch drainage', *Journal of Hydrology,* 179, pp. 37-66.

Dunne, T. (1983) 'Relation of field studies and modeling in the prediction of strom runoff', *Journal of Hydrology,* 65, pp. 25-48.

Efron, B. and Tibshirani, R. (1993) *An introduction to the bootstrap.* Boca Raton, Florida: Chapman & Hall/CRC.

Eggelsmann, R. (1988) *8th International Peat Congress.* Leningrad: International Peat Society.

Ekström, M., Fowler, H. J., Kilsby, C. G. P. D. and Jones, P. D. (2005) 'New estimates of future changes in extreme rainfall across the UK using regional climate model integrations. 2. Future estimates and use in impact studies', *Journal of Hydrology,* 300, pp. 234-251.

Environment Agency. (2009) *Ribble Catchment Flood Management Plan.* Warrington: Environment Agency

Evans, M., Allott, T., Holden, J., Flitcroft, C. and Bonn, A. (2005) *Understanding gully blocking in deep peat.* Castleton: Moors for the Future

Evans, M. G., Burt, T. P., Holden, J. and Adamson, J. K. (1999) 'Runoff generation and water table fluctuations in blanket peat: evidence from UK data spanning the dry summer of 1995', *Journal of Hydrology,* 221, pp. 141-160.

Evans, R. (1998) 'The erosional impacts of grazing animals', *Progress in Physical Geography,* 22, pp. 251-268.

Evrard, O., Bielders, C. L., Vandaele, K. and van Wesemael, B. (2007) 'Spatial and temporal variation of muddy floods in central Belgium, off-site impacts and potential control measures', *Catena,* 70, pp. 443-454.

Ewen, J. (2011) 'Hydrograph matching method for measuring model performance', *Journal of Hydrology,* 408, pp. 178-187.

Ewen, J. and Birkinshaw, S. J. (2007) 'Lumped hysteretic model for subsurface stormflow developed using downward approach', *Hydrological Processes,* 21, pp. 1496-1505.

Ewen, J., Geris, J., O'Donnell, G., Mayes, W. and O'Connell, E. (2010) *Multiscale Experimentation, Monitoring and Analysis of Long-term Land Use Changes and Flood Risk - EA project SC060092: Final Science Report.* Newcastle upon Tyne: Newcastle University

Ewen, J., Mayes, W. M., Quinn, P. F. and O'Connell, P. E. (2006a) *Evaluation of the potential for flood risk monitoring and assessment under the United Utilities SCaMP catchment management project. Final Report, EIT36-05-017.* English Nature

Ewen, J., O'Donnell, G., Burton, A. and O'Connell, E. (2006b) 'Errors and uncertainty in physically-based rainfall-runoff modelling of catchment change effects', *Journal of Hydrology,* 330, pp. 641-650.

Ewen, J., O'Donnell, G. and O'Connell, E. (2012) 'Role of river network in propagating effects of changes in rural land use/management to flood sites downstream', *Water Resources Research,* (In Internal Review).

Ewen, J. and Parkin, G. (1996) 'Validation of catchment models for predicting land-use and climate change impacts, 2. Case study for a Mediterranean catchment', *Journal of Hydrology* 175, pp. 595-613.

Ewen, J., Parkin, G. and O'Connell, P. E. (2000) 'SHETRAN: Distributed river basin flow and transport modeling system', *Journal of Hydrologic Engineering,* 5, (3), pp. 250-257.

Fisher, K. and Dawson, H. (2003) *Reducing uncertainty in river flood conveyance: Roughness review.* London, UK: DEFRA

Fohrer, N., Haverkamp, S., Eckhardt, K. and Frede, H. (2001) 'Hydrologic response to land use changes on the catchment scale', *Physics and Chemistry of the Earth (B): Hydrology, oceans, and atmosphere,* 26, pp. 577-582.

Forestry Commission. (1991) *Forests and water guidelines.* London: HMSO.

FRMRC2. (2011) *Flood Risk Management Research Consortium, Super Work Package 5: Land Use Management, Annual Report.*

FRMRC (2008) *The Flood Risk Management Research Consortium (FRMRC)* Available at: http://www.floodrisk.org.uk/ (Accessed: 01/10/2011).

Fuller, R. J. and Gough, S. J. (1999) 'Changes in sheep numbers in Britain: implications for bird populations', *Biological Conservation,* 91, pp. 73-89.

Furey, P. R. and Gupta, V. K. (2005) 'Effects of excess rainfall on the temporal variability of observed peak discharge power laws', *Advances in Water Resources,* 28, pp. 1240-1253.

Geomatics Group (2011) *Integrated spatial data*. Available at: http://www.geomatics-group.co.uk/geocms/homepage.aspx (Accessed: 01-10-2011).

Geris, J. R. M. C., Ewen, J., O'Donnell, G. M. and O'Connell, P. E. (2010) 'Monitoring and modelling the pre- and post-blocking hydrological response of moorland drains', *Role of Hydrology in Managing Consequences of a Changing Global Environment, Proc. 3rd BHS International Hydrology Symposium.* Newcastle upon Tyne, UK:Newcastle University.

Germann, P. F. (1990) 'Macropores and hydrologic hillslope processes', in Anderson, M. G. and Burt, T. P.(eds) *Process studies in hillslope hydrology.* Chichester: Wiley, pp. 327-363.

Gilman, K. (2002) *Modelling the effect of land use change in the upper Severn catchment on flood levels downstream.* Peterborough: English Nature

Gilman, K. and Newson, M. D. (1980) *Soil pipes and pipeflow: A hydrological study in upland Wales.* Cambridge, UK: Geobooks.

Goovaerts, P. (2000) 'Geostatistical approaches for incorporating elevation into the spatial interpolation of rainfall', *Journal of Hydrology,* 228, pp. 113-129.

Gorham, E. and Rochefort, L. (2003) 'Peatland restoration: a brief assessment with special reference to *Sphagnum* bogs', *Wetlands Ecology and Management,* 11, pp. 109-119.

Grant, S. A., Bolton, G. R. and Torvell, L. (1985) 'The responses of blanket bog vegetation to controlled grazing by hill sheep', *Journal of Applied Ecology,* 22, pp. 739-751.

Grayson, R., Holden, J. and Rose, R. (2010) 'Long-term change in storm hydrographs in response to peatland vegetation change', *Journal of Hydrology,* 389, pp. 336-343.

Grayson, R. B., Moore, I. D. and McMahon, T. A. (1992) 'Physically based hydrologic modeling: 2. Is the concept realistic?', *Water Resources Research,* 26, pp. 2659-2666.

Greenwood, K. L. and McKenzie, B. M. (2001) 'Grazing effects on soil physical properties and the consequences for pastures: a review', *Australian Journal of Experimental Agriculture,* 41, pp. 1231-1250.

Guertin, D. P., Barten, P. K. and Brooks, K. N. (1987) 'The peatland hydrologic impact model: development and testing', *Nordic Hydrology,* 18, pp. 79-100.

Guo, J. C. Y., Urbonas, B. and Stewart, K. (2001) 'Rain catch under wind and vegetal cover effects', *Journal of Hydrologic Engineering,* 6, pp. 29-33.

Gupta, V. K., Mantilla, R., Troutman, B. M., Dawdy, D. and Krajewski, W. F. (2010) 'Generalizing a nonlinear geophysical flood theory to medium-sized river networks', *Geophysical research Letters,* 37, pp. L11402.

Gupta, V. K., Ridriguez-Iturbe, I. and Wood, E. F. (1986) *Scale problems in hydrology.* Dordrecht: D. Reidel.

Gupta, V. K., Troutman, B. M. and Dawdy, D. R. (2007) 'Towards a nonlinear geophysical theory of floods in river networks: An overview of 20 years of progress', in A.A., T. and Elsner, J. B.(eds) *Nonlinear Dynamics in Geosciences.* New York: Springer, pp. 121–151.

Gustard, A. and Wesselink, A. J. (1993) 'Impact of land-use change on water resources: Balquhidder catchments', *Journal of Hydrology,* 145, pp. 389-401.

Halcrow. (2008) *The role of land use and land management in delivering flood risk management, Final Report.* Leeds:

Hamilton, A. S., Hutchinson, D. G. and Moore, R. D. (2000) 'Estimatig winter streamflow using conceptual streamflow model', *Journal of Cold Regions Engineering,* 14, pp. 158-175.

Heal, K. V., Stidson, R. T., Dickey, C. A., Cape, J. N. and Heal, M. R. (2004) 'New data for water losses from mature Sitka spruce plantations in temperate upland catchments', *Hydrological Sciences - Journal - des Sciences Hydrologiques,* 49, pp. 477-493.

Heathwaite, A. L., Burt, T. P. and Trudgill, S. T. (1989) *Regional Characterization of Water Quality.* Baltimore:IAHS Publication.

Heathwaite, A. L., Burt, T. P. and Trudgill, S. T. (1990) 'Land-use controls on sediment production in a lowland catchment, south-west England', in Boardsman, J., Foster, I. D. L. and Dearing, J. A.(eds) *Soil erosion on agricultural land.* Chichester, UK: John Wiley and Sons Ltd. .

Hemond, H. F. and Goldman, J. C. (1985) 'On non-Darcinian water flow in peat', *Journal of Ecology,* 73, pp. 579-584.

Henderson, F. M. (1966) *Open channel flow.* London: Collier Macmillan.

Herschy, R. W. (1995) *Streamflow Measurement, Second Edition.* New York: E and FN Spon, London.

Hess, T. M., Holman, I. P., Rose, S. C., Rosolova, Z. and Parrott, A. (2010) 'Estimating the impact of rural land management changes on catchment runoff generation in England and Wales', *Hydrological Processes,* 24, pp. 1357-1368.

Hewlett, J. D. and Pienhaar, L. (1973) *Symposium on use of small watersheds in determining effects of forest land use on water quality.* Kentucky:Lexington.

Hiscock, K. M., Lister, D. H., Boar, R. R. and Green, F. M. L. (2001) 'An integrated assessment of long-term changes in the hydrology of three lowland rivers in eastern England', *Journal of Environmental Management,* 61, pp. 195-214.

Hoag, R. S. and Price, J. S. (1997) 'The effects of matrix diffusion on solute transport and retardation in undistrubed peat in laboratory columns', *Journal of Contaminant Hydrology,* 28, pp. 193-205.

Holden, J. (2004) 'Hydrological connectivity of soil pipes determined by ground-penetrating radar tracer detection', *Earth Surface Processes and Landforms,* 29, pp. 437-442.

Holden, J. (2005a) 'Controls of soil pipe frequency in upland blanket peat', *Journal of Geophysical Research: Earth Surface,* 110, pp. F01002(1-11).

Holden, J. (2005b) 'Peatland hydrology and carbon release: why small-scale process matters', *Philosophical Transactions of the Royal Society,* 363, pp. 2891-2913.

Holden, J. (2005c) 'Piping and woody plants in peatlands: Cause or effect?', *Water Resources Research,* 41, pp. W06009(1-10).

Holden, J. (2006) 'Sediment and particulate carbon removal by pipe erosion increase over time in blanket peatlands as a consequence of land drainage', *Journal of Geophysical Research,* 111, pp. F02010.

Holden, J. (2009) 'Flow through macropores of different size classes in blanket peat', *Journal of Hydrology,* 364, pp. 342-348.

Holden, J. and Burt, T. P. (2002a) 'Infiltration, runoff and sediment production in blanket peat catchments: implications of field rainfall simulation experiments', *Hydrological Processes,* 16, pp. 2537-2557.

Holden, J. and Burt, T. P. (2002b) 'Laboratory experiments on drought and runoff in blanket peat ', *European Journal of Soil Science,* 53, pp. 675-689.

Holden, J. and Burt, T. P. (2003a) 'Hydraulic conductivity in upland blanket peat: measurement and variability', *Hydrological Processes,* 17, pp. 1227-1237.

Holden, J. and Burt, T. P. (2003b) 'Hydrological studies on blanket peat: the significance of the acrotelm-catotelm model', *Journal of Ecology,* 91, pp. 86-102.

Holden, J. and Burt, T. P. (2003c) 'Runoff production in blanket peat covered catchments', *Water Resources Research,* 39, (7), pp. 1191-1199.

Holden, J., Burt, T. P. and Cox, N. J. (2001) 'Macroporosity and infiltration in blanket peat: the implications of tension disc infiltrometer measurements', *Hydrological Processes,* 15, pp. 289-303.

Holden, J., Chapman, P. J. and Labadz, J. C. (2004) 'Artificial drainage of peatlands: hydrological and hydrochemical process and wetland restoration', *Progress in Physical Geography,* 28, (1), pp. 95-123.

Holden, J., Evans, M. G., Burt, T. P. and Horton, M. (2006) 'Impact of land drainage on peatland hydrology', *Journal of Environmental Quality,* 35, pp. 1764-1778.

Holden, J., Kirkby, M. J., Lane, S. N., Milledge, D. G., Brookes, C. J., Holden, V. and McDonald, A. T. (2008) 'Overland flow velocity and roughness properties in peatlands', *Water Resources Research,* 44, pp. W06415.

Holden, J., Shotbolt, L., Bonn, A., Burt, T. P., Chapman, P. J., Dougill, A. J., Fraser, E. D. G., Hubacek, K., Irvine, B., Kirkby, M. J., Reed, M. S., Prell, C., Stagl, S., Stringer, L. C., Turner, A. and Worrall, F. (2007) 'Environmental change in moorland landscapes', *Earth-Science Reviews,* 82, pp. 75-100.

Holden, J., Wallage, Z. E., Lane, S. N. and McDonald, A. T. (2011) 'Water table dynamics in undistrubed, drained and restored blanket peat', *Journal of Hydrology,* 402, pp. 103-114.

Holman, I. P., Hess, T. M. and Rose, S. C. (2011) 'A broad-scale assessment of the effect of improved soil management on catchment baseflow index', *Hydrological Processes,* 25, pp. 2563-2572.

Holman, I. P., Hollis, J. M., Bramley, M. E. and Thompson, T. R. E. (2003) 'The contribution of soil structural degradation to catchment flooding: a preliminary investigation of the 2000 floods in England and Wales', *Hydrology and Earth System Sciences,* 7, pp. 754-765.

Hooghoudt, S. B. (1940) *Algemeene beschouwing van het probleem van de detailontwatering en de infiltratie door middel van parallel loopende drains, greppels, slooten en kanalen.* 's Gravenhage

Hornby, A. S. (2000) *Oxford advanced learner's dictionary.* Oxford: University Press.

Houlbrooke, D. J., Paton, R. J., Littlejohn, R. P. and Morton, J. D. (2011) 'Land-use intensification in New Zealand: effects on soil properties and pasture production', *Journal of Agricultural Science,* 149, pp. 337-349.

Howorth, R. and Manning, C. (2005) *Land use change and the water environment of the West Weald landscape over a 30-year period (1971-2001).* Henfield: West Weald Landscape Project

Hubbart, J. A., Link, T. E., Gravelle, J. A. and Elliot, W. J. (2007) 'Timber Harvest Impacts on Water Yield in the Continental/Maritime Hydroclimatic Region of the United States ', *Forest Science,* 53, pp. 169-180.

Huisman, J. A., Breuer, L., Bormann, H., Bronstert, A., Croke, B. F. W., Frede, H.-G., Graff, T., Hubrechts, L., Jakeman, A. J., Kite, G., Lanini, J., Leavesley, G., Lettenmaier, D. P., Lindstrom, G., Seibert, J., Sivapalan, M., Viney, N. R. and Willems, P. (2009) 'Assessing the impact of land use change on hydrology by ensemble modeling (LUCHEM) III: Scenario analysis', *Advances in Water Resources,* 32, pp. 159-170.

Hulme, P. D., Merrell, B. G., Torvell, L., Fisher, J. M., Small, J. L. and Pakeman, R. J. (2002) 'Rehabilitation of degraded *Calluna vulgaris* (L.) Hull-dominated wet heath by controlled sheep grazing', *Biological Conservation,* 107, pp. 351-363.

Ilnicki, P. (1983) 'Bog transformation resulting from drainage', *International Symposium on peat utilization.* Bemidji, Minesota, pp 13-25

Ingram, H. A. P. (1978) 'Soil layers in mires: function and terminology', *Journal of Soil Science,* 29, pp. 224-227.

Ingram, H. A. P. (1983) 'Hydrology', in Gore, A. J. P.(ed), *Ecosystems of the World 4A, Mires: Swamp, bog, fen and moor.* Oxford, UK: Elsevier, pp. 67-158.

Ingram, H. A. P. (1992) 'Introduction to the ecohydrology of mires in the context of cultural perturbation', in Bragg, O. M., Hulme, P. D., Ingram, H. A. P. and Robertson, R. A.(eds) *Peatland Ecosystems and Man: An Impact Assessment. Proceedings of the BES/IPS symposium held in Dundee, September 1989* Department of Biological Sciences, University of Dundee, pp. 67-93.

Institute of Hydrology. (1976) *Water balance of the headwater catchments of the Wye and Severn 1970 - 1975.* Wallingford, UK: Institute of Hydrology

Institute of Hydrology. (1991) *Effects of upland afforestation on water resources: the Balquhider experiment 1981-1991.* Wallingford, UK: Institute of Hydrology

Jackson, B. M., Wheater, H. S., McIntyre, N., Chell, J., Francis, O. J., Frogbrook, Z., Marshall, M., Reynolds, B. and Solloway, I. (2008) 'The impact of upland land management on flooding: insights from a multiscale experimental and modelling programme', *Journal of Flood Risk Management,* 1, pp. 71-80.

Jakeman, A. J., Littlewood, I. G. and Whitehead, P. G. (1990) 'Computation of the instantaneous unit hydrograph and identifiable component flows with application to two small upland catchments', *Journal of Hydrology,* 117, pp. 275-300.

Jalbert, J., Mathevet, T. and Favre, A. C. (2011) 'Temporal uncertainty estimation of discharges from rating curves using variographic analysis', *Journal of Hydrology,* 397, pp. 83-92.

JBA Consulting. (2007) *Ripon land management project, final report.* Taunton: DEFRA

Johnson, R. H. (1987) *The geomorphology of north west England.* Manchester: Manchester University Press.

Johnson, R. H. and Whitehead, P. G. (1993) 'An introduction to the research in the Balquhidder experimental catchments', *Journal of Hydrology,* 145, pp. 231-238.

Jonczyk, J., Wilkinson, M., Rimmer, D. and Quinn, P. (2009) *Peatscapes: Monitoring of Hydrology and Water Quality at Geltsdale and Priorsdale, Report of Phase 1: Nov 2007 – Mar 2009.* Newcastle upon Tyne: Newcastle University

Jones, J. A. A., Richardson, J. M. and Jacob, H. J. (1997) 'Factors controlling the distribution of piping in Britain: a reconnaissance', *Geomorphology* 20, pp. 289-306.

Joosten, J. H. J. (1992) 'Bog regeneration in the Netherlands: a review', in Bragg, O. M., P.D., H., Ingram, H. A. P. and Robertson, R. A.(eds) *Peatland ecosystems and man: an impact assessment.* Dundee: University of Dundee / International Peat Society, pp. 367-373.

Kennedy, G. W. and Price, J. S. (2005) 'A conceptual model of volume change controls on the hydrology of cutover peats', *Journal of Hydrology,* 302, pp. 13-27.

Kiersch, B. (2001) 'Land use impacts on water resources: a literature review. Discussion Paper No. 1. Land-water linkages in rural watersheds*', Electronic Workshop.* Rome, Italy, pp.

Kirby, C., Newson, M. D. and Gilman, K. (1991) *Plynlimon research: the first two decades.* Wallingford: Institute of Hydrology

Kirchner, J. W. (2006) 'Getting the right answers for the right reasons: linking measurements, analyses, and models to advance the science of hydrology', *Water Resources Research,* 42, pp. W03S04.

Kirkby, M. J. (1993) 'Network hydrology and geomorphology', in Beven, K. and Kirkby, M. J.(eds) *Channel network hydrology.* Chichester, UK: Wiley & Sons, Ltd., pp. 1-11.

Kleeberg, H.-B. (1992) 'Regionalisierung in der Hydrologie (Regionalization in hydrology)', in Kleeberg, H.-B.(ed), *Ergebnisse von rundgesprachen der Deutschen forschungsgeminschaft.* Weinheim: VCH, pp. 444.

Kleinbaum, D. G., Kupper, L. L. and Muller, K. E. (1988) *Applied regression analysis and other multivariable methods.*Second ed Boston: PWS-KENT Publishing Company.

Klemes, V. (1983) 'Conceptualization and scale in hydrology ', *Journal of Hydrology,* 65, pp. 1-23.

Klemes, V. (1986) 'Dilettantism in hydrology: transition or destiny', *Water Resources Research,* 22, pp. 177S-188S.

Krecek, J. and Haigh, M. (2006) 'Headwater wetlands', in Krecek, J. and Haigh, M.(eds) *Environmental role of wetlands in headwaters.* Dordrecht: Springer, pp. 1-6.

Kundzewicz, Z. W. (2004) 'Searching for change in hydrological data', *Hydrological Sciences - Journal - des Sciences Hydrologiques,* 49, pp. 3-6.

Kundzewicz, Z. W. and Robson, A. J. (2004) 'Change detection in hydrological records - a review of the methodology', *Hydrological Sciences - Journal - des Sciences Hydrologiques,* 49, pp. 7-19.

La Barbera, P., Lanza, L. G. and Stagi, L. (2002) 'Tipping bucket mechanical errors and their influence on rainfall statistics and extremes', *Water Science and Technology,* 45, pp. 1-9.

Lamb, R. and Beven, K. (1997) 'Using interactive recession curve analysis to specify a general catchment storage model', *Hydrology and Earth System Sciences,* 1, pp. 101-113.

Lance, A. N. (1983) 'Performance of sheep on unburned and serially burned blanket bog in Western Ireland', *Journal of Applied Ecology,* 20, pp. 767-775.

Lane, P. N. J., Best, A. E., Hickel, K. and Zhang, L. (2005) 'The response of flow duration curves to afforestation', *Journal of Hydrology,* 310, pp. 253-265.

Lane, S. N. (2003) 'More floods, less rain? Changing hydrology in a Yorkshire context', in Atherden, M.(ed), *Global warming: a Yorkshire perspective.* York: PLACE Research Centre, York.

Lane, S. N. (2008) 'Slowing the floods in the UK Pennine uplands...a case of waiting for Godot?', *Journal of practical ecology and conservation,* 7.

Lane, S. N., Brookes, C. J., Hardy, R. J., Holden, J., James, T. D., Kirkby, M. J., McDonald, A. T., Tayefi, V. and Yu, D. (2003) 'Land management, flooding and environmental risk: new approaches to a very old question', *Forthcomin in Proc. CIWEM National Conference.*

Lane, S. N., Brookes, C. J., Kirkby, M. J. and Holden, J. (2004) 'A network-index-based version of TOPMODEL for use with high-resolution digital topographic data', *Hydrological Processes,* 18, pp. 191-201.

Langlands, J. P. and Bennett, I. L. (1973) 'Stocking intensity and pastoral production1. Changes in soil and vegetation of a sown pasture grazed by sheep at different stocking rates', *Journal of Agricultural Science,* 81, pp. 193-194.

LaRose, S., Price, J. and Rochefort, L. (1997) 'Rewetting of a cutover peatland: hydrologic assessment', *Wetlands,* 17, pp. 416-423.

Larson, L. W. and Peck, E. L. (1974) 'Accuracy of precipitation measurements for hydrologic modeling', *Water Resources Research,* 10, pp. 857-863.

Law, F. M. (1957) 'Measurement of rainfall, interception and evaporation losses in a plantation of Sitka Spruce trees', *International Association of Hydrological Sciences Publication,* 44, pp. 397-411.

Leonard, J., Mietton, M., Najib, H. and Gourbesville, P. (2000) 'Rating curve modelling with Manning's equation to manage instability and improve extrapolation', *Hydrological Sciences - Journal - des Sciences Hydrologiques,* 45, pp. 739-750.

Letts, M. G., Roulet, N. T., Comer, N. T., Skarupa, M. R. and Verseghy, D. L. (2000) 'Parametrization of peatland hydraulic properties for the Canadian land surface scheme', *Atmosphere-ocean,* 38, pp. 141-160.

Levavasseur, F., Bailly, J.S., Lagacherie, P., Colin, F. and Rabotin, M. (2012) 'Simulating the effects of spatial configurations of agricultural ditch drainage networks on surface runoff from agricultural catchments', *Hydrological Processes*, Article first published online: 24 Jan 2012.

Linsley, R. K., Kohler, M. A. and Paulhus, J. L. H. (1949) *Applied Hydrology.* New York: McGraw-Hill.

Luce, C. H. (2002) 'Hydrological processes and pathways affected by forest roads: what do we still need to learn?', *Hydrological Processes,* 16, pp. 2901-2904.

Mackay, A. W. and Tallis, J. H. (1994) 'The recent vegetational history of the Forest of Bowland, Lancashire, UK', *New Phytology,* 128, pp. 571-584.

Mackay, A. W. and Tallis, J. H. (1996) 'Summit-type blanket mire erosion in the Forest of Bowland, Lancashire, UK: Predisposing factors and implications for conservation', *Biological Conservation,* 76, pp. 31-44.

MacKinnon, D. and Tetzlaff, D. (2009) 'Conceptualising scale in regional studies and catchment science - Towards an integrated characterisation of spatial units', *Geography Compass,* 3, pp. 976-996.

Mallik, A. U. and Fitzpatrick, E. A. (1996) 'Thin section studies of Calluna heathland soils subject to prescribed burning', *Soil Use and Management,* 12, pp. 143-149.

Mallik, A. U., Gimingham, C. H. and Rahman, A. A. (1984) 'Ecological effects of heather burning, 1: Water infiltration, moisture retention and porosity of surface soil', *Journal of Ecology,* 72, pp. 767-776.

Marchand, J. P., Jarrett, R. D. and Jones, L. L. (1984) *Velocity profile, water-surface slope, and bed-material size for selected streams in Colorado.* Open-File Report: U.S. Geological Survey

Marshall, M. R., Francis, O. J., Frogbrook, Z. L., Jackson, B. M., McIntyre, N., Reynolds, B., Solloway, I., Wheater, H. S. and Chell, J. (2009) 'The impact of upland land

management on flooding: results from an improved pasture hillslope', *Hydrological Processes,* 23, pp. 464–475.

Mayes, W. M., Walsh, C. L., Bathurst, J. C., Kilsby, C. G., Quinn, P. F., Wilkinson, M. E., Daugherty, A. J. and O'Connell, P. E. (2006) 'Monitoring a flood event in a densely instrumented catchment, the Upper Eden, Cumbria, UK', *Water and Environment Journal,* 20, pp. 217-226.

McCuen, R. H., Knight, Z. and Cutter, A. G. (2006) 'Evaluation of the Nash–Sutcliffe efficiency index ', *Journal of Hydrologic Engineering* 11, pp. 597-602.

McDonald, A. T. (1973) 'Some views on the effects of peat drainage', *Scottish Forestry,* 27, pp. 315-327.

McDonnell, J. J., Sivapalan, M., Vache, K., Dunn, S., Grant, G., Haggerty, R., Hinz, C., Hooper, R., Kirchner, J., M.L., R., Selker, J. and Weiler, M. (2007) 'Moving beyond heterogeneity and process complexity: A new vision for watershed hydrology', *Water Resources Research,* 43, pp. W07301.

McGrath, M. and Smith, M. (2006) 'Sustainable Catchment Management Programme (SCaMP): from hilltop to tap*', BHS 9th National Hydrology Symposium.* Durham, UK, pp. 91-96.

McIntyre, N. and Marshall, M. (2010) 'Identification of rural land management signals in runoff response', *Hydrological Processes,* 24, pp. 3521-3534.

McIntyre, N., Young, P., Orellana, B., Marshall, M., Reynolds, B. and Wheater, H. (2011) 'Identification of nonlinearity in rainfall-flow response using data-based mechnistic modeling', *Water Resources Research,* 47, pp. W03515.

McMulloch, J. S. G. and Robinson, M. (1993) 'History of forest hydrology', *Journal of Hydrology,* 150, pp. 189-216.

McNally, G. (1997) 'Peatlands, power and post-industrial use', in Parkyn, L., Stoneman, R. E. and Ingram, H. A. P.(eds) *Conserving peatlands.* Oxon: CAB International, pp. 245-251.

Meyles, E. W., Williams, A. G., Ternan, J. L., Anderson, J. M. and Dowd, J. F. (2006) 'The influence of grazing on vegetation, soil properties and stream discharge in a small Dartmoor catchment, southwest England, UK', *Earth Surface Processes and Landforms,* 31, pp. 622-631.

Michel, J. C. (2010) 'The physical properties of peat: a key factor for modern growing media*', Mires and Peat.* Lamoura, France, International Mire Conservation Group and International Peat Society, pp.

Milne, R. and Brown, T. A. (1997) 'Carbon in the vegetation and soils of Great Britain', *Journal of Environmental Management,* 49, pp. 413-433.

Mitchell, R. J., Rose, R. J. and Palmer, S. C. F. (2008) 'Restoration of Calluna vulgaris on grass-dominated moorlands: The importance of disturbance, grazing and seeding', *Biological Conservation,* 141, pp. 2100-2111.

Molini, A., La Barbera, P., Lanza, L. G. and Stagi, L. (2001) 'Rainfall intermittency and the sampling error of tipping-bucket rain gauges', *Physics and Chemistry of the Earth,* 26, pp. 737–742.

Money, R. P. and Wheeler, B. D. (1999) 'Some critical questions concerning the restorability of damaged raised bogs', *Applied Vegetation Science,* 2, pp. 107-116.

Moore, P. D. and Bellamy, D. J. (1974) *Peatlands.* London: Paul Elek (Scientific Books) Ltd.

Morris, J. and Wheater, H. (2007) 'Catchment land-use', in Thorne, C. R., Evans, E. P. and Penning-Rowsell, E. C.(eds) *Future flooding and coastal erosion risks.* London: Thomas Telford Publishing.

Moussa, R., Voltz, M. and Andrieux, P. (2002) 'Effects of the spatial organization of agricultural management on the hydrological behaviour of a farmed catchment during flood events', *Hydrological Processes,* 16, pp. 393-412.

Mulqueen, J., Rodgers, M. and Killeen, E. (1997) 'A note on measuring the hydraulic conductivity in the field for drainage', *Irish Journal of Agricultural and Food Research,* 36, pp. 249-255.

Naef, F., Scherrer, S. and Weiler, M. (2002) 'A process based assessment of the potential to reduce flood runoff by land use change', *Journal of Hydrology,* 267, pp. 74-79.

Nash, J. E. and Sutcliffe, J. V. (1970) 'River flow forecasting through conceptual models part 1 - A discussion of principles', *Journal of Hydrology,* 10, pp. 282-290.

Nelder, J. A. and Mead, R. (1965) 'A simplex method for function minimization', *Computer Journal,* 7, pp. 308-313.

Nespor, V. and Sevruk, B. (1999) 'Estimation of wind-induced error of rainfall gauge measurements using a numerical simulation', *Journal of Atmospheric and Oceanic Technology,* 16, pp. 450-464.

Newson, M. D. (1981) 'Mountain streams', in Lewin, J.(ed), *British rivers.* London: George Allen and Unwin LTD.

Nieber, J. L. and Sidle, R. C. (2010) 'How do disconnected macropores in sloping soils facilitate preferential flow?', *Hydrological Processes,* 24, pp. 1582-1594.

Nilsson, B., Sidle, R. C., Klint, K. E., Bøggild, C. E. and Broholm, K. (2001) 'Mass transport and scale-dependent hydraulic tests in a heterogeneous glacial till-sandy aquifer system', *Journal of Hydrology,* 243, pp. 162-179.

Nuttle, W. K. and Hemond, H. F. (1988) 'Salt marsh hydrology: implications for biogechemical fluxes to the atmosphere and estuaries', *Global Biogechemical Cycles,* 2, pp. 1-13.

O'Connell, P. E., Beven, K. J., Carney, J. N., Clements, R. O., Ewen, J., Fowler, H., Harris, G. L., Hollis, J., Morris, J., O'Donnell, G. M., Packman, J. C., Parkin, A., Quinn, P. F., Rose, S. C., Shepherd, M. and Tellier, S. (2004) *Review of impacts of rural land use management on flood generation: Impact Study Report.* London, UK: DEFRA Flood Management Division

O'Connell, P. E., Ewen, J., O'Donnell, G. M. and Quinn, P. F. (2007a) 'Is there a link between agricultural land use management and flooding?', *Hydrology and Earth System Sciences,* 11, pp. 96-107.

O'Connell, P. E., Quinn, P. F., Bathurst, J. C., Parkin, G., Kilsby, C., Beven, K. J., Burt, T. P., Kirkby, M. J., Pickering, A., Robinson, M., Soulsby, C., Werritty, A. and Wilcock, D. (2007b) 'Catchment Hydrology and Sustainable Management (CHASM): an integrating methodological framework for prediction', *International Association of Scientific Hydrology Publication,* 309, (Predictions in Ungauged Basins: PUB Kick-off (Proceedings of the PUB Kick-off meeting held in Brasilia,20–22 November 2002).), pp. 53-62.

O'Connell, P. E., Quinn, P. F., Bathurst, J. C., Parkin, G., Kilsby, C. G., Beven, K. J., Burt, T. P., Kirkby, M. J., Tipping, E., Robinson, M., Soulsby, C., Werritty, A. and Wilcock, D. (2003) 'Catchment Hydrology and Sustainable Management (CHASM): an integrating methodological framework for prediction', *Geophysical Research Abstracts,* 5, pp. 14867.

O'Donnell, G., Ewen, J. and O'Connell, P. E. (2011) 'Sensitivity maps for impacts of land management on an extreme flood in the Hodder catchment, UK', *Physics and Chemistry of the Earth,* 36, pp. 630-637.

Oberlin, G. (1981) 'Influence du drainage et de l'assainissement rural sur l'hydrologie.', *CEMAGREF Bulletin,* 285, pp. 45-56.

Ours, D. P., Siegel, D. I. and Glaser, P. H. (1997) 'Chemical dilation and the dual porosity of humified bog peat', *Journal of Hydrology,* 196, pp. 348-360.

Owen, G. J. (2008) *Characterization of the channel network in the Hodder catchment for flood routing models.* MSc. thesis. Newcastle University.

Pakeman, R. J., Hulme, P. D., Torvell, L. and Fisher, J. M. (2003) 'Rehabilitation of degraded dry heather (*Calluna vulgaris* (L.) Hull) moorland by controlled sheep grazing', *Biological Conservation,* 114, pp. 389-400.

Park, J.-S., Graham, D., Butts, M. and Cluckie, I. (2010) 'Sensitivity of catchment management strategies for the River Parrett using a phsycially distributed model', *BHS 2010: Role of Hydrology in Managing Consequences of a Changing Global Environment, Proc. BHS Third International Symposium, 19th-23rd July 2010.* Newcastle University:British Hydrological Society.

Park, J. S., Ren, Q., Chen, Y., Cluckie, I. D., Butts, M. and Graham, D. (2009) *Hydroinformatics in Hydrology, Hydrogeology and Water Resources, Proc. Of Symposium of JS.4 at the Joint IAHS & IAH Convention.* Hyderabad, India:IAHS.

Parkin, G., O'Donnell, G., Ewen, J., Bathurst, J. C., O'Connell, P. E. and Lavabre, J. (1996) 'Validation of catchment models for predicting land-use and climate change impacts, 2. Case study for a Mediterranean catchment', *Journal of Hydrology,* 175, pp. 595-613.

Parkyn, L., Stoneman, R. E. and Ingram, H. A. P. (1997) *Conserving Peatlands.* Oxon: CAB International.

Parmentier, F. J. W., M.K., van der Molen, R.A.M. de Jeu, Hendriks, D. M. D. and Dolman, A. J. (2009) 'CO2 fluxes and evaporation on a peatland in the Netherlands appear not affected by water table fluctuations ', *Agricultural and Forest Meteorology,* 149, pp. 1202-1208.

Parrott, A., Brooks, W., Harmar, O. and Pygott, K. (2010) 'Role of rural land use management in flood and coastal risk management', *Journal of Flood Risk Management,* 2, pp. 272-284.

Peel, M. C. (2009) 'Hydrology: catchment vegetation and runoff', *Progress in Physical Geography,* 33, pp. 837-844.

Peel, M. C., Finlayson, B. L. and McMahon, T. A. (2007) 'Updated world map of the Köppen-Geiger climate classification', *Hydrology and Earth System Sciences,* 11, pp. 1633-1644.

Perry, M. and Hollis, D. (2005) 'Generation of monthly gridded data sets for a range of climatic variables over the UK', *International Journal of Climatology,* 25, pp. 1041-1054.

Pfister, L., Kwadijk, J., Musy, A., Bronstert, A. and Hoffman, L. (2004) 'Climate change, land use change and runoff prediction in the Rhine-Meuse basins', *River Research and Applications,* 20, pp. 229-241.

Pike, R. G., Redding, T. E., Wilford, D., Moore, R. D., Ice, G., Reiter, M. and Toews, D. A. A. (2010) 'Detecting and predicting changes in watersheds', in Pike, R. G., Redding, T. E., Moore, R. D., Winkler, R. D. and Bladon, K. D.(eds) *FORREX (Forum for Research and Extension in Natural Resources), Compendium of forest hydrology and geomorphology in British Columbia.* Victoria: Province of British Columbia.

Post, D. A., Jakeman, A. J., Littlewood, I. G., Whitehead, P. G. and Jayasuriya, M. D. A. (1996) 'Modelling land-cover-induced variations in hydrologic response: Picaninny Creek, Victoria', *Ecological Modelling,* 86, pp. 177-182.

Press, W. H., Teukolsky, S. A., Vetterling, W. T. and Flannery, B. P. (1992) *Numerical recipes in FORTRAN - The art of scientific computing.*Second ed Cambridge: Cambridge University Press.

Price, J. S. (1994) 'Water exchanges in a shorline Typha marsh on Lake Ontario', *Journal of Hydrology,* 155, pp. 407-428.

Price, J. S., Heathwaite, A. L. and Baird, A. J. (2003) 'Hydrological processes in abandoned and restored peatlands: an overview of management approaches', *Wetlands Ecology and Management,* 11, pp. 65-83.

Price, J. S. and Schlotzhauer, S. M. (1999) 'Importance of shrinkage and compression in determining water storage changes in peat: the case of a mined peatland', *Hydrological Processes,* 13, pp. 2591-2601.

Pringle, H. J. R. and Landsberg, J. (2004) 'Predicting the distribution of livestock grazing pressure in rangelands', *Austral Ecology,* 29, pp. 31-39.

Quinton, W. L., Hayashi, M. and Carey, S. K. (2008) 'Peat hydraulic conductivity in cold regions and its relation to pore size and geometry', *Hydrological Processes,* 22, pp. 2829-2837.

Radziejewski, M. and Kundzewicz, Z. W. (2004) 'Detectability of changes in hydrological records', *Hydrological Sciences - Journal - des Sciences Hydrologiques,* 49, pp. 39-51.

Ramchunder, S. J., Brown, L. E. and Holden, J. (2009) 'Environmental effects of drainage, drain-blocking and prescribed vegetation burning in UK upland peatlands', *Progress in Physical Geography,* 33, (1), pp. 49-79.

Ratto, M., Young, P. C., Romanowicz, R., Pappenberger, F., Saltelli, A. and Pagano, A. (2007) 'Uncertainty, sensitivity analysis and the role of data based mechanistic modeling in hydrology', *Hydrology and Earth System Sciences,* 11, pp. 1249-1266.

Rawes, M. (1983) 'Changes in two high altitude blanket bogs after cessation of sheep grazing', *Journal of Ecology,* 71, pp. 219-235.

Rawes, M. and Hobbs, R. (1979) 'Management of semi-natural blanket bog in the northern Pennines', *Journal of Ecology,* 67, pp. 789-807.

Reeve, A. S., Siegel, D. I. and Glaser, P. H. (2000) 'Simulating vertical flow in large peatlands', *Journal of Hydrology,* 227, pp. 207-217.

Reeve, A. S., Siegel, D. I. and Glaser, P. H. (2001) 'Simulating dispersive mixing in large peatlands', *Journal of Hydrology,* 242, pp. 103–114.

Richards, K. J. (1982) *Rivers: Form and process in alluvial channels.* London: Methuen.

Rizzuti, A. M., Cohen A.D. and Stack, E. M. (2004) 'Using hydraulic conductivity and micropetrography to assess water flow through peat-containing wetlands', *International Journal of Coal Geology,* 60, pp. 1-16.

Robertson, R. A. and Jowsey, P. C. (1968) 'Peat resources and development in the United Kingdom', *Third International Peat Congress.* Quebec, pp. 13-14.

Robinson, M. (1985) 'The hydrological effects of moorland gripping: a re-appraisal of the Moor House research', *Journal of Environmental Management,* 21, (201-211).

Robinson, M. (1986) 'Changes in catchment runoff following drainage and afforestation', *Journal of Hydrology,* 86, pp. 71-84.

Robinson, M. (1990) *Impact of improved land drainage on river flows.* Wallingford, UK: Institue of Hydrology

Robinson, M., Boardman, J., Evans, R., Heppell, K., Packman, J. and Leeks, G. (2000) 'Land use change', in Acreman, M.(ed), *The hydrology of the UK.* London: Routledge, pp. 303.

Robinson, M., Moore, R. E., Nisbet, T. R. and Blackie, J. R. (1998) *From moorland to forest: the Coalburn catchment experiment.* Wallingford: Institute of Hydrology

Robson, A. J. (2002) 'Evidence for trends in UK flooding', *Philosophical Transactions of the Royal Society,* 360, pp. 1327-1343.

Robson, A. J., Jones, T. K., Reed, D. W. and Bayliss, A. C. (1998) 'A study of national trend and variation in UK floods', *International Journal of Climatology,* 18, pp. 165-182.

Rochefort, L. and Price, J. (2003) 'Restoration of *Sphagnum* dominated peatlands', *Wetlands Ecology and Management,* 11, pp. 1-2.

Romanowicz, R. J., Young, P. C. and Beven, K. J. (2006) 'Data assimilation and adaptive forecasting of water levels in the river Severn catchment, United Kingdom', *Water Resources Research,* 42, pp. W06407.

Ronfort, C., Souchere, V., Martin, P., Sebillotte, C., Castellazzi, M. S., A., B., Meynard, J. M. and Laignel, B. (2011) 'Methodology for land use change scenario assessment for runoff impacts: A case study in a north-western European Loess belt region (Pays de Caux, France)', *Catena,* 86, pp. 36-48.

Ronkanen, A.-K. and Kløve, B. (2008) 'Hydraulics and flow modelling of water treatment wetlands constructed on peatlands in Northern Finland', *Water Research,* 42, pp. 3826-3836

Rosa, E. and Larocque, M. (2008) 'Investigating peat hydrological properties using field and laboratory methods: application to the Lanoraie peatland complex (southern Quebec, Canada)', *Hydrological Processes,* 22, pp. 1866-1875.

Rowell, T. A. (1988) *The peatland management handbook.* Research and survey in nature conservation, 14. Peterborough: Nature Conservancy Council

RSPB (2011a) *RSPB, Conservation project in the Forest of Bowland, Birds*. Available at: http://www.rspb.org.uk/ourwork/conservation/projects/bowland/birds/index.asp (Accessed: 25/01/2011).

RSPB. (2011b) *Scrape creation for wildlife.* Sandy, Bedfordshire, UK: RSPB

Rycroft, D. W., Williams, D. J. A. and Ingram, H. A. P. (1975) 'The transmission of water through peat: I. Review', *The Journal of Ecology,* 63, (2), pp. 535-556.

Sahin, V. and Hall, M. J. (1996) 'The effects of afforestation and deforestation on water yields', *Journal of Hydrology,* 178, pp. 293-309.

Samson, A. (1996) 'Floods and sheep - is there a link?', *Circulation: the newsletter of the British Hydrological Society,* 49, pp. 1-4.

Sansom, A. (1999) 'Upland vegetation management: the impacts of overstocking', *Water Science and Technology,* 39, pp. 85-92.

Schindler, D. W. (1998) 'Replication versus realism: the need for ecosystem-scale experiments', *Ecosystems,* 1, pp. 323-334.

Schlotzhauer, S. M. and Price, J. S. (1999) 'Soil water flow dynamics in a managed cutover peat field, Quebec: field and laboratory investigations.', *Water Resources Research,* 35, pp. 3675–3683.

Schmid, P. and Luthin, J. (1964) 'The drainage of sloping lands', *Journal of Geophysical Research,* 69, pp. 1525-1529.

Schulze, R. (2000) 'Transcending scales of space and time in impact studies of climate and climate change on agrohydrological responses', *Agriculture, Ecosystems and Environment,* 82, pp. 185-212.

Schwaerzel, K. and Bohl, H. P. (2003) 'An easily installable groundwater lysimeter to determine water balance components and hydraulic properties of peat soils', *Hydrology and Earth System Sciences,* 7, pp. 23-32.

Seibert, J. and McDonnell, J. J. (2002) 'On the dialog between experimentalist and modeler in catchment hydrology: Use of soft data for multi-criteria model calibration', *Water Resources Research*, pp. WR000978.

Shaman, J., Stieglitz, M. and Burns, D. (2004) 'Are big basins just the sum of small catchments?', *Hydrological Processes,* 18, pp. 3195-3206.

Shantz, M. A. and Price, J. S. (2006) 'Characterization of surface storage and runoff patterns following peatland restoration, Quebec Canada', *Hydrological Processes,* 20, pp. 3799-3814.

Shaw, E. M. (1988) *Hydrology in practice.*Second ed London, UK: Van Nostrand Reinhold (International) Co. Ltd

Shaw, E. M., Beven, K. J., Chappell, N. A. and Lamb, R. (2011) *Hydrology in practice.*Fourth ed Abingdon, UK: Spon Press.

Shaw, S. C., Wheeler, B. D., Kirby, P., Phillipson, P. and Edmunds, R. (1996) *Literature review of the historical effects of burning and grazing of blanket bog and upland wet heath.* Peterborough: English Nature

Shibchurn, A., Van Geel, P. J. and Kennedy, P. L. (2005) 'Impact of density on the hydraulic properties of peat and the time domain reflectometry (TDR) moisture calibration curve', *Canadian Geotechnical Journal,* 42, pp. 279-286.

Sidle, R. C. (2006) 'Field observations and process understanding in hydrology: essential components in scaling', *Hydrological Processes,* 20, pp. 1439-1445.

Siegel, D. I. and Glaser, P. H. (1987) 'Groundwater Flow in a Bog-Fen Complex, Lost River Peatland, Northern Minnesota', *Journal of Ecology,* 75, pp. 743-754.

Siriwardena, L., Finlayson, B. L. and McMahon, T. A. (2006) 'The impact of land use change on catchment hydrology in large catchments: The Comet river, Central Queensland, Australia', *Journal of Hydrology,* 326, pp. 199-214.

Sivapalan, M. (2003) 'Process complexity at hillslope scale, process simplicity at the watershed scale: is there a connection?', *Hydrological Processes,* 17, pp. 1037-1041.

Slaughter, C. W., Marks, D., Flerchinger, G. N., Van Vactor, S. S. and Burgess, M. (2001) 'Thrirty-five years of research data collection at the Reynolds Creek Experimental Watershed, Idaho, United States', *Water Resources Research,* 37, pp. 2819-2823.

Slumberger Water Services. (2010) 'Product Manual (Divers)', in Eijkelkamp Agrisearch Equipment(ed), Delft, Netherlands: Slumberger Water Services.

Smart, P. L. and Wilson, C. M. (1984) 'Two methods for the tracing of pipe flow on hillslopes', *Catena,* 11 pp. 159-168.

Smout, T. C. (1997) 'Bogs and people since 1600', in Parkyn, L., Stoneman, R. E. and Ingram, H. A. P.(eds) *Conserving Peatlands.* Oxon: CAB International, pp. 162-167.

Soulsby, C., Tetzlaff, D., Dunn, S. M. and Waldron, S. (2006) 'Scaling up and out in runoff process understanding: insights from nested experimental catchment studies', *Hydrological Processes,* 20, pp. 2461-2465.

Spieksma, J. F. M. (1999) 'Changes in the discharge pattern of a cutover raised bog during rewetting', *Hydrological Processes,* 13, pp. 1233-1246.

Stewart, A. J. A. and Lance, A. N. (1983) 'Moor-Draining: A review of impacts on land use', *Journal of Environmental Management,* 17, pp. 81-99.

Stewart, A. J. A. and Lance, A. N. (1991) 'Effects of moor-draining on the hydrology and vegetation of northern Pennine blanket bog', *Journal of Applied Ecology,* 28, pp. 1105-1117.

Sullivan, A., Ternan, J. L. and Williams, A. G. (2004) 'Land use change and hydrological response in the Camel catchment, Cornwall', *Applied Geography,* 24, pp. 119-137.

Surridge, B. W., Baird, A. J. and Heathwaite, A. L. (2005) 'Evaluating the quality of hydraulic conductivity estimates from piezometer slug tests in peat', *Hydrological Processes,* 19, pp. 1227-1244.

Taylor, C. J., Pedregal, D. J., Young, P. C. and Tych, W. (2007) 'Environmental time series analysis and forecasting with the Captain toolbox', *Environmental Modelling and Software,* 22, pp. 797-814. Internet: www.es.lancs.ac.uk/cres/captain.

Tetzlaff, D., Carey, S. K., Laudon, H. and McGuire, K. (2010) 'Catchment processes and heterogeneity at multiple scales - benchmarking observations, conceptualization and prediction', *Hydrological Processes,* 24, pp. 2203-2208.

Thiessen, A. H. (1911) 'Precipitation averages for large areas', *Monthly Weather Review,* 39, pp. 1082-1084.

Thomas, R. B. and Megahan, W. F. (1998) 'Peak flow responses to clear-cutting and roads in small and large basins, western Cascades, Oregon: A second opinion', *Water Resources Research,* 34, pp. 3393-3403.

Tian, Y., Singleton, P. L., Sheath, G. W., McCall, D. G. and Carlson, W. T. (1998) 'Modelling animal treading impacts on infiltration rate', *Proceedings of the New Zealand Grassland Association,* 60, pp. 149-152.

Tibbetts, T. E. (1968) 'Peat resources of the world. A review', *3rd International Peat Congress.* Quebec City, Quebec, pp. 8-23

Trettin, C. C., Amatya, D. M., Kaufman, C., Levine, N. and Morgan, R. T. (2008) 'Recognizing change in hydrologic functions and pathways due to historical agricultural use - Implications to hydrologic assesments and modeling', *The third interagency conference on research in watersheds.* Estes Park, Colorado, pp 8-11.

Troch, P. A., Carrillo, G. A., Heidbuchel, I., Rajagopal, S., Switanek, M., Volkmann, T. H. M. and Yaeger, M. (2009) 'Dealing with landscape heterogeneity in watershed hydrology: a review of recent progress toward new hydrological theory', *Geography Compass,* 3, pp. 375-392.

Tu, M., Hall, M. J., de Laat, P. J. M. and de Wit, M. J. M. (2005) 'Extreme floods in the Meuse river over the past century: aggravated by land-use changes?', *Physics and Chemistry of the Earth,* 30, pp. 267-276.

Tufnell, L. (1997) 'North-West England and the Isle of Man', in Wheeler, D. and Mayes, J.(eds) *Regional Climates of the British Isles.* Abingdon: Routledge, pp. 343.

Uhlenbrook, S., Holocher, J., Leibundgut, C. and Seibert, J. (1998) 'Using a conceptual rainfall-runoff model on different scales by comparing a headwater with larger basins', *International Association of Hydrological Sciences Publication,* 248, pp. 297-305.

United Utilities. (2008) *Stocks Reservoir.* Warrington: United Utilities

United Utilities (2011) *United Utilities, About SCaMP*. Available at: http://www.unitedutilities.com/AboutSCaMP.aspx (Accessed: 27/01/2011).

van Dijk, A. I. J. M., Pena-Arancibia, J. L. and Bruijnzeel, L. A. (2011) 'Top-down analysis of collated streamflow data from heterogeneous catchmetns leads to underestimation of land cover influence', *Hydrology and Earth System Sciences Discussions,* 8, pp. 4121-4150.

van Genuchten, M. T. (1980) 'A closed-form equation for predicting the hydraulic conductivity of unsaturated soils', *Soil Science Society of America Journal,* 44, pp. 892-898.

Van Seters, T. E. and Price, J. S. (2002) 'Towards a conceptual model of hydrological chagnes on an abandoned cutover bog, Quebec', *Hydrological Processes,* 16, pp. 1965-1981.

Ward, R. C. (1981) 'River systems and river regimes', in Lewin, J.(ed), *British rivers.* London: George Allen and Unwin LTD.

Westerberg, I., Guerrero, J. L., Seibert, J., Beven, K. J. and Halldin, S. (2011) 'Stage-discharge uncertainty derived with a non-stationary rating curve in the Choluteca River, Honduras', *Hydrological Processes,* 25, pp. 603-613.

Whalley, N., Iredale, R. S. and Clare, A. F. (2001) 'Reliability and uncertainty in flow measurement techniques - some current thinking', *Physics and Chemistry of the Earth,* 26, pp. 743-749.

Wheater, H. and Evans, E. (2009) 'Land use, water management and future flood risk', *Land Use Policy,* 26, pp. 251-264.

Whitehead, P. G. and Robinson, M. (1993) 'Experimental basin studies - an international and historical perspective of forest impacts', *Journal of Hydrology,* 145, pp. 217-230.

Wilby, R. L. (2006) 'When and where might climate change be detectable in UK river flows?', *Geophysical Research Letters,* 33, pp. L19407.

Wilby, R. L., Beven, K. J. and Reynard, N. S. (2008) 'Climate change and fluvial flood risk in the UK: more of the same?', *Hydrological Processes,* 22, pp. 2511-2523.

Wilkinson, M. E. (2009) *A multiscale nested experiment for understanding and prediction of high rainfall and flood response spatial behaviour in the Eden catchment, Cumbria, UK.* Ph.D. thesis. Newcastle University.

Williams, M. (1990) *Wetlands: a threatened landscape.* Oxford: Blackwell.

Wilson, C. M. and Smart, P. L. (1984) 'Pipes and pipe flow process in an upland catchment, Wales', *Catena,* 11, pp. 145-158.

Wilson, L., Wilson, J., Holden, J., Johnstone, I., Armstrong, A. and Morris, M. (2010) 'Recovery of water tables in Welsh blanket bog after drain blocking: discharge rates, time scales and the influence of local conditions', *Journal of Hydrology,* 391, pp. 377-386.

Wilson, L., Wilson, J. M. and Johnstone, I. (2011) 'The effect of blanket bog drainage on habitat condition and on sheep grazing, evidence from a Welsh upland bog', *Biological Conservation,* 144, pp. 199-201.

Wittenberg, H. (1999) 'Baseflow recession and recharge as nonlinear storage processes', *Hydrological Processes,* 13, pp. 715-726.

Woods, R. (2004) 'The impact of spatial scale on spatial variability in hydrologic response: experiments and ideas', *International Association of Scientific Hydrology Publication,* 287, pp. 153-167.

Woods, R. A., Grayson, R. B., Western, A. W., Duncan, M. J., Wilson, D. J., Young, R. I., Ibbitt, R. P., Henderson, R. D. and McMahon, T. A. (2001) 'Experimental design and initial results from the Mahurangi River Variability Experiment: MARVEX', in Lakshmi, V. and Albertson, J. D.(eds) *Observations and Modelling of Land Surface Hydrological Processes.* Washington: Water Resources Monographs, American Geophysical Union.

Worrall, F. and Adamson, J. K. (2008) 'The effect of burning and sheep grazing on soil water composition in a blanket bog: evidence for soil structural changes', *Hydrological Processes,* 22, pp. 2531-2541.

Worrall, F., Armstrong, A. and Adamson, J. K. (2007a) 'The effects of burning and sheep-grazing on water table depth and soil water quality in a upland peat', *Journal of Hydrology,* 339, pp. 1-14.

Worrall, F., Armstrong, A. and Holden, J. (2007b) 'Short-term impact of peat drain-blocking on water colour, dissolved organic carbon concentration, and water table depth', *Journal of Hydrology,* 337, pp. 315-325.

Worrall, F., Burt, T. P. and Adamson, J. K. (2007c) 'Change in runoff initiation probability over a severe drought in a peat soil - Implications for flowpaths', *Journal of Hydrology,* 345, pp. 16-26.

Worrall, F., Gibson, H. S. and Burt, T. P. (2007d) 'Modelling the impact of drainage and drain-blocking on dissolved organic carbon release from peatlands', *Journal of Hydrology,* 338, pp. 15-27.

Worrall, F., Reed, J., Warburton, J. and Burt, T. (2003) 'Carbon budget for a British upland peat catchment', *Science of the Total Environment,* 312, pp. 133-146.

Young, P. (2003) 'Top-down and data-based mechanistic modelling of rainfall-flow dynamics at the catchment scale', *Hydrological Processes,* 17, pp. 2195-2217.

Young, P. C. (1984) *Recursive estimation and time-series analysis.* Berlin: Springer-Verlag.

Young, P. C. (1992) 'Parallel processes in hydrology and water quality: a unified time-series approach', *Water and Environment Journal,* 6, pp. 598-612.

Young, P. C. (2001) 'Data based mechanistic modelling and validation of rainfall-flow processes', in Anderson, M. G. and Bates, P. D.(eds) *Model validation: perspective in hydrological science.* Chichester, UK: J. Wiley, pp. 117-161.

Young, P. C. (2002) 'Advances in real-time flood forecasting', *Philosophical Transactions of the Royal Society,* 360, pp. 1433-1450.

Young, P. C. (2004) *Hydrology: Science and practice for the 21st century.* London:British Hydrological Society.

Young, P. C. and Beven, K. J. (1994) 'Data-based mechanistic modelling and the rainfall-flow non-linearity', *Environmetrics,* 5, pp. 335-363.

Young, P. C. and Garnier, H. (2006) 'Identification and estimation of continuous-time, data-based mechanistic (DBM) models for environmental systems', *Environmental Modelling and Software,* 21, pp. 1055-1072.

Young, P. C., Jakeman, A. J. and Post, D. A. (1997) 'Recent advances in the data-based modelling and analysis of hydrological systems', *Water Science and Technology,* 36, pp. 99-116.

Young, P. C. and Tomlin, C. M. (2000) 'Data-based mechanistic modelling and adaptive flow forecasting', in Walshe, P., Lees, M.(ed), *Flood Forecasting: What Does Current Research Offer the Practitioner?* Vol. Occasional Paper 12 London: British Hydrological Society, pp. 26-40.

Young, R. A. and Voorhees, W. B. (1982) 'Soil erosion and runoff from planting to canopy development as influence by tractor wheel-traffic', *Transactions of the ASEA,* 25, pp. 708-712.

Yu, Z., Beilman, D. W., Frolking, S., MacDonald, G. M., Roulet, N. T., Camill, P. and Charman, D. J. (2011) 'Peatlands and their role in the global carbon cycle', *EOS, Transactions, American Geophysical Union,* 92, pp. 97-98.

Yu, Z., Loisel, J., Brosseau, D. P., Beilman, D. W. and Hunt, S. J. (2010) 'Global peatland dynamics since the Last Glacial Maximum', *Geophysical Research Letters,* 37, pp. L13402.

Zegre, N., Skaugset, A. E., Som, N. A., McDonnell, J. J. and Ganio, L. M. (2010) 'In lieu of the paired catchment approach: Hydrologic model change detection at the catchment scale', *Water Resources Research,* 46, pp. W11544.

Zegre, N. P. (2009) *Local and downstream effects of contemporary forest harvesting on streamflow and sediment yield.* PhD thesis. Oregon State Univesity.

Zhang, X., Drake, N. A. and Wainwright, J. (2004) 'Scaling issues in environmental modelling', in Wainwright, J. and Mulligan, M.(eds) *Environmental modelling.* Chichester: Wiley, pp. 319-334.

Zhao, Y. (2008) 'Livestock impacts on hydrological connectivity', Circulation: the newsletter of the British Hydrological Society, 97, p.16-17.

Appendix 1. Newcastle University Stream Gauges

This Appendix gives detailed information on the Newcastle University stream gauges.

For all stream gauges (Sections 1.1 – 1.23) the information includes:

- A table with general information about the gauge, such as location description, grid reference, elevation, upstream abstraction information, catchment area, related sites, the barometer used for corrections, installation date, record interval, and quality assurance notes
- A schematic figure of the location of the gauge in the Hodder catchment and a photograph of the gauge
- A table with information on the land use management changes upstream of the gauge
- A schematic of the river cross section at the location of the gauge
- A table with information regarding the rating curve, such as observed stage range, number of gaugings, percentage of the highest gauging stage of the maximum observed stage, and percentage of extrapolated time
- A plot of the observed data range, the discharge gaugings, and the extrapolated rating curve

CD-ROM WITH THIS INFORMATION FOR EACH GAUGE IS LOCATED IN BACK OF THESIS

Appendix 2. Statistical analyses related to Chapter 5

A.2.1 Non-linear Regression Lines

A.2.1.1 Introduction

As part of the SDD analysis a nonlinear (amoeba) regression was fitted through the recession data according to Equation A.2.1. The recession data are presented as extracted data pairs for the observed discharge (Q) and its rate of change (dQ/dt) for the recession parts of the hydrograph.

$$\frac{dQ}{dt} = mQ^n \qquad \text{(Equation A.2.1)}$$

For Equation A.2.1, the *m* and *n* parameters are optimised using a multidimensional downhill simplex optimisation method, based on Nelder and Mead (1965), as programmed for FORTRAN in the subroutine 'amoeba' (Press et al., 1992).

A full description of the analysis is given in Chapter 5. This appendix section describes the statistical analysis procedures and the results of the following tests related to the non-linear regressions of Equation A.2.1:

- Relating to Section 5.3.2 (see Figures 5.22-5.24) - yearly periods of the Footholme (FH), and Hodder Place (HP) gauges with long term data (12 pre-change years, 1 post-change year):

- Test for equality of the parameters m and n for all pre-change periods
- Test for equality of the parameters m and n for pre- and post- change period

These two tests are described in Sections A.2.1.2 and A.2.1.3 respectively.

- Relating to Section 5.4.1 - short term pre and post change periods for all gauges:

- Test for equality of the parameters m and n for pre- and post-change period (described in Section A.2.1.4)

For all tests the null hypothesis is that all samples are from the same population (i.e. there is no significant difference between all pre-change parameters and/or the pre- and post-change parameters of the regression lines).

Compared to the linear regression theory, significance testing for nonlinear regressions such as the amoeba regression is more complex. The non-linear theory is only approximate and obtaining meaningful results from non-linear statistical theories might not be viable. It would be possible to fit a linear model through the data and perform statistical tests of significance on these, though the physical interpretation of the regressions would be lost. In order to obtain the sampling properties of the parameter estimates from the non-linear regression, re-sampling techniques were employed as described in this Appendix. The so-called bootstrap method (e.g. Efron and Tibshirani, 1993) is versatile and allows for non-constant variance of the errors in a straightforward way. Common bootstrap procedures are parametric (fit a plausible distribution to the residuals and draw random samples from the distribution) and re-sampling (re-sample the actual residuals with replacement). Here, an empirical distribution is fitted to the residuals and random samples are drawn from this.

A.2.1.2 Hypothesis testing: equality of the *m* and *n* parameters for all pre change periods (long term records at Footholme and Hodder Place)

To test the hypothesis of equality of all *m* and *n* parameters for all pre-change periods, the variance of the different pre-change estimates can be compared with the average variance of the population parameters of the individual years, using an F test. Through bootstrapping (e.g. Efron and Tibshirani, 1993) it is possible to obtain estimates of the parameter properties such as the mean and variance, by estimating those properties through resampling.

For a given data set, the main bootstrap procedure is as follows:

1) Fit the model to the observed data set of size n and obtain parameter estimates *m* and *n* for the fitted model
2) Generate a random data sample of size n from the fitted model by generating the residuals using Monte Carlo sampling
3) Fit a model through the random sample of size n and obtain the 'bootstrap estimates ' of the *m* and *n* parameters

4) Repeat N times, with independent sequences of random numbers
5) Calculate the means, standard deviations and variances of the N 'bootstrap' estimates of the *m* and *n* parameters

To explain the bootstrap estimation procedure in more detail, an example is given for the data of a pre-change year (1996-1997) at Footholme.

During the first step, estimates of the *m* and *n* parameters were obtained from the observed data (-0.088 and 1.175 respectively).

There are two main approaches for the second step (2) of the bootstrap procedure. The first one involves fitting an appropriate distribution to the residuals; the second one involves resampling from the observed residuals. To find the appropriate approach, a good description of the residuals is needed first.

The residuals (ε) are defined as the estimates obtained by subtracting the observed responses (y_{obs}) from the predicted responses (y_{pred}), according to Equation A.2.2.

$$\varepsilon = y_{pred} - y_{obs} \qquad \text{(Equation A.2.2)}$$

Figure A.2.1 shows the residuals of the fitted model for the Footholme 1996-1997 recession data.

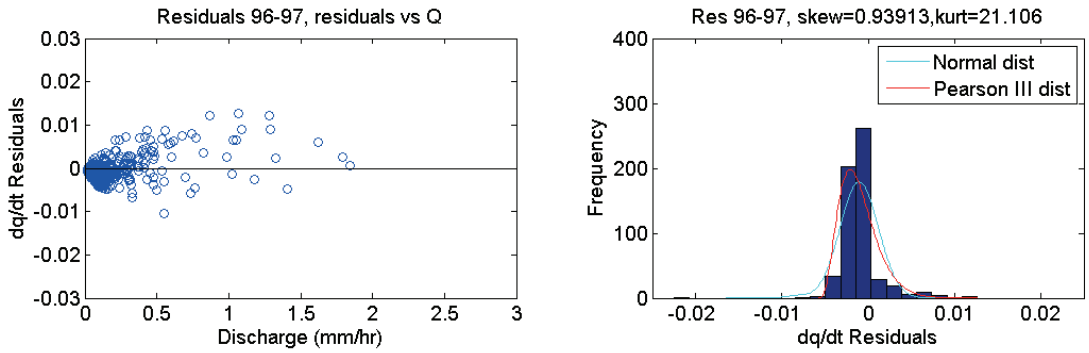

Figure A.2.1 Footholme 1996-1997 residuals of the fitted amoeba regression. Left: Discharge against residuals, Right: Scaled frequency diagram of the residuals with fitted Normal and Pearson III distributions

For the first approach to resampling the residuals, they need to be independently distributed, their variance should be constant across the range of the independent variable and they should follow a specific distribution, ideally normal. However, Figure A.2.1 (Left) shows that the variance of the residuals changes with the value of

discharge (the independent variable). In addition, an extensive analysis of the residuals showed that they could not be fitted satisfactorily with a normal distribution or any other distribution, such as the Pearson type III, that allows for some degree of skewness (asymmetry) and kurtosis ('peakedness') (Figure A.2.1 right).

As no suitable distribution could be identified to the residuals, it is preferred to resample from the observed residuals for the bootstrap procedure. Yet, for a specific discharge, it would be wrong to randomly sample from the full selection of residuals, because the residuals show some structure in their variance that should be accounted for. To represent the dependency of the variance of the residuals on the discharge, the observed residuals were subdivided into five classes, based on the discharge, in such a way that the variance is approximately constant within each class.

Figure A.2.2 (top) shows the five classes of discharge and the variation of the residuals within each of these classes. The middle plots of Figure A.2.2 show the frequency diagrams of the residuals for all five classes. From the top and middle plots it is clear that there is some bias in the residuals: e.g. for class 2 most residuals are negative and there is a high concentration of residuals around -0.0015. The bottom plots show the cumulative distribution of the residuals for each of the five classes, which represents any bias well.

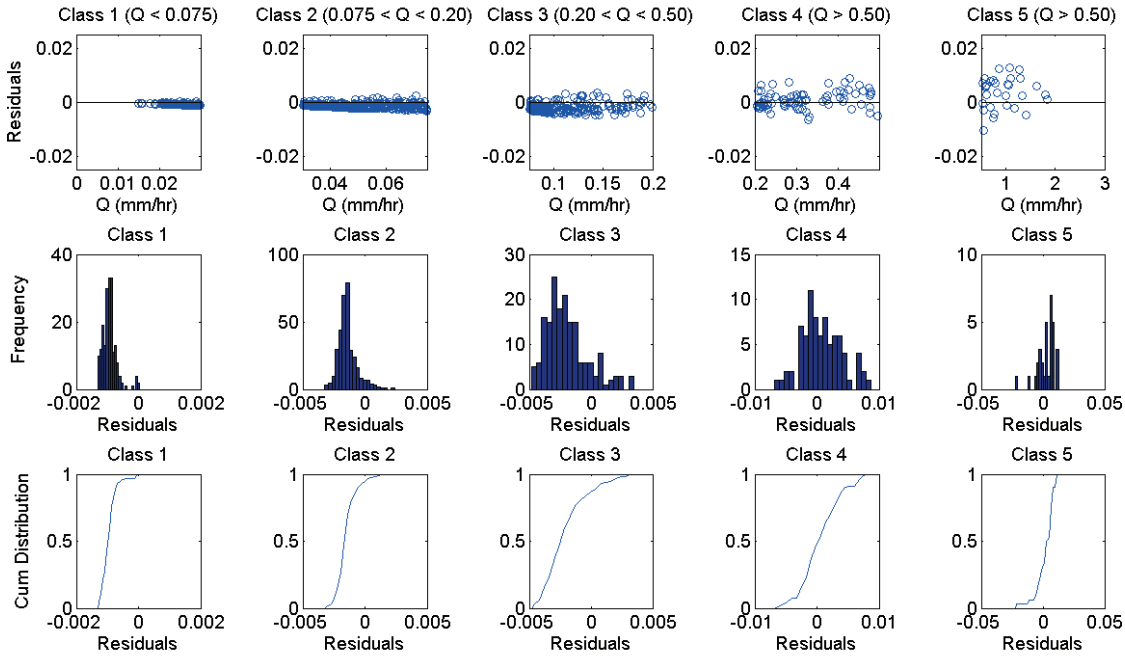

Figure A.2.2 Footholme 1996-1997 residuals of the fitted amoeba regression, subdivided in to five classes, according to discharge. Top: discharge against residuals, Middle: frequency diagram of the residuals, Bottom: cumulative distribution of the residuals

For each class, the corresponding cumulative distribution can be used to resample the residuals for the observed discharges within the class, so that the bias and distribution of the residuals is well represented in the bootstrap sample. This can be done by generating a uniformly distributed random number between 0 and 1 for each discharge value within a class (the cumulative distribution variable is uniformly distributed between 0 and 1), and obtaining the corresponding residual from the inverse of the cumulative distribution plot.

Using the fitted model with m= -0.088 and n=1.175, resampled values of dQ/dt can then be obtained for all observed discharge values.

Next, during step 3 of the bootstrap procedure, the m and n parameters of the resampled dataset can be estimated by applying the amoeba regression.

Figure A.2.3 shows the observed data and fitted amoeba regression for the Footholme 1996-1997 pre-change period in blue. It also shows five example resampled data sets and their corresponding fits. The m and n parameters of the bootstrap estimations are given in Table A.2.1

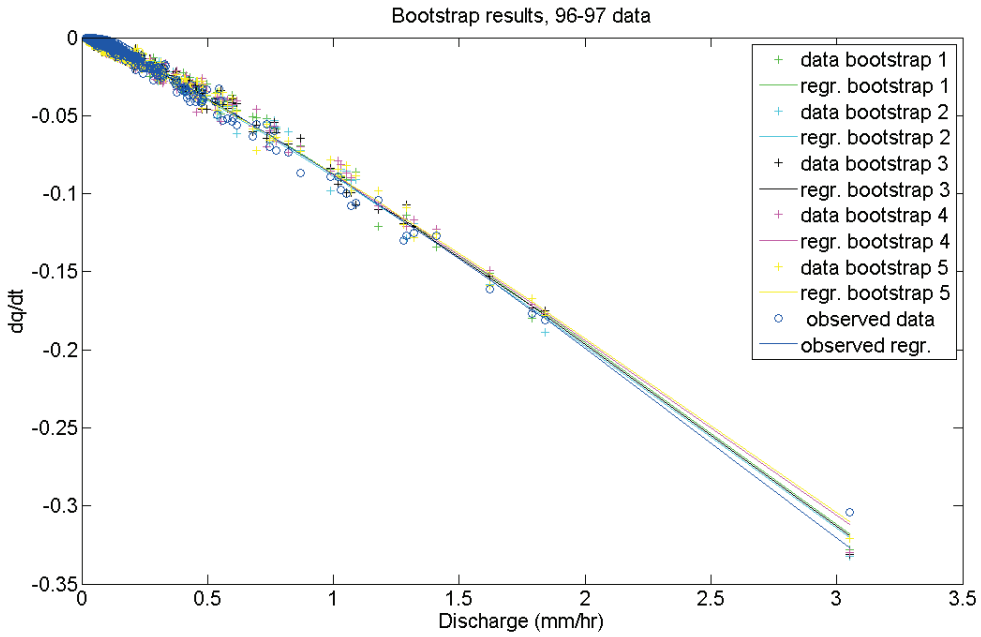

Figure A.2.3 Observed and fitted regression data (blue) and five bootstrap data sets with their corresponding fits.

Table A.2.1 *m* and *n* parameters of the amoeba regressions through the observed data and five bootstrap estimations

	Parameters	
Data set	**m**	**n**
Observed data	-0.08808	1.175119
Bootstrap estimation 1	-0.08750	1.157613
Bootstrap estimation 2	-0.08903	1.146144
Bootstrap estimation 3	-0.08806	1.154723
Bootstrap estimation 4	-0.08765	1.139903
Bootstrap estimation 5	-0.08743	1.134088

During step 4, the procedure is repeated N times, with N large enough so that the mean and variance of the m and n estimations remains constant. A test with different values of N revealed that when set at 1000, the properties of the *m* and *n* parameters remain stable and hence represent the population properties. The final step is then to obtain properties such as the mean and variance of the 1000 bootstrap estimated *m* and *n* parameters. The results of the bootstrap parameter estimations are given in Table A.2.2 for Footholme and Table A.2.3 for Hodder Place.

The F-test can be carried out to test the hypothesis of equality of all *m* and *n* parameters for all pre-change periods, by testing that the variance of the 12 pre-change estimates is equal to the average variance of the population parameters of the individual years. This is based on comparing the ratio of two variances ($F = S_1^2/S_2^2$, with $S_1^2 > S_2^2$). If there is no difference between the parameter variances of all pre-change years and the average parameter variances, the ratio of the variances will be (close to) 1. The null hypothesis of equal variances may be rejected when:

$F > F(\alpha, n_1\text{-}1, n_2\text{-}1)$

From the results in Tables A.2.2 and A.2.3 it may be concluded that all pre-change years are not statistically the same which can be attributed to the natural hydrological variability. For Footholme as well as Hodder Place the average variance of 1000 bootstrap estimated m and n parameters (highlighted in green) is much smaller than the variances of the 12 *m* and *n* parameters between years (highlighted in blue). For a 5% significance test, the ratio of the variances (F) should be smaller than 1.80. However, for Footholme the variance ratios for the *m* and *n* parameters are 16.79 and 9.40, respectively. For Hodder Place these are 22.35 and 19.57.

Table A.2.2 Footholme observed and bootstrap estimated *m* and *n* parameters for the pre-change periods in black and the post-change period in red. For the full pre-change period, the mean and variance of the observed *m* and *n* parameters, as well as the mean variance of the bootstrap estimations of each individual year are given.

	Observed parameters		Bootstrap results			
			mean		variance	
Period	***m***	***n***	***m***	***n***	***m***	***n***
Oct 1996 – Sep 1997, pre change	-0.0881	1.1748	-0.0883	1.1390	0.0000005	0.0000755
Oct 1997 – Sep 1998, pre change	-0.0881	1.2184	-0.0877	1.1802	0.0000008	0.0001109
Oct 1998 – Sep 1999, pre change	-0.0886	1.2773	-0.0871	1.2200	0.0000026	0.0002766
Oct 1999 – Sep 2000, pre change	-0.0847	1.1872	-0.0847	1.1427	0.0000007	0.0001122
Oct 2000 – Sep 2001, pre change	-0.0839	1.2565	-0.0831	1.1949	0.0000012	0.0002286
Oct 2001 – Sep 2002, pre change	-0.0829	1.2125	-0.0825	1.1524	0.0000008	0.0001136
Oct 2002 – Sep 2003, pre change	-0.0926	1.3079	-0.0912	1.2549	0.0000012	0.0001387
Oct 2003 – Sep 2004, pre change	-0.0891	1.2120	-0.0878	1.1513	0.0000010	0.0001400
Oct 2004 – Sep 2005, pre change	-0.0841	1.2278	-0.0828	1.1727	0.0000016	0.0002178
Oct 2005 – Sep 2006, pre change	-0.0926	1.2620	-0.0905	1.2024	0.0000022	0.0002224
Oct 2006 – Sep 2007, pre change	-0.0836	1.2857	-0.0833	1.2309	0.0000006	0.0001060
Oct 2007 – Sep 2008, pre change	-0.0814	1.2342	-0.0805	1.1836	0.0000011	0.0002064
mean	-0.0866	1.2380	-0.0858	1.1854	0.0000012	0.0001624
variance	0.0000201	0.0015266	0.0000170	0.0013438		
Sep 2009 - Aug 2010, post change	-0.0768	1.2558	-0.0767	1.2219	0.0000010	0.0002660

Table A.2.3 Hodder Place observed and bootstrap estimated *m* and *n* parameters for the pre-change periods in black and the post-change period in red. For the full pre-change period, the mean and variance of the observed *m* and *n* parameters, as well as the mean variance of the bootstrap estimations of each individual year are given.

	Observed parameters		Bootstrap results			
			mean		variance	
period	*m*	*n*	*m*	*n*	*m*	*n*
Oct 1996 - Sep 1997, pre change	-0.0783	1.3826	-0.0775	1.3408	0.0000020	0.0002747
Oct 1997 - Sep 1998, pre change	-0.0697	1.5335	-0.0678	1.4630	0.0000021	0.0004881
Oct 1998 - Sep 1999, pre change	-0.0852	1.5011	-0.0829	1.4454	0.0000023	0.0002845
Oct 1999 - Sep 2000, pre change	-0.0700	1.3636	-0.0699	1.3125	0.0000005	0.0001173
Oct 2000 - Sep 2001, pre change	-0.0667	1.3133	-0.0667	1.2633	0.0000006	0.0001610
Oct 2001 - Sep 2002, pre change	-0.0709	1.3183	-0.0697	1.2529	0.0000006	0.0001216
Oct 2002 - Sep 2003, pre change	-0.0772	1.4355	-0.0748	1.3702	0.0000018	0.0002602
Oct 2003 - Sep 2004, pre change	-0.0691	1.3066	-0.0685	1.2456	0.0000020	0.0004283
Oct 2004 - Sep 2005, pre change	-0.0707	1.4174	-0.0695	1.3689	0.0000022	0.0004091
Oct 2005 - Sep 2006, pre change	-0.0778	1.3858	-0.0753	1.3266	0.0000016	0.0002092
Oct 2006 - Sep 2007, pre change	-0.0655	1.3275	-0.0646	1.2625	0.0000016	0.0003927
Oct 2007 - Sep 2008, pre change	-0.0688	1.3486	-0.0682	1.2924	0.0000009	0.0001950
mean	-0.0725	1.3862	-0.0713	1.3287	0.0000015	0.0002785
variance	0.0000201	0.0015266	0.0000170	0.0013438		
Sep 2009 - Aug 2010, post change	-0.0768	1.2558	-0.0767	1.2219	0.0000012	0.0002713

A.2.1.3 Hypothesis testing: equality of the *m* and *n* pre- and post-change parameters (long term records at Footholme and Hodder Place)

The most direct approach is to test the difference in the mean of the 12 pre-change parameter estimates (one for each year of pre-change record) against the post changes parameter estimates (one year) using a two independent sample t-test with sample sizes 12 and 1, assuming that the populations have equal variances. As the variability of the parameters estimates about the mean can be partly due to sampling variability and partly due to variation between recessions, here it is not necessary to assume that all the pre-change parameters are equal.

The independent two sample t test for unequal sample sizes and equal variance follows equation A.2.3 (Chatfield and Collins, 2000):

$$t = \frac{\overline{x_{pre}} - \overline{x_{post}}}{S\sqrt{\frac{1}{n_{pre}} + \frac{1}{n_{post}}}} \qquad \text{(Equation A.2.3)}$$

for which $\overline{x_{pre}}$ and $\overline{x_{post}}$ are the mean pre and post change parameters, n_{pre} and n_{post} are the sample sizes of the pre and post change data sets, and:

$$S = \sqrt{\frac{(n_{pre}-1)S^2_{pre} + (n_{post}-1)S^2_{post}}{n_{pre}+n_{post}-2}} \qquad \text{(Equation A.2.4)}$$

where S^2_{pre} and S^2_{post} are the variances of the pre and post change samples respectively. The value of t follows the Student's t distribution with, (n_{pre} + n_{post} – 2) degrees of freedom (DF).

Table A.2.4 t-test results of m and n pre- versus post-change parameters for Footholme and Hodder Place

	Footholme, *m* parameter	**Footholme, *n* parameter**	**Hodder Place, *m* parameter**	**Hodder Place, *n* parameter**
$\overline{x_{pre}}$	-0.087	1.238	-0.072	1.386
$\overline{x_{post}}$	-0.077	1.256	-0.072	1.427
DF	11	11	11	11
S^2_{pre}	0.00001	0.00164	0.00003	0.00545
S	0.00372	0.04048	0.00581	0.07382
t	2.39176	0.40626	0.01872	0.51114
p	0.03575	0.69234	0.98540	0.61936

The results of the t-tests on the pre- versus post-change m and n parameters for FH and HP are shown in Table A.2.4. The table shows that, for FH, the post-change m parameter is significantly different from the pre-change m parameters at the 5% significance level (p=0.04), while there is no evidence against a hypothesis that the *n* parameter is the same for both periods (p=0.69). For HP both the pre- and post-change m and *n* parameters are statistically equivalent (p = 0.99 and 0.62 respectively).

However, the above test is applied separately to the individual *m* and *n* parameters, but the combination of the two fully describe the non-linear regressions. For this reason, the two parameters should be considered simultaneously. This can be done through the multivariate Hotelling T^2-test, as described by Chatfield and Collins (2000).

The Hotelling T^2-test follows the F distribution with (n_{pre} + n_{post} – p -1) degrees of freedom (DF). The F statistic can be calculated according to Equation A.2.5:

$$F = \frac{n_{pre}+ n_{post}-w-1}{w(n_{pre}+n_{post}-2)} \tau^2 \qquad \text{(Equation A.2.5)}$$

where:

$$\tau^2 = \frac{n_{pre}n_{post}}{n_{pre}+ n_{post}} (\overline{X_{pre}} - \overline{X_{post}})^T S^{-1} (\overline{X_{pre}} - \overline{X_{post}}) \qquad \text{(Equation A.2.6)}$$

for which the data matrix X_i is of order (n_i * *w*), and *S* is the covariance matrix, which is assumed to be the same for the two populations.

The results of the Hotelling T^2-test for FH and HP are shown in Table A.2.5. The table shows that for FH as well as HP, the *m* and *n* parameters simultaneously, are not significant at the 5% or 1% significance levels (p>0.05). From this it may be concluded that the Hotelling T^2-test has not provided the evidence against the null hypotheses of no difference between the pre- and post- change samples.

Table A.2.5 Hotelling T^2-test results of the multivariate pre- versus post-change parameters for Footholme and Hodder Place

	Footholme	Hodder Place
DF	11	11
F	3.66545	0.19338
p	0.06028	0.82691

The results of Section A.2.2 showed that it is not fully justified to just take the average results of the pre-change years, as there is some significant variability between years. Therefore, in addition to the three tests described above, Figure A.2.4 shows pair-wise bootstrap estimation variance ratios for the Footholme (top) and Hodder Place (bottom) *m* (left) and *n* (right) parameters of the individual years, including the post change years. The results are presented in frequency diagrams with the ratios of pre-change years in black and the ratios of post-change data with the pre-change years in red. The F statistics for the post change data fall within the range of all the pre-change years ratios, from which it may be concluded that no change has been detected.

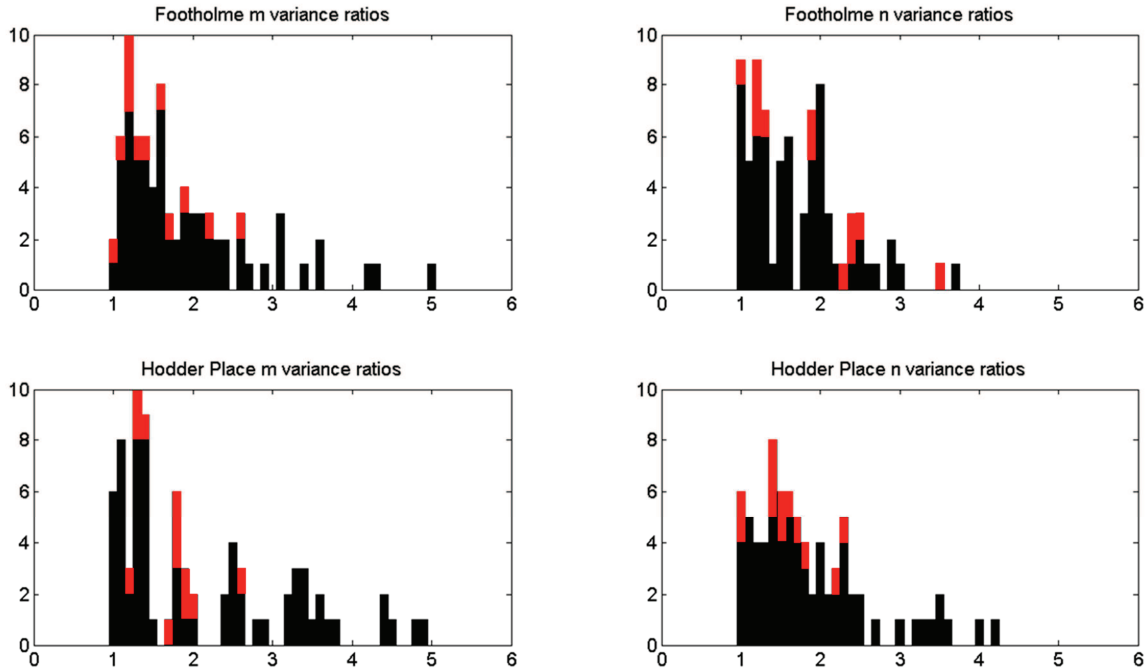

Figure A.2.4 Bootstrap estimation variance ratios between pre-change years (black) and post- and pre-change years in black. The variance ratios for *m* (left) and *n* (right) parameters are shown in the top two plots for Footholme and in the bottom two plots for Hodder Place.

A.2.1.4 Hypothesis testing: short term pre- and post- change records

The results in Section A.2.2 have shown that it is not possible to obtain meaningful results from statistical tests on the regressions if only short term data are available, as there is considerable variability between pre-change years due to natural hydrological variability. The available tests would therefore not be able to show where significant changes in the *m* and *n* parameters have occurred and where not. However, it is possible to look at a specific gauge in particular and compare the results of the

statistical tests with the results of other gauges nearby. Table A.2.6 (see also Figures 5.31-5.33) shows the *m* and *n* parameters of all short term pre- and post- change periods of the observed data, the bootstrap estimates with accompanying variances, and the results of the pre- versus post-change statistical test results of the bootstrap parameter variance ratio, as well as the t-test and Hotelling T^2 test on the bootstrap parameter means. All tests have been carried out as described in the previous two sections of this Appendix.

The gauges of CRO_mid, EAS_out and LOU_out have not undergone any land use/management change, but the data record has been subdivided into a 'pre-change' and a 'post-change' period, defined by the pre- and post-change periods of the nearest gauge that has undergone change. For CRO_mid this is CRO_sc5, for EAS_out this is CRO_out and for LOU_out this is LAN_out.

Table A.2.6 shows that the pre- and post-change parameter variance ratio of only a few gauges is close to 1, indicating that the variance is generally different between the two periods. In addition, the pre- and post- change parameter means are statistically different for the short-term records of all gauges ($p<0.01$), as a result of very high test statistics. However, this 'difference' seems to be especially large for CRO_sc5, a site which has been subjected to grip blocking, especially when the test results are compared with the neighbouring catchment CRO_mid which has not undergone any changes, and with the downstream site of CRO_weir. On the other hand, the test statistics of the three gauges for which no changes have occurred in the upstream area lie well within the range (or are even larger than) the test statistics of all other gauges (other than CRO_sc5) for which land use/management change did occur.

Table A.2.6 Short term observed and bootstrap estimated m and n parameters properties for the pre-and post-change periods for all gauges. Using the bootstrap parameter estimations, the results of the variance ratio, and the T-tests and Hotelling T2 tests on the means are also given.

Gauge	Area	Period	parameters		Bootstrap results				Variance Ratio		T test on means		Hotelling test on means
					mean		variance						
			m	*n*	*m*	*n*	*m*	*n*	*m*	*n*	*m*	*n*	
CRO_sc5	1.0	pre-change	-0.1546	1.4510	-0.1607	1.4128	0.0000068	0.0004506	2.80	1.33	393.48	131.50	304484.86
		post-change	-0.1189	1.3015	-0.1230	1.2782	0.0000024	0.0005981					
BRE_sap	1.7	pre-change	-0.1641	1.1013	-0.1678	1.0627	0.0000093	0.0009110	1.75	1.53	69.18	72.06	13031.40
		post-change	-0.1561	1.2111	-0.1595	1.1511	0.0000053	0.0005951					
LOS_mid	2.5	pre-change	-0.1198	1.6748	-0.1223	1.6211	0.0000075	0.0016708	1.83	2.07	44.41	64.71	10472.14
		post-change	-0.1169	1.7231	-0.1175	1.7229	0.0000041	0.0008078					
BRE_rhw	2.8	pre-change	-0.2013	1.2262	-0.2127	1.1705	0.0000253	0.0007682	3.90	2.40	85.40	100.64	41056.25
		post-change	-0.1883	1.3238	-0.1975	1.2754	0.0000065	0.0003203					
CRO_mid	3.6	pre-change	-0.1411	1.3798	-0.1487	1.2850	0.0000047	0.0005241	1.97	1.76	206.65	168.62	80864.54
		post-change	-0.1290	1.5070	-0.1313	1.4378	0.0000024	0.0002978					
HAR_out	4.9	pre-change	-0.1495	1.4422	-0.1504	1.4088	0.0000073	0.0013760	1.68	2.18	112.64	70.12	10850.25
		post-change	-0.1352	1.3513	-0.1383	1.3096	0.0000043	0.0006306					
WHI_mid	10.0	pre-change	-0.1323	1.3058	-0.1350	1.2775	0.0000035	0.0004035	1.35	1.06	78.00	91.78	8971.31
		post-change	-0.1367	1.2077	-0.1421	1.1939	0.0000047	0.0004265					
CRO_weir	10.4	pre-change	-0.1449	1.4999	-0.1466	1.3718	0.0000067	0.0005290	1.03	1.01	66.91	106.64	11435.67
		post-change	-0.1388	1.5579	-0.1388	1.4818	0.0000069	0.0005364					
BRE_out	11.0	pre-change	-0.1550	1.6911	-0.1569	1.6618	0.0000159	0.0022827	4.01	1.10	29.81	178.19	36535.48
		post-change	-0.1651	1.7431	-0.1526	1.3634	0.0000636	0.0025024					
EAS_out	13.3	pre-change	-0.1819	1.3301	-0.1820	1.2217	0.0000093	0.0006073	2.15	1.58	151.71	161.85	51134.66
		post-change	-0.1608	1.4493	-0.1643	1.3827	0.0000043	0.0003833					
WHI_out	13.6	pre-change	-0.1730	1.2304	-0.1745	1.1906	0.0000078	0.0005048	1.72	1.25	368.74	373.03	210851.28
		post-change	-0.1278	1.5450	-0.1337	1.5880	0.0000045	0.0006310					

Gauge	Area	Period	parameters		Bootstrap results				Variance Ratio		T test on means		Hotelling test on means
					mean		variance						
			m	*n*	*m*	*n*	*m*	*n*	*m*	*n*	*m*	*n*	
LAN_mid	15.0	pre-change	-0.1457	1.4793	-0.1459	1.3923	0.0000082	0.0008742	1.03	1.39	66.31	28.43	15876.32
		post-change	-0.1539	1.4987	-0.1543	1.4272	0.0000080	0.0006293					
CRO_out	21.1	pre-change	-0.1421	1.3940	-0.1473	1.3090	0.0000068	0.0009717	1.73	1.73	193.33	37.39	30017.55
		post-change	-0.1236	1.4167	-0.1273	1.3553	0.0000039	0.0005626					
Footholme	25.3	pre-change	-0.1503	1.3972	-0.1526	1.3634	0.0000051	0.0005248	1.35	1.99	4.67	36.70	2595.75
		post-change	-0.1485	1.3601	-0.1530	1.3308	0.0000038	0.0002641					
LAN_out	27.7	pre-change	-0.1409	1.5319	-0.1392	1.4215	0.0000065	0.0008024	1.60	1.00	82.83	151.12	92546.35
		post-change	-0.1468	1.6293	-0.1499	1.6127	0.0000103	0.0008012					
LOU_out	47.3	pre-change	-0.1327	1.2240	-0.1358	1.1402	0.0000083	0.0005272	1.70	1.50	51.24	100.92	8988.41
		post-change	-0.1307	1.3093	-0.1299	1.2348	0.0000049	0.0003509					
HOD_mid	110.3	pre-change	-0.1143	1.3551	-0.1149	1.2397	0.0000058	0.0006856	2.56	1.70	93.78	81.81	97566.15
		post-change	-0.1240	1.3681	-0.1283	1.3510	0.0000148	0.0011679					
Hodder Place	261.0	pre-change	-0.1048	1.4341	-0.1159	1.3095	0.0000029	0.0003582	1.73	1.08	119.22	39.06	31714.24
		post-change	-0.1050	1.4453	-0.1265	1.3419	0.0000049	0.0003329					

A.2.2 Peak Flow Regressions

A.2.2.1 Introduction

This section describes the statistical analysis procedures and the results of the following tests related to the linear regressions for peak flow:

- Relating to Section 5.3.4 - long term pre and post change periods (FH and HP):

  - Test for equality of slope and intercept of the linear regressions related to API at the time of peak and Peak Flow, for all pre-change periods
  - Test for equality of slope and intercept of the linear regressions related to observed and simulated peak flows, using parameters of all pre- and post-change periods

These two tests are described in Section A.2.2.2.

- Relating to Section 5.4.3 - short term pre and post change periods for all gauges:

  - Test for equality of slope and intercept of the linear regressions related to pre-change period observed and simulated peak flows, using parameters of all pre- and post-change periods

This test is described in Section A.2.2.3.

For all tests the null hypothesis is that all samples are from the same population (i.e. there is no significant difference between the slope and intercept of the regression lines).

A.2.2.2 ANOVA tests on linear regressions (long term records)

The full procedure of the ANOVA tests on linear regressions has been applied according to Holder (1985), Section 1.3.2. The test results in the tables below are according to the table on page 20 in Holder (1985).

The null hypothesis (equal slope and equal intercept) may be accepted when (Holder, 1985):

$$\frac{Difference\ in\ slopes\ mean\ square}{Residual\ mean\ square} < F(n-1, N-2n, 1-\propto) \quad \text{(Equation A.2.7)}$$

and:

$$\frac{Difference\ in\ intercept\ mean\ square}{Residual\ mean\ square} < F(n-1, N-2n, 1-\propto)$$ (Equation A.2.8)

where *n* is the number of data sets and *N* is the total number of data pairs.

The test results of the regressions of peak discharge on API for all pre-change years (see Figures 5.28 and 5.29) show that they are not all statistically the same (Tables A.2.7 and A.2.8). On the other hand, the test results of the regressions of simulated versus observed discharge (see Figure 5.30), using the SDD parameters of all pre-change as well as the post-change year show that they are all statistically the same (Tables A.2.9 - A.2.12). Hence, the comparison between observed and simulated peak flows, using parameters of pre- and post-change years is more appropriate for change detection in peak flows. The results also show that the post-change parameters are just as able to adequately predict the peak flow response as any set of pre-change parameters, and so there is no reason to suggest that the changes in LUM have had an effect on the peak flow response simulated by the SDD model.

Table A.2.7 Footholme ANOVA results, peak discharge versus API at peak time - linear regressions for pre-change years only

	Sum of Squares	DF	Mean Square	Mean Square Ratio	F (0.05)	P
Overall regression	1761.4560	1	1761.4560			
Difference in intercept	10142.5100	6	1690.4180	216.6777	2.1553	<0.000
Difference in slopes	3597.3200	6	599.5534	76.8507	2.1553	<0.000
Residual	1256.0470	161	7.8015			
Total	16757.3300	174				

Table A.2.8 Hodder Place ANOVA results, peak discharge versus API at peak time - linear regressions for pre-change years only

	Sum of Squares	DF	Mean Square	Mean Square Ratio	F (0.05)	P
Overall regression	879.3056	1	879.3056			
Difference in intercept	5605.0470	6	934.1744	406.4880	2.1553	<0.000
Difference in slopes	2249.7930	6	374.9655	163.1590	2.1553	<0.000
Residual	370.0037	161	2.2982			
Total	9104.1490	174				

Table A.2.9 Footholme ANOVA results, simulated discharge using parameters of other pre- and post-change years and the versus 0203 observed peak discharge - linear regressions

	Sum of Squares	DF	Mean Square	Mean Square Ratio	F (0.05)	P
Overall regression	57.4845	1	57.4845			
Difference in intercept	0.8091	7	0.1156	0.7394	2.0596	0.6388
Difference in slopes	0.1447	7	0.0207	0.1323	2.0596	0.9958
Residual	28.7620	184	0.1563			
Total	87.2000	199				

Table A.2.10 Footholme ANOVA results, simulated discharge using parameters of other pre- and post-change years versus 0607 observed peak discharge - linear regressions

	Sum of Squares	DF	Mean Square	Mean Square Ratio	F (0.05)	P
Overall regression	60.8868	1	60.8868			
Difference in intercept	2.0172	7	0.2882	1.5831	2.0596	0.1458
Difference in slopes	0.2566	7	0.0367	0.20139	2.0596	0.9848
Residual	33.4932	184	0.1820			
Total	96.6538	199				

Table A.2.11 Hodder Place ANOVA results, simulated discharge using parameters of other and post-pre-change years versus 0203 observed peak discharge - linear regressions

	Sum of Squares	DF	Mean Square	Mean Square Ratio	F (0.05)	P
Overall regression	23.9291	1	23.9291			
Difference in intercept	0.1612	7	0.0230	0.4404	2.0596	0.8757
Difference in slopes	0.0421	7	0.0060	0.1149	2.0596	0.9973
Residual	9.6199	184	0.0523			
Total	33.7522	199				

Table A.2.12 Hodder Place ANOVA results, simulated discharge using parameters of other and post-pre-change years versus 0607 observed peak discharge - linear regressions

	Sum of Squares	DF	Mean Square	Mean Square Ratio	F (0.05)	P
Overall regression	44.7662	1	60.8868			
Difference in intercept	0.4878	7	0.0697	1.1641	2.0596	0.3255
Difference in slopes	0.1037	7	0.0148	0.2475	2.0596	0.9724
Residual	11.0139	184	0.0599			
Total	56.3715	199				

A.2.2.3 t tests on linear regressions (short term records)

The t tests on the slope and intercept of the linear regressions of the simulated versus observed peak flows (Figure 5.36), based on the pre- and post-change parameters, have been applied according to Kleinbaum et al. (1988).

To test the equality of slopes, the test statistic t is given by Equation A.2.9:

$$t = \frac{slope_{pre} - slope_{post}}{S_{slope}} \qquad \text{(Equation A.2.9)}$$

where S_{slope} is an estimate of the standard deviation of the estimated difference between the two slopes (Kleinbaum et al., 1988), according to:

$${S_{slope}}^2 = {S_{P,YX}}^2 \left[\frac{1}{(n_{pre}-1){S_{Xpre}}^2} + \frac{1}{(n_{post}-1){S_{Xpost}}^2}\right] \qquad \text{(Equation A.2.10)}$$

for which ${S_{Xpre}}^2$ and ${S_{Xpost}}^2$ are the variances of the x data (here: observed peak flows) and ${S_{P,YX}}^2$ is a pooled estimate of the variance following:

$${S_{P,YX}}^2 = \frac{(n_{pre}-2){S_{YXpre}}^2 + (n_{post}-2){S_{YXpost}}^2}{(n_{pre}+n_{post}-4)} \qquad \text{(Equation A.2.11)}$$

where ${S_{YXpre}}^2$ and ${S_{YXpost}}^2$ are the residual mean square errors of the datasets.

To test the equality of intercepts, the test statistic T is given by Equation A.2.12:

$$t = \frac{intercept_{pre} - intercept_{post}}{S_{intercept}} \qquad \text{(Equation A.2.12)}$$

where $S_{intercept}$ is an estimate of the standard deviation of the estimated difference between the two intercepts (Kleinbaum et al., 1988), according to:

$${S_{intercept}}^2 = {S_{P,YX}}^2 \left[\frac{1}{n_{pre}} + \frac{1}{n_{post}} + \frac{{\bar{X}^2}_{pre}}{(n_{pre}-1){S_{Xpre}}^2} + \frac{{\bar{X}^2}_{post}}{(n_{post}-1){S_{Xpost}}^2}\right] \qquad \text{(Equation A.2.13)}$$

Both statistics will have the t distribution with $n_{pre} + n_{post} - 4$ degrees of freedom.

The test results in Table A.2.13 show, with three exceptions, that all pre- versus post-change slopes and intercepts are statistically the same, and no change has hence been detected. The exceptions are rejections of the null hypothesis regarding the slopes of the three sites that have relatively short pre- or post-change periods (CRO_out, HAR_out, and HOD_mid). It has been argued before that this may have resulted in

insufficient recession data for the optimisation of the pre- and post-change SDD parameters.

It is noted that visually the pre- versus post-change differences in slopes and intercepts are the highest for CRO_sc5 (Table A.2.13 and Figure 5.36). This is not reflected in the results of the statistical analyses, as the estimated standard deviations of the estimated differences between the slopes and intercepts of CRO_sc5 are relatively high, compared to those at the other sites (Table A.2.13).

Table A.2.13 T-test results on equality of slope and intercept of short term simulated peak flow using pre- and post-change parameters versus observed pre-change peak flows

location	Slope, pre	Slope, post	S_{slope}	T, slope	p, slope	Intercept, pre	Intercept, post	$S_{intercept}$	T, intercept	p, intercept
CRO_sc5	0.674	0.490	0.2113	0.874	0.387	0.626	0.800	0.2595	0.671	0.505
BRE_sap	0.845	0.733	0.0563	2.001	0.051	-0.210	-0.185	0.094	0.266	0.791
LOS-mid	1.365	1.372	0.0052	1.345	0.185	-0.336	-0.323	0.0199	0.638	0.527
BRE_rhw	1.016	0.954	0.0835	0.743	0.461	0.663	0.734	0.1118	0.642	0.524
CRO_mid	0.727	0.755	0.0932	0.307	0.760	1.188	1.061	0.1181	1.071	0.290
HAR_out	1.021	0.968	0.0161	3.286	0.011	0.232	0.259	0.0484	0.570	0.572
WHI_mid	1.019	0.977	0.0226	1.858	0.070	0.193	0.280	0.0712	1.225	0.227
CRO_weir	1.279	1.245	0.0345	0.982	0.331	0.006	0.004	0.0516	0.022	0.982
EAS_out	1.010	0.995	0.0409	0.360	0.721	0.360	0.250	0.0565	1.946	0.058
CRO_out	1.160	1.074	0.0421	2.036	0.048	0.081	0.065	0.0751	0.217	0.830
Footholme	1.024	1.004	0.0457	0.434	0.666	0.145	0.165	0.0827	0.241	0.811
LOU_out	0.621	0.644	0.0352	0.638	0.526	0.614	0.552	0.0625	0.996	0.324
HOD_mid	1.459	1.554	0.0263	3.616	0.001	-0.240	-0.277	0.0347	1.079	0.286
HP	1.024	1.024	0.0177	0.020	0.984	-0.117	-0.121	0.0463	0.077	0.939

References

Chatfield, C. and Collins, A. J. (2000) *Introduction to multivariate analysis.* Boca Raton, Florida: Chapman and Hall/CRC Press.

Efron, B. and Tibshirani, R. (1993) *An introduction to the bootstrap.* Boca Raton, Florida: Chapman & Hall/CRC.

Holder, R. L. (1985) *Multiple regression in hydrology.* Wallingford: Institute of Hydrology.

Kleinbaum, D. G., Kupper, L. L. and Muller, K. E. (1988) *Applied regression analysis and other multivariable methods.*Second ed Boston: PWS-KENT Publishing Company.

Nelder, J. A. and Mead, R. (1965) 'A simplex method for function minimization', *Computer Journal,* 7, pp. 308-313.

Press, W. H., Teukolsky, S. A., Vetterling, W. T. and Flannery, B. P. (1992) *Numerical recipes in FORTRAN - The art of scientific computing.*Second ed Cambridge: Cambridge University Press.

Appendix 3. Draft MURSAFF journal paper

This appendix provides a draft of a paper submitted to a hydrological journal.

Dialogue between field hydrologist and modeller: **new physically-based catchment model and its application to blocking open drains in peatland**

Authors: J.R.M.C. Geris, and J. Ewen

Abstract

Field hydrologists and catchment modellers face the challenge of capturing the complexity of the flows and storages observed in the field and incorporating the results into practical tools for catchment managers and regulators interested in problems such as flood risk. A new Model for Upland Runoff Storage and Flow Fields (MURSAFF) is developed based on a dialogue between a field hydrologist and a modeller. The aim is to improve the level of realism when modelling complex landscapes, and in particular to capture the geometry of the storage and flow fields and the dynamics of flow. The model uses a freeform polygon mesh that is developed interactively using field evidence and reports generated by the model. In its first application, MURSAFF is used to model the peatland landscape in the Sapling Clough headwater subcatchment (1.7 km^2) of the River Hodder catchment, NW England, UK. This has networks of open drains (grips) that were blocked under the United Utilities Sustainable Catchment Management Programme (SCaMP). The resulting simulations agree with field evidence that, immediately after blocking, there is only a small impact on peak flows. Some advantages of the MURSAFF approach, in relation to simulating the sensitivity to changes in land use and management, are demonstrated by comparing results for free-form polygon, square and TIN meshes.

Keywords: Rainfall-runoff Modelling; Physically-based; Land Use; Land Management; Peatlands

1. Introduction

Recent severe floods in Europe have raised concern and awareness about flood risk and have led to a call for improved flood prevention and mitigation strategies (e.g. DEFRA, 2005; Environment Agency, 2009; Pitt, 2008). Land Use and Management Change (LUMC) in rural upland areas has been proposed as a mechanism that could help prevent flooding (Evrard et al., 2007; Parrott et al., 2010; Wheater and Evans, 2009). This is based on evidence that some modern farming and management practices have been linked to an increase in flooding in upland areas (e.g. Holman et al., 2002). The practices include peatland drainage (Lane, 2001; Longfield and Macklin, 1999) and increased stocking densities for sheep and cattle (Lane, 2001; Meyles et al., 2006). Generally, the effect of distributed changes in land use and management on flooding is not well understood (O'Connell et al., 2004; O'Connell et al., 2007). There is a local effect on the rate of runoff from hillslopes and agricultural fields, but no clear evidence for a resulting accumulated effect on flooding at larger scales downstream.

The demonstration example in this paper is for blocking upland moorland drainage ditches in peatland. Drain blocking is being implemented extensively in the UK, with the aim of improving the environmental condition of moorlands (Holden et al., 2007). Schematic representations of a moorland drain are given in Fig. 1. As a result of drain blocking, small storage ponds are created upstream of the blocks and there is a change in the process of runoff generation. Field studies have found that the water table rises in the vicinity of the drain (LaRose et al., 1997; Worrall et al., 2007), but may not rise to the level that would have been expected if the site was left intact (Holden et al., 2011). At points located 0.5 m away from drains, Wilson et al. (2010) reported up to a 40% increase in the presence of surface water after blocking. Some studies have suggested that at hillslope and small catchment scales (a few hectares), there can be a decline in average and peak flow rates (Shantz and Price, 2006; Wilson et al., 2010; Worrall et al., 2007). The scale of impacts varies between sites and studies. However, based on a modelling study, Ballard et al. (2010) suggested that the impact could result in either an increase or decrease in peak flows, depending on the local conditions of the drains. There may also be a further layer of complexity at scales >1 km^2, where blocking of extensive irregular drainage networks results in a landscape with changing flow fields and (transient) storage patterns (Ballard et al., 2011; Lane et al., 2003).

Fiener et al. (2011) recently identified the influence of the organisation and interaction of man-made complex spatial patterns as one of the largest research gaps associated with the spatio-temporal patterns in land use and management affecting surface runoff response of agricultural catchments. This further highlights the need to improve the knowledge of the influence of complex spatial patterns and (dis-)connectivity and to implement this knowledge in new modelling tools (Fiener et al., 2011). The purpose here is therefore to model the geometrical complexity in the spatial arrangement of drains, their connectivity to the river network, and the distribution of water storages in the peat and as surface water (Geris et al., 2010).

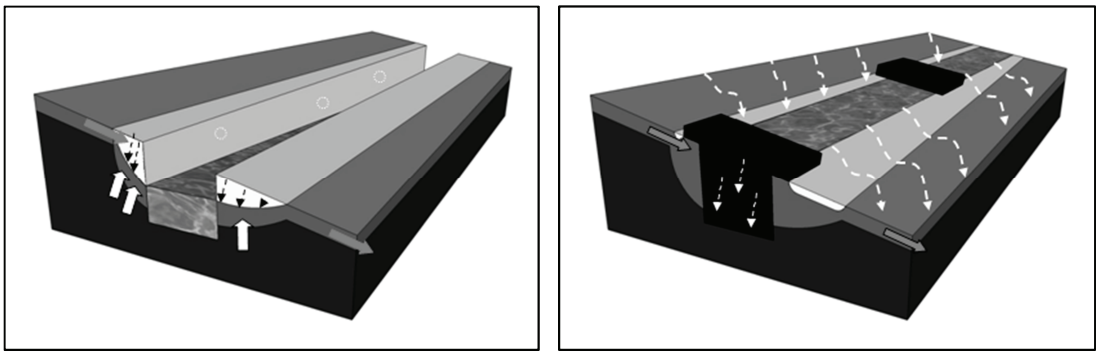

Figure 1. Schematic representation of an intact moorland drain (left) and a blocked drain (right), showing the within-channel water storage and the main flow directions (white arrows).

It is challenging for field hydrologists and modellers to agree on how to capture the complexity of the behaviour of drains and drain blocking within a model, for reasons that are well understood in terms of natural conflicts of interest between catchment managers, field hydrologists, and modellers (e.g. Beven, 1993; Dunn et al., 2008; Dunne, 1983; Klemeš, 1986a; Seibert and McDonnell, 2002): (1) catchment managers need reliable decision-support tools to give practical estimates for the aggregation and propagation of LUMC impacts; (2) field hydrologists know the realities of heterogeneity and complexity; and (3) catchment modellers have to deal with a tendency to value the perfection of particular, often quite limited, aspects of modelling over the need for complete models that can be used as practical tools. A particular problem faced when studying hydrology at small scales is that the available models are usually not able to adequately represent the complexity of the dominant local runoff generation processes and flow fields observed by field hydrologists (James et al., 2010; Kirchner, 2006; McDonnell et al., 2007). When studying LUMC, there is the further

problem that models calibrated accurately against observed data can give inaccurate predictions when used to estimate the impact of change, because they have the wrong sensitivities (Ewen et al., 2006; O'Connell et al., 2007).

It has been known for some time that distributed physically-based rainfall-runoff model based on property values measured in the field and laboratory are demanding to build and have limited success when tested against observations (Bathurst et al., 2004; James et al., 2010; Parkin et al., 1996). In recent years there has been a shift towards using field data in determining the model structure and field process-orientated models are increasingly being used for testing field hypotheses (e.g. Birkel et al., 2010; Clark et al., 2011; McMillan et al., 2011). The development of the new physically based model MURSAFF (Model for Upland Runoff Storage and Flow Fields) was also prompted by difficulties faced in reconciling field evidence about the effects that changes in land use management have on runoff with the way that the landscape and runoff are represented in catchment rainfall-runoff models. This problem arose in a combined field and modelling study focussing on the impact that changes made recently in upland rural land use and management in the Hodder catchment, northwest England, might have on the flood peaks downstream (Ewen et al., 2010).

The aim of this paper is to: (1) present the new physically-based modelling tool (MURSAFF) which is designed for investigating change impacts on the hydrological behaviour of geometrically complex environments while taking into account field observations, the needs of field hydrologists, and some of the concerns of hydrological modellers; and (2) investigate the short-term impact of drain blocking on runoff generation, flow connectivity, and catchment storage for drain blocking in the Sapling Clough (1.7 km^2) subcatchment of the River Hodder catchment.

2. Experimental Site Description

Sapling Clough is a moorland headwater catchment (Fig. 2). Its elevation ranges from 329 to 524 m and it receives approximately 1750 mm rainfall annually. Typical of UK moorland headwater catchments, it has a flashy discharge hydrograph. The catchment is primarily covered by blanket peat (classified as a histosol soil) with an average thickness of 1-3 m, underlain by carboniferous interbedded sequences of sandstones, silty mudstones and siltstone (Aitkenhead et al., 1992). The Winter Hill peat soil type

supports *Calluna, Molinia, Juncus* and *Spagnum* species. Owing to poor drainage properties of the peaty soil, the land is used mainly for game and some grazing, in addition to drinking water abstraction. Open drains were installed over approximately 35% of the catchment in the 1960s and 1970s, supported by the agricultural policy of that time, to improve the conditions for grazing and game. However, over time it has become clear that peatland drainage is largely inefficient and is sometimes detrimental to the quality of the environment (Stewart and Lance, 1983). Recently, the entire upper part of the Hodder catchment has been undergoing LUMC as part of the SCaMP programme (McGrath and Smith, 2006), which included blocking the drains in Sapling Clough during November 2008 (Fig. 2).

The Sapling Clough subcatchment has been monitored since June 2008 (Ewen et al., 2010). In addition to the two stream gauges (Fig. 2), there are two rain gauges nearby and an automatic weather station which supplies data for estimating evaporation. Data from these gauges are available at 15 min time intervals. Several field surveys were carried out to measure the cross-sectional profiles and network geometry for the drains and river channels, and the potential extra storage provided by ponds that develop upstream of the blocks.

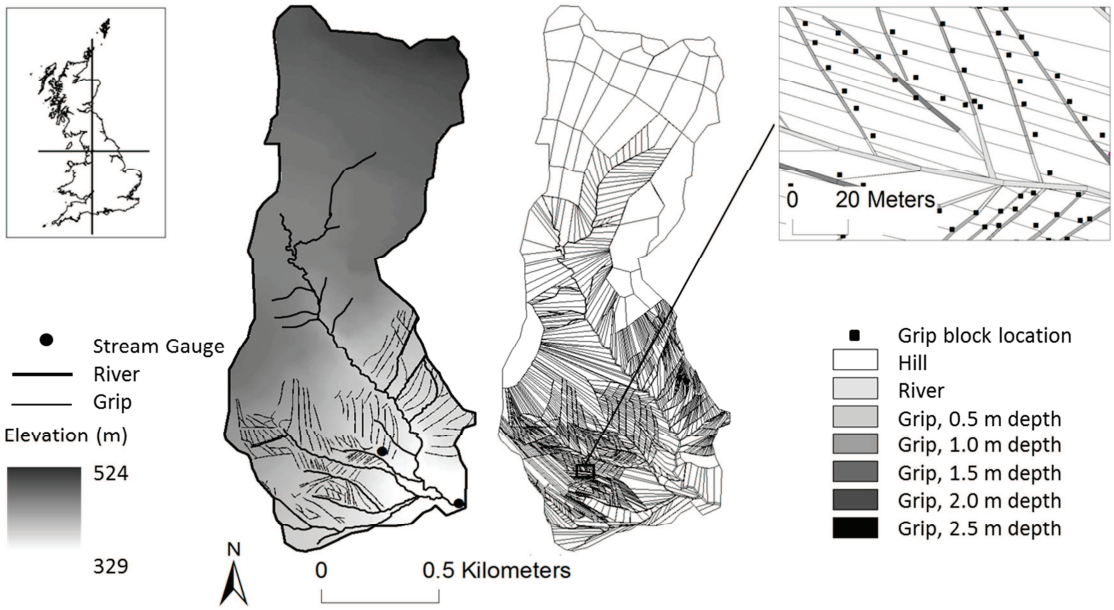

Figure 2. Sapling Clough catchment maps, showing elevation and the grips (left), and the MURSAFF mesh with shading showing the slab types (right). The zoom window shows the grip block locations, as mapped by the grip blocking machinery.

3. Grid Creation and Conceptual Design

It was clear from early on in the dialogue between the modeller and field hydrologist that the computational mesh types available in existing distributed catchment models (e.g. squares, rectangles and triangles) would make it difficult to represent the landscape and drain network. A more natural mesh was proposed by the field hydrologist. It is a significant undertaking to create and classify a computational mesh based directly on detailed local knowledge of a complex landscape. The irregular freeform polygon (FFP) mesh in Fig. 2 was created based on field observations and interpretations, in conjunction with digital information on the location of drains, blocks, and a 10 m Digital Elevation Model (DEM). The mesh comprises 3877 freeform polygon cells, called slabs, drawn with the aid of *ESRI* ARCGIS software. Its design depends largely on representing flow directions and having fine resolution where needed to capture spatial and temporal variations in storage and flow. The first step in creating the mesh was to draw the river and drain slabs. For the drain slabs, there are sub-types for unblocked and blocked conditions. The slabs for the unblocked condition have a channel and the slabs for the blocked condition have a pond. The second step in creating the mesh was to draw the hillslopes, taking into account topography, land use, and the main expected flow directions. To reduce the complexity of the models input data, the slabs were categorised into the seven basic types listed in the right hand side of Fig. 2.

4. Model Description

Once a draft version of the FFP mesh was available, storage and flow were discussed by the modeller and field hydrologist, and a model design developed. The main considerations for the modelling are:

1. it must use the nonlinear FFP mesh;
2. the need for incorporating detailed sub-grid descriptions for the geometry and hydrology within the polygon slabs; these are needed because very small scale features such as gross surface roughness due to heather clumping, and vertical stratification of porous media, can potentially play an important role;
3. the need for computational efficiency if large detailed grids are to be represented and simulations run for periods of several years;

4. the requirements of modern analytical tools, such as Algorithmic Differentiation; using these tools, work can get beyond the calibration/validation/application exercises that distributed models are usually limited to through the sheer effort required to set up and run them.

None of the existing approaches to modelling address all these considerations listed above. For example: integrated distributed modelling such as used in TOPMODEL (Beven and Freer, 2001; Beven and Kirkby, 1979) requires the behaviour within a cell to be quite simple to allow integration over the catchment; alternatively, GIS-based modelling (e.g. Miller et al., 2007) usually works with rectangular cells; and similarly, existing fully-distributed physically-based modelling (e.g. SHETRAN, Ewen et al., 2000) uses a mesh with limited cell geometry such as rectangles or triangles. Although triangular meshes are generally better at representing real terrain shapes (Bänninger, 2007; Vivoni et al., 2005), a large number of cells are needed to fully capture the geometrical complexity, and this can result in locally unrealistic flow fields. The model most similar to MURSAFF is MHYDAS (Moussa et al., 2002). This represents the catchment as a series of interconnected irregularly shaped field parts, based mainly on man-made hydrological discontinuities that are linked to the drainage network. For a fixed set of parameters, Lagacherie et al. (2010) recently demonstrated that the MHYDAS model performed significantly better using an irregularly shaped grid based on detailed field information, rather than one based on the information from a DEM only. MHYDAS has been applied to study the effects of artificial drainage networks (Levavasseur et al., 2012). However, the model has limitations in simulating flow directions as observed in the field. In addition, due to the nature of the model, the same grid cannot be used for both the unblocked and blocked cases because the network is represented as a series of linkages so cannot easily be adapted to represent ponding behind blocks such as pictured in Figure 1. The MURSAFF model was therefore developed.

The MURSAFF sub-grid properties and processes represented for a slab are listed in Table 1, and a schematic diagram of a cross-section through a slab is shown in Fig. 3. Quite a lot of detail can be specified for the sub-grid geometry and properties of a slab, including for vertical variations in physical properties, storages and flow rates. For clarity, not all this detail is shown in Fig. 3. Note that the ground surface can be incised

with a channel (which can exchange flow directly with adjacent slabs), or incised with ponds (which cannot exchange flow directly with adjacent slabs). Also note that the coarse texture for the surface can represented the effect of rills, vegetation clumps, etc. Some limitations are noted in the table, including the lack of a vegetation canopy to catch and store rainfall (not particularly relevant here) and the approach to representing overbank flow.

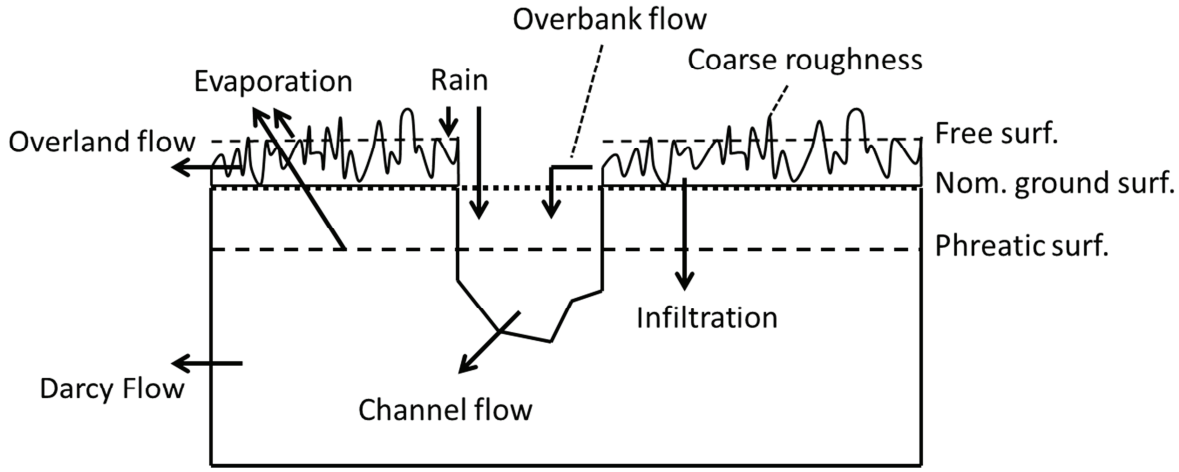

Figure 3 Schematic cross-section through a slab, showing storages and flows (if incised shape was pond instead of channel, diagram would be same but there would be no direct outflow of pond water)

Table 1 Slab properties and processes (z is elevation, which is zero at nominal ground level; t is time; * indicates parameters for slab)

Item	**Data**	**Symbol/ dependence**	**Equation**
Evaporation: actual		AE(t)	surface: AE = PE subsurface: AE = ε.PE
Evaporation: potential	Rate	PE(t)	
Infiltration		t	Rate equals k(0)
Overbank flow		t	Not included directly; incorporated within infiltration
Rainfall	Rainfall intensity	r(t)	
Subsurface capacity	Effective porosity	P(z)*	
Subsurface conductivity	Saturated hydraulic conductivity	k(z)*	
Subsurface flow		t	Darcy's law for flow through slab faces, depending on integral of k, driven by inter-slab ground

Item	Data	Symbol/ dependence	Equation
			surface elevation gradient
Subsurface storage fraction		ε(t)	Integral of P below phreatic surface, divided by total capacity
Surface flow: channel		t	Manning's equation, through slab faces, driven by inter-slab ground surface elevation gradient
Surface flow: overland		t	Manning's equation, through slab faces, depending on FP (representing rills etc.), driven by inter-slab ground surface elevation gradient
Surface capacity: channel	Plan area	CPA(z)*	
Surface capacity: pool	Plan area	PPA(z)*	
Surface pooling proportion	Fraction plan area ponded	FP(z)*	
Surface roughness: fine	Manning's exponent	n(z)*	
Surface storage: channel		t	Depth integral of CPA below free surface
Surface storage: ponding		t	Depth integral of FP below free surface
Surface storage: pool		t	Depth integral of PPA below free surface
Vegetation canopy		-	Not represented

Computationally, each slab has two storages, A and B where A is above the nominal ground level and B below. The channel and pools are incised into the ground, so lie below the nominal ground level. Both storages have a free water surface. The surface for A is the ponded surface and for B is the phreatic surface. A quasi-steady approach is used throughout the model, so the ponded, pooled and channel waters are in equilibrium with the adjacent porous media. This equilibrium means, for example, that the phreatic surface is continuous with the free surface in the pools and channel.

The main flow equations are Darcy's law and the Manning equation. Only one channel is allowed per slab, and this connects two faces of the slab's polygon. Overland and Darcy flow can take place through all the faces of the polygon.

A numerical model of this sort must be computationally efficient and unconditionally stable if it is to be of practical use. The direction of water flow depends on the ground slope and not the water elevations (a limitation of the prototype model), so the overall time-stepping solution can sweep through the mesh, from slab to slab, from high elevations to low. A fully-implicit mass-balance finite-difference approach is used for the slab calculations. Look-up tables are set up at the beginning of each simulation, to record solutions to the storage and flow equations that define the links between the various flows and the water surface elevations in the two storage compartments. These tables cover the full range of possible conditions that can exist in the slab (e.g. from very dry to saturated). When updating the water elevations for a slab, the current water storages and input rates are known, including the rates for rainfall, evaporation and flow from upstream. A simple form of mass balance calculation is carried out using this information and the result is entered into a table which returns the exact required fully-implicit solution, without requiring iteration.

Six depth-varying physical properties can be entered as parameters (marked by an asterisk in Table 1). Each slab type has its own set of physical properties, and the effect of LUMC is represented either by changing the properties directly or by changing the slab type (e.g. from unblocked or blocked subtypes for drains).

5. Grid Testing, Parameterisation and Calibration

Given that MURSAFF is designed to represent reality over a wide range of spatial scales, the demands for testing and improvement of the mesh are greater than they are for models that use a standard mesh and have a more limited range of applicability. The main aim in testing and improvement is to ensure that the slabs that are meant to exchange flow do exchange flow, and that networks that are intended to drain the catchment do drain the catchment. In the prototype version of MURSAFF there is also the difficulty that the directions of lateral flow are defined by the ground surface elevations, so care has to be taken that the node elevations for the slabs give a coherent draining mesh. This is similar to the problem faced in depitting a DEM when it is being used to create a channel drainage network.

There are six stages in testing and improvement: (1) identification and elimination of isolated polygon vertices, (2) identification and elimination of mismatched polygon

faces (add extra vertices if necessary), (3) find neighbouring slabs and matching faces, (4) walk and depit the drainage network, (5) apply general pit filling, and (6) walk and depit the entire mesh. For every stage, all improvements are checked against field observations.

Wherever possible, the physical properties take values from field observations or the literatures (see Geris, 2012). For example, the geometries for the river and drain channels and the drain storage ponds are from field surveys. The depth profile of the soil effective porosity (ranging from 0.2 at a depth of 0.5 m and below to 0.6 at the top of the soil profile) is based on values from the literature (e.g. Deeks et al., 2004; Reeve et al., 2001; Rizzuti et al., 2004). It is known that horizontal and vertical saturated hydraulic conductivity of peatland can exhibit great heterogeneity over short distances (Beckwith et al., 2003; Holden and Burt, 2003a), up to 2-3 orders of magnitude (Quinton et al., 2008), and can vary substantially between sites (Rycroft et al., 1975). Peatland soils generally have two main zones: the upper acrotelm, with a base of approximately 0.5 m depth, and the catotelm (Holden and Burt, 2003b). Within the acrotelm, substantial changes in the saturated hydraulic conductivity have been observed within the upper 5-10 cm. Given this complexity and variability, the saturated hydraulic conductivity of the vertical profile was set by optimisation against observed flow rates at the outlet from the subcatchment. During the optimisation, the lower acrotelm and the catotelm values were assumed to have conductivities of 0.01 and 0.0001, respectively, of that of the upper acrotelm layer. Calibration/validation used a split-sample approach (Klemeš, 1986b). The calibration of the hydraulic conductivity involved minimising the difference between the observed and simulated streamflow data at the catchment outlet for a full year of 15 min data starting 01/03/2009. The optimisation for calibration used a new “visual” metric based on the Nash Sutcliffe Efficiency (NSE) (Nash and Sutcliffe, 1970), calculated using the HMA (Hydrograph Matching Algorithm) from Ewen (2011). Small differences in timing are common when simulating flashy flows, and can have an unhelpfully disproportionately large effect on the NSE. In effect, the HMA was used to allow timing errors of up to 45 minutes (i.e. 3 time steps) to be neglected when calculating the NSE. Validation was for the period 01/08/2010 to 28/04/2011, inclusive. The result was a hydraulic conductivity of 5.86×10^{-3} m/s, with HMA-NSE values of 0.916 in calibration and 0.915 in validation; the

raw NSE values (which are not optimum because the model was calibrated to maximise HMA-NSE) were 0.80 and 0.64.

6. Results

Figure 4 shows the observed and simulated pre-blocking and post-blocking discharges (Q_{pre} and Q_{post}) for a relatively wet month (November 2009). There are only very small differences in timing, shape and amplitude between the pre- and post-blocking simulations, and overall good agreement with the observations. However, the peak flows are generally overestimated. The maximum reduction in peak flow is around 5%, for the relatively small event at 12/11/2009.

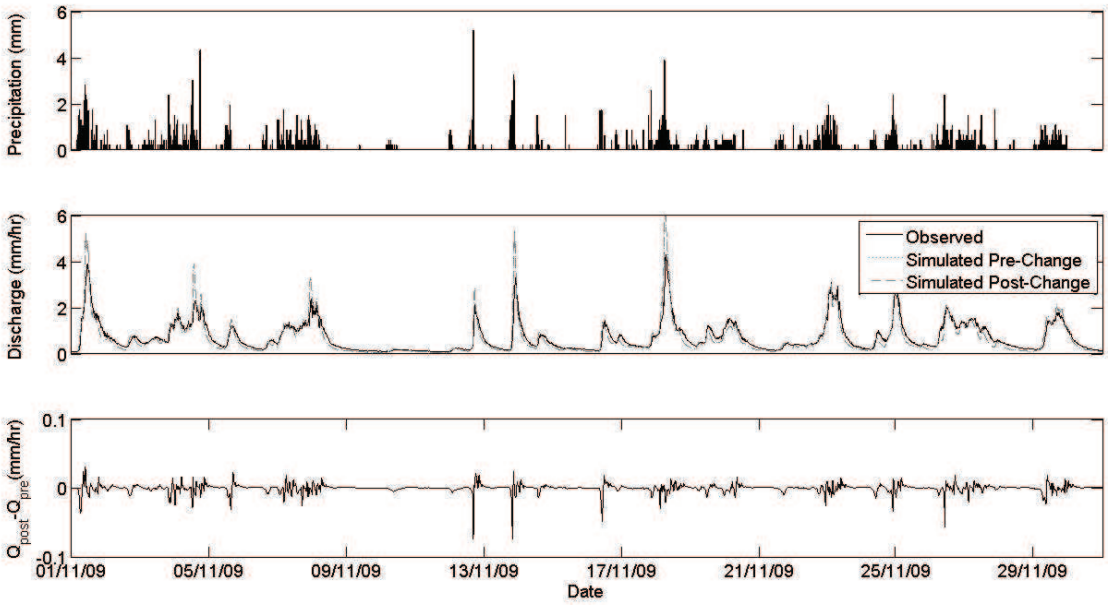

Figure 4 Observed precipitation (top), observed and simulated pre- and post-blocking discharge (middle), and difference between discharges (bottom), for Sapling Clough.

As a test of the general principle of mesh generation, square and triangular meshes were created for MURSAFF. Figure 5 shows that compared to the FFP mesh, these require many more cells to represent the drain network, and they distort the natural geometry and degrade some of the information from field observations. The square and triangular meshes were parameterised using the same property data and calibrated values as for the FFP mesh. However, to account for differences in slab size, the volume of the ponds had to be adjusted (especially for the 50m square mesh, where, for example, one slab can contain many drain ponds). The HMA-NSE metrics

for the calibration period were found to be 0.927, 0.926 and 0.927 for the 10m, 50m and TIN grids respectively (compared to 0.916 for the FFP mesh).

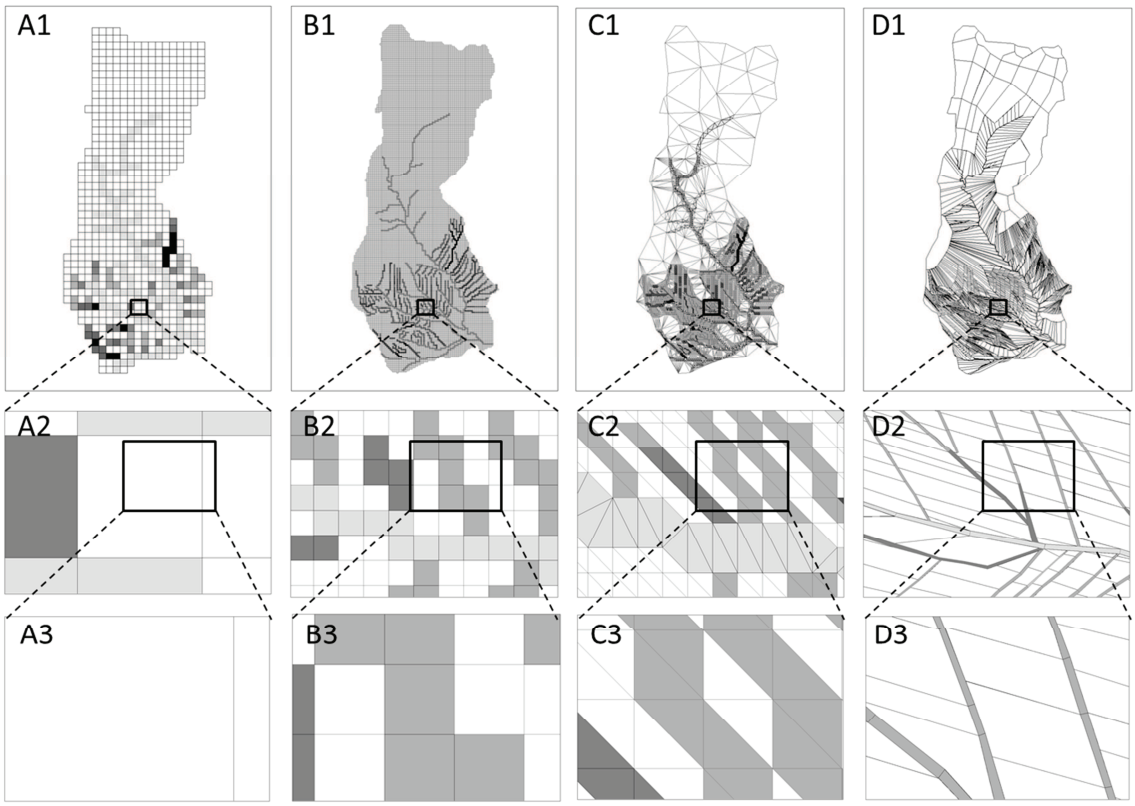

Figure 5 Four different meshes for Sapling Clough: rectangular 50 m (A, 711 slabs), rectangular 10 m (B, 16977 slabs), TIN (C, 7675 slabs) and the freeform polygon (FFP) (D, 3877 slabs), with zoom windows to demonstrate the level of detail represented by the grids.

Some results for the four grids are shown in Fig. 6, for the simulation of the impact of drain-blocking in the Sapling Clough catchment. One of the most noticeable results is that the simulated impact for discharge, i.e. Q_{post} - Q_{pre}, is considerably smaller for the FFP mesh than for the other three meshes (Fig. 6B). The FFP mesh was designed to give very small dynamic storage effects, to be consistent with the field observation that drains exert an effect within the porous media only very locally to the drains. Fig. 6C shows that on an area-average basis the dynamics within the slabs are fairly similar for three of the meshes, but for the 50m mesh there is considerable dampening of response. However, the area-average effects translate to quite different impacts on discharge because of the effects of the mesh geometry. For example, the slabs containing 1m deep slabs cover only a total of 0.5% of the catchment for the FFP mesh, but cover 4.7% for the 10m mesh, 5% for the 50m mesh, and 5.3% for the TIN mesh. In practice, the square and TIN meshes could be improved by reducing their slab sizes,

but the resulting meshes would have tens of thousands of slabs and be very expensive to run.

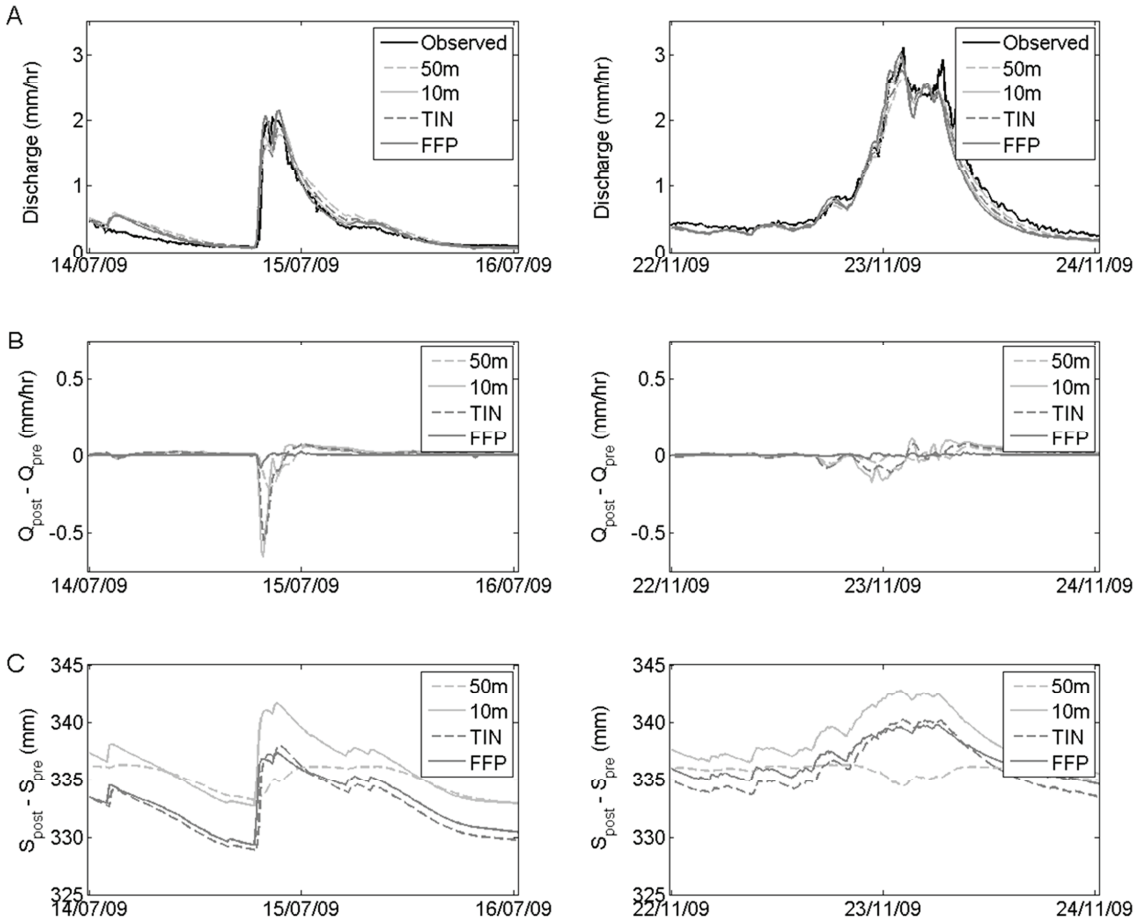

Figure 6 Example results for the four meshes for a summer (left) and a winter event (right): (A) observed and simulated post-blocking discharge; (B) simulated impact on discharge; (C) area-averaged simulated impact on depth of storage (mm water) for land area containing 1 m drains.

7. Discussion

There are two aspects to this work. First there is the development of the new physically-based catchment model MURSAFF (Model for Upland Runoff Storage And Flow Fields). Second, there is the application of the model to estimating the effects of land use management changes (LUMC). The example application described is a straightforward study of the short-term effect of blocking open drains in peatland. The problems of interest to catchment managers and field hydrologists, however, are often more subtle and demanding than this. For example, there is evidence that the effects of drain blocking may be different in the long term than in the short term (Spieksma, 1999; Worrall et al., 2007), so there is a need to model the variation of properties over

time. Also, the generally wetter antecedent conditions induced by drain blocking might, in time, give rise to more vigorous vegetation cover, and this will change the flow hydraulics, so vegetation changes may need to be modelled. There might also be some degree of resilience in the hydraulic catchment characteristics in responding to drain blocking, so feedback effects may need to be considered. Peat drainage has been associated with an increase in macropores and soil piping (Holden, 2005b), but it is unclear if and for how long this will remain active, so preferential flow may need to be modelled. And it is also noted that a restored peatland will not necessarily revert to an intact peatland, owing to irreversible changes in the physical properties as a result of draining (Holden, 2005a; Holden et al., 2011; Ramchunder et al., 2009), so, again, subtle variations in properties may need to be included in the modelling.

The question this raises is if the new model, or any other model, can rise to these challenges. In the work on developing the MURSAFF model, we have taken some very basic steps, aimed at being able to incorporate observations and interpretations from the field directly into a model, to give the field hydrologist better control over the modelling process. This has concentrated on the geometry of the landscape and channel system and led to the use of a freeform polygon mesh designed to capture the basic flow directions and hydrological elements that can be observed or interpreted in the field. Inevitable, this makes the process of generating the grid more difficult. It is, in effect, an interactive process, where the field hydrologist is aided by reasonably sophisticated, hydrologically-relevant, test results and reports generated by the model. MURSAFF provides opportunities for the field hydrologist to interpret and test field hypotheses about flow fields, runoff and storage.

In work going on in parallel with this modelling, detailed analyses of pre- and post-blocking hydrographs, measured at various scales using a large nested set flow gauges, have failed to detect any impact on discharge associated with drain blocking at catchment scales of approximately 1 km^2 and above (Ewen et al., 2010; Geris, 2012). Other studies, conducted by others using different techniques, have come to a similar conclusion (e.g. Ballard et al., 2010). The results from MURSAFF show that with the FFP mesh the predicted impact is very small, and is much smaller than predicted when a square or triangular mesh is used. In that sense, the modelling work has been successful. However, a wider perspective must be taken. At large scales, all the tested

meshes give similar results for discharge (e.g. they have roughly the same NSE-HMA performance metric when simulation is compared to observation). What is significantly different between them is the sensitivity to change, and this is closely related to the details of the representation of the dynamics of the near-drain subsurface (porous media) water storage. This confirms the assumption that a model for representing LUMC must take into account field knowledge and interpretations, and that geometry is important, but it does not confirm that the FFP mesh results give the right sensitivity for the right reason. In fact, the field evidence suggests that the hydraulic and storage properties of peat are highly variable and the flow paths complex, so encapsulating the correct formulation within a distributed model is difficult.

8. Conclusions

With the aim of predicting the effect of land use and management changes (LUMC), a new physically-based model has been built that allows the geometric complexity of the landscape to be represented more accurately than is possible using standard computation meshes such as squares, rectangles or triangles. The model, MURSAFF (Model for Upland Runoff Storage And Flow Fields) uses a freeform polygon mesh that is designed interactively by a field hydrologist in a multi-stage process that involves the use of field data, field interpretations, a DEM, and test reports generated by the model. The problem studied during the development process was the blocking of open drains (grips) in peatland at the Sapling Clough subcatchment (1.7 km^2) of the River Hodder catchment, northwest England.

The general concept behind this work is that predicting the effects of LUMC using distributed models is extremely difficult, so when creating and using models there should be as much direct involvement as possible by field hydrologists. Basically, the aim is to have a model that displays the right sensitivity to change for the right reasons. Note that this is a much more demanding aim than having a model that gives good metrics when calibrated against observed hydrographs. There are, inevitably, some limitations in any new model, and perhaps more here because of the considerable effort required to design and codifying the whole multi-stage process by which the freeform mesh is designed and implemented by the field hydrologist. However, the

benefit of having a freeform mesh was demonstrated, in that it (correctly) gives a smaller sensitivity to drain-blocking than square or triangular meshes that contain a similar number of computational cells. Also, the results for the freeform mesh were in agreement with field evidence, in that they predict that drain blocking has little effect on the peak discharge from the catchment.

Acknowledgements

Funding was provided by the UK Environment Agency under project SC060092. United Utilities, Jeff Walker (tenant farmer), and Glynn Roberts (game keeper) are thanked for providing land access and sharing their local knowledge. The authors are grateful to Prof. Enda O'Connell and Dr. Greg O'Donnell for discussions on this work.

References

Aitkenhead, N., McBridge, D., J., R.N. and Kimbell, S.F., 1992. Geology of the country around Garstang - memoir for 1:50 000 geological sheet 67 (England and Wales). In: B.G. Survey (Editor), British Geological Survey. HMSO, London.

Ballard, C.E., McIntyre, N. and Wheater, H., 2010. Peatland drain blocking: Can it reduce peak flood flows?, Role of Hydrology in Managing Consequences of a Changing Global Environment, Proc. 3rd BHS International Hydrology Symposium, Newcastle University, Newcastle upon Tyne, UK, pp. 6.

Ballard, C.E., McIntyre, N., Wheater, H.S., Holden, J. and Wallage, Z.E., 2011. Hydrological modelling of drained blanket peatland. J. Hydrol., 407(1-4): 81-93.

Bänninger, D., 2007. Technical Note: Water flow routing on irregular meshes. Hydrol. Earth Syst. Sci., 11(4): 1243-1247.

Bathurst, J.C., Ewen, J., Parkin, G., O'Connell, P.E. and Cooper, J.D., 2004. Validation of catchment models for predicting land-use and climate change impacts, 3. Blind validation for internal and outlet responses. J. Hydrol., 287(1-4): 74-94.

Beckwith, C.W., Baird, A.J. and Heathwaite, A.L., 2003. Anisotropy and depth-related heterogeneity of hydraulic conductivity in a bog peat. I: laboratory measurements. Hydrol. Process., 17(1): 89-101.

Beven, K., 1993. Prophecy, reality and uncertainty in distributed hydrological modelling. Adv. Water Resour., 16(1): 41-51.

Beven, K.J. and Freer, J., 2001. A dynamic TOPMODEL. Hydrol. Process., 15(10): 1993 – 2011.

Beven, K.J. and Kirkby, M.J., 1979. A physically based variable contributing area model of basin hydrology. Bull. Int. Assoc. Sci. Hydrol., 24(1): 43 – 69.

Birkel, C., Tetzlaff, D., Dunn, S.M. and Soulsby, C., 2010. Towards a simple dynamic process conceptualization in rainfall-runoff models using multi-criteria calibration and tracers in temperate, upland catchments. Hydrol. Process., 24(3): 260-275.

Clark, M.P., McMillan, H.K., Collins, D.B.G., Kevetski, D. and Woods, R.A., 2011. Hydrological field data from a modeller's perspective: Part 2: process-based evaluation of model hypotheses. Hydrol. Process., 25(4): 523-543.

Deeks, L.K. et al., 2004. Spatial variation of effective porosity and its implications for discharge in an upland headwater catchment in Scotland. J. Hydrol., 290(3-4): 217-228.

DEFRA, 2005. Making space for water, taking forward a new government strategy for flood and coastal erosion risk management in England, DEFRA, London.

Dunn, S.M. et al., 2008. Conceptualization in catchment modelling: simply learning? Hydrol. Process., 22(13): 2389-2393.

Dunne, T., 1983. Relation of field studies and modeling in the prediction of strom runoff. J. Hydrol., 65(1-3): 25-48.

Environment Agency, 2009. Flooding in England: A national assessment of flood risk, Environment Agency, Bristol.

Evrard, O., Bielders, C.L., Vandaele, K. and van Wesemael, B., 2007. Spatial and temporal variation of muddy floods in central Belgium, off-site impacts and potential control measures. Catena, 70: 443-454.

Ewen, J., 2011. Hydrograph matching method for measuring model performance. J. Hydrol., 408(1-2): 178-187.

Ewen, J., Geris, J., O'Donnell, G., Mayes, W. and O'Connell, E., 2010. Multiscale Experimentation, Monitoring and Analysis of Long-term Land Use Changes and Flood Risk - EA project SC060092: Final Science Report, Newcastle University, Newcastle upon Tyne.

Ewen, J., O'Donnell, G., Burton, A. and O'Connell, E., 2006. Errors and uncertainty in physically-based rainfall-runoff modelling of catchment change effects. J. Hydrol., 330(3-4): 641-650.

Ewen, J., Parkin, G. and O'Connell, P.E., 2000. SHETRAN: Distributed river basin flow and transport modeling system. J. Hydrol. Eng., 5(3): 250-257.

Fiener, P., Auerswald, K. and Van Oost, K., 2011. Spatio-temporal patterns in land use and management affecting surface runoff response of agricultural catchments - A review. Earth-Sci. Rev., 106(1-2): 92-104.

Geris, J.R.M.C., 2012. Multiscale impacts of land use/management changes on flood response in the river Hodder catchment, North-West England'. PhD Thesis, Newcastle University, Newcastle upon Tyne.

Geris, J.R.M.C., Ewen, J., O'Donnell, G.M. and O'Connell, P.E., 2010. Monitoring and modelling the pre- and post-blocking hydrological response of moorland drains, Role of Hydrology in Managing Consequences of a Changing Global Environment, Proc. 3rd BHS International Hydrology Symposium. Newcastle University, Newcastle upon Tyne, UK, pp. 6.

Holden, J., 2005a. Peatland hydrology and carbon release: why small-scale process matters. Philos. T. Roy. Soc. A, 363(1837): 2891-2913.

Holden, J., 2005b. Piping and woody plants in peatlands: Cause or effect? Water Resour. Res., 41: W06009(1-10).

Holden, J. and Burt, T.P., 2003a. Hydraulic conductivity in upland blanket peat: measurement and variability. Hydrol. Process., 17(6): 1227-1237.

Holden, J. and Burt, T.P., 2003b. Hydrological studies on blanket peat: the significance of the acrotelm-catotelm model. J. Ecol., 91(1): 86-102.

Holden, J. et al., 2007. Environmental change in moorland landscapes. Earth-Sci. Rev., 82(1-2): 75-100.

Holden, J., Wallage, Z.E., Lane, S.N. and McDonald, A.T., 2011. Water table dynamics in undistrubed, drained and restored blanket peat. J. Hydrol., 402(1-2): 103-114.

Holman, I.P., Hollis, J.M. and Thompson, T.R.E., 2002. Impact of agricultural soil conditions on floods - Autumn 2000, R&D Technical Report W5B-026/TR, Bristol

James, A.L., McDonnell, J.J., Tromp - van Meerveld, I. and Peters, N.E., 2010. Gypsies in the palace: experimentalist's view on the use of 3-D physics-based simulation of hillslope hydrological response. Hydrol. Process., 24(26): 3878-3893.

Kirchner, J.W., 2006. Getting the right answers for the right reasons: linking measurements, analyses, and models to advance the science of hydrology. Water Resour. Res., 42: W03S04.

Klemeš, V., 1986a. Dilettantism in hydrology: transition or destiny. Water Resour. Res., 22: 177S-188S.

Klemeš, V., 1986b. Operational testing of hydrological simulation methods. Hydrolog. Sci. J., 31(1): 13-24.

Lagacherie, P., Rabotin, M., Colin, F., Moussa, R. and Voltz, M., 2010. Geo-MHYDAS: A landscape discretization tool for distributed hydrological modeling of cultivated areas. Comput. Geosci., 36(8): 1021-1032.

Lane, S.N., 2001. More floods, less rain: changing hydrology in a Yorkshire context. The Yorkshire and Humber Region. Rev., 11(3): 18-19.

Lane, S.N. et al., 2003. Land management, flooding and environmental risk: new approaches to a very old question. In: CIWEM (Editor), Forthcomin. in Proc. CIWEM National Conference.

LaRose, S., Price, J. and Rochefort, L., 1997. Rewetting of a cutover peatland: hydrologic assessment. Wetlands, 17(3): 416-423.

Levavasseur, F., Bailly, J.S., Lagacherie, P., Colin, F. and Rabotin, M., 2012. Simulating the effects of spatial configurations of agricultural ditch drainage networks on surface runoff from agricultural catchments. Hydrol. Process., Article first published online: 24 Jan 2012.

Longfield, S.A. and Macklin, M.G., 1999. The influence of recent environmental change on flooding and sediment fluxes in the Yorkshire Ouse basin. Hydrol. Process., 13(7): 1051-1066.

McDonnell, J.J. et al., 2007. Moving beyond heterogeneity and process complexity: A new vision for watershed hydrology. Water Resour. Res., 43: W07301.

McGrath, M. and Smith, M., 2006. Sustainable Catchment Management Programme (SCaMP): from hilltop to tap, BHS 9th National Hydrology Symposium, Durham, UK, pp. 91-96.

McMillan, H.K., Clark, M.P., Bowden, W.B., Duncan, M.J. and Woods, R.A., 2011. Hydrological field data from a modeller's perspective: Part 1. Diagnostic tests for model structure. Hydrol. Process., 25(4): 511-522.

Meyles, E.W., Williams, A.G., Ternan, J.L., Anderson, J.M. and Dowd, J.F., 2006. The influence of grazing on vegetation, soil properties and stream discharge in a small Dartmoor catchment, southwest England, UK. Earth Surf. Proc. Land., 31(5): 622-631.

Miller, S.N. et al., 2007. The Automated Geospatial Watershed Assessment tool. Environ. Modell. Softw., 22(3): 365-377.

Moussa, R., Voltz, M. and Andrieux, P., 2002. Effects of the spatial organization of agricultural management on the hydrological behaviour of a farmed catchment during flood events. Hydrol. Process., 16(2): 393-412.

Nash, J.E. and Sutcliffe, J.V., 1970. River flow forecasting through conceptual models part 1 - A discussion of principles. J. Hydrol., 10(3): 282-290.

O'Connell, P.E. et al., 2004. Review of impacts of rural land use management on flood generation: Impact Study Report, DEFRA Flood Management Division, London, UK.

O'Connell, P.E., Ewen, J., O'Donnell, G.M. and Quinn, P.F., 2007. Is there a link between agricultural land use management and flooding? Hydrol. Earth Syst. Sci., 11(1): 96-107.

Parkin, G. et al., 1996. Validation of catchment models for predicting land-use and climate change impacts, 2. Case study for a Mediterranean catchment. J. Hydrol., 175(1-4): 595-613.

Parrott, A., Brooks, W., Harmar, O. and Pygott, K., 2010. Role of rural land use management in flood and coastal risk management. J. Flood Risk Manag., 2(4): 272-284.

Pitt, M., 2008. The Pitt Review. Learning lessons from the 2007 floods, Cabinet Office, London.

Quinton, W.L., Hayashi, M. and Carey, S.K., 2008. Peat hydraulic conductivity in cold regions and its relation to pore size and geometry. Hydrol. Process., 22(15): 2829-2837.

Ramchunder, S.J., Brown, L.E. and Holden, J., 2009. Environmental effects of drainage, drain-blocking and prescribed vegetation burning in UK upland peatlands. Prog. Phys. Geog., 33(1): 49-79.

Reeve, A.S., Siegel, D.I. and Glaser, P.H., 2001. Simulating dispersive mixing in large peatlands. J. Hydrol., 242(1-2): 103–114.

Rizzuti, A.M., Cohen A.D. and Stack, E.M., 2004. Using hydraulic conductivity and micropetrography to assess water flow through peat-containing wetlands. Int. J. Coal Geol., 60(1): 1-16.

Rycroft, D.W., Williams, D.J.A. and Ingram, H.A.P., 1975. The transmission of water through peat: I. Review. J. Ecol., 63(2): 535-556.

Seibert, J. and McDonnell, J.J., 2002. On the dialog between experimentalist and modeler in catchment hydrology: Use of soft data for multi-criteria model calibration. Water Resour. Res.: WR000978.

Shantz, M.A. and Price, J.S., 2006. Characterization of surface storage and runoff patterns following peatland restoration, Quebec Canada. Hydrol. Process., 20(18): 3799-3814.

Spieksma, J.F.M., 1999. Changes in the discharge pattern of a cutover raised bog during rewetting. Hydrol. Process., 13(8): 1233-1246.

Stewart, A.J.A. and Lance, A.N., 1983. Moor-Draining: A review of impacts on land use. J. Environ. Manage., 17(1): 81-99.

Vivoni, E.R., Ivanov, V.Y., Bras, R.L. and Entekhabi, D., 2005. On the effects of triangulated terrain resolution on distributed hydrologic model response. Hydrol. Process., 19(11): 2101-2122.

Wheater, H. and Evans, E., 2009. Land use, water management and future flood risk. Land Use Policy, 26 (S1): S251-S264.

Wilson, L. et al., 2010. Recovery of water tables in Welsh blanket bog after drain blocking: discharge rates, time scales and the influence of local conditions. J. Hydrol., 391(3-4): 377-386.

Worrall, F., Armstrong, A. and Holden, J., 2007. Short-term impact of peat drain-blocking on water colour, dissolved organic carbon concentration, and water table depth. J. Hydrol., 337(3-4): 315-325.

Appendix 4. MURSAFF Grid Improvement Stages

This Appendix describes the 10 stages of the MURSAFF set-up and simulation, using the example grid as shown in Figure A.4.1. It is noted that during all steps in the grid automatic improvement, the changes are checked against field observations and interpretations to ensure that the grid will represent reality in the flow directions. Figure A.4.1 shows an example section of a grid, with cell numbers 1-11 and the elevation in brackets. Cells 8-11 are classified as 'river' slabs, the other cells as 'hill' slabs. The catchment outlet is the left face of cell 8.

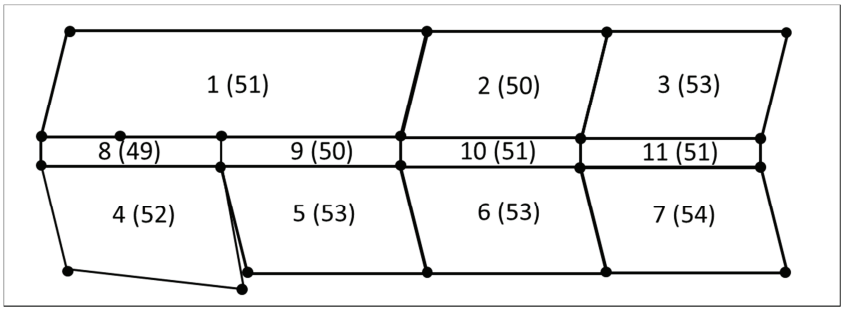

Figure A.4.1 Example grid for correction

The following steps are taken to test and improve the pavement file and set it up for the MURSAFF simulation:

1) Identification of any isolated vertices

Stage 1 involves the identification and correction of isolated vertices. Isolated vertices are expected on the catchment boundaries (blue vertices, Figure A.4.2). Those isolated vertices within the grid are either mismatched (red vertices, cells 4 and 5, Figure A.4.2) or redundant (red vertex, cell 1, Figure A.4.2) and are corrected.

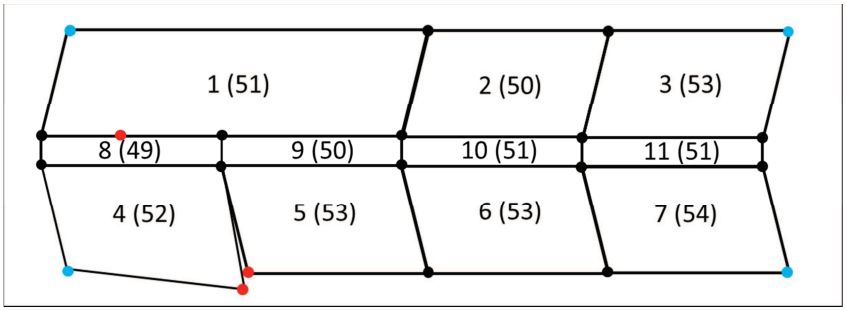

Figure A.6.2 Example grid, stage 1

2) Check for mismatched faces and add extra vertices if necessary

For the example grid this involves splitting the bottom face of cell 1 (red face, Figure A.4.3). into two by adding an additional vertex so that cell 1 has a face that matches with cell 8 and one with cell 9.

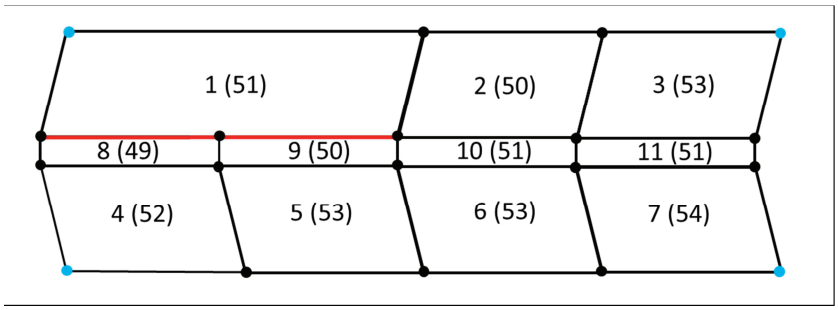

Figure A.4.3 Example grid, stage 2

3) Find neighbouring slabs and matching faces

The neighbouring slabs and matching faces for the example grid are indicated by the green lines in Figure A.4.4.

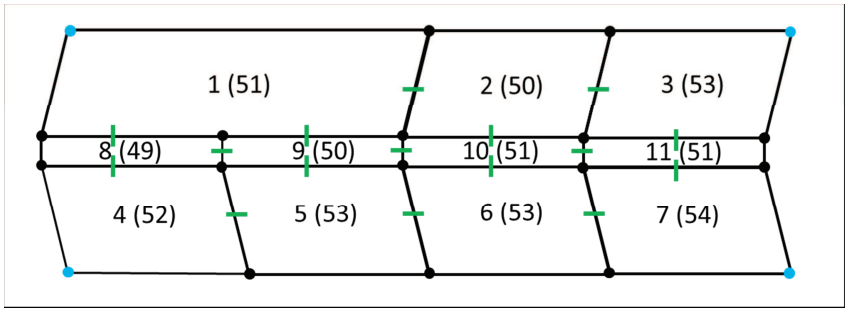

Figure A.4.4 Example grid, stage 3

4) Walk and depit the drainage network

The drainage network outlet is defined in the pavement input file, which holds all information on the grids. The pavement file also specifies which cell types constitute the river network. During stage four, MURSAFF walks the river network (in an upstream direction) and adjusts the elevation of network cells when needed (based on a predefined increment, e.g. 0.1 m). For the example grid, this involves increasing the elevation of cell 11 so that there will be flow from cell 11 to cell 10 (see Figure A.4.5).

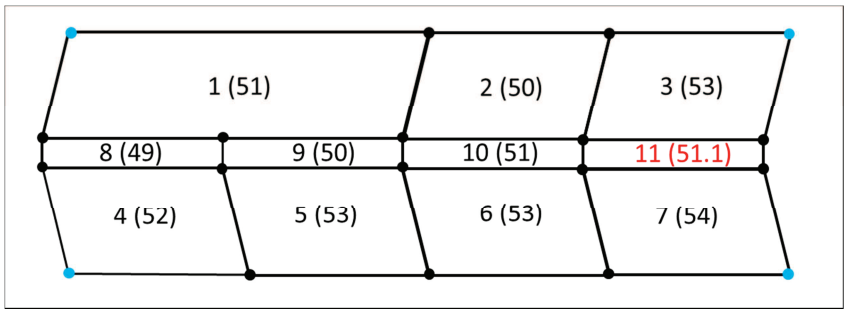

Figure A.4.5 Example grid, stage 4

5) General pit filling

During this stage the grid cells constituting the hillslope slabs are checked for pits. For the example grid, this would involve raising the elevation from 50 to 51 (see Figure A.4.6)

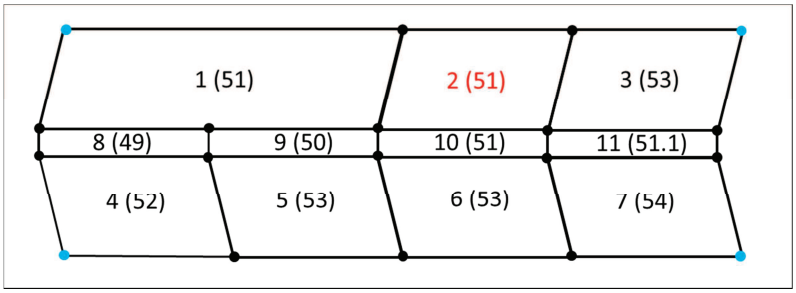

Figure A.4.6 Example grid, stage 5

6) Walk and depit the pavement

During stage 6, MURSAFF walks the entire grid (including hillslopes) and adjusts the elevation of network cells when needed (based on a predefined increment, e.g. 0.1 m) so that all cells have outflows. For the example grid, this involves raising the elevation of cell 2 from 51 to 51.1, so that there is flow from cell 2 to cells 1 and 10.

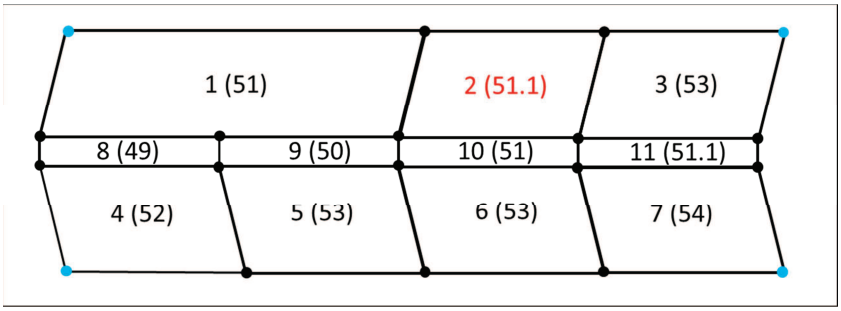

Figure A.4.7 Example grid, stage 6

7) Find flow directions

During stage 7, MURSAFF establishes the flow directions based on the corrected elevations. For the example grid the flow directions are indicated by the orange arrows.

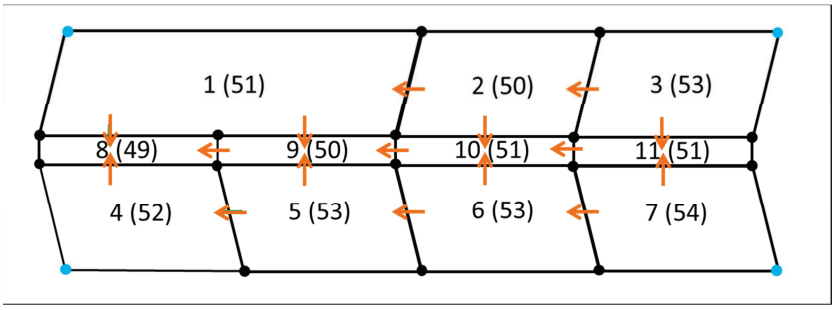

Figure A.4.8 Example grid, stage 7

8) Calculate areas for slabs

9) Read and set-up property tables

10) Run simulation

Appendix 5. Additional results of empirical changes at the mini scale on the downstream HP peak flow, related to Section 7.3.2

This appendix serves as a supplement to the analyses of the propagation of empirical mini scale impacts in Section 7.3.2. Here, the downstream impacts on peak flow are presented of empirical changes in all different mini scale subcatchments in the Hodder catchment. For four storms, Tables A.5.1, A.5.2 and A.5.3 show the downstream impacts on the peak flow of HP of the 1 hr delay, 15% change and a combination of the two, respectively.

Table A.5.1 Impact on Hodder Place Peak flow of 1 hr delay changes at the different subcatchments

IMPACT at HP, from 1 hr delay at subcatchment	**October 2008**		**January 2009**		**July 2009**		**November 2009**	
	Delay Q_p (hr)	ΔQ_p (m^3/s)*	Delay Q_p (hr)	ΔQ_p (m^3/s)*	Delay Q_p (hr)	ΔQ_p (m^3/s)*	Delay Q_p (hr)	ΔQ_p (m^3/s)*
LAN_out	0.25	+1.02 (+0.4%)	0.00	-1.23 (-0.8%)	1.25	-3.93 (-8.9%)	0.25	-7.19 (-2.7%)
Footholme	0.75	-1.18 (-0.4%)	0.00	+1.95 (+1.2%)	0.00	-1.62 (-3.7%)	0.25	-4.67 (-1.8%)
CRO_out	0.00	-5.52 (-2.0%)	0.25	-4.04 (-2.5%)	0.00	+0.04 (+0.1%)	0.25	-9.20 (-3.5%)
EAS_out	0.00	-2.55 (-1.0%)	0.00	-0.06 (<0.0%)	0.00	+0.02 (<0.0%)	0.25	-5.81 (-2.2%)
LOU_out	0.25	-8.14 (-3.0%)	0.25	-3.82 (-9.5%)	1.00	-4.23 (-9.5%)	0.50	-11.56 (-4.4%)
LAN_out + FH + CRO_out	1.00	-1.45 (-0.6%)	0.25	-3.29 (-2.0%)	1.25	-7.37 (-16.6%	0.75	-14.83 (-5.7%)

* Percentage change of pre-change peak flow in brackets

Table A.5.2 Impact on Hodder Place Peak flow of 15% changes at the different subcatchments

IMPACT at HP, from 15% change at subcatchment	October 2008		January 2009		July 2009		November 2009	
	Delay Q_p (hr)	ΔQ_p (m^3/s)*	Delay Q_p (hr)	ΔQ_p (m^3/s)*	Delay Q_p (hr)	ΔQ_p (m^3/s)*	Delay Q_p (hr)	ΔQ_p (m^3/s)*
LAN_out	0.00	-3.46 (-1.4%)	0.00	-2.28 (-1.4%)	0.00	-2.83 (-6.4%)	0.00	-3.24 (-1.2%)
Footholme	0.00	-6.01 (-2.3%)	0.00	-2.95 (-1.8%)	0.00	-0.47 (-1.1%)	0.00	-4.32 (-1.7%)
CRO_out	0.00	-3.11 (-1.2%)	0.00	-2.50 (-1.5%)	0.00	+0.22 (+0.5%)	0.00	-4.43 (-1.7%)
EAS_out	0.00	-1.65 (-0.6%)	0.00	-1.19 (-0.7%)	0.00	+0.11 (+0.3%)	0.00	-2.70 (-1.0%)
LOU_out	0.00	-9.53 (-3.6%)	0.00	-4.08 (-2.5%)	0.00	-1.29 (-2.9%)	0.00	-7.55 (-2.9%)
LAN_out + FH + CRO_out	0.00	-12.36 (-4.6%)	0.00	-7.73 (-4.7%)	0.00	-3.09 (-7.0%)	0.00	-12.00 (-4.6%)

* Percentage change of pre-change peak flow in brackets

Table A.5.3 Impact on Hodder Place Peak flow of 1 hr and 15% changes at the different subcatchments

IMPACT at HP, from 15% change +1hr delay at subcatchment	October 2008		January 2009		July 2009		November 2009	
	Delay Q_p (hr)	ΔQ_p (m^3/s)*	Delay Q_p (hr)	ΔQ_p (m^3/s)*	Delay Q_p (hr)	ΔQ_p (m^3/s)*	Delay Q_p (hr)	ΔQ_p (m^3/s)*
LAN_out	0.25	-2.48 (-0.9%)	0.00	-3.34 (-2.0%)	1.25	-6.11 (-13.8%)	0.25	-9.48 (-3.6%)
Footholme	0.75	-6.64 (-2.5%)	0.25	-1.25 (-0.8%)	0.00	-1.72 (-3.9%)	0.25	-8.27 (-3.2%)
CRO_out	0.00	-7.80 (-2.9%)	0.25	-6.01 (-3.7%)	0.00	+0.26 (+0.6%)	0.00	-12.36 (-4.7%)
EAS_out	0.00	-3.82 (-1.4%)	0.00	-1.24 (-0.8%)	0.00	+0.13 (+0.3%)	0.25	-7.73 (-3.0%)
LOU_out	0.25	-19.12 (-7.2%)	0.25	-7.39 (-4.5%)	0.25	-5.03 (-11.3%)	0.25	-18.10 (-6.9%)
1.00	-13.62 (-5.1%)	0.25	-10.49 (-6.4%)	1.25	-9.80 (-22.1%)	0.75	-25.08 (-9.6%)	1.00

* Percentage change of pre-change peak flow in brackets

A.1.1 BRE_grip/BRE_grip_weir

Gauge name	BRE_grip (superseded by BRE_grip_weir at 01/12/08)
Description:	The outlet of a grip in Sapling Clough, headwater of River Brennand sub catchment. BRE_grip_weir is located 5 m downstream of channel site BRE_grip.
Grid reference:	SD 62692 55949 (BRE_grip), and SD 62690 55949 (BRE_grip_weir)
Elevation:	383.6 m (BRE_grip), and 380.6 m (BRE_grip_weir)
Abstractions:	-
Catchment area:	0.0014 km^2 (process scale)
Related sites:	Upstream: - Downstream: BRE_sap, BRE_out, Footholme (EA), Hodder Place (EA)
Baro used for correction:	Baro_Footholme
Installation Date:	15/05/2008 (BRE_grip), 01/12/2008 (BRE_grip_weir)
Record Interval:	5 min
QA notes:	The data from BRE_grip_weir are unreliable for 06/06/2009 – 25/06/2009 as a result of weir leakage

Location in Hodder Area	Photo of weir and gauge, upstream direction
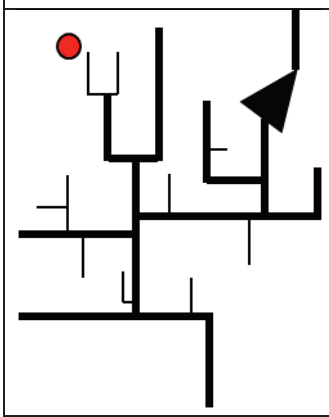	

UU SCaMP interventions	Stocking density	Grip blocking	Tree planting
Timing	Spring 08	November 2008	-
Area affected (%)	100	100	-

Rating Curve

The weir at BRE_grip/BRE_grip_weir is a v-notch weir build according to British Standard 3680, Part 4A (BSI, 1981). The geometrical details of the weir are given below.

Schematic representation of the v-notch weir at BRE_grip_weir

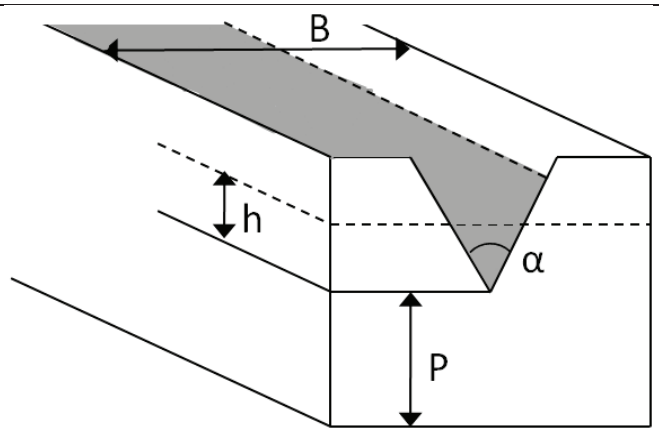

B	1.2
α	90
p (upstream)	0.42
p (downstream)	0.53
Maximum height above crest	0.39
Distance gauge to weir	1.35

The discharge Q (m^3/s) is calculated from stage h (m) according to the Kindsvater-Shen formula (BSI, 1981):

$$Q = C_e \frac{8}{15} \tan\frac{\alpha}{2} \sqrt{2 g_n h_e^{5/2}}$$

where h_e is the effective head above the crest (m), and g_n is the acceleration due to gravity (m/s^2), and the coefficient of discharge C_e has been determined by experiments as a function of P, B and h_e (BSI, 1981).

A.1.2 BRE_out

Gauge name	Brennand Outlet
Description:	River Brennand Outlet, subcatchment of River Dunsop
Grid reference:	SD 65271 53214
Elevation:	172.7 m
Abstractions:	Upstream abstractions as part of United Utilities' Dunsop abstraction system
Catchment area:	11.0 km^2 (mini scale)
Related sites:	Upstream: BRE_grip/BRE_grip_weir, BRE_sap, BRE_rhw Downstream: Footholme (EA), Hodder Place (EA)
Baro used for correction:	Baro_Footholme
Installation Date:	07/12/2007
Record Interval:	15 min
QA notes:	In low flows this gauge may be above the river water surface. The gauge was initially installed at 07/12/2007, but the baro only recorded from 23/01/2008, so the full time record only starts at 23/01/2008. Diver changed at 25/06/2009. Unreliable data between 06/06/2009 – 25/06/2009 as a result of livestock disturbance. Gauge relocated at 25/06/2009.

Location in Hodder Area	Photo of gauge, downstream direction
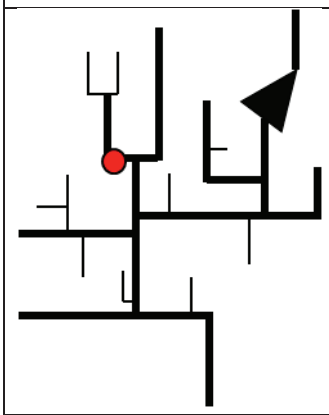	

UU SCaMP interventions	Stocking density	Grip blocking	Tree planting
Timing	Spring 08	November 08	Spring 08
Area affected (%)	100	15	5

Cross-section (from EPR)

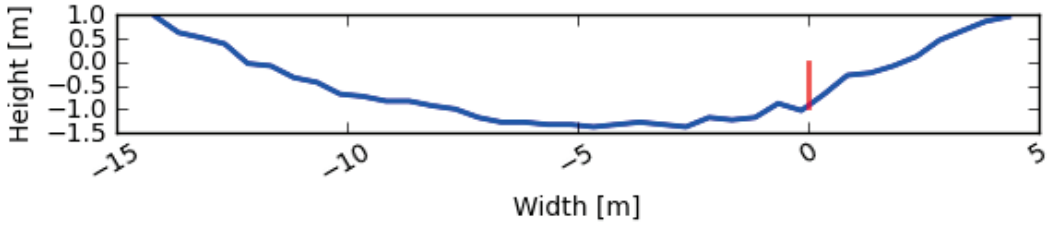

Rating Curve

Observed stage range (m):	-0.930 – 0.565
Number of gaugings:	8
Percentage highest gauging of maximum observed stage peak (%):	25.1
Percentage of time extrapolated (%):	2.0

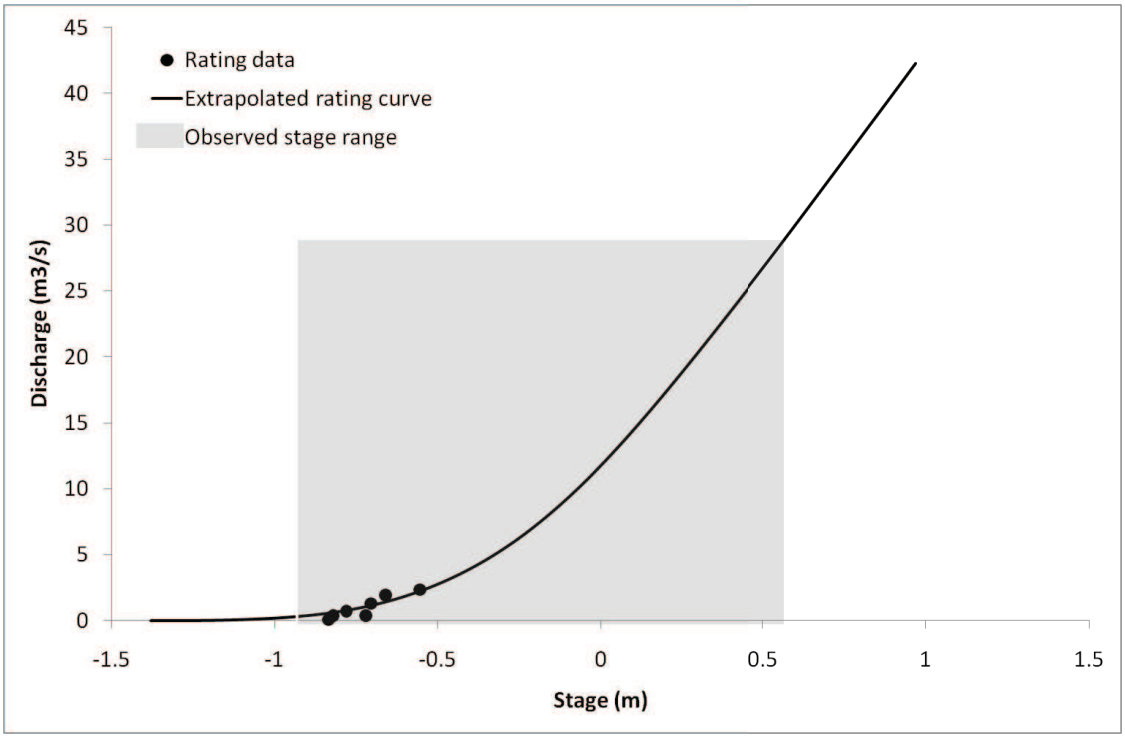

A.1.3 BRE_rhw

Gauge name	Brennand Round Hill Water
Description:	Outlet of Round Hill Water, a headwater of River Brennand
Grid reference:	SD 63136 55751
Elevation:	333.7 m
Catchment area:	2.8 km^2 (micro scale)
Abstractions:	-
Related sites:	Upstream: - Downstream: BRE_out, Footholme, Hodder Place
Baro used for correction:	Baro_Footholme
Installation Date:	15/05/2008
Record Interval:	5 min
QA notes:	-

Location in Hodder Area	Photo of gauge, downstream direction
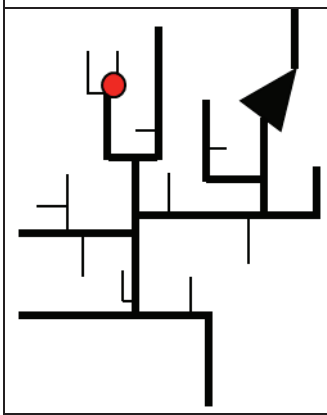	

UU SCaMP interventions	Stocking density	Grip blocking	Tree planting
Timing	Spring 08	November 08	-
Area affected (%)	100	20	-

Cross-section (from EPR, 2010)

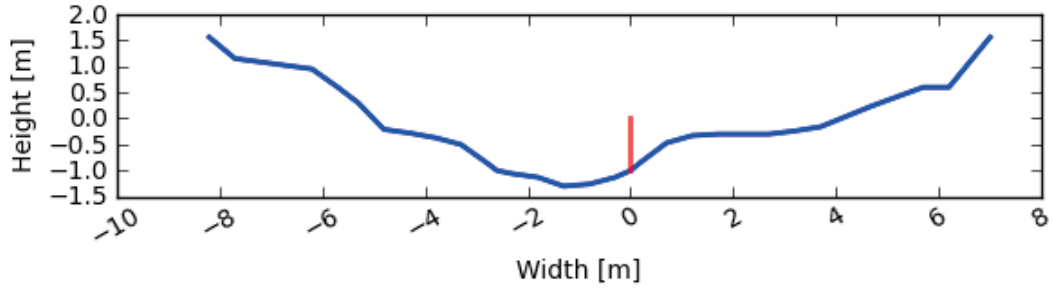

Rating Curve

Observed stage range (m):	-0.985 – 0.015
Number of gaugings:	10
Percentage highest gauging of maximum observed stage peak (%):	47.0
Percentage of time extrapolated (%):	<1

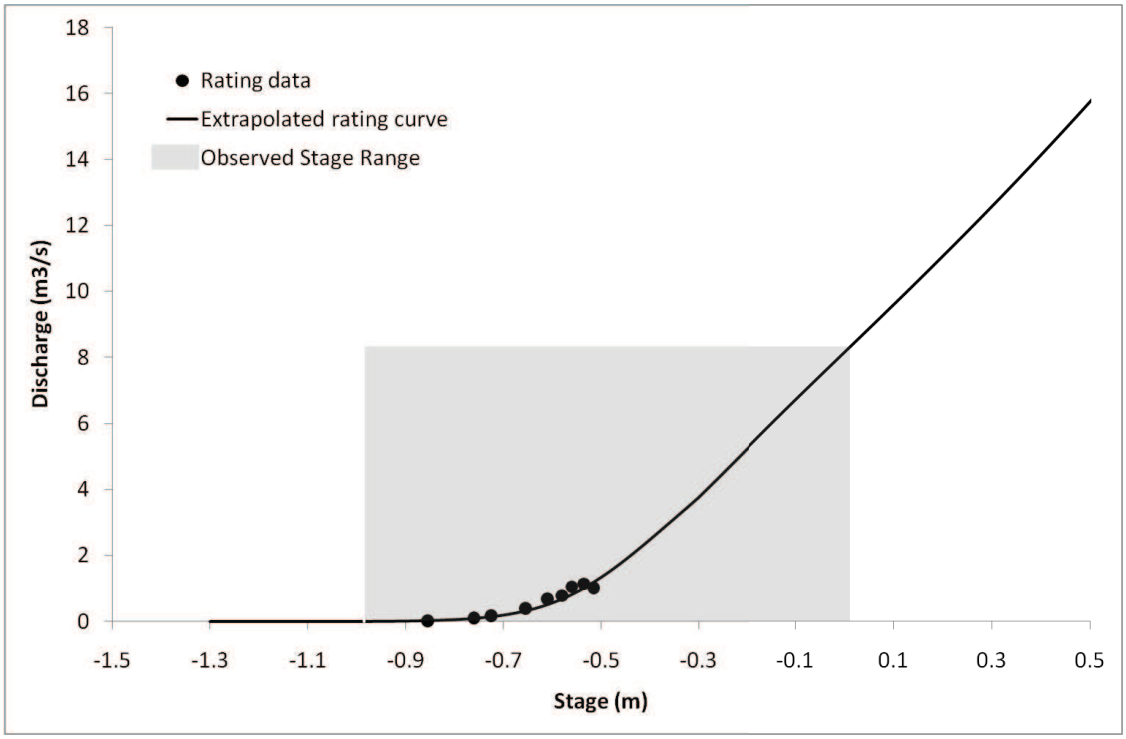

A.1.4 BRE_sap

Gauge name	Brennand Sapling Clough
Description:	Outlet of Sapling Clough, a headwater of River Brennand
Grid reference:	SD 62960 55717
Elevation:	339.9 m
Catchment area:	1.7 km^2 (micro scale)
Abstractions:	-
Related sites:	Upstream: BRE_grip/BRE_grip_weir Downstream: BRE_out, Footholme, Hodder Place
Baro used for correction:	Baro_Footholme
Installation Date:	05/06/2008
Record Interval:	5 min
QA notes:	-

Location in Hodder Area	Photo of gauge, downstream direction
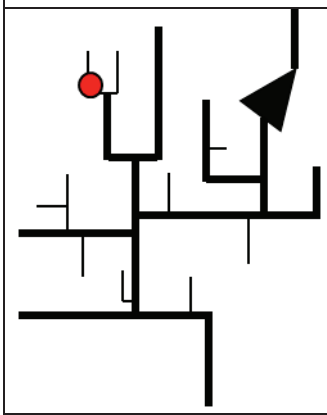	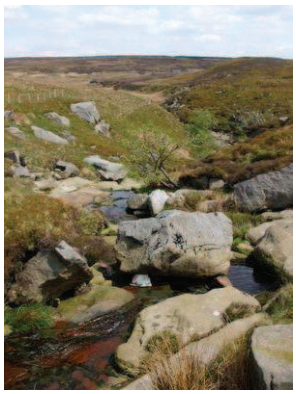

UU SCaMP interventions	Stocking density	Grip blocking	Tree planting
Timing	Spring 08	November 08	-
Area affected (%)	100	35	-

Cross-section (from EPR)

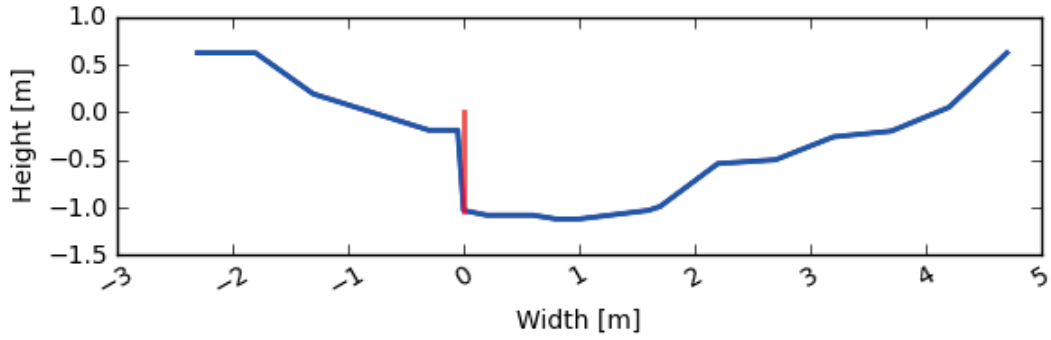

Rating Curve

Observed stage range (m):	-1.015 – 0.215
Number of gaugings:	12
Percentage highest gauging of maximum observed stage peak (%):	31.9
Percentage of time extrapolated (%):	3.9

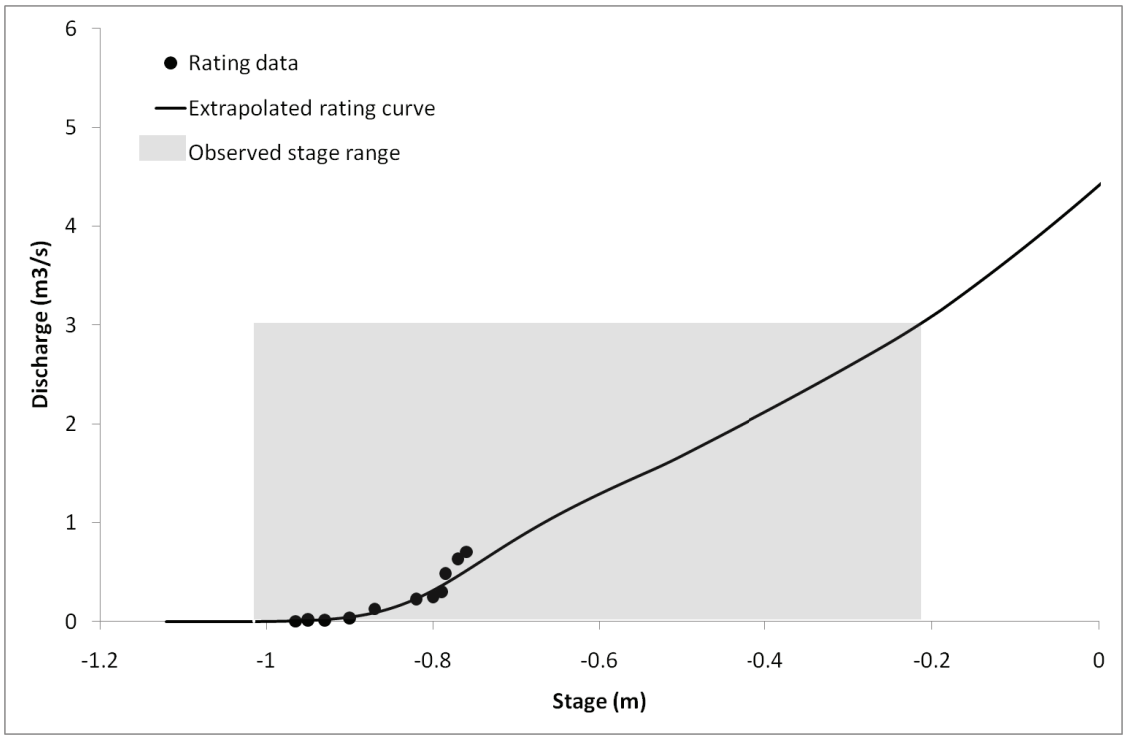

A.1.5 CRO_mid

Gauge name	Mid Croasdale
Description:	Mid Croasdale Brook, just upstream of confluence with Swine Clough
Grid reference:	SD 68673 56607
Elevation:	243.1 m
Catchment area:	3.6 km^2 (micro scale)
Abstractions:	-
Related sites:	Upstream: none Downstream: CRO_out, HOD_mid, Hodder Place
Baro used for correction:	Baro_Croasdale
Installation Date:	06/12/2007
Record Interval:	5 min (7 min from 06/12/2007 - 13/03/2008)
QA notes:	The gauge was initially installed at 06/12/2007, but the baro only recorded from 23/01/2008, so the full time record only starts at 23/01/2008. Missing data from 27/04/2010 – 31/05/2010 as a result of equipment failure.

Location in Hodder Area	Photo of gauge, downstream direction
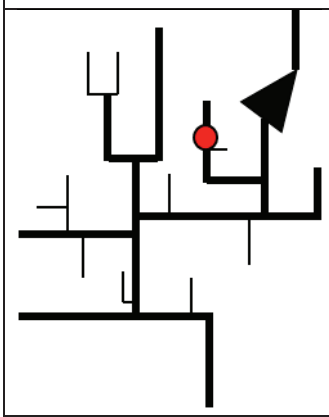	

UU SCaMP interventions	Stocking density	Grip blocking	Tree planting
Timing	February 09	-	-
Area affected (%)	100	-	-

Cross-section (from EPR, 2010)

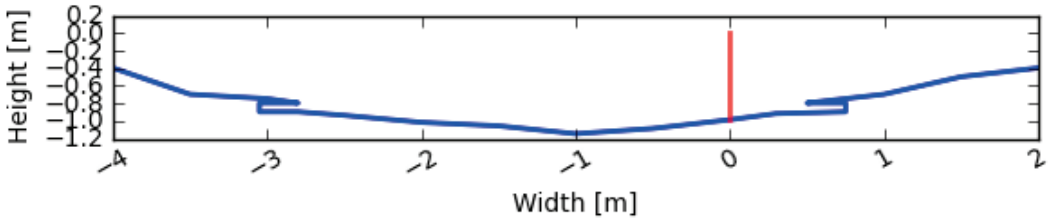

Rating Curve

Observed stage range (m):	-0.868 – 0.034
Number of gaugings:	8
Percentage highest gauging of maximum observed stage peak (%):	54.7
Percentage of time extrapolated (%):	1.4

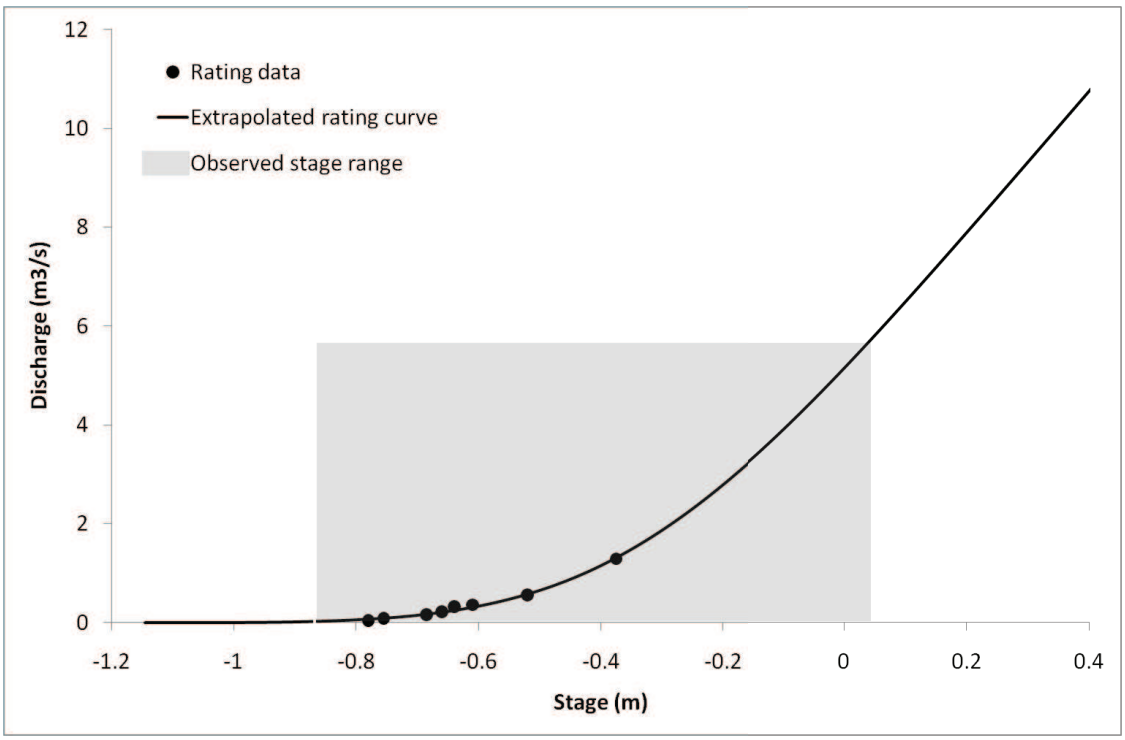

A.1.6 CRO_out

Gauge name	Croasdale Brook outlet
Description:	Outlet of Croasdale Brook
Grid reference:	SD 71216 52496
Elevation:	136.6 m
Catchment area:	21.1 km^2 (mini scale)
Abstractions:	-
Related sites:	Upstream: CRO_mid, CRO_sc1, CRO_sc2, CRO_sc3, CRO_sc4, CRO_sc5, Croasdale weir (EA) Downstream: HOD_mid, Hodder Place
Baro used for correction:	Baro_Footholme
Installation Date:	03/10/2008
Record Interval:	5 min
QA notes:	-

Location in Hodder Area	Photo of gauge, downstream direction
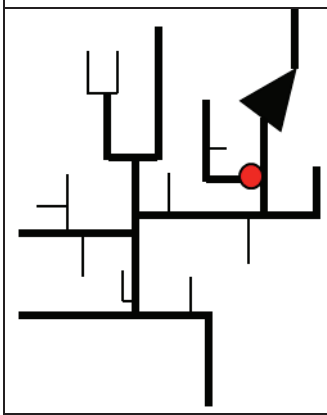	

UU SCaMP interventions	Stocking density	Grip blocking	Tree planting
Timing	Spring 09	February 09	-
Area affected (%)	45.4	2	-

Cross-section (from EPR, 2010)

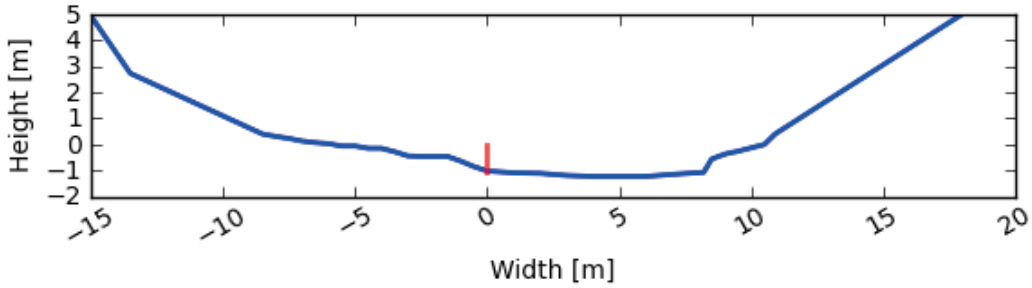

Rating Curve

Observed stage range (m):	-1.020 – 0.419
Number of gaugings:	7
Percentage highest gauging of maximum observed stage peak (%):	48.6
Percentage of time extrapolated (%):	1.3

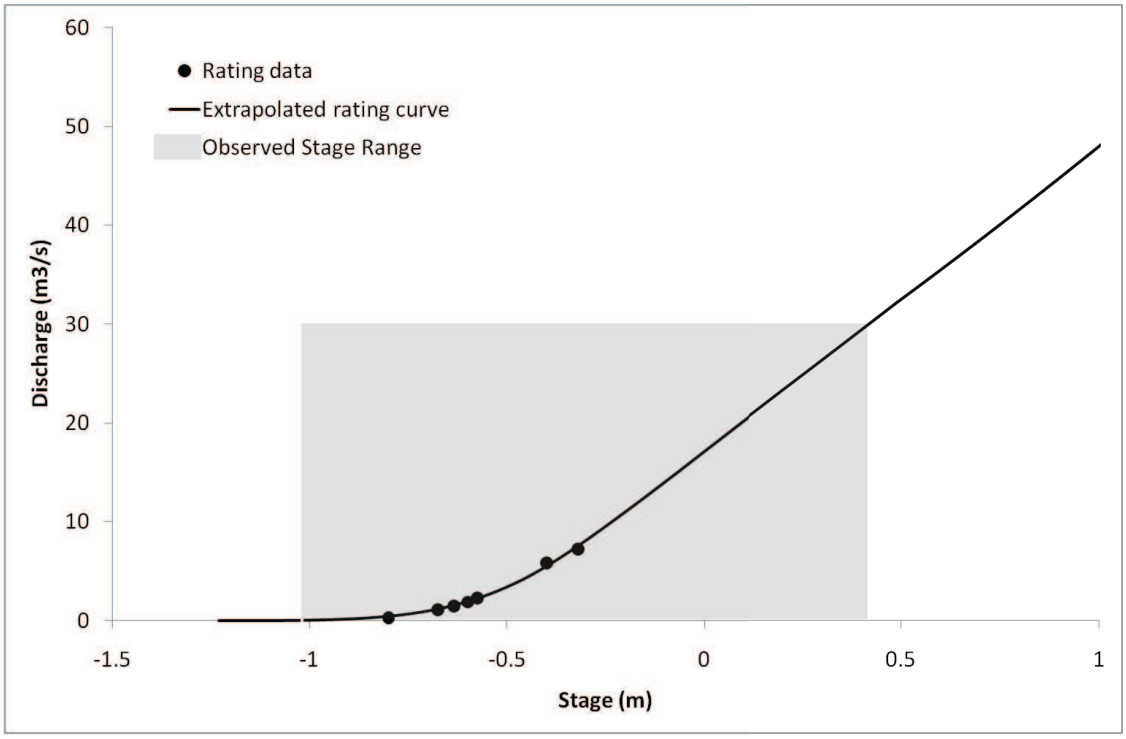

A.1.7 CRO_sc1

Gauge name	Swine Clough, top of grip, Croasdale Brook
Description:	At the top of the grip in the headwaters of Swine Clough in the Croasdale Brook catchment
Grid reference:	SD 69508 57348
Elevation:	411.3 m
Catchment area:	0.08 km^2 (process scale)
Abstractions:	-
Related sites:	Upstream: - Downstream: CRO_sc2, CRO_sc3,CRO_sc5, CRO_out, Croasdale weir (EA) HOD_mid, Hodder Place
Baro used for correction:	Baro_Croasdale
Installation Date:	07/12/2007
Record Interval:	5 min (7 min from 06/12/2007 - 23/01/2008)
QA notes:	The gauge was initially installed at 06/12/2007, but the baro only recorded from 23/01/2008, so the full time record only starts at 23/01/2008. In addition, the diver changed at 23/01/2008

Location in Hodder Area	Photo of gauge, downstream direction, post blocking
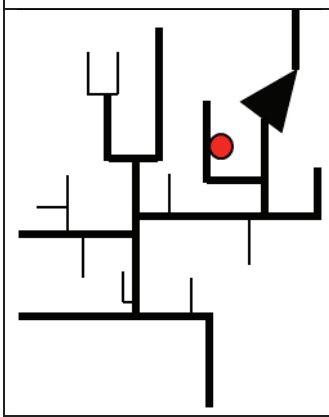	

UU SCaMP interventions	Stocking density	Grip blocking	Tree planting
Timing	Spring 09	February 09	-
Area affected (%)	100	100	-

Cross-section (from EPR, 2010)

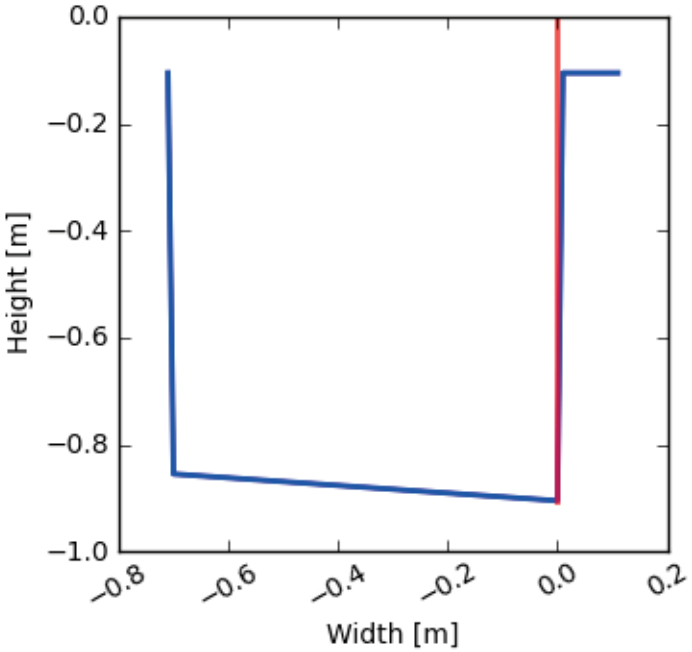

No rating curve available – stage used only in analyses

A.1.8 CRO_sc2

Gauge name	Swine Clough, bottom of grip, Croasdale Brook
Description:	At the bottom of the grip in the headwaters of Swine Clough in the Croasdale Brook catchment
Grid reference:	SD 69335 57247
Elevation:	411.3 m
Catchment area:	0.15 km^2 (process scale)
Abstractions:	-
Related sites:	Upstream: CRO_sc1 Downstream: CRO_sc3,CRO_sc5, CRO_out, Croasdale weir (EA) HOD_mid, Hodder Place
Baro used for correction:	Baro_Croasdale
Installation Date:	07/12/2007
Record Interval:	5 min (7 min from 06/12/2007 – 23/01/2008)
QA notes:	The gauge was initially installed at 07/12/2007, but the baro only recorded from 23/01/2008, so the full time record only starts at 23/01/2008. In addition, the diver changed at 23/01/2008

Location in Hodder Area	Photo of gauge, upstream direction, pre blocking
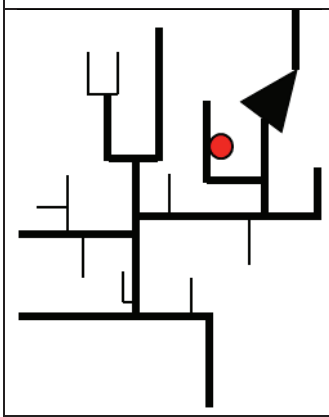	

UU ScaMP interventions	Stocking density	Grip blocking	Tree planting
Timing	Spring 09	February 09	-
Area affected (%)	100	100	-

Cross-section (from EPR, 2010)

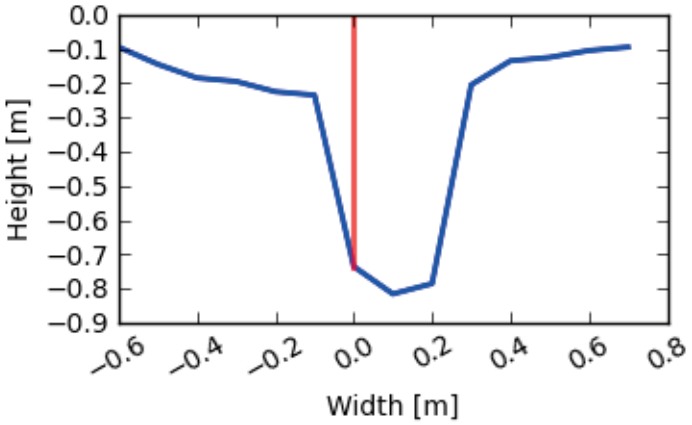

No rating curve available – stage used only in analyses

A.1.9 CRO_sc3

Gauge name	Swine Clough, outlet of a side grip, Croasdale Brook
Description:	At the outlet of a side grip in the headwaters of Swine Clough in the Croasdale Brook catchment
Grid reference:	SD 692323 57249
Elevation:	395.8 m
Catchment area:	0.015 km^2 (process scale)
Abstractions:	-
Related sites:	Upstream: none Downstream: CRO_sc5, CRO_out, Croasdale weir (EA) HOD_mid, Hodder Place
Baro used for correction:	Baro_Croasdale
Installation Date:	07/12/2007
Record Interval:	5 min (7 min from 06/12/2007 – 23/01/2008)
QA notes:	The gauge was initially installed at 06/12/2007, but the baro only recorded from 23/01/2008, so the full time record only starts at 23/01/2008. In addition, the diver changed at 23/01/2008; unreliable data as a result of livestock disturbance from 12/06/2008 – 01/07/2008; missing data from 17/10/2009-09/12/2009 as a result of equipment failure; diver changed at 09/12/2009

Location in Hodder Area	Photo of gauge, downstream direction, post blocking
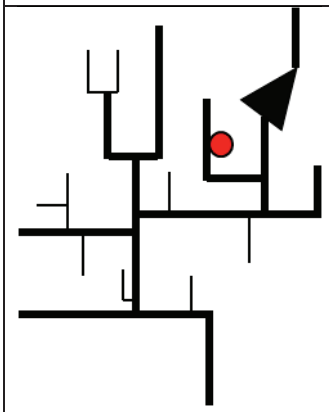	

UU ScaMP interventions	Stocking density	Grip blocking	Tree planting
Timing	Spring 09	February 09	-
Area affected (%)	100	100	-

Cross-section (from EPR, 2010)

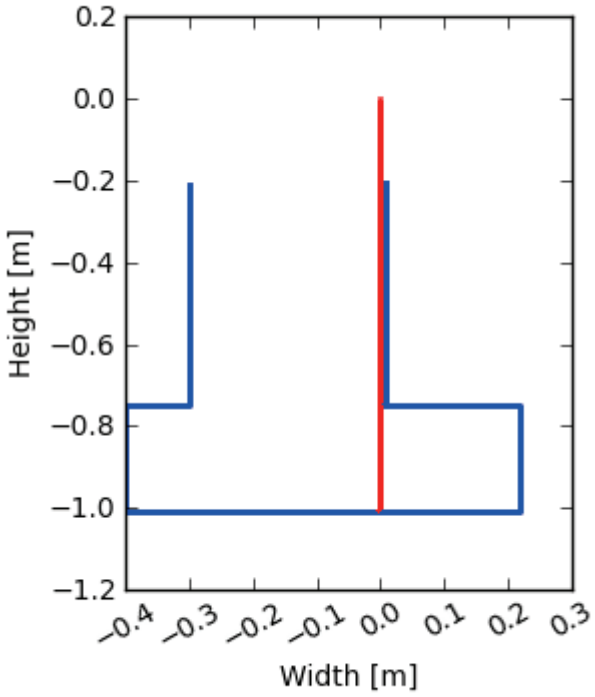

No rating curve available – stage used only in analyses

A.1.10 CRO_sc4

Gauge name	Swine Clough
Description:	At the top of Swine Clough, before the confluence with the grip, in the Croasdale Brook catchment
Grid reference:	SD 69119 57102
Elevation:	370.4 m
Catchment area:	0.10 km^2 (process scale)
Abstractions:	-
Related sites:	Upstream: none Downstream: CRO_sc5, CRO_out, Croasdale weir (EA) HOD_mid, Hodder Place
Baro used for correction:	Baro_Croasdale
Installation Date:	07/12/2007
Record Interval:	5 min (7 min from 06/12/2007 - 23/01/2008)
QA notes:	The gauge was initially installed at 06/12/2007, but the baro only recorded from 23/01/2008, so the full time record only starts at 23/01/2008. In addition, the diver changed at 23/01/2008. Between 02/04/2010 – 31/05/2010 unreliable data as a result of equipment failure (clock out of sync). Missing data from 08/06/2010 – 12/08/2010 as a result of equipment failure

Location in Hodder Area	Photo of gauge, upstream direction
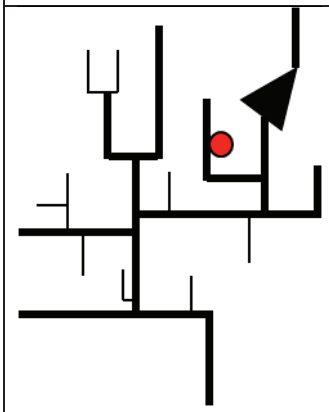	

UU SCaMP interventions	Stocking density	Grip blocking	Tree planting
Timing	Spring 09	-	-
Area affected (%)	100	-	-

Cross-section (from EPR, 2010)

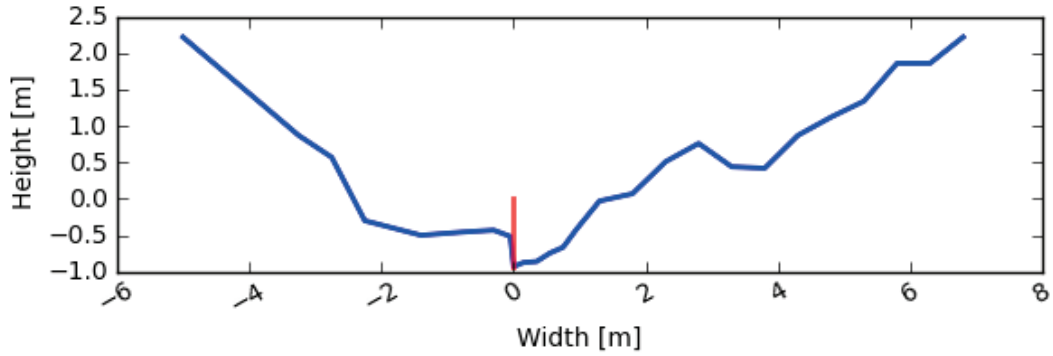

Rating Curve

Observed stage range (m):	-0.93 -0.43
Number of gaugings:	6
Percentage highest gauging of maximum observed stage peak (%):	61.2
Percentage of time extrapolated (%):	1.5

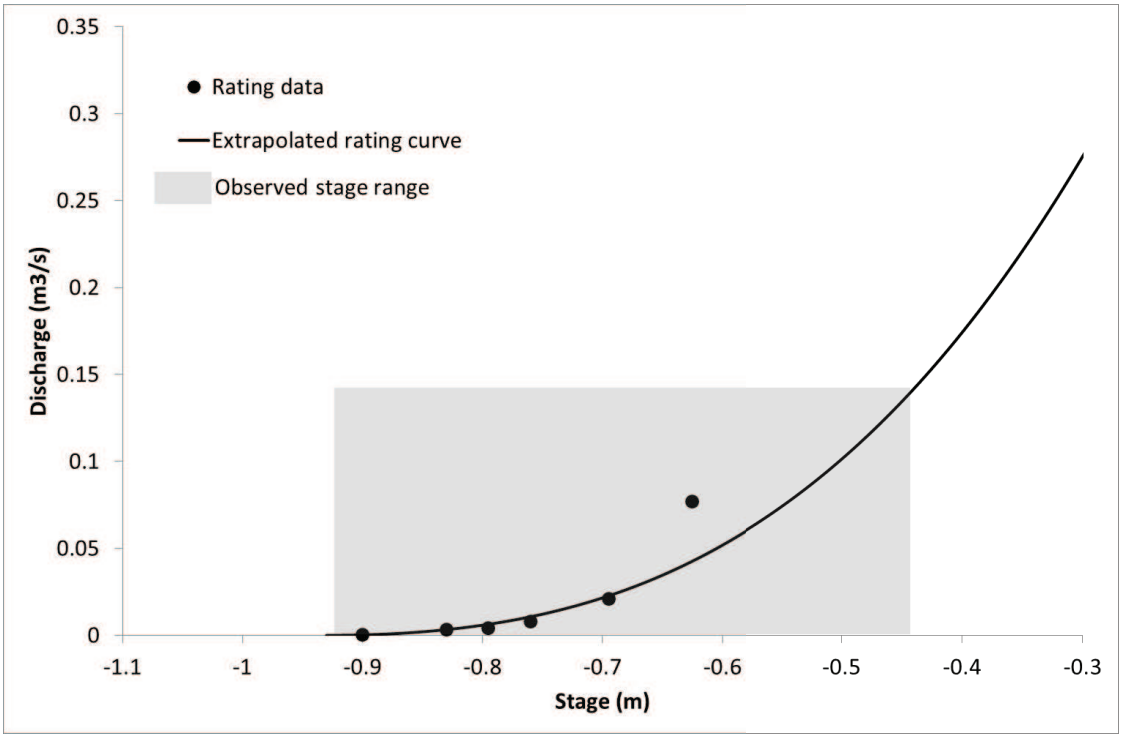

A.1.11 CRO_sc5

Gauge name	Croasdale Brook outlet
Description:	Outlet of Swine Clough in the Croasdale Brook catchment
Grid reference:	SD 68734 56678
Elevation:	255.73 m
Catchment area:	0.5 km^2 (micro scale)
Abstractions:	-
Related sites:	Upstream: CRO_sc1, CRO_sc2, CRO_sc3, CRO_sc4, Downstream: CRO_out, Croasdale weir (EA) HOD_mid, Hodder Place
Baro used for correction:	Baro_Croasdale
Installation Date:	07/12/2007
Record Interval:	5 min (7 min from 06/12/2007 - 13/03/2008)
QA notes:	The gauge was initially installed at 06/12/2007, but the baro only recorded from 23/01/2008, so the full time record only starts at 23/01/2008

Location in Hodder Area	Photo of gauge, downstream direction
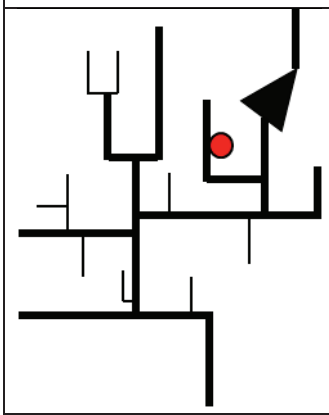	

UU SCaMP interventions	Stocking density	Grip blocking	Tree planting
Timing	Spring 09	February 09	-
Area affected (%)	100	35	-

Cross-section (from EPR, 2010)

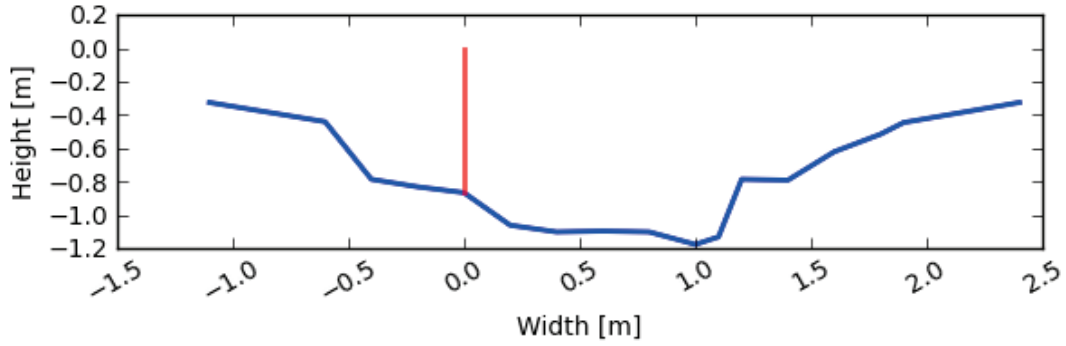

Rating Curve

Observed stage range (m):	-0.86 – (-0.35)
Number of gaugings:	7
Percentage highest gauging of maximum observed stage peak (%):	61.4
Percentage of time extrapolated (%):	2.1

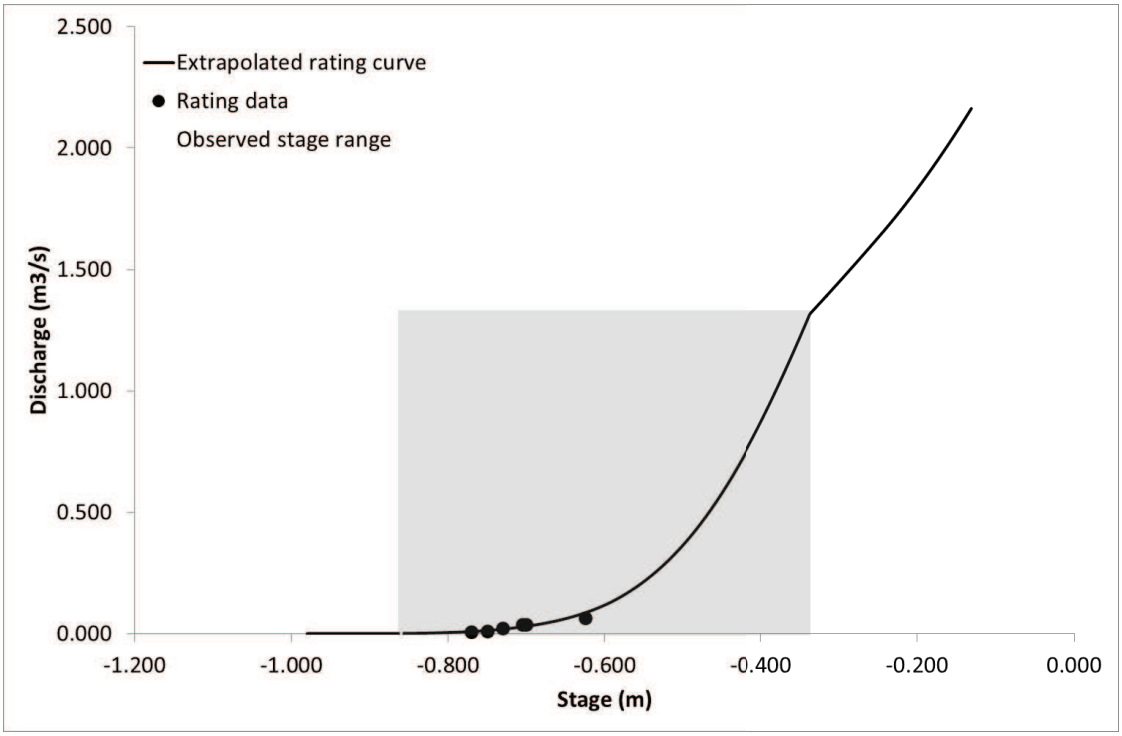

A.1.12 EAS_out

Gauge name	Easington Outlet
Description:	Outlet of Easington Brook
Grid reference:	SD 70781 50341
Elevation:	134.0 m
Abstractions:	-
Catchment area:	13.3 km^2 (mini scale)
Related sites:	Upstream: - Downstream: HOD_mid, Hodder Place (EA)
Baro used for correction:	Baro_Footholme
Installation Date:	19/06/2008
Record Interval:	5 min
QA notes:	-

Location in Hodder Area	Photo of gauge, downstream direction
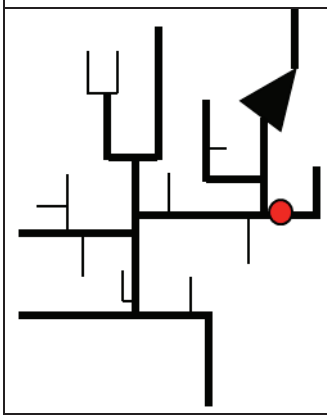	

UU SCaMP interventions	Stocking density	Grip blocking	Tree planting
Timing	-	-	-
Area affected (%)	-	-	-

Cross-section (from EPR)

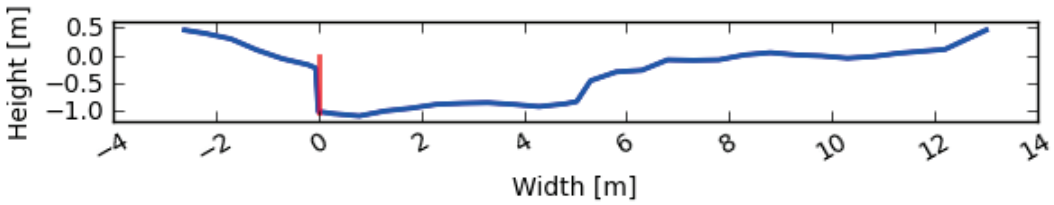

Rating Curve

Observed stage range (m):	-1.020 -0.494
Number of gaugings:	8
Percentage highest gauging of maximum observed stage peak (%):	43.6
Percentage of time extrapolated (%):	2.4

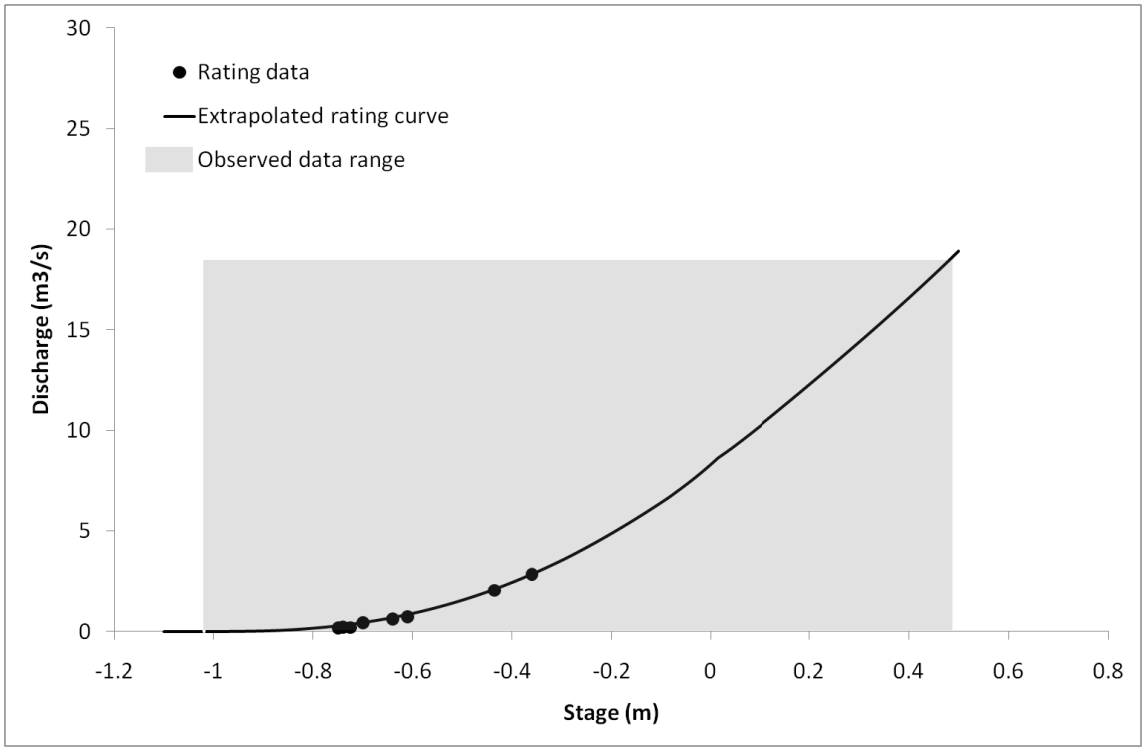

A.1.13 HAR_out

Gauge name	Hareden Outlet
Description:	Hareden Brook Outlet, a tributary of Langden Brook
Grid reference:	SD 64226 56588
Elevation:	147.4 m
Abstractions:	Upstream abstractions as part of United Utilities' Bowland abstraction system
Catchment area:	4.9 km^2 (micro scale)
Related sites:	Upstream: -. Downstream: LAN_out, Hodder Place (EA)
Baro used for correction:	Baro_Footholme
Installation Date:	20/05/2008
Record Interval:	5 min
QA notes:	Missing data from 03/10/2008 – 15/12/2008 as a result of vandalism, new diver from 09/12/2008

Location in Hodder Area	Photo of gauge, downstream direction
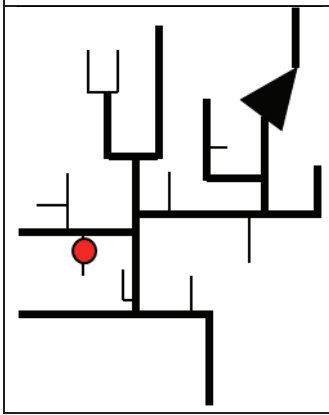	

UU SCaMP interventions	Stocking density	Grip blocking	Tree planting
Timing	February 09	-	February 09
Area affected (%)	100	-	NA

Cross-section (from EPR)

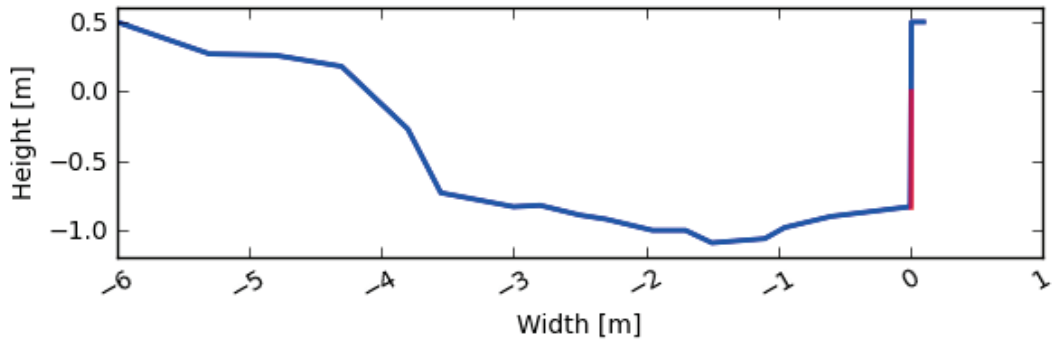

Rating Curve

Observed stage range (m):	-0.775 – 0.102
Number of gaugings:	6
Percentage highest gauging of maximum observed stage peak (%):	37.0
Percentage of time extrapolated (%):	1.6

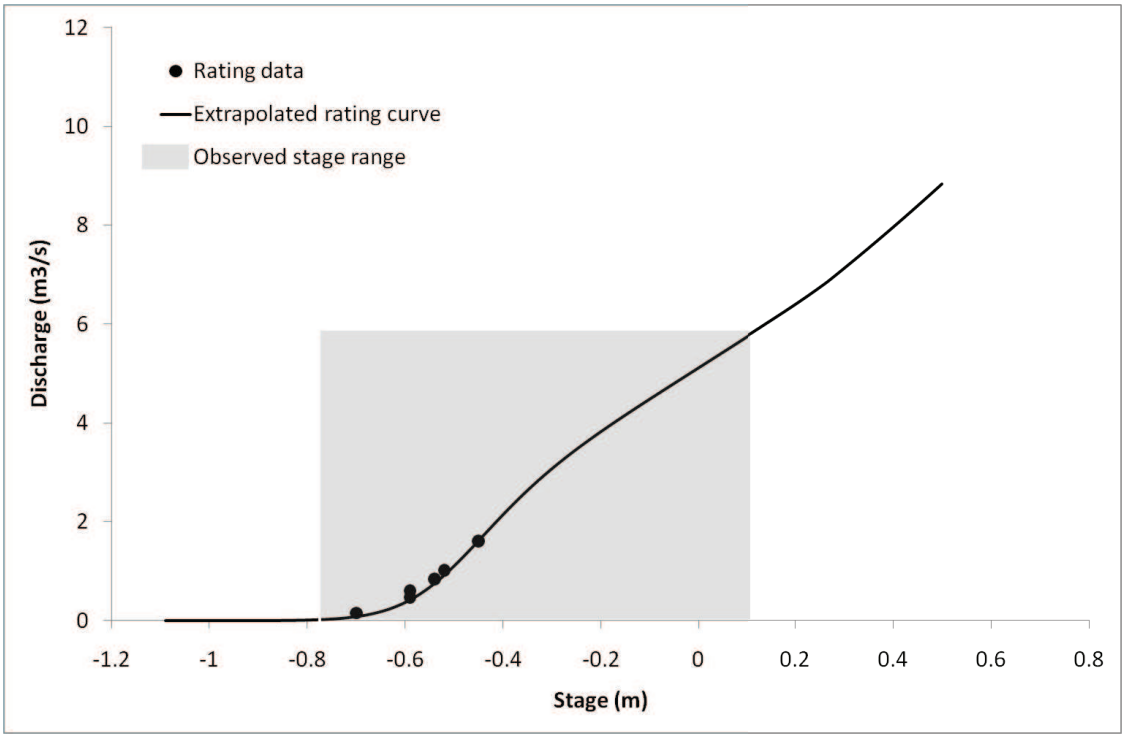

A.1.14 HOD_mid

Gauge name	Mid Hodder
Description:	Mid River Hodder, just upstream of the confluence with River Dunsop
Grid reference:	SD 66343 50031
Elevation:	116.1 m
Abstractions:	Upstream abstractions as part of United Utilities' abstraction system at Stocks Reservoir
Catchment area:	110.3 km^2 (meso scale)
Related sites:	Upstream: CRO_sc1, CRO_sc2, CRO_sc3, CRO_sc4, CRO_sc5, CRO_mid, Croasdale Weir (EA), CRO_out, EAS_out, Stocks Reservoir (EA) Downstream: Hodder Place (EA)
Baro used for correction:	Baro_Footholme
Installation Date:	20/06/2008
Record Interval:	5 min
QA notes:	Missing data from 03/02/2010 – 12/08/2010 as a result of equipment failure

Location in Hodder Area	Photo of gauge, downstream direction
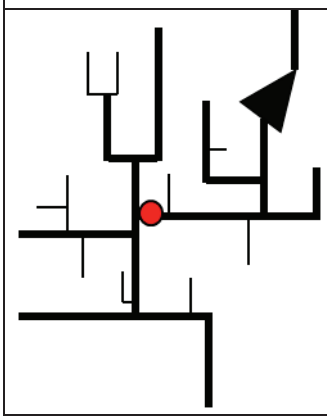	

UU SCaMP interventions	Stocking density	Grip blocking	Tree planting
Timing	February 09	February 09	-
Area affected (%)	1	<1	-

Cross-section (from EPR)

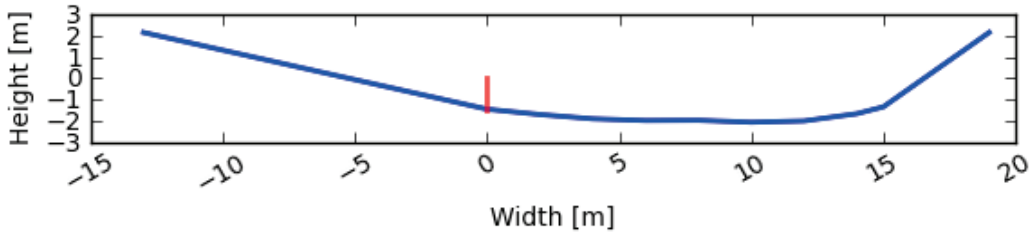

Rating Curve

Observed stage range (m):	-1.440 – 1.100
Number of gaugings:	8
Percentage highest gauging of maximum observed stage peak (%):	59.3
Percentage of time extrapolated (%):	<1

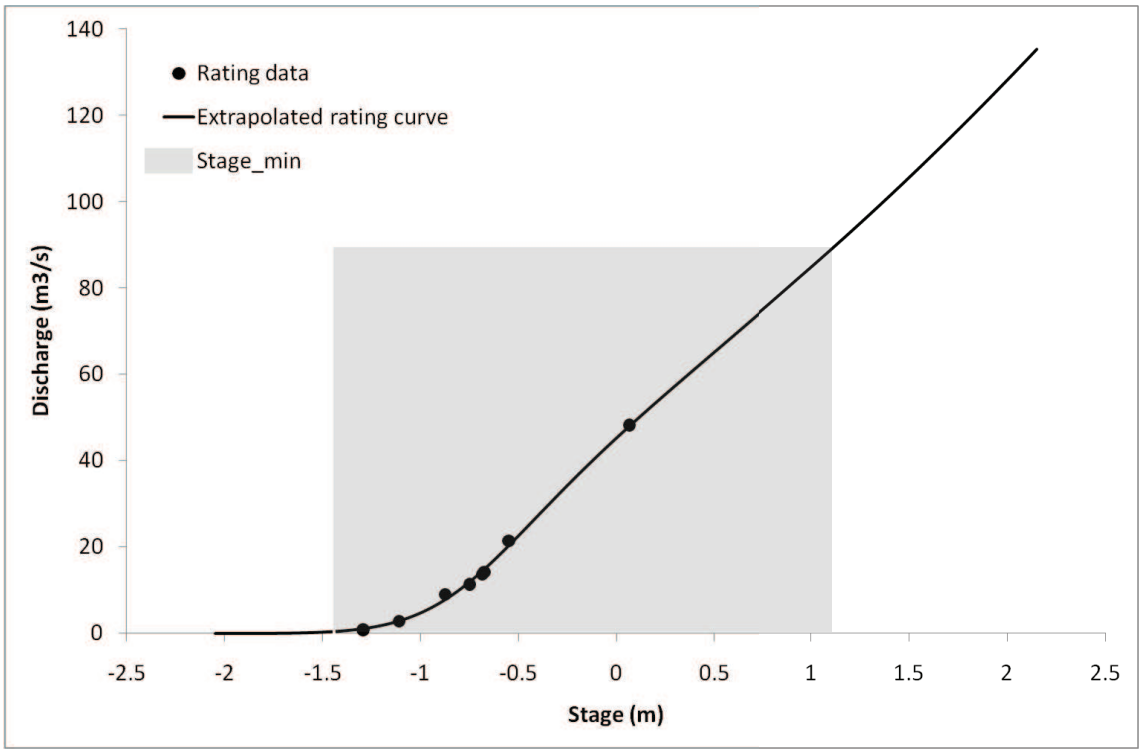

A.1.15 LAN_mid

Gauge name	Mid Langden
Description:	Mid Langden Brook, just upstream of the confluence with Losterdale Brook
Grid reference:	SD 63131 51083
Elevation:	165.9 m
Abstractions:	Upstream abstractions as part of United Utilities' Bowland abstraction system
Catchment area:	15.0 km^2 (mini scale)
Related sites:	Upstream: - Downstream: LAN_out, Hodder Place (EA)
Baro used for correction:	Baro_Footholme
Installation Date:	19/05/2008
Record Interval:	5 min
QA notes:	A telemetered 'frog logger' was installed adjacent to the current logger at 23/04/2010

Location in Hodder Area	Photo of gauge, downstream direction
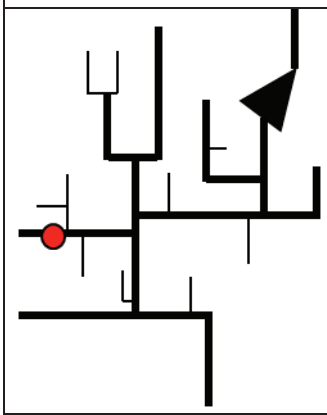	

UU SCaMP interventions	Stocking density	Grip blocking	Tree planting
Timing	February 09	-	Mar 09
Area affected (%)	100	-	<1

Cross-section (from EPR)

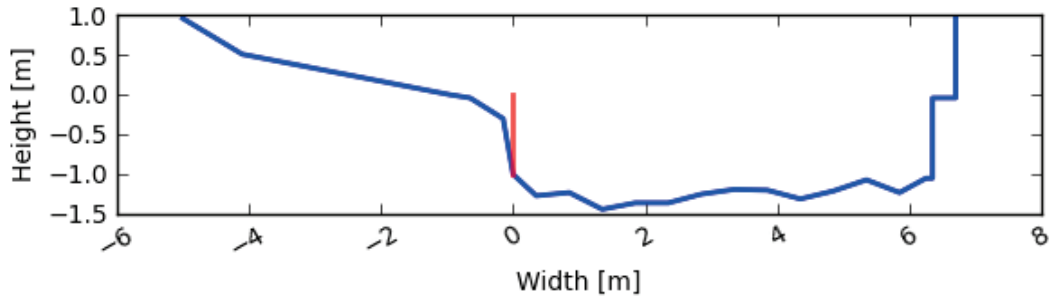

Rating Curve

Observed stage range (m):	-1.005 - -0.045
Number of gaugings:	9
Percentage highest gauging of maximum observed stage peak (%):	33.3
Percentage of time extrapolated (%):	4.7

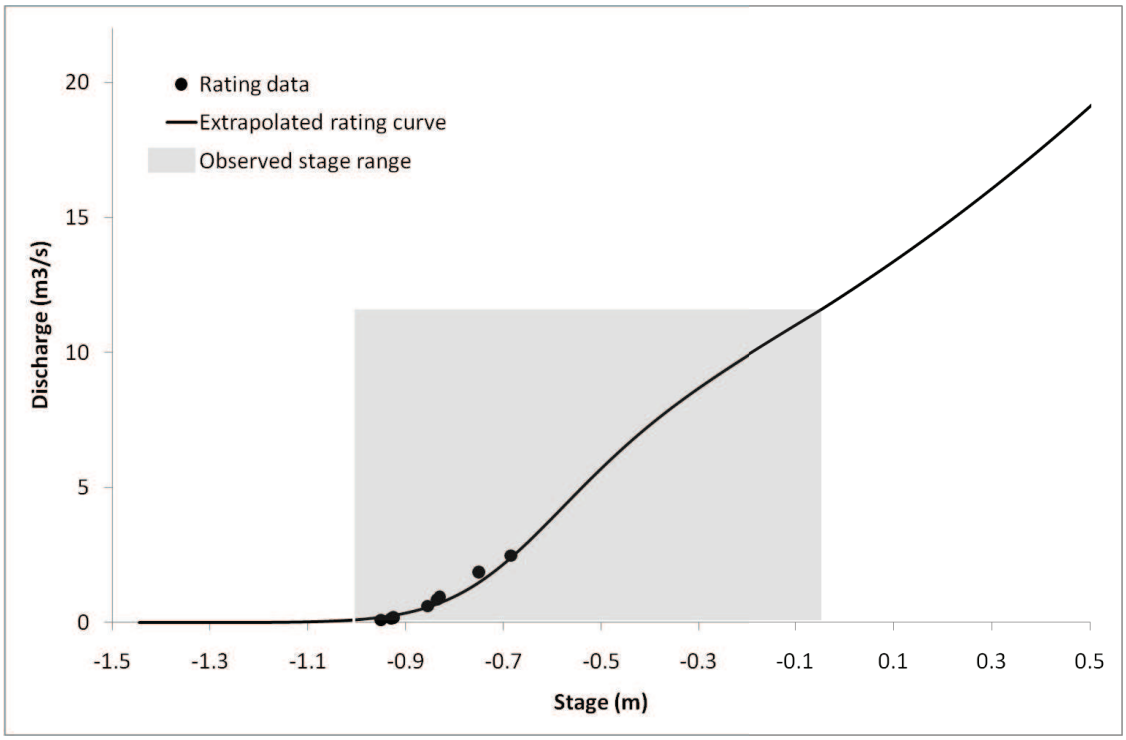

A.1.16 LAN_out

Gauge name	Langden Outlet
Description:	Langden Brook Outlet
Grid reference:	SD 65932 49334
Elevation:	117.4 m
Abstractions:	Upstream abstractions as part of United Utilities' Bowland abstraction system
Catchment area:	27.7 km^2 (mini scale)
Related sites:	Upstream: LOS_stock/LOS_stock_weir, LOS_mid, LOS_out, LAN_mid, HAR_out Downstream: Hodder Place (EA)
Baro used for correction:	Baro_Footholme
Installation Date:	21/05/2008
Record Interval:	15 min
QA notes:	-

Location in Hodder Area	Photo of gauge location, upstream direction
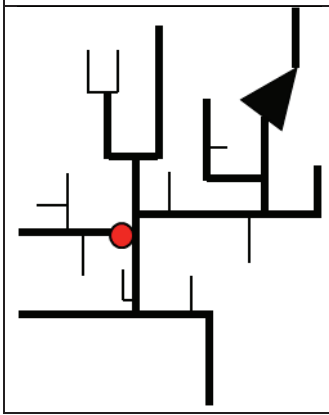	

UU SCaMP interventions	Stocking density	Grip blocking	Tree planting
Timing	February 09	-	March 09
Area affected (%)	85	-	<1

Cross-section (from EPR)

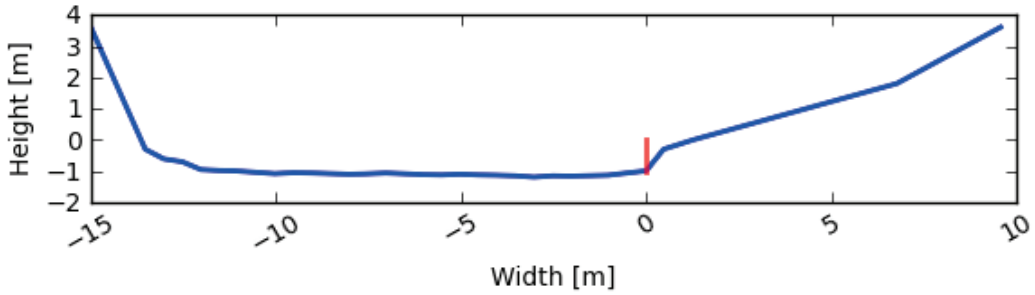

Rating Curve

Observed stage range (m):	-0.985 – 0.177
Number of gaugings:	8
Percentage highest gauging of maximum observed stage peak (%):	66.7
Percentage of time extrapolated (%):	<1

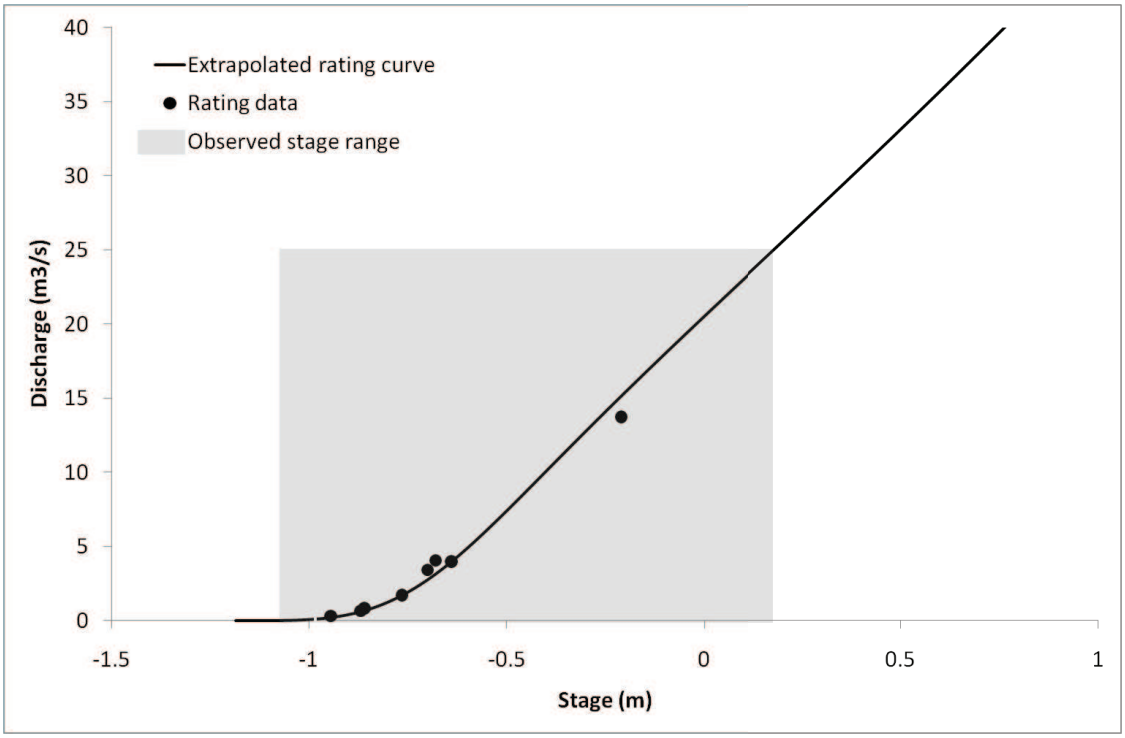

A.1.17 LOS_mid

Gauge name	Mid Losterdale
Description:	Mid Losterdale Brook, just upstream of the confluence with Swine Clough (monitored for stocking density changes and tree planting)
Grid reference:	SD 62743 52049
Elevation:	187.9 m
Abstractions:	-
Catchment area:	2.5 km^2 (micro scale)
Related sites:	Upstream: - Downstream: LOS_out, LAN_out, Hodder Place (EA)
Baro used for correction:	Baro_Footholme
Installation Date:	05/06/2008
Record Interval:	5 min
QA notes:	Missing data from 25/12/2008 – 13/01/2009 as a result of equipment failure, diver changed at 03/02/2010

Location in Hodder Area	Photo of gauge, downstream direction
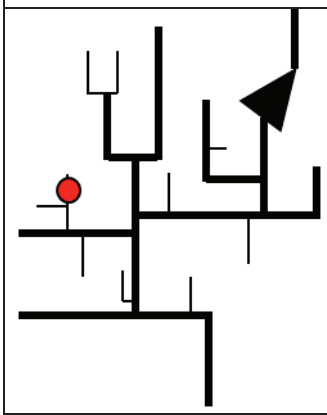	

UU SCaMP interventions	Stocking density	Grip blocking	Tree planting
Timing	February 09	-	-
Area affected (%)	100	-	-

Cross-section (from EPR)

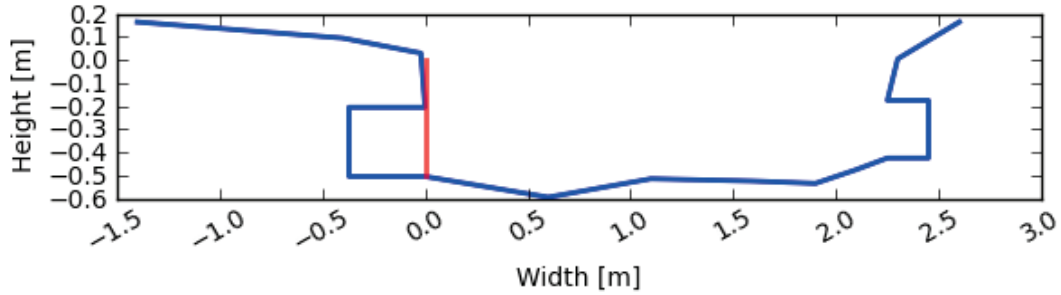

Rating Curve

Observed stage range (m):	-0.505 – 0.328
Number of gaugings:	8
Percentage highest gauging of maximum observed stage peak (%):	50.4
Percentage of time extrapolated (%):	1.0

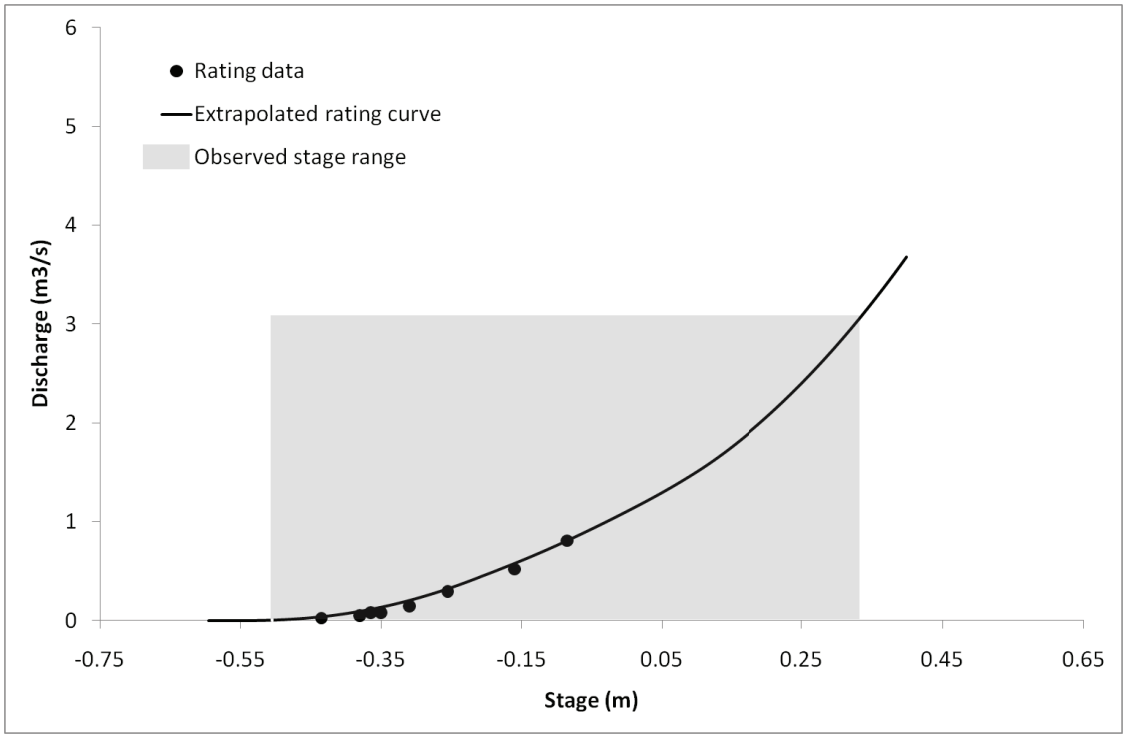

A.1.18 LOS_out

Gauge name	Losterdale Outlet
Description:	Losterdale Brook Outlet, a tributary of Langden Brook
Grid reference:	SD 63203 51219
Elevation:	165.2 m
Abstractions:	Upstream abstractions as part of United Utilities' Bowland abstraction system
Catchment area:	4.0 km^2 (micro scale)
Related sites:	Upstream: LOS_stock/LOS_stock_weir, LOS_mid Downstream: LAN_out, Hodder Place (EA)
Baro used for correction:	Baro_Footholme
Installation Date:	05/06/2008
Record Interval:	5 min
QA notes:	Missing data from 24/01/2010 – 02/02/2010 and 03/07/2010 – 14/07/2010 as a result of equipment failure. Data post 24/01/2010 questionable as a result of the equipment failure: sensor potentially damaged by frost

Location in Hodder Area	Photo of gauge, downstream direction
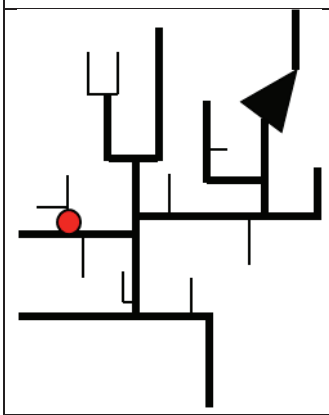	

UU SCaMP interventions	Stocking density	Grip blocking	Tree planting
Timing	February 09	-	March 09
Area affected (%)	100	-	<1

Cross-section (from EPR)

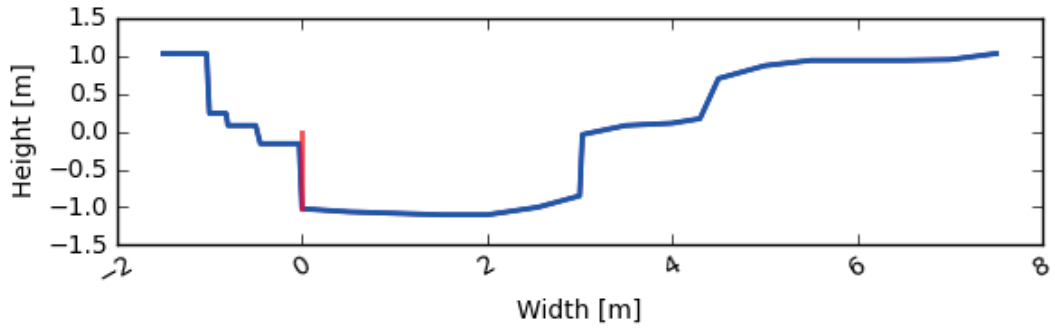

Rating Curve

Observed stage range (m):	-1.010 -0.001
Number of gaugings:	7
Percentage highest gauging of maximum observed stage peak (%):	37.1
Percentage of time extrapolated (%):	4.6

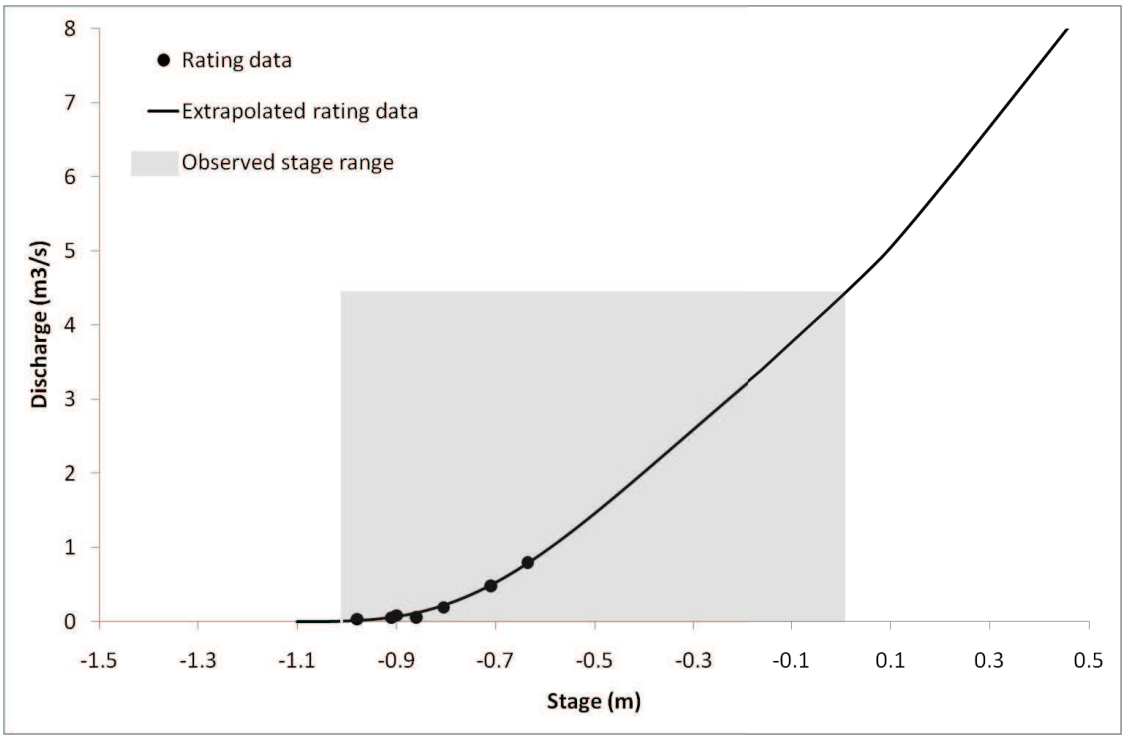

A.1.19 LOS_stock/LOS_stock_weir

Gauge name	LOS_stock and LOS_stock_weir
Description:	LOS_stock is located at the outlet of Swine Clough, a headwater of Losterdale Brook, in the Langden Brook subcatchment. LOS_stock_weir is located about 500 m upstream of LOS_stock, in a headwater of Swine Clough.
Grid reference:	LOS_stock: SD 62721 52025
Elevation:	LOS_stock: 197.7
Abstractions:	-
Catchment area:	LOS_stock: 0.12 km^2 (process scale) LOS_stock_weir: 1.00 km^2 (micro scale)
Related sites:	Upstream: none Downstream: LOS_out, LAN_out, Hodder Place (EA)
Baro used for correction:	Baro_Footholme
Installation Date:	03/06/2008 (LOS_stock), 25/11/2008 (LOS_stock_weir)
Record Interval:	5 min
QA notes:	LOS_stock has missing data from 03/10/2008 - 09/12/2008 as a result of equipment failure. The diver was replaced at 09/12/2008. The data of LOS_stock_weir are unreliable at 09/12/2009 as a result of weir maintenance.

LOS_stock:

Location in Hodder Area	Photo of gauge, downstream direction
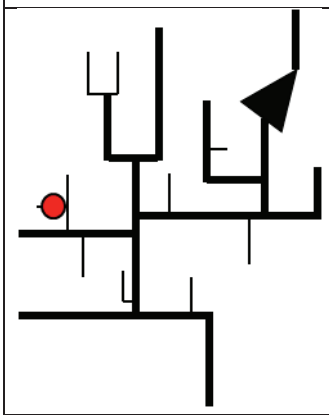	

UU SCaMP interventions	Stocking density	Grip blocking	Tree planting
Timing	February 2009	-	March 2009
Area affected (%)	100	-	5

LOS_stock_weir:

Location in Hodder Area	Photo of weir and gauge, upstream direction
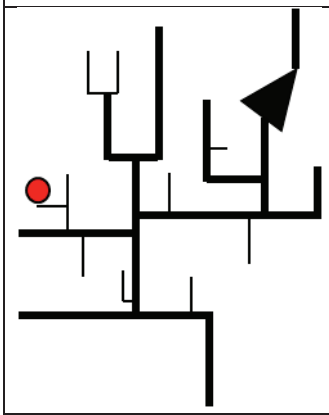	

UU SCaMP interventions	Stocking density	Grip blocking	Tree planting
Timing	February 2009	-	February 2009
Area affected (%)	100	-	5

Rating Curve

No rating curve available for LOS_stock as this site was considered redundant after the installation of the LOS_stock_weir.

The weir at LOS_stock_weir is a rectangular weir build according to British Standard 3680, Part 4A (BSI, 1981). The geometrical details of the weir are given below.

Schematic representation of the v-notch weir at WHI_tree_weir

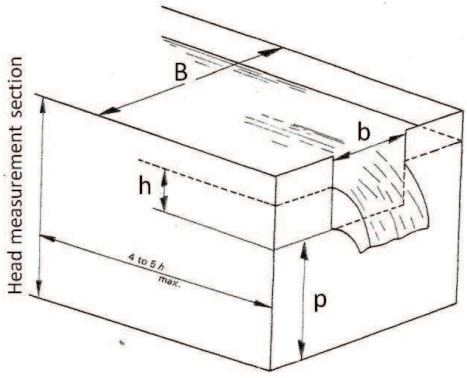

B	1.4
b	0.8
p (upstream)	0.345
p (downstream)	0.560
Maximum height above crest	0.45
Distance gauge to weir	0.65

For rectangular thin plate weirs the discharge Q ($m^3\ s^{-1}$) can be calculated from stage h (m) according to the Kindsvater-Carter formula:

$$Q = C_e \frac{2}{3} \sqrt{2g_n} b_e h_e^{3/2}$$

where C_e is the coefficient of discharge (-), b_e is the effective width (m), h_e is the effective head (m), and g_n is the acceleration due to gravity (9.81 m/s^2).

A.1.20 LOU_out

Gauge name	Loud Outlet
Sub catchment:	Outlet of River Loud
Grid reference:	SD 64889 43056
Elevation:	86.5 m
Catchment area:	47.3 km^2 (mini scale)
Abstractions:	-
Related sites:	Upstream: none
	Downstream: Hodder Place
Baro used for correction:	Baro_Loud
Installation Date:	11/06/2008
Record Interval:	15 min
QA notes:	-

Location in Hodder Area	Photo of gauge, downstream direction
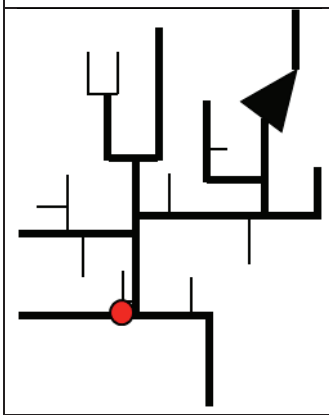	

UU SCaMP interventions	Stocking density	Grip blocking	Tree planting
Timing	-	-	-
Area affected (%)	-	-	-

Cross-section (from EPR)

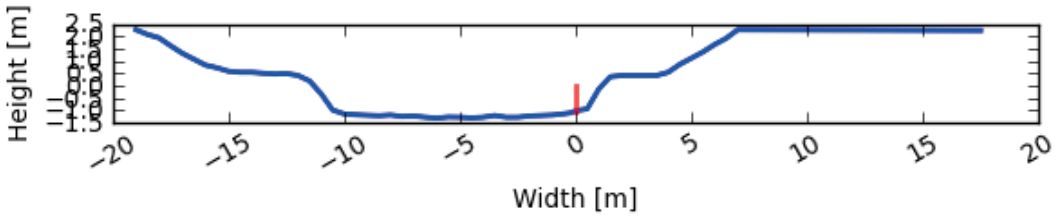

Rating Curve

Observed stage range (m):	-1.00 – 1.56
Number of gaugings:	6
Percentage highest gauging of maximum observed stage peak (%):	53.9
Percentage of time extrapolated (%):	0.2

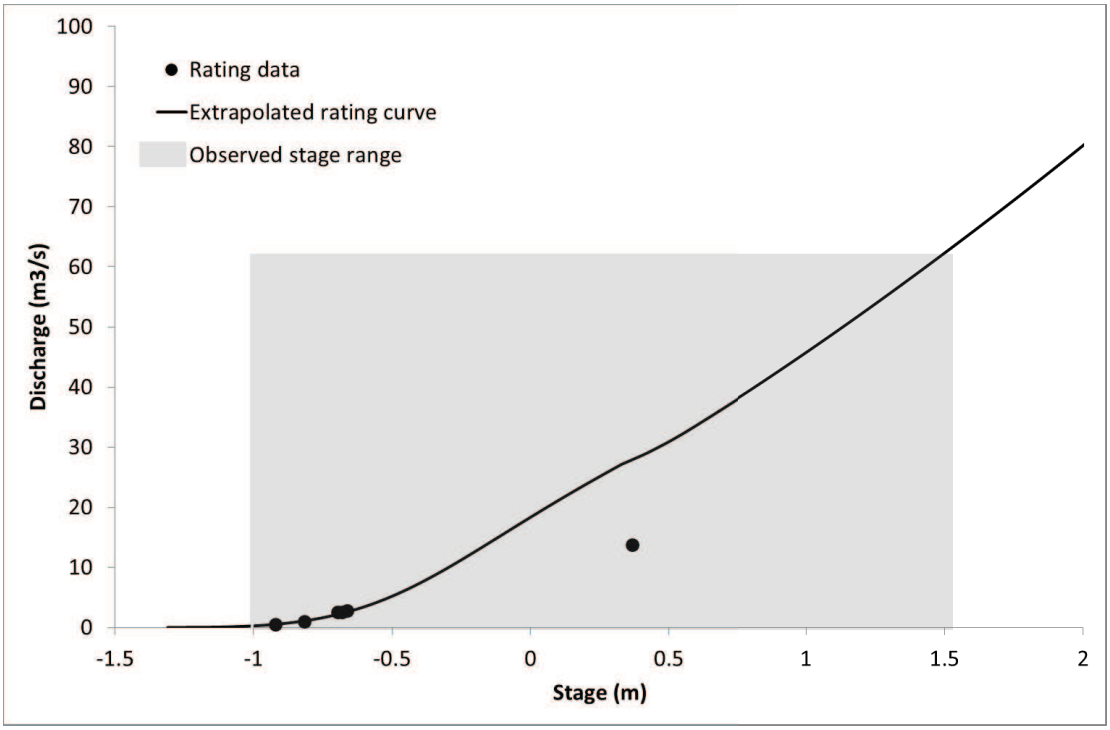

A.1.21 WHI_mid

Gauge name	Mid Whitendale
Description:	Mid River Whitendale, upstream of the confluence with a stream draining from Blue Scar (monitored for tree planting)
Grid reference:	SD 66061 54633
Elevation:	205.0 m
Abstractions:	Upstream abstractions as part of United Utilities' Dunsop abstraction system
Catchment area:	10.0 km^2 (mini scale)
Related sites:	Upstream: - Downstream: WHI_out, Footholme (EA), Hodder Place (EA)
Baro used for correction:	Baro_Footholme
Installation Date:	11/06/2008
Record Interval:	15 min
QA notes:	Gauge maintenance at 26/02/2009 where datum shifted -19.5 cm

Location in Hodder Area	Photo of gauge, downstream direction
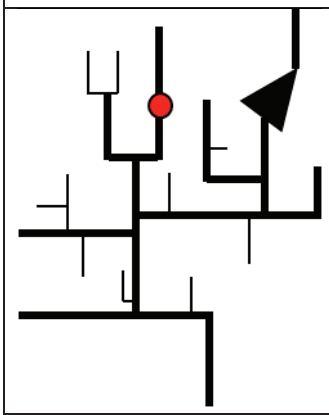	

UU SCaMP interventions	Stocking density	Grip blocking	Tree planting
Timing	Spring 08	2005	Spring 08
Area affected (%)	100	NA	5

Cross-section (from EPR)

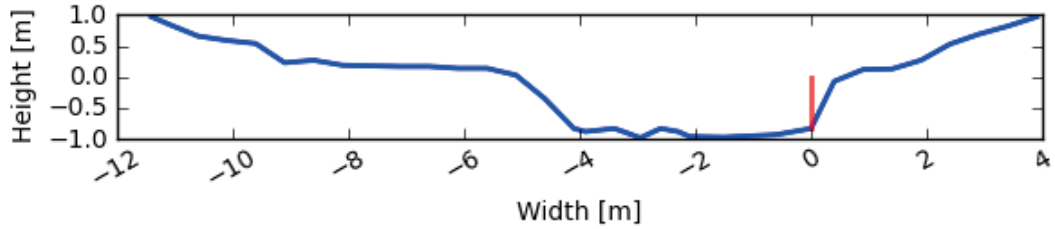

Rating Curve

Observed stage range (m):	-0.830 – 0.522
Number of gaugings:	6
Percentage highest gauging of maximum observed stage peak (%):	43.3
Percentage of time extrapolated (%):	3.7

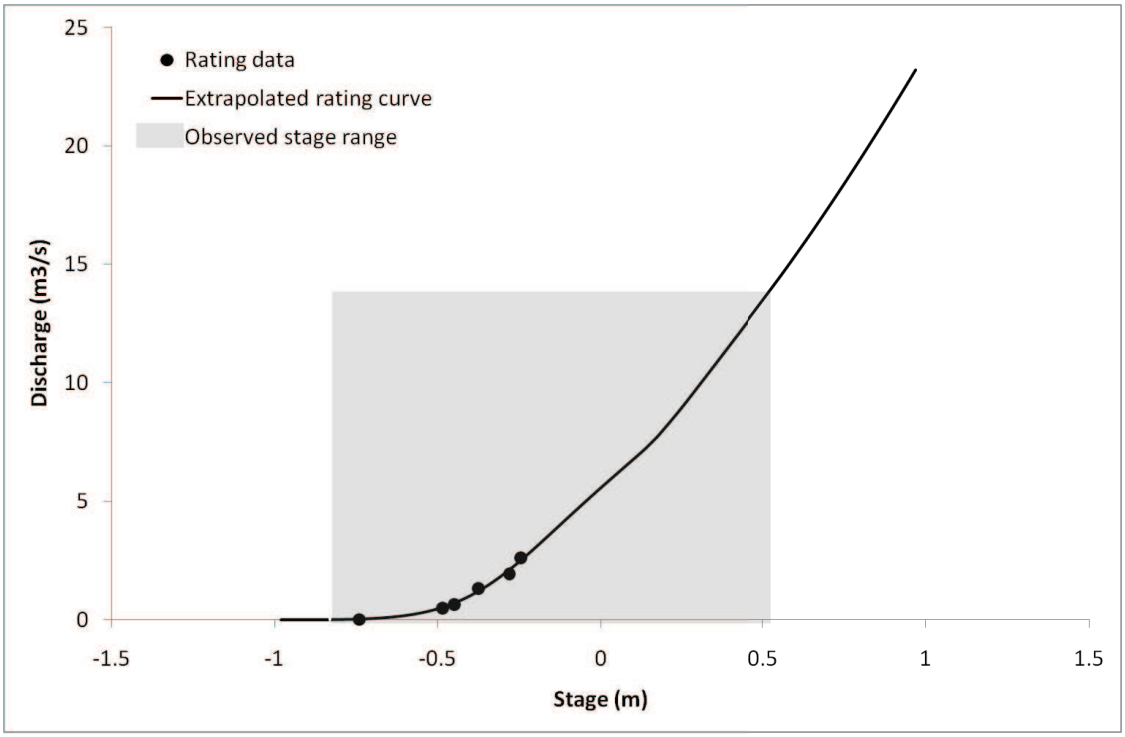

A.1.23 WHI_out

Gauge name	Whitendale Outlet
Description:	River Whitendale Outlet, subcatchment of River Dunsop
Grid reference:	SD 65326 53231
Elevation:	177.9 m
Abstractions:	Upstream abstractions as part of United Utilities' Dunsop abstraction system
Catchment area:	13.6 km^2 (mini scale)
Related sites:	Upstream: WHI_tree/WHI_tree_weir Downstream: Footholme (EA), Hodder Place (EA)
Baro used for correction:	Baro_Footholme
Installation Date:	07/12/2007
Record Interval:	15 min
QA notes:	In low flows this gauge may be above the river water surface. The gauge was initially installed at 07/12/2007, but the baro only recorded from 23/01/2008, so the full time record only starts at 23/01/2008.

Location in Hodder Area	Photo of gauge, downstream direction
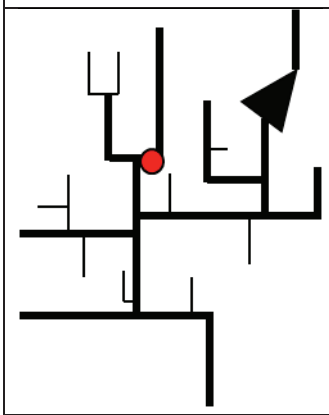	

UU SCaMP interventions	Stocking density	Grip blocking	Tree planting
Timing	Spring 08	2005	Spring 08
Area affected (%)	100	NA	5

Cross-section (from EPR)

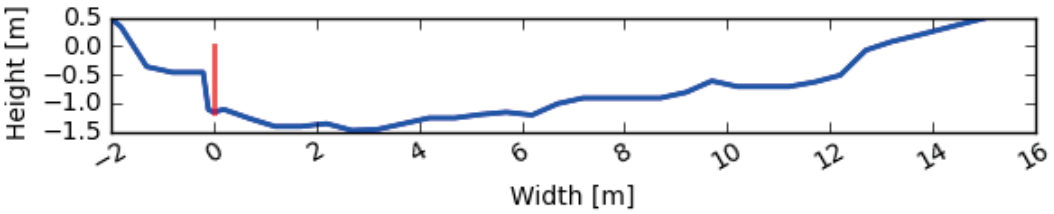

Rating Curve

Observed stage range (m):	-1.155 – 0.177
Number of gaugings:	9
Percentage highest gauging of maximum observed stage peak (%):	49.8
Percentage of time extrapolated (%):	2.2

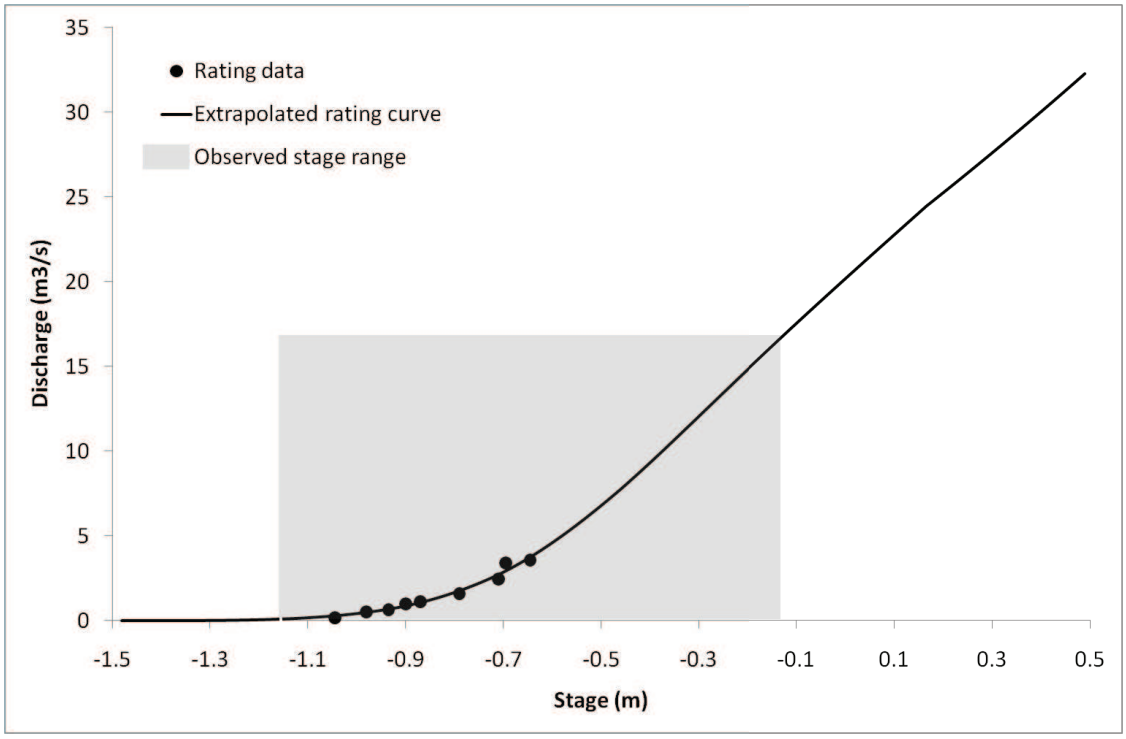

A.1.22 WHI_tree/WHI_tree_weir

Gauge name	WHI_tree (superseded by WHI_tree_weir at 25/11/08)
Description:	The outlet of a stream draining Blue Scar at Middle Knoll in the Whitendale subcatchment. WHI_tree_weir is located 18 m downstream of channel site WHI_tree
Grid reference:	SD 66030 54663 (WHI_tree), and SD 66041 54647 (WHI_tree_weir)
Elevation:	208.4 m (WHI_tree), and 205.5 (WHI_tree_weir)
Abstractions:	-
Catchment area:	0.06 km^2 (process scale)
Related sites:	Upstream: - Downstream: WHI_out, Footholme (EA), Hodder Place (EA)
Baro used for correction:	Baro_Footholme
Installation Date:	03/06/2008 (WHI_tree), 25/11/2008 (WHI_tree_weir)
Record Interval:	5 min
QA notes:	-

Location in Hodder Area	Photo of weir and gauge, upstream direction
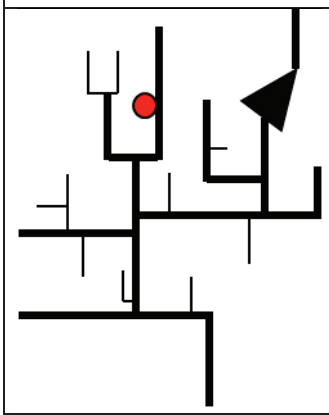	

UU SCaMP interventions	Stocking density	Grip blocking	Tree planting
Timing	-	-	Spring 2008
Area affected (%)	-	-	100

Rating Curve

The weir at WHI_tree/WHI_tree_weir is a v-notch weir build according to British Standard 3680, Part 4A (BSI, 1981). The geometrical details of the weir are given below.

Schematic representation of the v-notch weir at WHI_tree_weir

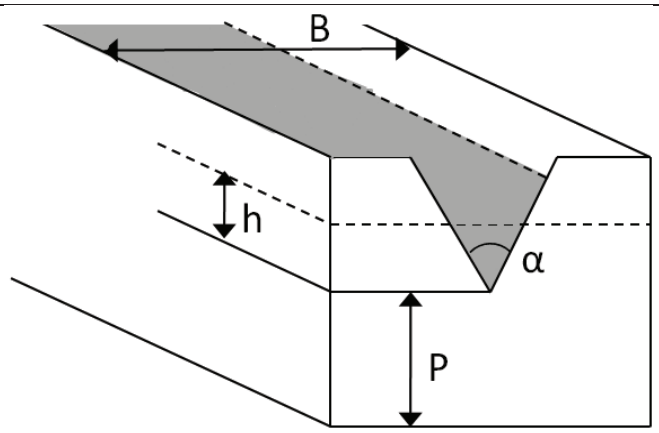

B	0.85
α	90
p (upstream)	0.135
p (downstream)	0.3
Maximum height above crest	0.28
Distance gauge to weir	1.15

The discharge Q (m^3/s) is calculated from stage h (m) according to the Kindsvater-Shen formula (BSI, 1981):

$$Q = C_e \frac{8}{15} \tan\frac{\alpha}{2} \sqrt{2 g_n h_e^{5/2}}$$

where h_e is the effective head above the crest (m), and g_n is the acceleration due to gravity (m/s^2), and the coefficient of discharge C_e has been determined by experiments as a function of P, B and h_e (BSI, 1981).

A.1.1 BRE_grip/BRE_grip_weir

Gauge name	BRE_grip (superseded by BRE_grip_weir at 01/12/08)
Description:	The outlet of a grip in Sapling Clough, headwater of River Brennand sub catchment. BRE_grip_weir is located 5 m downstream of channel site BRE_grip.
Grid reference:	SD 62692 55949 (BRE_grip), and SD 62690 55949 (BRE_grip_weir)
Elevation:	383.6 m (BRE_grip), and 380.6 m (BRE_grip_weir)
Abstractions:	-
Catchment area:	0.0014 km^2 (process scale)
Related sites:	Upstream: - Downstream: BRE_sap, BRE_out, Footholme (EA), Hodder Place (EA)
Baro used for correction:	Baro_Footholme
Installation Date:	15/05/2008 (BRE_grip), 01/12/2008 (BRE_grip_weir)
Record Interval:	5 min
QA notes:	The data from BRE_grip_weir are unreliable for 06/06/2009 – 25/06/2009 as a result of weir leakage

Location in Hodder Area	Photo of weir and gauge, upstream direction
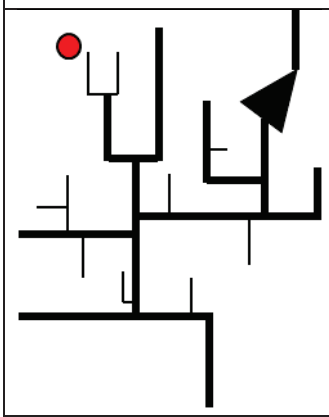	

UU SCaMP interventions	Stocking density	Grip blocking	Tree planting
Timing	Spring 08	November 2008	-
Area affected (%)	100	100	-

Rating Curve

The weir at BRE_grip/BRE_grip_weir is a v-notch weir build according to British Standard 3680, Part 4A (BSI, 1981). The geometrical details of the weir are given below.

Schematic representation of the v-notch weir at BRE_grip_weir

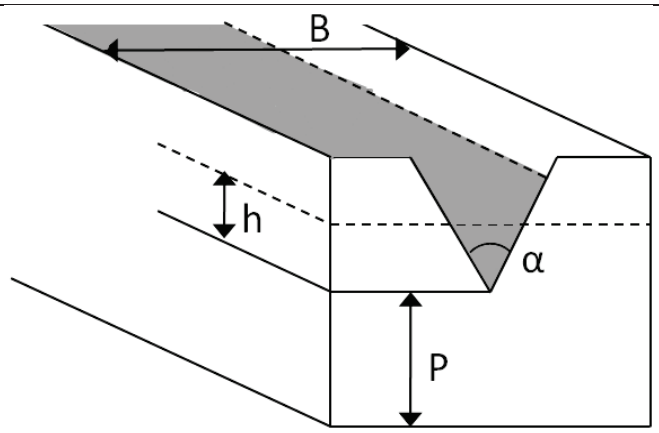

B	1.2
α	90
p (upstream)	0.42
p (downstream)	0.53
Maximum height above crest	0.39
Distance gauge to weir	1.35

The discharge Q (m^3/s) is calculated from stage h (m) according to the Kindsvater-Shen formula (BSI, 1981):

$$Q = C_e \frac{8}{15} \tan\frac{\alpha}{2} \sqrt{2 g_n h_e^{5/2}}$$

where h_e is the effective head above the crest (m), and g_n is the acceleration due to gravity (m/s^2), and the coefficient of discharge C_e has been determined by experiments as a function of P, B and h_e (BSI, 1981).

A.1.2 BRE_out

Gauge name	Brennand Outlet
Description:	River Brennand Outlet, subcatchment of River Dunsop
Grid reference:	SD 65271 53214
Elevation:	172.7 m
Abstractions:	Upstream abstractions as part of United Utilities' Dunsop abstraction system
Catchment area:	11.0 km^2 (mini scale)
Related sites:	Upstream: BRE_grip/BRE_grip_weir, BRE_sap, BRE_rhw Downstream: Footholme (EA), Hodder Place (EA)
Baro used for correction:	Baro_Footholme
Installation Date:	07/12/2007
Record Interval:	15 min
QA notes:	In low flows this gauge may be above the river water surface. The gauge was initially installed at 07/12/2007, but the baro only recorded from 23/01/2008, so the full time record only starts at 23/01/2008. Diver changed at 25/06/2009. Unreliable data between 06/06/2009 – 25/06/2009 as a result of livestock disturbance. Gauge relocated at 25/06/2009.

Location in Hodder Area	Photo of gauge, downstream direction
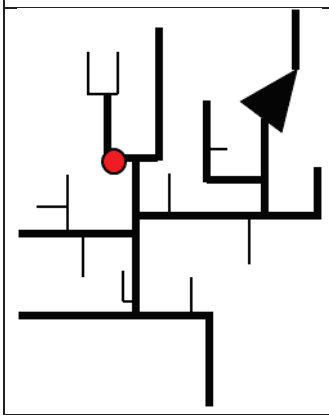	

UU SCaMP interventions	Stocking density	Grip blocking	Tree planting
Timing	Spring 08	November 08	Spring 08
Area affected (%)	100	15	5

Cross-section (from EPR)

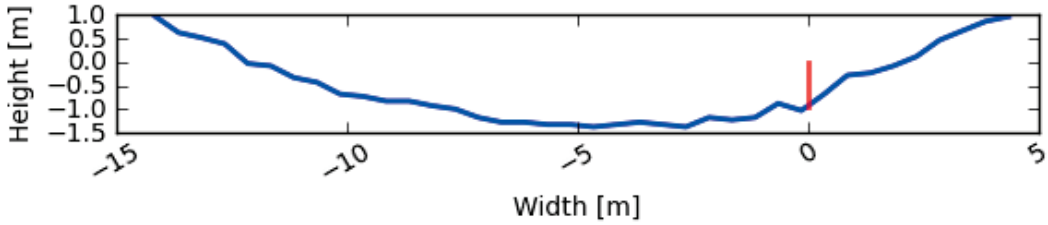

Rating Curve

Observed stage range (m):	-0.930 – 0.565
Number of gaugings:	8
Percentage highest gauging of maximum observed stage peak (%):	25.1
Percentage of time extrapolated (%):	2.0

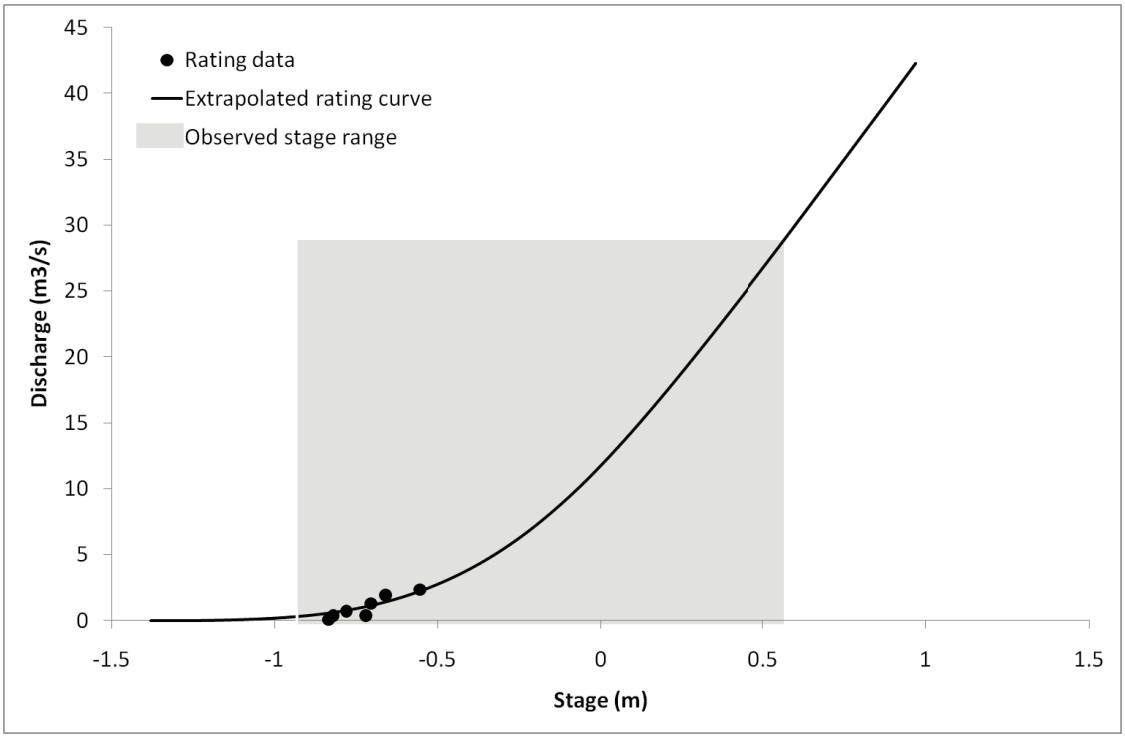

A.1.3 BRE_rhw

Gauge name	Brennand Round Hill Water
Description:	Outlet of Round Hill Water, a headwater of River Brennand
Grid reference:	SD 63136 55751
Elevation:	333.7 m
Catchment area:	2.8 km^2 (micro scale)
Abstractions:	-
Related sites:	Upstream: - Downstream: BRE_out, Footholme, Hodder Place
Baro used for correction:	Baro_Footholme
Installation Date:	15/05/2008
Record Interval:	5 min
QA notes:	-

Location in Hodder Area	Photo of gauge, downstream direction
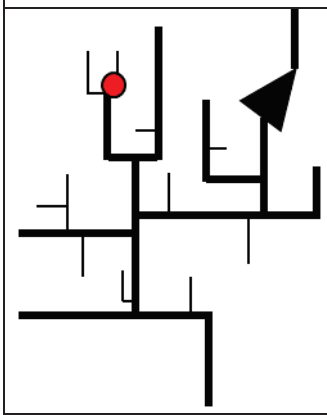	

UU SCaMP interventions	Stocking density	Grip blocking	Tree planting
Timing	Spring 08	November 08	-
Area affected (%)	100	20	-

Cross-section (from EPR, 2010)

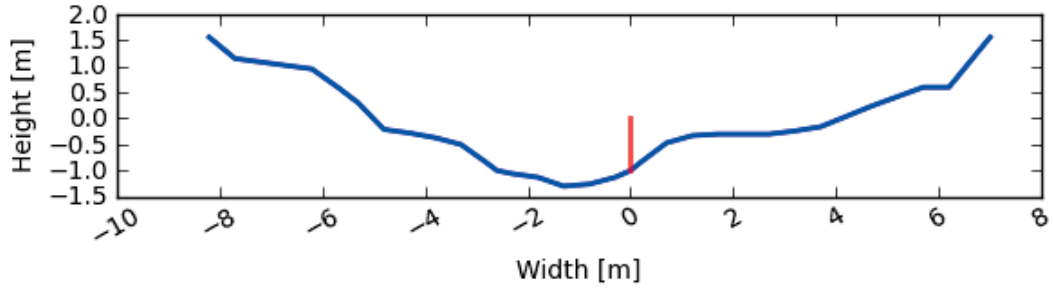

Rating Curve

Observed stage range (m):	-0.985 – 0.015
Number of gaugings:	10
Percentage highest gauging of maximum observed stage peak (%):	47.0
Percentage of time extrapolated (%):	<1

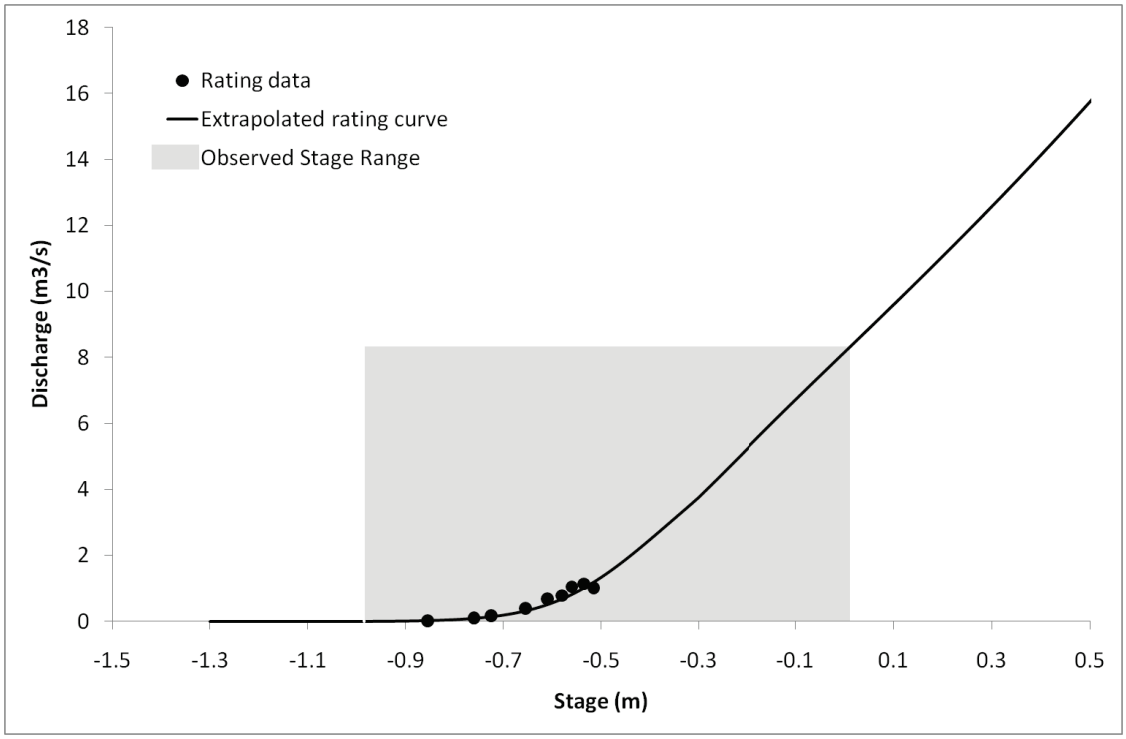

A.1.4 BRE_sap

Gauge name	Brennand Sapling Clough
Description:	Outlet of Sapling Clough, a headwater of River Brennand
Grid reference:	SD 62960 55717
Elevation:	339.9 m
Catchment area:	1.7 km^2 (micro scale)
Abstractions:	-
Related sites:	Upstream: BRE_grip/BRE_grip_weir Downstream: BRE_out, Footholme, Hodder Place
Baro used for correction:	Baro_Footholme
Installation Date:	05/06/2008
Record Interval:	5 min
QA notes:	-

Location in Hodder Area	Photo of gauge, downstream direction
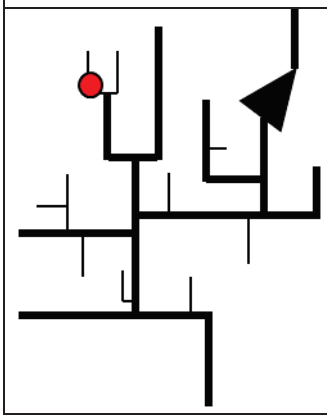	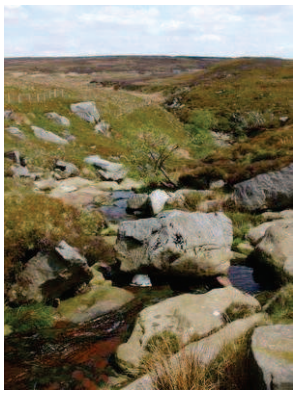

UU SCaMP interventions	Stocking density	Grip blocking	Tree planting
Timing	Spring 08	November 08	-
Area affected (%)	100	35	-

Cross-section (from EPR)

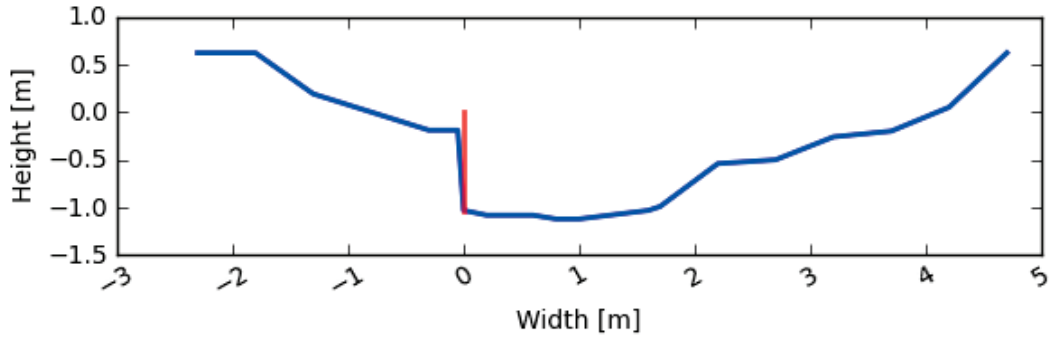

Rating Curve

Observed stage range (m):	-1.015 – 0.215
Number of gaugings:	12
Percentage highest gauging of maximum observed stage peak (%):	31.9
Percentage of time extrapolated (%):	3.9

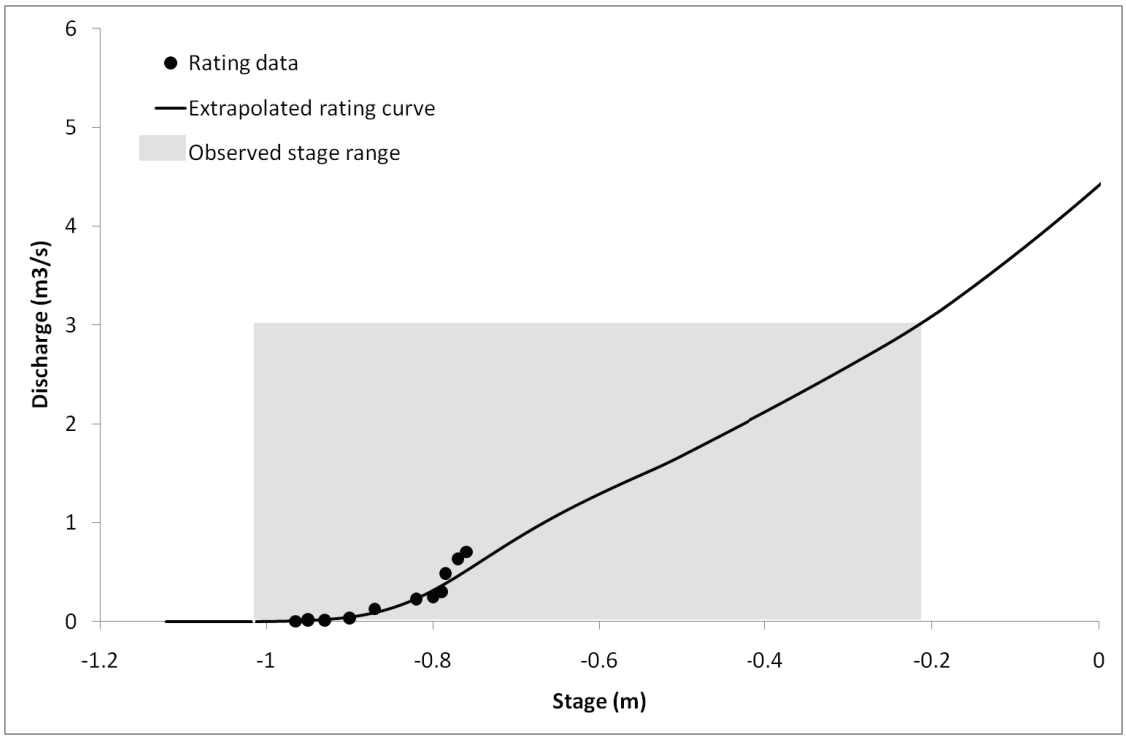

A.1.5 CRO_mid

Gauge name	Mid Croasdale
Description:	Mid Croasdale Brook, just upstream of confluence with Swine Clough
Grid reference:	SD 68673 56607
Elevation:	243.1 m
Catchment area:	3.6 km^2 (micro scale)
Abstractions:	-
Related sites:	Upstream: none Downstream: CRO_out, HOD_mid, Hodder Place
Baro used for correction:	Baro_Croasdale
Installation Date:	06/12/2007
Record Interval:	5 min (7 min from 06/12/2007 - 13/03/2008)
QA notes:	The gauge was initially installed at 06/12/2007, but the baro only recorded from 23/01/2008, so the full time record only starts at 23/01/2008. Missing data from 27/04/2010 – 31/05/2010 as a result of equipment failure.

Location in Hodder Area	Photo of gauge, downstream direction
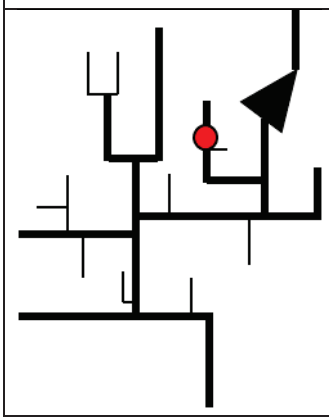	

UU SCaMP interventions	Stocking density	Grip blocking	Tree planting
Timing	February 09	-	-
Area affected (%)	100	-	-

Cross-section (from EPR, 2010)

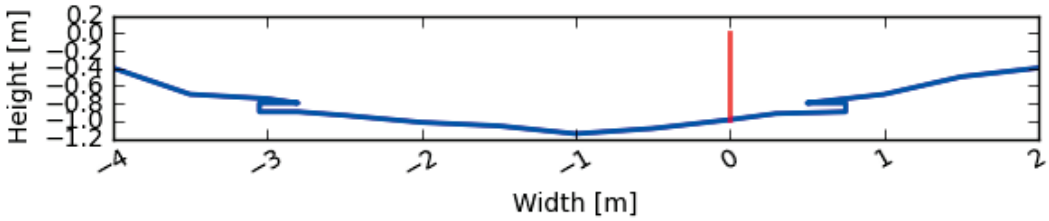

Rating Curve

Observed stage range (m):	-0.868 – 0.034
Number of gaugings:	8
Percentage highest gauging of maximum observed stage peak (%):	54.7
Percentage of time extrapolated (%):	1.4

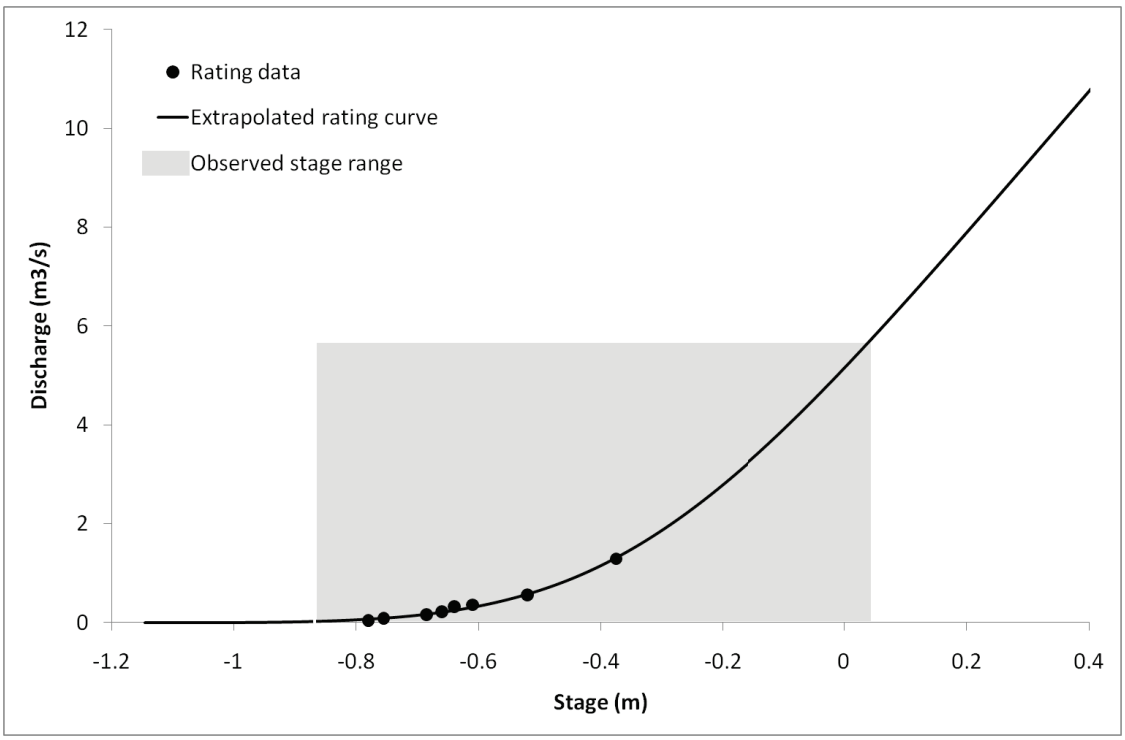

A.1.6 CRO_out

Gauge name	Croasdale Brook outlet
Description:	Outlet of Croasdale Brook
Grid reference:	SD 71216 52496
Elevation:	136.6 m
Catchment area:	21.1 km^2 (mini scale)
Abstractions:	-
Related sites:	Upstream: CRO_mid, CRO_sc1, CRO_sc2, CRO_sc3, CRO_sc4, CRO_sc5, Croasdale weir (EA) Downstream: HOD_mid, Hodder Place
Baro used for correction:	Baro_Footholme
Installation Date:	03/10/2008
Record Interval:	5 min
QA notes:	-

Location in Hodder Area	Photo of gauge, downstream direction
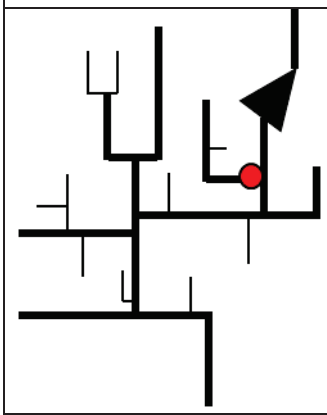	

UU SCaMP interventions	Stocking density	Grip blocking	Tree planting
Timing	Spring 09	February 09	-
Area affected (%)	45.4	2	-

Cross-section (from EPR, 2010)

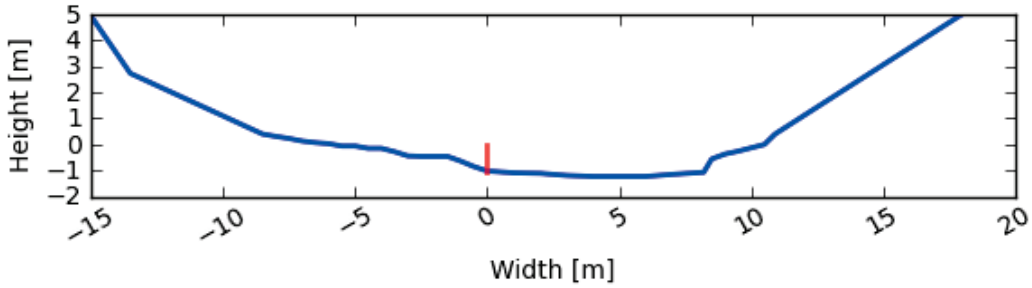

Rating Curve

Observed stage range (m):	-1.020 – 0.419
Number of gaugings:	7
Percentage highest gauging of maximum observed stage peak (%):	48.6
Percentage of time extrapolated (%):	1.3

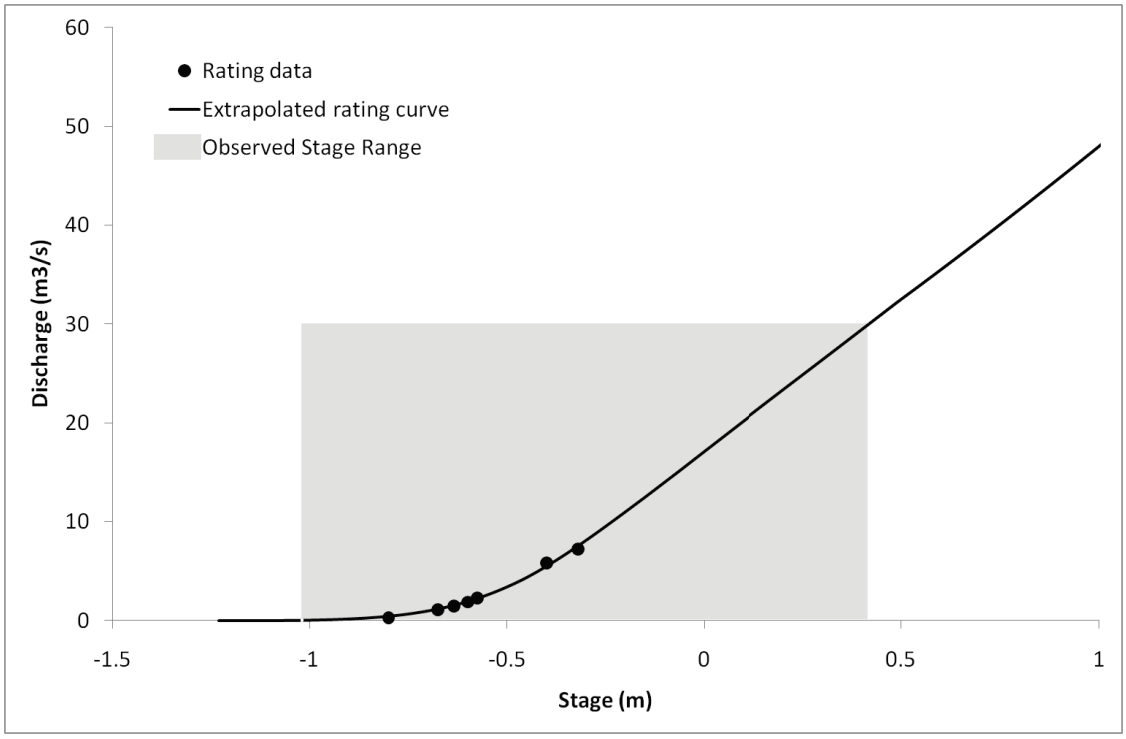

A.1.7 CRO_sc1

Gauge name	Swine Clough, top of grip, Croasdale Brook
Description:	At the top of the grip in the headwaters of Swine Clough in the Croasdale Brook catchment
Grid reference:	SD 69508 57348
Elevation:	411.3 m
Catchment area:	0.08 km^2 (process scale)
Abstractions:	-
Related sites:	Upstream: - Downstream: CRO_sc2, CRO_sc3,CRO_sc5, CRO_out, Croasdale weir (EA) HOD_mid, Hodder Place
Baro used for correction:	Baro_Croasdale
Installation Date:	07/12/2007
Record Interval:	5 min (7 min from 06/12/2007 - 23/01/2008)
QA notes:	The gauge was initially installed at 06/12/2007, but the baro only recorded from 23/01/2008, so the full time record only starts at 23/01/2008. In addition, the diver changed at 23/01/2008

Location in Hodder Area	Photo of gauge, downstream direction, post blocking
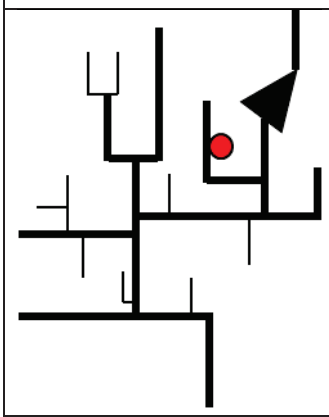	

UU SCaMP interventions	Stocking density	Grip blocking	Tree planting
Timing	Spring 09	February 09	-
Area affected (%)	100	100	-

Cross-section (from EPR, 2010)

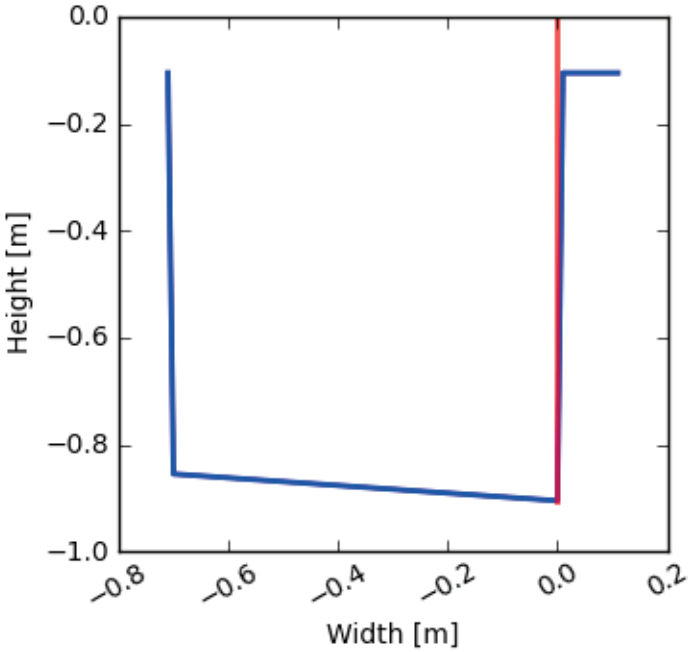

No rating curve available – stage used only in analyses

A.1.8 CRO_sc2

Gauge name	Swine Clough, bottom of grip, Croasdale Brook
Description:	At the bottom of the grip in the headwaters of Swine Clough in the Croasdale Brook catchment
Grid reference:	SD 69335 57247
Elevation:	411.3 m
Catchment area:	0.15 km^2 (process scale)
Abstractions:	-
Related sites:	Upstream: CRO_sc1 Downstream: CRO_sc3,CRO_sc5, CRO_out, Croasdale weir (EA) HOD_mid, Hodder Place
Baro used for correction:	Baro_Croasdale
Installation Date:	07/12/2007
Record Interval:	5 min (7 min from 06/12/2007 – 23/01/2008)
QA notes:	The gauge was initially installed at 07/12/2007, but the baro only recorded from 23/01/2008, so the full time record only starts at 23/01/2008. In addition, the diver changed at 23/01/2008

Location in Hodder Area	Photo of gauge, upstream direction, pre blocking
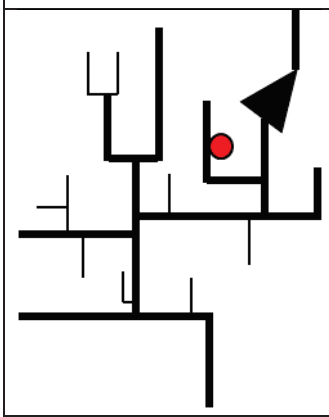	

UU ScaMP interventions	Stocking density	Grip blocking	Tree planting
Timing	Spring 09	February 09	-
Area affected (%)	100	100	-

Cross-section (from EPR, 2010)

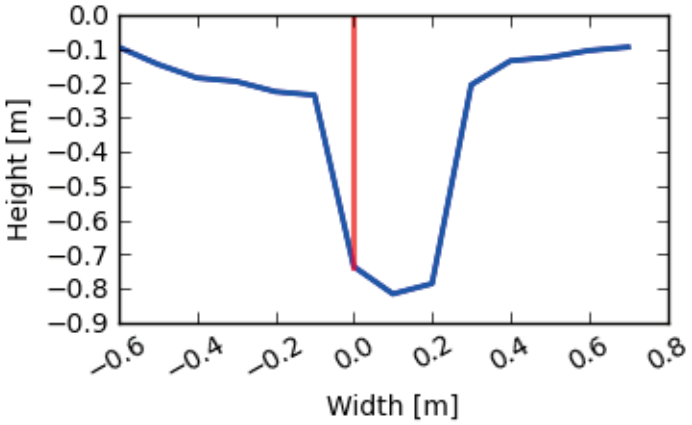

No rating curve available – stage used only in analyses

A.1.9 CRO_sc3

Gauge name	Swine Clough, outlet of a side grip, Croasdale Brook
Description:	At the outlet of a side grip in the headwaters of Swine Clough in the Croasdale Brook catchment
Grid reference:	SD 692323 57249
Elevation:	395.8 m
Catchment area:	0.015 km^2 (process scale)
Abstractions:	-
Related sites:	Upstream: none Downstream: CRO_sc5, CRO_out, Croasdale weir (EA) HOD_mid, Hodder Place
Baro used for correction:	Baro_Croasdale
Installation Date:	07/12/2007
Record Interval:	5 min (7 min from 06/12/2007 – 23/01/2008)
QA notes:	The gauge was initially installed at 06/12/2007, but the baro only recorded from 23/01/2008, so the full time record only starts at 23/01/2008. In addition, the diver changed at 23/01/2008; unreliable data as a result of livestock disturbance from 12/06/2008 – 01/07/2008; missing data from 17/10/2009-09/12/2009 as a result of equipment failure; diver changed at 09/12/2009

Location in Hodder Area	Photo of gauge, downstream direction, post blocking
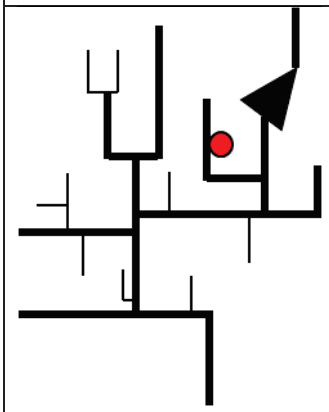	

UU ScaMP interventions	Stocking density	Grip blocking	Tree planting
Timing	Spring 09	February 09	-
Area affected (%)	100	100	-

Cross-section (from EPR, 2010)

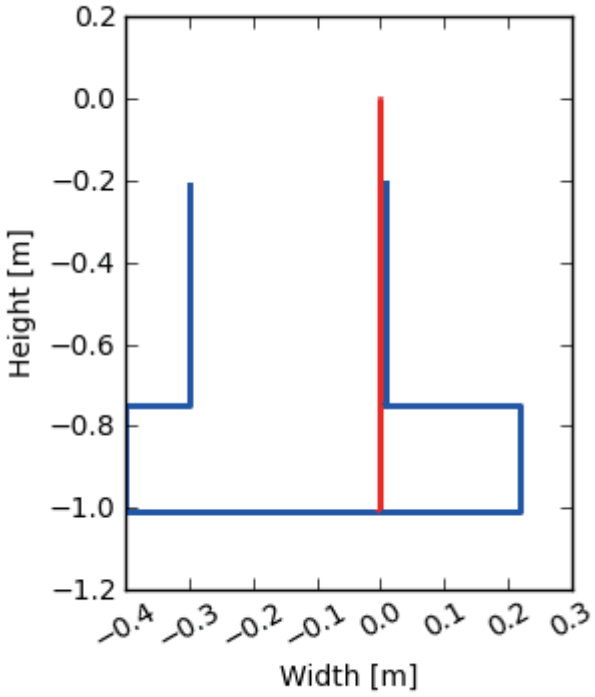

No rating curve available – stage used only in analyses

A.1.10 CRO_sc4

Gauge name	Swine Clough
Description:	At the top of Swine Clough, before the confluence with the grip, in the Croasdale Brook catchment
Grid reference:	SD 69119 57102
Elevation:	370.4 m
Catchment area:	0.10 km^2 (process scale)
Abstractions:	-
Related sites:	Upstream: none Downstream: CRO_sc5, CRO_out, Croasdale weir (EA) HOD_mid, Hodder Place
Baro used for correction:	Baro_Croasdale
Installation Date:	07/12/2007
Record Interval:	5 min (7 min from 06/12/2007 - 23/01/2008)
QA notes:	The gauge was initially installed at 06/12/2007, but the baro only recorded from 23/01/2008, so the full time record only starts at 23/01/2008. In addition, the diver changed at 23/01/2008. Between 02/04/2010 – 31/05/2010 unreliable data as a result of equipment failure (clock out of sync). Missing data from 08/06/2010 – 12/08/2010 as a result of equipment failure

Location in Hodder Area	Photo of gauge, upstream direction
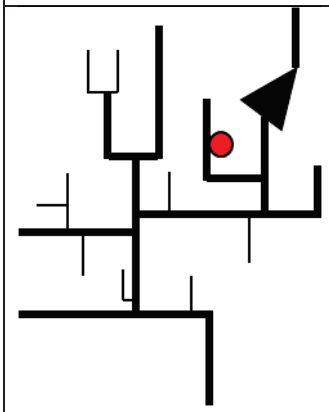	

UU SCaMP interventions	Stocking density	Grip blocking	Tree planting
Timing	Spring 09	-	-
Area affected (%)	100	-	-

Cross-section (from EPR, 2010)

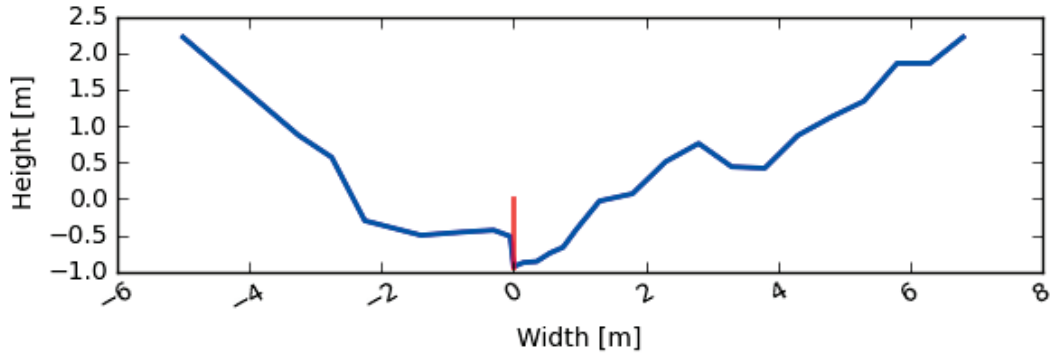

Rating Curve

Observed stage range (m):	-0.93 -0.43
Number of gaugings:	6
Percentage highest gauging of maximum observed stage peak (%):	61.2
Percentage of time extrapolated (%):	1.5

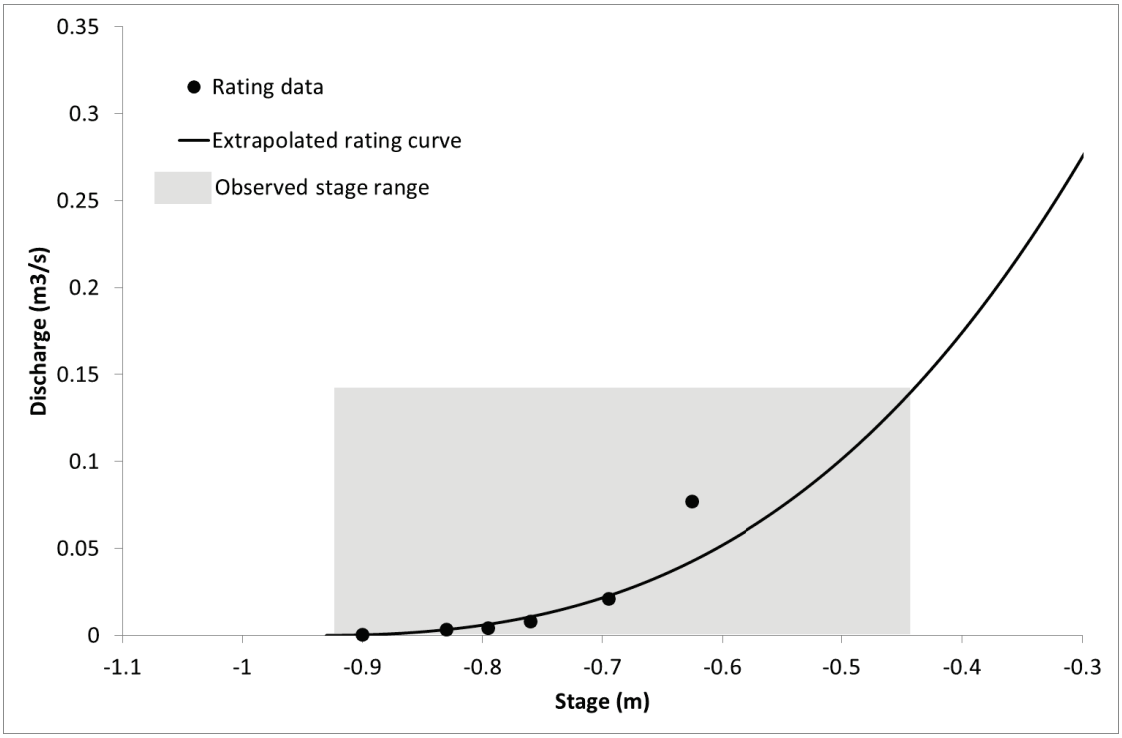

A.1.11 CRO_sc5

Gauge name	Croasdale Brook outlet
Description:	Outlet of Swine Clough in the Croasdale Brook catchment
Grid reference:	SD 68734 56678
Elevation:	255.73 m
Catchment area:	0.5 km^2 (micro scale)
Abstractions:	-
Related sites:	Upstream: CRO_sc1, CRO_sc2, CRO_sc3, CRO_sc4, Downstream: CRO_out, Croasdale weir (EA) HOD_mid, Hodder Place
Baro used for correction:	Baro_Croasdale
Installation Date:	07/12/2007
Record Interval:	5 min (7 min from 06/12/2007 - 13/03/2008)
QA notes:	The gauge was initially installed at 06/12/2007, but the baro only recorded from 23/01/2008, so the full time record only starts at 23/01/2008

Location in Hodder Area	Photo of gauge, downstream direction
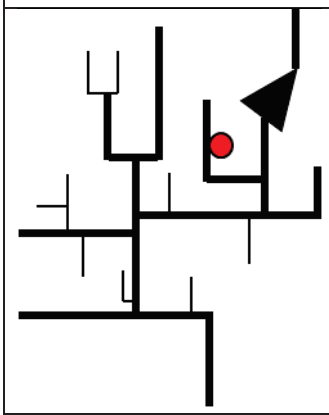	

UU SCaMP interventions	Stocking density	Grip blocking	Tree planting
Timing	Spring 09	February 09	-
Area affected (%)	100	35	-

Cross-section (from EPR, 2010)

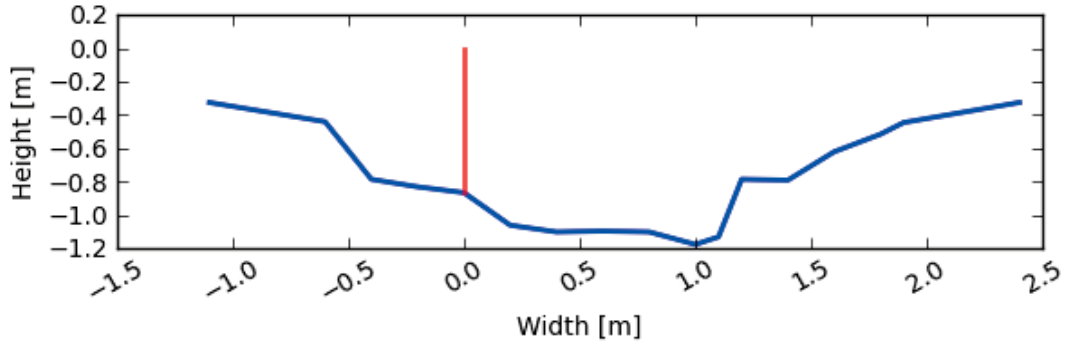

Rating Curve

Observed stage range (m):	-0.86 – (-0.35)
Number of gaugings:	7
Percentage highest gauging of maximum observed stage peak (%):	61.4
Percentage of time extrapolated (%):	2.1

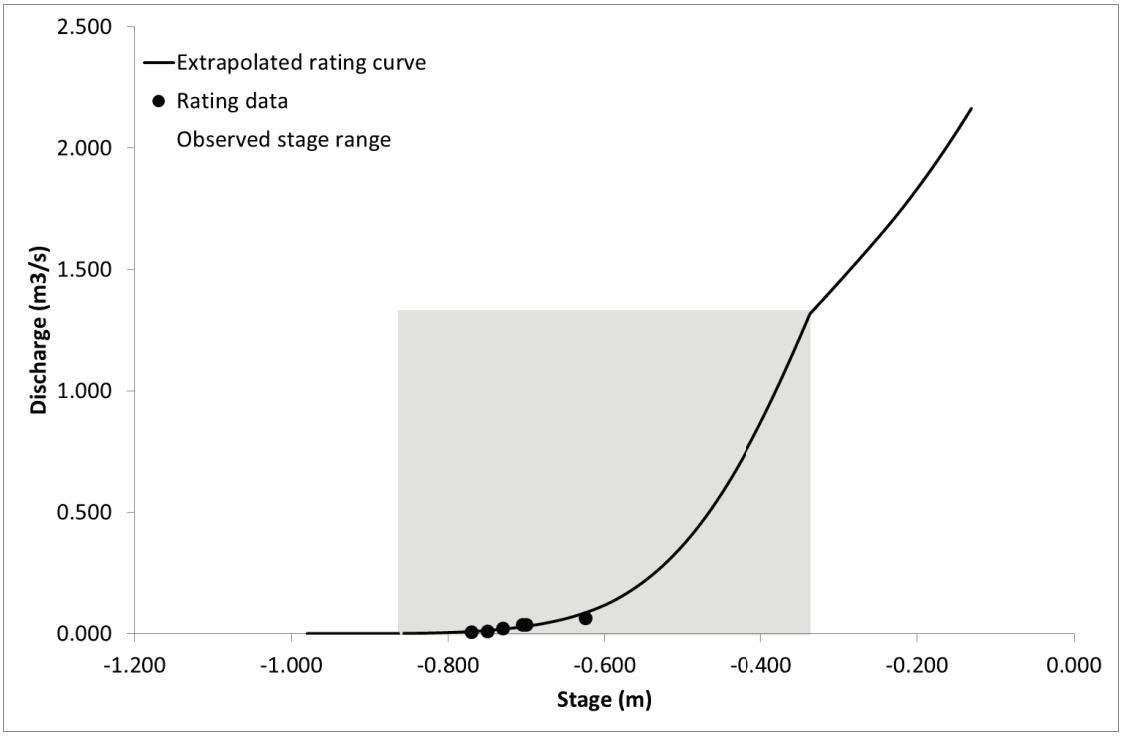

A.1.12 EAS_out

Gauge name	Easington Outlet
Description:	Outlet of Easington Brook
Grid reference:	SD 70781 50341
Elevation:	134.0 m
Abstractions:	-
Catchment area:	13.3 km^2 (mini scale)
Related sites:	Upstream: - Downstream: HOD_mid, Hodder Place (EA)
Baro used for correction:	Baro_Footholme
Installation Date:	19/06/2008
Record Interval:	5 min
QA notes:	-

Location in Hodder Area	Photo of gauge, downstream direction
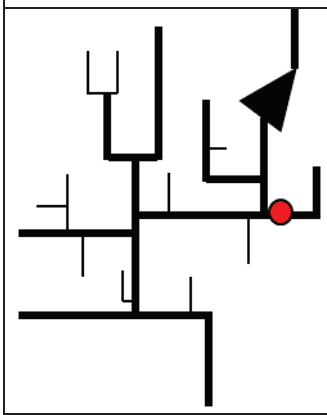	

UU SCaMP interventions	Stocking density	Grip blocking	Tree planting
Timing	-	-	-
Area affected (%)	-	-	-

Cross-section (from EPR)

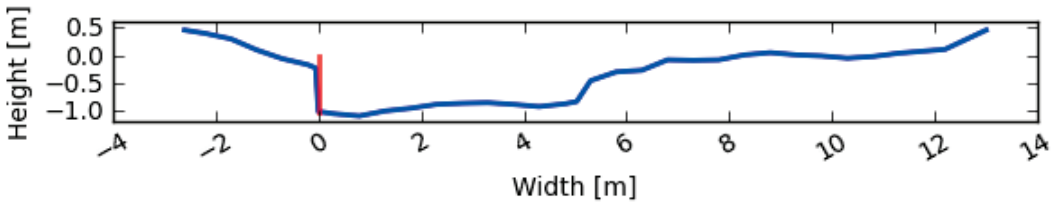

Rating Curve

Observed stage range (m):	-1.020 -0.494
Number of gaugings:	8
Percentage highest gauging of maximum observed stage peak (%):	43.6
Percentage of time extrapolated (%):	2.4

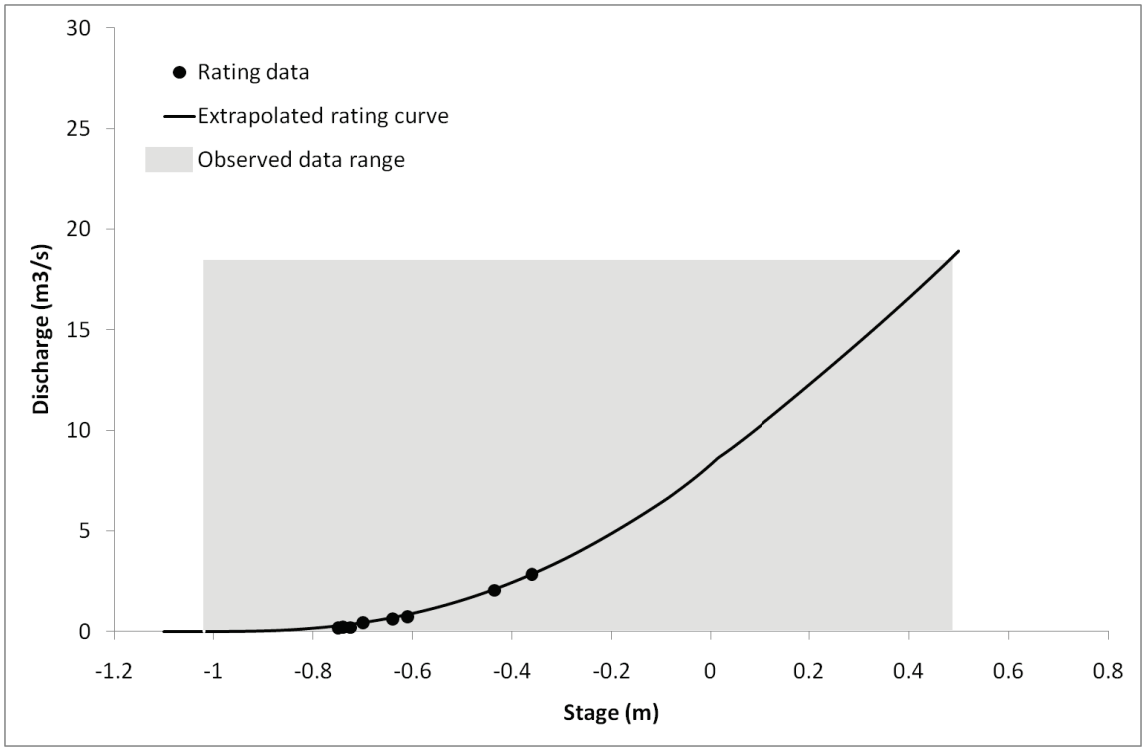

A.1.13 HAR_out

Gauge name	Hareden Outlet
Description:	Hareden Brook Outlet, a tributary of Langden Brook
Grid reference:	SD 64226 56588
Elevation:	147.4 m
Abstractions:	Upstream abstractions as part of United Utilities' Bowland abstraction system
Catchment area:	4.9 km^2 (micro scale)
Related sites:	Upstream: -. Downstream: LAN_out, Hodder Place (EA)
Baro used for correction:	Baro_Footholme
Installation Date:	20/05/2008
Record Interval:	5 min
QA notes:	Missing data from 03/10/2008 – 15/12/2008 as a result of vandalism, new diver from 09/12/2008

Location in Hodder Area	Photo of gauge, downstream direction
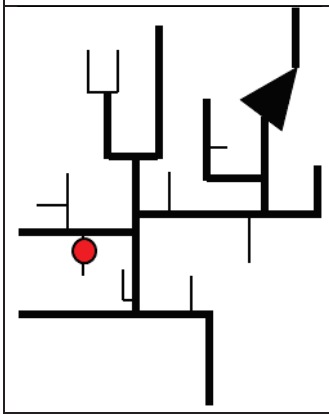	

UU SCaMP interventions	Stocking density	Grip blocking	Tree planting
Timing	February 09	-	February 09
Area affected (%)	100	-	NA

Cross-section (from EPR)

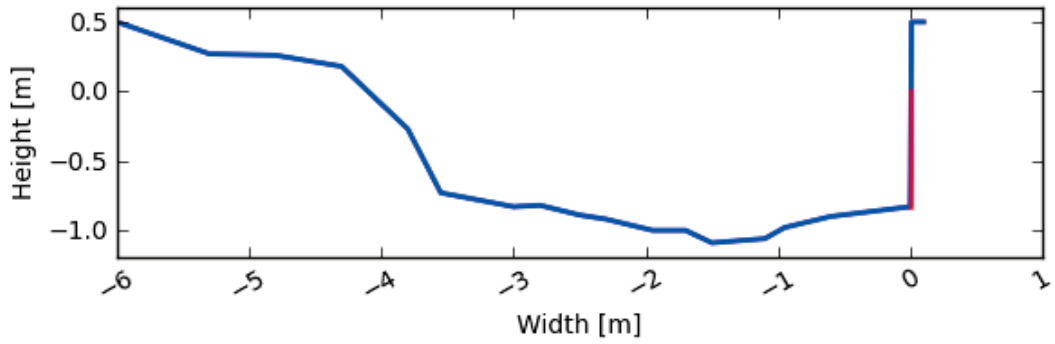

Rating Curve

Observed stage range (m):	-0.775 – 0.102
Number of gaugings:	6
Percentage highest gauging of maximum observed stage peak (%):	37.0
Percentage of time extrapolated (%):	1.6

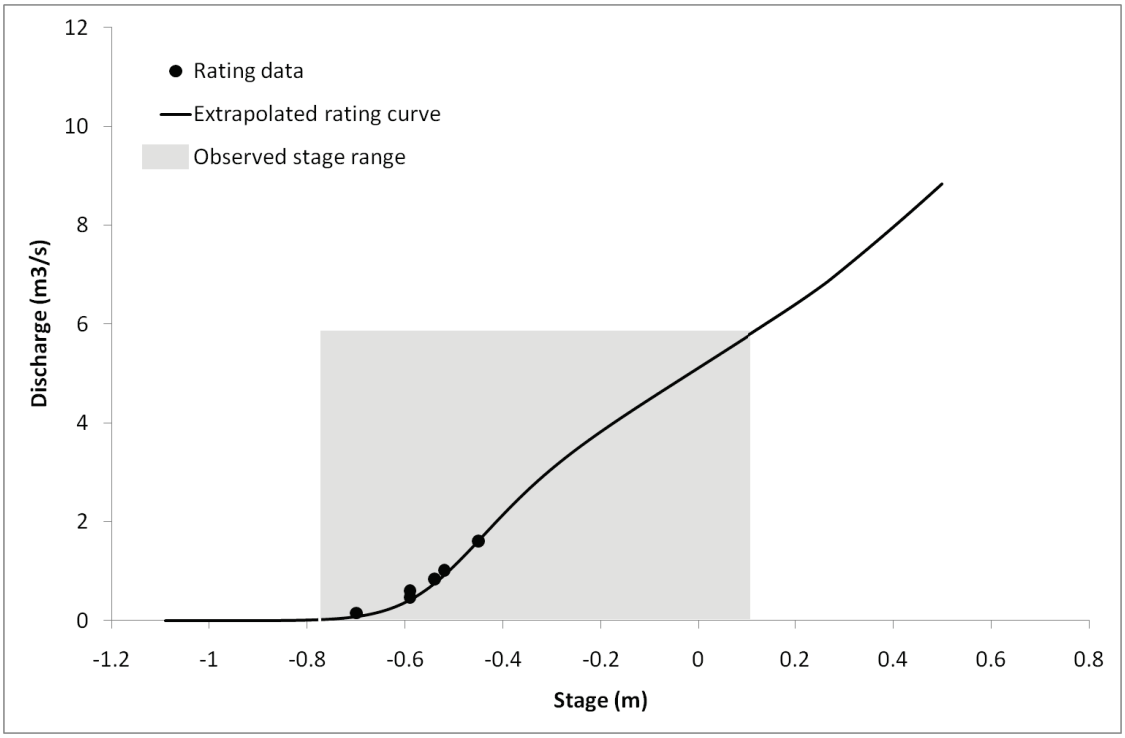

A.1.14 HOD_mid

Gauge name	Mid Hodder
Description:	Mid River Hodder, just upstream of the confluence with River Dunsop
Grid reference:	SD 66343 50031
Elevation:	116.1 m
Abstractions:	Upstream abstractions as part of United Utilities' abstraction system at Stocks Reservoir
Catchment area:	110.3 km^2 (meso scale)
Related sites:	Upstream: CRO_sc1, CRO_sc2, CRO_sc3, CRO_sc4, CRO_sc5, CRO_mid, Croasdale Weir (EA), CRO_out, EAS_out, Stocks Reservoir (EA) Downstream: Hodder Place (EA)
Baro used for correction:	Baro_Footholme
Installation Date:	20/06/2008
Record Interval:	5 min
QA notes:	Missing data from 03/02/2010 – 12/08/2010 as a result of equipment failure

Location in Hodder Area	Photo of gauge, downstream direction
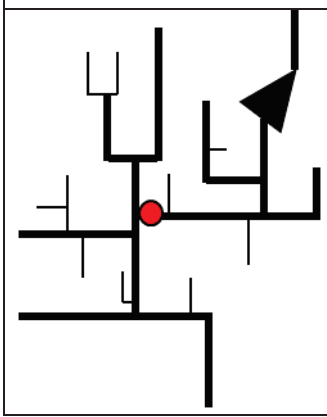	

UU SCaMP interventions	Stocking density	Grip blocking	Tree planting
Timing	February 09	February 09	-
Area affected (%)	1	<1	-

Cross-section (from EPR)

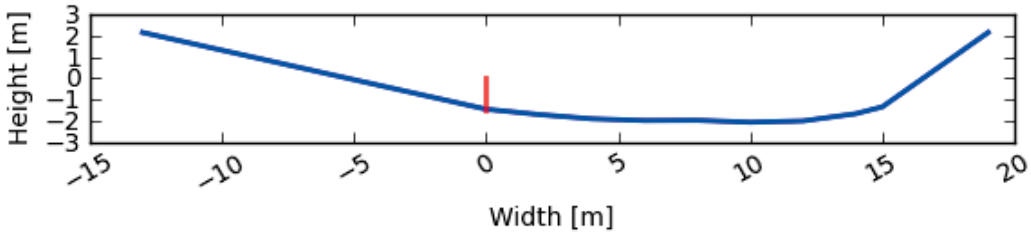

Rating Curve

Observed stage range (m):	-1.440 – 1.100
Number of gaugings:	8
Percentage highest gauging of maximum observed stage peak (%):	59.3
Percentage of time extrapolated (%):	<1

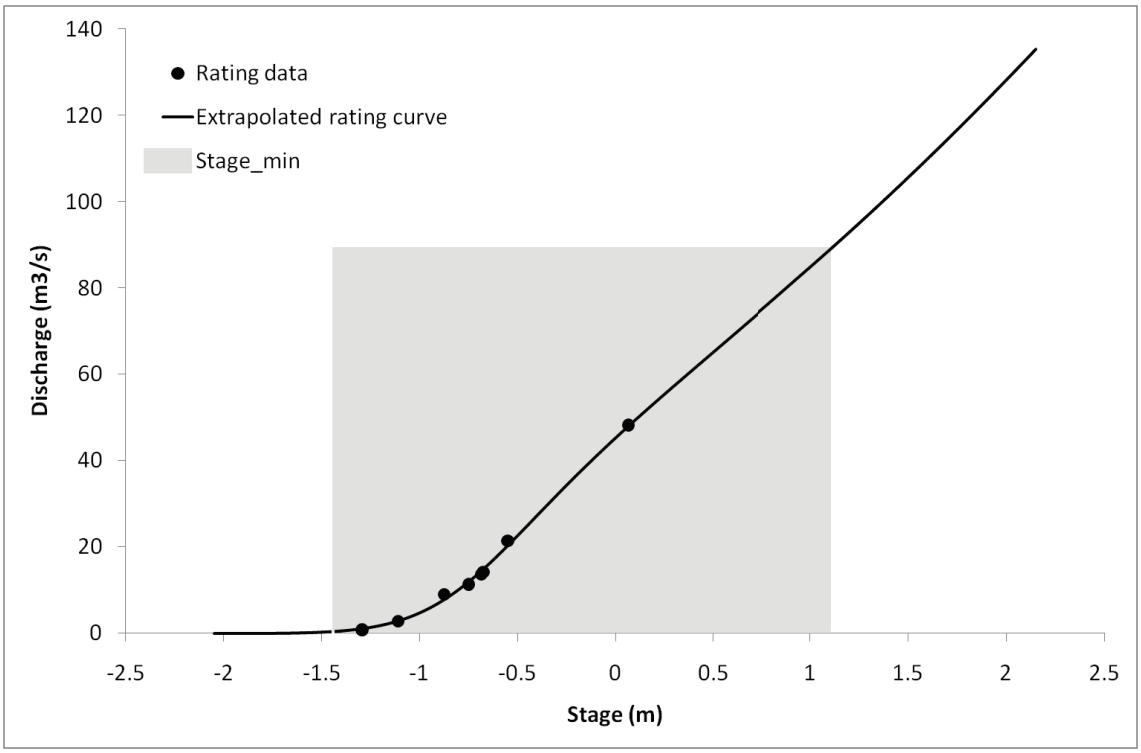

A.1.15 LAN_mid

Gauge name	Mid Langden
Description:	Mid Langden Brook, just upstream of the confluence with Losterdale Brook
Grid reference:	SD 63131 51083
Elevation:	165.9 m
Abstractions:	Upstream abstractions as part of United Utilities' Bowland abstraction system
Catchment area:	15.0 km^2 (mini scale)
Related sites:	Upstream: - Downstream: LAN_out, Hodder Place (EA)
Baro used for correction:	Baro_Footholme
Installation Date:	19/05/2008
Record Interval:	5 min
QA notes:	A telemetered 'frog logger' was installed adjacent to the current logger at 23/04/2010

Location in Hodder Area	Photo of gauge, downstream direction
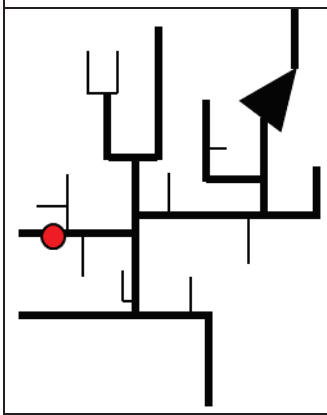	

UU SCaMP interventions	Stocking density	Grip blocking	Tree planting
Timing	February 09	-	Mar 09
Area affected (%)	100	-	<1

Cross-section (from EPR)

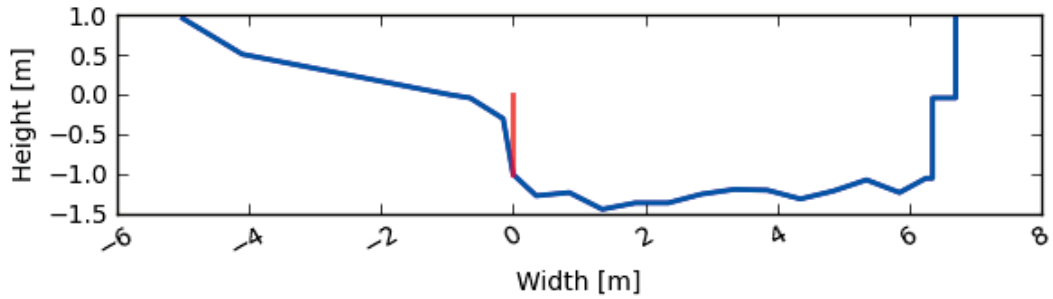

Rating Curve

Observed stage range (m):	-1.005 - -0.045
Number of gaugings:	9
Percentage highest gauging of maximum observed stage peak (%):	33.3
Percentage of time extrapolated (%):	4.7

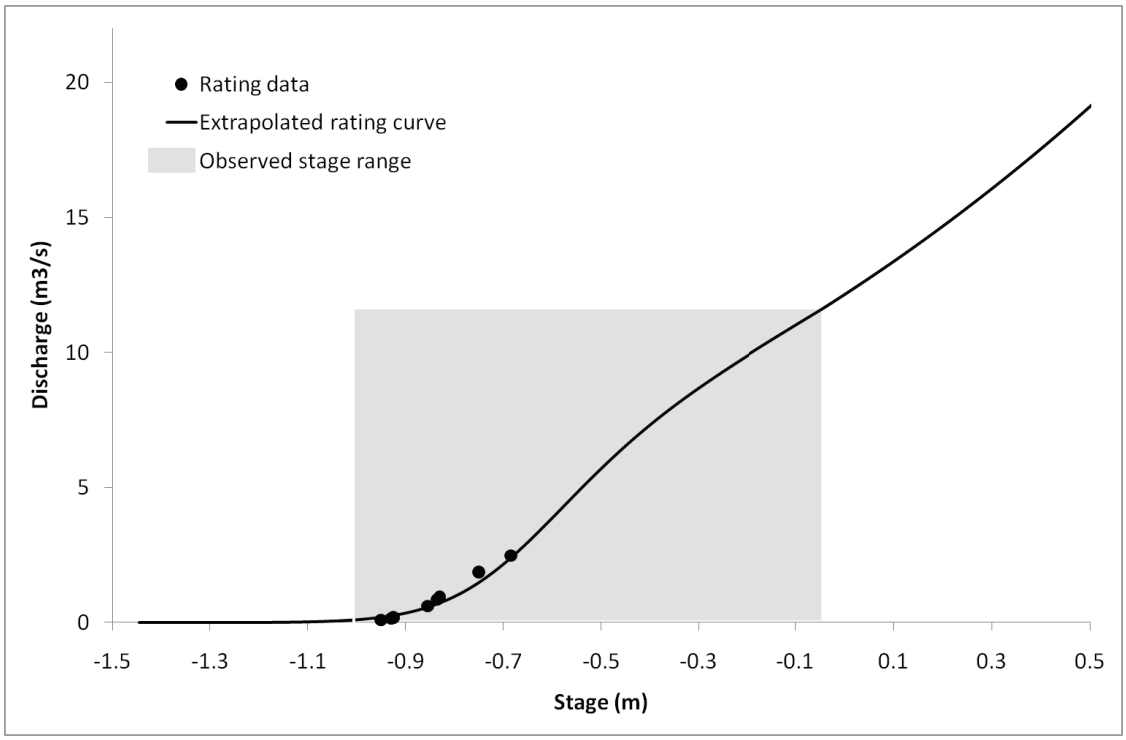

A.1.16 LAN_out

Gauge name	Langden Outlet
Description:	Langden Brook Outlet
Grid reference:	SD 65932 49334
Elevation:	117.4 m
Abstractions:	Upstream abstractions as part of United Utilities' Bowland abstraction system
Catchment area:	27.7 km^2 (mini scale)
Related sites:	Upstream: LOS_stock/LOS_stock_weir, LOS_mid, LOS_out, LAN_mid, HAR_out Downstream: Hodder Place (EA)
Baro used for correction:	Baro_Footholme
Installation Date:	21/05/2008
Record Interval:	15 min
QA notes:	-

Location in Hodder Area	Photo of gauge location, upstream direction
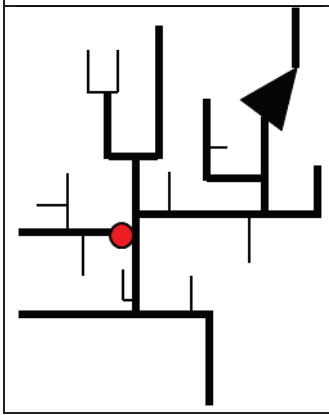	

UU SCaMP interventions	Stocking density	Grip blocking	Tree planting
Timing	February 09	-	March 09
Area affected (%)	85	-	<1

Cross-section (from EPR)

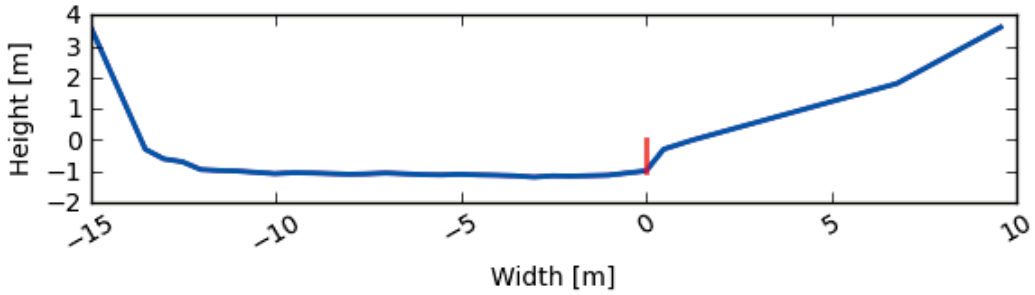

Rating Curve

Observed stage range (m):	-0.985 – 0.177
Number of gaugings:	8
Percentage highest gauging of maximum observed stage peak (%):	66.7
Percentage of time extrapolated (%):	<1

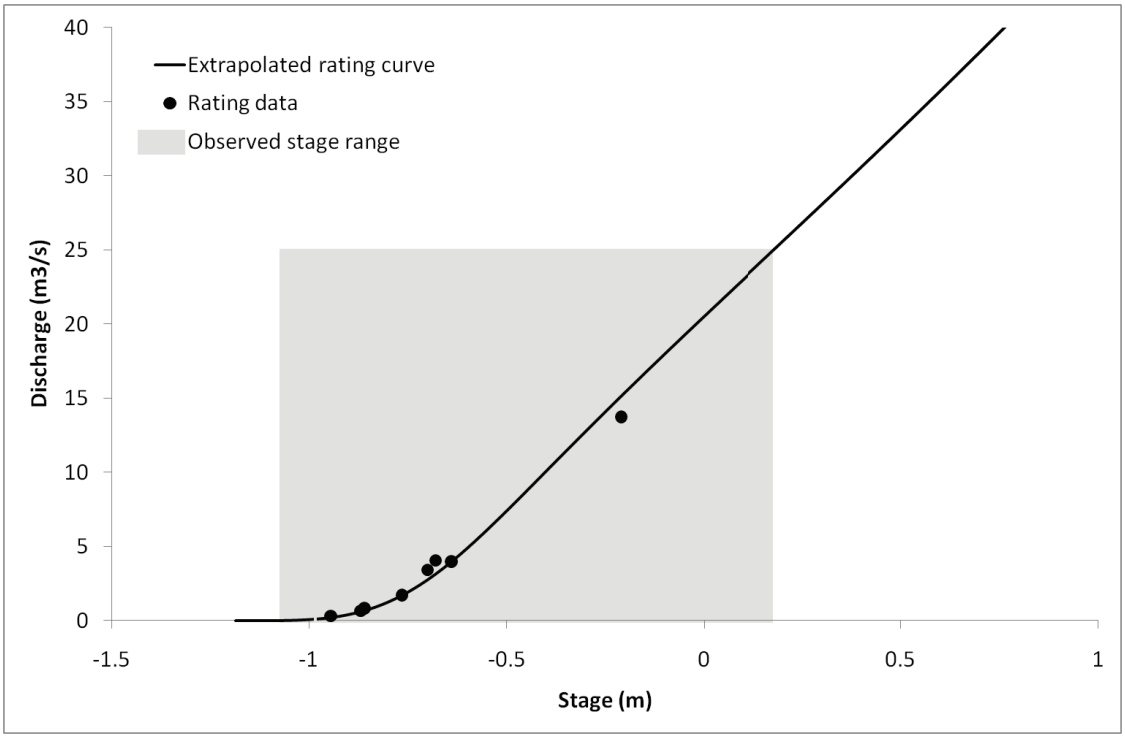

A.1.17 LOS_mid

Gauge name	Mid Losterdale
Description:	Mid Losterdale Brook, just upstream of the confluence with Swine Clough (monitored for stocking density changes and tree planting)
Grid reference:	SD 62743 52049
Elevation:	187.9 m
Abstractions:	-
Catchment area:	2.5 km^2 (micro scale)
Related sites:	Upstream: - Downstream: LOS_out, LAN_out, Hodder Place (EA)
Baro used for correction:	Baro_Footholme
Installation Date:	05/06/2008
Record Interval:	5 min
QA notes:	Missing data from 25/12/2008 – 13/01/2009 as a result of equipment failure, diver changed at 03/02/2010

Location in Hodder Area	Photo of gauge, downstream direction
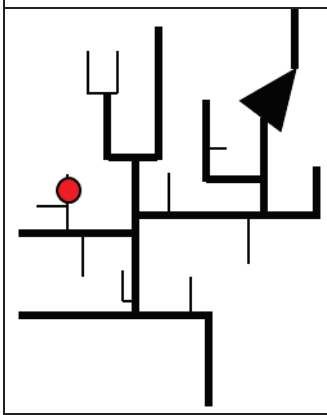	

UU SCaMP interventions	Stocking density	Grip blocking	Tree planting
Timing	February 09	-	-
Area affected (%)	100	-	-

Cross-section (from EPR)

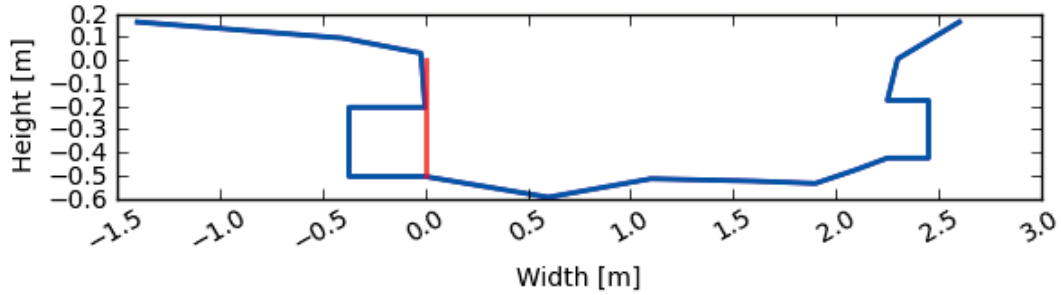

Rating Curve

Observed stage range (m):	-0.505 – 0.328
Number of gaugings:	8
Percentage highest gauging of maximum observed stage peak (%):	50.4
Percentage of time extrapolated (%):	1.0

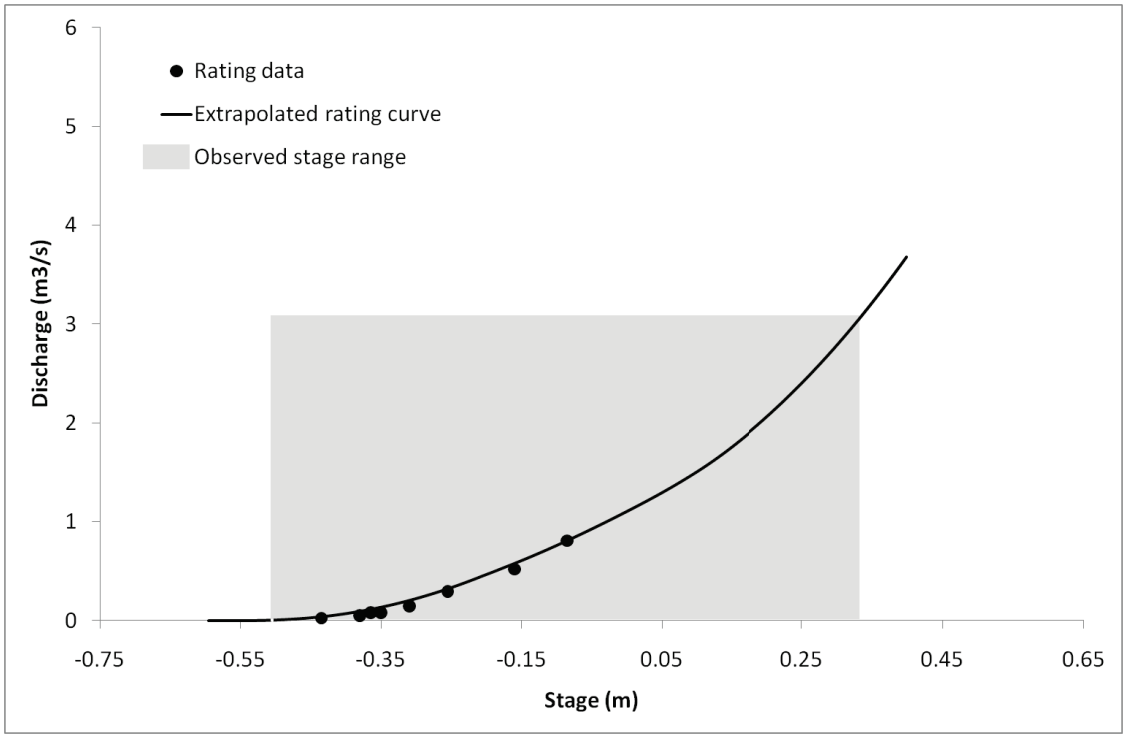

A.1.18 LOS_out

Gauge name	Losterdale Outlet
Description:	Losterdale Brook Outlet, a tributary of Langden Brook
Grid reference:	SD 63203 51219
Elevation:	165.2 m
Abstractions:	Upstream abstractions as part of United Utilities' Bowland abstraction system
Catchment area:	4.0 km^2 (micro scale)
Related sites:	Upstream: LOS_stock/LOS_stock_weir, LOS_mid Downstream: LAN_out, Hodder Place (EA)
Baro used for correction:	Baro_Footholme
Installation Date:	05/06/2008
Record Interval:	5 min
QA notes:	Missing data from 24/01/2010 – 02/02/2010 and 03/07/2010 – 14/07/2010 as a result of equipment failure. Data post 24/01/2010 questionable as a result of the equipment failure: sensor potentially damaged by frost

Location in Hodder Area	Photo of gauge, downstream direction
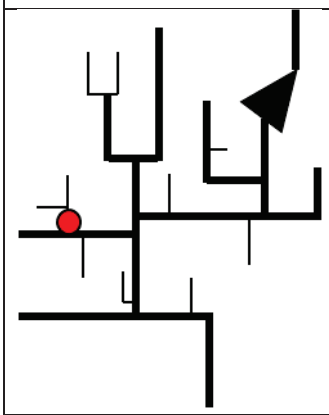	

UU SCaMP interventions	Stocking density	Grip blocking	Tree planting
Timing	February 09	-	March 09
Area affected (%)	100	-	<1

Cross-section (from EPR)

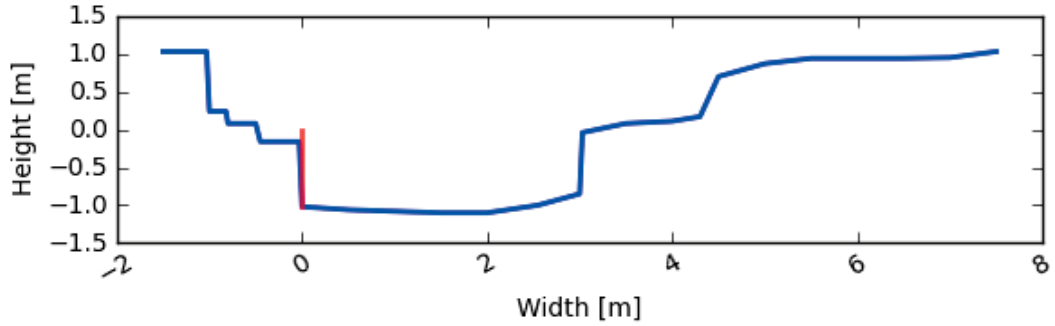

Rating Curve

Observed stage range (m):	-1.010 -0.001
Number of gaugings:	7
Percentage highest gauging of maximum observed stage peak (%):	37.1
Percentage of time extrapolated (%):	4.6

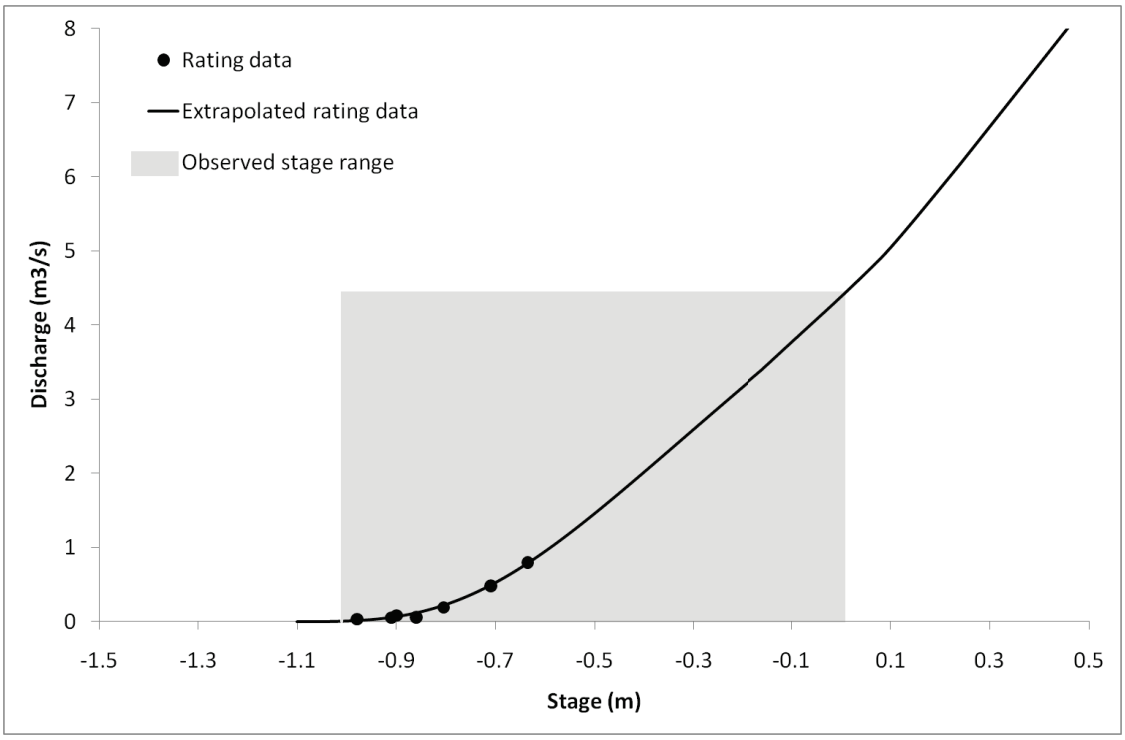

A.1.19 LOS_stock/LOS_stock_weir

Gauge name	LOS_stock and LOS_stock_weir
Description:	LOS_stock is located at the outlet of Swine Clough, a headwater of Losterdale Brook, in the Langden Brook subcatchment. LOS_stock_weir is located about 500 m upstream of LOS_stock, in a headwater of Swine Clough.
Grid reference:	LOS_stock: SD 62721 52025
Elevation:	LOS_stock: 197.7
Abstractions:	-
Catchment area:	LOS_stock: 0.12 km^2 (process scale) LOS_stock_weir: 1.00 km^2 (micro scale)
Related sites:	Upstream: none Downstream: LOS_out, LAN_out, Hodder Place (EA)
Baro used for correction:	Baro_Footholme
Installation Date:	03/06/2008 (LOS_stock), 25/11/2008 (LOS_stock_weir)
Record Interval:	5 min
QA notes:	LOS_stock has missing data from 03/10/2008 - 09/12/2008 as a result of equipment failure. The diver was replaced at 09/12/2008. The data of LOS_stock_weir are unreliable at 09/12/2009 as a result of weir maintenance.

LOS_stock:

Location in Hodder Area	Photo of gauge, downstream direction
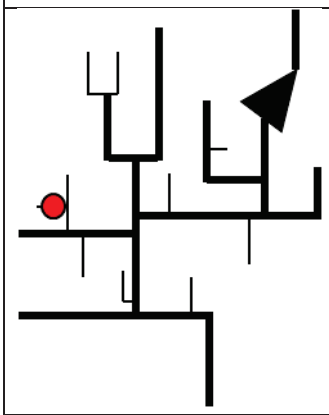	

UU SCaMP interventions	Stocking density	Grip blocking	Tree planting
Timing	February 2009	-	March 2009
Area affected (%)	100	-	5

LOS_stock_weir:

Location in Hodder Area	Photo of weir and gauge, upstream direction
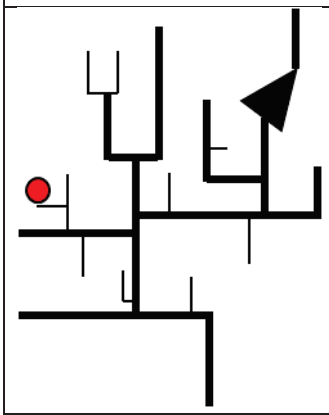	

UU SCaMP interventions	Stocking density	Grip blocking	Tree planting
Timing	February 2009	-	February 2009
Area affected (%)	100	-	5

Rating Curve

No rating curve available for LOS_stock as this site was considered redundant after the installation of the LOS_stock_weir.

The weir at LOS_stock_weir is a rectangular weir build according to British Standard 3680, Part 4A (BSI, 1981). The geometrical details of the weir are given below.

Schematic representation of the v-notch weir at WHI_tree_weir

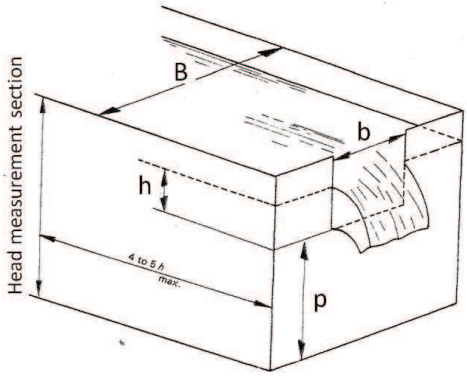

B	1.4
b	0.8
p (upstream)	0.345
p (downstream)	0.560
Maximum height above crest	0.45
Distance gauge to weir	0.65

For rectangular thin plate weirs the discharge Q ($m^3\ s^{-1}$) can be calculated from stage h (m) according to the Kindsvater-Carter formula:

$$Q = C_e \frac{2}{3} \sqrt{2g_n} b_e h_e^{3/2}$$

where C_e is the coefficient of discharge (-), b_e is the effective width (m), h_e is the effective head (m), and g_n is the acceleration due to gravity (9.81 m/s^2).

A.1.20 LOU_out

Gauge name	Loud Outlet
Sub catchment:	Outlet of River Loud
Grid reference:	SD 64889 43056
Elevation:	86.5 m
Catchment area:	47.3 km^2 (mini scale)
Abstractions:	-
Related sites:	Upstream: none
	Downstream: Hodder Place
Baro used for correction:	Baro_Loud
Installation Date:	11/06/2008
Record Interval:	15 min
QA notes:	-

Location in Hodder Area	Photo of gauge, downstream direction
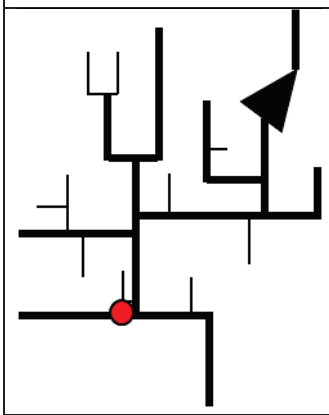	

UU SCaMP interventions	Stocking density	Grip blocking	Tree planting
Timing	-	-	-
Area affected (%)	-	-	-

Cross-section (from EPR)

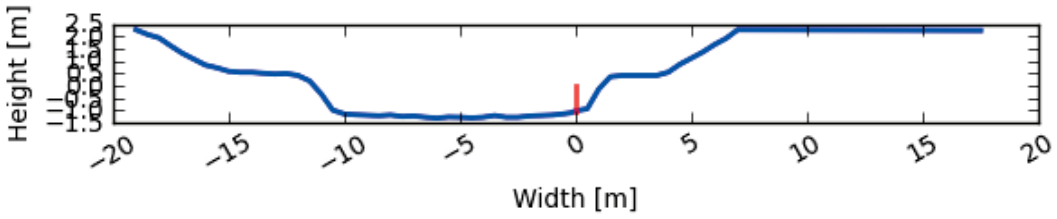

Rating Curve

Observed stage range (m):	-1.00 – 1.56
Number of gaugings:	6
Percentage highest gauging of maximum observed stage peak (%):	53.9
Percentage of time extrapolated (%):	0.2

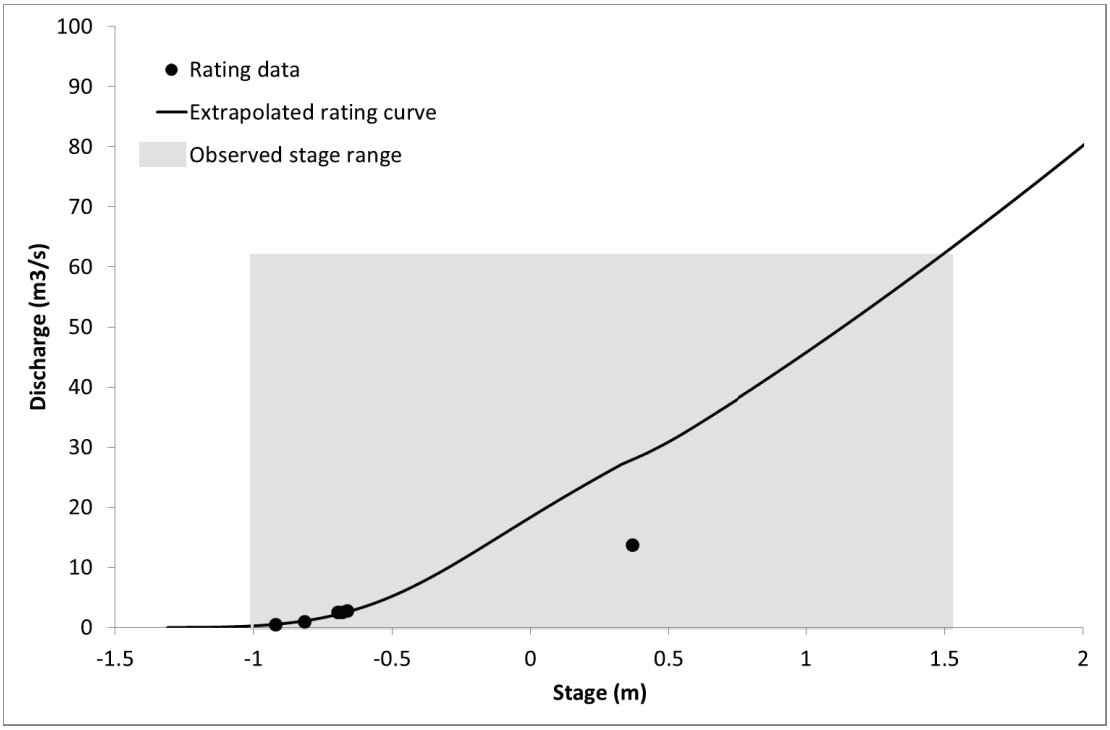

A.1.21 WHI_mid

Gauge name	Mid Whitendale
Description:	Mid River Whitendale, upstream of the confluence with a stream draining from Blue Scar (monitored for tree planting)
Grid reference:	SD 66061 54633
Elevation:	205.0 m
Abstractions:	Upstream abstractions as part of United Utilities' Dunsop abstraction system
Catchment area:	10.0 km^2 (mini scale)
Related sites:	Upstream: - Downstream: WHI_out, Footholme (EA), Hodder Place (EA)
Baro used for correction:	Baro_Footholme
Installation Date:	11/06/2008
Record Interval:	15 min
QA notes:	Gauge maintenance at 26/02/2009 where datum shifted -19.5 cm

Location in Hodder Area	Photo of gauge, downstream direction
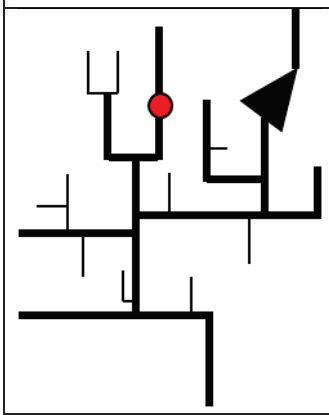	

UU SCaMP interventions	Stocking density	Grip blocking	Tree planting
Timing	Spring 08	2005	Spring 08
Area affected (%)	100	NA	5

Cross-section (from EPR)

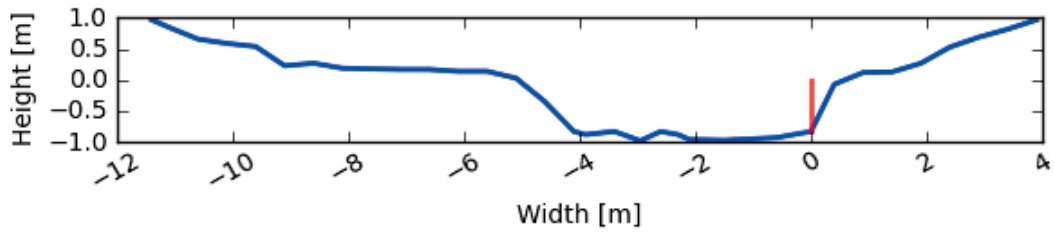

Rating Curve

Observed stage range (m):	-0.830 – 0.522
Number of gaugings:	6
Percentage highest gauging of maximum observed stage peak (%):	43.3
Percentage of time extrapolated (%):	3.7

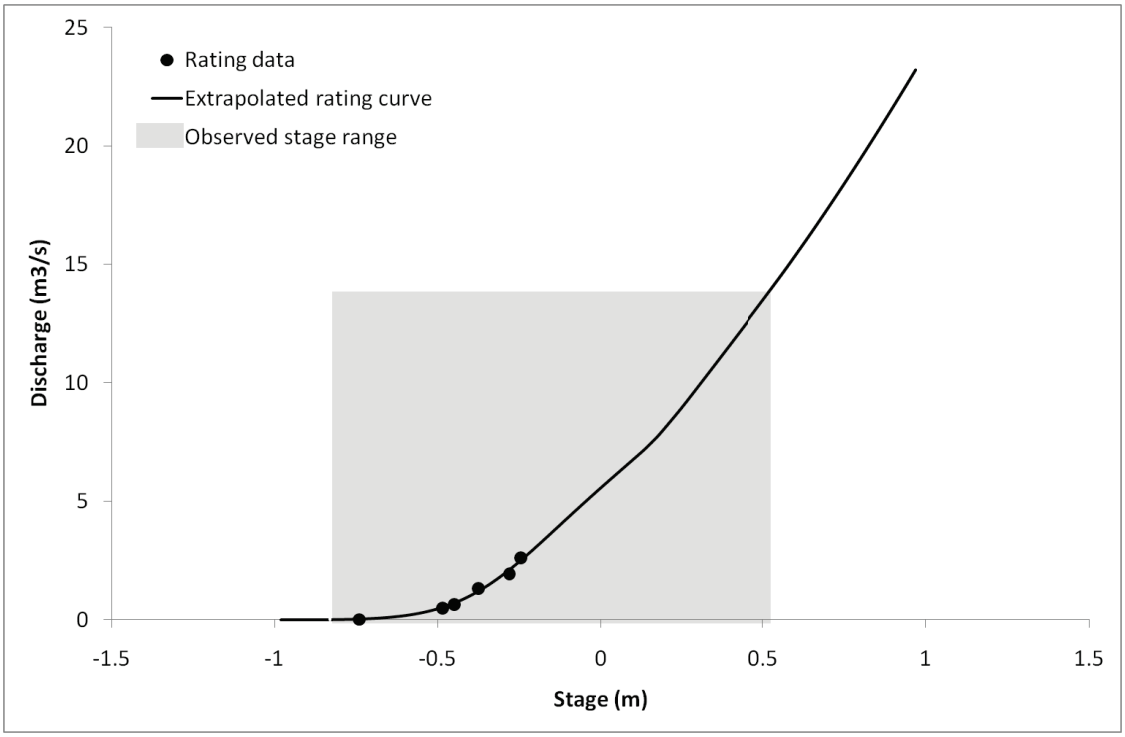

A.1.23 WHI_out

Gauge name	Whitendale Outlet
Description:	River Whitendale Outlet, subcatchment of River Dunsop
Grid reference:	SD 65326 53231
Elevation:	177.9 m
Abstractions:	Upstream abstractions as part of United Utilities' Dunsop abstraction system
Catchment area:	13.6 km^2 (mini scale)
Related sites:	Upstream: WHI_tree/WHI_tree_weir Downstream: Footholme (EA), Hodder Place (EA)
Baro used for correction:	Baro_Footholme
Installation Date:	07/12/2007
Record Interval:	15 min
QA notes:	In low flows this gauge may be above the river water surface. The gauge was initially installed at 07/12/2007, but the baro only recorded from 23/01/2008, so the full time record only starts at 23/01/2008.

Location in Hodder Area	Photo of gauge, downstream direction
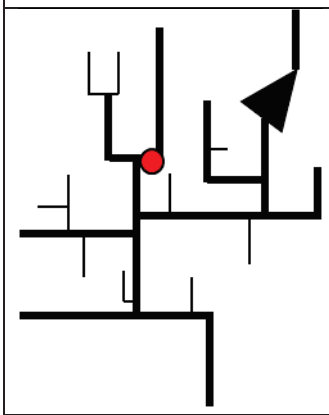	

UU SCaMP interventions	Stocking density	Grip blocking	Tree planting
Timing	Spring 08	2005	Spring 08
Area affected (%)	100	NA	5

Cross-section (from EPR)

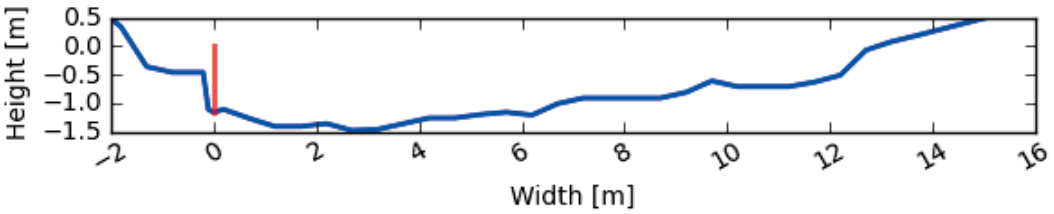

Rating Curve

Observed stage range (m):	-1.155 – 0.177
Number of gaugings:	9
Percentage highest gauging of maximum observed stage peak (%):	49.8
Percentage of time extrapolated (%):	2.2

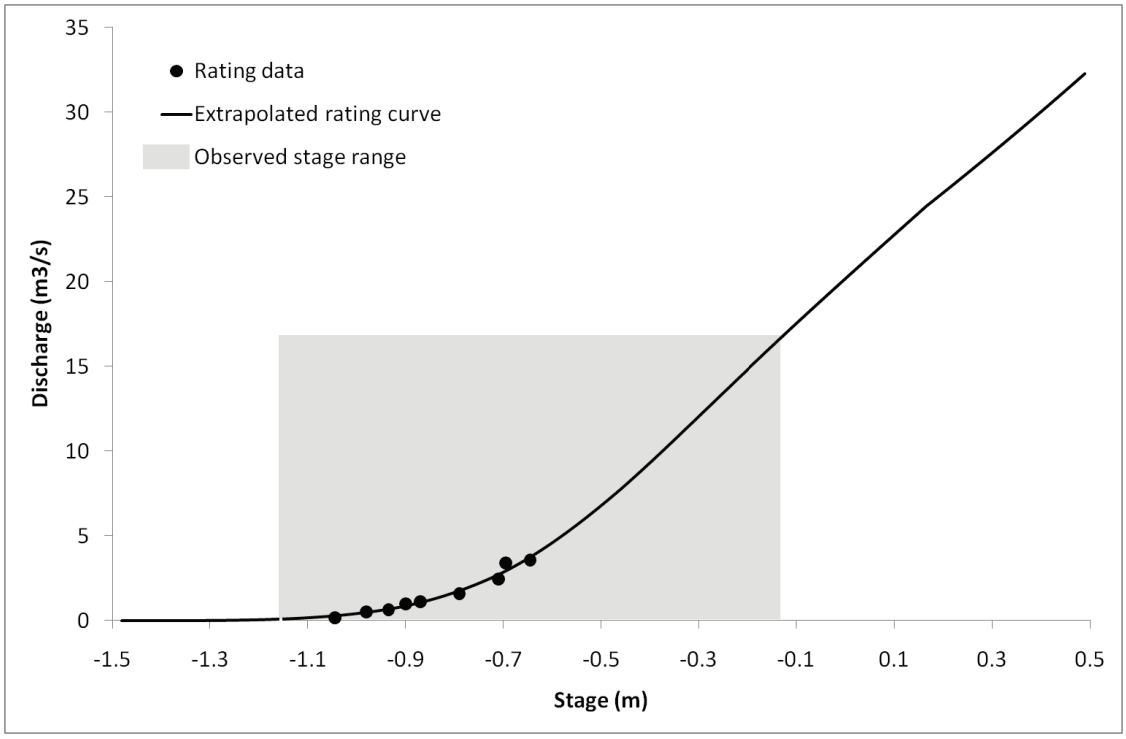

A.1.22 WHI_tree/WHI_tree_weir

Gauge name	WHI_tree (superseded by WHI_tree_weir at 25/11/08)
Description:	The outlet of a stream draining Blue Scar at Middle Knoll in the Whitendale subcatchment. WHI_tree_weir is located 18 m downstream of channel site WHI_tree
Grid reference:	SD 66030 54663 (WHI_tree), and SD 66041 54647 (WHI_tree_weir)
Elevation:	208.4 m (WHI_tree), and 205.5 (WHI_tree_weir)
Abstractions:	-
Catchment area:	0.06 km^2 (process scale)
Related sites:	Upstream: - Downstream: WHI_out, Footholme (EA), Hodder Place (EA)
Baro used for correction:	Baro_Footholme
Installation Date:	03/06/2008 (WHI_tree), 25/11/2008 (WHI_tree_weir)
Record Interval:	5 min
QA notes:	-

Location in Hodder Area	Photo of weir and gauge, upstream direction
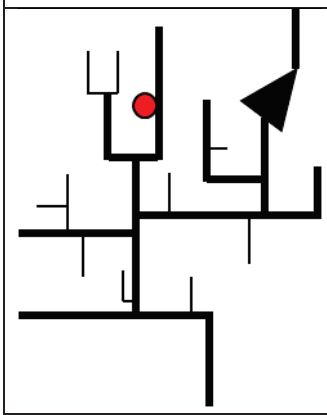	

UU SCaMP interventions	Stocking density	Grip blocking	Tree planting
Timing	-	-	Spring 2008
Area affected (%)	-	-	100

Rating Curve

The weir at WHI_tree/WHI_tree_weir is a v-notch weir build according to British Standard 3680, Part 4A (BSI, 1981). The geometrical details of the weir are given below.

Schematic representation of the v-notch weir at WHI_tree_weir

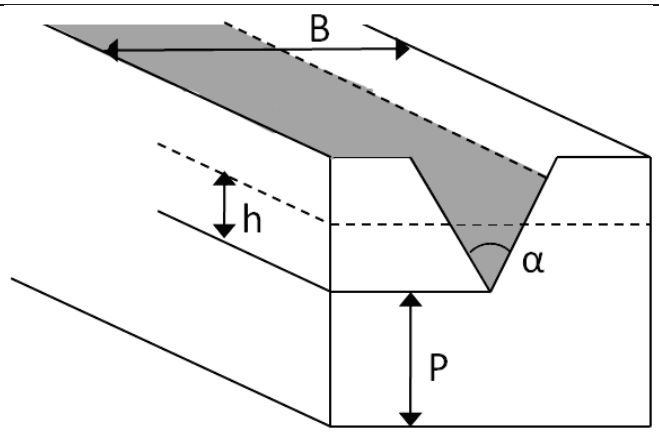

B	0.85
α	90
p (upstream)	0.135
p (downstream)	0.3
Maximum height above crest	0.28
Distance gauge to weir	1.15

The discharge Q (m^3/s) is calculated from stage h (m) according to the Kindsvater-Shen formula (BSI, 1981):

$$Q = C_e \frac{8}{15} \tan\frac{\alpha}{2} \sqrt{2 g_n h_e^{5/2}}$$

where h_e is the effective head above the crest (m), and g_n is the acceleration due to gravity (m/s^2), and the coefficient of discharge C_e has been determined by experiments as a function of P, B and h_e (BSI, 1981).